Agreement INGV-DPC 2007-2009

Project S4: ITALIAN STRONG MOTION DATA BASE

Responsibles: Francesca Pacor, INGV Milano – Pavia
and Roberto Paolucci, Politecnico Milano

http://esse4.mi.ingv.it

Deliverable # 7

APPLICATION OF SURFACE-WAVES METHODS FOR SEISMIC SITE CHARACTERIZATION OF ITACA STATIONS

Annexes: Technical Reports

June 2010

edited by:

UR4 Sebastiano Foti, Politecnico di Torino

UR8 Stefano Parolai, Helmholtz Centre Potsdam GFZ German Research Centre for Geosciences

UR7 Dario Albarello, Università di Siena

Contributors

UR1 – INGV Milano

Rodolfo Puglia

UR2 – INGV Roma

Giuliano Milana, Giuseppe Di Giulio, Fabrizio Cara, Paola Bordoni, Riccardo Azzara, Francesco Bergamaschi

UR4 – Politecnico di Torino

Paolo Bergamo, Cesare Comina (Università di Torino), Sebastiano Foti, Margherita Maraschini, Ken Tokeshi

UR7 – Università di Siena

Dario Albarello, Enrico Lunedei, Domenico Pileggi, David Rossi

UR8 – Helmholtz Centre Potsdam GFZ German Research Centre for Geosciences

Stefano Parolai, Matteo Picozzi

Shear waves velocity measurements at Assergi (GSA) site

The velocity profile for the R.A.N. station of Assergi (GSA) was derived by MASW and microtremor measurements performed in the vicinity of the station. Due to the large available space we performed both 1D (active and passive) and 2D array analysis.
1D data were collected by three data loggers Geometrics-GEODE interconnected in a LAN configuration. The GEODE is a 24 channels instrument based on a 24 bits AD converter. The data acquisition is driven by a laptop PC that is also used as data storage unit, data are stored in SEG2 binary format. The geophones used are GEOSPACE vertical geophones with a natural frequency of 4.5 Hz. Active data were collected using a linear deployment based on 72 channels with two geophones spacing of 2 meters and a minigun as active source. Minigun shots were performed at both sides of each deployment with two offsets (20 meters, 10 meter), an extra shot was performed at the center of the array. The symmetry in shots layout allows verifying the monodimensional behavior of the investigated site as required by MASW technique. Sampling rate was set at 0.125 ms with a record duration of 2 seconds (16000 points). For the passive 1D approach was used with the same array geometry; in this case we collected 20 noise windows of 30 seconds length with a sampling rate of 2 ms.
For 2D arrays we used 12 stand alone seismic instruments based on Reftek 130 (24 bits) and Lennartz Marslite (21 bits) data loggers. Each unit, synchronized using GPS receivers, was operating in continuous recording mode with a sampling rate of 200-250 samples per second. Data were recorded in a native binary format and converted in SEGY or SEG2 format. The recording units were connected to Lennartz LE3D-5s seismometers with a natural frequency of 0.2 Hz. and high sensitivity (400 V/m/s). To reduce the bias introduced by possible errors in sensors location, the station's position is determined by differential GPS measurements obtained performing a real time kinematic survey with a Leica Systems 1200 GNSS instrument. The differential corrections are obtained through a GPRS connection to a network of reference stations (www.italpos.it). The positioning system consents to operate in navigation mode. It provide in real time distance and azimuth between any couple of points in the array. This feature allows to draw the array geometry in advance and to easily find the positions of the recording stations on the field. With this approach the error in positioning can be lowered to few (5-10) centimeters.
Data were processed in order to find the experimental dispersion curve for Rayleigh waves. For 1D and 2D array data three different computer codes were used: Optim R.e.m.i, Geopsy (www.geopsy.org) and software developed by INGV researcher.
For the inversion of the dispersion curve we used the Neighbourhood Algorithm in order to invert the experimental curves (*www.geopsy.org*). The results of data analysis are shown in figures 1 and 2.

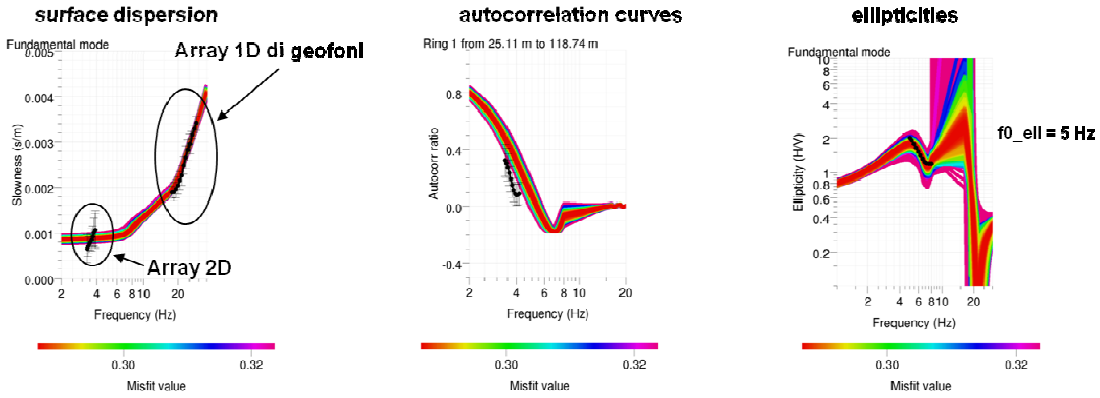

Figure 1 – Experimental dispersion curve, autocorrelation and ellipticity results.

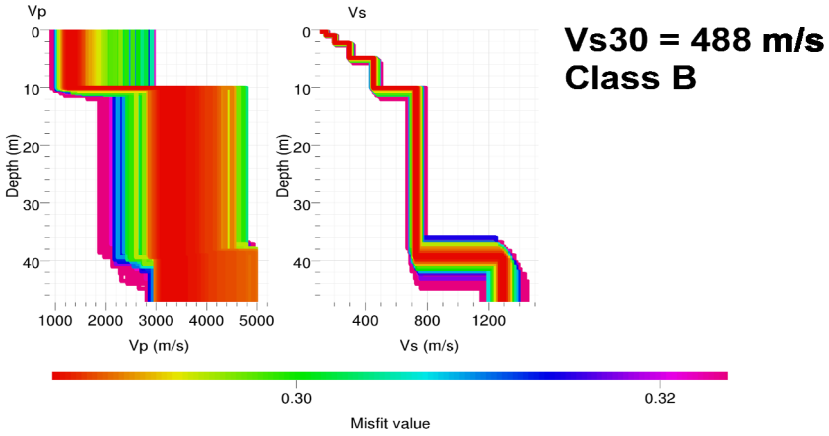

Figure 2 – Inverted Vp and Vs best models.

Figure 1 illustrates the fit between experimental and theoretical curves. We performed a joint inversion of dispersion curve, autocorrelation curve derived by ESAC techniques, and ellipticity function to better constraint the deeper layers. The ellipciticy function was derived as the average of HVNSR results fro the 12 array stations. We use the decreasing branch of the HVNSR starting from the resonance frequency.

The inverted best models of figure 2 show some velocity increase in the first 10 meters and a deeper layer with Vs velocity of about 600 m/s. A deeper interface at about 40 meters is related to a faster layer with a velocity of 1300 m/s. The results of inversion are quite stable in terms of Vs and the investigated depth are well constrained by the geometry of the array.

The passive data can be partially affected by the presence of strong disturbances related to the highway viaduct running very close to the site.

Shear waves velocity measurements at Avezzano (AVZ) site

The velocity profile for the R.A.N. station of Avezzano (AVZ) was derived by MASW and microtremor measurements performed in the vicinity of the station. Due to the large available space we performed 2D array analysis.
For the 2D array we used 14 stand alone seismic instruments based on Reftek 130 (24 bits) and Lennartz Marslite (21 bits) data loggers with a maximun array aperture of about 1 km. Each unit, synchronized using GPS receivers, was operating in continuous recording mode with a sampling rate of 200-250 samples per second. Data were recorded in a native binary format and converted in SEGY or SEG2 format. The recording units were connected to Lennartz LE3D-5s seismometers with a natural frequency of 0.2 Hz. and high sensitivity (400 V/m/s). To reduce the bias introduced by possible errors in sensors location, the station's position is determined by differential GPS measurements obtained performing a real time kinematic survey with a Leica Systems 1200 GNSS instrument. The differential corrections are obtained through a GPRS connection to a network of reference stations (www.italpos.it). The positioning system consents to operate in navigation mode. It provide in real time distance and azimuth between any couple of points in the array. This feature allows to draw the array geometry in advance and to easily find the positions of the recording stations on the field. With this approach the error in positioning can be lowered to few (5-10) centimeters.
Data were processed in order to find the experimental dispersion curve for Rayleigh waves using the Geopsy (www.geopsy.org) software.
For the inversion of the dispersion curve we used the Neighbourhood Algorithm in order to invert the experimental curves (*www.geopsy.org*). The results of data analysis are shown in figures 1 and 2.

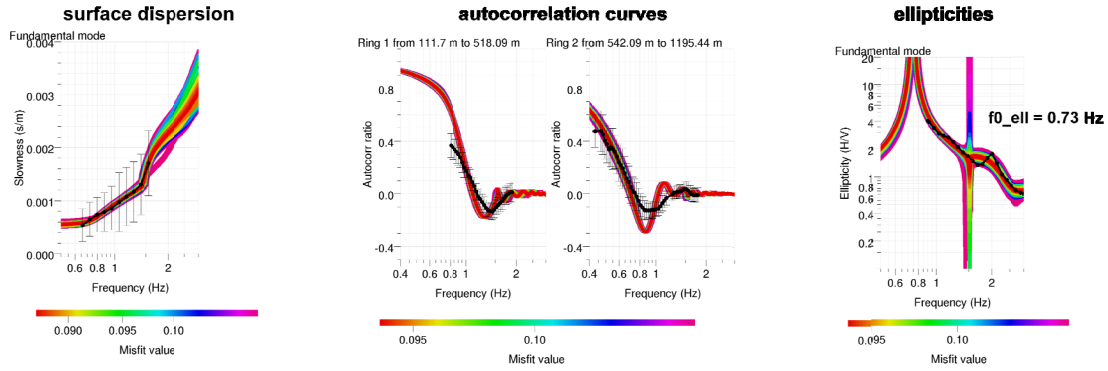

Figure 1 – Experimental dispersion curve, autocorrelation and ellipticity results.

Figure 1 illustrates the fit between experimental and theoretical curves. We performed a joint inversion of dispersion curve, autocorrelation curve derived by ESAC techniques, and ellipticity function to better constraint the deeper layers. The ellipcitiy function was derived as the average of HVNSR results fro the 14 array stations. We use the decreasing branch of the HVNSR starting from the resonance frequency.

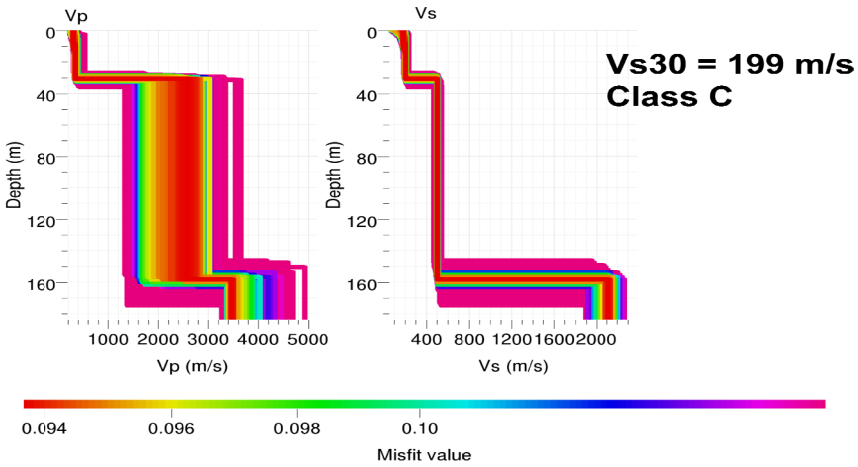

Figure 2 – Inverted Vp and Vs best models.

The inverted best models in figure 2 show low velocity layer (200 m/s) for the first 35 meters and a deeper layer with Vs velocity of about 500 m/s that extends down to 160 meters where the bedrock is found. The bedrock depth is compatible with those observed using seismic profiles found in literature.

Shear waves velocity measurements at Bibbiena nuova (BBN) site

The velocity profile for the R.A.N. station of Bibbiena Nuova (BBN) was derived by MASW and microtremor measurements performed in the vicinity of the station. Due to the limited available space only a 1D array was deployed in a layout with total length of respectively 70 meters.
Data were collected by three data loggers Geometrics-GEODE interconnected in a LAN configuration. The GEODE is a 24 channels instrument based on a 24 bits AD converter. The data acquisition is driven by a laptop PC that is also used as data storage unit, data are stored in SEG2 binary format. The geophones used are GEOSPACE vertical geophones with a natural frequency of 4.5 Hz.
Data were collected using a linear deployment based on 71 channels with two geophones spacing of 1 and 2 meters and a minigun as active source. Minigun shots were performed at both sides of each deployment with two offsets (15 meters, 1 meter), an extra shot was performed at the center of the array. The symmetry in shots layout allows verifying the monodimensional behavior of the investigated site as required by MASW technique. Sampling rate was set at 0.125 ms with a record duration of 2 seconds (16000 points).
Also passive 1D approach was used with the same array geometry; in this case we collected 20 noise windows of 30 seconds length with a sampling rate of 2 ms.
Data were processed in order to find the experimental dispersion curve for Rayleigh waves. For 1D array data three different computer codes were used: Optim R.e.m.i, Geopsy (www.geopsy.org) and software developed by INGV researcher.
For the inversion of the dispersion curve we used the Neighbourhood Algorithm in order to invert the experimental curves (*www.geopsy.org*). The results of data analysis are shown in figure 1.

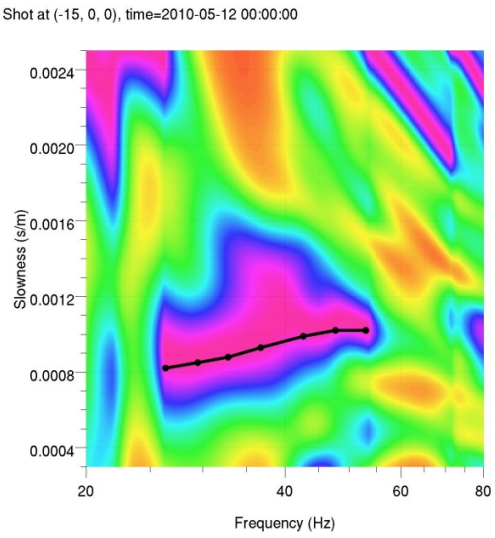

Figure 1 – Experimental dispersion curve.

The figure illustrates as the phase velocity remains almost constant in a broad frequency range (25-50 Hz) with an average value of around 1000 m/s, moreover the HVNSR result

does not show any resonance peak in the entire frequency range. Consequently the site can be assumed as a stiff site (soil class A).
The data collected in this site were quite complicated by the presence of a water fall almost aligned to the deployment. The fall was generating an acoustic disturbance reflected by a constant velocity (about 350 m/s) peak in the frequency-slowness domain. This features made difficult the use of passive data. Another problem arises from lateral geological variation in outcropping terrain.

Shear waves velocity measurements at Borgo Ottomila (BTT2) site

The velocity profile for the R.A.N. station of Borgo Ottomila (Btt2) was derived by MASW and microtremor measurements performed in the vicinity of the station. Due to the large available space we performed 2D array analysis.
For the 2D array we used 14 stand alone seismic instruments based on Reftek 130 (24 bits) and Lennartz Marslite (21 bits) data loggers with a maximun array aperture of about 1 km. Each unit, synchronized using GPS receivers, was operating in continuous recording mode with a sampling rate of 200-250 samples per second. Data were recorded in a native binary format and converted in SEGY or SEG2 format. The recording units were connected to Lennartz LE3D-5s seismometers with a natural frequency of 0.2 Hz. and high sensitivity (400 V/m/s). To reduce the bias introduced by possible errors in sensors location, the station's position is determined by differential GPS measurements obtained performing a real time kinematic survey with a Leica Systems 1200 GNSS instrument. The differential corrections are obtained through a GPRS connection to a network of reference stations (www.italpos.it). The positioning system consents to operate in navigation mode. It provide in real time distance and azimuth between any couple of points in the array. This feature allows to draw the array geometry in advance and to easily find the positions of the recording stations on the field. With this approach the error in positioning can be lowered to few (5-10) centimeters.
Data were processed in order to find the experimental dispersion curve for Rayleigh waves using the Geopsy (www.geopsy.org) software.
For the inversion of the dispersion curve we used the Neighbourhood Algorithm in order to invert the experimental curves (*www.geopsy.org*). The results of data analysis are shown in figures 1 and 2.

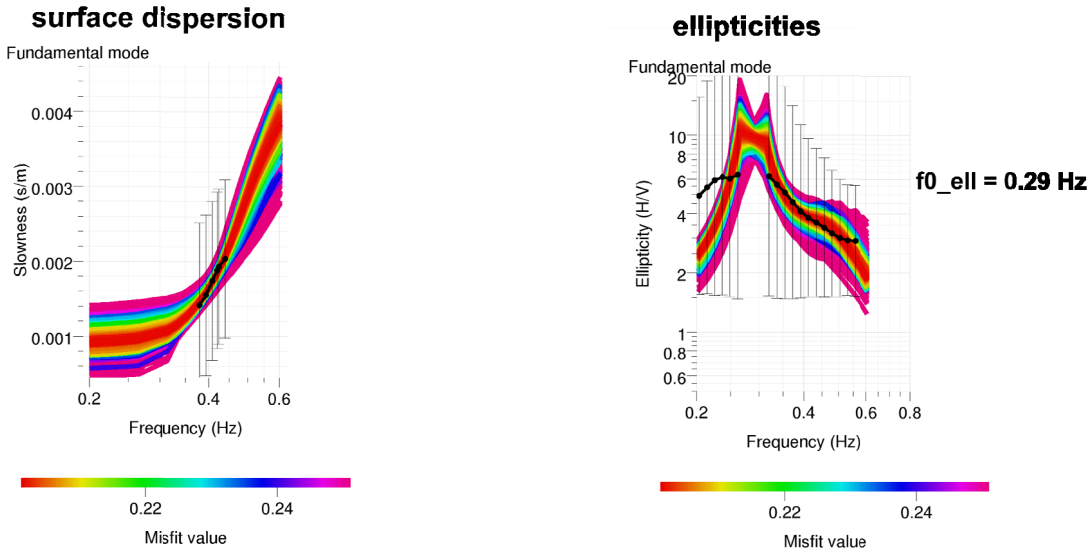

Figure 1 – Experimental dispersion curve and ellipticity results.

Figure 1 illustrates the fit between experimental and theoretical curves. We performed a joint inversion of dispersion curve and ellipticity function to better constraint the deeper layers. The ellipcitiy function was derived as the average of HVNSR results from the 14 array stations. We use the left and right branch of the HVNSR near the resonance frequency.

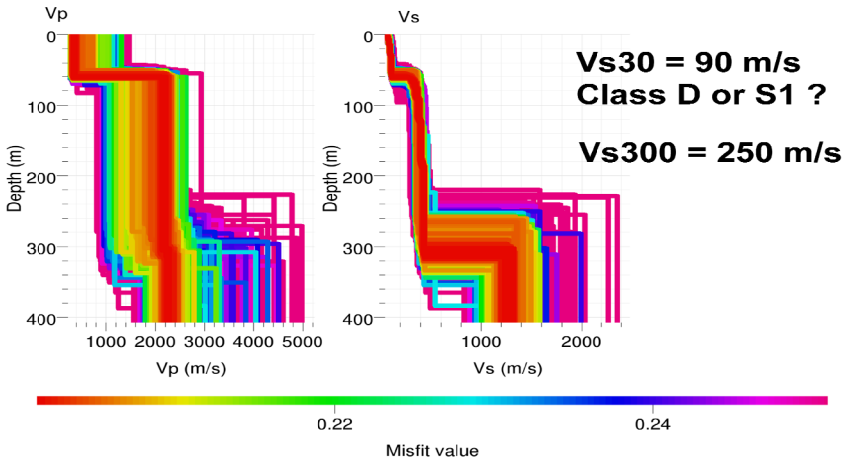

Figure 2 – Inverted Vp and Vs best models.

The inverted best models in figure 2 show a very low velocity layer (about 100 m/s) for the first 60 meters and a deeper layer with Vs velocity increasing from 270 to 450 m/s down to 300 meters where the bedrock is found. The very low velocity surface layer is in good agreement with geotechnical data available for the area. The bedrock depth is also confirmed by seismic profiles found in literature.

Shear waves velocity measurements at Cassino (CSS) site

The velocity profile for the R.A.N. station of Cassino (CSS) was derived by MASW and microtremor measurements performed in the vicinity of the station. Due to the limited available space only a 1D array was deployed.
Data were collected by three data loggers Geometrics-GEODE interconnected in a LAN configuration. The GEODE is a 24 channels instrument based on a 24 bits AD converter. The data acquisition is driven by a laptop PC that is also used as data storage unit, data are stored in SEG2 binary format. The geophones used are GEOSPACE vertical geophones with a natural frequency of 4.5 Hz.
Data were collected using a linear deployment based on 54 channels with geophones spacing of 1 meter and a minigun as active source. Minigun shots were performed at both side of deployment with two offsets (15 meters, 1 meter), an extra shot was performed at the center of the array. The symmetry in shots layout allows verifying the monodimensional behavior of the investigated site as required by MASW technique. Sampling rate was set at 0.125 ms with a record duration of 2 seconds (16000 points).
Data were processed in order to find the experimental dispersion curve for Rayleigh waves. For 1D array data three different computer codes were used: Optim R.e.m.i, Geopsy (www.geopsy.org) and software developed by INGV researcher.
For the inversion of the dispersion curve we used the Neighbourhood Algorithm in order to invert the experimental curves (*www.geopsy.org*). The results of data inversion are shown in figure 1 where the dispersion curves and the inverted best models are represented.

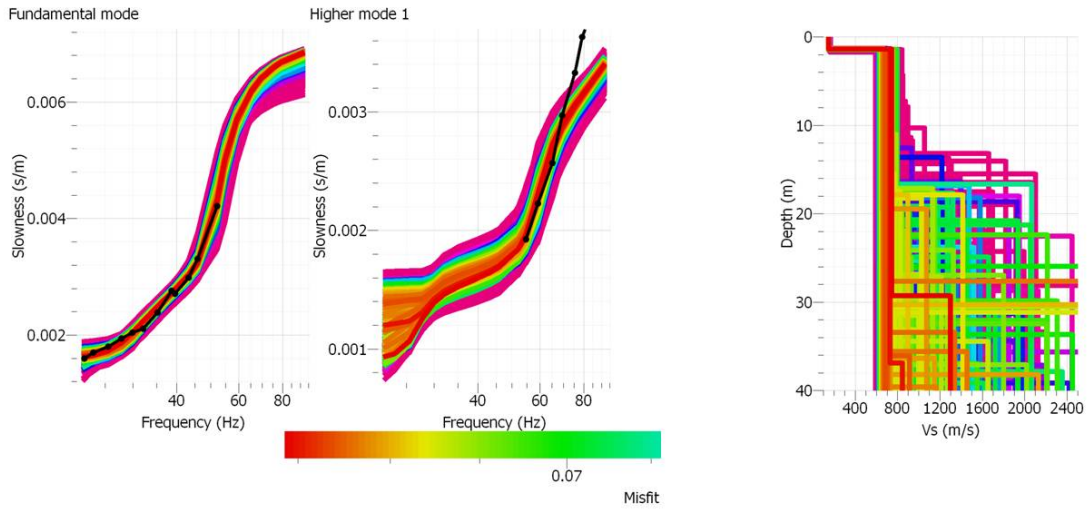

Figure 1 – Experimental versus inverted dispersion curves and best Vs inverted models.

The inverted Vs velocity models show a very thin low velocity surface layer over a stiff material with a velocity above 600 m/s. Due to the limited extension of the array the bedrock depth is not very constrained and the velocity discontinuity shown by some of the best models between 30 and 40 meters is not very reliable.

In this case we did not perform a joint inversion of dispersion curves and of HVNSR data due to the absence of a clear resonance peak in microtremor spectral ratio that is characterized by a broad peak in the 2-5 Hz frequency range. In the site is present a cultural noise source (water pumps) that can bias the HVNSR results and make difficult the use of passive approach in array analysis.

Shear waves velocity measurements at Dicomano (DCM) site

The velocity profile for the R.A.N. station of Dicomano (DCM) was derived by MASW and microtremor measurements performed in the vicinity of the station. Due to the limited available space only a 1D array was deployed in two layouts with maximum total length of respectively 71 and141 meters.
Data were collected by three data loggers Geometrics-GEODE interconnected in a LAN configuration. The GEODE is a 24 channels instrument based on a 24 bits AD converter. The data acquisition is driven by a laptop PC that is also used as data storage unit, data are stored in SEG2 binary format. The geophones used are GEOSPACE vertical geophones with a natural frequency of 4.5 Hz.
Data were collected using a linear deployment based on 72 channels with two geophones spacing of 1 and 2 meters and a minigun as active source. Minigun shots were performed at both sides of each deployment with two offsets (20 meters, 10 meter), an extra shot was performed at the center of the array. The symmetry in shots layout allows verifying the monodimensional behavior of the investigated site as required by MASW technique. Sampling rate was set at 0.125 ms with a record duration of 2 seconds (16000 points).
Also passive 1D approach was used with the same array geometry; in this case we collected 20 noise windows of 30 seconds length with a sampling rate of 2 ms.
Data were processed in order to find the experimental dispersion curve for Rayleigh waves. For 1D array data three different computer codes were used: Optim R.e.m.i, Geopsy (www.geopsy.org) and software developed by INGV researcher.
For the inversion of the dispersion curve we used the Neighbourhood Algorithm in order to invert the experimental curves (*www.geopsy.org*). The results of data analysis are shown in figure 1.

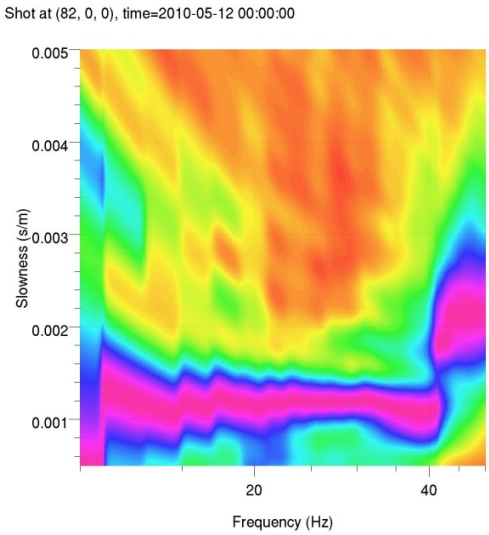

Figure 1 – Experimental dispersion curve.

The figure illustrates as the phase velocity remains almost constant in a broad frequency range (up to 40 Hz) with a value of around 1000 m/s. Consequently the site can be assumed as a stiff site (soil class A). The dispersive velocity branch above 40 Hz can be

related to some very thin slow layer. This feature is only observed at the first geophones at one side of the deployment and is probability due to some filling material or some weathered layer. This is confirmed by HVNSR results that show a resonance peak only in the high frequency range (20-25 Hz). The effects of this thin layer are probably not affecting the R.A.N. station that is few meters apart from the array deployment and is mounted on a concrete pillar with a small foundation.

Shear waves velocity measurements at Rieti (RTI) site

The velocity profile for the R.A.N. station of Rieti (RTI) was derived by MASW and microtremor measurements performed in the vicinity of the station. Due to the large available space we performed both 1D (active and passive) and 2D array analysis.

1D data were collected by three data loggers Geometrics-GEODE interconnected in a LAN configuration. The GEODE is a 24 channels instrument based on a 24 bits AD converter. The data acquisition is driven by a laptop PC that is also used as data storage unit, data are stored in SEG2 binary format. The geophones used are GEOSPACE vertical geophones with a natural frequency of 4.5 Hz. Active data were collected using a linear deployment based on 72 channels with two geophones spacing of 2 meters and a minigun as active source. Minigun shots were performed at both sides of each deployment with three offsets (40 meters, 20 meters, 1 meter), an extra shot was performed at the center of the array. The symmetry in shots layout allows verifying the monodimensional behavior of the investigated site as required by MASW technique. Sampling rate was set at 0.125 ms with a record duration of 2 seconds (16000 points). For the passive 1D approach was used with the same array geometry; in this case we collected 20 noise windows of 30 seconds length with a sampling rate of 2 ms. Some test was also performed using a moving vehicle as a source at one end of the linear deployment.

For 2D arrays we used 13 stand alone seismic instruments based on Reftek 130 (24 bits) and Lennartz Marslite (21 bits) data loggers with a maximum array aperture of about 200 meters. Each unit, synchronized using GPS receivers, was operating in continuous recording mode with a sampling rate of 200-250 samples per second. Data were recorded in a native binary format and converted in SEGY or SEG2 format. The recording units were connected to Lennartz LE3D-5s seismometers with a natural frequency of 0.2 Hz. and high sensitivity (400 V/m/s). To reduce the bias introduced by possible errors in sensors location, the station's position is determined by differential GPS measurements obtained performing a real time kinematic survey with a Leica Systems 1200 GNSS instrument. The differential corrections are obtained through a GPRS connection to a network of reference stations (www.italpos.it). The positioning system consents to operate in navigation mode. It provide in real time distance and azimuth between any couple of points in the array. This feature allows to draw the array geometry in advance and to easily find the positions of the recording stations on the field. With this approach the error in positioning can be lowered to few (5-10) centimeters.

Data were processed in order to find the experimental dispersion curve for Rayleigh waves. For 1D and 2D array data three different computer codes were used: Optim R.e.m.i, Geopsy (www.geopsy.org) and software developed by INGV researcher.

For the inversion of the dispersion curve we used the Neighbourhood Algorithm in order to invert the experimental curves (*www.geopsy.org*). The results of data analysis are shown in figures 1 and 2.

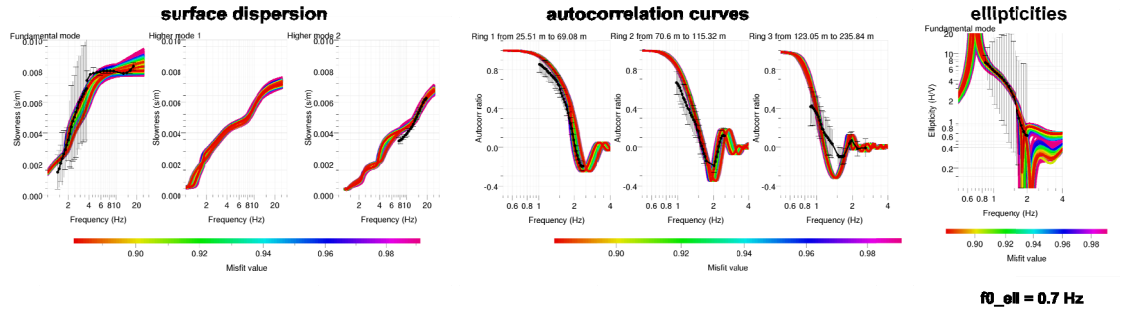

Figure 1 – Experimental dispersion curve, autocorrelation and ellipticity results.

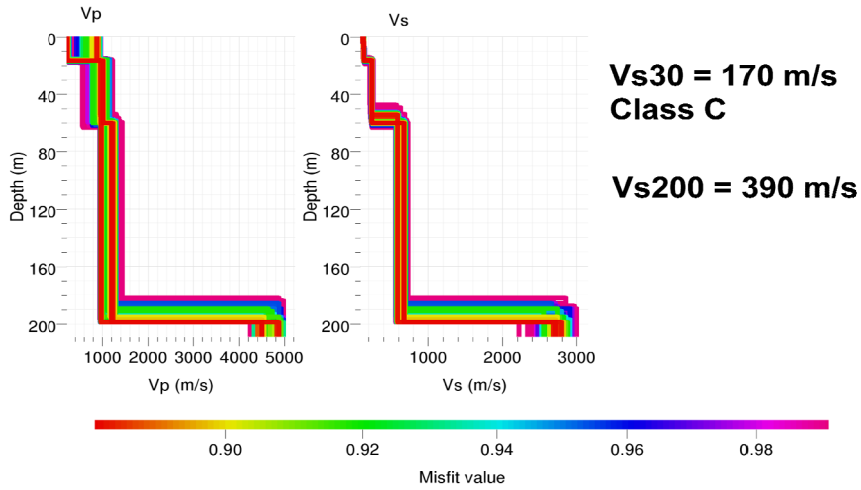

Figure 2 – Inverted Vp and Vs best models.

Figure 1 illustrates the fit between experimental and theoretical curves. We performed a joint inversion of dispersion curve, autocorrelation curve derived by ESAC techniques, and ellipticity function to better constraint the deeper layers. The ellipciticy function was derived as the average of HVNSR results fro the 13 array stations. We use the decreasing branch of the HVNSR starting from the resonance frequency.

The inverted best models show a first low velocity (140 m/s) layer with thickness of about 16 meters and a deeper 40 meters thick layer with velocity of about 250 m/s. A third layer with a velocity of 670 m/s extends down to the bedrock located at a depth of about 200 meters. The results of inversion are quite stable in terms of Vs and the investigated depth are well constrained by the geometry of the array.

APPLICATION OF SURFACE WAVE METHODS FOR SEISMIC SITE CHARACTERIZATION

L'AQUILA - VALLE ATERNO - FIUME ATERNO (AQA)

Responsible:
Sebastiano Foti

Co-workers:
Giovanni Bianchi
Margherita Maraschini
Paolo Bergamo

FINAL REPORT

Turin, 13/1/2010

INDEX

1 Introduction

In this report a summary of the results obtained for the characterization of the accelerometric station of L'Aquila - valle Aterno - fiume Aterno of the RAN within Project S4 is presented. The analysis was performed using active surface wave method and refraction method.

The map of the site and the array and its location are shown in Figure 1 and Figure 2. According to geological information a shallow bedrock is expected.

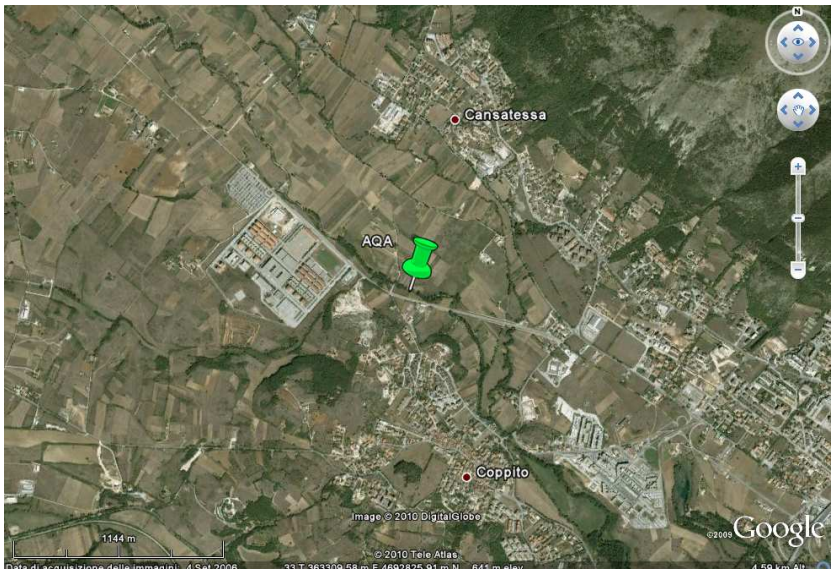

Figure 1 L'Aquila - valle Aterno - fiume Aterno: map

Figure 2 L'Aquila - valle Aterno - fiume Aterno: map of the array and its location

Goal of the seismic tests is the estimation of the S-wave velocity profile of the subsoil, and in particular the position of the bedrock. The presence of stiff seismic interfaces between the sediments and the shallow bedrock can cause a relevance of higher modes in the

surface wave experimental dispersion curve which has be taken into account in order to provide reliable results.

The primary use of surface wave testing is related to site characterization in terms of shear wave velocity profile. The V_S profile is of primary interest for seismic site response studies and for studies of vibration of foundations and vibration transmission in soils. Other applications are related to the prediction of settlements and to soil-structure interaction.

With respect to the evaluation of seismic site response, it is worth noting the affinity between the model used for the interpretation of surface wave tests and the model adopted for most site responses study. Indeed the application of equivalent linear elastic methods is often associated with layered models (e.g. the code SHAKE and all similar approaches). This affinity is also particularly important in the light of equivalence problems, which arise because of non-uniqueness of the solution in inverse problems. Indeed profiles which are equivalent in terms of Rayleigh wave propagation are also equivalent in term of seismic amplification (Foti et al., 2009).

Many seismic building codes introduce the weighted average of the shear wave velocity profile in the shallowest 30m as to discriminate class of soils to which a similar site amplification effect can be associated. The so-called $V_{S,30}$ can be evaluated very efficiently with surface wave method also because its average nature does not require the high level of accuracy that can be obtained with seismic borehole methods.

In the following a methodological summary of techniques and the description of the results is presented.

For Further explanation of surface wave methodologies, see document: Project S4: ITALIAN STRONG MOTION DATA BASE, Deliverable # 6, Application of Surface wave methods for seismic site characterization, May 2009.

2 Surface wave method

Surface wave method (S.W.M.) is based on the geometrical dispersion, which makes Rayleigh wave velocity frequency dependent in vertically heterogeneous media. High frequency (short wavelength) Rayleigh waves propagate in shallow zones close to the free surface and are informative about their mechanical properties, whereas low frequency (long wavelength) components involve deeper layers. Surface wave tests are typically devoted to the determination of a small strain stiffness profile for the site under investigation. Consequently the dispersion curve will be associated to the variation of medium parameters with depth.

The calculation of the dispersion curve from model parameters is the so called forward problem. Surface wave propagation can be seen as the combination of multiple modes of propagation, i.e. more than one possible velocity can be associated to each frequency value. Including higher modes in the inversion process allows the penetration depth to be increased and a more accurate subsoil profile to be retrieved.

If the dispersion curve is estimated on the basis of experimental data, it is then possible to solve the inverse problem, i.e. the model parameters are identified on the basis of the experimental data collected on the boundary of the medium. The result of the surface wave method is a one-dimensional S wave velocity soil profile.

The standard procedure for surface wave tests is reported in Figure 3. It can be subdivided into three main steps:

1. acquisition of experimental data;
2. signal processing to obtain the experimental dispersion curve;
3. inversion process to estimate shear wave velocity profile at the site.

It is very important to recognize that the above steps are strongly interconnected and their interaction must be adequately accounted for during the whole interpretation process.

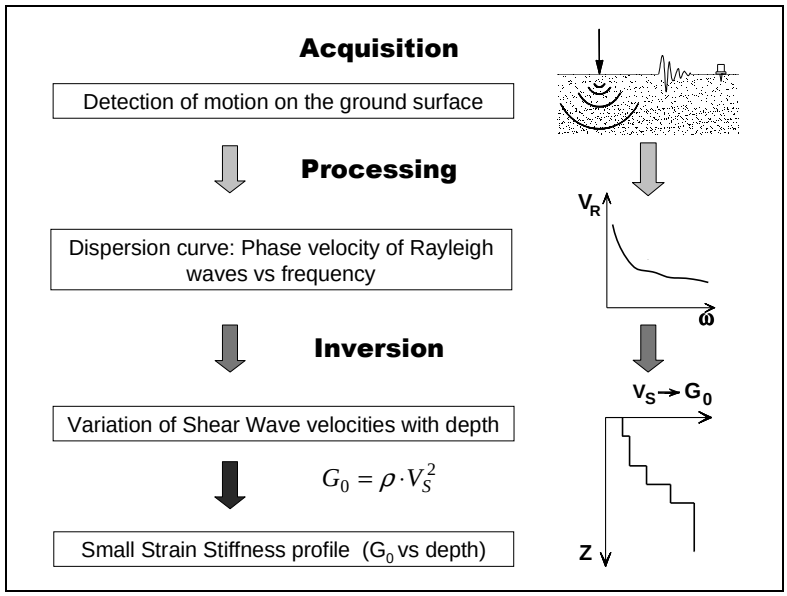

Figure 3 – Flow chart of surface wave tests.

2.1 Acquisition

Active surface wave tests (MASW) and refraction tests at L'Aquila - valle Aterno - fiume Aterno have been performed in May 2009 within the project S4 for the characterization of RAN sites.

Characteristics of sensors are reported in Table 1.

Test	GEOPHONE TYPE	NATURAL FREQUENCY	GEOPHONE NUMBER
MASW/Refraction	vertical SENSOR SM-6/U-B	4,5 Hz	24

Table 1 L'Aquila - valle Aterno - fiume Aterno: receiver characteristics

The acquisition array could not be placed very close to the accelerometric station because the station is located in an inaccessible spot on the left bank of Aterno river: the array was laid on the right bank.

The spacing between geophones (1.5 m) has been dictated by available testing space at the testing locations, which was very limited because of the presence of cultivated fields. The total length of the array is 34.5m. The source is a 5kg sledge hammer. Geometry parameters are summarized in Table 2.

Test	GEOF. N.	SPACING	SOURCE TYPE	ACQUISITION WINDOW	SAMPLING INTERVAL	STACK
MASW	24	1.5 m	Hammer	T = 2 s	Δt = 0.5 ms	10
Refraction	24	1.5 m	Hammer	T =1 s	Δt = 0.03125 ms	8

Table 2 L'Aquila - valle Aterno - fiume Aterno: Acquisition parameters

Note that both surveys were performed with the same testing geometry: in this case (survey line close to the river) we expect the P-wave seismic refraction method to provide relevant information with respect to the position of the water table .

2.2 Processing of surface waves

The processing allows the experimental dispersion curve to be determined.

Multichannel data are processed using a double Fourier Transform, which generates the frequency-wave number spectrum, where the multimodal dispersion curve is easily extracted as the location of spectral maxima.

2.3 Inversion of surface waves

The solution of the inverse Rayleigh problem is the final step in test interpretation. The solution of the forward problem forms the basis of any inversion strategy; the forward problem consists in the calculation of the function whose zeros are dispersion curves of a given model. Assuming a model for the soil deposit, model parameters of the best fitting subsoil profile are obtained minimizing an object function.

The subsoil is modelled as a horizontally layered medium overlaying a halfspace, with constant parameter in the interior of each layer and linear elastic behaviour. Model parameters are thickness, S-wave velocity, P-wave velocity (or Poisson coefficient), and density of each layer and the halfspace. The inversion is performed on S-wave velocities and thicknesses, whereas for the other parameters realistic values are chosen a priori. The number of layer is chosen applying minimum parameterization criterion.

In surface wave analysis it is very common to perform the inversions using only the fundamental mode of propagation. This approach is based on the assumption that the prevailing mode of propagation is the fundamental one; if this is partially true for normal dispersive sites, in several real cases the experimental dispersion curve is on the contrary the result of the superposition of several modes. This may happen in particular when velocity inversions or strong velocity contrasts are present in the shear wave velocity profile. In these stratigraphic conditions the inversion of the only fundamental mode will produce significant errors; moreover all the information contained in higher propagating

modes is not used in the inversion process. Therefore, the fundamental mode inversion does not use all the available information, and this affects the result accuracy.

The use of higher modes in the inversion can be helpful both in the low frequency range, in order to increase the investigation depth and to avoid the overestimation of the bedrock velocity, and in the high frequency range in order to provide a more consistent interpretation of shallow interfaces and increase model parameter resolution.

In this work a multimodal misfit function has been used. This function is based on the Haskell-Thomson method for dispersion curve calculation (Thomson 1950, Haskell 1953, Herrmann e Wang 1980, Herrmann 2002). For a given subsoil model, and an experimental data, the misfit of the model is the L^1 norm of the vector containing the absolute value of the determinant of the Haskell-Thomson matrix (which is zeros in correspondence of all the modes of the dispersion curves of the numerical model) evaluated in correspondence of the experimental data (Maraschini et al. 2008). The misfit function adopted has the advantage of being able to include any dispersive event present in the data without the need of specifying to which mode the data points belong to, avoiding errors arising from mode misidentification, in particular in the low frequency range.

This misfit function is applied in a Global Search Methods (GSM), in order to reduce the possibility of falling in local minima. A uniform random search is applied; ranges for the inversion have been chosen, for the different sites, based on the experimental dispersion curves; in particular the range of the S-wave half space velocity is close to the maximum surface wave velocity retrieved on experimental data.

The results of the inversion are reported as the ensemble of the twenty shear wave velocity profiles which present the minimum misfits with respect to the experimental dispersion curve. In the Figures reported a representation based on the misfit is adopted for velocity profiles, so that the darkest colour corresponds to the profile whose dispersion curve has the lowest misfit and better approximation to the reference one; instead for dispersion curves the coloured surface under imposed to the experimental one is a misfit surface, whose zeros are synthetic dispersion curve of the best fitting model.

2.4 Numerical code

The numerical codes used for processing and inversion of surface waves are non commercial codes, implemented at Politecnico di Torino.

3 L'Aquila - valle Aterno - fiume Aterno – Refraction results

As the acquisition was performed on the banks of Aterno river it is very likely that refraction tests will give information about the depth of the water table.
Figure 4 shows the three shots that have been considered for the inversion: for both shots at the extremes of the array the presence of noise has conditioned the first-break arrival times picking, so that these values for offset greater than 20 m are not reliable. In such conditions only the velocities of the two shallower layers and the depth of their interface can be identified: note that as the velocity of the deeper layer is close to P-wave velocity in water the interface probably points out the depth of water table (see Table 3).

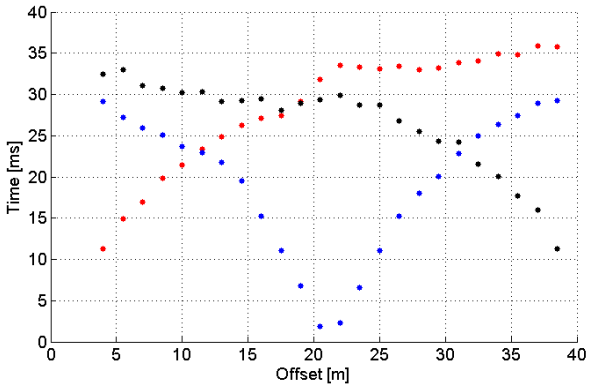

Figure 4 L'Aquila - valle Aterno - fiume Aterno – First breaks of the three shots considered

P-wave velocity (m/s)	Thickness (m)
343	2.7
1280	-

Table 3 Velocity models retrieved by refraction survey

4 L'Aquila - valle Aterno - fiume Aterno – Surface wave results

In Figure 5 an example of the f-k spectrum of the data collected at L'Aquila - valle Aterno - fiume Aterno is presented.

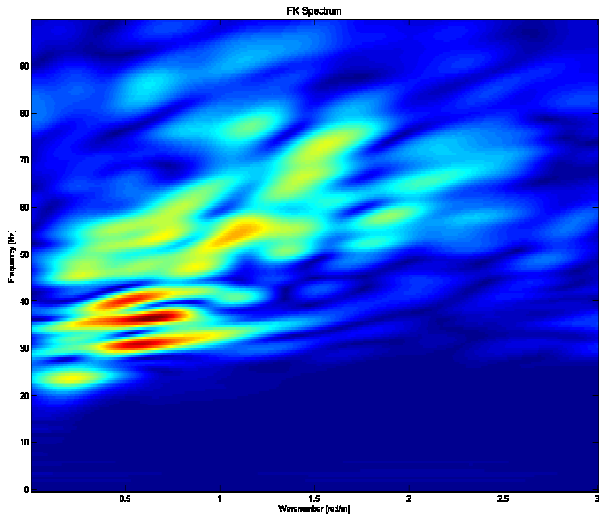

Figure 5 – L'Aquila - valle Aterno - fiume Aterno – example of f-k spectrum

From the f-k spectra, several dispersion curves can be retrieved. From all these curves an average curve is estimated (Figure 6).

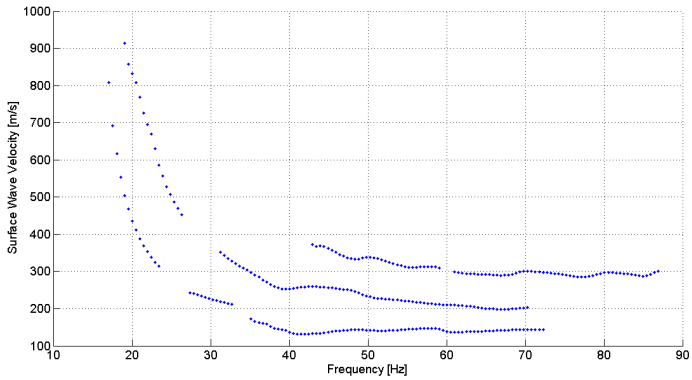

Figure 6 – L'Aquila - valle Aterno - fiume Aterno - Average apparent dispersion curve

The experimental dispersion curve includes three branches: the steep velocity increase in the low frequency range which can be observed in two branches is probably due to a jump on higher modes in that range.
Data were inverted using a multimodal stochastic approach, the best fitting profiles are plotted in Figure 7 a), profile colour depends on the misfit, from yellow to blue (best fitting profile). In Figure 7 b) the best fitting profile is compared with the refraction result, and in Figure 8 the experimental dispersion curve is compared with the determinant surface of the best fitting model. We can note that the experimental points follow the minima of the determinant surface, and the low frequency part of the experimental dispersion curve tends to go to on higher modes, probably due to the marked impedance contrast between topsoil and bedrock. It can be noted that the refraction results are not in full agreement with the surface wave results: this is due to the fact that P-waves are sensitive to the presence of water while Rayleigh waves are not, so that the depth of water table is identified by refraction tests but not by surface wave tests.

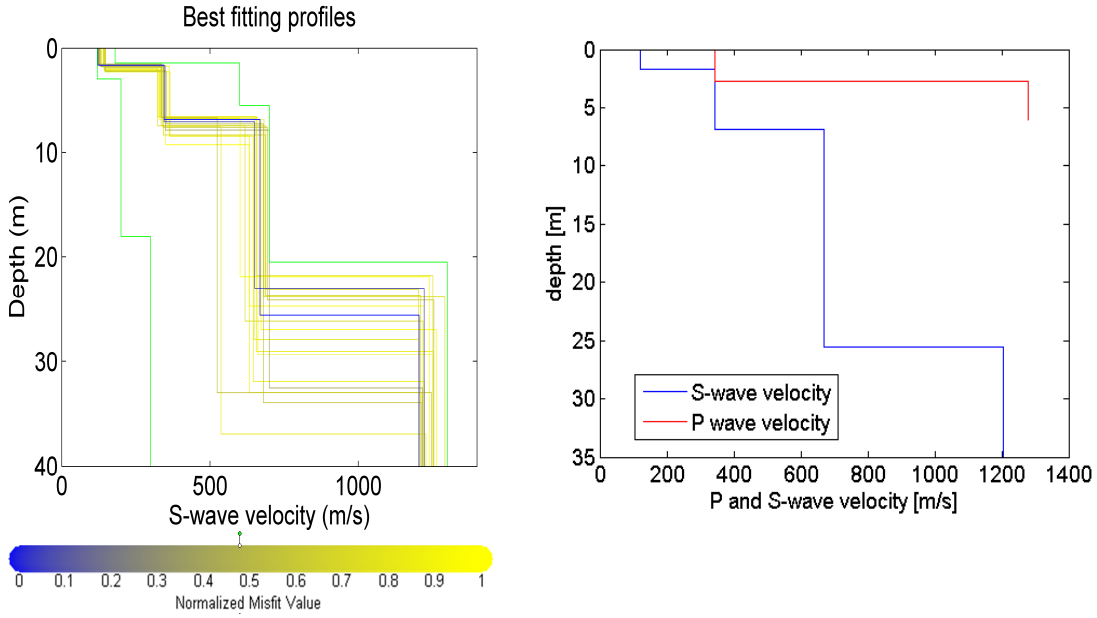

Figure 7 – L'Aquila - valle Aterno - fiume Aterno – a) Monte Carlo results (from yellow to blue) of the inversion with the boundaries in green. b) L'Aquila - valle Aterno - fiume Aterno – Best fitting profile (blue) compared with the refraction result (red).

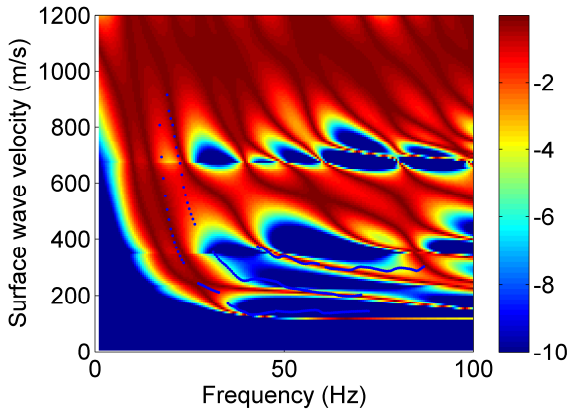

Figure 8 L'Aquila - valle Aterno - fiume Aterno – Experimental dispersion curve compared with the misfit surface of the best fitting model

The parameters of the best fitting profile are summarized in Table 4.

Vs (m/s)	Thickness (m)	Poisson coefficient	Density (T/m^3)
121	1.7	0.3	1.8
345	5.2	0.3	1.8
668	18.7	0.3	1.8
1204	-	0.2	2

Table 4 L'Aquila - valle Aterno - fiume Aterno: subsoil parameters of the best fitting profile.

References

Project S4: ITALIAN STRONG MOTION DATA BASE, Deliverable # 6, Application of Surface wave methods for seismic site characterization, May 2009.

Foti S., Comina C., Boiero D., Socco L.V. (2009) "Non uniqueness in surface wave inversion and consequences on seismic site response analyses", Soil Dynamics and Earthquake Engineering, Vol. 29 (6), 982-993.

Haskell, N., 1964, Radiation pattern of surface waves from point sources in a multilayered medium: Bulletin of seismological society of America, 54, no. 1, 377-393.

Herrmann, R. B., and C. Y. Wang, 1980, A numerical study of p-, sv- and sh- wave generation in a plane layered medium: Bulletin of seismological society of America, 70, no. 4, 1015-1036.

Herrmann, R. B., 2002, SURF code, www.eas.slu.edu/People/RBHerrmann/.

Maraschini, M., F. Ernst, D. Boiero, S. Foti, and L.V. Socco, 2008, A new approach for multimodal inversion of Rayleigh and Scholte waves: Proceedings of EAGE Rome, expanded abstract.

Thomson, W. T, 1950., Transmission of elastic waves through a stratified solid medium: Journal of Applied Physics, 21, no. 89.

APPLICATION OF SURFACE WAVE METHODS FOR SEISMIC SITE CHARACTERIZATION

CATANIA (PIANA) (CAT)

Responsible:
Sebastiano Foti

Co-workers:
Giovanni Bianchi
Cesare Comina
Margherita Maraschini
Ken Tokeshi
Paolo Bergamo

FINAL REPORT

Turin, 02/02/2010

INDEX

1 Introduction

In this report a summary of the results obtained for the characterization of the accelerometric station of Catania (Piana) of the RAN within Project S4 is presented. The analysis was performed using active and passive surface wave method .

Catania (Piana) RAN station lies on the alluvial plane of Catania, approximately 3.5 km from the sea. No shallow bedrock is expected, but a sequence of soft layers made up of alluvial deposits with a S-wave velocity increasing with depth.

The map, site location and measurements arrays are shown in Figure1, Figure 2 and Figure 3.

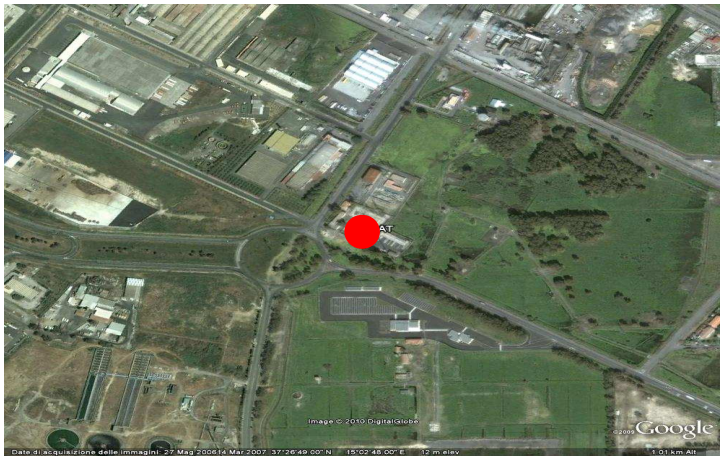

Figure 1 Catania (Piana): site map

Figure 2 Catania (Piana): array map. The red line represents the active measurements array; the black circle and the red circle represent the two circles along which receivers for passive measurements were arranged.

Figure 3 Catania (Piana): site location and active measurement array.

Goal of the seismic tests is the estimation of the S-wave velocity profile of the subsoil. Both passive and active surface wave tests were performed in order to increase the investigation depth, as no shallow bedrock is expected.

The primary use of surface wave testing is related to site characterization in terms of shear wave velocity profile. The V_S profile is of primary interest for seismic site response studies and for studies of vibration of foundations and vibration transmission in soils. Other applications are related to the prediction of settlements and to soil-structure interaction.

With respect to the evaluation of seismic site response, it is worth noting the affinity between the model used for the interpretation of surface wave tests and the model adopted for most site responses study. Indeed the application of equivalent linear elastic methods is often associated with layered models (e.g. the code SHAKE and all similar approaches). This affinity is also particularly important in the light of equivalence problems, which arise because of non-uniqueness of the solution in inverse problems. Indeed profiles which are equivalent in terms of Rayleigh wave propagation are also equivalent in term of seismic amplification (Foti et al., 2009).

Many seismic building codes introduce the weighted average of the shear wave velocity profile in the shallowest 30m as to discriminate class of soils to which a similar site amplification effect can be associated. The so-called $V_{S,30}$ can be evaluated very efficiently with surface wave method also because its average nature does not require the high level of accuracy that can be obtained with seismic borehole methods.

In the following a methodological summary of techniques and the description of the results is presented.

For Further explanation of surface wave methodologies, see document: Project S4: ITALIAN STRONG MOTION DATA BASE, Deliverable # 6, Application of Surface wave methods for seismic site characterization, May 2009.

2 Surface wave method

Surface wave method (S.W.M.) is based on the geometrical dispersion, which makes Rayleigh wave velocity frequency dependent in vertically heterogeneous media. High frequency (short wavelength) Rayleigh waves propagate in shallow zones close to the free surface and are informative about their mechanical properties, whereas low frequency (long wavelength) components involve deeper layers. Surface wave tests are typically devoted to the determination of a small strain stiffness profile for the site under investigation. Consequently the dispersion curve will be associated to the variation of medium parameters with depth.

The calculation of the dispersion curve from model parameters is the so called forward problem. Surface wave propagation can be seen as the combination of multiple modes of propagation, i.e. more than one possible velocity can be associated to each frequency value. Including higher modes in the inversion process allows the penetration depth to be increased and a more accurate subsoil profile to be retrieved.

If the dispersion curve is estimated on the basis of experimental data, it is then possible to solve the inverse problem, i.e. the model parameters are identified on the basis of the experimental data collected on the boundary of the medium. The result of the surface wave method is a one-dimensional S wave velocity soil profile.

The standard procedure for surface wave tests is reported in Figure 4. It can be subdivided into three main steps:

1. acquisition of experimental data;
2. signal processing to obtain the experimental dispersion curve;
3. inversion process to estimate shear wave velocity profile at the site.

It is very important to recognize that the above steps are strongly interconnected and their interaction must be adequately accounted for during the whole interpretation process.

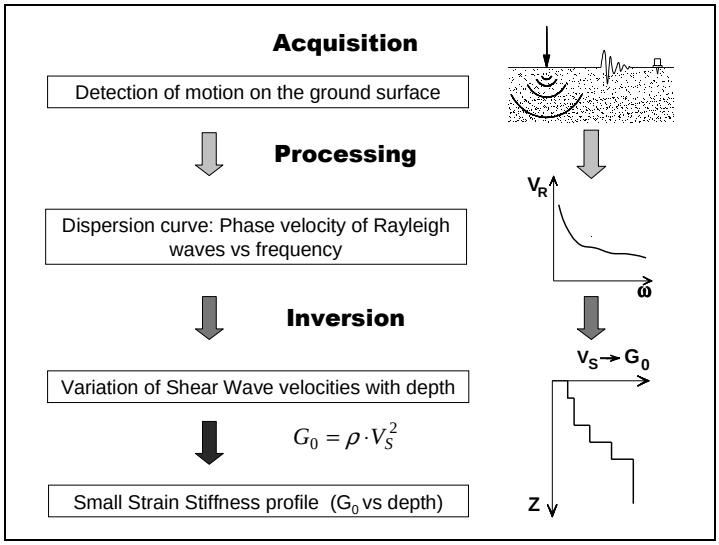

Figure 4 – Flow chart of surface wave tests.

2.1 Acquisition

Active (MASW) and passive surface wave tests at Catania (Piana) have been performed in May 2009 within the project S4 for the characterization of RAN sites.

Characteristics of sensors are reported in Table 1.

Test	GEOPHONE TYPE	NATURAL FREQUENCY	GEOPHONE NUMBER
MASW	vertical SENSOR SM-6/U-B	4,5 Hz	48
Passive surface wave tests	three components 3D HS1 GEO-SPACE	2 Hz	4
	vertical HS1 GEO-SPACE	2 Hz	12

Table 1 Catania (Piana): receiver characteristics

Acquisition geometry is shown in Figure 5. 48 receivers were used for active tests, with a spacing of 1.5 m between neighbouring geophones, so that the total length of the array is 70.5 m. The source is a 5kg sledge hammer. 16 receivers were used for passive tests: one three components geophones was placed at the centre of the array and three others were disposed along a circle whose radius is 9 m; 12 vertical geophones were arranged along the outer circle whose radius is 25 m. Acquisition parameters are summarized in Table 2

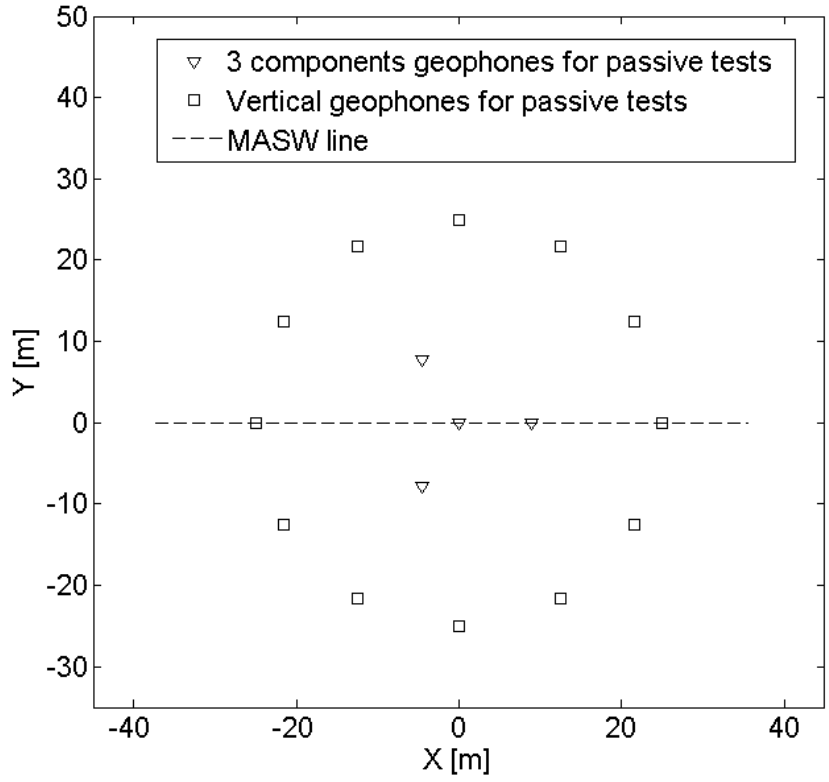

Figure 5 – Acquisition geometry.

Test	GEOF. N.	SPACING	SOURCE TYPE	ACQUISITION WINDOW	SAMPLING INTERVAL	STACK
MASW	48	1.5 m	Hammer	T = 2 s	Δt = 0.5 ms	10
Passive tests	16	-	-	T =524 s	Δt = 8 ms	1

Table 2 Catania (Piana): Acquisition parameters

2.2 Processing of active surface wave data

The processing allows the experimental dispersion curve to be determined.

Multichannel data are processed using a double Fourier Transform, which generates the frequency-wave number spectrum, where the multimodal dispersion curve is easily extracted as the location of spectral maxima.

2.3 Processing of passive surface wave data

The phase velocity of the surface waves can be extracted from noise recordings by using different methods: among them, the most frequently used are the Beam-Forming Method (BFM) (Lacoss et al., 1969) and the Maximum Likelihood Method (MLM) (Capon, 1969). Here we will illustrate the Beam-Forming Method which was used to process passive surface wave data. For further explanation on passive surface wave methodologies, see document: Project S4: ITALIAN STRONG MOTION DATA BASE, Deliverable # 6, Application of Surface wave methods for seismic site characterization, May 2009.

The estimate of the F-K spectra $P_b(f,\mathrm{k})$ by the BFM is given by:

$$P_b(f,k) = \sum_{l,m=1}^{n} \phi_{lm} \exp\{ik(X_l - X_m\} \ ,$$

where f is the frequency, k the two-dimensional horizontal wavenumber vector, n the number of sensors, ϕ_{lm} the estimate of the cross-power spectra between the l^{th} and the m^{th} data, and X_i and X_m, are the coordinates of the l^{th} and m^{th} sensors, respectively.

From the peak in the F-K spectrum occurring at coordinates k_{xo} and k_{yo} for a certain frequency $f_{0,}$ the phase velocity c_0 can be calculated by:

$$c_0 = \frac{2\pi f_0}{\sqrt{k_{xo}{}^2 + k_{yo}{}^2}}$$

so that, again, an experimental dispersion curve is retrieved.

Figure 6 shows an example of F-K analysis results obtained by processing passive surface wave data with Beam-Forming Method: white dots indicate the position of the maximum used to estimate the phase velocity while the white circle joins points with the same k values.

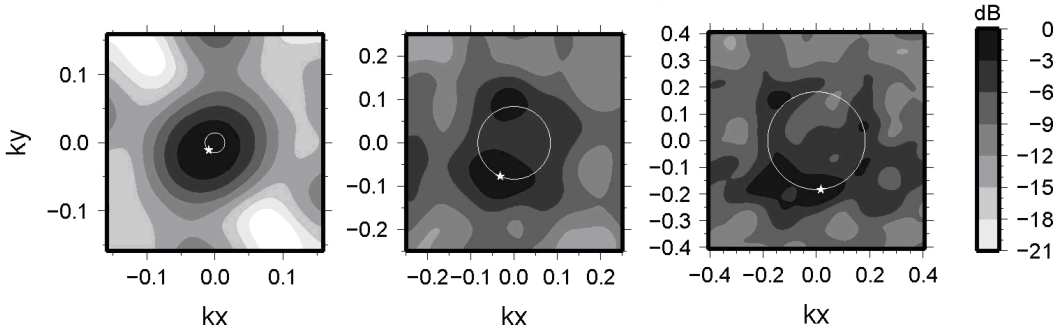

Figure 6 – Example of results from F-K analysis s for 2.5 Hz, 3.9 Hz, and 6.5 Hz. White dots indicate the position of the maximum used to estimate the phase velocity. The white circle joins points with the same k

2.4 Inversion of surface waves

The solution of the inverse Rayleigh problem is the final step in test interpretation. The solution of the forward problem forms the basis of any inversion strategy; the forward problem consists in the calculation of the function whose zeros are dispersion curves of a given model. Assuming a model for the soil deposit, model parameters of the best fitting subsoil profile are obtained minimizing an object function.

The subsoil is modelled as a horizontally layered medium overlaying a halfspace, with constant parameter in the interior of each layer and linear elastic behaviour. Model parameters are thickness, S-wave velocity, P-wave velocity (or Poisson coefficient), and density of each layer and the halfspace. The inversion is performed on S-wave velocities and thicknesses, whereas for the other parameters realistic values are chosen a priori. The number of layer is chosen applying minimum parameterization criterion.

In surface wave analysis it is very common to perform the inversions using only the fundamental mode of propagation. This approach is based on the assumption that the prevailing mode of propagation is the fundamental one; if this is partially true for normal dispersive sites, in several real cases the experimental dispersion curve is on the contrary the result of the superposition of several modes. This may happen in particular when velocity inversions or strong velocity contrasts are present in the shear wave velocity profile. In these stratigraphic conditions the inversion of the only fundamental mode will produce significant errors; moreover all the information contained in higher propagating modes is not used in the inversion process. Therefore, the fundamental mode inversion does not use all the available information, and this affects the result accuracy.

The use of higher modes in the inversion can be helpful both in the low frequency range, in order to increase the investigation depth and to avoid the overestimation of the bedrock velocity, and in the high frequency range in order to provide a more consistent interpretation of shallow interfaces and increase model parameter resolution.

In this work a multimodal misfit function has been used. This function is based on the Haskell-Thomson method for dispersion curve calculation (Thomson 1950, Haskell 1953, Herrmann e Wang 1980, Herrmann 2002). For a given subsoil model, and an experimental data, the misfit of the model is the L^1 norm of the vector containing the absolute value of the determinant of the Haskell-Thomson matrix (which is zeros in correspondence of all the modes of the dispersion curves of the numerical model) evaluated in correspondence of the experimental data (Maraschini et al. 2008). The misfit function adopted has the

advantage of being able to include any dispersive event present in the data without the need of specifying to which mode the data points belong to, avoiding errors arising from mode misidentification, in particular in the low frequency range.

This misfit function is applied in a Global Search Methods (GSM), in order to reduce the possibility of falling in local minima. A uniform random search is applied; ranges for the inversion have been chosen, for the different sites, based on the experimental dispersion curves; in particular the range of the S-wave half space velocity is close to the maximum surface wave velocity retrieved on experimental data.

The results of the inversion are reported as the ensemble of the best shear wave velocity profiles chosen according to a chi-square test (see Socco et al., 2008). It can be assumed that the experimental dispersion curve is affected by a Gaussian error with a known standard deviation, so that the probability density function of data $\rho_D(d)$ can be described by a discrete m-dimensional Gaussian (where *m* are the model parameters) and the sample variance variable of each random vector (dispersion curve) extracted from the data pdf is distributed according to a chi-square probability density. According to these assumptions we adopt a misfit function with the structure of a chi-square and this allows a statistical test to be applied to the variances of the synthetic dispersion curves with respect to the experimental one d_{obs}. Assuming that the best fitting curve d_{opt} belongs to the distribution $\rho_D(d_{obs})$ all models belonging to the distribution $\rho_D(d_{opt})$ and consistent with the data within a fixed level of confidence α are selected. As the ratio between chi-square variables follows a Fisher distribution a one–tailed F test can be performed:

$$F_{\alpha}(dof_{dopt}, dof_{g(m)}) < \frac{\chi^2_{dopt}}{\chi^2_{g(m)}}$$

where α is the chosen level of confidence, dof_{dopt} and $dof_{g(m)}$ are the degrees of freedom of the Fischer distribution and χ^2_{dopt} and $\chi^2_{g(m)}$ are the misfit of the best fitting curve and the misfit of all the others respectively. All models passing such test are selected. In the figures reported a representation based on the misfit is adopted for velocity profiles, so that the darkest colour corresponds to the profile whose dispersion curve has the lowest misfit and better approximation to the reference one; instead for dispersion curves the coloured surface under imposed to the experimental one is a misfit surface, whose zeros are synthetic dispersion curve of the best fitting model.

2.5 Numerical code

The numerical codes used for processing and inversion of surface waves are non commercial codes, implemented at Politecnico di Torino.

3 Catania (Piana) – Surface wave results

In Figure 7 an example of the f-k spectrum from active data collected at Catania (Piana) is presented.

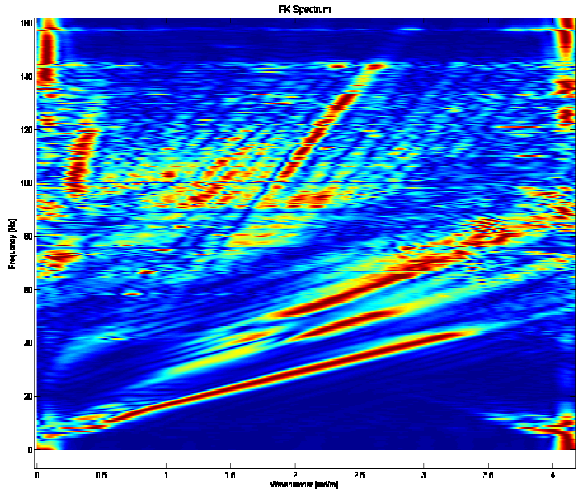

Figure 7 Catania (Piana) – example of f-k spectrum

From the f-k spectra of active and passive data, several dispersion curves can be retrieved. From all these curves an average curve is estimated (Figure 8).

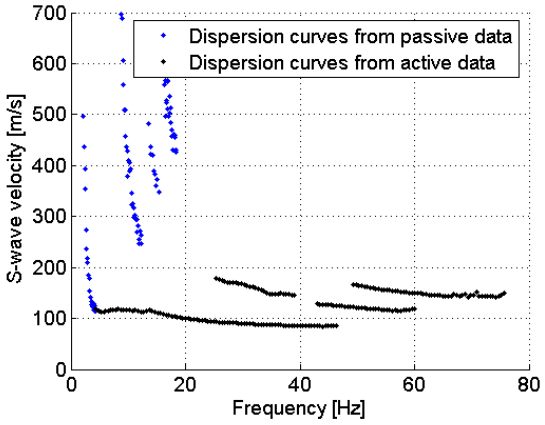

Figure 8 – Catania (Piana) -Average apparent dispersion curve

Very likely the apparent dispersion curve is characterized by the presence of four propagation modes: all of them show a steep velocity increase in the low frequency range. It should also be noticed that the low frequency part of the dispersion curve has been retrieved by processing passive data which allow a greater investigation depth.
Data were inverted using a multimodal stochastic approach, the best fitting profiles are plotted in Figure 9 a), profile colour depends on the misfit, from yellow to blue (best fitting profile). In Figure 9 b) the best fitting profile is compared with the results of a DH test previously performed on the same site. In Figure 10 the experimental dispersion curve is compared with the determinant surface of the best fitting model. Moreover it can be noted that the surface wave method results are in fairly good agreement with the DH test profile, particularly in the shallower part of the profile itself.

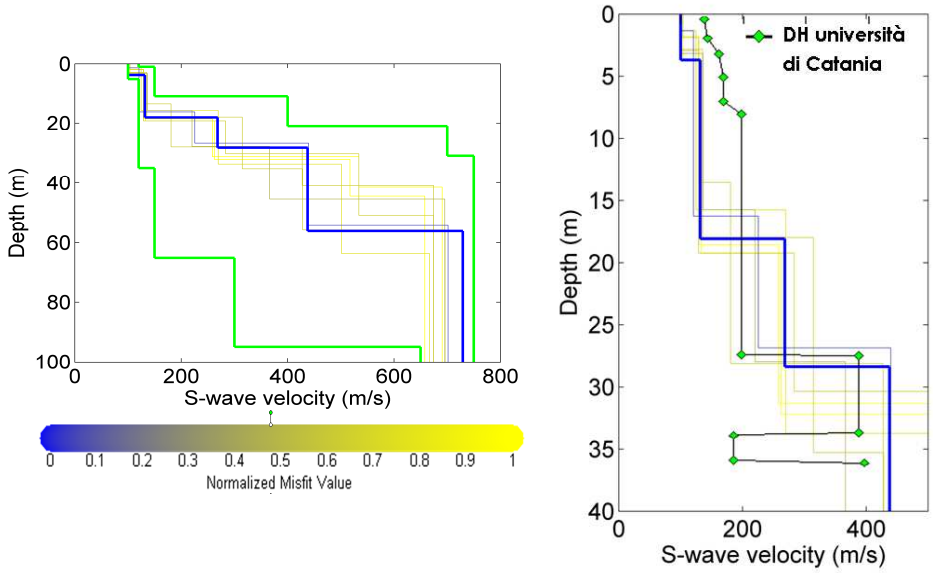

Figure 9 Catania (Piana) – a) Monte Carlo results (from yellow to blue) of the inversion with the boundaries (green). b) Catania (Piana) – Best fitting profiles compared with the refraction result (black).

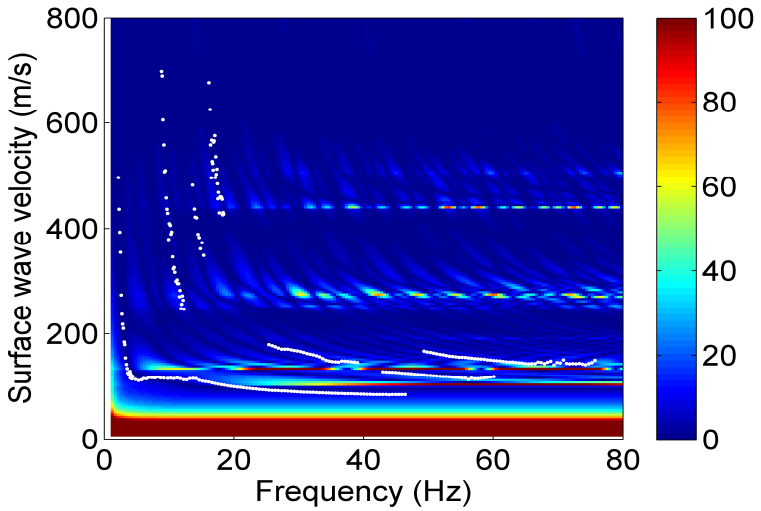

Figure 10 Catania – Experimental dispersion curve compared with the misfit surface of the best fitting model

The parameters of the best fitting profile are summarized in Table 4.

Vs (m/s)	Thickness (m)	Poisson coefficient	Density (T/m^3)
100	3.7	0.3	1.8
132	14.4	0.3	1.8
268	10.3	0.3	1.8
438	27.8	0.3	1.8
730	-	0.3	1.8

Table 3 Catania (Piana): subsoil parameters of the best fitting profile.

References

Project S4: ITALIAN STRONG MOTION DATA BASE, Deliverable # 6, Application of Surface wave methods for seismic site characterization, May 2009.

Foti S., Comina C., Boiero D., Socco L.V. (2009) "Non uniqueness in surface wave inversion and consequences on seismic site response analyses", Soil Dynamics and Earthquake Engineering, Vol. 29 (6), 982-993.

Haskell, N., 1964, Radiation pattern of surface waves from point sources in a multilayered medium: Bulletin of seismological society of America, 54, no. 1, 377-393.

Herrmann, R. B., and C. Y. Wang, 1980, A numerical study of p-, sv- and sh- wave generation in a plane layered medium: Bulletin of seismological society of America, 70, no. 4, 1015-1036.

Herrmann, R. B., 2002, SURF code, www.eas.slu.edu/People/RBHerrmann/.

Maraschini, M., F. Ernst, D. Boiero, S. Foti, and L.V. Socco, 2008, A new approach for multimodal inversion of Rayleigh and Scholte waves: Proceedings of EAGE Rome, expanded abstract.

Thomson, W. T, 1950., Transmission of elastic waves through a stratified solid medium: Journal of Applied Physics, 21, no. 89.

APPLICATION OF SURFACE WAVE METHODS FOR SEISMIC SITE CHARACTERIZATION

CALTAGIRONE (CLG)

Responsible:
Sebastiano Foti

Co-workers:
Giovanni Bianchi
Paolo Bergamo
Margherita Maraschini
Ken Tokeshi
Cesare Comina

FINAL REPORT

Turin, 11/02/2010

INDEX

1 Introduction

In this report a summary of the results obtained for the characterization of the accelerometric station of Caltagirone of the RAN within Project S4 is presented. The analysis was performed using active and passive surface wave method and refraction method.

Caltagirone RAN station is located within the built-up area of the town: a limited zone of rock alteration and vegetation soil is expected above the bedrock.

The map, site location and measurements arrays are shown in Figure1, Figure 2 and Figure 3.

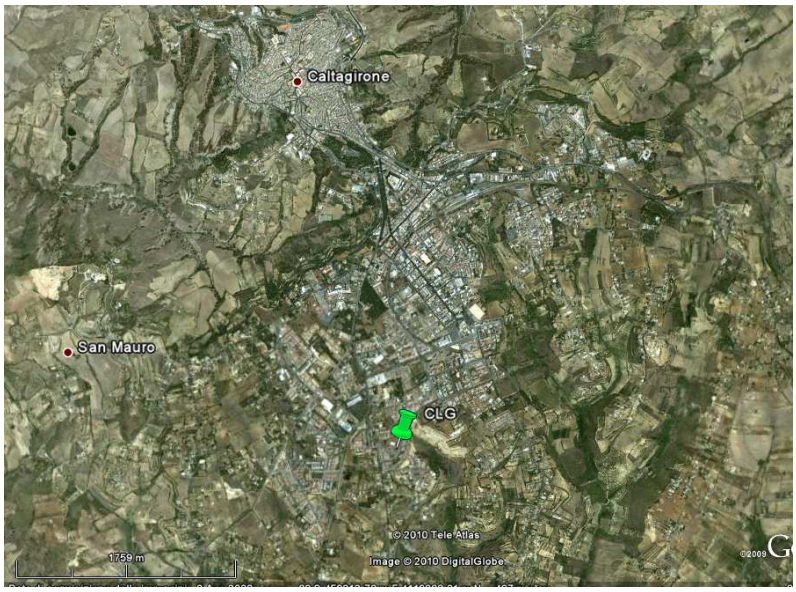

Figure 1 Caltagirone: maps

Figure 2 Caltagirone: array map. The yellow line represents the active measurements array; the red triangle and the white triangle represent the two triangles along which receivers for passive measurements were arranged.

Figure 3 Caltagirone: site location and active measurement array.

Goal of the seismic tests is the estimation of the S-wave velocity profile of the subsoil, and in particular the position of the bedrock. The presence of stiff seismic interfaces between the sediments and the shallow bedrock can cause a relevance of higher modes in the surface wave experimental dispersion curve which has be taken into account in order to provide reliable results.

The primary use of surface wave testing is related to site characterization in terms of shear wave velocity profile. The V_S profile is of primary interest for seismic site response studies and for studies of vibration of foundations and vibration transmission in soils. Other applications are related to the prediction of settlements and to soil-structure interaction.

With respect to the evaluation of seismic site response, it is worth noting the affinity between the model used for the interpretation of surface wave tests and the model adopted for most site responses study. Indeed the application of equivalent linear elastic methods is often associated with layered models (e.g. the code SHAKE and all similar approaches). This affinity is also particularly important in the light of equivalence problems, which arise because of non-uniqueness of the solution in inverse problems. Indeed profiles which are equivalent in terms of Rayleigh wave propagation are also equivalent in term of seismic amplification (Foti et al., 2009).

Many seismic building codes introduce the weighted average of the shear wave velocity profile in the shallowest 30m as to discriminate class of soils to which a similar site amplification effect can be associated. The so-called $V_{S,30}$ can be evaluated very efficiently with surface wave method also because its average nature does not require the high level of accuracy that can be obtained with seismic borehole methods.

In the following a methodological summary of techniques and the description of the results is presented.

For Further explanation of surface wave methodologies, see document: Project S4: ITALIAN STRONG MOTION DATA BASE, Deliverable # 6, Application of Surface wave methods for seismic site characterization, May 2009.

2 Surface wave method

Surface wave method (S.W.M.) is based on the geometrical dispersion, which makes Rayleigh wave velocity frequency dependent in vertically heterogeneous media. High frequency (short wavelength) Rayleigh waves propagate in shallow zones close to the free surface and are informative about their mechanical properties, whereas low frequency (long wavelength) components involve deeper layers. Surface wave tests are typically devoted to the determination of a small strain stiffness profile for the site under investigation. Consequently the dispersion curve will be associated to the variation of medium parameters with depth.

The calculation of the dispersion curve from model parameters is the so called forward problem. Surface wave propagation can be seen as the combination of multiple modes of propagation, i.e. more than one possible velocity can be associated to each frequency value. Including higher modes in the inversion process allows the penetration depth to be increased and a more accurate subsoil profile to be retrieved.

If the dispersion curve is estimated on the basis of experimental data, it is then possible to solve the inverse problem, i.e. the model parameters are identified on the basis of the experimental data collected on the boundary of the medium. The result of the surface wave method is a one-dimensional S wave velocity soil profile.

The standard procedure for surface wave tests is reported in Figure 4. It can be subdivided into three main steps:

1. acquisition of experimental data;
2. signal processing to obtain the experimental dispersion curve;
3. inversion process to estimate shear wave velocity profile at the site.

It is very important to recognize that the above steps are strongly interconnected and their interaction must be adequately accounted for during the whole interpretation process.

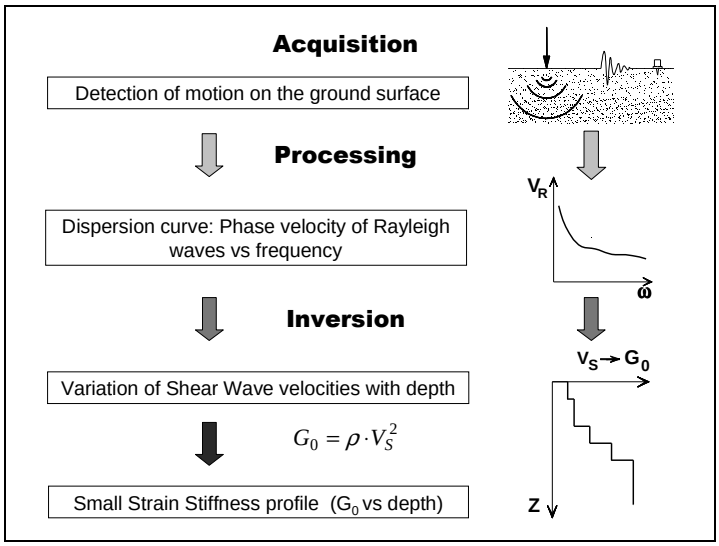

Figure 4 – Flow chart of surface wave tests.

2.1 Acquisition

Active (MASW) and passive surface wave tests and refraction surveys at Caltagirone have been performed in May 2009 within the project S4 for the characterization of RAN sites.

Characteristics of sensors are reported in Table 1.

Test	GEOPHONE TYPE	NATURAL FREQUENCY	GEOPHONE NUMBER
MASW/Refraction survey	vertical SENSOR SM-6/U-B	4,5 Hz	48
Passive surface wave tests	three components 3D HS1 GEO-SPACE	2 Hz	4
	vertical HS1 GEO-SPACE	2 Hz	12

Table 1 Caltagirone: receiver characteristics

48 receivers were used for active tests, with a spacing of 1 m between neighbouring geophones, so that the total length of the array is 47 m. The source is a 5kg sledge hammer. This array was used for refraction surveys as well. 16 receivers were used for passive tests: 12 vertical geophones were arranged along an isosceles triangle whose basis is 15 m long and the other two sides are 24 m long; one three components geophones was placed at the centre of this triangle and three others were disposed on the vertexes of a smaller triangle inscrittible within the first one. Arrays for passive measurements are shown in Figure 5; acquisition parameters are summarized in Table 2

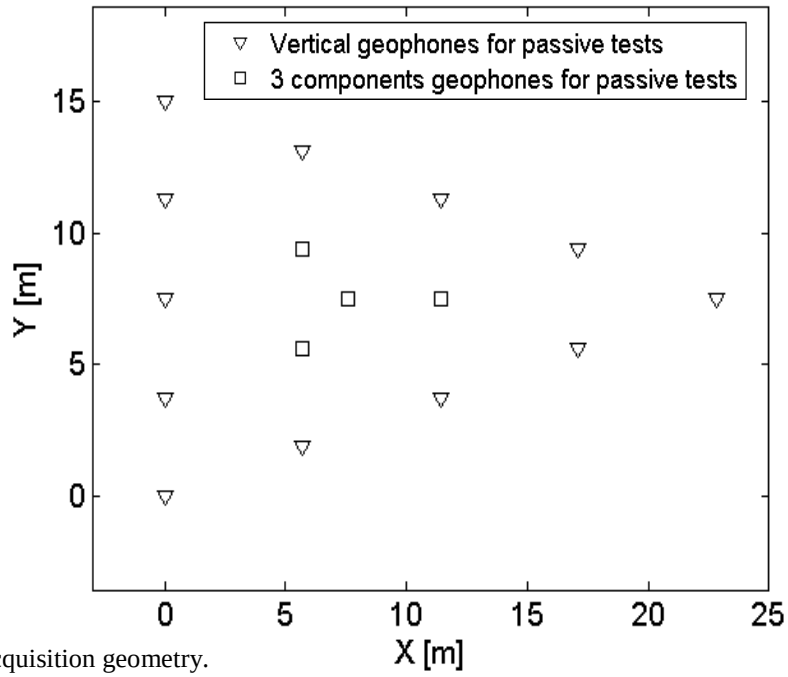

Figure 5 – Acquisition geometry.

Test	GEOF. N.	SPACING	SOURCE TYPE	ACQUISITION WINDOW	SAMPLING INTERVAL	STACK
MASW	48	1 m	Hammer	T = 2 s	Δt = 0.5 ms	10
Passive tests	16	-	-	T =524 s	Δt = 8 ms	1
Refraction surveys	48	1 m	Hammer	T = 1 s	Δt = 62.5 μs	10

Table 2 Caltagirone: Acquisition parameters

2.2 Processing of active surface wave data

The processing allows the experimental dispersion curve to be determined.

Multichannel data are processed using a double Fourier Transform, which generates the frequency-wave number spectrum, where the multimodal dispersion curve is easily extracted as the location of spectral maxima.

2.3 Processing of passive surface wave data

The phase velocity of the surface waves can be extracted from noise recordings by using different methods: among them, the most frequently used are the Beam-Forming Method (BFM) (Lacoss et al., 1969) and the Maximum Likelihood Method (MLM) (Capon, 1969). Here we will illustrate the Beam-Forming Method which was used to process passive surface wave data. For further explanation on passive surface wave methodologies, see document: Project S4: ITALIAN STRONG MOTION DATA BASE, Deliverable # 6, Application of Surface wave methods for seismic site characterization, May 2009.

The estimate of the F-K spectra $P_b(f,\mathrm{k})$ by the BFM is given by:

$$P_b(f,k) = \sum_{l,m=1}^{n} \phi_{lm} \exp\{ik(X_l - X_m\} \ ,$$

where f is the frequency, k the two-dimensional horizontal wavenumber vector, n the number of sensors, ϕ_{lm} the estimate of the cross-power spectra between the l^{th} and the m^{th} data, and X_i and X_m, are the coordinates of the l^{th} and m^{th} sensors, respectively.

From the peak in the F-K spectrum occurring at coordinates k_{xo} and k_{yo} for a certain frequency $f_{0,}$ the phase velocity c_0 can be calculated by:

$$c_0 = \frac{2\pi f_0}{\sqrt{k_{xo}{}^2 + k_{yo}{}^2}}$$

so that, again, an experimental dispersion curve is retrieved.

Figure 6 shows an example of F-K analysis results obtained by processing passive surface wave data with Beam-Forming Method: white dots indicate the position of the maximum used to estimate the phase velocity while the white circle joins points with the same k values.

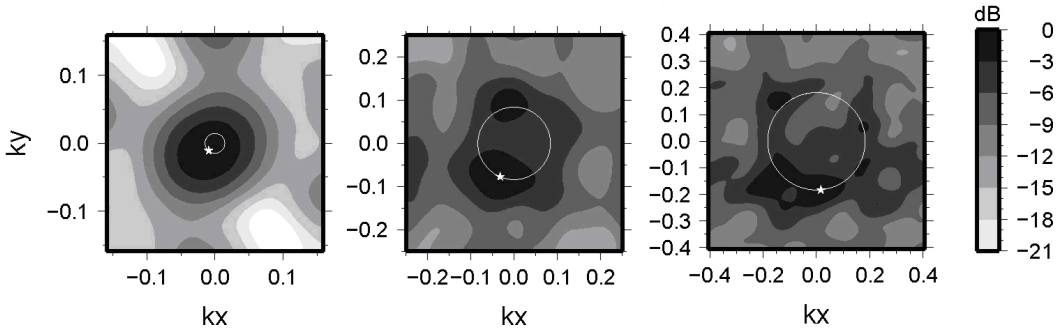

Figure 6 – Example of results from F-K analysis s for 2.5 Hz, 3.9 Hz, and 6.5 Hz. White dots indicate the position of the maximum used to estimate the phase velocity. The white circle joins points with the same k

2.4 Inversion of surface waves

The solution of the inverse Rayleigh problem is the final step in test interpretation. The solution of the forward problem forms the basis of any inversion strategy; the forward problem consists in the calculation of the function whose zeros are dispersion curves of a given model. Assuming a model for the soil deposit, model parameters of the best fitting subsoil profile are obtained minimizing an object function.

The subsoil is modelled as a horizontally layered medium overlaying a halfspace, with constant parameter in the interior of each layer and linear elastic behaviour. Model parameters are thickness, S-wave velocity, P-wave velocity (or Poisson coefficient), and density of each layer and the halfspace. The inversion is performed on S-wave velocities and thicknesses, whereas for the other parameters realistic values are chosen a priori. The number of layer is chosen applying minimum parameterization criterion.

In surface wave analysis it is very common to perform the inversions using only the fundamental mode of propagation. This approach is based on the assumption that the prevailing mode of propagation is the fundamental one; if this is partially true for normal dispersive sites, in several real cases the experimental dispersion curve is on the contrary the result of the superposition of several modes. This may happen in particular when velocity inversions or strong velocity contrasts are present in the shear wave velocity profile. In these stratigraphic conditions the inversion of the only fundamental mode will produce significant errors; moreover all the information contained in higher propagating modes is not used in the inversion process. Therefore, the fundamental mode inversion does not use all the available information, and this affects the result accuracy.

The use of higher modes in the inversion can be helpful both in the low frequency range, in order to increase the investigation depth and to avoid the overestimation of the bedrock velocity, and in the high frequency range in order to provide a more consistent interpretation of shallow interfaces and increase model parameter resolution.

In this work a multimodal misfit function has been used. This function is based on the Haskell-Thomson method for dispersion curve calculation (Thomson 1950, Haskell 1953, Herrmann e Wang 1980, Herrmann 2002). For a given subsoil model, and an experimental data, the misfit of the model is the L^1 norm of the vector containing the absolute value of the determinant of the Haskell-Thomson matrix (which is zeros in correspondence of all the modes of the dispersion curves of the numerical model) evaluated in correspondence of

the experimental data (Maraschini et al. 2008). The misfit function adopted has the advantage of being able to include any dispersive event present in the data without the need of specifying to which mode the data points belong to, avoiding errors arising from mode misidentification, in particular in the low frequency range.

This misfit function is applied in a Global Search Methods (GSM), in order to reduce the possibility of falling in local minima. A uniform random search is applied; ranges for the inversion have been chosen, for the different sites, based on the experimental dispersion curves; in particular the range of the S-wave half space velocity is close to the maximum surface wave velocity retrieved on experimental data.

The results of the inversion are reported as the ensemble of the best shear wave velocity profiles chosen according to a chi-square test (see Socco et al., 2008). It can be assumed that the experimental dispersion curve is affected by a Gaussian error with a known standard deviation, so that the probability density function of data $\rho_D(d)$ can be described by a discrete m-dimensional Gaussian (where *m* are the model parameters) and the sample variance variable of each random vector (dispersion curve) extracted from the data pdf is distributed according to a chi-square probability density. According to these assumptions we adopt a misfit function with the structure of a chi-square and this allows a statistical test to be applied to the variances of the synthetic dispersion curves with respect to the experimental one d_{obs}. Assuming that the best fitting curve d_{opt} belongs to the distribution $\rho_D(d_{obs})$ all models belonging to the distribution $\rho_D(d_{opt})$ and consistent with the data within a fixed level of confidence α are selected. As the ratio between chi-square variables follows a Fisher distribution a one–tailed F test can be performed:

$$F_\alpha(dof_{dopt}, dof_{g(m)}) < \frac{\chi^2_{dopt}}{\chi^2_{g(m)}}$$

where α is the chosen level of confidence, dof_{dopt} and $dof_{g(m)}$ are the degrees of freedom of the Fischer distribution and χ^2_{dopt} and $\chi^2_{g(m)}$ are the misfit of the best fitting curve and the misfit of all the others respectively. All models passing such test are selected. In the figures reported a representation based on the misfit is adopted for velocity profiles, so that the darkest colour corresponds to the profile whose dispersion curve has the lowest misfit and better approximation to the reference one; instead for dispersion curves the coloured surface under imposed to the experimental one is a misfit surface, whose zeros are synthetic dispersion curve of the best fitting model.

2.5 Numerical code

The numerical codes used for processing and inversion of surface waves are non commercial codes, implemented at Politecnico di Torino.

3 Caltagirone – Refraction results

5 shots were considered for refraction survey: two of them with the source at the edges of the array and three with the source at intermediate positions along the survey line. First-break arrival times are shown in Figure 7.

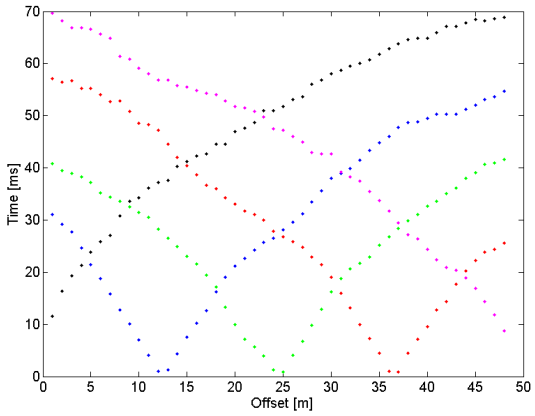

Figure 7 Caltagirone – First breaks of the five considered shots

A three layers model is identified: the weathering layer has a P-wave velocity of 373 m/s and its thickness grows thin from 5.7 m to 2.2 m towards the end of the array. The intermediate layer is characterized by a P-wave velocity of approximately 750 m/s and a thickness of 6.5 m increasing to 8.9 m toward the end of the array; the lowest layer has a P-wave velocity of 1423 m/s. The average profile features are summarized in Table 3.

P-wave velocity (m/s)	Thickness (m)
373	3.9
750	7.7
1423	-

Table 3 Velocity models retrieved by refraction survey

4 Caltagirone – Surface wave results

In Figure 8 an example of the f-k spectrum of the active data collected at Caltagirone is presented.

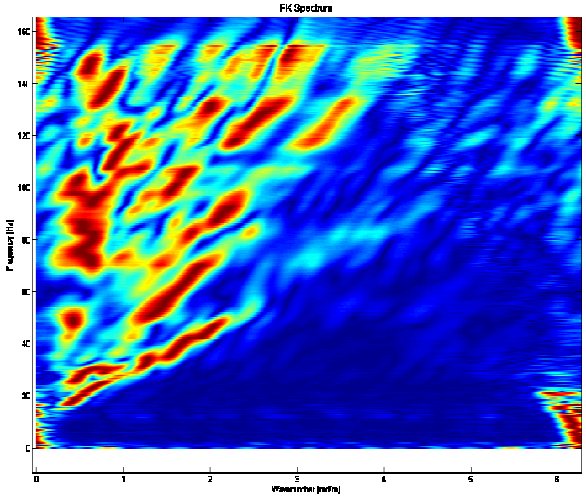

Figure 8 Caltagirone – example of f-k spectrum

From the f-k spectra, several dispersion curves can be retrieved. From all these curves an average curve is estimated (Figure 9).

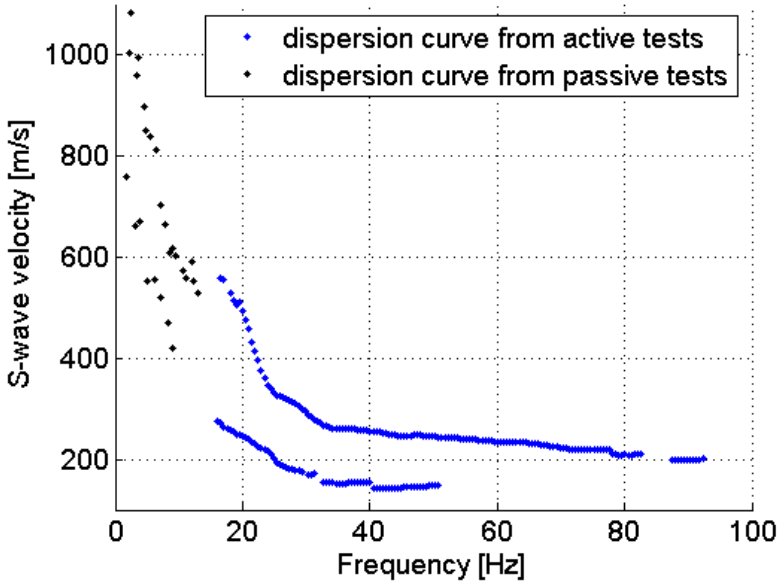

Figure 9 – Caltagirone - Average apparent dispersion curve

The apparent dispersion curve is made up of four branches – two from active data and two from passive data – which probably follow two propagation modes: note that one branch is characterized by a steep velocity increase at about 20 Hz, probably jumping from one mode to another.

Data were inverted using a multimodal stochastic approach, the best fitting profiles are plotted in Figure 10 a), profile colour depends on the misfit, from yellow to blue (best fitting profile). In Figure 10 b) the best fitting profile is compared with the refraction result, and in Figure 11 the experimental dispersion curve is compared with the determinant surface of the best fitting model. We can note that the experimental points fall into the minima of the determinant surface, and that a branch of the apparent dispersion curve jumps from the 1st to the 2nd higher mode at around 20 Hz, probably because of the impedance contrast between topsoil and bedrock. Moreover it can be noted that the position of the first two interfaces is in good agreement with the refraction results.

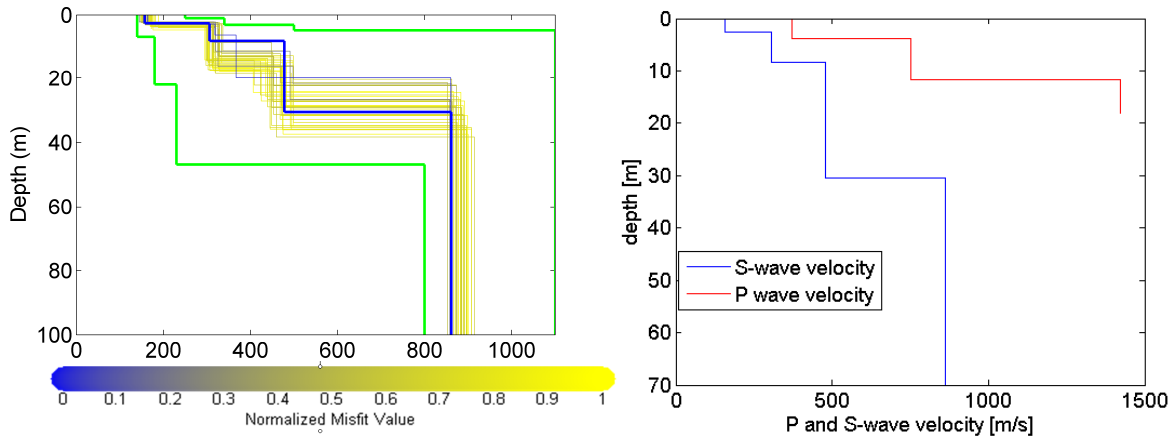

Figure 10 Caltagirone – a) Monte Carlo results (from yellow to blue) of the inversion with the boundaries (green). b) Caltagirone – Best fitting profile (blue) compared with the refraction result (red).

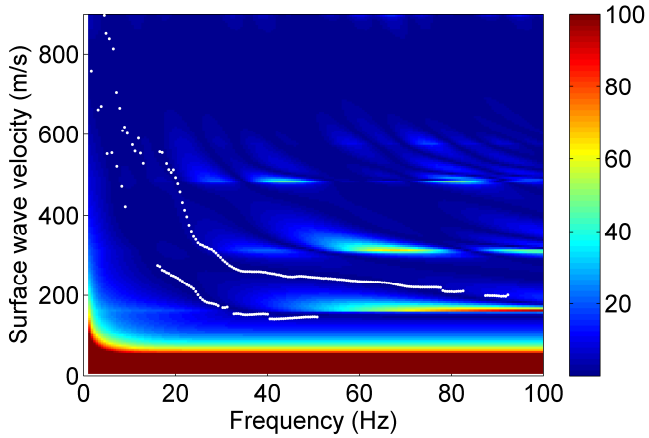

Figure 11 Caltagirone – Experimental dispersion curve compared with the misfit surface of the best fitting model

The parameters of the best fitting profile are summarized in Table 4.

Vs (m/s)	Thickness (m)	Poisson coefficient	Density (T/m^3)
157	2.5	0.3	1.8
305	5.7	0.3	1.8
477	22.1	0.3	1.8
861		0.3	1.8

Table 4 Caltagirone: subsoil parameters of the best fitting profile.

References

Project S4: ITALIAN STRONG MOTION DATA BASE, Deliverable # 6, Application of Surface wave methods for seismic site characterization, May 2009.

Foti S., Comina C., Boiero D., Socco L.V. (2009) "Non uniqueness in surface wave inversion and consequences on seismic site response analyses", Soil Dynamics and Earthquake Engineering, Vol. 29 (6), 982-993.

Haskell, N., 1964, Radiation pattern of surface waves from point sources in a multilayered medium: Bulletin of seismological society of America, 54, no. 1, 377-393.

Herrmann, R. B., and C. Y. Wang, 1980, A numerical study of p-, sv- and sh- wave generation in a plane layered medium: Bulletin of seismological society of America, 70, no. 4, 1015-1036.

Herrmann, R. B., 2002, SURF code, www.eas.slu.edu/People/RBHerrmann/.

Maraschini, M., F. Ernst, D. Boiero, S. Foti, and L.V. Socco, 2008, A new approach for multimodal inversion of Rayleigh and Scholte waves: Proceedings of EAGE Rome, expanded abstract.

Thomson, W. T, 1950., Transmission of elastic waves through a stratified solid medium: Journal of Applied Physics, 21, no. 89.

APPLICATION OF SURFACE WAVE METHODS FOR SEISMIC SITE CHARACTERIZATION

GELA (GEA)

Responsible:
Sebastiano Foti

Co-workers:
Giovanni Bianchi
Margherita Maraschini
Paolo Bergamo

FINAL REPORT

Turin, 15/01/2010

INDEX

1 Introduction

In this report a summary of the results obtained for the characterization of the accelerometric station of Gela of the RAN within Project S4 is presented. The analysis was performed using active surface wave method and refraction method.

Gela RAN station is placed in an alluvial plane bordered by the sea: according to available geological information the soil is made up of present and recent alluvial deposits followed by clays and marls. No shallow bedrock is expected.

The map of the site and the array and its location are shown in Figure 1 and Figure 2.

Figure 1 Gela: map

Figure 2 Gela: map of the array and its location

Goal of the seismic tests is the estimation of the S-wave velocity profile of the subsoil. The possible presence of S-wave velocity inversions between adjacent layers can cause an

anomalous energy distribution on the apparent dispersion curve: this has to be taken into account in order to provide reliable results.

The primary use of surface wave testing is related to site characterization in terms of shear wave velocity profile. The V_S profile is of primary interest for seismic site response studies and for studies of vibration of foundations and vibration transmission in soils. Other applications are related to the prediction of settlements and to soil-structure interaction.

With respect to the evaluation of seismic site response, it is worth noting the affinity between the model used for the interpretation of surface wave tests and the model adopted for most site responses study. Indeed the application of equivalent linear elastic methods is often associated with layered models (e.g. the code SHAKE and all similar approaches). This affinity is also particularly important in the light of equivalence problems, which arise because of non-uniqueness of the solution in inverse problems. Indeed profiles which are equivalent in terms of Rayleigh wave propagation are also equivalent in term of seismic amplification (Foti et al., 2009).

Many seismic building codes introduce the weighted average of the shear wave velocity profile in the shallowest 30m as to discriminate class of soils to which a similar site amplification effect can be associated. The so-called $V_{S,30}$ can be evaluated very efficiently with surface wave method also because its average nature does not require the high level of accuracy that can be obtained with seismic borehole methods.

In the following a methodological summary of techniques and the description of the results is presented.

For Further explanation of surface wave methodologies, see document: Project S4: ITALIAN STRONG MOTION DATA BASE, Deliverable # 6, Application of Surface wave methods for seismic site characterization, May 2009.

2 Surface wave method

Surface wave method (S.W.M.) is based on the geometrical dispersion, which makes Rayleigh wave velocity frequency dependent in vertically heterogeneous media. High frequency (short wavelength) Rayleigh waves propagate in shallow zones close to the free surface and are informative about their mechanical properties, whereas low frequency (long wavelength) components involve deeper layers. Surface wave tests are typically devoted to the determination of a small strain stiffness profile for the site under investigation. Consequently the dispersion curve will be associated to the variation of medium parameters with depth.

The calculation of the dispersion curve from model parameters is the so called forward problem. Surface wave propagation can be seen as the combination of multiple modes of propagation, i.e. more than one possible velocity can be associated to each frequency value. Including higher modes in the inversion process allows the penetration depth to be increased and a more accurate subsoil profile to be retrieved.

If the dispersion curve is estimated on the basis of experimental data, it is then possible to solve the inverse problem, i.e. the model parameters are identified on the basis of the

experimental data collected on the boundary of the medium. The result of the surface wave method is a one-dimensional S wave velocity soil profile.

The standard procedure for surface wave tests is reported in Figure 3. It can be subdivided into three main steps:

1. acquisition of experimental data;
2. signal processing to obtain the experimental dispersion curve;
3. inversion process to estimate shear wave velocity profile at the site.

It is very important to recognize that the above steps are strongly interconnected and their interaction must be adequately accounted for during the whole interpretation process.

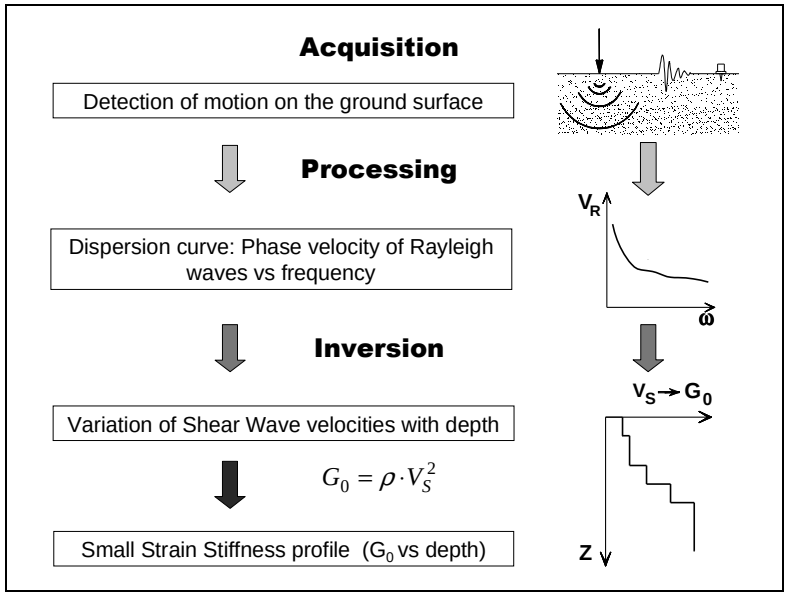

Figure 3 – Flow chart of surface wave tests.

2.1 Acquisition

Active surface wave tests (MASW) and refraction tests at Gela have been performed in May 2009 within the project S4 for the characterization of RAN sites.

Characteristics of sensors are reported in Table 1.

Test	GEOPHONE TYPE	NATURAL FREQUENCY	GEOPHONE NUMBER
MASW/Refraction	vertical SENSOR SM-6/U-B	4,5 Hz	48

Table 1 Gela: receiver characteristics

The measuring array is located in an uncultivated area on a gentle slope in the alluvial plane: 48 geophones were used, with a spacing between geophones of 1.5 m. The total length of the array is 70.5m. The source is a 5kg sledge hammer. Geometry parameters are summarized in Table 2.

Test	GEOF. N.	SPACING	SOURCE TYPE	ACQUISITION WINDOW	SAMPLING INTERVAL	STACK
MASW	48	1.5 m	Hammer	T = 2 s	Δt = 0.5 ms	10
Refraction	48	1.5 m	Hammer	T =1 s	Δt = 0.0625 ms	10

Table 2 Gela: Acquisition parameters

The acquisition array is located in an alluvial plane at approximately 2.6 km from the coast at about 17 m on sea level, so that the water table is expected to be quite shallow. As this site is characterized by the superposition of alluvial deposits, the usefulness of P-wave seismic refraction survey is not to locate the bedrock but to provide information on water table depth.

2.2 Processing of surface waves

The processing allows the experimental dispersion curve to be determined.

Multichannel data are processed using a double Fourier Transform, which generates the frequency-wave number spectrum, where the multimodal dispersion curve is easily extracted as the location of spectral maxima.

2.3 Inversion of surface waves

The solution of the inverse Rayleigh problem is the final step in test interpretation. The solution of the forward problem forms the basis of any inversion strategy; the forward problem consists in the calculation of the function whose zeros are dispersion curves of a given model. Assuming a model for the soil deposit, model parameters of the best fitting subsoil profile are obtained minimizing an object function.

The subsoil is modelled as a horizontally layered medium overlaying a halfspace, with constant parameter in the interior of each layer and linear elastic behaviour. Model parameters are thickness, S-wave velocity, P-wave velocity (or Poisson coefficient), and density of each layer and the halfspace. The inversion is performed on S-wave velocities and thicknesses, whereas for the other parameters realistic values are chosen a priori. The number of layer is chosen applying minimum parameterization criterion.

In surface wave analysis it is very common to perform the inversions using only the fundamental mode of propagation. This approach is based on the assumption that the prevailing mode of propagation is the fundamental one; if this is partially true for normal dispersive sites, in several real cases the experimental dispersion curve is on the contrary the result of the superposition of several modes. This may happen in particular when velocity inversions or strong velocity contrasts are present in the shear wave velocity profile. In these stratigraphic conditions the inversion of the only fundamental mode will

produce significant errors; moreover all the information contained in higher propagating modes is not used in the inversion process. Therefore, the fundamental mode inversion does not use all the available information, and this affects the result accuracy.

The use of higher modes in the inversion can be helpful both in the low frequency range, in order to increase the investigation depth and to avoid the overestimation of the bedrock velocity, and in the high frequency range in order to provide a more consistent interpretation of shallow interfaces and increase model parameter resolution.

In this work a multimodal misfit function has been used. This function is based on the Haskell-Thomson method for dispersion curve calculation (Thomson 1950, Haskell 1953, Herrmann e Wang 1980, Herrmann 2002). For a given subsoil model, and an experimental data, the misfit of the model is the L^1 norm of the vector containing the absolute value of the determinant of the Haskell-Thomson matrix (which is zeros in correspondence of all the modes of the dispersion curves of the numerical model) evaluated in correspondence of the experimental data (Maraschini et al. 2008). The misfit function adopted has the advantage of being able to include any dispersive event present in the data without the need of specifying to which mode the data points belong to, avoiding errors arising from mode misidentification, in particular in the low frequency range.

This misfit function is applied in a Global Search Methods (GSM), in order to reduce the possibility of falling in local minima. A uniform random search is applied; ranges for the inversion have been chosen, for the different sites, based on the experimental dispersion curves; in particular the range of the S-wave half space velocity is close to the maximum surface wave velocity retrieved on experimental data.

The results of the inversion are reported as the ensemble of the best shear wave velocity profiles chosen according to a chi-square test (see Socco et al., 2008). It can be assumed that the experimental dispersion curve is affected by a Gaussian error with a known standard deviation, so that the probability density function of data $\rho_D(d)$ can be described by a discrete m-dimensional Gaussian (where m are the model parameters) and the sample variance variable of each random vector (dispersion curve) extracted from the data pdf is distributed according to a chi-square probability density. According to these assumptions we adopt a misfit function with the structure of a chi-square and this allows a statistical test to be applied to the variances of the synthetic dispersion curves with respect to the experimental one d_{obs}. Assuming that the best fitting curve d_{opt} belongs to the distribution $\rho_D(d_{obs})$ all models belonging to the distribution $\rho_D(d_{opt})$ and consistent with the data within a fixed level of confidence α are selected. As the ratio between chi-square variables follows a Fisher distribution a one–tailed F test can be performed:

$$F_\alpha(dof_{dopt}, dof_{g(m)}) < \frac{\chi^2_{dopt}}{\chi^2_{g(m)}}$$

where α is the chosen level of confidence, dof_{dopt} and $dof_{g(m)}$ are the degrees of freedom of the Fischer distribution and χ^2_{dopt} and $\chi^2_{g(m)}$ are the misfit of the best fitting curve and the misfit of all the others respectively. All models passing such test are selected. In the figures reported a representation based on the misfit is adopted for velocity profiles, so that the darkest colour corresponds to the profile whose dispersion curve has the lowest misfit and better approximation to the reference one; instead for dispersion curves the coloured surface under imposed to the experimental one is a misfit surface, whose zeros are synthetic dispersion curve of the best fitting model.

2.4 Numerical code

The numerical codes used for processing and inversion of surface waves are non commercial codes, implemented at Politecnico di Torino.

3 Gela – Refraction results

Five shots were considered for the inversion, two of them with the source located at the extremes of the survey line (2 m from the first geophone) and three with the source within the survey line (at one quarter, in the middle and at three quarters of the array). The first breaks of these shots are shown in Figure 4.

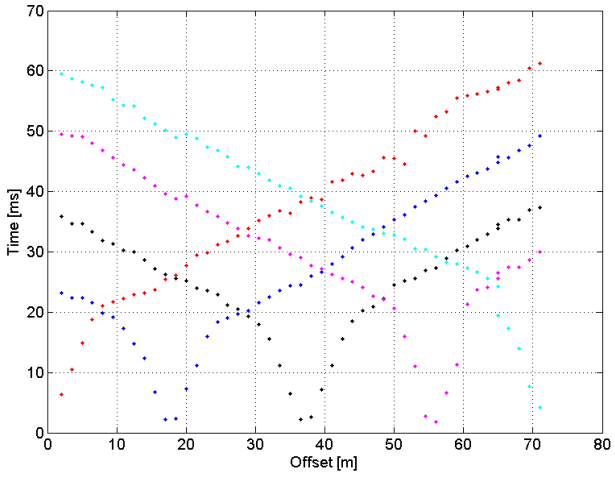

Figure 4 Gela – First breaks of the five shots considered

The presence of velocity inversions and of the water table can be excluded.
All five shots were considered for the inversion, yielding a P-wave velocity model with a first layer thickness decreasing from 3.7 to 2.9 m: the first layer velocity is 390 m/s, the deeper layer velocity is 1656 m/s. As the shallower layer grows thin following the slope of soil and being the second layer velocity quite close to the P-wave velocity in water it is very likely that the interface between the two layers corresponds to the water table depth. Parameters are summarized in Table 3.

P-wave velocity (m/s)	Thickness (m)
390	3.7 – 2.9
1656	-

Table 3 Velocity models retrieved by refraction survey

4 Gela – Surface wave results

In Figure 5 an example of the f-k spectrum of the data collected at Gela with the picked dispersion curve is presented.

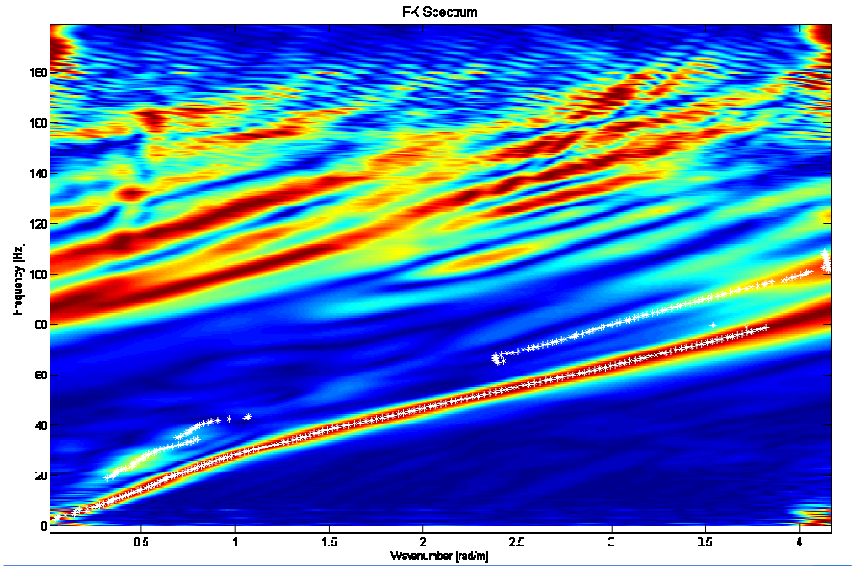

Figure 5 Gela – example of f-k spectrum

From the f-k spectra, several dispersion curves can be retrieved. From all these curves an average curve is estimated (Figure 6).

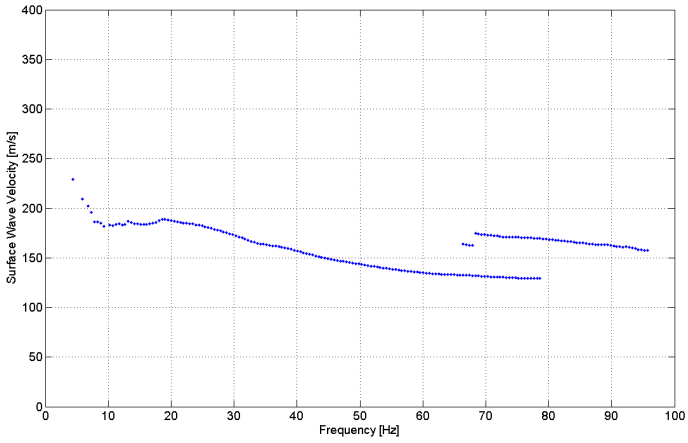

Figure 6 – Gela -Average apparent dispersion curve

The experimental dispersion curves is made up of two branches, one of them ranging from 5 to 80 Hz with velocities between 140 and 240 m/s and the other one with frequencies between 70 and 95 Hz and velocities between 150 and 180 m/s. The first branch is characterized by the presence of a hump at about 20 Hz which may indicate a velocity inversion.

Data were inverted using a multimodal stochastic approach, the 20 best fitting profiles are plotted in Figure 7 a), profile colour depends on the misfit, from yellow to blue (best fitting profile). In Figure 7 b) the best fitting profile is compared with the refraction result, and in Figure 8 the experimental dispersion curve is compared with the determinant surface of the best fitting model. We can note that the experimental points follow in the minima of the determinant surface, and that at around 10 m depth a velocity inversion actually occurs. Note also that the refraction results are not in full agreement with the surface wave results: this is due to the fact that P-waves are sensitive to the presence of water while Rayleigh waves are not, so that the depth of water table is identified by refraction tests but not by surface wave tests.

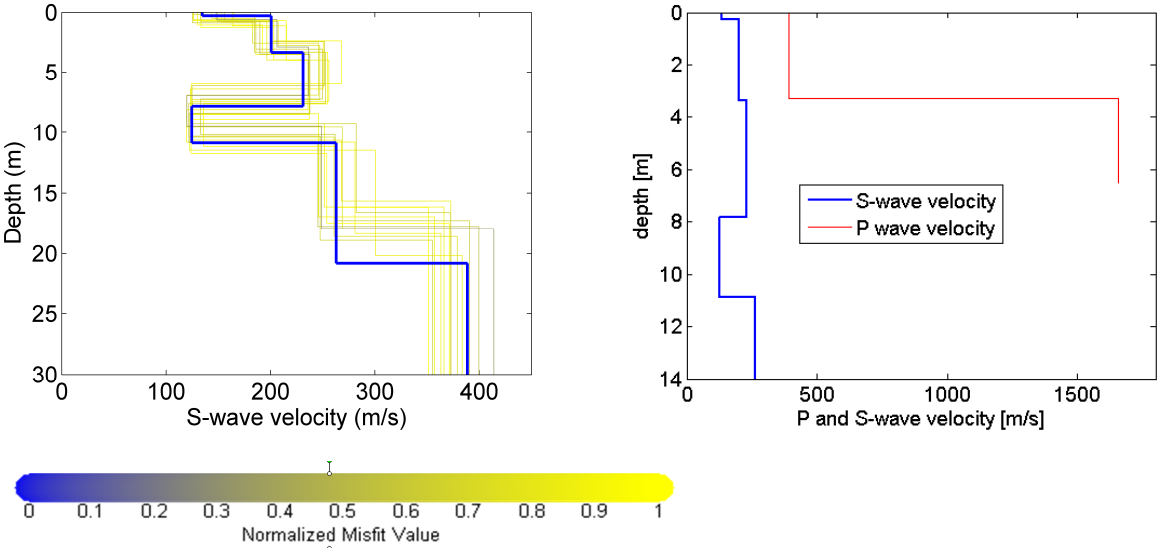

Figure 7 Gela – a) Monte Carlo results (from yellow to blue) of the inversion. b) Gela – Best fitting profile (blue) compared with the refraction result (red).

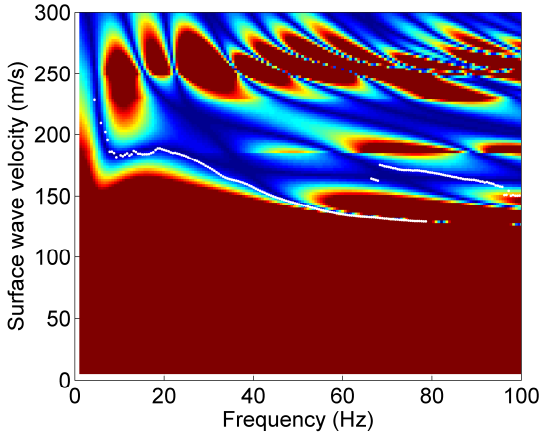

Figure 8 Gela – Experimental dispersion curve compared with the misfit surface of the best fitting model

The parameters of the best fitting profile are summarized in Table 4.

Vs (m/s)	Thickness (m)	Poisson coefficient	Density (T/m^3)
135	0.3	0.3	1.8
201	3.1	0.3	1.8
231	4.5	0.3	1.8
125	3.0	0.3	1.8
263	9.9	0.3	1.8
389	-	0.3	1.8

Table 4 Gela: subsoil parameters of the best fitting profile.

References

Project S4: ITALIAN STRONG MOTION DATA BASE, Deliverable # 6, Application of Surface wave methods for seismic site characterization, May 2009.

Foti S., Comina C., Boiero D., Socco L.V. (2009) "Non uniqueness in surface wave inversion and consequences on seismic site response analyses", Soil Dynamics and Earthquake Engineering, Vol. 29 (6), 982-993.

Haskell, N., 1964, Radiation pattern of surface waves from point sources in a multilayered medium: Bulletin of seismological society of America, 54, no. 1, 377-393.

Herrmann, R. B., and C. Y. Wang, 1980, A numerical study of p-, sv- and sh- wave generation in a plane layered medium: Bulletin of seismological society of America, 70, no. 4, 1015-1036.

Herrmann, R. B., 2002, SURF code, www.eas.slu.edu/People/RBHerrmann/.

Maraschini, M., F. Ernst, D. Boiero, S. Foti, and L.V. Socco, 2008, A new approach for multimodal inversion of Rayleigh and Scholte waves: Proceedings of EAGE Rome, expanded abstract.

Socco, L.V. and Boiero D., 2008, Improved Monte Carlo inversion of surface wave data: Geophysical Prospecting, **56**, no.3, 357-371.

Thomson, W. T, 1950., Transmission of elastic waves through a stratified solid medium: Journal of Applied Physics, 21, no. 89.

APPLICATION OF SURFACE WAVE METHODS FOR SEISMIC SITE CHARACTERIZATION

CONDOMINIO EX ATER - GEMONA

Responsible:
Sebastiano Foti

Co-workers:
Claudio Piatti

FINAL REPORT

Turin, 26/4/2010

INDEX

1 Introduction

In this report a summary of the results obtained for the characterization of the site of the temporary accelerometric station Condominio Ex Ater (Gemona del Friuli) within the project PRIN 2007 “Prediction of ground motion and generation of shaking maps in the near-fault region of an earthquake” is presented. The analysis was performed using active surface wave method.

The map and the site location are shown in Figure 1 and Figure 2.

According to little a priori geological information available, gravels deposits are expected for tens of meter of depth below ground surface.

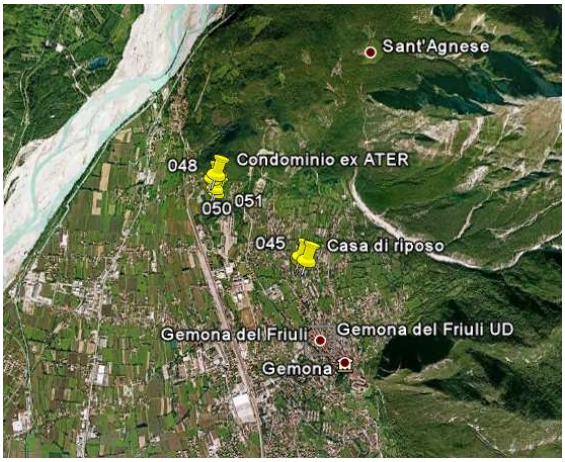

Figure 1 Gemona del Friuli: map

Figure 2 Condominio Ex Ater: site location

Goal of the seismic tests is the estimation of the S-wave velocity profile of the subsoil.

The primary use of surface wave testing is related to site characterization in terms of shear wave velocity profile. The V_S profile is of primary interest for seismic site response studies and for studies of vibration of foundations and vibration transmission in soils. Other applications are related to the prediction of settlements and to soil-structure interaction.

With respect to the evaluation of seismic site response, it is worth noting the affinity between the model used for the interpretation of surface wave tests and the model adopted for most site responses study. Indeed the application of equivalent linear elastic methods is often associated with layered models (e.g. the code SHAKE and all similar approaches). This affinity is also particularly important in the light of equivalence problems, which arise because of non-uniqueness of the solution in inverse problems. Indeed profiles which are equivalent in terms of Rayleigh wave propagation are also equivalent in term of seismic amplification (Foti et al., 2009).

Many seismic building codes introduce the weighted average of the shear wave velocity profile in the shallowest 30m as to discriminate class of soils to which a similar site amplification effect can be associated. The so-called $V_{S,30}$ can be evaluated very efficiently with surface wave method also because its average nature does not require the high level of accuracy that can be obtained with seismic borehole methods.

In the following a methodological summary of techniques and the description of the results is presented.

For further explanation of surface wave methodologies, see document: Project S4: ITALIAN STRONG MOTION DATA BASE, Deliverable # 6, Application of Surface wave methods for seismic site characterization, May 2009.

2 Surface wave method

Surface wave method (S.W.M.) is based on the geometrical dispersion, which makes Rayleigh wave velocity frequency dependent in vertically heterogeneous media. High frequency (short wavelength) Rayleigh waves propagate in shallow zones close to the free surface and are informative about their mechanical properties, whereas low frequency (long wavelength) components involve deeper layers. Surface wave tests are typically devoted to the determination of a small strain stiffness profile for the site under investigation. Consequently the dispersion curve will be associated to the variation of medium parameters with depth.

The calculation of the dispersion curve from model parameters is the so called forward problem. Surface wave propagation can be seen as the combination of multiple modes of propagation, i.e. more than one possible velocity can be associated to each frequency value.

If the dispersion curve is estimated on the basis of experimental data, it is then possible to solve the inverse problem, i.e. the model parameters are identified on the basis of the experimental data collected on the boundary of the medium. The result of the surface wave method is a one-dimensional S wave velocity soil profile.

The standard procedure for surface wave tests is reported in Figure 3. It can be subdivided into three main steps:

1. acquisition of experimental data;
2. signal processing to obtain the experimental dispersion curve;
3. inversion process to estimate shear wave velocity profile at the site.

It is very important to recognize that the above steps are strongly interconnected and their interaction must be adequately accounted for during the whole interpretation process.

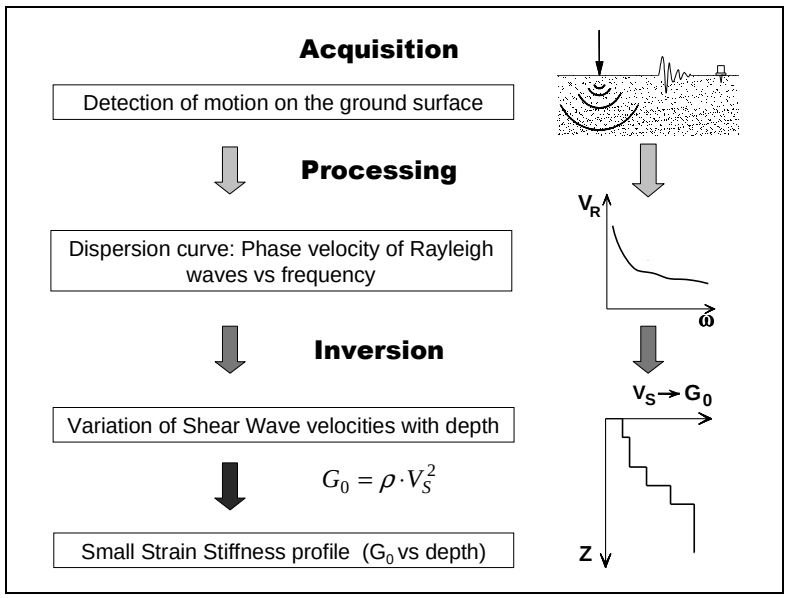

Figure 3 – Flow chart of surface wave tests.

2.1 Acquisition

Active surface wave tests (MASW) tests at Condominio Ex Ater have been performed in September 2009.

Characteristics of sensors are reported in Table 1.

Test	GEOPHONE TYPE	NATURAL FREQUENCY	GEOPHONE NUMBER
MASW/Refraction	vertical SENSOR SM-6/U-B	4,5 Hz	48

Table 1 Condominio Ex Ater: receiver characteristics

The total length of the array is 141 m. The source is a 5kg sledge hammer. Geometry parameters are summarized in Table 2.

Test	GEOF. N.	SPACING	SOURCE TYPE	ACQUISITION WINDOW	SAMPLING INTERVAL	STACK
MASW	48	3.0 m	Hammer	T = 2 s	Δt = 0.5 ms	20

Table 2 Condominio Ex Ater: acquisition parameters

2.2 Processing of surface waves

The processing allows the experimental dispersion curve to be determined.

Multichannel data are processed using a double Fourier Transform, which generates the frequency-wave number spectrum, where the dispersion curve is easily extracted as the location of spectral maxima.

2.3 Inversion of surface waves

The solution of the inverse Rayleigh problem is the final step in test interpretation. The solution of the forward problem forms the basis of any inversion strategy; the forward problem consists in the calculation of the function whose zeros are dispersion curves of a given model. Assuming a model for the soil deposit, model parameters of the best fitting subsoil profile are obtained minimizing an object function.

The subsoil is modelled as a horizontally layered medium overlaying a halfspace, with constant parameter in the interior of each layer and linear elastic behaviour. Model parameters are thickness, S-wave velocity, P-wave velocity (or Poisson coefficient), and density of each layer and the halfspace. The inversion is performed on S-wave velocities and thicknesses, whereas for the other parameters realistic values are chosen a priori. The number of layer is chosen applying minimum parameterization criterion.

In surface wave analysis it is very common to perform the inversions using only the fundamental mode of propagation. This approach is based on the assumption that the prevailing mode of propagation is the fundamental one; if this is partially true for normal dispersive sites, in several real cases the experimental dispersion curve is on the contrary the result of the superposition of several modes. This may happen in particular when velocity inversions or strong velocity contrasts are present in the shear wave velocity profile. In these stratigraphic conditions the inversion of the only fundamental mode will produce significant errors; moreover all the information contained in higher propagating modes is not used in the inversion process.

The use of higher modes in the inversion can be helpful both in the low frequency range, in order to increase the investigation depth and to avoid the overestimation of the bedrock velocity, and in the high frequency range in order to provide a more consistent interpretation of shallow interfaces and increase model parameter resolution.

In this work a Monte Carlo Global Search Method (GSM) has been adopted to perform the inversion, in order to reduce the possibility of falling in local minima. The Monte Carlo approach used exploits a particular property of the solution and permits to increase the efficiency with respect to traditional Monte Carlo approaches (Socco and Boiero 2008). Ranges for the inversion have been chosen, for the different sites, based on the experimental dispersion curves.

The results of the inversion are reported as the ensemble of the shear wave velocity profiles selected accordingly to experimental data uncertainties and degrees of freedom of the problem at a certain level of confidence through a statistical test (Socco and Boiero 2008). In the figures reported a representation based on the misfit is adopted for velocity profiles, so that the darkest colour corresponds to the profile whose dispersion curve has the lowest misfit and better approximation to the reference one; the same holds for the corresponding dispersion curves.

2.4 Numerical code

The numerical codes used for processing and inversion of surface waves are non commercial codes, implemented at Politecnico di Torino.

3 Condominio Ex Ater – Surface wave results

In Figure 4 an example of the f-k spectrum of the data collected at Condominio Ex Ater is presented.

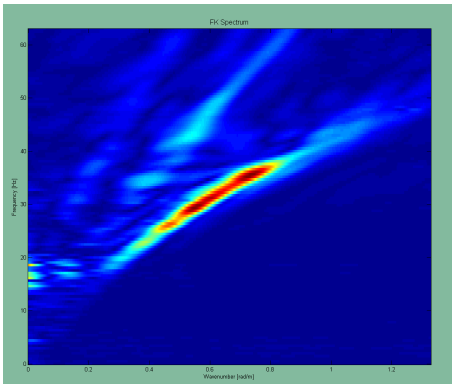

Figure 4 Condominio Ex Ater – example of f-k spectrum

From the f-k spectra, several dispersion curves can be retrieved. From all these curves an average curve is estimated (Figure 5).

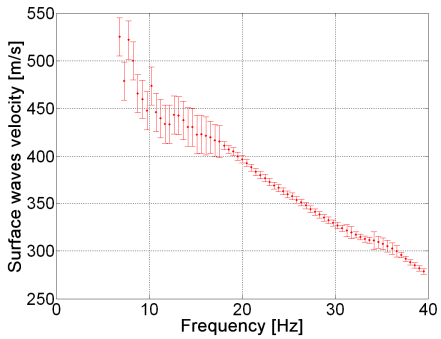

Figure 5 – Condominio Ex Ater -Average apparent dispersion curve

Observing the dispersion curve larger uncertainties can be observed in the low frequency range with respect to higher frequencies, due to weaker signal to noise ratio at low frequencies.
The best fitting profiles resulting from the Monte Carlo inversion at a confidence level of 1% (Socco and Boiero 2008) are plotted in Figure 6a, profile colour depends on the misfit, from yellow to blue (best fitting profile). In Figure 6b the corresponding dispersion curves are represented. In Figure 7 the experimental dispersion curve is compared with the dispersion curve of the best fitting model.

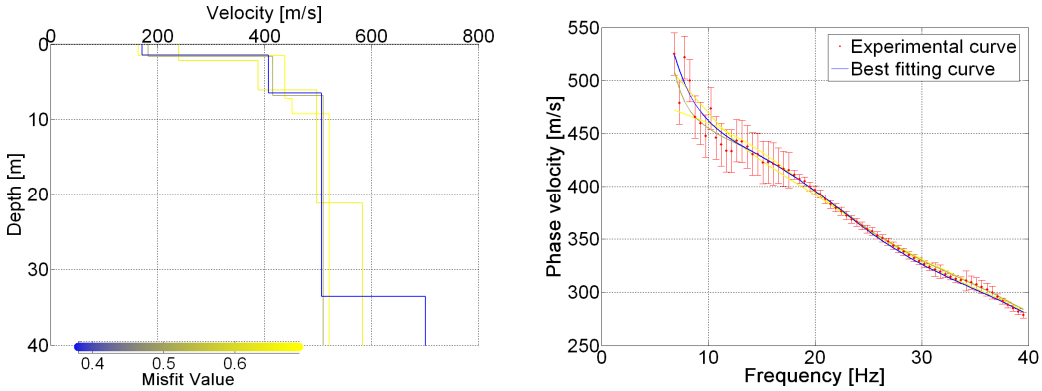

Figure 6 Condominio Ex Ater – a) final profiles (from yellow to blue) b) corresponding dispersion curves.

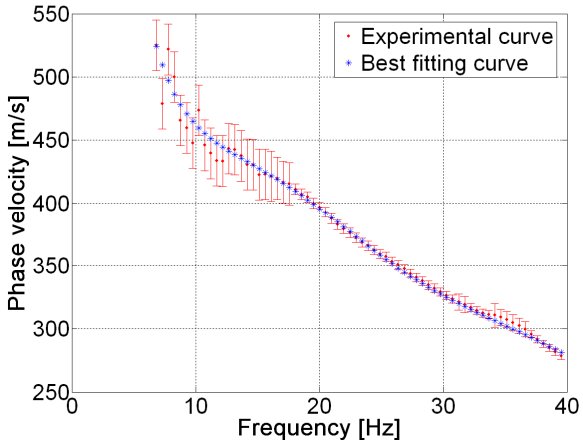

Figure 7 Condominio Ex Ater – Experimental dispersion curve compared with the best fitting curve

The parameters of the best fitting profile are summarized in Table 3.

Vs (m/s)	Thickness (m)	Poisson coefficient	Density (t/m^3)
171	1.5	0.25	1.8
407	5.0	0.33	1.9
507	27	0.45	2.0
701	-	0.45	2.0

Table 3 Condominio Ex Ater: subsoil parameters of the best fitting profile.

References

Project S4: ITALIAN STRONG MOTION DATA BASE, Deliverable # 6, Application of Surface wave methods for seismic site characterization, May 2009.

Foti S., Comina C., Boiero D., Socco L.V. (2009) "Non uniqueness in surface wave inversion and consequences on seismic site response analyses", Soil Dynamics and Earthquake Engineering, Vol. 29 (6), 982-993.

Socco L.V., Boiero D. (2008) “Improved Monte Carlo inversion of surface wave data”, Geophysical Prospecting, Vol. 56, 357-371.

APPLICATION OF SURFACE WAVE METHODS FOR SEISMIC SITE CHARACTERIZATION

GENOVA (GNV)

Responsible:
Sebastiano Foti

Co-workers:
Giovanni Bianchi
Cesare Comina
Margherita Maraschini

FINAL REPORT

Turin, 31/7/2009

INDEX

1 Introduction

In this report a summary of the results obtained for the characterization of the accelerometric station of Genova of the RAN within Project S4 is presented. The analysis was performed using active surface wave method and refraction method.

The map and the site location are shown in Figure 1. According to geological information a shallow bedrock is expected.

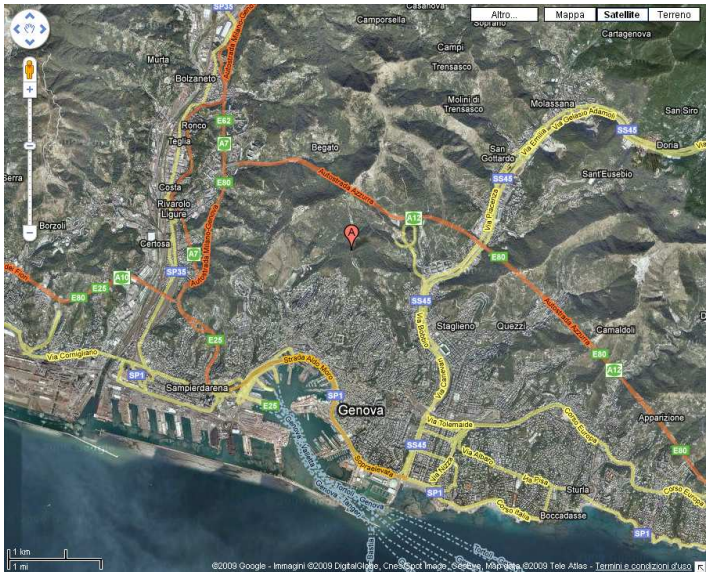

a) b)

Figure 1 Genova: a) map b) site location

Goal of the seismic tests is the estimation of the S-wave velocity profile of the subsoil, and in particular the position of the bedrock. The presence of stiff seismic interfaces between the sediments and the shallow bedrock can cause a relevance of higher modes in the surface wave experimental dispersion curve which has be taken into account in order to provide reliable results.

The primary use of surface wave testing is related to site characterization in terms of shear wave velocity profile. The V_S profile is of primary interest for seismic site response studies and for studies of vibration of foundations and vibration transmission in soils. Other applications are related to the prediction of settlements and to soil-structure interaction.

With respect to the evaluation of seismic site response, it is worth noticing the affinity between the model used for the interpretation of surface wave tests and the model adopted for most site responses study. Indeed the application of equivalent linear elastic methods is often associated with layered models (e.g. the code SHAKE and all similar approaches). This affinity is also particularly important in the light of equivalence problems, which arise because of non-uniqueness of the solution in inverse problems. Indeed profiles which are

equivalent in terms of Rayleigh wave propagation are also equivalent in term of seismic amplification (Foti et al., 2009).

Many seismic building codes introduce the weighted average of the shear wave velocity profile in the shallowest 30m as to discriminate class of soils to which a similar site amplification effect can be associated. The so-called $V_{S,30}$ can be evaluated very efficiently with surface wave method also because its average nature does not require the high level of accuracy that can be obtained with seismic borehole methods.

In the following a methodological summary of techniques and the description of the results is presented.

For Further explanation of surface wave methodologies, see document: Project S4: ITALIAN STRONG MOTION DATA BASE, Deliverable # 6, Application of Surface wave methods for seismic site characterization, May 2009.

2 Surface wave method

Surface wave method (S.W.M.) is based on the geometrical dispersion, which makes Rayleigh wave velocity frequency dependent in vertically heterogeneous media. High frequency (short wavelength) Rayleigh waves propagate in shallow zones close to the free surface and are informative about their mechanical properties, whereas low frequency (long wavelength) components involve deeper layers. Surface wave tests are typically devoted to the determination of a small strain stiffness profile for the site under investigation. Consequently the dispersion curve will be associated to the variation of medium parameters with depth.

The calculation of the dispersion curve from model parameters is the so called forward problem. Surface wave propagation can be seen as the combination of multiple modes of propagation, i.e. more than one possible velocity can be associated to each frequency value. Including higher modes in the inversion process allows the penetration depth to be increased and a more accurate subsoil profile to be retrieved.

If the dispersion curve is estimated on the basis of experimental data, it is then possible to solve the inverse problem, i.e. the model parameters are identified on the basis of the experimental data collected on the boundary of the medium. The result of the surface wave method is a one-dimensional S wave velocity soil profile.

The standard procedure for surface wave tests is reported in Figure 2. It can be subdivided into three main steps:

1. acquisition of experimental data;
2. signal processing to obtain the experimental dispersion curve;
3. inversion process to estimate shear wave velocity profile at the site.

It is very important to recognize that the above steps are strongly interconnected and their interaction must be adequately accounted for during the whole interpretation process.

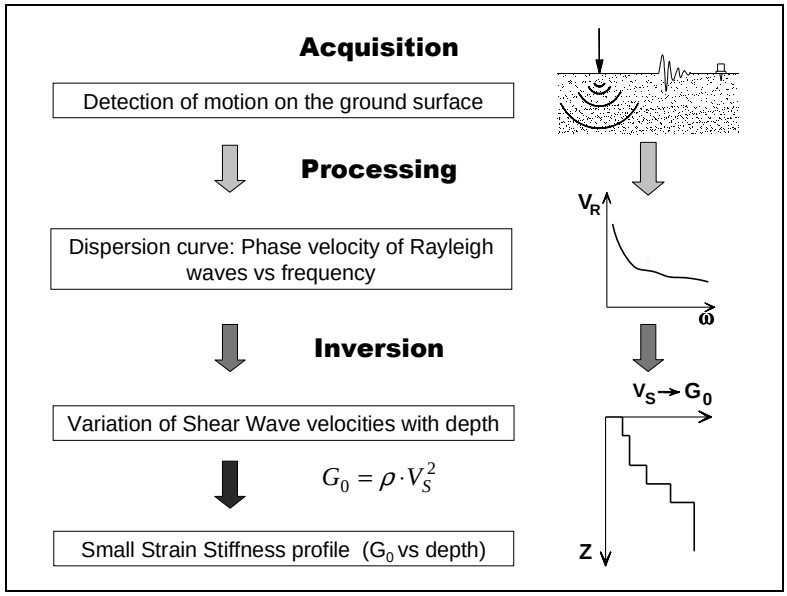

Figure 2 – Flow chart of surface wave tests.

2.1 Acquisition

Active surface wave tests (MASW) and refraction tests at Genova have been performed in October 2008 within the project S4 for the characterization of RAN sites.

Characteristics of sensors used are reported in Table 1.

Test	GEOPHONE TYPE	NATURAL FREQUENCY	GEOPHONE NUMBER
MASW/ Refraction	vertical SENSOR SM-6/U-B	4,5 Hz	48

Table 1 Genova: receiver characteristics

The total length of the array is 23.5m. The source is a 5kg sledge hammer. Geometry parameters are summarized in Table 2.

Test	GEOF. N.	SPACING	SOURCE TYPE	ACQUISITION WINDOW	SAMPLING INTERVAL
MASW	48	0.5 m	Hammer	T = 0.512 s	Δt = 0.25 ms
Refraction	48	0.5 m	Hammer	T =0.256 s	Δt = 0.03125 ms

Table 2 Genova: Acquisition parameters

Since a shallow bedrock is expected at this site, the synergies between surface wave active methods and P-wave refraction surveys are relevant. Indeed both surveys can be performed with the same testing configuration. In particular P-wave seismic refraction method can in

this situation provide relevant information with respect to the position of the interface between the soil cover and the bedrock.

2.2 Processing of surface waves

The processing allows the experimental dispersion curve to be determined.

Multichannel data are processed using a double Fourier Transform, which generates the frequency-wave number spectrum, where the multimodal dispersion curve is easily extracted as the location of spectral maxima.

2.3 Inversion of surface waves

The solution of the inverse Rayleigh problem is the final step in test interpretation. The solution of the forward problem forms the basis of any inversion strategy; the forward problem consists in the calculation of the function whose zeros are dispersion curves of a given model. Assuming a model for the soil deposit, model parameters of the best fitting subsoil profile are obtained minimizing an object function.

The subsoil is modelled as a horizontally layered medium overlaying a halfspace, with constant parameter in the interior of each layer and linear elastic behaviour. Model parameters are thickness, S-wave velocity, P-wave velocity (or Poisson coefficient), and density of each layer and the halfspace. The inversion is performed on S-wave velocities and thicknesses, whereas for the other parameters realistic values are chosen a priori. The number of layer is chosen applying minimum parameterization criterion.

In surface wave analysis it is very common to perform the inversions using only the fundamental mode of propagation. This approach is based on the assumption that the prevailing mode of propagation is the fundamental one; if this is partially true for normal dispersive sites, in several real cases the experimental dispersion curve is on the contrary the result of the superposition of several modes. This may happen in particular when velocity inversions or strong velocity contrasts are present in the shear wave velocity profile. In these stratigraphic conditions the inversion of the only fundamental mode will produce significant errors; moreover all the information contained in higher propagating modes is not used in the inversion process. Therefore, the fundamental mode inversion does not use all the available information, and this affects the result accuracy.

The use of higher modes in the inversion can be helpful both in the low frequency range, in order to increase the investigation depth and to avoid the overestimation of the bedrock velocity, and in the high frequency range in order to provide a more consistent interpretation of shallow interfaces and increase model parameter resolution.

In this work a multimodal misfit function has been used. This function is based on the Haskell-Thomson method for dispersion curve calculation (Thomson 1950, Haskell 1953, Herrmann e Wang 1980, Herrmann 2002). For a given subsoil model, and an experimental data, the misfit of the model is the L^1 norm of the vector containing the absolute value of the determinant of the Haskell-Thomson matrix (which is zeros in correspondence of all the modes of the dispersion curves of the numerical model) evaluated in correspondence of the experimental data (Maraschini et al. 2008). The misfit function adopted has the advantage of being able to include any dispersive event present in the data without the need of specifying to which mode the data points belong to, avoiding errors arising from mode misidentification, in particular in the low frequency range.

This misfit function is applied in a Global Search Methods (GSM), in order to reduce the possibility of falling in local minima. A uniform random search is applied; ranges for the inversion have been chosen, for the different sites, based on the experimental dispersion curves; in particular the range of the S-wave half space velocity is close to the maximum surface wave velocity retrieved on experimental data.

The results of the inversion are reported as the ensemble of the twenty shear wave velocity profiles which present the minimum misfits with respect to the experimental dispersion curve. In the figures reported a representation based on the misfit is adopted for velocity profiles, so that the darkest colour corresponds to the profile whose dispersion curve has the lowest misfit and better approximation to the reference one; instead for dispersion curves the coloured surface under imposed to the experimental one is a misfit surface, whose zeros are synthetic dispersion curve of the best fitting model.

2.4 Numerical code

The numerical codes used for processing and inversion of surface waves are non commercial codes, implemented at Politecnico di Torino.

3 Genova – Refraction results

The first breaks of the considered shots are shown in Figure 3.

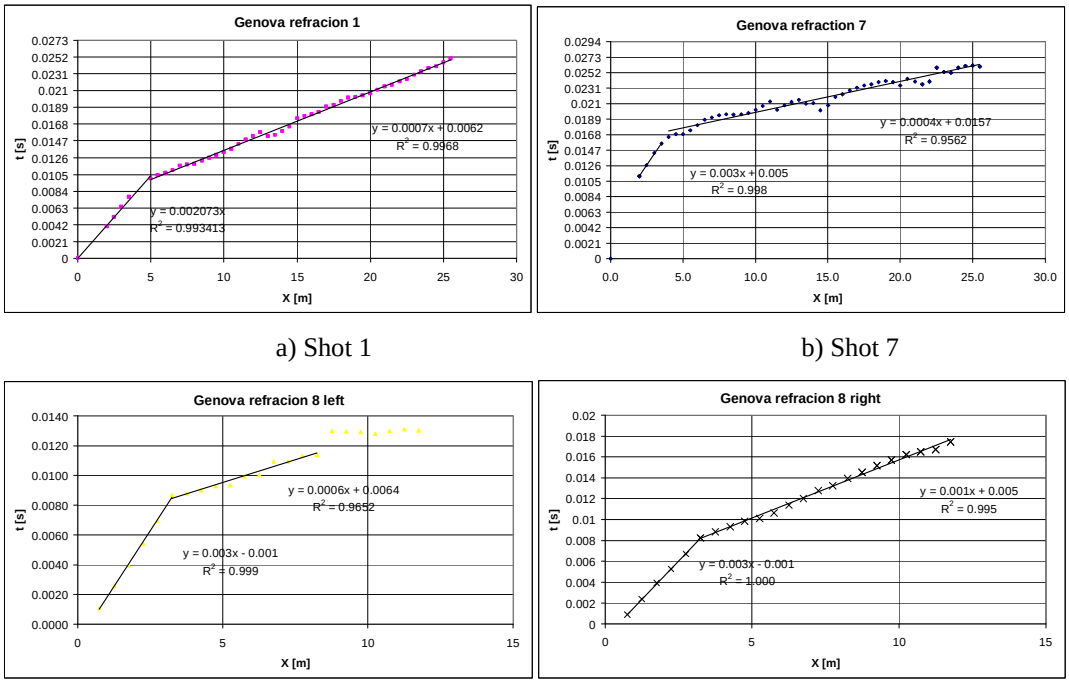

a) Shot 1 b) Shot 7

c) Shot 8 left d) Shot 8 right

Figure 3 Genova – First breaks of the considered shots

For all the analysis, a 1 layer over a halfspace model is identified; parameters are summarized in Table 3.

Shot 1		Shot 7		Shot 8 left		Shot 8 right	
P-wave velocity (m/s)	Thickness (m)	P-wave velocity (m/s)	Thickness (m)	P-wave velocity (m/s)	Thickness (m)	P-wave velocity (m/s)	Thickness (m)
476.2	1.6	370.4	0.4	333.3	1.1	344.8	0.8
1369.9		2398.1		1628.7		909.1	

Table 3 Parameters of the soil profiles obtained by refraction tests.

For the comparison with surface wave results, an average profile is considered.

4 Genova – Surface wave results

Several dispersion curves can be retrieved from data. From all these curves an average curve is estimated (Figure 4).

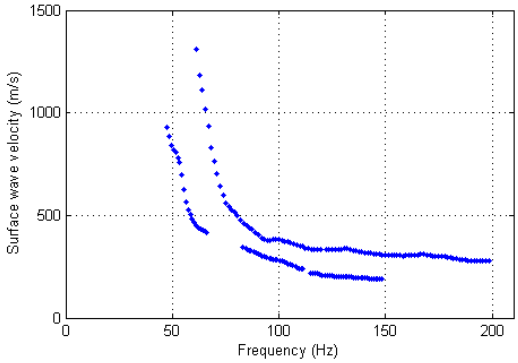

Figure 4 – Genova -Average apparent dispersion curve

Two modes of the apparent dispersion curve can be picked in the f-k spectrum.
Data were inverted using a multimodal stochastic approach, which considers at first the slowest branch of the apparent dispersion curve, and then refines the result considering both modes. The 20 best fitting profiles are plotted in Figure 5 a), profile colour depends on the misfit, from yellow to blue (best fitting profile). In Figure 5 b) the best fitting profile is compared with the refraction result, and in Figure 6 the experimental dispersion curve is compared with the determinant surface of the best fitting model. We can note that the experimental points of both branches follow in the minima of the determinant surface, and the low frequency part of the experimental branches tends to go to the first and the second higher modes respectively, probably due to the marked impedance contrast between topsoil and bedrock. Moreover it can be noted that the position of the first interface is in good agreement with the refraction results.

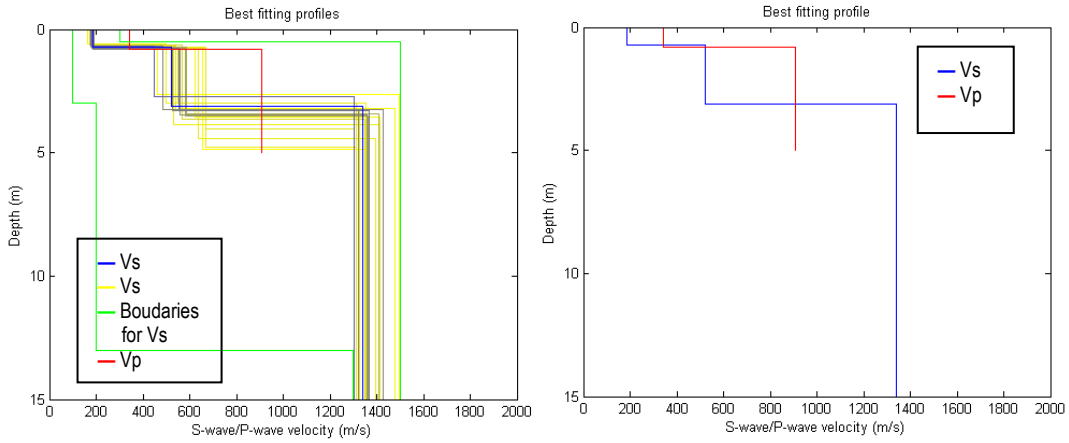

Figure 5 Genova – a) Monte Carlo results (from yellow to blue) of the inversion with the boundaries (green) compared with the refraction result (red). b) Genova – Best fitting profile (blue) compared with the refraction result (red).

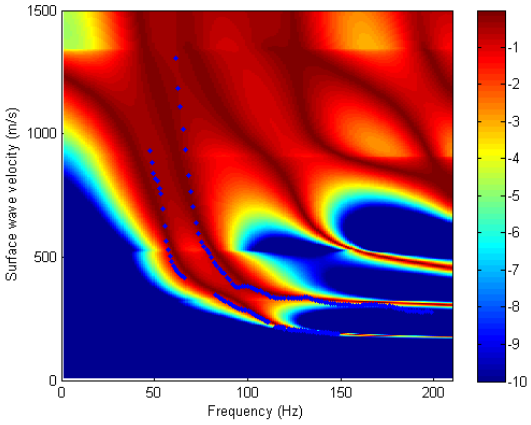

Figure 6 Genova – Experimental dispersion curve compared with the misfit surface of the best fitting model

The parameters of the best fitting profile are summarized in Table 4.

Vs (m/s)	Thickness (m)	Poisson coefficient	Density (T/m^3)
185	0.7	0.25	1.8
522	2.4	0.25	2.1
1338	-	0.25	2.1

Table 4 Genova: subsoil parameters of the best fitting profile.

References

Project S4: ITALIAN STRONG MOTION DATA BASE, Deliverable # 6, Application of Surface wave methods for seismic site characterization, May 2009.

Foti S., Comina C., Boiero D., Socco L.V. (2009) "Non uniqueness in surface wave inversion and consequences on seismic site response analyses", Soil Dynamics and Earthquake Engineering, Vol. 29 (6), 982-993.

Haskell, N., 1964, Radiation pattern of surface waves from point sources in a multilayered medium: Bulletin of seismological society of America, 54, no. 1, 377-393.

Herrmann, R. B., and C. Y. Wang, 1980, A numerical study of p-, sv- and sh- wave generation in a plane layered medium: Bulletin of seismological society of America, 70, no. 4, 1015-1036.

Herrmann, R. B., 2002, SURF code, www.eas.slu.edu/People/RBHerrmann/.

Maraschini, M., F. Ernst, D. Boiero, S. Foti, and L.V. Socco, 2008, A new approach for multimodal inversion of Rayleigh and Scholte waves: Proceedings of EAGE Rome, expanded abstract.

Thomson, W. T, 1950., Transmission of elastic waves through a stratified solid medium: Journal of Applied Physics, 21, no. 89.

APPLICATION OF SURFACE WAVE METHODS FOR SEISMIC SITE CHARACTERIZATION

ISPICA (ISI)

Responsible:
Sebastiano Foti

Co-workers:
Giovanni Bianchi
Margherita Maraschini
Paolo Bergamo

FINAL REPORT

Turin, 18/01/2010

INDEX

1 Introduction

In this report a summary of the results obtained for the characterization of the accelerometric station of Ispica of the RAN within Project S4 is presented. The analysis was performed using active surface wave method and refraction method.

Ispica RAN station is classified as rock outcrop and a very limited zone of rock alteration and vegetation soil was expected above the limestone bedrock.

The map and the site location are shown in Figure1 and Figure 2. According to geological information a very shallow bedrock is expected.

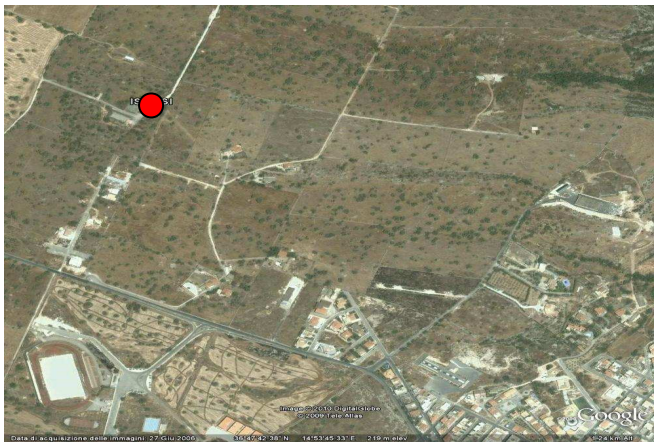

Figure 1 Ispica: map

Figure 2 Ispica: RAN station and survey line.

Goal of the seismic tests is the estimation of the S-wave velocity profile of the subsoil, and in particular the position of the bedrock. The presence of stiff seismic interfaces between the sediments and the shallow bedrock can cause a relevance of higher modes in the surface wave experimental dispersion curve which has be taken into account in order to provide reliable results.

The primary use of surface wave testing is related to site characterization in terms of shear wave velocity profile. The V_S profile is of primary interest for seismic site response studies and for studies of vibration of foundations and vibration transmission in soils. Other applications are related to the prediction of settlements and to soil-structure interaction.

With respect to the evaluation of seismic site response, it is worth noting the affinity between the model used for the interpretation of surface wave tests and the model adopted for most site responses study. Indeed the application of equivalent linear elastic methods is often associated with layered models (e.g. the code SHAKE and all similar approaches). This affinity is also particularly important in the light of equivalence problems, which arise because of non-uniqueness of the solution in inverse problems. Indeed profiles which are equivalent in terms of Rayleigh wave propagation are also equivalent in term of seismic amplification (Foti et al., 2009).

Many seismic building codes introduce the weighted average of the shear wave velocity profile in the shallowest 30m as to discriminate class of soils to which a similar site amplification effect can be associated. The so-called $V_{S,30}$ can be evaluated very efficiently with surface wave method also because its average nature does not require the high level of accuracy that can be obtained with seismic borehole methods.

In the following a methodological summary of techniques and the description of the results is presented.

For Further explanation of surface wave methodologies, see document: Project S4: ITALIAN STRONG MOTION DATA BASE, Deliverable # 6, Application of Surface wave methods for seismic site characterization, May 2009.

2 Surface wave method

Surface wave method (S.W.M.) is based on the geometrical dispersion, which makes Rayleigh wave velocity frequency dependent in vertically heterogeneous media. High frequency (short wavelength) Rayleigh waves propagate in shallow zones close to the free surface and are informative about their mechanical properties, whereas low frequency (long wavelength) components involve deeper layers. Surface wave tests are typically devoted to the determination of a small strain stiffness profile for the site under investigation. Consequently the dispersion curve will be associated to the variation of medium parameters with depth.

The calculation of the dispersion curve from model parameters is the so called forward problem. Surface wave propagation can be seen as the combination of multiple modes of propagation, i.e. more than one possible velocity can be associated to each frequency value. Including higher modes in the inversion process allows the penetration depth to be increased and a more accurate subsoil profile to be retrieved.

If the dispersion curve is estimated on the basis of experimental data, it is then possible to solve the inverse problem, i.e. the model parameters are identified on the basis of the experimental data collected on the boundary of the medium. The result of the surface wave method is a one-dimensional S wave velocity soil profile.

The standard procedure for surface wave tests is reported in Figure 3. It can be subdivided into three main steps:

1. acquisition of experimental data;
2. signal processing to obtain the experimental dispersion curve;
3. inversion process to estimate shear wave velocity profile at the site.

It is very important to recognize that the above steps are strongly interconnected and their interaction must be adequately accounted for during the whole interpretation process.

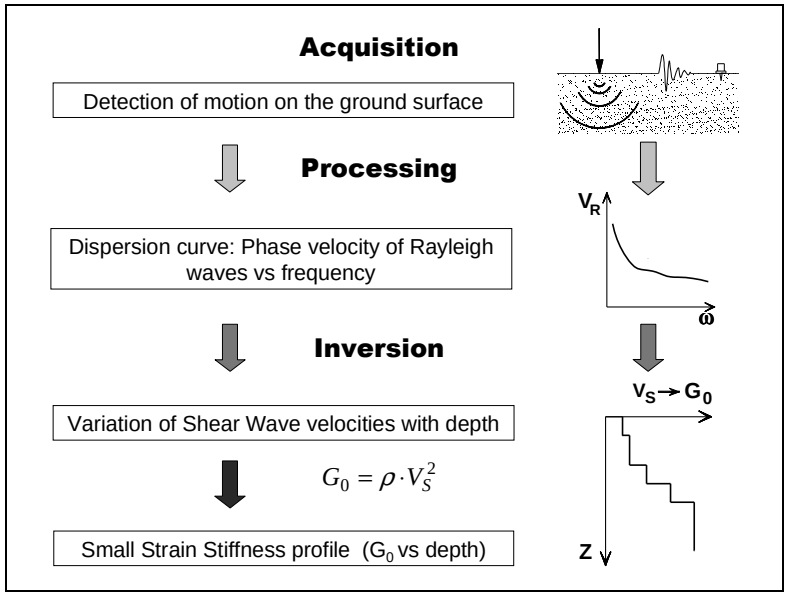

Figure 3 – Flow chart of surface wave tests.

2.1 Acquisition

Active surface wave tests (MASW) and refraction tests at Ispica have been performed in May 2009 within the project S4 for the characterization of RAN sites.

Characteristics of sensors are reported in Table 1.

Test	GEOPHONE TYPE	NATURAL FREQUENCY	GEOPHONE NUMBER
MASW/Refraction	vertical SENSOR SM-6/U-B	4,5 Hz	24

Table 1 Ispica: receiver characteristics

Acquisition geometry was influenced by the presence of underground fresh-water tanks of Ispica aqueduct: the measuring array is relatively short (24 geophones with a spacing of 1 m between neighbouring receivers) as a vary shallow bedrock is expected. The total length of the array is 23 m. The source is a 5kg sledge hammer. Geometry parameters are summarized in Table 2.

Test	GEOF. N.	SPACING	SOURCE TYPE	ACQUISITION WINDOW	SAMPLING INTERVAL	STACK
MASW	24	1 m	Hammer	T = 2 s	Δt = 0.5 ms	10
Refraction	24	1 m	Hammer	T =0.5 s	Δt = 0.03125 ms	10

Table 2 Ispica: Acquisition parameters

Since a shallow bedrock is expected at this site, the synergies between surface wave active methods and P-wave refraction surveys are relevant. Indeed both surveys can be performed with the same testing configuration. In particular P-wave seismic refraction method can in this situation provide relevant information with respect to the position of the interface between the soil cover and the bedrock.

2.2 Processing of surface waves

The processing allows the experimental dispersion curve to be determined.

Multichannel data are processed using a double Fourier Transform, which generates the frequency-wave number spectrum, where the multimodal dispersion curve is easily extracted as the location of spectral maxima.

2.3 Inversion of surface waves

The solution of the inverse Rayleigh problem is the final step in test interpretation. The solution of the forward problem forms the basis of any inversion strategy; the forward problem consists in the calculation of the function whose zeros are dispersion curves of a given model. Assuming a model for the soil deposit, model parameters of the best fitting subsoil profile are obtained minimizing an object function.

The subsoil is modelled as a horizontally layered medium overlaying a halfspace, with constant parameter in the interior of each layer and linear elastic behaviour. Model parameters are thickness, S-wave velocity, P-wave velocity (or Poisson coefficient), and density of each layer and the halfspace. The inversion is performed on S-wave velocities and thicknesses, whereas for the other parameters realistic values are chosen a priori. The number of layer is chosen applying minimum parameterization criterion.

In surface wave analysis it is very common to perform the inversions using only the fundamental mode of propagation. This approach is based on the assumption that the prevailing mode of propagation is the fundamental one; if this is partially true for normal dispersive sites, in several real cases the experimental dispersion curve is on the contrary the result of the superposition of several modes. This may happen in particular when velocity inversions or strong velocity contrasts are present in the shear wave velocity

profile. In these stratigraphic conditions the inversion of the only fundamental mode will produce significant errors; moreover all the information contained in higher propagating modes is not used in the inversion process. Therefore, the fundamental mode inversion does not use all the available information, and this affects the result accuracy.

The use of higher modes in the inversion can be helpful both in the low frequency range, in order to increase the investigation depth and to avoid the overestimation of the bedrock velocity, and in the high frequency range in order to provide a more consistent interpretation of shallow interfaces and increase model parameter resolution.

In this work a multimodal misfit function has been used. This function is based on the Haskell-Thomson method for dispersion curve calculation (Thomson 1950, Haskell 1953, Herrmann e Wang 1980, Herrmann 2002). For a given subsoil model, and an experimental data, the misfit of the model is the L^1 norm of the vector containing the absolute value of the determinant of the Haskell-Thomson matrix (which is zeros in correspondence of all the modes of the dispersion curves of the numerical model) evaluated in correspondence of the experimental data (Maraschini et al. 2008). The misfit function adopted has the advantage of being able to include any dispersive event present in the data without the need of specifying to which mode the data points belong to, avoiding errors arising from mode misidentification, in particular in the low frequency range.

This misfit function is applied in a Global Search Methods (GSM), in order to reduce the possibility of falling in local minima. A uniform random search is applied; ranges for the inversion have been chosen, for the different sites, based on the experimental dispersion curves; in particular the range of the S-wave half space velocity is close to the maximum surface wave velocity retrieved on experimental data.

The results of the inversion are reported as the ensemble of the best shear wave velocity profiles chosen according to a chi-square test (see Socco et al., 2008). It can be assumed that the experimental dispersion curve is affected by a Gaussian error with a known standard deviation, so that the probability density function of data $\rho_D(d)$ can be described by a discrete m-dimensional Gaussian (where m are the model parameters) and the sample variance variable of each random vector (dispersion curve) extracted from the data pdf is distributed according to a chi-square probability density. According to these assumptions we adopt a misfit function with the structure of a chi-square and this allows a statistical test to be applied to the variances of the synthetic dispersion curves with respect to the experimental one d_{obs}. Assuming that the best fitting curve d_{opt} belongs to the distribution $\rho_D(d_{obs})$ all models belonging to the distribution $\rho_D(d_{opt})$ and consistent with the data within a fixed level of confidence α are selected. As the ratio between chi-square variables follows a Fisher distribution a one–tailed F test can be performed:

$$F_\alpha(dof_{dopt}, dof_{g(m)}) < \frac{\chi^2_{dopt}}{\chi^2_{g(m)}}$$

where α is the chosen level of confidence, dof_{dopt} and $dof_{g(m)}$ are the degrees of freedom of the Fischer distribution and χ^2_{dopt} and $\chi^2_{g(m)}$ are the misfit of the best fitting curve and the misfit of all the others respectively. All models passing such test are selected. In the figures reported a representation based on the misfit is adopted for velocity profiles, so that the darkest colour corresponds to the profile whose dispersion curve has the lowest misfit and better approximation to the reference one; instead for dispersion curves the coloured

surface under imposed to the experimental one is a misfit surface, whose zeros are synthetic dispersion curve of the best fitting model.

2.4 Numerical code

The numerical codes used for processing and inversion of surface waves are non commercial codes, implemented at Politecnico di Torino.

3 Ispica – Refraction results

The presence of velocity inversions and of the water table can be excluded.
Three shots were considered for the inversion: one with source at the beginning of the survey line, one with the source at its end and one with the source in the middle of the array. As no lateral variation is expected, the first-break times of the three shots were averaged according to the offset obtaining the following mean dromocrone:

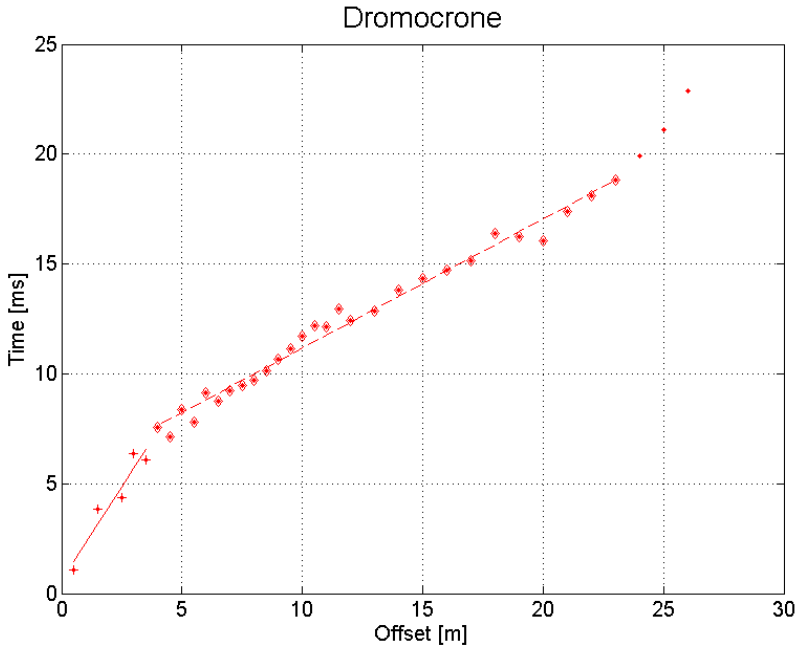

Figure 4 Ispica – mean dromocrone

A 2 layer model is clearly identified: a thin softer layer, probably made up vegetation soil mixed with altered rock, lays on the limestone bedrock. Table 3 summarizes the P-wave velocity model parameters.

P-wave velocity (m/s)	Thickness (m)
590	1.6
1700	-

Table 3 Velocity models retrieved by refraction survey

4 Ispica – Surface wave results

In Figure 5 an example of the f-k spectrum of the data collected at Ispica is presented.

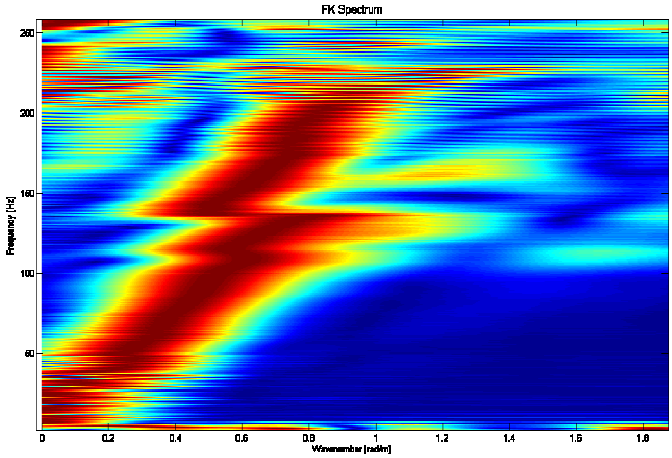

Figure 5 Ispica – example of f-k spectrum

From the f-k spectra, several dispersion curves can be retrieved. From all these curves an average curve is estimated (Figure 6).

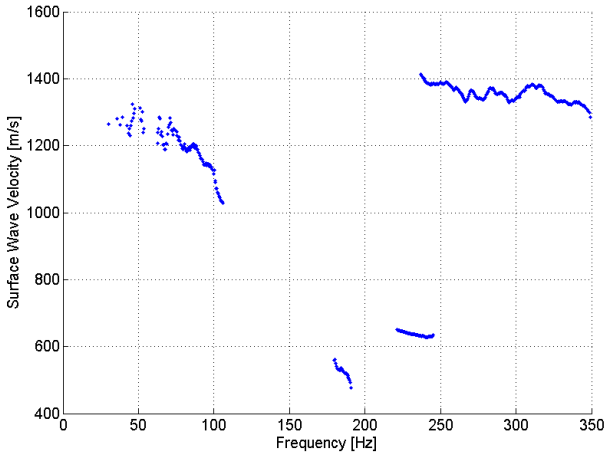

Figure 6 – Ispica -Average apparent dispersion curve

The dispersion curve is noisy and made up of two main branches, with velocities between 1000 and 1400 m/s and frequencies in the ranges 25-100 Hz and 250-350 Hz, and two minor braches with lower velocities (500 – 700 Hz) and with frequencies within 170 – 250 Hz. It is not possible to attribute a priori any branch to a particular mode. The appearance of the apparent dispersion curve is probably due to the high velocity contrast between the bedrock and the covering layer.
Data were inverted using a multimodal stochastic approach, the 20 best fitting profiles are plotted in Figure 7 a), profile colour depends on the misfit, from yellow to blue (best fitting profile). In Figure 7 b) the best fitting profile is compared with the refraction result, and in Figure 8 the experimental dispersion curve is compared with the determinant surface of the

best fitting model. We can note that the experimental points follow in the minima of the determinant surface: two branches are superimposed to the fundamental mode, one to the first higher mode and another one to the second higher mode. Moreover it can be noted that the position of the first interface is in fairly good agreement with the refraction results

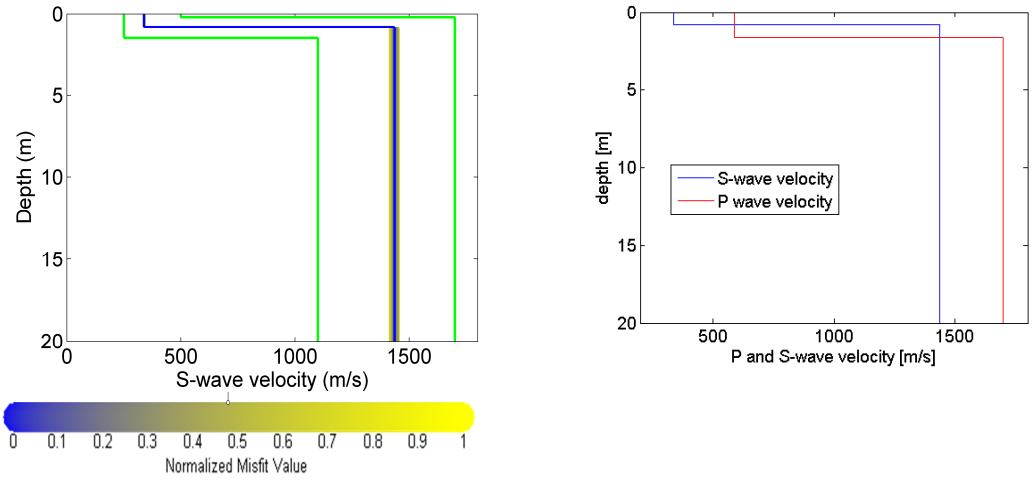

Figure 7 Ispica – a) Monte Carlo results (from yellow to blue) of the inversion with the boundaries (green). b) Ispica – Best fitting profile (blue) compared with the refraction result (red).

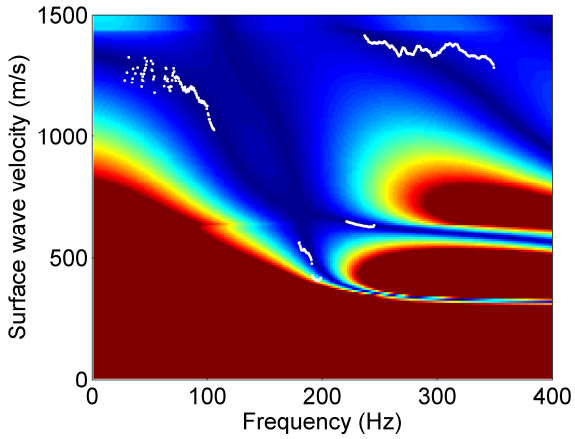

Figure 8 Ispica – Experimental dispersion curve compared with the misfit surface of the best fitting model

Again, a two layer profile is retrieved: the shallower layer has a S-wave velocity of approximately 340 m/s and is 0.9 m thick; the bedrock below is characterized by a S-wave velocity of 1400 m/s. The parameters of the best fitting profile are summarized in Table 4.

Vs (m/s)	Thickness (m)	Poisson coefficient	Density (T/m^3)
338	0.8	0.3	1.8
1435	-	0.3	1.8

Table 4 Ispica: subsoil parameters of the best fitting profile.

References

Project S4: ITALIAN STRONG MOTION DATA BASE, Deliverable # 6, Application of Surface wave methods for seismic site characterization, May 2009.

Foti S., Comina C., Boiero D., Socco L.V. (2009) "Non uniqueness in surface wave inversion and consequences on seismic site response analyses", Soil Dynamics and Earthquake Engineering, Vol. 29 (6), 982-993.

Haskell, N., 1964, Radiation pattern of surface waves from point sources in a multilayered medium: Bulletin of seismological society of America, 54, no. 1, 377-393.

Herrmann, R. B., and C. Y. Wang, 1980, A numerical study of p-, sv- and sh- wave generation in a plane layered medium: Bulletin of seismological society of America, 70, no. 4, 1015-1036.

Herrmann, R. B., 2002, SURF code, www.eas.slu.edu/People/RBHerrmann/.

Maraschini, M., F. Ernst, D. Boiero, S. Foti, and L.V. Socco, 2008, A new approach for multimodal inversion of Rayleigh and Scholte waves: Proceedings of EAGE Rome, expanded abstract.

Thomson, W. T, 1950., Transmission of elastic waves through a stratified solid medium: Journal of Applied Physics, 21, no. 89.

APPLICATION OF SURFACE WAVE METHODS FOR SEISMIC SITE CHARACTERIZATION

NOTO (NTE)

Responsible:
Sebastiano Foti

Co-workers:
Giovanni Bianchi
Margherita Maraschini
Paolo Bergamo

FINAL REPORT

Turin, 15/01/2010

INDEX

1 Introduction

In this report a summary of the results obtained for the characterization of the accelerometric station of Noto of the RAN within Project S4 is presented. The analysis was performed using active surface wave method and refraction method.

Noto RAN station is classified as rock outcrop and a very limited zone of rock alteration and vegetation soil was expected above the calctufa bedrock.

The map of the site and the array and its location are shown in Figure 1 and Figure 2.

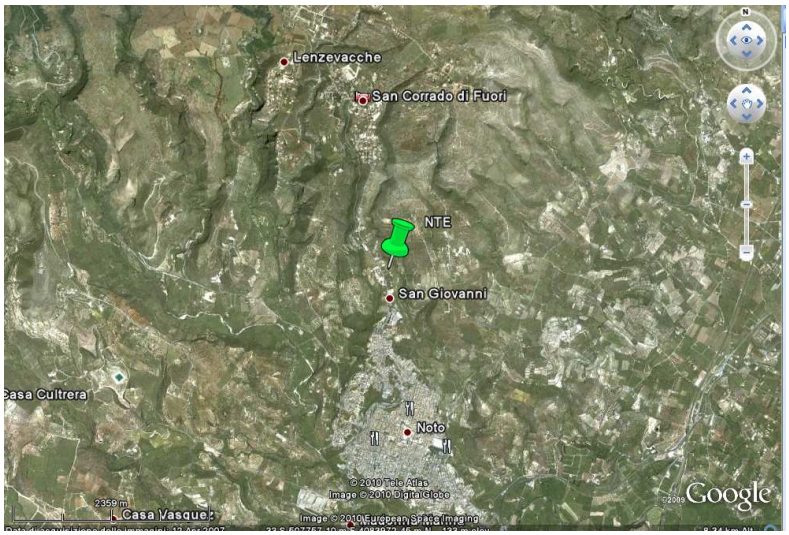

Figure 1 Noto: maps

Figure 2 Noto: map of the array and its location

Goal of the seismic tests is the estimation of the S-wave velocity profile of the subsoil, and in particular the position of the bedrock . The presence of stiff seismic interfaces between the sediments and the shallow bedrock can cause a relevance of higher modes in the

surface wave experimental dispersion curve which has be taken into account in order to provide reliable results.

The primary use of surface wave testing is related to site characterization in terms of shear wave velocity profile. The V_S profile is of primary interest for seismic site response studies and for studies of vibration of foundations and vibration transmission in soils. Other applications are related to the prediction of settlements and to soil-structure interaction.

With respect to the evaluation of seismic site response, it is worth noting the affinity between the model used for the interpretation of surface wave tests and the model adopted for most site responses study. Indeed the application of equivalent linear elastic methods is often associated with layered models (e.g. the code SHAKE and all similar approaches). This affinity is also particularly important in the light of equivalence problems, which arise because of non-uniqueness of the solution in inverse problems. Indeed profiles which are equivalent in terms of Rayleigh wave propagation are also equivalent in term of seismic amplification (Foti et al., 2009).

Many seismic building codes introduce the weighted average of the shear wave velocity profile in the shallowest 30m as to discriminate class of soils to which a similar site amplification effect can be associated. The so-called $V_{S,30}$ can be evaluated very efficiently with surface wave method also because its average nature does not require the high level of accuracy that can be obtained with seismic borehole methods.

In the following a methodological summary of techniques and the description of the results is presented.

For Further explanation of surface wave methodologies, see document: Project S4: ITALIAN STRONG MOTION DATA BASE, Deliverable # 6, Application of Surface wave methods for seismic site characterization, May 2009.

2 Surface wave method

Surface wave method (S.W.M.) is based on the geometrical dispersion, which makes Rayleigh wave velocity frequency dependent in vertically heterogeneous media. High frequency (short wavelength) Rayleigh waves propagate in shallow zones close to the free surface and are informative about their mechanical properties, whereas low frequency (long wavelength) components involve deeper layers. Surface wave tests are typically devoted to the determination of a small strain stiffness profile for the site under investigation. Consequently the dispersion curve will be associated to the variation of medium parameters with depth.

The calculation of the dispersion curve from model parameters is the so called forward problem. Surface wave propagation can be seen as the combination of multiple modes of propagation, i.e. more than one possible velocity can be associated to each frequency value. Including higher modes in the inversion process allows the penetration depth to be increased and a more accurate subsoil profile to be retrieved.

If the dispersion curve is estimated on the basis of experimental data, it is then possible to solve the inverse problem, i.e. the model parameters are identified on the basis of the

experimental data collected on the boundary of the medium. The result of the surface wave method is a one-dimensional S wave velocity soil profile.

The standard procedure for surface wave tests is reported in Figure 3. It can be subdivided into three main steps:

1. acquisition of experimental data;
2. signal processing to obtain the experimental dispersion curve;
3. inversion process to estimate shear wave velocity profile at the site.

It is very important to recognize that the above steps are strongly interconnected and their interaction must be adequately accounted for during the whole interpretation process.

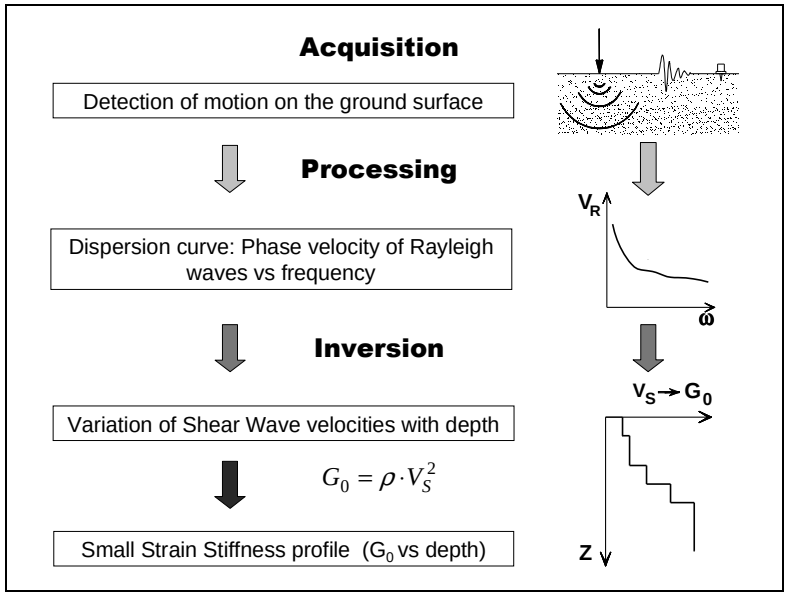

Figure 3 – Flow chart of surface wave tests.

2.1 Acquisition

Active surface wave tests (MASW) and refraction tests at Noto have been performed in May 2009 within the project S4 for the characterization of RAN sites.

Characteristics of sensors are reported in Table 1.

Test	GEOPHONE TYPE	NATURAL FREQUENCY	GEOPHONE NUMBER
MASW/Refraction	vertical SENSOR SM-6/U-B	4,5 Hz	24

Table 1 Noto: receiver characteristics

The acquisition geometry was influenced by the limited size of areas without concrete covering on the site: a 24 geophones array was used with a spacing between geophones of 0.8 m. The total length of the array is 18.4 m. The source is a 5 kg sledge hammer. Geometry parameters are summarized in Table 2.

Test	GEOF. N.	SPACING	SOURCE TYPE	ACQUISITION WINDOW	SAMPLING INTERVAL	STACK
MASW	24	0.8 m	Hammer	T = 1 s	Δt = 0.25 ms	10
Refraction	24	0.8 m	Hammer	T = 0.5 s	Δt = 0.03125 ms	10

Table 2 Noto: Acquisition parameters

2.2 Processing of surface waves

The processing allows the experimental dispersion curve to be determined.

Multichannel data are processed using a double Fourier Transform, which generates the frequency-wave number spectrum, where the multimodal dispersion curve is easily extracted as the location of spectral maxima.

2.3 Inversion of surface waves

The solution of the inverse Rayleigh problem is the final step in test interpretation. The solution of the forward problem forms the basis of any inversion strategy; the forward problem consists in the calculation of the function whose zeros are dispersion curves of a given model. Assuming a model for the soil deposit, model parameters of the best fitting subsoil profile are obtained minimizing an object function.

The subsoil is modelled as a horizontally layered medium overlaying a halfspace, with constant parameter in the interior of each layer and linear elastic behaviour. Model parameters are thickness, S-wave velocity, P-wave velocity (or Poisson coefficient), and density of each layer and the halfspace. The inversion is performed on S-wave velocities and thicknesses, whereas for the other parameters realistic values are chosen a priori. The number of layer is chosen applying minimum parameterization criterion.

In surface wave analysis it is very common to perform the inversions using only the fundamental mode of propagation. This approach is based on the assumption that the prevailing mode of propagation is the fundamental one; if this is partially true for normal dispersive sites, in several real cases the experimental dispersion curve is on the contrary the result of the superposition of several modes. This may happen in particular when velocity inversions or strong velocity contrasts are present in the shear wave velocity profile. In these stratigraphic conditions the inversion of the only fundamental mode will produce significant errors; moreover all the information contained in higher propagating modes is not used in the inversion process. Therefore, the fundamental mode inversion does not use all the available information, and this affects the result accuracy.

The use of higher modes in the inversion can be helpful both in the low frequency range, in order to increase the investigation depth and to avoid the overestimation of the bedrock

velocity, and in the high frequency range in order to provide a more consistent interpretation of shallow interfaces and increase model parameter resolution.

In this work a multimodal misfit function has been used. This function is based on the Haskell-Thomson method for dispersion curve calculation (Thomson 1950, Haskell 1953, Herrmann e Wang 1980, Herrmann 2002). For a given subsoil model, and an experimental data, the misfit of the model is the L^1 norm of the vector containing the absolute value of the determinant of the Haskell-Thomson matrix (which is zeros in correspondence of all the modes of the dispersion curves of the numerical model) evaluated in correspondence of the experimental data (Maraschini et al. 2008). The misfit function adopted has the advantage of being able to include any dispersive event present in the data without the need of specifying to which mode the data points belong to, avoiding errors arising from mode misidentification, in particular in the low frequency range.

This misfit function is applied in a Global Search Methods (GSM), in order to reduce the possibility of falling in local minima. A uniform random search is applied; ranges for the inversion have been chosen, for the different sites, based on the experimental dispersion curves; in particular the range of the S-wave half space velocity is close to the maximum surface wave velocity retrieved on experimental data.

The results of the inversion are reported as the ensemble of the best shear wave velocity profiles chosen according to a chi-square test (see Socco et al., 2008). It can be assumed that the experimental dispersion curve is affected by a Gaussian error with a known standard deviation, so that the probability density function of data $\rho_D(d)$ can be described by a discrete m-dimensional Gaussian (where m are the model parameters) and the sample variance variable of each random vector (dispersion curve) extracted from the data pdf is distributed according to a chi-square probability density. According to these assumptions we adopt a misfit function with the structure of a chi-square and this allows a statistical test to be applied to the variances of the synthetic dispersion curves with respect to the experimental one d_{obs}. Assuming that the best fitting curve d_{opt} belongs to the distribution $\rho_D(d_{obs})$ all models belonging to the distribution $\rho_D(d_{opt})$ and consistent with the data within a fixed level of confidence α are selected. As the ratio between chi-square variables follows a Fisher distribution a one–tailed F test can be performed:

$$F_{\alpha}(dof_{dopt}, dof_{g(m)}) < \frac{\chi^2_{dopt}}{\chi^2_{g(m)}}$$

where α is the chosen level of confidence, dof_{dopt} and $dof_{g(m)}$ are the degrees of freedom of the Fischer distribution and χ^2_{dopt} and $\chi^2_{g(m)}$ are the misfit of the best fitting curve and the misfit of all the others respectively. All models passing such test are selected. In the figures reported a representation based on the misfit is adopted for velocity profiles, so that the darkest colour corresponds to the profile whose dispersion curve has the lowest misfit and better approximation to the reference one; instead for dispersion curves the coloured surface under imposed to the experimental one is a misfit surface, whose zeros are synthetic dispersion curve of the best fitting model.

2.4 Numerical code

The numerical codes used for processing and inversion of surface waves are non commercial codes, implemented at Politecnico di Torino.

3 Noto – Refraction results

The presence of velocity inversions can be excluded.
Two shots were considered for the inversion, one of them with the source at the beginning of the array, the other one with the source at the end of the survey line. The limited length of the array (18.4 m) allows a very limited penetration depth. The first breaks of the considered shots are shown in Figure 4.

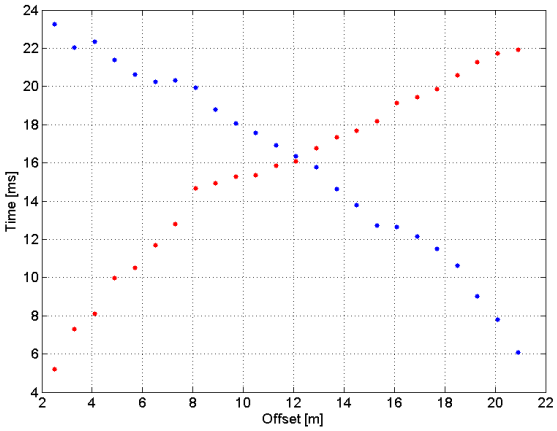

Figure 4 Noto – First breaks of the two shots considered

A two layer P-wave profile was retrieved: the upper layer has velocity of 612 m/s while the lower one shows a velocity of 1438 m/s. The thickness of the 1st layer varies between 2.42 m (at beginning of the array) and 3.1 m (at the end of the array) : parameters are summarized in Table 3.

P-wave velocity (m/s)	Average thickness (m)
612	2.8
1438	-

Table 3 Velocity models retrieved by refraction survey

4 Noto – Surface wave results

In Figure 5 an example of the f-k spectrum of the data collected at Noto is presented.

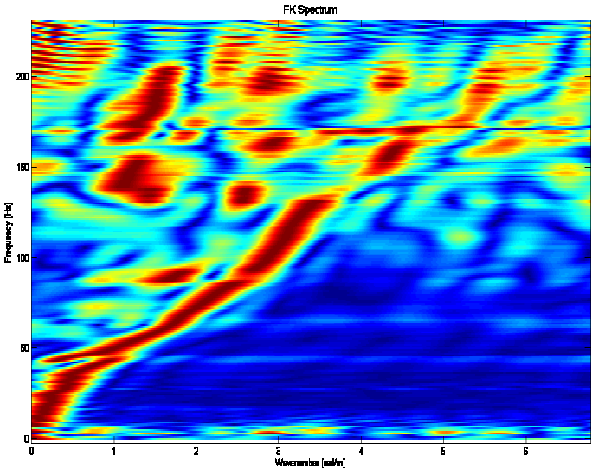

Figure 5 Noto – example of f-k spectrum

From the f-k spectra, several dispersion curves can be retrieved. From all these curves an average curve is estimated (Figure 6).

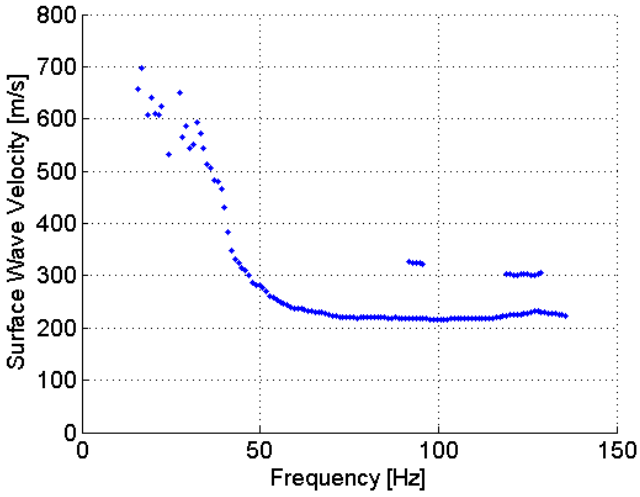

Figure 6 Noto - Average apparent dispersion curve

The experimental dispersion curve is composed of a main branch and two small branches with higher velocities: note that the main branch shows a steep velocity increase in the low frequency range probably due to a jump on the first higher mode in that range. All branches were used for the inversion.
Data were inverted using a multimodal stochastic approach, the 20 best fitting profiles are plotted in Figure 7 a), profile colour depends on the misfit, from yellow to blue (best fitting profile). In Figure 7 b) the best fitting profile is compared with the refraction result, and in Figure 8 the experimental dispersion curve is compared with the determinant surface of the best fitting model. We can note that the experimental points fall in the minima of the determinant surface, and the low frequency part of the experimental dispersion curve tends to go to the first higher mode, probably due to the impedance contrast between topsoil and bedrock.

The obtained S-wave profile shows an interface between the soft shallower layer at about 2 m depth and a gradual velocity increase below this depth. The bedrock, probably made up of calctufa, is at about 7 m depth.
From Figure 7 it can be noted that the position of the second interface is in good agreement with the refraction results.

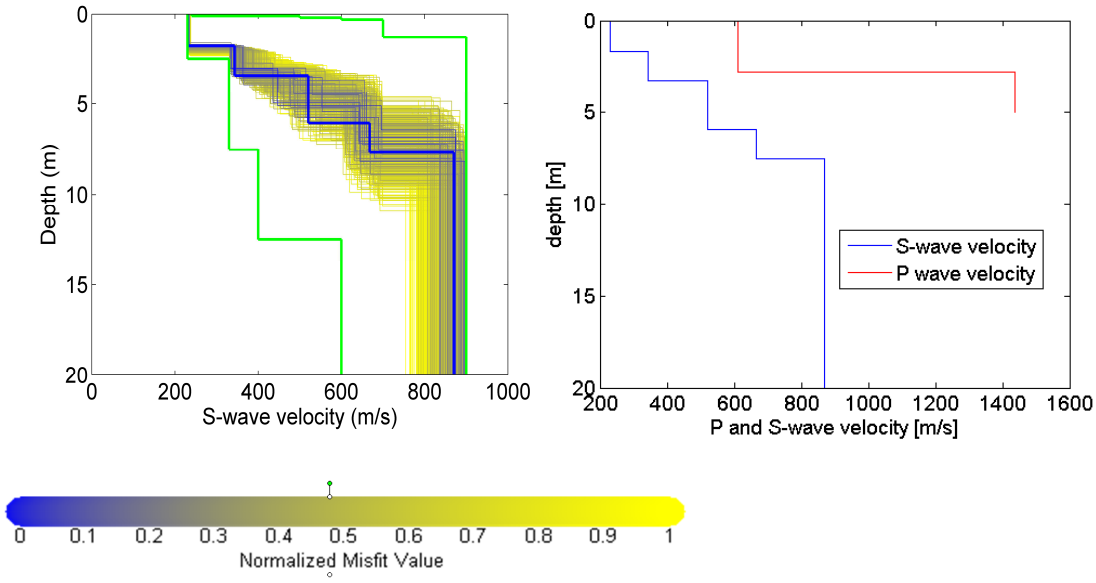

Figure 7 Noto – a) Monte Carlo results (from yellow to blue) of the inversion with the boundaries (green) compared with the refraction result (red). b) Noto – Best fitting profile (blue) compared with the refraction result (red).

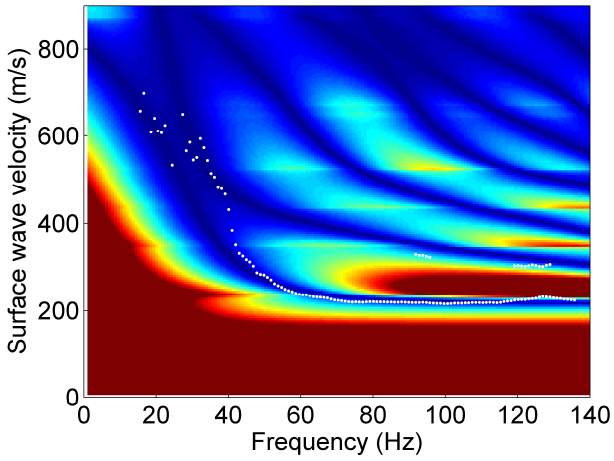

Figure 8 Noto – Experimental dispersion curve compared with the misfit surface of the best fitting mode

The parameters of the best fitting profile are summarized in Table 4.

Vs (m/s)	Thickness (m)	Poisson coefficient	Density (T/m^3)
231	1.8	0.3	1.8
343	1.6	0.3	1.8
520	2.6	0.3	1.8
668	1.6	0.3	1.8
870	-	0.3	2.0

Table 4: Noto: subsoil parameters of the best fitting profile

References

Project S4: ITALIAN STRONG MOTION DATA BASE, Deliverable # 6, Application of Surface wave methods for seismic site characterization, May 2009.

Foti S., Comina C., Boiero D., Socco L.V. (2009) "Non uniqueness in surface wave inversion and consequences on seismic site response analyses", Soil Dynamics and Earthquake Engineering, Vol. 29 (6), 982-993.

Haskell, N., 1964, Radiation pattern of surface waves from point sources in a multilayered medium: Bulletin of seismological society of America, 54, no. 1, 377-393.

Herrmann, R. B., and C. Y. Wang, 1980, A numerical study of p-, sv- and sh- wave generation in a plane layered medium: Bulletin of seismological society of America, 70, no. 4, 1015-1036.

Herrmann, R. B., 2002, SURF code, www.eas.slu.edu/People/RBHerrmann/.

Maraschini, M., F. Ernst, D. Boiero, S. Foti, and L.V. Socco, 2008, A new approach for multimodal inversion of Rayleigh and Scholte waves: Proceedings of EAGE Rome, expanded abstract.

Thomson, W. T, 1950., Transmission of elastic waves through a stratified solid medium: Journal of Applied Physics, 21, no. 89.

APPLICATION OF SURFACE WAVE METHODS FOR SEISMIC SITE CHARACTERIZATION

PACHINO (PCH)

Responsible:
Sebastiano Foti

Co-workers:
Giovanni Bianchi
Paolo Bergamo
Margherita Maraschini

FINAL REPORT

Turin, 11/02/2010

INDEX

1 Introduction

In this report a summary of the results obtained for the characterization of the accelerometric station of Pachino of the RAN within Project S4 is presented. The analysis was performed using active surface wave method and refraction method.

Pachino RAN station is classified as rock outcrop and a very limited zone of rock alteration and vegetation soil was expected above the limestone bedrock.

The map and the site location are shown in Figure 1 and Figure 2. According to geological information a shallow bedrock is expected.

Figure 1 Pachino: map

Figure 2 Pachino: map of the array (white line) and site location

Goal of the seismic tests is the estimation of the S-wave velocity profile of the subsoil, and in particular the position of the bedrock. The presence of stiff seismic interfaces between the sediments and the shallow bedrock can cause a relevance of higher modes in the surface wave experimental dispersion curve which has be taken into account in order to provide reliable results.

The primary use of surface wave testing is related to site characterization in terms of shear wave velocity profile. The V_S profile is of primary interest for seismic site response studies and for studies of vibration of foundations and vibration transmission in soils. Other applications are related to the prediction of settlements and to soil-structure interaction.

With respect to the evaluation of seismic site response, it is worth noting the affinity between the model used for the interpretation of surface wave tests and the model adopted for most site responses study. Indeed the application of equivalent linear elastic methods is often associated with layered models (e.g. the code SHAKE and all similar approaches). This affinity is also particularly important in the light of equivalence problems, which arise because of non-uniqueness of the solution in inverse problems. Indeed profiles which are equivalent in terms of Rayleigh wave propagation are also equivalent in term of seismic amplification (Foti et al., 2009).

Many seismic building codes introduce the weighted average of the shear wave velocity profile in the shallowest 30m as to discriminate class of soils to which a similar site amplification effect can be associated. The so-called $V_{S,30}$ can be evaluated very efficiently with surface wave method also because its average nature does not require the high level of accuracy that can be obtained with seismic borehole methods.

In the following a methodological summary of techniques and the description of the results is presented.

For Further explanation of surface wave methodologies, see document: Project S4: ITALIAN STRONG MOTION DATA BASE, Deliverable # 6, Application of Surface wave methods for seismic site characterization, May 2009.

2 Surface wave method

Surface wave method (S.W.M.) is based on the geometrical dispersion, which makes Rayleigh wave velocity frequency dependent in vertically heterogeneous media. High frequency (short wavelength) Rayleigh waves propagate in shallow zones close to the free surface and are informative about their mechanical properties, whereas low frequency (long wavelength) components involve deeper layers. Surface wave tests are typically devoted to the determination of a small strain stiffness profile for the site under investigation. Consequently the dispersion curve will be associated to the variation of medium parameters with depth.

The calculation of the dispersion curve from model parameters is the so called forward problem. Surface wave propagation can be seen as the combination of multiple modes of propagation, i.e. more than one possible velocity can be associated to each frequency value. Including higher modes in the inversion process allows the penetration depth to be increased and a more accurate subsoil profile to be retrieved.

If the dispersion curve is estimated on the basis of experimental data, it is then possible to solve the inverse problem, i.e. the model parameters are identified on the basis of the experimental data collected on the boundary of the medium. The result of the surface wave method is a one-dimensional S wave velocity soil profile.

The standard procedure for surface wave tests is reported in Figure 3. It can be subdivided into three main steps:

1. acquisition of experimental data;
2. signal processing to obtain the experimental dispersion curve;
3. inversion process to estimate shear wave velocity profile at the site.

It is very important to recognize that the above steps are strongly interconnected and their interaction must be adequately accounted for during the whole interpretation process.

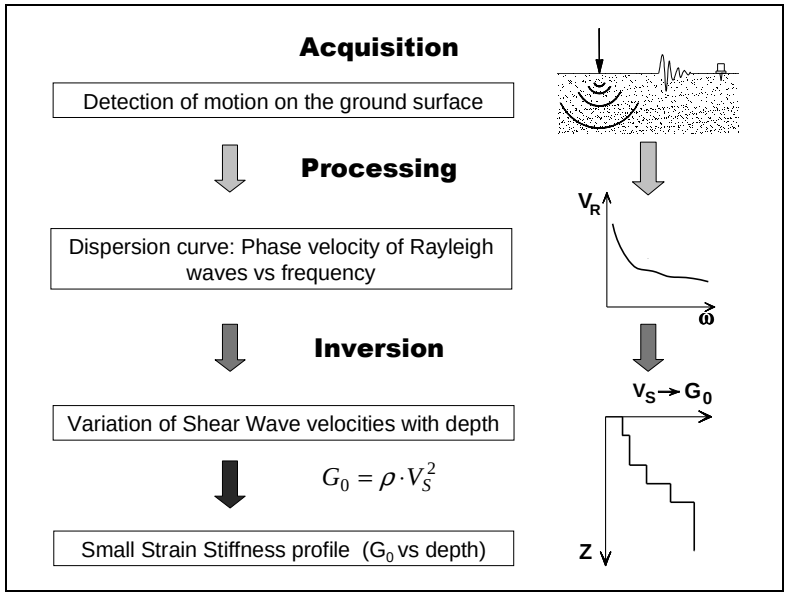

Figure 3 – Flow chart of surface wave tests.

2.1 Acquisition

Active surface wave tests (MASW) and refraction tests at Pachino have been performed in May 2009 within the project S4 for the characterization of RAN sites.

Characteristics of sensors are reported in Table 1.

Test	GEOPHONE TYPE	NATURAL FREQUENCY	GEOPHONE NUMBER
MASW/Refraction	vertical SENSOR SM-6/U-B	4,5 Hz	24

Table 1 Pachino: receiver characteristics

24 receivers were used for both MASW and refraction survey, with a spacing between neighbouring geophones of 1 m. The total length of the array is 23 m. The source is a 5kg sledge hammer. Geometry parameters are summarized in Table 2.

Test	GEOF. N.	SPACING	SOURCE TYPE	ACQUISITION WINDOW	SAMPLING INTERVAL	STACK
MASW	24	1 m	Hammer	T = 2 s	Δt = 0.5 ms	10
Refraction	24	1 m	Hammer	T = 0.5 s	Δt = 0.03125 ms	10

Table 2 Pachino: Acquisition parameters

Since a shallow bedrock is expected at this site, the synergies between surface wave active methods and P-wave refraction surveys are relevant. Indeed both surveys can be performed with the same testing configuration.

2.2 Processing of surface waves

The processing allows the experimental dispersion curve to be determined.

Multichannel data are processed using a double Fourier Transform, which generates the frequency-wave number spectrum, where the multimodal dispersion curve is easily extracted as the location of spectral maxima.

2.3 Inversion of surface waves

The solution of the inverse Rayleigh problem is the final step in test interpretation. The solution of the forward problem forms the basis of any inversion strategy; the forward problem consists in the calculation of the function whose zeros are dispersion curves of a given model. Assuming a model for the soil deposit, model parameters of the best fitting subsoil profile are obtained minimizing an object function.

The subsoil is modelled as a horizontally layered medium overlaying a halfspace, with constant parameter in the interior of each layer and linear elastic behaviour. Model parameters are thickness, S-wave velocity, P-wave velocity (or Poisson coefficient), and density of each layer and the halfspace. The inversion is performed on S-wave velocities and thicknesses, whereas for the other parameters realistic values are chosen a priori. The number of layer is chosen applying minimum parameterization criterion.

In surface wave analysis it is very common to perform the inversions using only the fundamental mode of propagation. This approach is based on the assumption that the prevailing mode of propagation is the fundamental one; if this is partially true for normal dispersive sites, in several real cases the experimental dispersion curve is on the contrary the result of the superposition of several modes. This may happen in particular when velocity inversions or strong velocity contrasts are present in the shear wave velocity profile. In these stratigraphic conditions the inversion of the only fundamental mode will produce significant errors; moreover all the information contained in higher propagating

modes is not used in the inversion process. Therefore, the fundamental mode inversion does not use all the available information, and this affects the result accuracy.

The use of higher modes in the inversion can be helpful both in the low frequency range, in order to increase the investigation depth and to avoid the overestimation of the bedrock velocity, and in the high frequency range in order to provide a more consistent interpretation of shallow interfaces and increase model parameter resolution.

In this work a multimodal misfit function has been used. This function is based on the Haskell-Thomson method for dispersion curve calculation (Thomson 1950, Haskell 1953, Herrmann e Wang 1980, Herrmann 2002). For a given subsoil model, and an experimental data, the misfit of the model is the L^1 norm of the vector containing the absolute value of the determinant of the Haskell-Thomson matrix (which is zeros in correspondence of all the modes of the dispersion curves of the numerical model) evaluated in correspondence of the experimental data (Maraschini et al. 2008). The misfit function adopted has the advantage of being able to include any dispersive event present in the data without the need of specifying to which mode the data points belong to, avoiding errors arising from mode misidentification, in particular in the low frequency range.

This misfit function is applied in a Global Search Methods (GSM), in order to reduce the possibility of falling in local minima. A uniform random search is applied; ranges for the inversion have been chosen, for the different sites, based on the experimental dispersion curves; in particular the range of the S-wave half space velocity is close to the maximum surface wave velocity retrieved on experimental data.

The results of the inversion are reported as the ensemble of the best shear wave velocity profiles chosen according to a chi-square test (see Socco et al., 2008). It can be assumed that the experimental dispersion curve is affected by a Gaussian error with a known standard deviation, so that the probability density function of data $\rho_D(d)$ can be described by a discrete m-dimensional Gaussian (where m are the model parameters) and the sample variance variable of each random vector (dispersion curve) extracted from the data pdf is distributed according to a chi-square probability density. According to these assumptions we adopt a misfit function with the structure of a chi-square and this allows a statistical test to be applied to the variances of the synthetic dispersion curves with respect to the experimental one d_{obs}. Assuming that the best fitting curve d_{opt} belongs to the distribution $\rho_D(d_{obs})$ all models belonging to the distribution $\rho_D(d_{opt})$ and consistent with the data within a fixed level of confidence α are selected. As the ratio between chi-square variables follows a Fisher distribution a one–tailed F test can be performed:

$$F_\alpha(dof_{dopt}, dof_{g(m)}) < \frac{\chi^2_{dopt}}{\chi^2_{g(m)}}$$

where α is the chosen level of confidence, dof_{dopt} and $dof_{g(m)}$ are the degrees of freedom of the Fischer distribution and χ^2_{dopt} and $\chi^2_{g(m)}$ are the misfit of the best fitting curve and the misfit of all the others respectively. All models passing such test are selected. In the figures reported a representation based on the misfit is adopted for velocity profiles, so that the darkest colour corresponds to the profile whose dispersion curve has the lowest misfit and better approximation to the reference one; instead for dispersion curves the coloured surface under imposed to the experimental one is a misfit surface, whose zeros are synthetic dispersion curve of the best fitting model.

2.4 Numerical code

The numerical codes used for processing and inversion of surface waves are non commercial codes, implemented at Politecnico di Torino.

3 Pachino – Refraction results

Two shots were considered for refraction surveys, one with the source at the beginning of the array and the other one with the source at the end of the array. The first-break arrival times are represented in Figure 4.

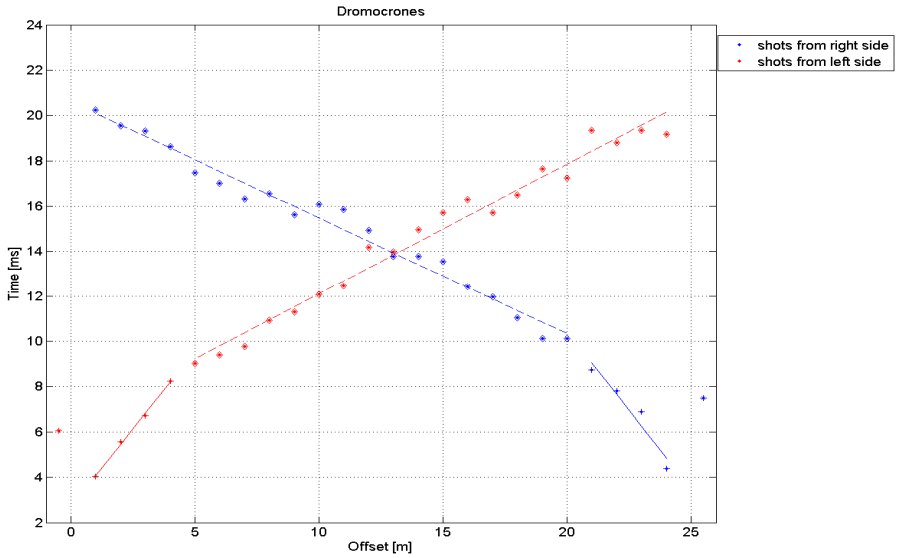

Figure 4 Pachino – First breaks of the two shots considered

A one layer over a halfspace model is identified: the weathering layer has a P-wave velocity of 560 m/s and a thickness increasing from 1.7 m to 2.1 m towards the end of the array, while the lower layer has a P-wave velocity of 1787 m/s. The poor penetration depth of the survey is due to the limited length of the measuring array (23 m). Refraction survey results are summarized in Table 3.

P-wave velocity (m/s)	Thickness (m)
560	1.9
1787	-

Table 3 Velocity models retrieved by refraction survey

4 Pachino – Surface wave results

In Figure 5 an example of the f-k spectrum of the data collected at Pachino with the picked dispersion curve is presented.

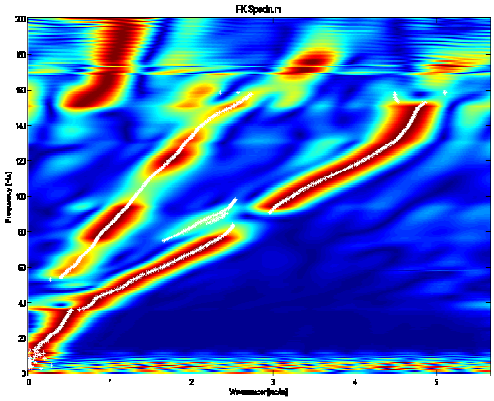

Figure 5 Pachino – example of f-k spectrum

From the f-k spectra, several dispersion curves can be retrieved. From all these curves an average curve is estimated (Figure 6).

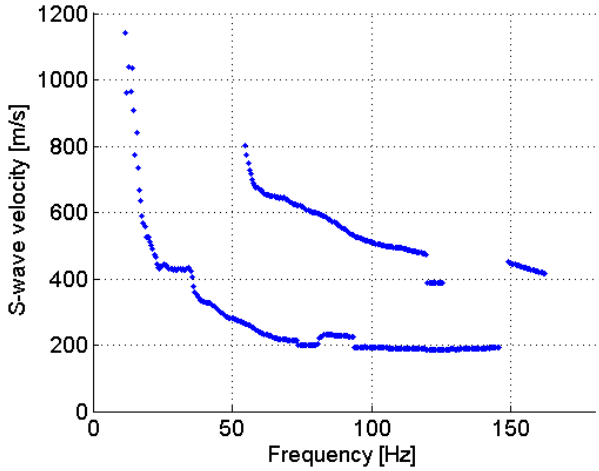

Figure 6 – Pachino - Average apparent dispersion curve

The apparent dispersion curve is made up of two branches: both of them present a steep velocity increase at low frequencies, probably due to a marked velocity contrast between weathering layers and the bedrock.
Data were inverted using a multimodal stochastic approach, the best fitting profiles are plotted in Figure 7 a), profile colour depends on the misfit, from yellow to blue (best fitting profile). In Figure 7 b) the best fitting profile is compared with the refraction result, and in Figure 8 the experimental dispersion curve is compared with the determinant surface of the best fitting model. We can note that the experimental points fall into the minima of the determinant surface, and the low frequency part of the main branch of the experimental dispersion curve tends to go to the first higher mode, probably due to the marked

impedance contrast between topsoil and bedrock. Moreover it can be noted that the position of the first interface is in good agreement with the refraction results.

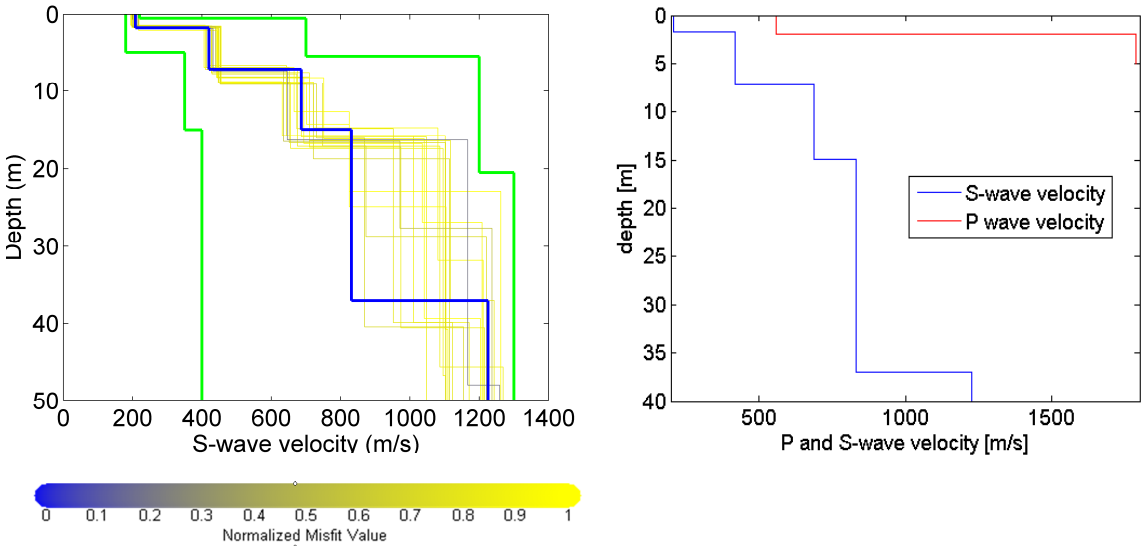

Figure 7 Pachino – a) Monte Carlo results (from yellow to blue) of the inversion with the boundaries (green). b) Pachino – Best fitting profile (blue) compared with the refraction result (red).

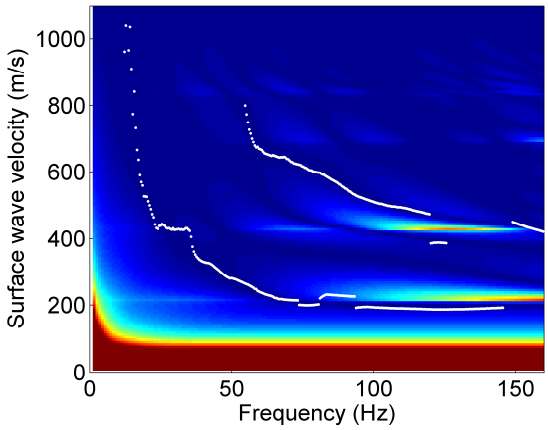

Figure 8 Pachino – Experimental dispersion curve compared with the misfit surface of the best fitting model

The parameters of the best fitting profile are summarized in Table 4.

Vs (m/s)	Thickness (m)	Poisson coefficient	Density (T/m^3)
208	1.7	0.3	1.8
421	5.5	0.3	1.8
687	7.8	0.3	1.8
832	22.1	0.3	1.8
1226	-	0.3	1.8

Table 4 Pachino: subsoil parameters of the best fitting profile.

References

Project S4: ITALIAN STRONG MOTION DATA BASE, Deliverable # 6, Application of Surface wave methods for seismic site characterization, May 2009.

Foti S., Comina C., Boiero D., Socco L.V. (2009) "Non uniqueness in surface wave inversion and consequences on seismic site response analyses", Soil Dynamics and Earthquake Engineering, Vol. 29 (6), 982-993.

Haskell, N., 1964, Radiation pattern of surface waves from point sources in a multilayered medium: Bulletin of seismological society of America, 54, no. 1, 377-393.

Herrmann, R. B., and C. Y. Wang, 1980, A numerical study of p-, sv- and sh- wave generation in a plane layered medium: Bulletin of seismological society of America, 70, no. 4, 1015-1036.

Herrmann, R. B., 2002, SURF code, www.eas.slu.edu/People/RBHerrmann/.

Maraschini, M., F. Ernst, D. Boiero, S. Foti, and L.V. Socco, 2008, A new approach for multimodal inversion of Rayleigh and Scholte waves: Proceedings of EAGE Rome, expanded abstract.

Thomson, W. T, 1950., Transmission of elastic waves through a stratified solid medium: Journal of Applied Physics, 21, no. 89.

APPLICATION OF SURFACE WAVE METHODS FOR SEISMIC SITE CHARACTERIZATION

PALAZZOLO ACREIDE (PLZ)

Responsible:
Sebastiano Foti

Co-workers:
Giovanni Bianchi
Paolo Bergamo
Margherita Maraschini

FINAL REPORT

Turin, 11/02/2010

INDEX

1 Introduction

In this report a summary of the results obtained for the characterization of the accelerometric station of Palazzolo Acreide of the RAN within Project S4 is presented. The analysis was performed using active surface wave method and refraction method.

Palazzolo Acreide RAN station is classified as rock outcrop and a very limited zone of rock alteration and vegetation soil was expected above the limestone bedrock.

The map and the site location are shown in Figure 1 and Figure 2. According to geological information a shallow bedrock is expected.

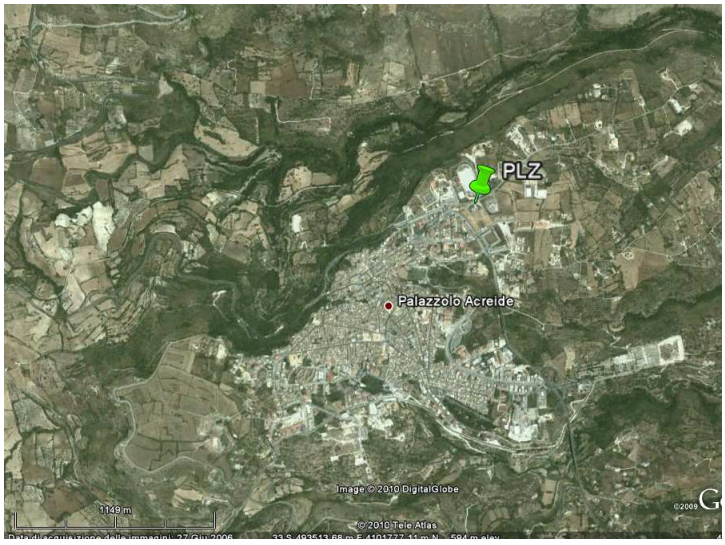

Figure 1 Palazzolo Acreide: map

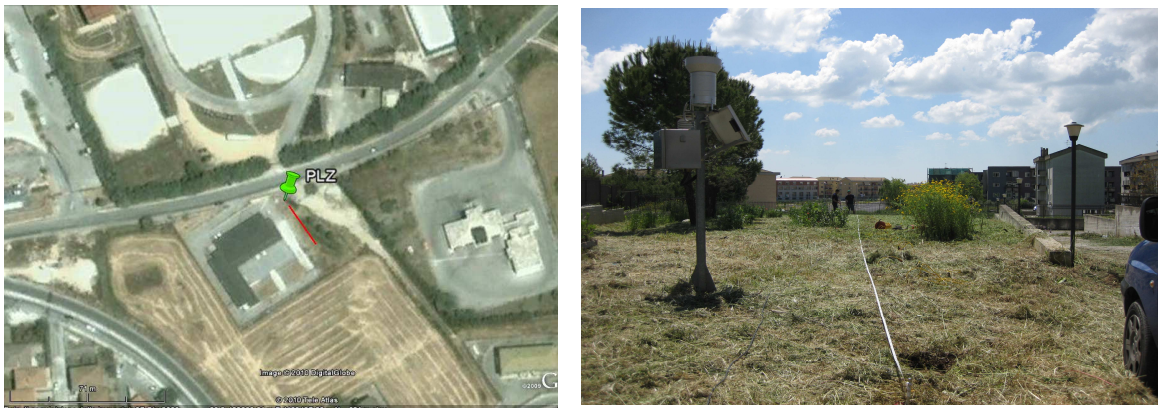

Figure 2 Palazzolo Acreide: map of the array (red line) and site location

Goal of the seismic tests is the estimation of the S-wave velocity profile of the subsoil, and in particular the position of the bedrock. The presence of stiff seismic interfaces between the sediments and the shallow bedrock can cause a relevance of higher modes in the

surface wave experimental dispersion curve which has be taken into account in order to provide reliable results.

The primary use of surface wave testing is related to site characterization in terms of shear wave velocity profile. The V_S profile is of primary interest for seismic site response studies and for studies of vibration of foundations and vibration transmission in soils. Other applications are related to the prediction of settlements and to soil-structure interaction.

With respect to the evaluation of seismic site response, it is worth noting the affinity between the model used for the interpretation of surface wave tests and the model adopted for most site responses study. Indeed the application of equivalent linear elastic methods is often associated with layered models (e.g. the code SHAKE and all similar approaches). This affinity is also particularly important in the light of equivalence problems, which arise because of non-uniqueness of the solution in inverse problems. Indeed profiles which are equivalent in terms of Rayleigh wave propagation are also equivalent in term of seismic amplification (Foti et al., 2009).

Many seismic building codes introduce the weighted average of the shear wave velocity profile in the shallowest 30m as to discriminate class of soils to which a similar site amplification effect can be associated. The so-called $V_{S,30}$ can be evaluated very efficiently with surface wave method also because its average nature does not require the high level of accuracy that can be obtained with seismic borehole methods.

In the following a methodological summary of techniques and the description of the results is presented.

For Further explanation of surface wave methodologies, see document: Project S4: ITALIAN STRONG MOTION DATA BASE, Deliverable # 6, Application of Surface wave methods for seismic site characterization, May 2009.

2 Surface wave method

Surface wave method (S.W.M.) is based on the geometrical dispersion, which makes Rayleigh wave velocity frequency dependent in vertically heterogeneous media. High frequency (short wavelength) Rayleigh waves propagate in shallow zones close to the free surface and are informative about their mechanical properties, whereas low frequency (long wavelength) components involve deeper layers. Surface wave tests are typically devoted to the determination of a small strain stiffness profile for the site under investigation. Consequently the dispersion curve will be associated to the variation of medium parameters with depth.

The calculation of the dispersion curve from model parameters is the so called forward problem. Surface wave propagation can be seen as the combination of multiple modes of propagation, i.e. more than one possible velocity can be associated to each frequency value. Including higher modes in the inversion process allows the penetration depth to be increased and a more accurate subsoil profile to be retrieved.

If the dispersion curve is estimated on the basis of experimental data, it is then possible to solve the inverse problem, i.e. the model parameters are identified on the basis of the experimental data collected on the boundary of the medium. The result of the surface wave method is a one-dimensional S wave velocity soil profile.

The standard procedure for surface wave tests is reported in Figure 3. It can be subdivided into three main steps:

1. acquisition of experimental data;
2. signal processing to obtain the experimental dispersion curve;
3. inversion process to estimate shear wave velocity profile at the site.

It is very important to recognize that the above steps are strongly interconnected and their interaction must be adequately accounted for during the whole interpretation process.

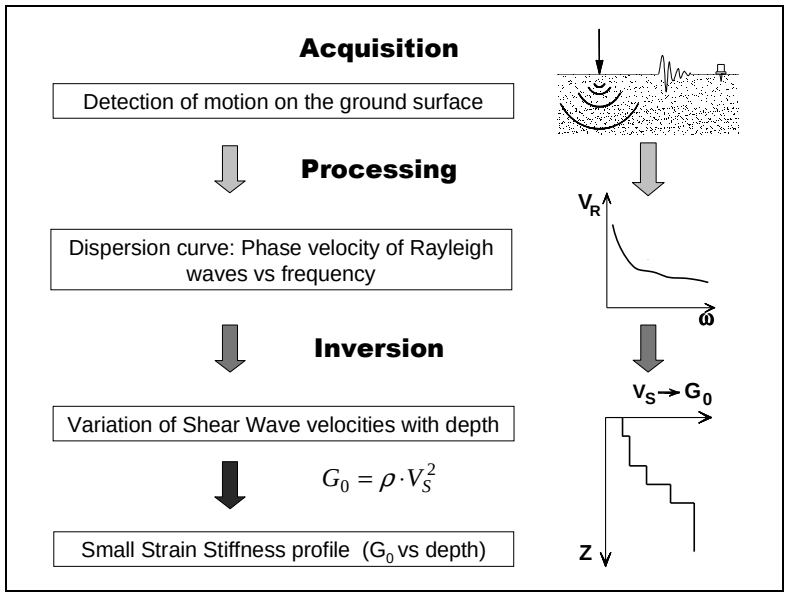

Figure 3 – Flow chart of surface wave tests.

2.1 Acquisition

Active surface wave tests (MASW) and refraction tests at Palazzolo Acreide have been performed in May 2009 within the project S4 for the characterization of RAN sites.

Characteristics of sensors are reported in Table 1.

Test	GEOPHONE TYPE	NATURAL FREQUENCY	GEOPHONE NUMBER
MASW/Refraction	vertical SENSOR SM-6/U-B	4,5 Hz	24

Table 1 Palazzolo Acreide: receiver characteristics

24 receivers were used for both MASW and refraction survey, with a spacing between neighbouring geophones of 1 m. The total length of the array is 23 m. The source is a 5kg sledge hammer. Geometry parameters are summarized in Table 2.

Test	GEOF. N.	SPACING	SOURCE TYPE	ACQUISITION WINDOW	SAMPLING INTERVAL	STACK
MASW	24	1 m	Hammer	T = 2 s	Δt = 0.5 ms	10
Refraction	24	1 m	Hammer	T = 0.5 s	Δt = 0.03125 ms	10

Table 2 Palazzolo Acreide: Acquisition parameters

Since a shallow bedrock is expected at this site, the synergies between surface wave active methods and P-wave refraction surveys are relevant. Indeed both surveys can be performed with the same testing configuration.

2.2 Processing of surface waves

The processing allows the experimental dispersion curve to be determined.

Multichannel data are processed using a double Fourier Transform, which generates the frequency-wave number spectrum, where the multimodal dispersion curve is easily extracted as the location of spectral maxima.

2.3 Inversion of surface waves

The solution of the inverse Rayleigh problem is the final step in test interpretation. The solution of the forward problem forms the basis of any inversion strategy; the forward problem consists in the calculation of the function whose zeros are dispersion curves of a given model. Assuming a model for the soil deposit, model parameters of the best fitting subsoil profile are obtained minimizing an object function.

The subsoil is modelled as a horizontally layered medium overlaying a halfspace, with constant parameter in the interior of each layer and linear elastic behaviour. Model parameters are thickness, S-wave velocity, P-wave velocity (or Poisson coefficient), and density of each layer and the halfspace. The inversion is performed on S-wave velocities and thicknesses, whereas for the other parameters realistic values are chosen a priori. The number of layer is chosen applying minimum parameterization criterion.

In surface wave analysis it is very common to perform the inversions using only the fundamental mode of propagation. This approach is based on the assumption that the prevailing mode of propagation is the fundamental one; if this is partially true for normal dispersive sites, in several real cases the experimental dispersion curve is on the contrary the result of the superposition of several modes. This may happen in particular when velocity inversions or strong velocity contrasts are present in the shear wave velocity profile. In these stratigraphic conditions the inversion of the only fundamental mode will produce significant errors; moreover all the information contained in higher propagating modes is not used in the inversion process. Therefore, the fundamental mode inversion does not use all the available information, and this affects the result accuracy.

The use of higher modes in the inversion can be helpful both in the low frequency range, in order to increase the investigation depth and to avoid the overestimation of the bedrock velocity, and in the high frequency range in order to provide a more consistent interpretation of shallow interfaces and increase model parameter resolution.

In this work a multimodal misfit function has been used. This function is based on the Haskell-Thomson method for dispersion curve calculation (Thomson 1950, Haskell 1953, Herrmann e Wang 1980, Herrmann 2002). For a given subsoil model, and an experimental data, the misfit of the model is the L^1 norm of the vector containing the absolute value of the determinant of the Haskell-Thomson matrix (which is zeros in correspondence of all the modes of the dispersion curves of the numerical model) evaluated in correspondence of the experimental data (Maraschini et al. 2008). The misfit function adopted has the advantage of being able to include any dispersive event present in the data without the need of specifying to which mode the data points belong to, avoiding errors arising from mode misidentification, in particular in the low frequency range.

This misfit function is applied in a Global Search Methods (GSM), in order to reduce the possibility of falling in local minima. A uniform random search is applied; ranges for the inversion have been chosen, for the different sites, based on the experimental dispersion curves; in particular the range of the S-wave half space velocity is close to the maximum surface wave velocity retrieved on experimental data.

The results of the inversion are reported as the ensemble of the best shear wave velocity profiles chosen according to a chi-square test (see Socco et al., 2008). It can be assumed that the experimental dispersion curve is affected by a Gaussian error with a known standard deviation, so that the probability density function of data $\rho_D(d)$ can be described by a discrete m-dimensional Gaussian (where m are the model parameters) and the sample variance variable of each random vector (dispersion curve) extracted from the data pdf is distributed according to a chi-square probability density. According to these assumptions we adopt a misfit function with the structure of a chi-square and this allows a statistical test to be applied to the variances of the synthetic dispersion curves with respect to the experimental one d_{obs}. Assuming that the best fitting curve d_{opt} belongs to the distribution $\rho_D(d_{obs})$ all models belonging to the distribution $\rho_D(d_{opt})$ and consistent with the data within a fixed level of confidence α are selected. As the ratio between chi-square variables follows a Fisher distribution a one–tailed F test can be performed:

$$F_\alpha(dof_{dopt}, dof_{g(m)}) < \frac{\chi^2_{dopt}}{\chi^2_{g(m)}}$$

where α is the chosen level of confidence, dof_{dopt} and $dof_{g(m)}$ are the degrees of freedom of the Fischer distribution and χ^2_{dopt} and $\chi^2_{g(m)}$ are the misfit of the best fitting curve and the misfit of all the others respectively. All models passing such test are selected. In the figures reported a representation based on the misfit is adopted for velocity profiles, so that the darkest colour corresponds to the profile whose dispersion curve has the lowest misfit and better approximation to the reference one; instead for dispersion curves the coloured surface under imposed to the experimental one is a misfit surface, whose zeros are synthetic dispersion curve of the best fitting model.

2.4 Numerical code

The numerical codes used for processing and inversion of surface waves are non commercial codes, implemented at Politecnico di Torino.

3 Palazzolo Acreide – Refraction results

Three shots were considered for refraction surveys, one with the source at the beginning of the array, one with the source at the end of the array and the third one with the source in the centre of the array. The first-break arrival times are represented in Figure 4.

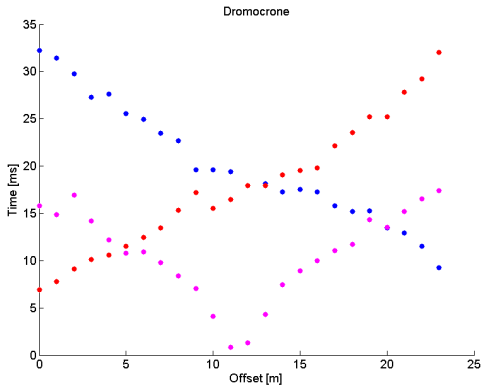

Figure 4 Palazzolo Acreide – First breaks of the three shots considered

A one layer over a halfspace model is identified: the weathering layer has a P-wave velocity of 324 m/s and a thickness increasing from 0.65 m to 1.45 m towards the end of the array, while the lower layer has a P-wave velocity of 1049 m/s. The poor penetration depth of the survey is due to the limited length of the measuring array (23 m). Refraction survey results are summarized in Table 3.

P-wave velocity (m/s)	Thickness (m)
324	1.1
1049	-

Table 3 Velocity models retrieved by refraction survey

4 Palazzolo Acreide – Surface wave results

In Figure 5 an example of the f-k spectrum of the data collected at Palazzolo Acreide is presented.

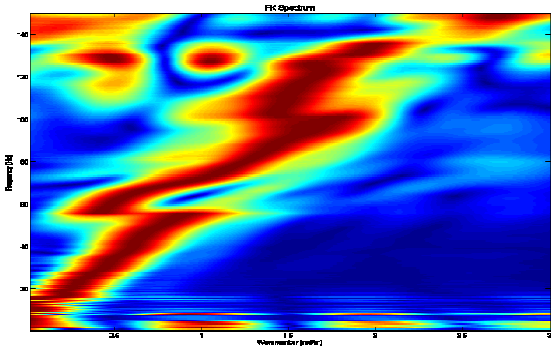

Figure 5 Palazzolo Acreide – example of f-k spectrum

From the f-k spectra, several dispersion curves can be retrieved. From all these curves an average curve is estimated (Figure 6).

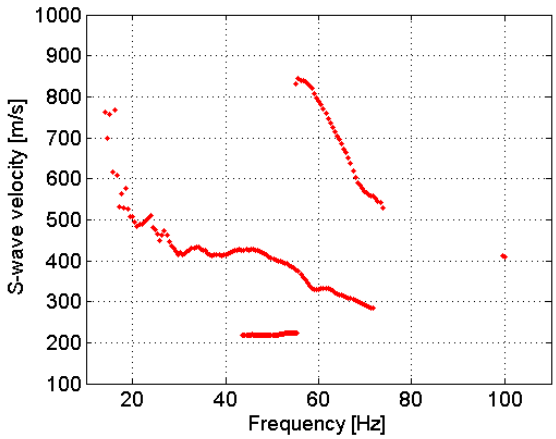

Figure 6 – Palazzolo Acreide - Average apparent dispersion curve

The apparent dispersion curve is made up of three branches, probably belonging to three different propagation modes.
Data were inverted using a multimodal stochastic approach, the best fitting profiles are plotted in Figure 7 a), profile colour depends on the misfit, from yellow to blue (best fitting profile). In Figure 7 b) the best fitting profile is compared with the refraction result, and in Figure 8 the experimental dispersion curve is compared with the determinant surface of the best fitting model. We can note that the experimental points fall into the minima of the determinant surface, and that the three branches actually belong to three different propagation modes, with the exception of the 2nd branch which at around 20 Hz jumps from the 1st higher mode to the fundamental one. Moreover it can be noted that the position of the first interface is in good agreement with the refraction results.

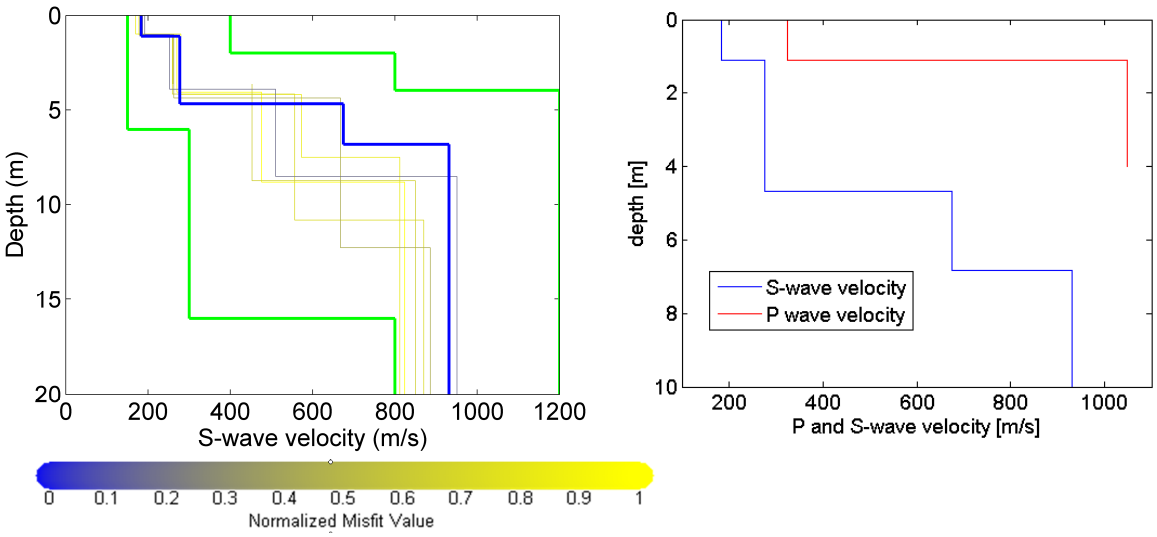

Figure 7 Palazzolo Acreide – a) Monte Carlo results (from yellow to blue) of the inversion with the boundaries (green). b) Palazzolo Acreide – Best fitting profile (blue) compared with the refraction result (red).

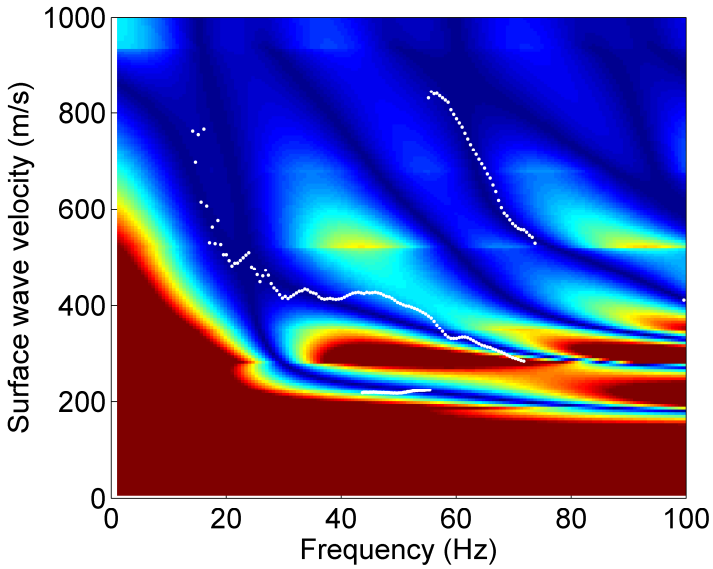

Figure 8 Palazzolo Acreide – Experimental dispersion curve compared with the misfit surface of the best fitting model

The parameters of the best fitting profile are summarized in Table 4.

Vs (m/s)	Thickness (m)	Poisson coefficient	Density (T/m^3)
183	1.1	0.3	1.8
277	3.6	0.3	1.8
675	2.1	0.3	1.8
931	-	0.3	1.8

Table 4 Palazzolo Acreide: subsoil parameters of the best fitting profile.

References

Project S4: ITALIAN STRONG MOTION DATA BASE, Deliverable # 6, Application of Surface wave methods for seismic site characterization, May 2009.

Foti S., Comina C., Boiero D., Socco L.V. (2009) "Non uniqueness in surface wave inversion and consequences on seismic site response analyses", Soil Dynamics and Earthquake Engineering, Vol. 29 (6), 982-993.

Haskell, N., 1964, Radiation pattern of surface waves from point sources in a multilayered medium: Bulletin of seismological society of America, 54, no. 1, 377-393.

Herrmann, R. B., and C. Y. Wang, 1980, A numerical study of p-, sv- and sh- wave generation in a plane layered medium: Bulletin of seismological society of America, 70, no. 4, 1015-1036.

Herrmann, R. B., 2002, SURF code, www.eas.slu.edu/People/RBHerrmann/.

Maraschini, M., F. Ernst, D. Boiero, S. Foti, and L.V. Socco, 2008, A new approach for multimodal inversion of Rayleigh and Scholte waves: Proceedings of EAGE Rome, expanded abstract.

Thomson, W. T, 1950., Transmission of elastic waves through a stratified solid medium: Journal of Applied Physics, 21, no. 89.

APPLICATION OF SURFACE WAVE METHODS FOR SEISMIC SITE CHARACTERIZATION

PINEROLO (PNR)

Responsible:
Sebastiano Foti

Co-workers:
Giovanni Bianchi
Cesare Comina
Margherita Maraschini

FINAL REPORT

Turin, 31/7/2009

INDEX

1 Introduction

In this report a summary of the results obtained for the characterization of the accelerometric station of Pinerolo of the RAN within Project S4 is presented. The analysis was performed using active surface wave method and seismic refraction tests.
From available boreholes nearby the site, some information on the stratigraphy can be obtained: the topsoil thickness is about 1m; below this layer, a layer of about 10m thick of coarse gravel with fine materials is present; the water table is in this layer. From 10 to 15m a layer composed by pebbles and gravel in silty sand is present. From 15 to 20m there is a sandy silt layer with inclusions of alterate rock.

The map and the site location are shown in Figure 1 and Figure 2.

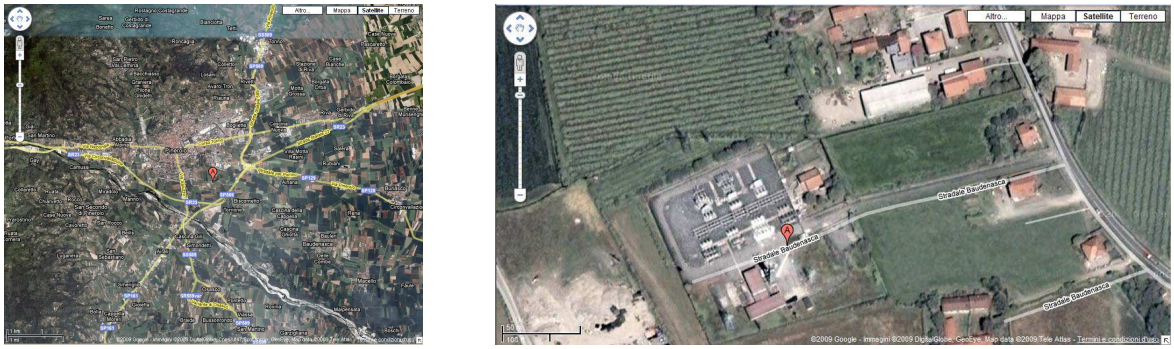

Figure 1 Pinerolo: maps

Figure 2 Pinerolo: site location

Goal of the seismic tests is the estimation of the S-wave velocity profile of the subsoil.

The primary use of surface wave testing is related to site characterization in terms of shear wave velocity profile. The V_S profile is of primary interest for seismic site response studies and for studies of vibration of foundations and vibration transmission in soils. Other applications are related to the prediction of settlements and to soil-structure interaction.

With respect to the evaluation of seismic site response, it is worth noting the affinity between the model used for the interpretation of surface wave tests and the model adopted for most site responses study. Indeed the application of equivalent linear elastic methods is often associated with layered models (e.g. the code SHAKE and all similar approaches). This affinity is also particularly important in the light of equivalence problems, which arise because of non-uniqueness of the solution in inverse problems. Indeed profiles which are equivalent in terms of Rayleigh wave propagation are also equivalent in term of seismic amplification (Foti et al., 2009).

Many seismic building codes introduce the weighted average of the shear wave velocity profile in the shallowest 30m as to discriminate class of soils to which a similar site amplification effect can be associated. The so-called $V_{S,30}$ can be evaluated very efficiently with surface wave method also because its average nature does not require the high level of accuracy that can be obtained with seismic borehole methods.

In the following a methodological summary of techniques and the description of the results is presented.

For Further explanation of surface wave methodologies, see document: Project S4: ITALIAN STRONG MOTION DATA BASE, Deliverable # 6, Application of Surface wave methods for seismic site characterization, May 2009.

2 Surface wave method

Surface wave method (S.W.M.) is based on the geometrical dispersion, which makes Rayleigh wave velocity frequency dependent in vertically heterogeneous media. High frequency (short wavelength) Rayleigh waves propagate in shallow zones close to the free surface and are informative about their mechanical properties, whereas low frequency (long wavelength) components involve deeper layers. Surface wave tests are typically devoted to the determination of a small strain stiffness profile for the site under investigation. Consequently the dispersion curve will be associated to the variation of medium parameters with depth.

The calculation of the dispersion curve from model parameters is the so called forward problem. Surface wave propagation can be seen as the combination of multiple modes of propagation, i.e. more than one possible velocity can be associated to each frequency value. Including higher modes in the inversion process allows the penetration depth to be increased and a more accurate subsoil profile to be retrieved.

If the dispersion curve is estimated on the basis of experimental data, it is then possible to solve the inverse problem, i.e. the model parameters are identified on the basis of the experimental data collected on the boundary of the medium. The result of the surface wave method is a one-dimensional S wave velocity soil profile.

The standard procedure for surface wave tests is reported in Figure 3. It can be subdivided into three main steps:

1. acquisition of experimental data;
2. signal processing to obtain the experimental dispersion curve;

3. inversion process to estimate shear wave velocity profile at the site.

It is very important to recognize that the above steps are strongly interconnected and their interaction must be adequately accounted for during the whole interpretation process.

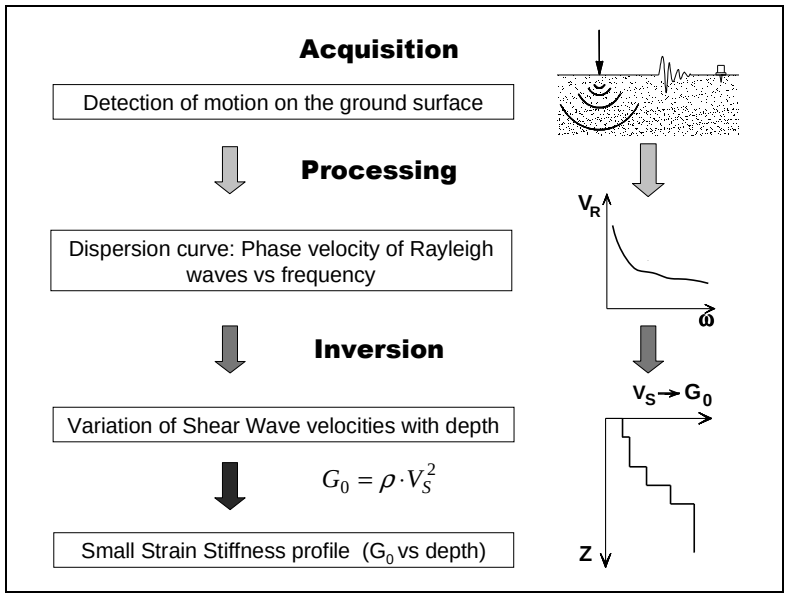

Figure 3 – Flow chart of surface wave tests.

2.1 Acquisition

Active surface wave tests (MASW) and refraction tests at Pinerolo have been performed within the project S4 for the characterization of RAN sites.

Characteristics of sensors are reported in Table 1.

Test	GEOPHONE TYPE	NATURAL FREQUENCY	GEOPHONE NUMBER
MASW/Refraction	vertical SENSOR SM-6/U-B	4,5 Hz	48

Table 1 Pinerolo: receiver characteristics

The total length of the array is 47 m. The source is a 5 kg sledge hammer. Geometry parameters are summarized in Table 2.

Test	GEOF. N.	SPACING	SOURCE TYPE	ACQUISITION WINDOW	SAMPLING INTERVAL	STACK
MASW	48	1 m	Hammer	T = 0.512/1.024 s	Δt = 0.03125/0.5 ms	10
Refraction	48	1 m	Hammer	T =0.512s	Δt = 0.03125ms	10

Table 2 Pinerolo: Acquisition parameters

Since a shallow bedrock is expected at this site, the synergies between surface wave active methods and P-wave refraction surveys are relevant. Indeed both surveys can be performed with the same testing configuration. In particular P-wave seismic refraction method can in this situation provide relevant information with respect to the position of the interface between the soil cover and the bedrock.

2.2 Processing of surface waves

The processing allows the experimental dispersion curve to be determined.

Multichannel data are processed using a double Fourier Transform, which generates the frequency-wave number spectrum, where the multimodal dispersion curve is easily extracted as the location of spectral maxima.

2.3 Inversion of surface waves

The solution of the inverse Rayleigh problem is the final step in test interpretation. The solution of the forward problem forms the basis of any inversion strategy; the forward problem consists in the calculation of the function whose zeros are dispersion curves of a given model. Assuming a model for the soil deposit, model parameters of the best fitting subsoil profile are obtained minimizing an object function.

The subsoil is modelled as a horizontally layered medium overlaying a halfspace, with constant parameter in the interior of each layer and linear elastic behaviour. Model parameters are thickness, S-wave velocity, P-wave velocity (or Poisson coefficient), and density of each layer and the halfspace. The inversion is performed on S-wave velocities and thicknesses, whereas for the other parameters realistic values are chosen a priori. The number of layer is chosen applying minimum parameterization criterion.

In surface wave analysis it is very common to perform the inversions using only the fundamental mode of propagation. This approach is based on the assumption that the prevailing mode of propagation is the fundamental one; if this is partially true for normal dispersive sites, in several real cases the experimental dispersion curve is on the contrary the result of the superposition of several modes. This may happen in particular when velocity inversions or strong velocity contrasts are present in the shear wave velocity profile. In these stratigraphic conditions the inversion of the only fundamental mode will produce significant errors; moreover all the information contained in higher propagating modes is not used in the inversion process. Therefore, the fundamental mode inversion does not use all the available information, and this affects the result accuracy.

The use of higher modes in the inversion can be helpful both in the low frequency range, in order to increase the investigation depth and to avoid the overestimation of the bedrock velocity, and in the high frequency range in order to provide a more consistent interpretation of shallow interfaces and increase model parameter resolution.

In this work a multimodal misfit function has been used. This function is based on the Haskell-Thomson method for dispersion curve calculation (Thomson 1950, Haskell 1953, Herrmann e Wang 1980, Herrmann 2002). For a given subsoil model, and an experimental data, the misfit of the model is the L^1 norm of the vector containing the absolute value of the determinant of the Haskell-Thomson matrix (which is zeros in correspondence of all the modes of the dispersion curves of the numerical model) evaluated in correspondence of

the experimental data (Maraschini et al. 2008). The misfit function adopted has the advantage of being able to include any dispersive event present in the data without the need of specifying to which mode the data points belong to, avoiding errors arising from mode misidentification, in particular in the low frequency range.

This misfit function is applied in a Global Search Methods (GSM), in order to reduce the possibility of falling in local minima. A uniform random search is applied; ranges for the inversion have been chosen, for the different sites, based on the experimental dispersion curves; in particular the range of the S-wave half space velocity is close to the maximum surface wave velocity retrieved on experimental data.

The results of the inversion are reported as the ensemble of the twenty shear wave velocity profiles which present the minimum misfits with respect to the experimental dispersion curve. In the figures reported a representation based on the misfit is adopted for velocity profiles, so that the darkest colour corresponds to the profile whose dispersion curve has the lowest misfit and better approximation to the reference one; instead for dispersion curves the coloured surface under imposed to the experimental one is a misfit surface, whose zeros are synthetic dispersion curve of the best fitting model.

2.4 Numerical code

The numerical codes used for processing and inversion of surface waves are non commercial codes, implemented at Politecnico di Torino.

3 Pinerolo – Refraction results

Several acquisition have been performed for refraction tests. The main goal of the refraction survey is the estimation of the water table position (Foti e Strobbia 2002). An example of first breaks is shown in Figure 4a) and soil profiles obtained by refraction survey are shown in Figure 4 b).

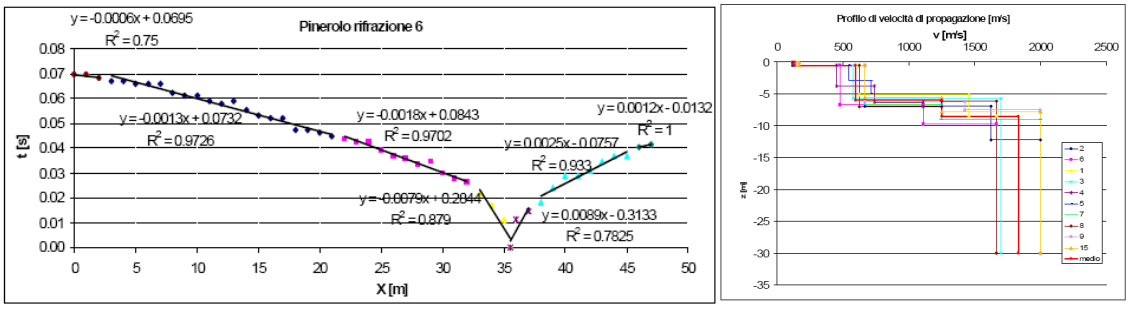

a) b)

Figure 4 Pinerolo – a)Example of first breaks b) profiles obtained by refraction tests

The soil profiles obtained by the refraction tests are in good agreement between each other. The average profile is plotted in red. The soil parameters are summarized in Table 3.

Average profile	
P-wave velocity (m/s)	Thickness (m)
110	0.5
600	5.5
1300	2.5
1860	-

Table 3 Average soil profile by refraction surveys

The second interface corresponds to the position of the water table.

4 Pinerolo – Surface wave results

In Figure 5 an example of the f-k spectrum of the data collected at Pinerolo is presented.

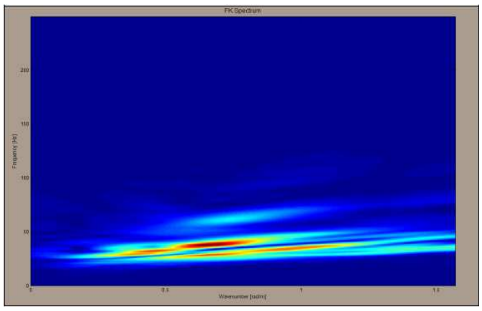

Figure 5 a) Pinerolo – example of f-k spectrum

From the f-k spectra, several dispersion curves can be retrieved. From all these curves an average curve is estimated (Figure 6).

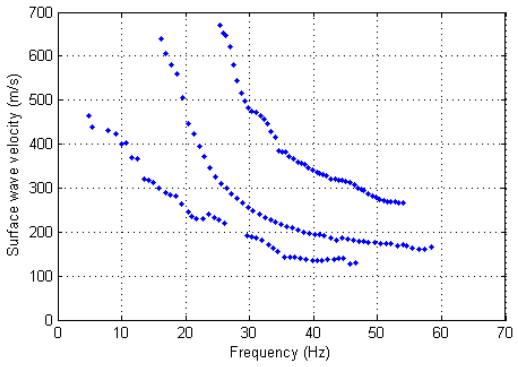

Figure 6 – Pinerolo -Average apparent dispersion curve

Three different branches are considered in the inversion.
Data were inverted using a multimodal stochastic approach, the 20 best fitting profiles are plotted in Figure 7 a), profile colour depends on the misfit, from yellow to blue (best fitting profile). In Figure 7 b) the best fitting profile is compared with the refraction result, and in

Figure 8 the experimental dispersion curve is compared with the determinant surface of the best fitting model.
We can note that the experimental points of all the branches follow in the minima of the determinant surface, even if the fitting of the low frequency part of the higher modes is not good. Moreover it can be noted that the position of both interfaces is in good agreement with the refraction results.

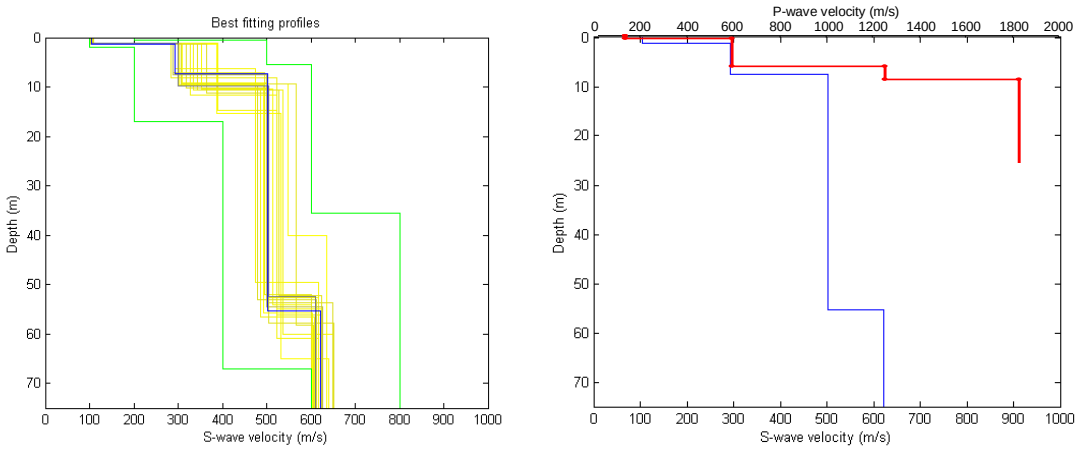

Figure 7 Pinerolo – a) Monte Carlo results (from yellow to blue) of the inversion with the boundaries (green). b) Pinerolo – Best fitting profile (blue) compared with the refraction result (red).

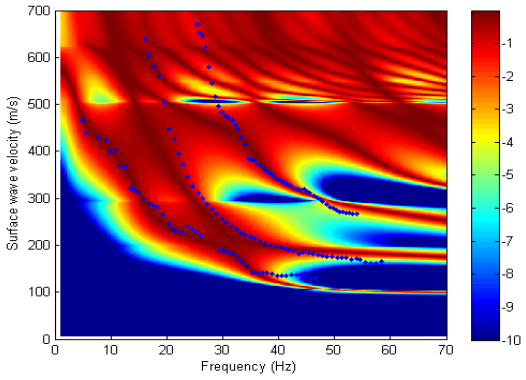

Figure 8 Pinerolo – Experimental dispersion curve compared with the misfit surface of the best fitting model

The parameters of the best fitting profile are summarized in Table 4.

Vs (m/s)	Thickness (m)	Poisson coefficient	Density (T/m^3)
104	1.3	0.3	1.8
292	6.1	0.3	1.8
503	48.0	0.45	1.8
621	-	0.45	1.8

Table 4 Pinerolo: subsoil parameters of the best fitting profile.

References

Project S4: ITALIAN STRONG MOTION DATA BASE, Deliverable # 6, Application of Surface wave methods for seismic site characterization, May 2009.

Foti S., Comina C., Boiero D., Socco L.V. (2009) "Non uniqueness in surface wave inversion and consequences on seismic site response analyses", Soil Dynamics and Earthquake Engineering, Vol. 29 (6), 982-993.

Foti S., Strobbia C. (2002) "Some notes on model parameters for surface wave data inversion", Proc. of SAGEEP 2002, Las Vegas, USA, February 10-14, CD-Rom.

Haskell, N., 1964, Radiation pattern of surface waves from point sources in a multilayered medium: Bulletin of seismological society of America, 54, no. 1, 377-393.

Herrmann, R. B., and C. Y. Wang, 1980, A numerical study of p-, sv- and sh- wave generation in a plane layered medium: Bulletin of seismological society of America, 70, no. 4, 1015-1036.

Herrmann, R. B., 2002, SURF code, www.eas.slu.edu/People/RBHerrmann/.

Maraschini, M., F. Ernst, D. Boiero, S. Foti, and L.V. Socco, 2008, A new approach for multimodal inversion of Rayleigh and Scholte waves: Proceedings of EAGE Rome, expanded abstract.

Thomson, W. T, 1950., Transmission of elastic waves through a stratified solid medium: Journal of Applied Physics, 21, no. 89.

APPLICATION OF SURFACE WAVE METHODS FOR SEISMIC SITE CHARACTERIZATION

PATTI (PTT)

Responsible:
Sebastiano Foti

Co-workers:
Giovanni Bianchi
Paolo Bergamo
Margherita Maraschini

FINAL REPORT

Turin, 11/02/2010

INDEX

1 Introduction

In this report a summary of the results obtained for the characterization of the accelerometric station of Patti of the RAN within Project S4 is presented. The analysis was performed using active surface wave method and refraction method.

Patti RAN station is located on a slope outside of the city centre in agricultural soil.

The map, site location and measurements arrays are shown in Figure1, Figure 2 and Figure 3.

Figure 1 Patti: map

Figure 2 Patti: array map. The red line represents the active measurements array.

Figure 3 Patti: site location and active measurement array.

Goal of the seismic tests is the estimation of the S-wave velocity profile of the subsoil, and in particular the position of the bedrock. The presence of stiff seismic interfaces between the sediments and the shallow bedrock can cause a relevance of higher modes in the surface wave experimental dispersion curve which has be taken into account in order to provide reliable results.

The primary use of surface wave testing is related to site characterization in terms of shear wave velocity profile. The V_S profile is of primary interest for seismic site response studies and for studies of vibration of foundations and vibration transmission in soils. Other applications are related to the prediction of settlements and to soil-structure interaction.

With respect to the evaluation of seismic site response, it is worth noting the affinity between the model used for the interpretation of surface wave tests and the model adopted for most site responses study. Indeed the application of equivalent linear elastic methods is often associated with layered models (e.g. the code SHAKE and all similar approaches). This affinity is also particularly important in the light of equivalence problems, which arise because of non-uniqueness of the solution in inverse problems. Indeed profiles which are equivalent in terms of Rayleigh wave propagation are also equivalent in term of seismic amplification (Foti et al., 2009).

Many seismic building codes introduce the weighted average of the shear wave velocity profile in the shallowest 30m as to discriminate class of soils to which a similar site amplification effect can be associated. The so-called $V_{S,30}$ can be evaluated very efficiently with surface wave method also because its average nature does not require the high level of accuracy that can be obtained with seismic borehole methods.

In the following a methodological summary of techniques and the description of the results is presented.

For Further explanation of surface wave methodologies, see document: Project S4: ITALIAN STRONG MOTION DATA BASE, Deliverable # 6, Application of Surface wave methods for seismic site characterization, May 2009.

2 Surface wave method

Surface wave method (S.W.M.) is based on the geometrical dispersion, which makes Rayleigh wave velocity frequency dependent in vertically heterogeneous media. High frequency (short wavelength) Rayleigh waves propagate in shallow zones close to the free surface and are informative about their mechanical properties, whereas low frequency (long wavelength) components involve deeper layers. Surface wave tests are typically devoted to the determination of a small strain stiffness profile for the site under investigation. Consequently the dispersion curve will be associated to the variation of medium parameters with depth.

The calculation of the dispersion curve from model parameters is the so called forward problem. Surface wave propagation can be seen as the combination of multiple modes of propagation, i.e. more than one possible velocity can be associated to each frequency value. Including higher modes in the inversion process allows the penetration depth to be increased and a more accurate subsoil profile to be retrieved.

If the dispersion curve is estimated on the basis of experimental data, it is then possible to solve the inverse problem, i.e. the model parameters are identified on the basis of the experimental data collected on the boundary of the medium. The result of the surface wave method is a one-dimensional S wave velocity soil profile.

The standard procedure for surface wave tests is reported in Figure 4. It can be subdivided into three main steps:

1. acquisition of experimental data;
2. signal processing to obtain the experimental dispersion curve;
3. inversion process to estimate shear wave velocity profile at the site.

It is very important to recognize that the above steps are strongly interconnected and their interaction must be adequately accounted for during the whole interpretation process.

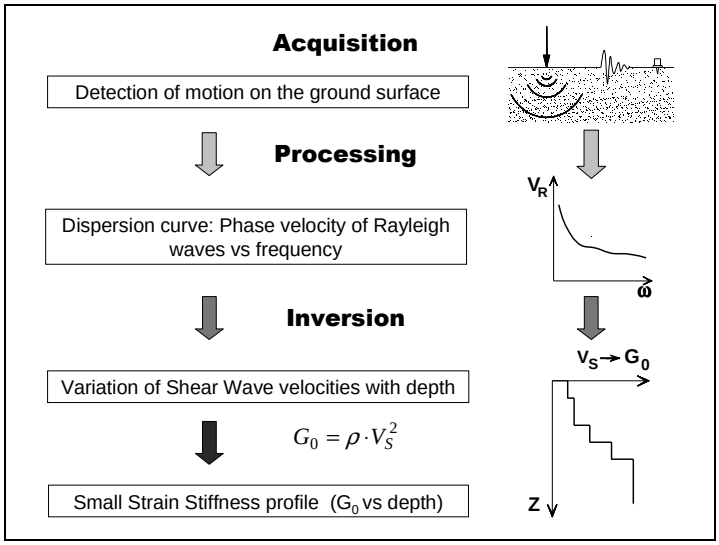

Figure 4 – Flow chart of surface wave tests.

2.1 Acquisition

Active (MASW) surface wave tests and refraction surveys at Patti have been performed in May 2009 within the project S4 for the characterization of RAN sites.

Characteristics of sensors are reported in Table 1.

Test	GEOPHONE TYPE	NATURAL FREQUENCY	GEOPHONE NUMBER
MASW/Refraction survey	vertical SENSOR SM-6/U-B	4,5 Hz	24

Table 1 Patti: receiver characteristics

24 receivers were used for active tests, with a spacing of 1 m between neighbouring geophones, so that the total length of the array is 23 m. The source is a 5kg sledge hammer. This array was used for refraction surveys as well. Acquisition parameters are summarized in Table 2.

Test	GEOF. N.	SPACING	SOURCE TYPE	ACQUISITION WINDOW	SAMPLING INTERVAL	STACK
MASW	24	1 m	Hammer	T = 2 s	Δt = 0.5 ms	10
Refraction surveys	24	1 m	Hammer	T = 1 s	Δt = 62.5 μs	1

Table 2 Patti: Acquisition parameters

2.2 Processing of active surface wave data

The processing allows the experimental dispersion curve to be determined.

Multichannel data are processed using a double Fourier Transform, which generates the frequency-wave number spectrum, where the multimodal dispersion curve is easily extracted as the location of spectral maxima.

2.3 Inversion of surface waves

The solution of the inverse Rayleigh problem is the final step in test interpretation. The solution of the forward problem forms the basis of any inversion strategy; the forward problem consists in the calculation of the function whose zeros are dispersion curves of a given model. Assuming a model for the soil deposit, model parameters of the best fitting subsoil profile are obtained minimizing an object function.

The subsoil is modelled as a horizontally layered medium overlaying a halfspace, with constant parameter in the interior of each layer and linear elastic behaviour. Model parameters are thickness, S-wave velocity, P-wave velocity (or Poisson coefficient), and density of each layer and the halfspace. The inversion is performed on S-wave velocities and thicknesses, whereas for the other parameters realistic values are chosen a priori. The number of layer is chosen applying minimum parameterization criterion.

In surface wave analysis it is very common to perform the inversions using only the fundamental mode of propagation. This approach is based on the assumption that the prevailing mode of propagation is the fundamental one; if this is partially true for normal dispersive sites, in several real cases the experimental dispersion curve is on the contrary the result of the superposition of several modes. This may happen in particular when velocity inversions or strong velocity contrasts are present in the shear wave velocity profile. In these stratigraphic conditions the inversion of the only fundamental mode will produce significant errors; moreover all the information contained in higher propagating modes is not used in the inversion process. Therefore, the fundamental mode inversion does not use all the available information, and this affects the result accuracy.

The use of higher modes in the inversion can be helpful both in the low frequency range, in order to increase the investigation depth and to avoid the overestimation of the bedrock velocity, and in the high frequency range in order to provide a more consistent interpretation of shallow interfaces and increase model parameter resolution.

In this work a multimodal misfit function has been used. This function is based on the Haskell-Thomson method for dispersion curve calculation (Thomson 1950, Haskell 1953, Herrmann e Wang 1980, Herrmann 2002). For a given subsoil model, and an experimental data, the misfit of the model is the L^1 norm of the vector containing the absolute value of the determinant of the Haskell-Thomson matrix (which is zeros in correspondence of all the modes of the dispersion curves of the numerical model) evaluated in correspondence of the experimental data (Maraschini et al. 2008). The misfit function adopted has the advantage of being able to include any dispersive event present in the data without the need of specifying to which mode the data points belong to, avoiding errors arising from mode misidentification, in particular in the low frequency range.

This misfit function is applied in a Global Search Methods (GSM), in order to reduce the possibility of falling in local minima. A uniform random search is applied; ranges for the inversion have been chosen, for the different sites, based on the experimental dispersion curves; in particular the range of the S-wave half space velocity is close to the maximum surface wave velocity retrieved on experimental data.

The results of the inversion are reported as the ensemble of the best shear wave velocity profiles chosen according to a chi-square test (see Socco et al., 2008). It can be assumed that the experimental dispersion curve is affected by a Gaussian error with a known standard deviation, so that the probability density function of data $\rho_D(d)$ can be described by a discrete m-dimensional Gaussian (where m are the model parameters) and the sample variance variable of each random vector (dispersion curve) extracted from the data pdf is distributed according to a chi-square probability density. According to these assumptions we adopt a misfit function with the structure of a chi-square and this allows a statistical test to be applied to the variances of the synthetic dispersion curves with respect to the experimental one d_{obs}. Assuming that the best fitting curve d_{opt} belongs to the distribution $\rho_D(d_{obs})$ all models belonging to the distribution $\rho_D(d_{opt})$ and consistent with the data within a fixed level of confidence α are selected. As the ratio between chi-square variables follows a Fisher distribution a one–tailed F test can be performed:

$$F_\alpha(dof_{dopt}, dof_{g(m)}) < \frac{\chi^2_{dopt}}{\chi^2_{g(m)}}$$

where α is the chosen level of confidence, dof_{dopt} and $dof_{g(m)}$ are the degrees of freedom of the Fischer distribution and χ^2_{dopt} and $\chi^2_{g(m)}$ are the misfit of the best fitting curve and the misfit of all the others respectively. All models passing such test are selected. In the figures reported a representation based on the misfit is adopted for velocity profiles, so that the darkest colour corresponds to the profile whose dispersion curve has the lowest misfit and better approximation to the reference one; instead for dispersion curves the coloured surface under imposed to the experimental one is a misfit surface, whose zeros are synthetic dispersion curve of the best fitting model.

2.4 Numerical code

The numerical codes used for processing and inversion of surface waves are non commercial codes, implemented at Politecnico di Torino.

3 Patti – Refraction results

Three shots were considered for refraction survey: two of them with the source at the edges of the array and one with the source at intermediate positions along the survey line. First-break arrival times are shown in Figure 5.

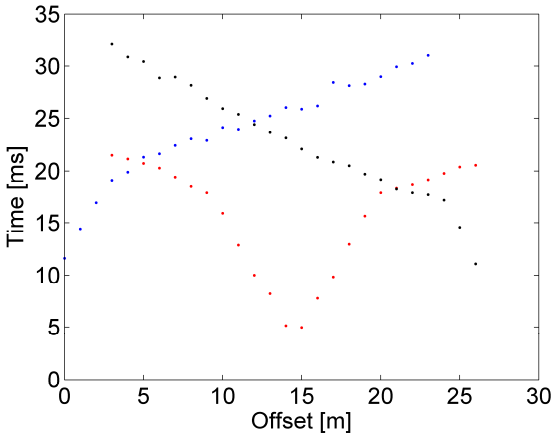

Figure 5 Patti – First breaks of the five considered shots

A two layers model is identified: the weathering layer has a P-wave velocity of 350 m/s and its thickness grows thin from 3.2 m to 2.3 m towards the end of the array following the slope of the ground. The halfspace has a P-wave velocity of 1554 m/s. The average profile features are summarized in Table 3.

P-wave velocity (m/s)	Thickness (m)
350	2.8
1554	-

Table 3 Velocity models retrieved by refraction survey

4 Patti – Surface wave results

In Figure 6 an example of the f-k spectrum of the active data collected at Patti is presented.

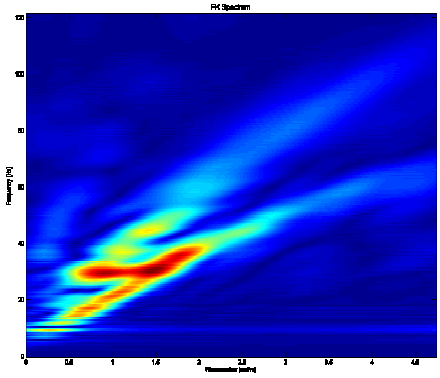

Figure 6 Patti – example of f-k spectrum

From the f-k spectra, several dispersion curves can be retrieved. From all these curves an average curve is estimated (Figure 7).

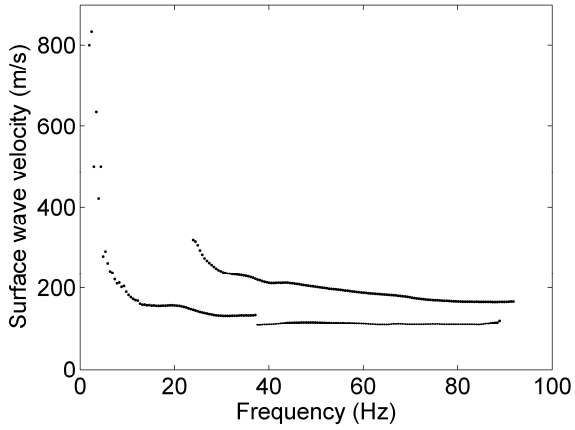

Figure 7 – Patti - Average apparent dispersion curve

The apparent dispersion curve is made up of two branches which follow two propagation modes.
Data were inverted using a multimodal stochastic approach, the best fitting profiles are plotted in Figure 8 a), profile colour depends on the misfit, from yellow to blue (best fitting profile). In Figure 8 b) the best fitting profile is compared with the refraction result, and in Figure 9 the experimental dispersion curve is compared with the determinant surface of the best fitting model. We can note that the experimental points fall into the minima of the determinant surface. Moreover it can be noted that the position of the first interface is in good agreement with the refraction results.

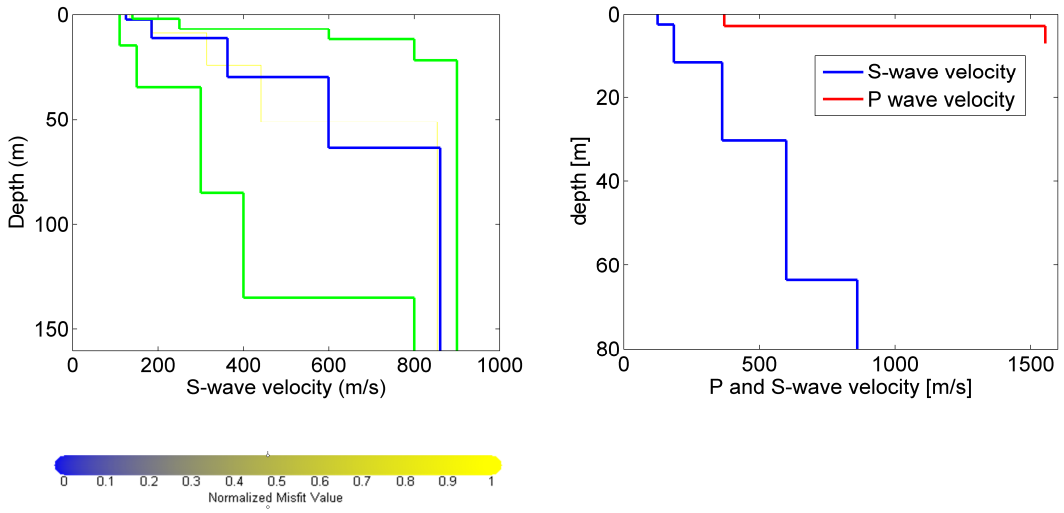

Figure 8 Patti – a) Monte Carlo results (from yellow to blue) of the inversion with the boundaries (green). b) Patti – Best fitting profile (blue) compared with the refraction result (red).

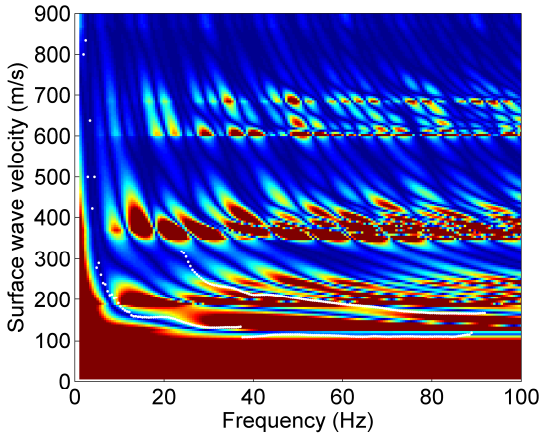

Figure 9 Patti – Experimental dispersion curve compared with the misfit surface of the best fitting model

The parameters of the best fitting profile are summarized in Table 4.

Vs (m/s)	Thickness (m)	Poisson coefficient	Density (T/m^3)
125	2.4	0.3	1.8
185	9.2	0.3	1.8
363	18.8	0.3	1.8
599	33.3	0.3	1.8
861			

Table 4 Patti: subsoil parameters of the best fitting profile.

References

Project S4: ITALIAN STRONG MOTION DATA BASE, Deliverable # 6, Application of Surface wave methods for seismic site characterization, May 2009.

Foti S., Comina C., Boiero D., Socco L.V. (2009) "Non uniqueness in surface wave inversion and consequences on seismic site response analyses", Soil Dynamics and Earthquake Engineering, Vol. 29 (6), 982-993.

Haskell, N., 1964, Radiation pattern of surface waves from point sources in a multilayered medium: Bulletin of seismological society of America, 54, no. 1, 377-393.

Herrmann, R. B., and C. Y. Wang, 1980, A numerical study of p-, sv- and sh- wave generation in a plane layered medium: Bulletin of seismological society of America, 70, no. 4, 1015-1036.

Herrmann, R. B., 2002, SURF code, www.eas.slu.edu/People/RBHerrmann/.

Maraschini, M., F. Ernst, D. Boiero, S. Foti, and L.V. Socco, 2008, A new approach for multimodal inversion of Rayleigh and Scholte waves: Proceedings of EAGE Rome, expanded abstract.

Thomson, W. T, 1950., Transmission of elastic waves through a stratified solid medium: Journal of Applied Physics, 21, no. 89.

APPLICATION OF SURFACE WAVE METHODS FOR SEISMIC SITE CHARACTERIZATION

RAGUSA (RGS)

Responsible:
Sebastiano Foti

Co-workers:
Giovanni Bianchi
Paolo Bergamo
Margherita Maraschini

FINAL REPORT

Turin, 11/02/2010

INDEX

1 Introduction

In this report a summary of the results obtained for the characterization of the accelerometric station of Ragusa of the RAN within Project S4 is presented. The analysis was performed using active surface wave method.

Ragusa RAN station is located on a calcareous rock outcrop, close to the city centre.

The map, site location and measurements arrays are shown in Figure1, Figure 2 and Figure 3.

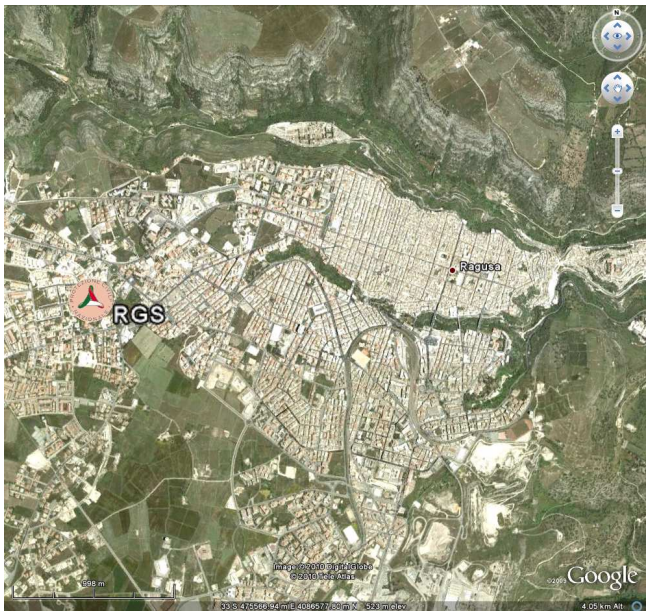

Figure 1 Ragusa: map

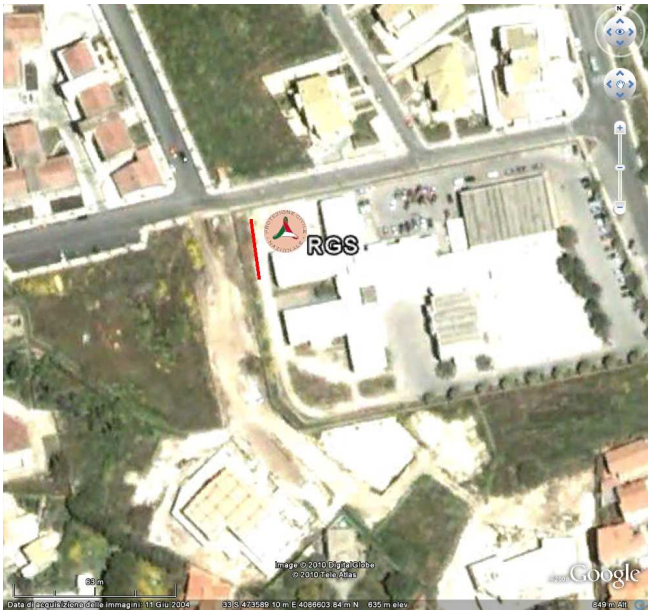

Figure 2 Ragusa: array map. The red line represents the active measurements array.

Figure 3 Ragusa: site location and active measurement array.

Goal of the seismic tests is the estimation of the S-wave velocity profile of the subsoil, and in particular the position of the bedrock. The presence of stiff seismic interfaces between the sediments and the shallow bedrock can cause a relevance of higher modes in the surface wave experimental dispersion curve which has be taken into account in order to provide reliable results.

The primary use of surface wave testing is related to site characterization in terms of shear wave velocity profile. The V_S profile is of primary interest for seismic site response studies and for studies of vibration of foundations and vibration transmission in soils. Other applications are related to the prediction of settlements and to soil-structure interaction.

With respect to the evaluation of seismic site response, it is worth noting the affinity between the model used for the interpretation of surface wave tests and the model adopted for most site responses study. Indeed the application of equivalent linear elastic methods is often associated with layered models (e.g. the code SHAKE and all similar approaches). This affinity is also particularly important in the light of equivalence problems, which arise because of non-uniqueness of the solution in inverse problems. Indeed profiles which are equivalent in terms of Rayleigh wave propagation are also equivalent in term of seismic amplification (Foti et al., 2009).

Many seismic building codes introduce the weighted average of the shear wave velocity profile in the shallowest 30m as to discriminate class of soils to which a similar site amplification effect can be associated. The so-called $V_{S,30}$ can be evaluated very efficiently with surface wave method also because its average nature does not require the high level of accuracy that can be obtained with seismic borehole methods.

In the following a methodological summary of techniques and the description of the results is presented.

For Further explanation of surface wave methodologies, see document: Project S4: ITALIAN STRONG MOTION DATA BASE, Deliverable # 6, Application of Surface wave methods for seismic site characterization, May 2009.

2 Surface wave method

Surface wave method (S.W.M.) is based on the geometrical dispersion, which makes Rayleigh wave velocity frequency dependent in vertically heterogeneous media. High frequency (short wavelength) Rayleigh waves propagate in shallow zones close to the free surface and are informative about their mechanical properties, whereas low frequency (long wavelength) components involve deeper layers. Surface wave tests are typically devoted to the determination of a small strain stiffness profile for the site under investigation. Consequently the dispersion curve will be associated to the variation of medium parameters with depth.

The calculation of the dispersion curve from model parameters is the so called forward problem. Surface wave propagation can be seen as the combination of multiple modes of propagation, i.e. more than one possible velocity can be associated to each frequency value. Including higher modes in the inversion process allows the penetration depth to be increased and a more accurate subsoil profile to be retrieved.

If the dispersion curve is estimated on the basis of experimental data, it is then possible to solve the inverse problem, i.e. the model parameters are identified on the basis of the experimental data collected on the boundary of the medium. The result of the surface wave method is a one-dimensional S wave velocity soil profile.

The standard procedure for surface wave tests is reported in Figure 4. It can be subdivided into three main steps:

1. acquisition of experimental data;
2. signal processing to obtain the experimental dispersion curve;
3. inversion process to estimate shear wave velocity profile at the site.

It is very important to recognize that the above steps are strongly interconnected and their interaction must be adequately accounted for during the whole interpretation process.

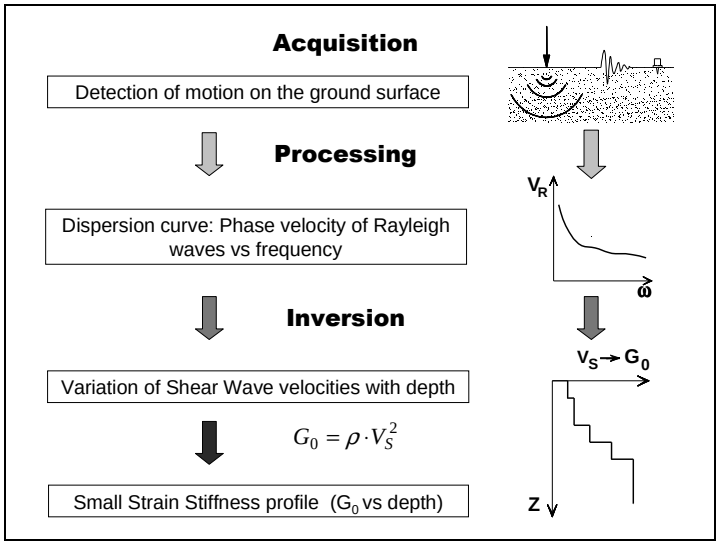

Figure 4 – Flow chart of surface wave tests.

2.1 Acquisition

Active (MASW) surface wave tests at Ragusa have been performed in May 2009 within the project S4 for the characterization of RAN sites.

Characteristics of sensors are reported in Table 1.

Test	GEOPHONE TYPE	NATURAL FREQUENCY	GEOPHONE NUMBER
MASW	vertical SENSOR SM-6/U-B	4,5 Hz	24

Table 1 Ragusa: receiver characteristics

24 receivers were used for active tests, with a spacing of 1 m between neighbouring geophones, so that the total length of the array is 23 m. The source is a 5kg sledge hammer. This array was used for refraction surveys as well. Acquisition parameters are summarized in Table 2.

Test	GEOF. N.	SPACING	SOURCE TYPE	ACQUISITION WINDOW	SAMPLING INTERVAL	STACK
MASW	24	1 m	Hammer	T = 1 s	Δt = 0.25 ms	10

Table 2 Ragusa: Acquisition parameters

2.2 Processing of active surface wave data

The processing allows the experimental dispersion curve to be determined.

Multichannel data are processed using a double Fourier Transform, which generates the frequency-wave number spectrum, where the multimodal dispersion curve is easily extracted as the location of spectral maxima.

2.3 Inversion of surface waves

The solution of the inverse Rayleigh problem is the final step in test interpretation. The solution of the forward problem forms the basis of any inversion strategy; the forward problem consists in the calculation of the function whose zeros are dispersion curves of a given model. Assuming a model for the soil deposit, model parameters of the best fitting subsoil profile are obtained minimizing an object function.

The subsoil is modelled as a horizontally layered medium overlaying a halfspace, with constant parameter in the interior of each layer and linear elastic behaviour. Model parameters are thickness, S-wave velocity, P-wave velocity (or Poisson coefficient), and density of each layer and the halfspace. The inversion is performed on S-wave velocities and thicknesses, whereas for the other parameters realistic values are chosen a priori. The number of layer is chosen applying minimum parameterization criterion.

In surface wave analysis it is very common to perform the inversions using only the fundamental mode of propagation. This approach is based on the assumption that the prevailing mode of propagation is the fundamental one; if this is partially true for normal dispersive sites, in several real cases the experimental dispersion curve is on the contrary

the result of the superposition of several modes. This may happen in particular when velocity inversions or strong velocity contrasts are present in the shear wave velocity profile. In these stratigraphic conditions the inversion of the only fundamental mode will produce significant errors; moreover all the information contained in higher propagating modes is not used in the inversion process. Therefore, the fundamental mode inversion does not use all the available information, and this affects the result accuracy.

The use of higher modes in the inversion can be helpful both in the low frequency range, in order to increase the investigation depth and to avoid the overestimation of the bedrock velocity, and in the high frequency range in order to provide a more consistent interpretation of shallow interfaces and increase model parameter resolution.

In this work a multimodal misfit function has been used. This function is based on the Haskell-Thomson method for dispersion curve calculation (Thomson 1950, Haskell 1953, Herrmann e Wang 1980, Herrmann 2002). For a given subsoil model, and an experimental data, the misfit of the model is the L^1 norm of the vector containing the absolute value of the determinant of the Haskell-Thomson matrix (which is zeros in correspondence of all the modes of the dispersion curves of the numerical model) evaluated in correspondence of the experimental data (Maraschini et al. 2008). The misfit function adopted has the advantage of being able to include any dispersive event present in the data without the need of specifying to which mode the data points belong to, avoiding errors arising from mode misidentification, in particular in the low frequency range.

This misfit function is applied in a Global Search Methods (GSM), in order to reduce the possibility of falling in local minima. A uniform random search is applied; ranges for the inversion have been chosen, for the different sites, based on the experimental dispersion curves; in particular the range of the S-wave half space velocity is close to the maximum surface wave velocity retrieved on experimental data.

The results of the inversion are reported as the ensemble of the best shear wave velocity profiles chosen according to a chi-square test (see Socco et al., 2008). It can be assumed that the experimental dispersion curve is affected by a Gaussian error with a known standard deviation, so that the probability density function of data $\rho_D(d)$ can be described by a discrete m-dimensional Gaussian (where m are the model parameters) and the sample variance variable of each random vector (dispersion curve) extracted from the data pdf is distributed according to a chi-square probability density. According to these assumptions we adopt a misfit function with the structure of a chi-square and this allows a statistical test to be applied to the variances of the synthetic dispersion curves with respect to the experimental one d_{obs}. Assuming that the best fitting curve d_{opt} belongs to the distribution $\rho_D(d_{obs})$ all models belonging to the distribution $\rho_D(d_{opt})$ and consistent with the data within a fixed level of confidence α are selected. As the ratio between chi-square variables follows a Fisher distribution a one–tailed F test can be performed:

$$F_{\alpha}(dof_{dopt}, dof_{g(m)}) < \frac{\chi^2_{dopt}}{\chi^2_{g(m)}}$$

where α is the chosen level of confidence, dof_{dopt} and $dof_{g(m)}$ are the degrees of freedom of the Fischer distribution and χ^2_{dopt} and $\chi^2_{g(m)}$ are the misfit of the best fitting curve and the misfit of all the others respectively. All models passing such test are selected. In the figures reported a representation based on the misfit is adopted for velocity profiles, so that the darkest colour corresponds to the profile whose dispersion curve has the lowest misfit

and better approximation to the reference one; instead for dispersion curves the coloured surface under imposed to the experimental one is a misfit surface, whose zeros are synthetic dispersion curve of the best fitting model.

2.4 Numerical code

The numerical codes used for processing and inversion of surface waves are non commercial codes, implemented at Politecnico di Torino.

3 Ragusa – Surface wave results

In Figure 5 an example of the f-k spectrum of the active data collected at Ragusa is presented.

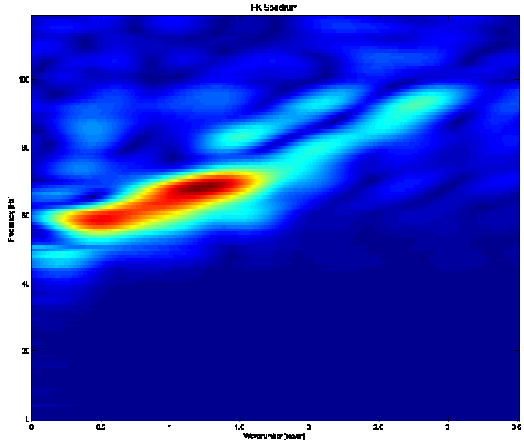

Figure 5 Ragusa – example of f-k spectrum

From the f-k spectra, several dispersion curves can be retrieved. From all these curves an average curve is estimated (Figure 6).

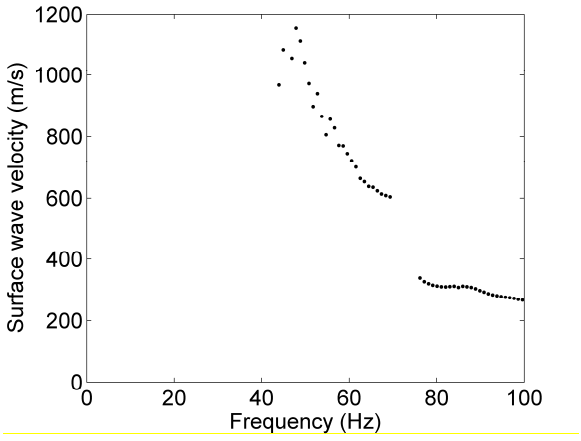

Figure 6 – Ragusa - Average apparent dispersion curve

The apparent dispersion curve is made up of two branches which probably follow two propagation modes: note that one branch is characterized by a steep velocity increase probably jumping from one mode to another.
Data were inverted using a multimodal stochastic approach, the best fitting profiles are plotted in Figure 7, profile colour depends on the misfit, from yellow to blue (best fitting profile). In Figure 8 the experimental dispersion curve is compared with the determinant surface of the best fitting model. We can note that the experimental points fall into the minima of the determinant surface, and that a branch of the apparent dispersion curve jumps from the fundamental to the 1st higher mode, probably because of the impedance contrast between topsoil and bedrock.

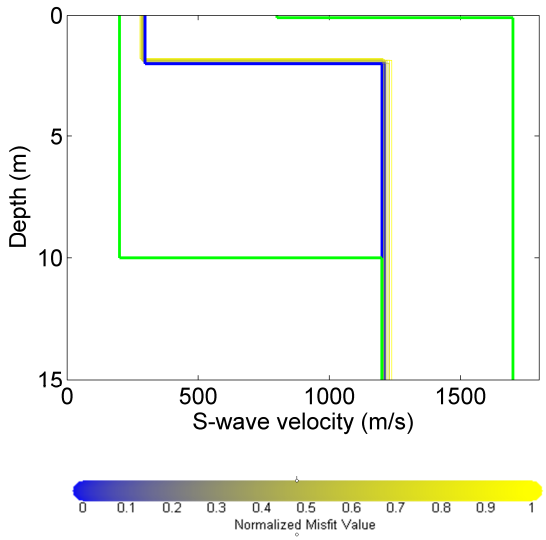

Figure 7 Ragusa – Monte Carlo results (from yellow to blue) of the inversion with the boundaries (green).

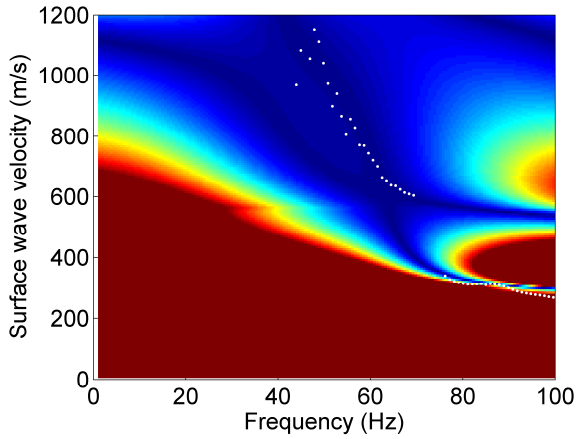

Figure 8 Ragusa – Experimental dispersion curve compared with the misfit surface of the best fitting model

The parameters of the best fitting profile are summarized in Table 4.

Vs (m/s)	Thickness (m)	Poisson coefficient	Density (T/m^3)
297	2.0	0.3	1.8
1201	-	0.3	1.8

Table 3 Ragusa: subsoil parameters of the best fitting profile.

References

Project S4: ITALIAN STRONG MOTION DATA BASE, Deliverable # 6, Application of Surface wave methods for seismic site characterization, May 2009.

Foti S., Comina C., Boiero D., Socco L.V. (2009) "Non uniqueness in surface wave inversion and consequences on seismic site response analyses", Soil Dynamics and Earthquake Engineering, Vol. 29 (6), 982-993.

Haskell, N., 1964, Radiation pattern of surface waves from point sources in a multilayered medium: Bulletin of seismological society of America, 54, no. 1, 377-393.

Herrmann, R. B., and C. Y. Wang, 1980, A numerical study of p-, sv- and sh- wave generation in a plane layered medium: Bulletin of seismological society of America, 70, no. 4, 1015-1036.

Herrmann, R. B., 2002, SURF code, www.eas.slu.edu/People/RBHerrmann/.

Maraschini, M., F. Ernst, D. Boiero, S. Foti, and L.V. Socco, 2008, A new approach for multimodal inversion of Rayleigh and Scholte waves: Proceedings of EAGE Rome, expanded abstract.

Thomson, W. T, 1950., Transmission of elastic waves through a stratified solid medium: Journal of Applied Physics, 21, no. 89.

APPLICATION OF SURFACE WAVE METHODS FOR SEISMIC SITE CHARACTERIZATION

RONCO SCRIVIA (RNS)

Responsible:
Sebastiano Foti

Co-workers:
Giovanni Bianchi
Cesare Comina
Margherita Maraschini

FINAL REPORT

Turin, 31/7/2009

INDEX

1 Introduction

In this report a summary of the results obtained for the characterization of the accelerometric station of Ronco Scrivia of the RAN within Project S4 is presented. The analysis was performed using active surface wave method and refraction method.

Ronco Scrivia RAN station is classified as rock outcrop and a very limited zone of rock alteration and vegetation soil was expected above the bedrock. There is the presence of shale alternated with sandstone outcrop.

The map and the site location are shown in Figure 1 and Figure 2. According to geological information a shallow bedrock is expected.

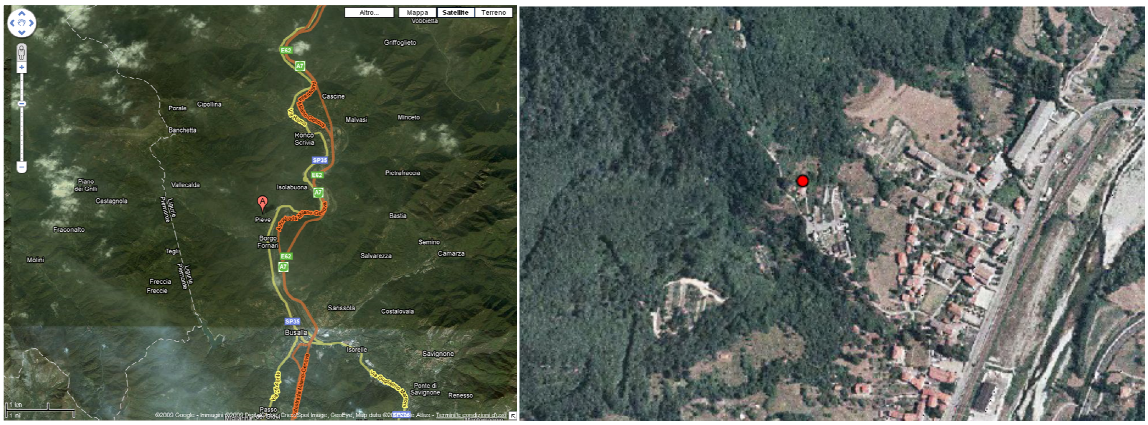

Figure 1 Ronco Scrivia: maps

Figure 2 Ronco Scrivia: site location

Goal of the seismic tests is the estimation of the S-wave velocity profile of the subsoil, and in particular the position of the bedrock. The presence of stiff seismic interfaces between the sediments and the shallow bedrock can cause a relevance of higher modes in the surface wave experimental dispersion curve which has be taken into account in order to provide reliable results.

The primary use of surface wave testing is related to site characterization in terms of shear wave velocity profile. The V_S profile is of primary interest for seismic site response studies and for studies of vibration of foundations and vibration transmission in soils. Other applications are related to the prediction of settlements and to soil-structure interaction.

With respect to the evaluation of seismic site response, it is worth noting the affinity between the model used for the interpretation of surface wave tests and the model adopted for most site responses study. Indeed the application of equivalent linear elastic methods is often associated with layered models (e.g. the code SHAKE and all similar approaches). This affinity is also particularly important in the light of equivalence problems, which arise because of non-uniqueness of the solution in inverse problems. Indeed profiles which are equivalent in terms of Rayleigh wave propagation are also equivalent in term of seismic amplification (Foti et al., 2009).

Many seismic building codes introduce the weighted average of the shear wave velocity profile in the shallowest 30m as to discriminate class of soils to which a similar site amplification effect can be associated. The so-called $V_{S,30}$ can be evaluated very efficiently with surface wave method also because its average nature does not require the high level of accuracy that can be obtained with seismic borehole methods.

In the following a methodological summary of techniques and the description of the results is presented.

For Further explanation of surface wave methodologies, see document: Project S4: ITALIAN STRONG MOTION DATA BASE, Deliverable # 6, Application of Surface wave methods for seismic site characterization, May 2009.

2 Surface wave method

Surface wave method (S.W.M.) is based on the geometrical dispersion, which makes Rayleigh wave velocity frequency dependent in vertically heterogeneous media. High frequency (short wavelength) Rayleigh waves propagate in shallow zones close to the free surface and are informative about their mechanical properties, whereas low frequency (long wavelength) components involve deeper layers. Surface wave tests are typically devoted to the determination of a small strain stiffness profile for the site under investigation. Consequently the dispersion curve will be associated to the variation of medium parameters with depth.

The calculation of the dispersion curve from model parameters is the so called forward problem. Surface wave propagation can be seen as the combination of multiple modes of propagation, i.e. more than one possible velocity can be associated to each frequency value. Including higher modes in the inversion process allows the penetration depth to be increased and a more accurate subsoil profile to be retrieved.

If the dispersion curve is estimated on the basis of experimental data, it is then possible to solve the inverse problem, i.e. the model parameters are identified on the basis of the experimental data collected on the boundary of the medium. The result of the surface wave method is a one-dimensional S wave velocity soil profile.

The standard procedure for surface wave tests is reported in Figure 3. It can be subdivided into three main steps:

1. acquisition of experimental data;
2. signal processing to obtain the experimental dispersion curve;
3. inversion process to estimate shear wave velocity profile at the site.

It is very important to recognize that the above steps are strongly interconnected and their interaction must be adequately accounted for during the whole interpretation process.

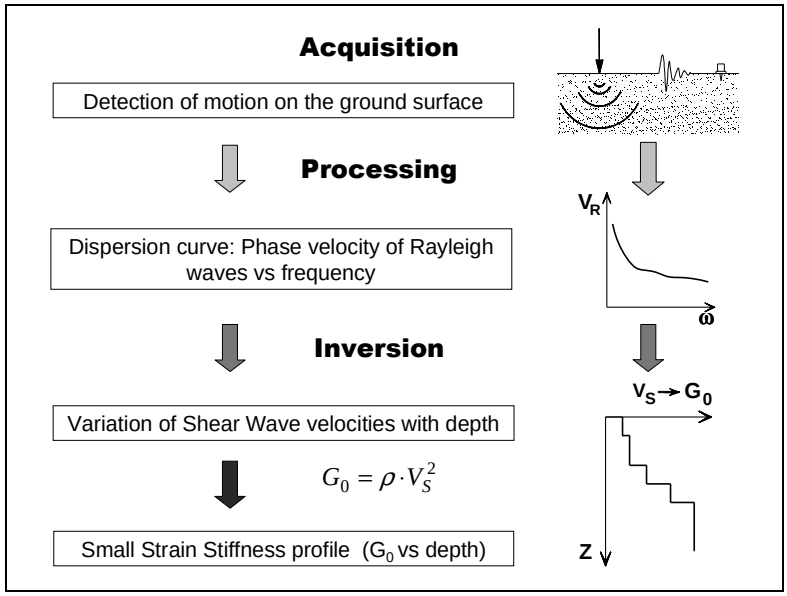

Figure 3 – Flow chart of surface wave tests.

2.1 Acquisition

Active surface wave tests (MASW) and refraction tests at Ronco Scrivia have been performed in October 2008 within the project S4 for the characterization of RAN sites.

Characteristics of sensors are reported in Table 1.

Test	GEOPHONE TYPE	NATURAL FREQUENCY	GEOPHONE NUMBER
MASW/Refraction	vertical SENSOR SM-6/U-B	4,5 Hz	48

Table 1 Ronco Scrivia: receiver characteristics

Acquisition geometry was influenced by the slope and the presence of an embankment.

The spacing between geophones (0.5 m) has been dictated by available testing space at the testing locations, which was very limited because the station is placed close to an urbanised area. The total length of the array is 23.5m. The source is a 5kg sledge hammer. Geometry parameters are summarized in Table 2.

Test	GEOF. N.	SPACING	SOURCE TYPE	ACQUISITION WINDOW	SAMPLING INTERVAL	STACK
MASW	48	0.5 m	Hammer	T = 0.512 s	Δt = 0.25 ms	10
Refraction	48	0.5 m	Hammer	T =0.256 s	Δt = 0.03125 ms	15

Table 2 Ronco Scrivia: Acquisition parameters

Since a shallow bedrock is expected at this site, the synergies between surface wave active methods and P-wave refraction surveys are relevant. Indeed both surveys can be performed with the same testing configuration. In particular P-wave seismic refraction method can in this situation provide relevant information with respect to the position of the interface between the soil cover and the bedrock.

2.2 Processing of surface waves

The processing allows the experimental dispersion curve to be determined.

Multichannel data are processed using a double Fourier Transform, which generates the frequency-wave number spectrum, where the multimodal dispersion curve is easily extracted as the location of spectral maxima.

2.3 Inversion of surface waves

The solution of the inverse Rayleigh problem is the final step in test interpretation. The solution of the forward problem forms the basis of any inversion strategy; the forward problem consists in the calculation of the function whose zeros are dispersion curves of a given model. Assuming a model for the soil deposit, model parameters of the best fitting subsoil profile are obtained minimizing an object function.

The subsoil is modelled as a horizontally layered medium overlaying a halfspace, with constant parameter in the interior of each layer and linear elastic behaviour. Model parameters are thickness, S-wave velocity, P-wave velocity (or Poisson coefficient), and density of each layer and the halfspace. The inversion is performed on S-wave velocities and thicknesses, whereas for the other parameters realistic values are chosen a priori. The number of layer is chosen applying minimum parameterization criterion.

In surface wave analysis it is very common to perform the inversions using only the fundamental mode of propagation. This approach is based on the assumption that the prevailing mode of propagation is the fundamental one; if this is partially true for normal dispersive sites, in several real cases the experimental dispersion curve is on the contrary the result of the superposition of several modes. This may happen in particular when velocity inversions or strong velocity contrasts are present in the shear wave velocity profile. In these stratigraphic conditions the inversion of the only fundamental mode will produce significant errors; moreover all the information contained in higher propagating modes is not used in the inversion process. Therefore, the fundamental mode inversion does not use all the available information, and this affects the result accuracy.

The use of higher modes in the inversion can be helpful both in the low frequency range, in order to increase the investigation depth and to avoid the overestimation of the bedrock velocity, and in the high frequency range in order to provide a more consistent interpretation of shallow interfaces and increase model parameter resolution.

In this work a multimodal misfit function has been used. This function is based on the Haskell-Thomson method for dispersion curve calculation (Thomson 1950, Haskell 1953, Herrmann e Wang 1980, Herrmann 2002). For a given subsoil model, and an experimental data, the misfit of the model is the L^1 norm of the vector containing the absolute value of the determinant of the Haskell-Thomson matrix (which is zeros in correspondence of all the modes of the dispersion curves of the numerical model) evaluated in correspondence of

the experimental data (Maraschini et al. 2008). The misfit function adopted has the advantage of being able to include any dispersive event present in the data without the need of specifying to which mode the data points belong to, avoiding errors arising from mode misidentification, in particular in the low frequency range.

This misfit function is applied in a Global Search Methods (GSM), in order to reduce the possibility of falling in local minima. A uniform random search is applied; ranges for the inversion have been chosen, for the different sites, based on the experimental dispersion curves; in particular the range of the S-wave half space velocity is close to the maximum surface wave velocity retrieved on experimental data.

The results of the inversion are reported as the ensemble of the twenty shear wave velocity profiles which present the minimum misfits with respect to the experimental dispersion curve. In the figures reported a representation based on the misfit is adopted for velocity profiles, so that the darkest colour corresponds to the profile whose dispersion curve has the lowest misfit and better approximation to the reference one; instead for dispersion curves the coloured surface under imposed to the experimental one is a misfit surface, whose zeros are synthetic dispersion curve of the best fitting model.

2.4 Numerical code

The numerical codes used for processing and inversion of surface waves are non commercial codes, implemented at Politecnico di Torino.

3 Ronco Scrivia – Refraction results

The presence of velocity inversions and of the water table can be excluded.
Due to the presence of an embankment, only two shots have been considered for the inversion, moreover for shot 38 (the source is in the centre of the array) only the 24 receivers far form this embankment and for shot 37 (the source is in the end of the array far from the embankment) only 29 receivers have been used for the analysis. The shortness of the array allows a very limited penetration depth. The first breaks of the considered shots are shown in Figure 4.

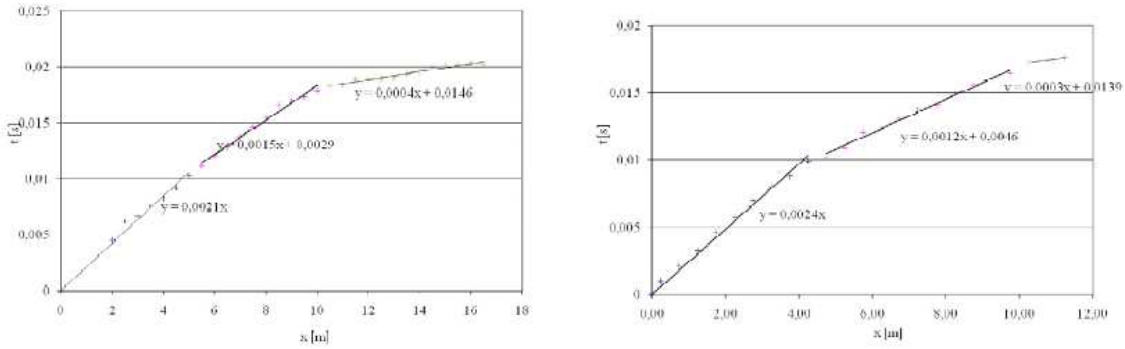

a) Shot 37 b) Shot 38

Figure 4 Ronco Scrivia – First breaks of the two shots considered

For both model, a 2 layer over a halfspace model is identified; parameters are summarized in Table 3.

Shot 37		Shot 38	
P-wave velocity (m/s)	Thickness (m)	P-wave velocity (m/s)	Thickness (m)
480	1.0	420	1.2
670	3.6	830	3.7
2500	-	3300	-

Table 3 Velocity models retrieved by refraction survey

The results of the two profiles are coherent, identifying a soft layer on the top, of about 1m thickness, a stiffer layer below, and the halfspace at about 4,5-5m depth.
For the comparison with surface wave results, an average profile is considered.

4 Ronco Scrivia – Surface wave results

In Figure 5 an example of the f-k spectrum of the data collected at Ronco Scrivia with the picked dispersion curve is presented.

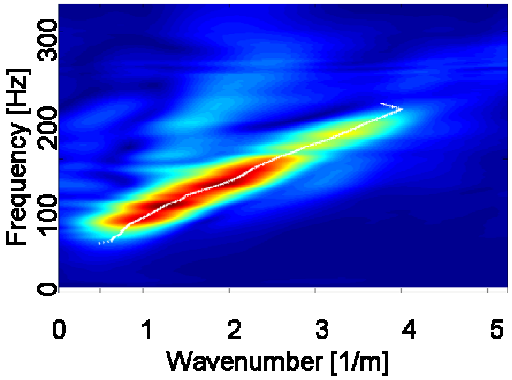

Figure 5 Ronco Scrivia – example of f-k spectrum

From the f-k spectra, several dispersion curves can be retrieved. From all these curves an average curve is estimated (Figure 6).

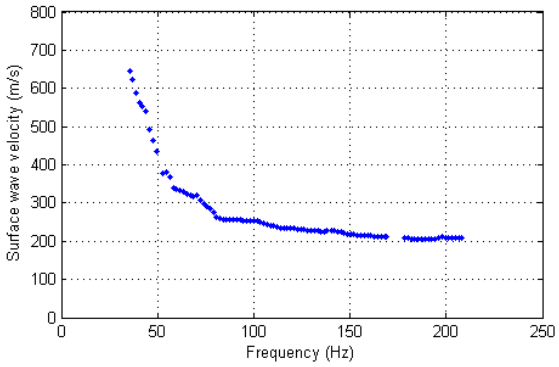

Figure 6 – Ronco Scrivia -Average apparent dispersion curve

Observing the dispersion curve a steep velocity increase in the low frequency range, that can be due to a jump on the first higher mode in the that range can be observed.
Data were inverted using a multimodal stochastic approach, the 20 best fitting profiles are plotted in Figure 7 a), profile colour depends on the misfit, from yellow to blue (best fitting profile). In Figure 7 the best fitting profile is compared with the refraction result, and in Figure 8 the experimental dispersion curve is compared with the determinant surface of the best fitting model. We can note that the experimental points follow in the minima of the determinant surface, and the low frequency part of the experimental dispersion curve tends to go to the first higher mode, probably due to the marked impedance contrast between topsoil and bedrock. Moreover it can be noted that the position of the first interface is in good agreement with the refraction results, and the position of the second interface is acceptable.

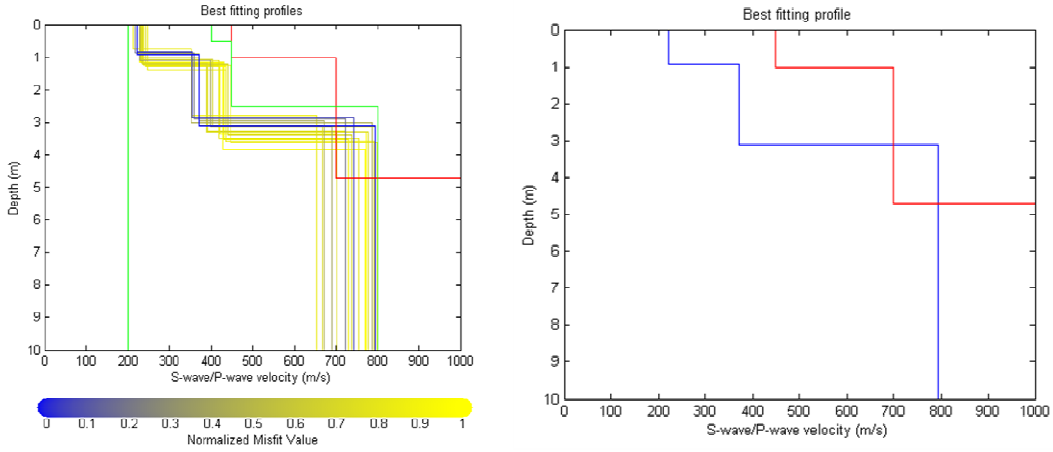

Figure 7 Ronco Scrivia – a) Monte Carlo results (from yellow to blue) of the inversion with the boundaries (green) compared with the refraction result (red). b) Ronco Scrivia – Best fitting profile (blue) compared with the refraction result (red).

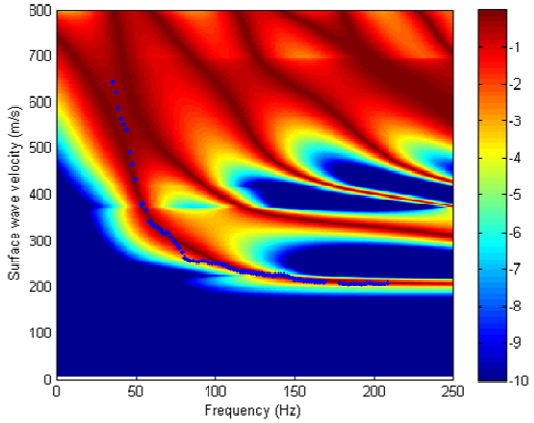

Figure 8 Ronco Scrivia – Experimental dispersion curve compared with the misfit surface of the best fitting model

The parameters of the best fitting profile are summarized in Table 4.

Vs (m/s)	Thickness (m)	Poisson coefficient	Density (T/m^3)
222	0.9	0.3	1.8
371	2.2	0.3	1.8
795	-	0.3	1.8

Table 4 Ronco Scrivia: subsoil parameters of the best fitting profile.

References

Project S4: ITALIAN STRONG MOTION DATA BASE, Deliverable # 6, Application of Surface wave methods for seismic site characterization, May 2009.

Foti S., Comina C., Boiero D., Socco L.V. (2009) "Non uniqueness in surface wave inversion and consequences on seismic site response analyses", Soil Dynamics and Earthquake Engineering, Vol. 29 (6), 982-993.

Haskell, N., 1964, Radiation pattern of surface waves from point sources in a multilayered medium: Bulletin of seismological society of America, 54, no. 1, 377-393.

Herrmann, R. B., and C. Y. Wang, 1980, A numerical study of p-, sv- and sh- wave generation in a plane layered medium: Bulletin of seismological society of America, 70, no. 4, 1015-1036.

Herrmann, R. B., 2002, SURF code, www.eas.slu.edu/People/RBHerrmann/.

Maraschini, M., F. Ernst, D. Boiero, S. Foti, and L.V. Socco, 2008, A new approach for multimodal inversion of Rayleigh and Scholte waves: Proceedings of EAGE Rome, expanded abstract.

Thomson, W. T, 1950., Transmission of elastic waves through a stratified solid medium: Journal of Applied Physics, 21, no. 89.

APPLICATION OF SURFACE WAVE METHODS FOR SEISMIC SITE CHARACTERIZATION

SANTA CROCE (SCR)

Responsible:
Sebastiano Foti

Co-workers:
Giovanni Bianchi
Paolo Bergamo
Margherita Maraschini

FINAL REPORT

Turin, 11/02/2010

INDEX

1 Introduction

In this report a summary of the results obtained for the characterization of the accelerometric station of Santa Croce of the RAN within Project S4 is presented. The analysis was performed using active surface wave method.

Santa Croce RAN station is located in an uncultivated area near the city centre. A thin weathering layer is expected to lie upon the bedrock.

The map, site location and measurements arrays are shown in Figure1, Figure 2 and Figure 3.

Figure 1 Santa Croce: maps

Figure 2 Santa Croce: array map. The red line represents the active measurements array.

Figure 3 Santa Croce: site location and active measurement array.

Goal of the seismic tests is the estimation of the S-wave velocity profile of the subsoil, and in particular the position of the bedrock. The presence of stiff seismic interfaces between the sediments and the shallow bedrock can cause a relevance of higher modes in the surface wave experimental dispersion curve which has be taken into account in order to provide reliable results.

The primary use of surface wave testing is related to site characterization in terms of shear wave velocity profile. The V_S profile is of primary interest for seismic site response studies and for studies of vibration of foundations and vibration transmission in soils. Other applications are related to the prediction of settlements and to soil-structure interaction.

With respect to the evaluation of seismic site response, it is worth noting the affinity between the model used for the interpretation of surface wave tests and the model adopted for most site responses study. Indeed the application of equivalent linear elastic methods is often associated with layered models (e.g. the code SHAKE and all similar approaches). This affinity is also particularly important in the light of equivalence problems, which arise because of non-uniqueness of the solution in inverse problems. Indeed profiles which are equivalent in terms of Rayleigh wave propagation are also equivalent in term of seismic amplification (Foti et al., 2009).

Many seismic building codes introduce the weighted average of the shear wave velocity profile in the shallowest 30m as to discriminate class of soils to which a similar site amplification effect can be associated. The so-called $V_{S,30}$ can be evaluated very efficiently with surface wave method also because its average nature does not require the high level of accuracy that can be obtained with seismic borehole methods.

In the following a methodological summary of techniques and the description of the results is presented.

For Further explanation of surface wave methodologies, see document: Project S4: ITALIAN STRONG MOTION DATA BASE, Deliverable # 6, Application of Surface wave methods for seismic site characterization, May 2009.

2 Surface wave method

Surface wave method (S.W.M.) is based on the geometrical dispersion, which makes Rayleigh wave velocity frequency dependent in vertically heterogeneous media. High frequency (short wavelength) Rayleigh waves propagate in shallow zones close to the free surface and are informative about their mechanical properties, whereas low frequency (long wavelength) components involve deeper layers. Surface wave tests are typically devoted to the determination of a small strain stiffness profile for the site under investigation. Consequently the dispersion curve will be associated to the variation of medium parameters with depth.

The calculation of the dispersion curve from model parameters is the so called forward problem. Surface wave propagation can be seen as the combination of multiple modes of propagation, i.e. more than one possible velocity can be associated to each frequency value. Including higher modes in the inversion process allows the penetration depth to be increased and a more accurate subsoil profile to be retrieved.

If the dispersion curve is estimated on the basis of experimental data, it is then possible to solve the inverse problem, i.e. the model parameters are identified on the basis of the experimental data collected on the boundary of the medium. The result of the surface wave method is a one-dimensional S wave velocity soil profile.

The standard procedure for surface wave tests is reported in Figure 4. It can be subdivided into three main steps:

1. acquisition of experimental data;
2. signal processing to obtain the experimental dispersion curve;
3. inversion process to estimate shear wave velocity profile at the site.

It is very important to recognize that the above steps are strongly interconnected and their interaction must be adequately accounted for during the whole interpretation process.

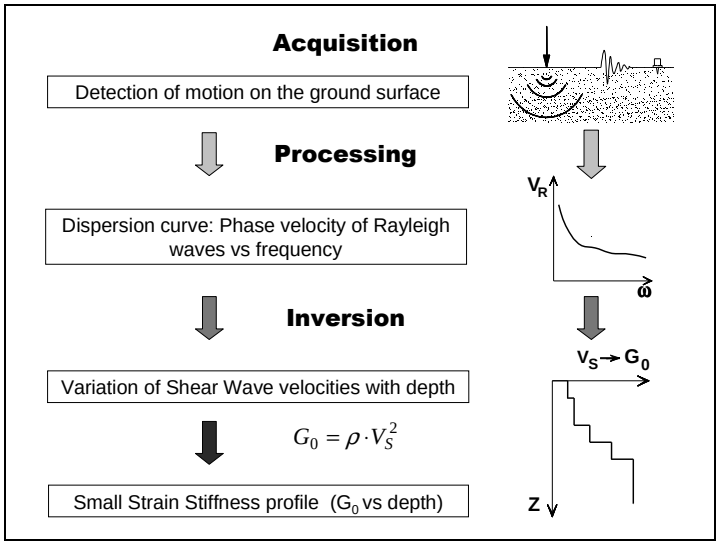

Figure 4 – Flow chart of surface wave tests.

2.1 Acquisition

Active (MASW) surface wave tests at Santa Croce have been performed in May 2009 within the project S4 for the characterization of RAN sites.

Characteristics of sensors are reported in Table 1.

Test	GEOPHONE TYPE	NATURAL FREQUENCY	GEOPHONE NUMBER
MASW	vertical SENSOR SM-6/U-B	4,5 Hz	24

Table 1 Santa Croce: receiver characteristics

24 receivers were used for active tests, with a spacing of 1 m between neighbouring geophones, so that the total length of the array is 23 m. The source is a 5kg sledge hammer. Acquisition parameters are summarized in Table 2

Test	GEOF. N.	SPACING	SOURCE TYPE	ACQUISITION WINDOW	SAMPLING INTERVAL	STACK
MASW	24	1 m	Hammer	T = 2 s	Δt = 0.5 ms	10

Table 2 Santa Croce: Acquisition parameters

2.2 Processing of active surface wave data

The processing allows the experimental dispersion curve to be determined.

Multichannel data are processed using a double Fourier Transform, which generates the frequency-wave number spectrum, where the multimodal dispersion curve is easily extracted as the location of spectral maxima.

2.3 Inversion of surface waves

The solution of the inverse Rayleigh problem is the final step in test interpretation. The solution of the forward problem forms the basis of any inversion strategy; the forward problem consists in the calculation of the function whose zeros are dispersion curves of a given model. Assuming a model for the soil deposit, model parameters of the best fitting subsoil profile are obtained minimizing an object function.

The subsoil is modelled as a horizontally layered medium overlaying a halfspace, with constant parameter in the interior of each layer and linear elastic behaviour. Model parameters are thickness, S-wave velocity, P-wave velocity (or Poisson coefficient), and density of each layer and the halfspace. The inversion is performed on S-wave velocities and thicknesses, whereas for the other parameters realistic values are chosen a priori. The number of layer is chosen applying minimum parameterization criterion.

In surface wave analysis it is very common to perform the inversions using only the fundamental mode of propagation. This approach is based on the assumption that the prevailing mode of propagation is the fundamental one; if this is partially true for normal

dispersive sites, in several real cases the experimental dispersion curve is on the contrary the result of the superposition of several modes. This may happen in particular when velocity inversions or strong velocity contrasts are present in the shear wave velocity profile. In these stratigraphic conditions the inversion of the only fundamental mode will produce significant errors; moreover all the information contained in higher propagating modes is not used in the inversion process. Therefore, the fundamental mode inversion does not use all the available information, and this affects the result accuracy.

The use of higher modes in the inversion can be helpful both in the low frequency range, in order to increase the investigation depth and to avoid the overestimation of the bedrock velocity, and in the high frequency range in order to provide a more consistent interpretation of shallow interfaces and increase model parameter resolution.

In this work a multimodal misfit function has been used. This function is based on the Haskell-Thomson method for dispersion curve calculation (Thomson 1950, Haskell 1953, Herrmann e Wang 1980, Herrmann 2002). For a given subsoil model, and an experimental data, the misfit of the model is the L^1 norm of the vector containing the absolute value of the determinant of the Haskell-Thomson matrix (which is zeros in correspondence of all the modes of the dispersion curves of the numerical model) evaluated in correspondence of the experimental data (Maraschini et al. 2008). The misfit function adopted has the advantage of being able to include any dispersive event present in the data without the need of specifying to which mode the data points belong to, avoiding errors arising from mode misidentification, in particular in the low frequency range.

This misfit function is applied in a Global Search Methods (GSM), in order to reduce the possibility of falling in local minima. A uniform random search is applied; ranges for the inversion have been chosen, for the different sites, based on the experimental dispersion curves; in particular the range of the S-wave half space velocity is close to the maximum surface wave velocity retrieved on experimental data.

The results of the inversion are reported as the ensemble of the best shear wave velocity profiles chosen according to a chi-square test (see Socco et al., 2008). It can be assumed that the experimental dispersion curve is affected by a Gaussian error with a known standard deviation, so that the probability density function of data $\rho_D(d)$ can be described by a discrete m-dimensional Gaussian (where m are the model parameters) and the sample variance variable of each random vector (dispersion curve) extracted from the data pdf is distributed according to a chi-square probability density. According to these assumptions we adopt a misfit function with the structure of a chi-square and this allows a statistical test to be applied to the variances of the synthetic dispersion curves with respect to the experimental one d_{obs}. Assuming that the best fitting curve d_{opt} belongs to the distribution $\rho_D(d_{obs})$ all models belonging to the distribution $\rho_D(d_{opt})$ and consistent with the data within a fixed level of confidence α are selected. As the ratio between chi-square variables follows a Fisher distribution a one–tailed F test can be performed:

$$F_\alpha(dof_{dopt}, dof_{g(m)}) < \frac{\chi^2_{dopt}}{\chi^2_{g(m)}}$$

where α is the chosen level of confidence, dof_{dopt} and $dof_{g(m)}$ are the degrees of freedom of the Fischer distribution and χ^2_{dopt} and $\chi^2_{g(m)}$ are the misfit of the best fitting curve and the misfit of all the others respectively. All models passing such test are selected. In the figures reported a representation based on the misfit is adopted for velocity profiles, so that

the darkest colour corresponds to the profile whose dispersion curve has the lowest misfit and better approximation to the reference one; instead for dispersion curves the coloured surface under imposed to the experimental one is a misfit surface, whose zeros are synthetic dispersion curve of the best fitting model.

2.4 Numerical code

The numerical codes used for processing and inversion of surface waves are non commercial codes, implemented at Politecnico di Torino.

3 Santa Croce – Surface wave results

In Figure 5 an example of the f-k spectrum of the active data collected at Santa Croce is presented.

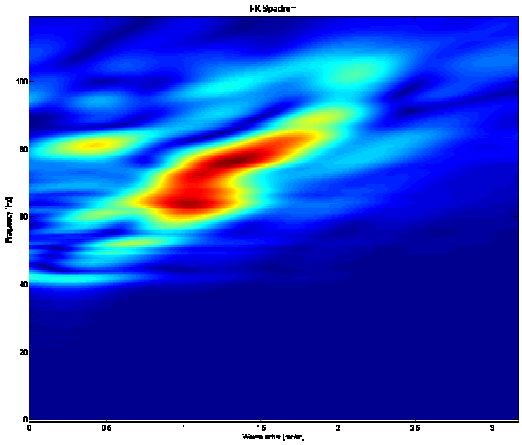

Figure 5 Santa Croce – example of f-k spectrum

From the f-k spectra, two dispersion curves can be retrieved. From all these curves an average curve is estimated (Figure 6).

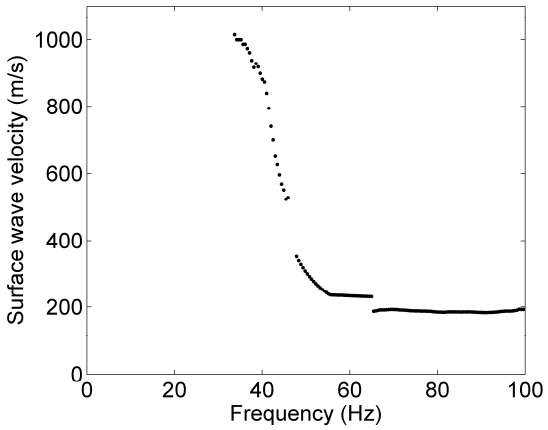

Figure 6 – Santa Croce - Average apparent dispersion curve

The apparent dispersion curve is made up of two branches which probably follow two propagation modes: note that one branch is characterized by a steep velocity increase at about 40 Hz, probably jumping from one mode to another.
Data were inverted using a multimodal stochastic approach, the best fitting profiles are plotted in Figure 7, profile colour depends on the misfit, from yellow to blue (best fitting profile). In Figure 8 the experimental dispersion curve is compared with the determinant surface of the best fitting model. We can note that the experimental points fall into the minima of the determinant surface, and that a branch of the apparent dispersion curve jumps from fundamental mode to the to the 1st higher mode at around 40 Hz, probably because of the impedance contrast between topsoil and bedrock.

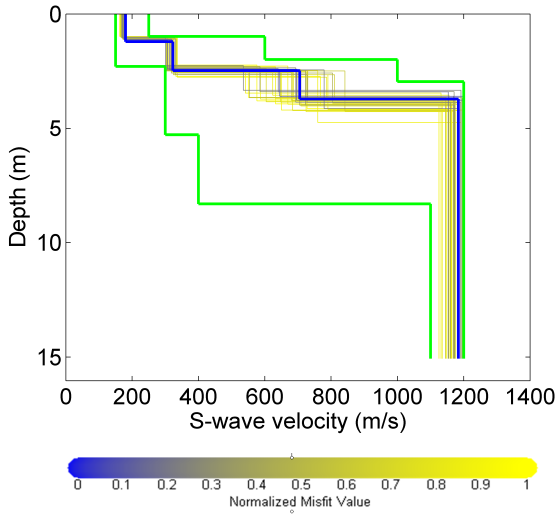

Figure 7 Santa Croce – Monte Carlo results (from yellow to blue) of the inversion with the boundaries (green).

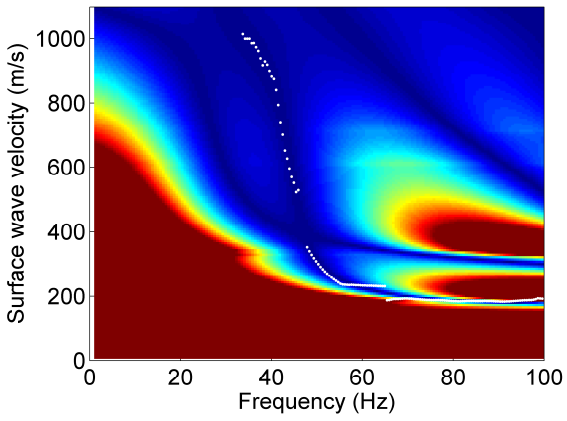

Figure 8 Santa Croce – Experimental dispersion curve compared with the misfit surface of the best fitting model

The parameters of the best fitting profile are summarized in Table 4.

Vs (m/s)	Thickness (m)	Poisson coefficient	Density (T/m^3)
180	1.2	0.3	1.8
323	1.2	0.3	1.8
705	1.3	0.3	1.8
1184		0.3	1.8

Table 3 Santa Croce: subsoil parameters of the best fitting profile.

References

Project S4: ITALIAN STRONG MOTION DATA BASE, Deliverable # 6, Application of Surface wave methods for seismic site characterization, May 2009.

Foti S., Comina C., Boiero D., Socco L.V. (2009) "Non uniqueness in surface wave inversion and consequences on seismic site response analyses", Soil Dynamics and Earthquake Engineering, Vol. 29 (6), 982-993.

Haskell, N., 1964, Radiation pattern of surface waves from point sources in a multilayered medium: Bulletin of seismological society of America, 54, no. 1, 377-393.

Herrmann, R. B., and C. Y. Wang, 1980, A numerical study of p-, sv- and sh- wave generation in a plane layered medium: Bulletin of seismological society of America, 70, no. 4, 1015-1036.

Herrmann, R. B., 2002, SURF code, www.eas.slu.edu/People/RBHerrmann/.

Maraschini, M., F. Ernst, D. Boiero, S. Foti, and L.V. Socco, 2008, A new approach for multimodal inversion of Rayleigh and Scholte waves: Proceedings of EAGE Rome, expanded abstract.

Thomson, W. T, 1950., Transmission of elastic waves through a stratified solid medium: Journal of Applied Physics, 21, no. 89.

APPLICATION OF SURFACE WAVE METHODS FOR SEISMIC SITE CHARACTERIZATION

SESTRI LEVANTE (SEL)

Responsible:
Sebastiano Foti

Co-workers:
Giovanni Bianchi
Cesare Comina
Margherita Maraschini

FINAL REPORT

Turin, 31/7/2009

INDEX

1 Introduction

In this report a summary of the results obtained for the characterization of the accelerometric station of Sestri Levante of the RAN within Project S4 is presented. The analysis was performed using active surface wave method, the refraction data was not used, because a velocity inversion is expected.

The map and the site location are shown in Figure 1 and Figure 2. A stiff superficial layer, composed by gravels and pebbles, can be observed, which is used for the passage of trucks (Figure 2). According to geological information a shallow bedrock is expected.

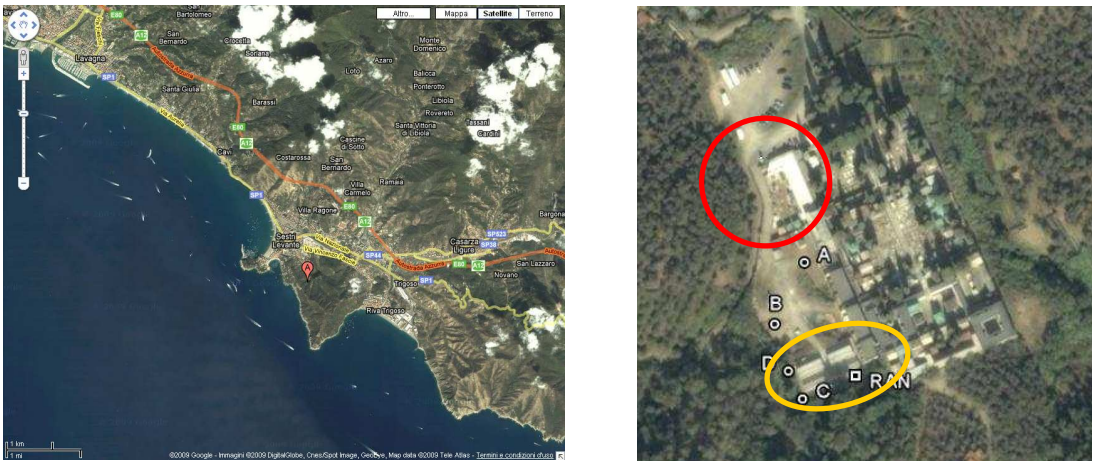

Figure 1 Sestri Levante: maps

Figure 2 Sestri Levante: site location

Goal of the seismic tests is the estimation of the S-wave velocity profile of the subsoil, and in particular the position of the bedrock.

The primary use of surface wave testing is related to site characterization in terms of shear wave velocity profile. The V_S profile is of primary interest for seismic site response studies and for studies of vibration of foundations and vibration transmission in soils. Other applications are related to the prediction of settlements and to soil-structure interaction.

With respect to the evaluation of seismic site response, it is worth noting the affinity between the model used for the interpretation of surface wave tests and the model adopted for most site responses study. Indeed the application of equivalent linear elastic methods is often associated with layered models (e.g. the code SHAKE and all similar approaches). This affinity is also particularly important in the light of equivalence problems, which arise because of non-uniqueness of the solution in inverse problems. Indeed profiles which are equivalent in terms of Rayleigh wave propagation are also equivalent in term of seismic amplification (Foti et al., 2009).

Many seismic building codes introduce the weighted average of the shear wave velocity profile in the shallowest 30m as to discriminate class of soils to which a similar site amplification effect can be associated. The so-called $V_{S,30}$ can be evaluated very efficiently with surface wave method also because its average nature does not require the high level of accuracy that can be obtained with seismic borehole methods.

In the following a methodological summary of techniques and the description of the results is presented.

For Further explanation of surface wave methodologies, see document: Project S4: ITALIAN STRONG MOTION DATA BASE, Deliverable # 6, Application of Surface wave methods for seismic site characterization, May 2009.

2 Surface wave method

Surface wave method (S.W.M.) is based on the geometrical dispersion, which makes Rayleigh wave velocity frequency dependent in vertically heterogeneous media. High frequency (short wavelength) Rayleigh waves propagate in shallow zones close to the free surface and are informative about their mechanical properties, whereas low frequency (long wavelength) components involve deeper layers. Surface wave tests are typically devoted to the determination of a small strain stiffness profile for the site under investigation. Consequently the dispersion curve will be associated to the variation of medium parameters with depth.

The calculation of the dispersion curve from model parameters is the so called forward problem. Surface wave propagation can be seen as the combination of multiple modes of propagation, i.e. more than one possible velocity can be associated to each frequency value. Including higher modes in the inversion process allows the penetration depth to be increased and a more accurate subsoil profile to be retrieved.

If the dispersion curve is estimated on the basis of experimental data, it is then possible to solve the inverse problem, i.e. the model parameters are identified on the basis of the experimental data collected on the boundary of the medium. The result of the surface wave method is a one-dimensional S wave velocity soil profile.

The standard procedure for surface wave tests is reported in Figure 3. It can be subdivided into three main steps:

1. acquisition of experimental data;
2. signal processing to obtain the experimental dispersion curve;
3. inversion process to estimate shear wave velocity profile at the site.

It is very important to recognize that the above steps are strongly interconnected and their interaction must be adequately accounted for during the whole interpretation process.

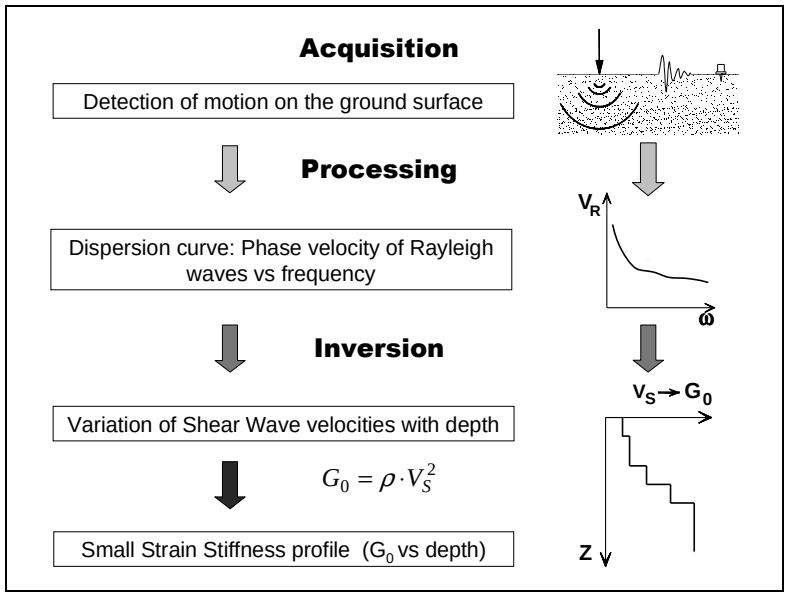

Figure 3 – Flow chart of surface wave tests.

2.1 Acquisition

Active surface wave tests (MASW) and refraction tests at Sestri Levante have been performed in October 2008 within the project S4 for the characterization of RAN sites.

Characteristics of sensors are reported in Table 1.

Test	GEOPHONE TYPE	NATURAL FREQUENCY	GEOPHONE NUMBER
MASW/Refraction	vertical SENSOR SM-6/U-B	4,5 Hz	48

Table 1 Sestri Levante: receiver characteristics

The total length of the array is 32.9m. The source is a 5kg sledge hammer. Geometry parameters are summarized in Table 2.

Test	GEOF. N.	SPACING	SOURCE TYPE	ACQUISITION WINDOW	SAMPLING INTERVAL	STACK
MASW	48	0.7 m	Hammer	T = 0.512 s	Δt = 0.25 ms	10/12/15

Table 2 Sestri Levante: Acquisition parameters

2.2 Processing of surface waves

The processing allows the experimental dispersion curve to be determined.

Multichannel data are processed using a double Fourier Transform, which generates the frequency-wave number spectrum, where the multimodal dispersion curve is easily extracted as the location of spectral maxima.

2.3 Inversion of surface waves

The solution of the inverse Rayleigh problem is the final step in test interpretation. The solution of the forward problem forms the basis of any inversion strategy; the forward problem consists in the calculation of the function whose zeros are dispersion curves of a given model. Assuming a model for the soil deposit, model parameters of the best fitting subsoil profile are obtained minimizing an object function.

The subsoil is modelled as a horizontally layered medium overlaying a halfspace, with constant parameter in the interior of each layer and linear elastic behaviour. Model parameters are thickness, S-wave velocity, P-wave velocity (or Poisson coefficient), and density of each layer and the halfspace. The inversion is performed on S-wave velocities and thicknesses, whereas for the other parameters realistic values are chosen a priori. The number of layer is chosen applying minimum parameterization criterion.

In surface wave analysis it is very common to perform the inversions using only the fundamental mode of propagation. This approach is based on the assumption that the prevailing mode of propagation is the fundamental one; if this is partially true for normal dispersive sites, in several real cases the experimental dispersion curve is on the contrary the result of the superposition of several modes. This may happen in particular when velocity inversions or strong velocity contrasts are present in the shear wave velocity profile. In these stratigraphic conditions the inversion of the only fundamental mode will produce significant errors; moreover all the information contained in higher propagating modes is not used in the inversion process. Therefore, the fundamental mode inversion does not use all the available information, and this affects the result accuracy.

The use of higher modes in the inversion can be helpful both in the low frequency range, in order to increase the investigation depth and to avoid the overestimation of the bedrock velocity, and in the high frequency range in order to provide a more consistent interpretation of shallow interfaces and increase model parameter resolution.

In this work a multimodal misfit function has been used. This function is based on the Haskell-Thomson method for dispersion curve calculation (Thomson 1950, Haskell 1953, Herrmann e Wang 1980, Herrmann 2002). For a given subsoil model, and an experimental data, the misfit of the model is the L^1 norm of the vector containing the absolute value of the determinant of the Haskell-Thomson matrix (which is zeros in correspondence of all

the modes of the dispersion curves of the numerical model) evaluated in correspondence of the experimental data (Maraschini et al. 2008). The misfit function adopted has the advantage of being able to include any dispersive event present in the data without the need of specifying to which mode the data points belong to, avoiding errors arising from mode misidentification, in particular in the low frequency range.

This misfit function is applied in a Global Search Methods (GSM), in order to reduce the possibility of falling in local minima. A uniform random search is applied; ranges for the inversion have been chosen, for the different sites, based on the experimental dispersion curves; in particular the range of the S-wave half space velocity is close to the maximum surface wave velocity retrieved on experimental data.

The results of the inversion are reported as the ensemble of the twenty shear wave velocity profiles which present the minimum misfits with respect to the experimental dispersion curve. In the figures reported a representation based on the misfit is adopted for velocity profiles, so that the darkest colour corresponds to the profile whose dispersion curve has the lowest misfit and better approximation to the reference one; instead for dispersion curves the coloured surface under imposed to the experimental one is a misfit surface, whose zeros are synthetic dispersion curve of the best fitting model.

2.4 Numerical code

The numerical codes used for processing and inversion of surface waves are non commercial codes, implemented at Politecnico di Torino.

3 Sestri Levante – Surface wave results

The presence of stiff seismic interfaces between the sediments and the shallow bedrock, and of a stiff layer on the top, which is expected at the site location, can cause a relevance of higher mode generation in the surface wave apparent dispersion curve which must be taken into account in order to provide reliable results.
In Figure 4 an example of the f-k spectrum of the data collected at Sestri Levante is presented.

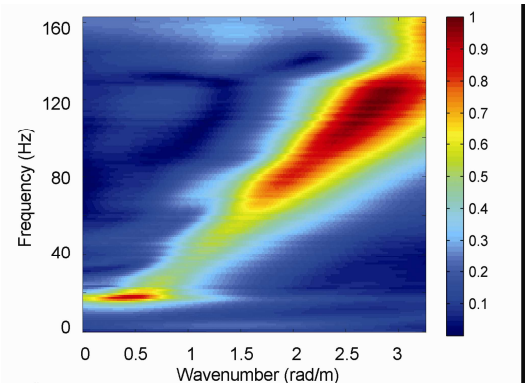

Figure 4 Sestri Levante – example of f-k spectrum

From the f-k spectra, several dispersion curves can be retrieved. From all these curves an average curve is estimated (Figure 5).

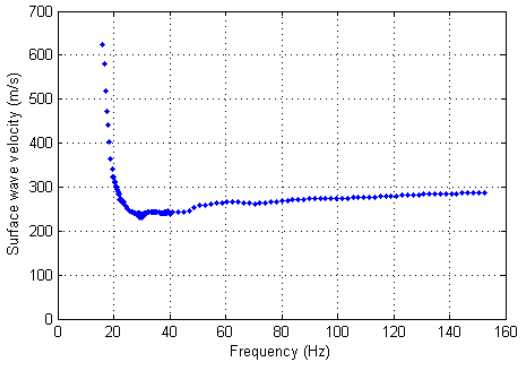

Figure 5 – Sestri Levante -Average apparent dispersion curve

Observing the dispersion curve, a steep velocity increase in the low frequency range, that can be due to a jump on the first higher mode in that range, and a velocity increase in the high frequency range, that can be due to a velocity inversion, can be remarked.
Data were inverted using a multimodal stochastic approach, the 20 best fitting profiles are plotted in Figure 6 a), profile colour depends on the misfit, from yellow to blue (best fitting profile). In Figure 7 the experimental dispersion curve is compared with the determinant surface of the best fitting model. We can note that the experimental points follow in the minima of the determinant surface.

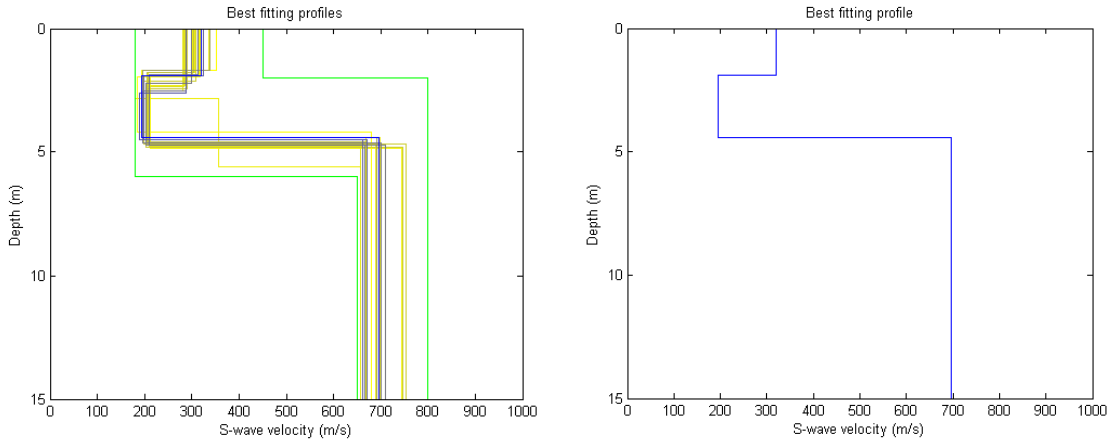

Figure 6 Sestri Levante – a) Monte Carlo results (from yellow to blue) of the inversion with the boundaries (green) b) Sestri Levante – Best fitting profile

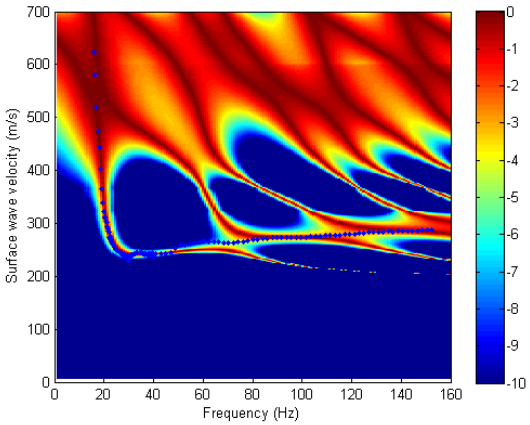

Figure 7 Sestri Levante – Experimental dispersion curve compared with the misfit surface of the best fitting model

The parameters of the best fitting profile are summarized in Table 3.

Vs (m/s)	Thickness (m)	Poisson coefficient	Density (T/m^3)
321	1.9	0.3	1.8
194	2.5	0.3	1.8
697		0.3	1.8

Table 3 Sestri Levante: subsoil parameters of the best fitting profile.

References

Project S4: ITALIAN STRONG MOTION DATA BASE, Deliverable # 6, Application of Surface wave methods for seismic site characterization, May 2009.

Foti S., Comina C., Boiero D., Socco L.V. (2009) "Non uniqueness in surface wave inversion and consequences on seismic site response analyses", Soil Dynamics and Earthquake Engineering, Vol. 29 (6), 982-993.

Haskell, N., 1964, Radiation pattern of surface waves from point sources in a multilayered medium: Bulletin of seismological society of America, 54, no. 1, 377-393.

Herrmann, R. B., and C. Y. Wang, 1980, A numerical study of p-, sv- and sh- wave generation in a plane layered medium: Bulletin of seismological society of America, 70, no. 4, 1015-1036.

Herrmann, R. B., 2002, SURF code, www.eas.slu.edu/People/RBHerrmann/.

Maraschini, M., F. Ernst, D. Boiero, S. Foti, and L.V. Socco, 2008, A new approach for multimodal inversion of Rayleigh and Scholte waves: Proceedings of EAGE Rome, expanded abstract.

Thomson, W. T, 1950., Transmission of elastic waves through a stratified solid medium: Journal of Applied Physics, 21, no. 89.

APPLICATION OF SURFACE WAVE METHODS FOR SEISMIC SITE CHARACTERIZATION

TORTORICI (TOR)

Responsible:
Sebastiano Foti

Co-workers:
Giovanni Bianchi
Margherita Maraschini
Paolo Bergamo

FINAL REPORT

Turin, 19/01/2010

INDEX

1 Introduction

In this report a summary of the results obtained for the characterization of the accelerometric station of Tortorici of the RAN within Project S4 is presented. The analysis was performed using active surface wave method and refraction method.

Tortorici RAN station is located on a hillside outside the urban area of Tortorici: a limited zone of rock alteration and vegetation soil is expected above the bedrock.

The map and the site location are shown in Figure 1 and Figure 2.

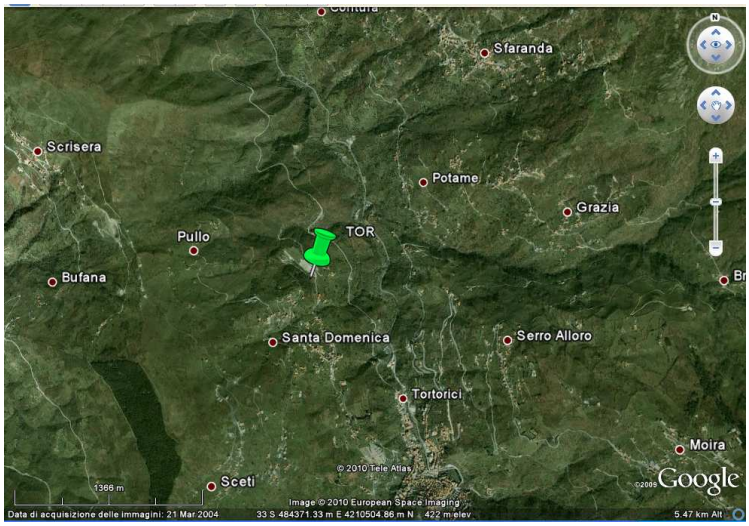

Figure 1 Tortorici: map

Figure 2 Tortorici: acquisition array

Goal of the seismic tests is the estimation of the S-wave velocity profile of the subsoil, and in particular the position of the bedrock . The presence of stiff seismic interfaces between the sediments and the shallow bedrock can cause a relevance of higher modes in the surface wave experimental dispersion curve which has be taken into account in order to provide reliable results.

The primary use of surface wave testing is related to site characterization in terms of shear wave velocity profile. The V_S profile is of primary interest for seismic site response studies and for studies of vibration of foundations and vibration transmission in soils. Other applications are related to the prediction of settlements and to soil-structure interaction.

With respect to the evaluation of seismic site response, it is worth noting the affinity between the model used for the interpretation of surface wave tests and the model adopted for most site responses study. Indeed the application of equivalent linear elastic methods is often associated with layered models (e.g. the code SHAKE and all similar approaches). This affinity is also particularly important in the light of equivalence problems, which arise because of non-uniqueness of the solution in inverse problems. Indeed profiles which are equivalent in terms of Rayleigh wave propagation are also equivalent in term of seismic amplification (Foti et al., 2009).

Many seismic building codes introduce the weighted average of the shear wave velocity profile in the shallowest 30m as to discriminate class of soils to which a similar site amplification effect can be associated. The so-called $V_{S,30}$ can be evaluated very efficiently with surface wave method also because its average nature does not require the high level of accuracy that can be obtained with seismic borehole methods.

In the following a methodological summary of techniques and the description of the results is presented.

For Further explanation of surface wave methodologies, see document: Project S4: ITALIAN STRONG MOTION DATA BASE, Deliverable # 6, Application of Surface wave methods for seismic site characterization, May 2009.

2 Surface wave method

Surface wave method (S.W.M.) is based on the geometrical dispersion, which makes Rayleigh wave velocity frequency dependent in vertically heterogeneous media. High frequency (short wavelength) Rayleigh waves propagate in shallow zones close to the free surface and are informative about their mechanical properties, whereas low frequency (long wavelength) components involve deeper layers. Surface wave tests are typically devoted to the determination of a small strain stiffness profile for the site under investigation. Consequently the dispersion curve will be associated to the variation of medium parameters with depth.

The calculation of the dispersion curve from model parameters is the so called forward problem. Surface wave propagation can be seen as the combination of multiple modes of propagation, i.e. more than one possible velocity can be associated to each frequency value. Including higher modes in the inversion process allows the penetration depth to be increased and a more accurate subsoil profile to be retrieved.

If the dispersion curve is estimated on the basis of experimental data, it is then possible to solve the inverse problem, i.e. the model parameters are identified on the basis of the experimental data collected on the boundary of the medium. The result of the surface wave method is a one-dimensional S wave velocity soil profile.

The standard procedure for surface wave tests is reported in Figure 3. It can be subdivided into three main steps:

1. acquisition of experimental data;
2. signal processing to obtain the experimental dispersion curve;
3. inversion process to estimate shear wave velocity profile at the site.

It is very important to recognize that the above steps are strongly interconnected and their interaction must be adequately accounted for during the whole interpretation process.

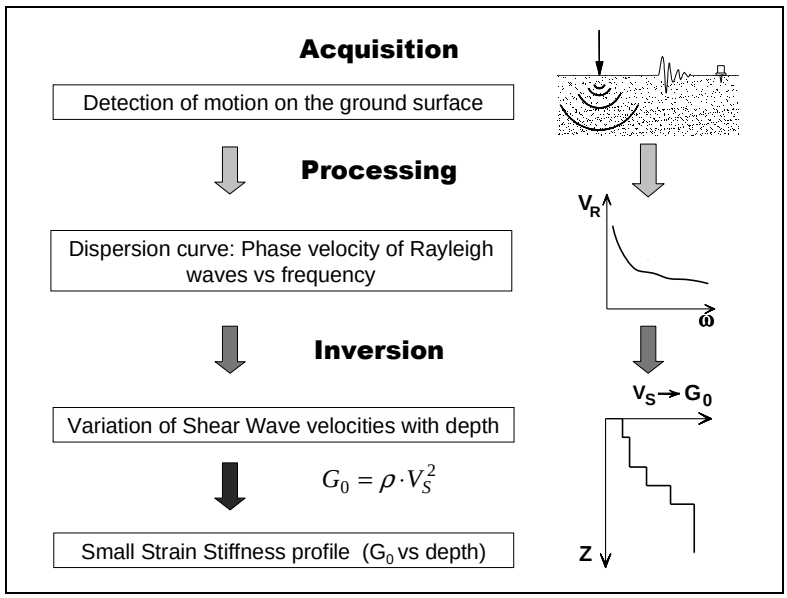

Figure 3 – Flow chart of surface wave tests.

2.1 Acquisition

Active surface wave tests (MASW) and refraction tests at Tortorici have been performed in May 2009 within the project S4 for the characterization of RAN sites.

Characteristics of sensors are reported in Table 1.

Test	GEOPHONE TYPE	NATURAL FREQUENCY	GEOPHONE NUMBER
MASW/Refraction	vertical SENSOR SM-6/U-B	4,5 Hz	24

Table 1 Tortorici: receiver characteristics

Acquisition array was placed on a soccer pitch very close to the RAN station: two different acquisition geometries were arranged. In the first case a spacing between geophones of 1 m was chosen, so that the overall length of the survey line is 23 m: then the spacing between neighbouring receivers was doubled yielding a 46 m long survey line. In both cases 24 receivers were used. Refraction tests were performed using both configurations, MASW

tests were carried out using the 46 m long acquisition geometry. In both cases a 5kg sledge hammer was used as source. Acquisition parameters are summarized in Table 2.

Test	GEOF. N.	SPACING	SOURCE TYPE	ACQUISITION WINDOW	SAMPLING INTERVAL	STACK
MASW	24	2 m	Hammer	T = 2 s	Δt = 0.5 ms	5
Refraction	24	1- 2 m	Hammer	T =1 s	Δt = 0.0625 ms	5

Table 2 Tortorici: Acquisition parameters

The acquisition was performed on a soccer pitch which lies on a terracing carried out along the hillside: P-wave refraction tests were carried out in order to locate the border between the filling material of the terracing and the hillside and to retrieve possible lateral variations.

2.2 Processing of surface waves

The processing allows the experimental dispersion curve to be determined.

Multichannel data are processed using a double Fourier Transform, which generates the frequency-wave number spectrum, where the multimodal dispersion curve is easily extracted as the location of spectral maxima.

2.3 Inversion of surface waves

The solution of the inverse Rayleigh problem is the final step in test interpretation. The solution of the forward problem forms the basis of any inversion strategy; the forward problem consists in the calculation of the function whose zeros are dispersion curves of a given model. Assuming a model for the soil deposit, model parameters of the best fitting subsoil profile are obtained minimizing an object function.

The subsoil is modelled as a horizontally layered medium overlaying a halfspace, with constant parameter in the interior of each layer and linear elastic behaviour. Model parameters are thickness, S-wave velocity, P-wave velocity (or Poisson coefficient), and density of each layer and the halfspace. The inversion is performed on S-wave velocities and thicknesses, whereas for the other parameters realistic values are chosen a priori. The number of layer is chosen applying minimum parameterization criterion.

In surface wave analysis it is very common to perform the inversions using only the fundamental mode of propagation. This approach is based on the assumption that the prevailing mode of propagation is the fundamental one; if this is partially true for normal dispersive sites, in several real cases the experimental dispersion curve is on the contrary the result of the superposition of several modes. This may happen in particular when velocity inversions or strong velocity contrasts are present in the shear wave velocity profile. In these stratigraphic conditions the inversion of the only fundamental mode will produce significant errors; moreover all the information contained in higher propagating

modes is not used in the inversion process. Therefore, the fundamental mode inversion does not use all the available information, and this affects the result accuracy.

The use of higher modes in the inversion can be helpful both in the low frequency range, in order to increase the investigation depth and to avoid the overestimation of the bedrock velocity, and in the high frequency range in order to provide a more consistent interpretation of shallow interfaces and increase model parameter resolution.

In this work a multimodal misfit function has been used. This function is based on the Haskell-Thomson method for dispersion curve calculation (Thomson 1950, Haskell 1953, Herrmann e Wang 1980, Herrmann 2002). For a given subsoil model, and an experimental data, the misfit of the model is the L^1 norm of the vector containing the absolute value of the determinant of the Haskell-Thomson matrix (which is zeros in correspondence of all the modes of the dispersion curves of the numerical model) evaluated in correspondence of the experimental data (Maraschini et al. 2008). The misfit function adopted has the advantage of being able to include any dispersive event present in the data without the need of specifying to which mode the data points belong to, avoiding errors arising from mode misidentification, in particular in the low frequency range.

This misfit function is applied in a Global Search Methods (GSM), in order to reduce the possibility of falling in local minima. A uniform random search is applied; ranges for the inversion have been chosen, for the different sites, based on the experimental dispersion curves; in particular the range of the S-wave half space velocity is close to the maximum surface wave velocity retrieved on experimental data.

The results of the inversion are reported as the ensemble of the best shear wave velocity profiles chosen according to a chi-square test (see Socco et al., 2008). It can be assumed that the experimental dispersion curve is affected by a Gaussian error with a known standard deviation, so that the probability density function of data $\rho_D(d)$ can be described by a discrete m-dimensional Gaussian (where m are the model parameters) and the sample variance variable of each random vector (dispersion curve) extracted from the data pdf is distributed according to a chi-square probability density. According to these assumptions we adopt a misfit function with the structure of a chi-square and this allows a statistical test to be applied to the variances of the synthetic dispersion curves with respect to the experimental one d_{obs}. Assuming that the best fitting curve d_{opt} belongs to the distribution $\rho_D(d_{obs})$ all models belonging to the distribution $\rho_D(d_{opt})$ and consistent with the data within a fixed level of confidence α are selected. As the ratio between chi-square variables follows a Fisher distribution a one–tailed F test can be performed:

$$F_\alpha(dof_{dopt}, dof_{g(m)}) < \frac{\chi^2_{dopt}}{\chi^2_{g(m)}}$$

where α is the chosen level of confidence, dof_{dopt} and $dof_{g(m)}$ are the degrees of freedom of the Fischer distribution and χ^2_{dopt} and $\chi^2_{g(m)}$ are the misfit of the best fitting curve and the misfit of all the others respectively. All models passing such test are selected. In the figures reported a representation based on the misfit is adopted for velocity profiles, so that the darkest colour corresponds to the profile whose dispersion curve has the lowest misfit and better approximation to the reference one; instead for dispersion curves the coloured surface under imposed to the experimental one is a misfit surface, whose zeros are synthetic dispersion curve of the best fitting model.

2.4 Numerical code

The numerical codes used for processing and inversion of surface waves are non commercial codes, implemented at Politecnico di Torino.

3 Tortorici – Refraction results

Three shots were considered for the inversion: two of them were acquired using the 23 m long acquisition array and the source is located at the beginning and at the end of the array itself; the third shot was acquired using the 46 m long measuring geometry, the source is in the middle of the array.
The dromocrones represented in Figure 4 point out the presence of a 3 layered model with lateral variations: the first layer, whose P-wave velocity is approximately 549 m/s, has a thickness decreasing from 1 to 0.3 m towards the end of the array; the intermediate layer is characterized by a P-wave velocity of about 830 m/s and a thickness of around 3.9 m increasing towards the end of the array; the deeper layer has P-wave velocity of 1646 m/s.

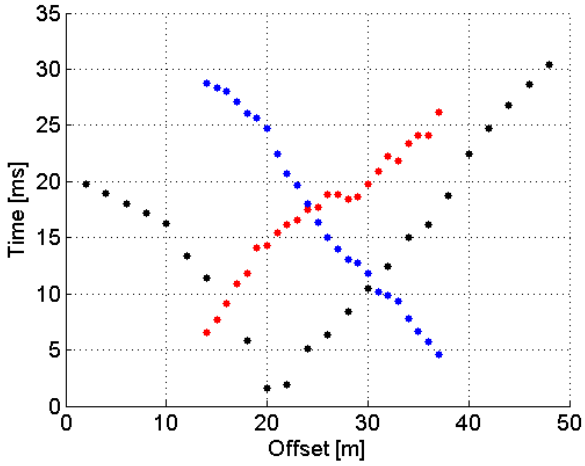

Figure 4 Tortorici – First breaks of the three considered shots

Parameters are summarized in Table 3.

P-wave velocity (m/s)	Average thickness (m)
549	0.7
834	3.9
1646	-

Table 3 Velocity models retrieved by refraction survey

4 Tortorici – Surface wave results

In Figure 5 an example of the f-k spectrum of the data collected at Tortorici is presented.

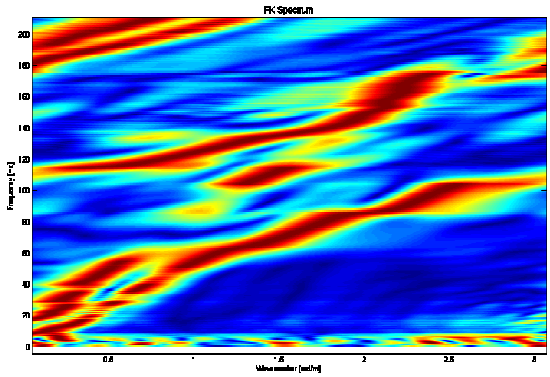

Figure 5 Tortorici – example of f-k spectrum

From the f-k spectra, several dispersion curves can be retrieved. From all these curves an average curve is estimated (Figure 6).

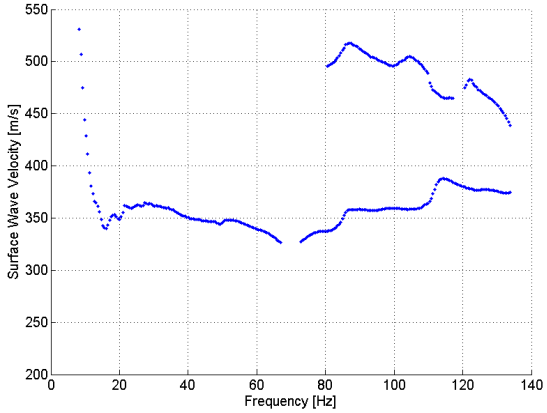

Figure 6 Tortorici -Average apparent dispersion curve

The apparent dispersion curve is made up of three branches: their irregular appearance is probably due to velocity contrasts and velocity inversions (the hump at about 20 Hz very likely points out a velocity inversion). Very probably all branches jump from one mode to another.

Data were inverted using a multimodal stochastic approach, the best fitting profiles are plotted in Figure 7 a), profile colour depends on the misfit, from yellow to blue (best fitting profile). In Figure 7 b) the best fitting profile is compared with the refraction result, and in Figure 8 the experimental dispersion curve is compared with the determinant surface of the best fitting model. We can note that the experimental points fall into the minima of the determinant surface: one of the three branches of the apparent dispersion curve follow the fundamental mode, another one jumps from the fundamental to higher modes while the third one follows the 5^{th} and the 6^{th} higher modes.

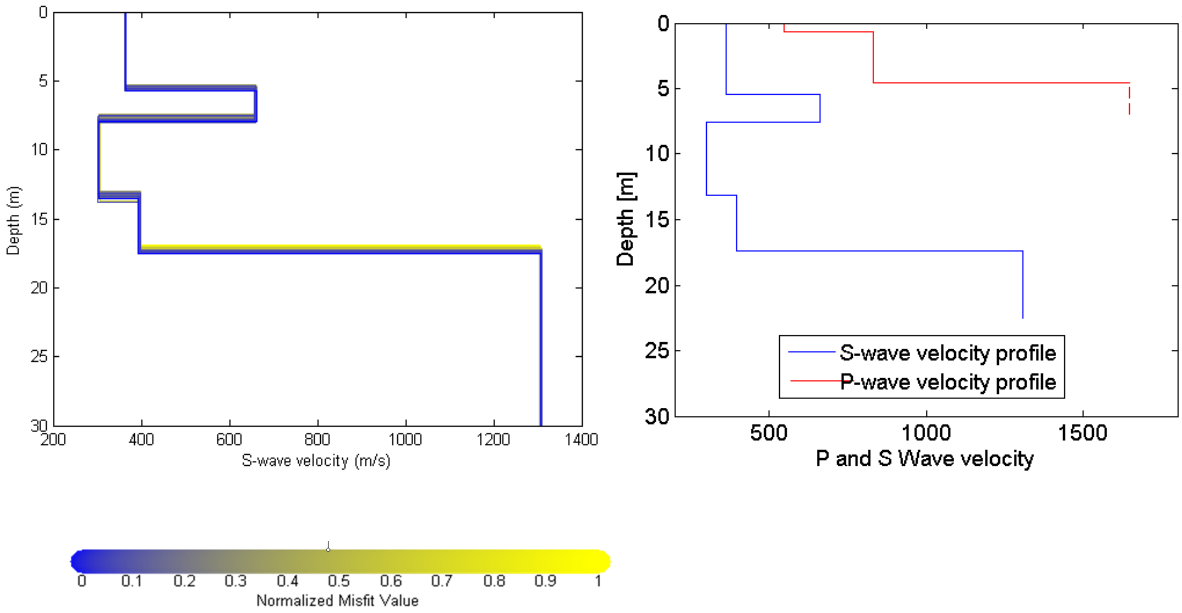

Figure 7 Tortorici – a) Monte Carlo results (from yellow to blue) of the inversion . b) Best fitting profile (blue) compared with the refraction result (red).

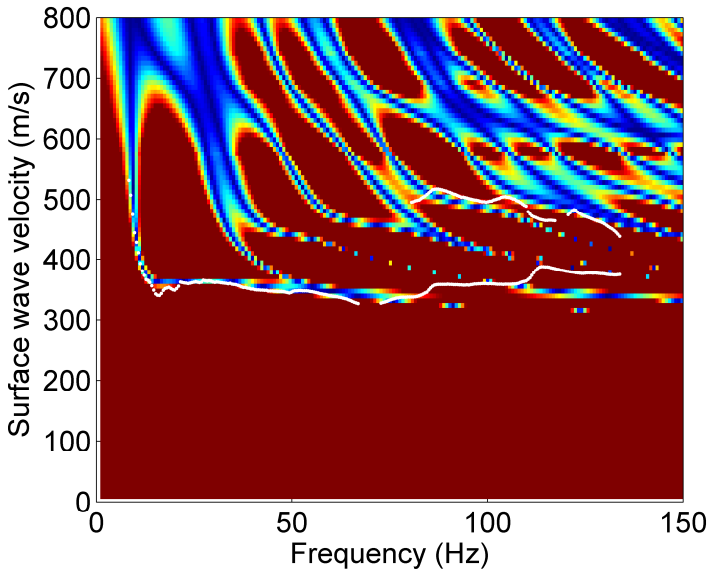

Figure 8 Tortorici – Experimental dispersion curve compared with the misfit surface of the best fitting model

The retrieved S-wave soil profile is characterized by a velocity inversion at 7.6 m depth: the bedrock interface is located at 17.4 m depth. Note also that the interface between the 2nd and the 3rd layer is in fairly good agreement with the refraction results.

The parameters of the best fitting profile are summarized in Table 4

Vs (m/s)	Thickness (m)	Poisson coefficient	Density (T/m^3)
365	5.7	0.3	1.8
662	2.2	0.3	1.8
303	5.5	0.3	1.8
393	4.0	0.3	1.8
1308	-	0.3	1.8

Table 4 Tortorici: subsoil parameters of the best fitting profile.

References

Project S4: ITALIAN STRONG MOTION DATA BASE, Deliverable # 6, Application of Surface wave methods for seismic site characterization, May 2009.

Foti S., Comina C., Boiero D., Socco L.V. (2009) "Non uniqueness in surface wave inversion and consequences on seismic site response analyses", Soil Dynamics and Earthquake Engineering, Vol. 29 (6), 982-993.

Haskell, N., 1964, Radiation pattern of surface waves from point sources in a multilayered medium: Bulletin of seismological society of America, 54, no. 1, 377-393.

Herrmann, R. B., and C. Y. Wang, 1980, A numerical study of p-, sv- and sh- wave generation in a plane layered medium: Bulletin of seismological society of America, 70, no. 4, 1015-1036.

Herrmann, R. B., 2002, SURF code, www.eas.slu.edu/People/RBHerrmann/.

Maraschini, M., F. Ernst, D. Boiero, S. Foti, and L.V. Socco, 2008, A new approach for multimodal inversion of Rayleigh and Scholte waves: Proceedings of EAGE Rome, expanded abstract.

Thomson, W. T, 1950., Transmission of elastic waves through a stratified solid medium: Journal of Applied Physics, 21, no. 89.

APPLICATION OF SURFACE WAVE METHODS FOR SEISMIC SITE CHARACTERIZATION

MESSINA TORRE FARO (TRF)

Responsible:
Sebastiano Foti

Co-workers:
Giovanni Bianchi
Margherita Maraschini
Paolo Bergamo

FINAL REPORT

Turin, 15/01/2010

INDEX

1 Introduction

In this report a summary of the results obtained for the characterization of the accelerometric station of Messina Torre Faro of the RAN within Project S4 is presented. The analysis was performed using active surface wave method.

Messina Torre Faro RAN station lies on an alluvial plane at approximately 300 m from the sea: no shallow bedrock is expected.

The map of the site and the array and its location are shown in Figure 1 and Figure 2.

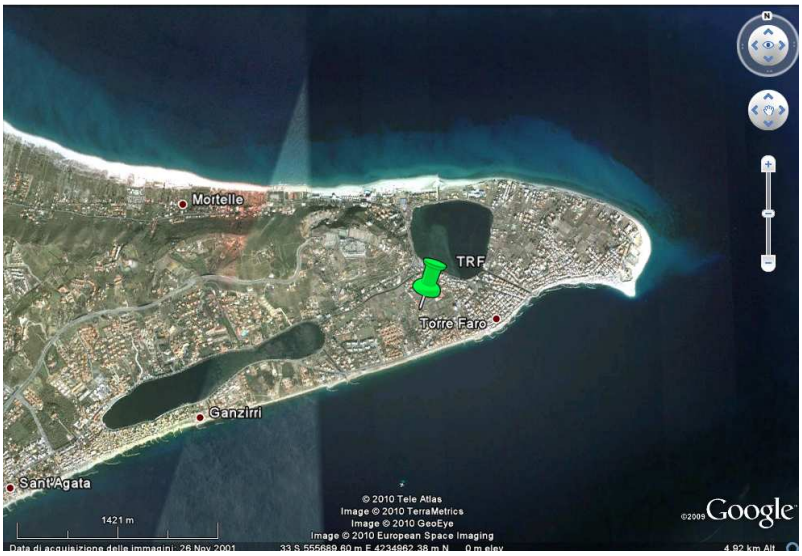

Figure 1 Messina Torre Faro: map

Figure 2 Messina Torre Faro: map of the array and its location

Goal of the seismic tests is the estimation of the S-wave velocity profile of the subsoil of the area surrounding the RAN station. No shallow bedrock is expected, as the station is located on a plane made up of soft alluvial deposits: S-wave velocities are supposed to be quite low.

The primary use of surface wave testing is related to site characterization in terms of shear wave velocity profile. The V_S profile is of primary interest for seismic site response studies

and for studies of vibration of foundations and vibration transmission in soils. Other applications are related to the prediction of settlements and to soil-structure interaction.

With respect to the evaluation of seismic site response, it is worth noting the affinity between the model used for the interpretation of surface wave tests and the model adopted for most site responses study. Indeed the application of equivalent linear elastic methods is often associated with layered models (e.g. the code SHAKE and all similar approaches). This affinity is also particularly important in the light of equivalence problems, which arise because of non-uniqueness of the solution in inverse problems. Indeed profiles which are equivalent in terms of Rayleigh wave propagation are also equivalent in term of seismic amplification (Foti et al., 2009).

Many seismic building codes introduce the weighted average of the shear wave velocity profile in the shallowest 30m as to discriminate class of soils to which a similar site amplification effect can be associated. The so-called $V_{S,30}$ can be evaluated very efficiently with surface wave method also because its average nature does not require the high level of accuracy that can be obtained with seismic borehole methods.

In the following a methodological summary of techniques and the description of the results is presented.

For Further explanation of surface wave methodologies, see document: Project S4: ITALIAN STRONG MOTION DATA BASE, Deliverable # 6, Application of Surface wave methods for seismic site characterization, May 2009.

2 Surface wave method

Surface wave method (S.W.M.) is based on the geometrical dispersion, which makes Rayleigh wave velocity frequency dependent in vertically heterogeneous media. High frequency (short wavelength) Rayleigh waves propagate in shallow zones close to the free surface and are informative about their mechanical properties, whereas low frequency (long wavelength) components involve deeper layers. Surface wave tests are typically devoted to the determination of a small strain stiffness profile for the site under investigation. Consequently the dispersion curve will be associated to the variation of medium parameters with depth.

The calculation of the dispersion curve from model parameters is the so called forward problem. Surface wave propagation can be seen as the combination of multiple modes of propagation, i.e. more than one possible velocity can be associated to each frequency value. Including higher modes in the inversion process allows the penetration depth to be increased and a more accurate subsoil profile to be retrieved.

If the dispersion curve is estimated on the basis of experimental data, it is then possible to solve the inverse problem, i.e. the model parameters are identified on the basis of the experimental data collected on the boundary of the medium. The result of the surface wave method is a one-dimensional S wave velocity soil profile.

The standard procedure for surface wave tests is reported in Figure 3. It can be subdivided into three main steps:

1. acquisition of experimental data;
2. signal processing to obtain the experimental dispersion curve;
3. inversion process to estimate shear wave velocity profile at the site.

It is very important to recognize that the above steps are strongly interconnected and their interaction must be adequately accounted for during the whole interpretation process.

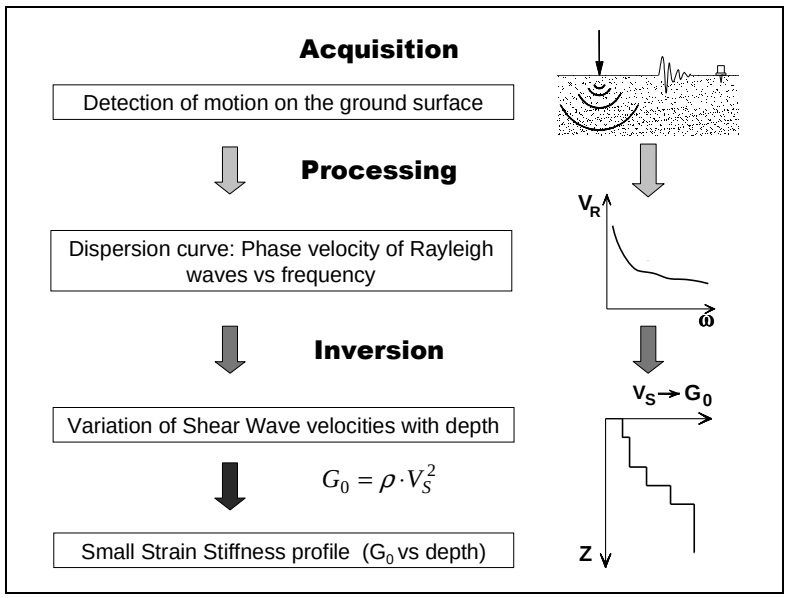

Figure 3 – Flow chart of surface wave tests.

2.1 Acquisition

Active surface wave tests (MASW) at Messina Torre Faro have been performed in May 2009 within the project S4 for the characterization of RAN sites.

Characteristics of sensors are reported in Table 1.

Test	GEOPHONE TYPE	NATURAL FREQUENCY	GEOPHONE NUMBER
MASW	vertical SENSOR SM-6/U-B	4,5 Hz	24

Table 1 Messina Torre Faro: receiver characteristics

The acquisition geometry was influence by the limited size of the uncultivated area close to the station where the survey was performed: the measuring array is made up of 24 geophones with a spacing of 1.75 m between neighbouring receivers. The total length of the array is 40.25 m, the source is a 5kg sledge hammer. Geometry parameters are summarized in Table 2.

Test	GEOF. N.	SPACING	SOURCE TYPE	ACQUISITION WINDOW	SAMPLING INTERVAL	STACK
MASW	24	1.75 m	Hammer	T = 2 s	Δt = 0.5 ms	10

Table 2 Messina Torre Faro: Acquisition parameters

2.2 Processing of surface waves

The processing allows the experimental dispersion curve to be determined.

Multichannel data are processed using a double Fourier Transform, which generates the frequency-wave number spectrum, where the multimodal dispersion curve is easily extracted as the location of spectral maxima.

2.3 Inversion of surface waves

The solution of the inverse Rayleigh problem is the final step in test interpretation. The solution of the forward problem forms the basis of any inversion strategy; the forward problem consists in the calculation of the function whose zeros are dispersion curves of a given model. Assuming a model for the soil deposit, model parameters of the best fitting subsoil profile are obtained minimizing an object function.

The subsoil is modelled as a horizontally layered medium overlaying a halfspace, with constant parameter in the interior of each layer and linear elastic behaviour. Model parameters are thickness, S-wave velocity, P-wave velocity (or Poisson coefficient), and density of each layer and the halfspace. The inversion is performed on S-wave velocities and thicknesses, whereas for the other parameters realistic values are chosen a priori. The number of layer is chosen applying minimum parameterization criterion.

In surface wave analysis it is very common to perform the inversions using only the fundamental mode of propagation. This approach is based on the assumption that the prevailing mode of propagation is the fundamental one; if this is partially true for normal dispersive sites, in several real cases the experimental dispersion curve is on the contrary the result of the superposition of several modes. This may happen in particular when velocity inversions or strong velocity contrasts are present in the shear wave velocity profile. In these stratigraphic conditions the inversion of the only fundamental mode will produce significant errors; moreover all the information contained in higher propagating modes is not used in the inversion process. Therefore, the fundamental mode inversion does not use all the available information, and this affects the result accuracy.

The use of higher modes in the inversion can be helpful both in the low frequency range, in order to increase the investigation depth and to avoid the overestimation of the bedrock velocity, and in the high frequency range in order to provide a more consistent interpretation of shallow interfaces and increase model parameter resolution.

In this work a multimodal misfit function has been used. This function is based on the Haskell-Thomson method for dispersion curve calculation (Thomson 1950, Haskell 1953, Herrmann e Wang 1980, Herrmann 2002). For a given subsoil model, and an experimental data, the misfit of the model is the L^1 norm of the vector containing the absolute value of

the determinant of the Haskell-Thomson matrix (which is zeros in correspondence of all the modes of the dispersion curves of the numerical model) evaluated in correspondence of the experimental data (Maraschini et al. 2008). The misfit function adopted has the advantage of being able to include any dispersive event present in the data without the need of specifying to which mode the data points belong to, avoiding errors arising from mode misidentification, in particular in the low frequency range.

This misfit function is applied in a Global Search Methods (GSM), in order to reduce the possibility of falling in local minima. A uniform random search is applied; ranges for the inversion have been chosen, for the different sites, based on the experimental dispersion curves; in particular the range of the S-wave half space velocity is close to the maximum surface wave velocity retrieved on experimental data.

The results of the inversion are reported as the ensemble of the best shear wave velocity profiles chosen according to a chi-square test (see Socco et al., 2008). It can be assumed that the experimental dispersion curve is affected by a Gaussian error with a known standard deviation, so that the probability density function of data $\rho_D(d)$ can be described by a discrete m-dimensional Gaussian and the sample variance variable of each random vector (dispersion curve) extracted from the data pdf is distributed according to a chi-square probability density. According to these assumptions we adopt a misfit function with the structure of a chi-square and this allows a statistical test to be applied to the variances of the synthetic dispersion curves with respect to the experimental one d_{obs}. Assuming that the best fitting curve d_{opt} belongs to the distribution $\rho_D(d_{obs})$ all models belonging to the distribution $\rho_D(d_{opt})$ and consistent with the data within a fixed level of confidence α are selected. As the ratio between chi-square variables follows a Fisher distribution a one–tailed F test can be performed:

$$F_\alpha(dof_{dopt}, dof_{g(m)}) < \frac{\chi^2_{dopt}}{\chi^2_{g(m)}}$$

where α is the chosen level of confidence, dof_{dopt} and $dof_{g(m)}$ are the degrees of freedom of the Fischer distribution and χ^2_{dopt} and $\chi^2_{g(m)}$ are the misfit of the best fitting curve and the misfit of all the others respectively. All models passing such test are selected. In the figures reported a representation based on the misfit is adopted for velocity profiles, so that the darkest colour corresponds to the profile whose dispersion curve has the lowest misfit and better approximation to the reference one; instead for dispersion curves the coloured surface under imposed to the experimental one is a misfit surface, whose zeros are synthetic dispersion curve of the best fitting model.

2.4 Numerical code

The numerical codes used for processing and inversion of surface waves are non commercial codes, implemented at Politecnico di Torino.

3 Messina Torre Faro– Surface wave results

In Figure 4 an example of the f-k spectrum of the data collected at Messina Torre Faro is presented.

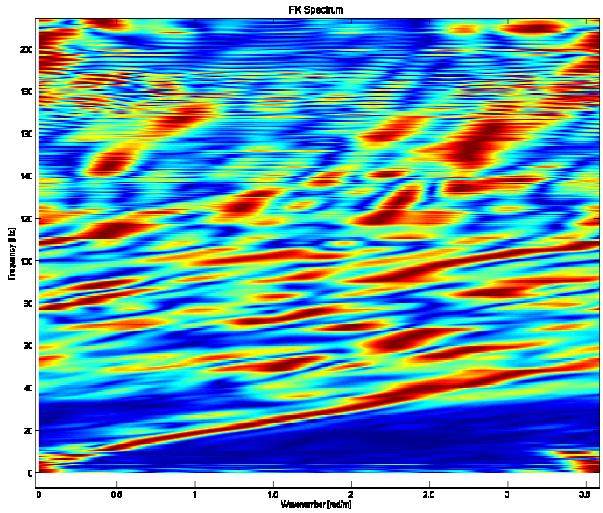

Figure 4 Messina Torre Faro – example of f-k spectrum

From the f-k spectra, several dispersion curves can be retrieved. From all these curves an average curve is estimated (Figure 5).

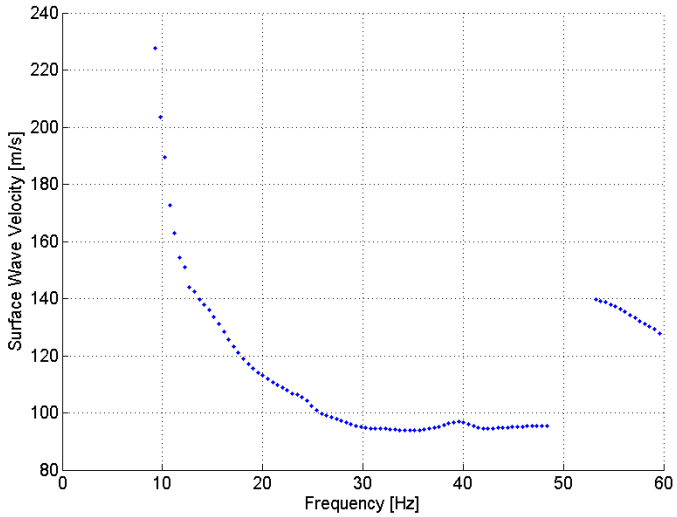

Figure 5 – Messina Torre Faro -Average apparent dispersion curve

The experimental dispersion curve (see Figure 6) is made up of one main branch, which probably corresponds to the fundamental mode, and of a minor branch which probably lies on a higher mode.
Data were inverted using a multimodal stochastic approach, the best fitting profiles are plotted in Figure 6, profile colour depends on the misfit, from yellow to blue (best fitting profile). In Figure 7 the experimental dispersion curve is compared with the determinant surface of the best fitting model. We can note that the experimental points fall into the minima of the determinant surface: the main and the minor branch are actually superimposed to the fundamental mode and to the first higher mode, respectively.

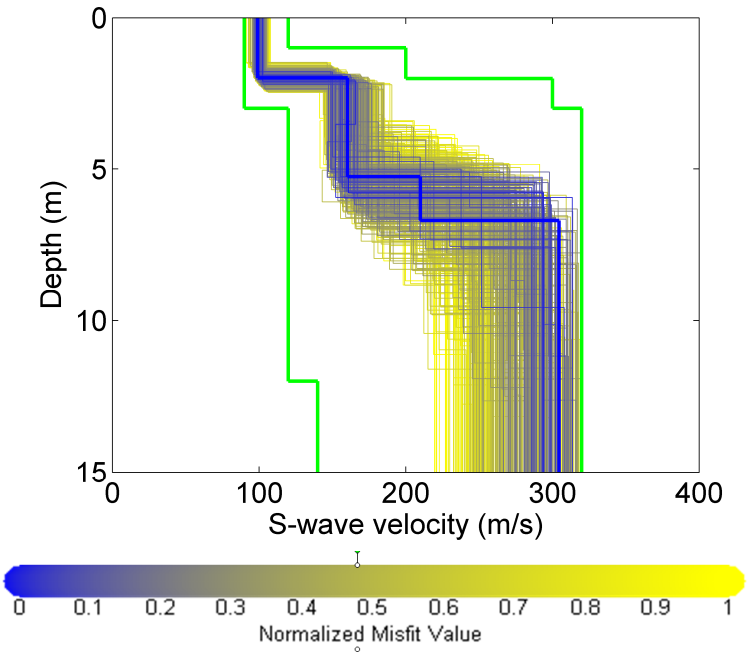

Figure 6 Messina Torre Faro – Monte Carlo results (from yellow to blue) of the inversion with the boundaries (green) .

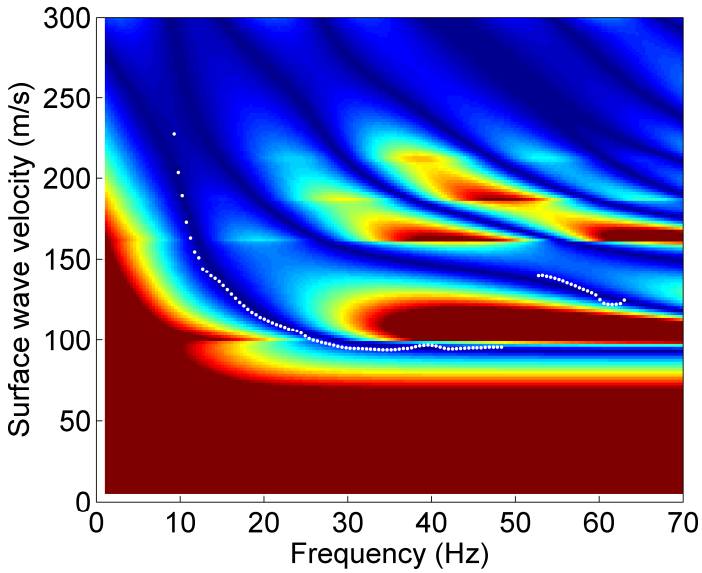

Figure 7 Messina Torre Faro – Experimental dispersion curve compared with the misfit surface of the best fitting model

The retrieved S-wave velocity profile is characterized by a very soft shallow layer (Vs is about 100 m/s) followed by a 4 m thick layer with a Vs of approximately 160 m/s: then the S-wave velocity increases progressively with depth until a stiffer layer is reached at around 8 m depth.

The parameters of the best fitting profile are summarized in Table 3.

Vs (m/s)	Thickness (m)	Poisson coefficient	Density (T/m^3)
99	2	0.3	1.8
160	3.3	0.3	1.8
210	1.4	0.3	1.8
306	-	0.3	1.8

Table 3 Messina Torre Faro: subsoil parameters of the best fitting profile.

References

Project S4: ITALIAN STRONG MOTION DATA BASE, Deliverable # 6, Application of Surface wave methods for seismic site characterization, May 2009.

Foti S., Comina C., Boiero D., Socco L.V. (2009) "Non uniqueness in surface wave inversion and consequences on seismic site response analyses", Soil Dynamics and Earthquake Engineering, Vol. 29 (6), 982-993.

Haskell, N., 1964, Radiation pattern of surface waves from point sources in a multilayered medium: Bulletin of seismological society of America, 54, no. 1, 377-393.

Herrmann, R. B., and C. Y. Wang, 1980, A numerical study of p-, sv- and sh- wave generation in a plane layered medium: Bulletin of seismological society of America, 70, no. 4, 1015-1036.

Herrmann, R. B., 2002, SURF code, www.eas.slu.edu/People/RBHerrmann/.

Maraschini, M., F. Ernst, D. Boiero, S. Foti, and L.V. Socco, 2008, A new approach for multimodal inversion of Rayleigh and Scholte waves: Proceedings of EAGE Rome, expanded abstract.

Thomson, W. T, 1950., Transmission of elastic waves through a stratified solid medium: Journal of Applied Physics, 21, no. 89.

APPLICATION OF SURFACE WAVE METHODS FOR SEISMIC SITE CHARACTERIZATION

TORTONA (TRT)

Responsible:
Sebastiano Foti

Co-workers:
Margherita Maraschini
Cesare Comina

FINAL REPORT

Turin, 11/02/2010

INDEX

1 Introduction

In this report a summary of the results obtained for the characterization of the accelerometric station of Tortona of the RAN within Project S4 is presented. The analysis was performed using active and passive surface wave method and refraction tomography method.

Tortona RAN station is located on a hillside outside the urban area of Tortona. The map, site location and measurements arrays are shown in Figure1, Figure 2 and Figure 3.

Figure 1 Tortona: map.

Figure 2 Tortona: array map. The yellow line represents the active measurements array; the red circle the passive measurement array.

Figure 3 Tortona: site location and RAN station.

Goal of the seismic tests is the estimation of the S-wave velocity profile of the subsoil, and in particular the position of the bedrock. The presence of stiff seismic interfaces between the sediments and the shallow bedrock can cause a relevance of higher modes in the surface wave experimental dispersion curve which has be taken into account in order to provide reliable results.

The primary use of surface wave testing is related to site characterization in terms of shear wave velocity profile. The V_S profile is of primary interest for seismic site response studies and for studies of vibration of foundations and vibration transmission in soils. Other applications are related to the prediction of settlements and to soil-structure interaction.

With respect to the evaluation of seismic site response, it is worth noting the affinity between the model used for the interpretation of surface wave tests and the model adopted for most site responses study. Indeed the application of equivalent linear elastic methods is often associated with layered models (e.g. the code SHAKE and all similar approaches). This affinity is also particularly important in the light of equivalence problems, which arise because of non-uniqueness of the solution in inverse problems. Indeed profiles which are equivalent in terms of Rayleigh wave propagation are also equivalent in term of seismic amplification (Foti et al., 2009).

Many seismic building codes introduce the weighted average of the shear wave velocity profile in the shallowest 30m as to discriminate class of soils to which a similar site amplification effect can be associated. The so-called $V_{S,30}$ can be evaluated very efficiently with surface wave method also because its average nature does not require the high level of accuracy that can be obtained with seismic borehole methods.

In the following a methodological summary of techniques and the description of the results is presented.

For Further explanation of surface wave methodologies, see document: Project S4: ITALIAN STRONG MOTION DATA BASE, Deliverable # 6, Application of Surface wave methods for seismic site characterization, May 2009.

2 Surface wave method

Surface wave method (S.W.M.) is based on the geometrical dispersion, which makes Rayleigh wave velocity frequency dependent in vertically heterogeneous media. High frequency (short wavelength) Rayleigh waves propagate in shallow zones close to the free surface and are informative about their mechanical properties, whereas low frequency (long wavelength) components involve deeper layers. Surface wave tests are typically devoted to the determination of a small strain stiffness profile for the site under investigation. Consequently the dispersion curve will be associated to the variation of medium parameters with depth.

The calculation of the dispersion curve from model parameters is the so called forward problem. Surface wave propagation can be seen as the combination of multiple modes of propagation, i.e. more than one possible velocity can be associated to each frequency value. Including higher modes in the inversion process allows the penetration depth to be increased and a more accurate subsoil profile to be retrieved.

If the dispersion curve is estimated on the basis of experimental data, it is then possible to solve the inverse problem, i.e. the model parameters are identified on the basis of the experimental data collected on the boundary of the medium. The result of the surface wave method is a one-dimensional S wave velocity soil profile.

The standard procedure for surface wave tests is reported in Figure 4. It can be subdivided into three main steps:

1. acquisition of experimental data;
2. signal processing to obtain the experimental dispersion curve;
3. inversion process to estimate shear wave velocity profile at the site.

It is very important to recognize that the above steps are strongly interconnected and their interaction must be adequately accounted for during the whole interpretation process.

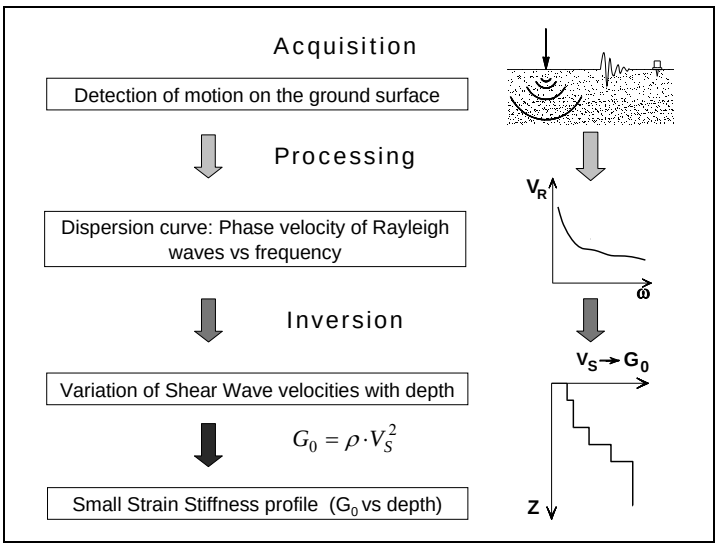

Figure 4 – Flow chart of surface wave tests.

2.1 Acquisition

Active (MASW), passive surface wave tests and refraction surveys at Tortona have been performed in September 2009 within the project S4 for the characterization of RAN sites.

Characteristics of sensors are reported in Table 1.

Test	GEOPHONE TYPE	NATURAL FREQUENCY	GEOPHONE NUMBER
MASW/Refraction survey	vertical SENSOR SM-6/U-B	4,5 Hz	48
Passive Surface Wave tests	vertical HS1 GEO-SPACE	2 Hz	12

Table 1 Tortona: receiver characteristics

For Active tests 48 receivers, with a spacing of 1 m between neighbouring geophones, were used so that the total length of the array is 47 m. The source was a 5kg sledge hammer. This array was used for refraction tomography survey as well. For passive tests 12 vertical geophones were arranged equal-spaced along a circle of 24 m diameter. Acquisition parameters for the surveys are summarized in Table 2.

Test	GEOF. N.	SPACING	SOURCE TYPE	ACQUISITION WINDOW	SAMPLING INTERVAL	STACK
MASW	48	1 m	Hammer	T = 2 s	Δt = 0.5 ms	10
Passive tests	12	-	-	T =524 s	Δt = 8 ms	1
Refraction surveys	48	1 m	Hammer	T = 0.512 s	Δt = 31.25 μs	10

Table 2 Tortona: Acquisition parameters

2.2 Processing of active surface wave data

The processing allows the experimental dispersion curve to be determined.

Multichannel data are processed using a double Fourier Transform, which generates the frequency-wave number spectrum, where the multimodal dispersion curve is easily extracted as the location of spectral maxima.

2.3 Processing of passive surface wave data

The phase velocity of the surface waves can be extracted from noise recordings by using different methods: among them, the most frequently used are the Beam-Forming Method (BFM) (Lacoss et al., 1969) and the Maximum Likelihood Method (MLM) (Capon, 1969). Here we will illustrate the Beam-Forming Method which was used to process passive surface wave data. For further explanation on passive surface wave methodologies, see document: Project S4: ITALIAN STRONG MOTION DATA BASE, Deliverable # 6, Application of Surface wave methods for seismic site characterization, May 2009.

The estimate of the F-K spectra $P_b(f,\mathrm{k})$ by the BFM is given by:

$$P_b(f,k) = \sum_{l,m=1}^{n} \phi_{lm} \exp\{ik(X_l - X_m\} \ ,$$

where f is the frequency, k the two-dimensional horizontal wavenumber vector, n the number of sensors, ϕ_{lm} the estimate of the cross-power spectra between the l^{th} and the m^{th} data, and X_i and X_m, are the coordinates of the l^{th} and m^{th} sensors, respectively.

From the peak in the F-K spectrum occurring at coordinates k_{xo} and k_{yo} for a certain frequency $f_{0,}$ the phase velocity c_0 can be calculated by:

$$c_0 = \frac{2\pi f_0}{\sqrt{k_{xo}{}^2 + k_{yo}{}^2}}$$

so that, again, an experimental dispersion curve is retrieved.

Figure 5 shows an example of F-K analysis results obtained by processing passive surface wave data with Beam-Forming Method.

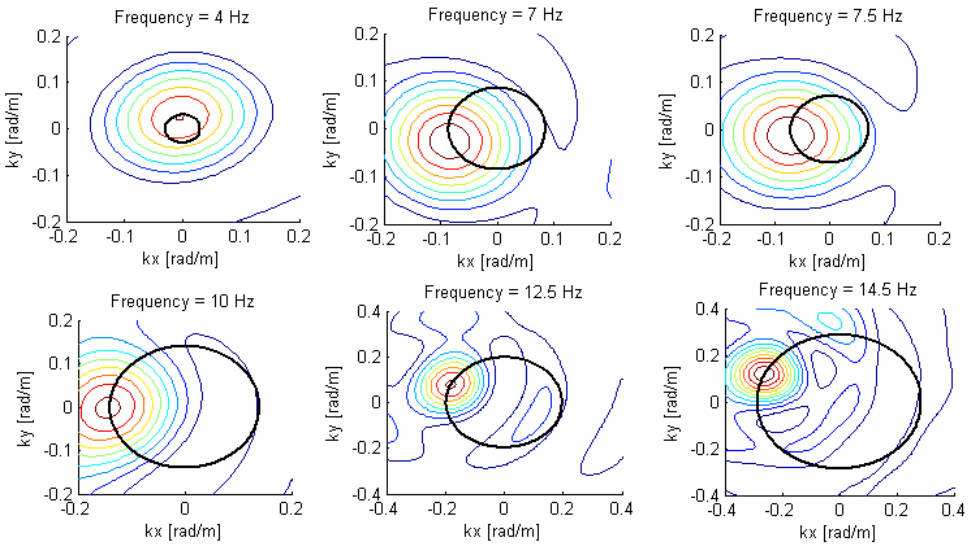

Figure 5 – Example of results from F-K analysis for some frequencies. The black circle joins points with the same k while the position of the maximum is used to estimate the phase velocity.

2.4 Inversion of surface waves

The solution of the inverse Rayleigh problem is the final step in test interpretation. The solution of the forward problem forms the basis of any inversion strategy; the forward problem consists in the calculation of the function whose zeros are dispersion curves of a given model. Assuming a model for the soil deposit, model parameters of the best fitting subsoil profile are obtained minimizing an object function.

The subsoil is modelled as a horizontally layered medium overlaying a halfspace, with constant parameter in the interior of each layer and linear elastic behaviour. Model parameters are thickness, S-wave velocity, P-wave velocity (or Poisson coefficient), and density of each layer and the halfspace. The inversion is performed on S-wave velocities

and thicknesses, whereas for the other parameters realistic values are chosen a priori. The number of layer is chosen applying minimum parameterization criterion.

In surface wave analysis it is very common to perform the inversions using only the fundamental mode of propagation. This approach is based on the assumption that the prevailing mode of propagation is the fundamental one; if this is partially true for normal dispersive sites, in several real cases the experimental dispersion curve is on the contrary the result of the superposition of several modes. This may happen in particular when velocity inversions or strong velocity contrasts are present in the shear wave velocity profile. In these stratigraphic conditions the inversion of the only fundamental mode will produce significant errors; moreover all the information contained in higher propagating modes is not used in the inversion process. Therefore, the fundamental mode inversion does not use all the available information, and this affects the result accuracy.

The use of higher modes in the inversion can be helpful both in the low frequency range, in order to increase the investigation depth and to avoid the overestimation of the bedrock velocity, and in the high frequency range in order to provide a more consistent interpretation of shallow interfaces and increase model parameter resolution.

In this work a multimodal misfit function has been used. This function is based on the Haskell-Thomson method for dispersion curve calculation (Thomson 1950, Haskell 1953, Herrmann e Wang 1980, Herrmann 2002). For a given subsoil model, and an experimental data, the misfit of the model is the L^1 norm of the vector containing the absolute value of the determinant of the Haskell-Thomson matrix (which is zeros in correspondence of all the modes of the dispersion curves of the numerical model) evaluated in correspondence of the experimental data (Maraschini et al. 2008). The misfit function adopted has the advantage of being able to include any dispersive event present in the data without the need of specifying to which mode the data points belong to, avoiding errors arising from mode misidentification, in particular in the low frequency range.

This misfit function is applied in a Global Search Methods (GSM), in order to reduce the possibility of falling in local minima. A uniform random search is applied; ranges for the inversion have been chosen, for the different sites, based on the experimental dispersion curves; in particular the range of the S-wave half space velocity is close to the maximum surface wave velocity retrieved on experimental data.

The results of the inversion are reported as the ensemble of the twenty shear wave velocity profiles which present the minimum misfits with respect to the experimental dispersion curve. In the figures reported a representation based on the misfit is adopted for velocity profiles, so that the darkest colour corresponds to the profile whose dispersion curve has the lowest misfit and better approximation to the reference one; instead for dispersion curves the coloured surface under imposed to the experimental one is a misfit surface, whose zeros are synthetic dispersion curve of the best fitting model.

2.5 Numerical code

The numerical codes used for processing and inversion of surface waves are non commercial codes, implemented at Politecnico di Torino. For refraction tomography the code Rayfract® has been used.

3 Tortona – Refraction results

5 shots were considered for refraction survey: two of them with the source at the edges of the array and three with the source at intermediate positions along the survey line. First-break arrival times are shown in Figure 6 while the tomographic interpretation is shown in Figure 7.

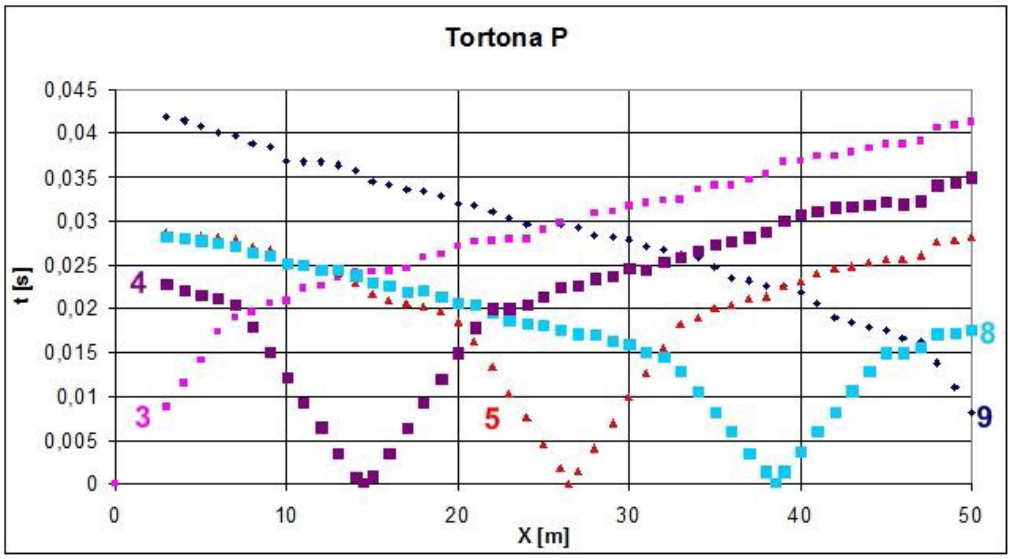

Figure 6 Tortona – First breaks of the five considered shots

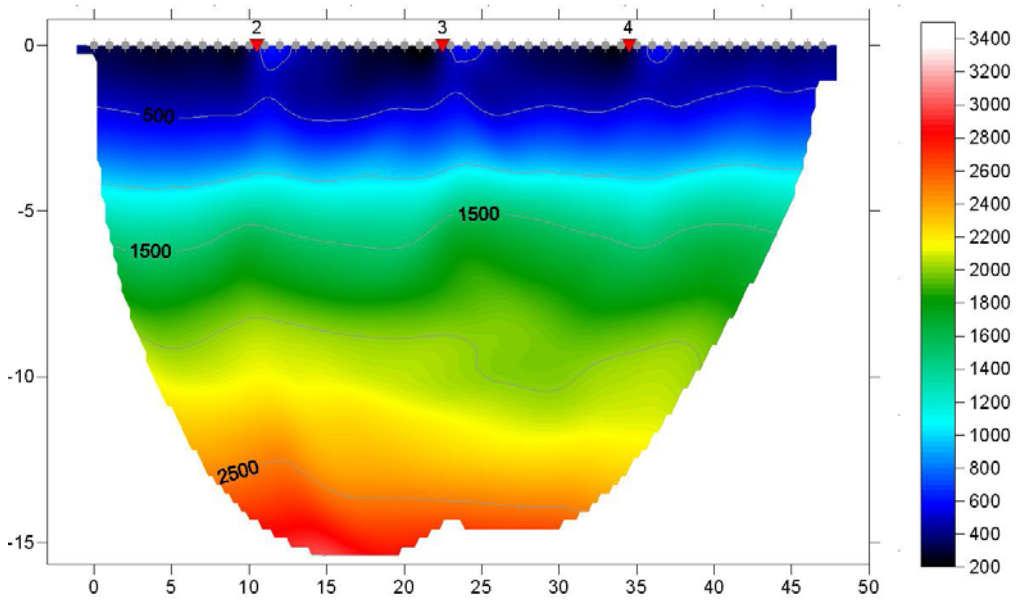

Figure 7 Tortona – P wave tomography result

A three layers model can be roughly identified from the refraction tomography: the shallow layer has a P-wave velocity of 480 m/s and a thickness of about 4.5 m above the water table which is the intermediate layer and is characterized by a P-wave velocity of approximately 1500 m/s slowly increasing till an average depth of about 12 m; the lowest

layer has a P-wave velocity of 2200 m/s and is gently dipping on the right side of the array. The average profile features are summarized in Table 3.

P-wave velocity (m/s)	Thickness (m)
480	4.5
1500	7.5
2200	-

Table 3 Velocity model retrieved by refraction survey

4 Tortona – Surface wave results

In Figure 8 an example of the f-k spectrum of the active data collected at Tortona is presented.

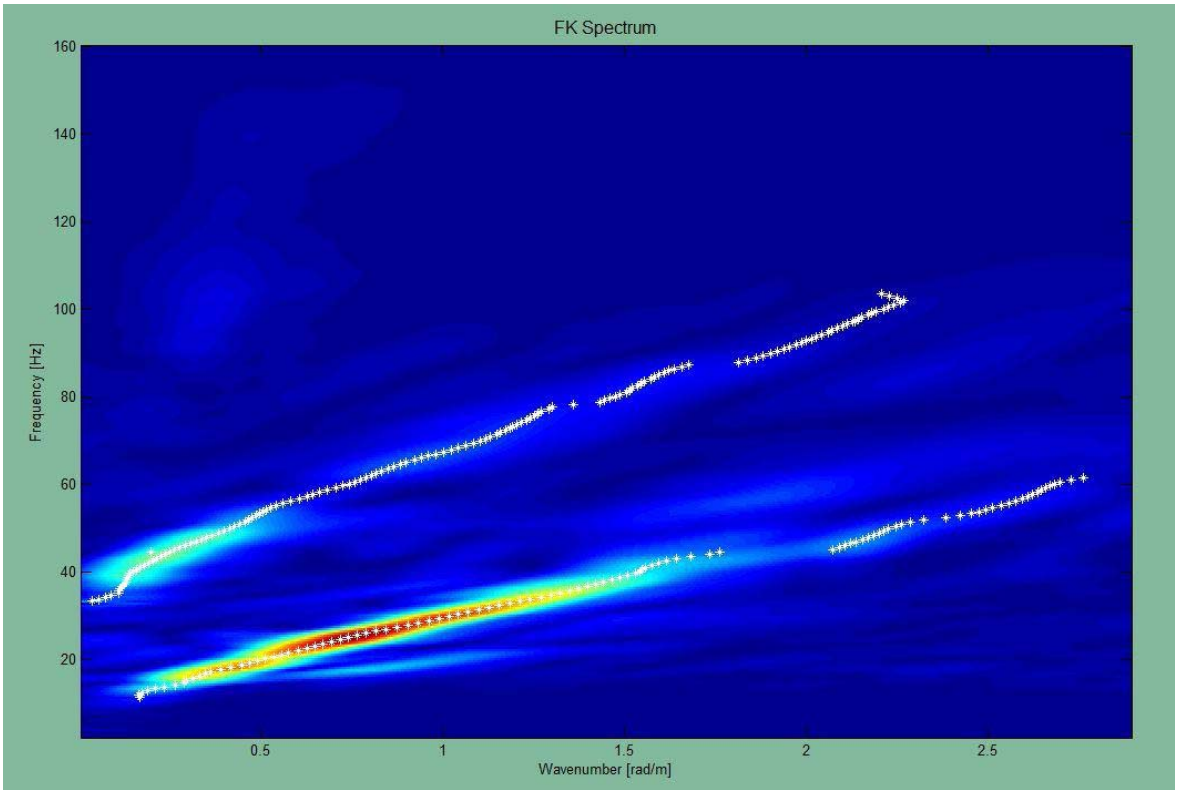

Figure 8 Tortona – example of f-k spectrum

From the f-k spectra, several dispersion curves can be retrieved. From all these curves an average curve is estimated (Figure 9).
The apparent dispersion curve is made up of two branches – two from active data and one from passive data – which probably follow two propagation modes.
Data were inverted using a multimodal stochastic approach, the best fitting profiles are plotted in Figure 10 left), profile colour depends on the misfit, from yellow to blue (best fitting profile). In Figure 10 rigth) the best fitting profile is compared with the mean profile from refraction tomography result, and in Figure 11 the experimental dispersion curve is

compared with the determinant surface of the best fitting model. We can note that the experimental points fall into the minima of the determinant surface. Moreover it can be noted that the position of the bedrock interface is in good agreement with the refraction results.

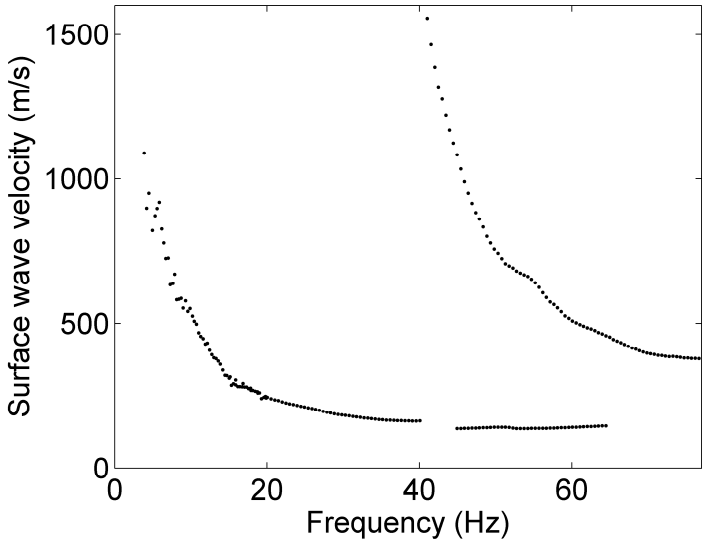

Figure 9 – Tortona - Average apparent dispersion curve from active and passive tests.

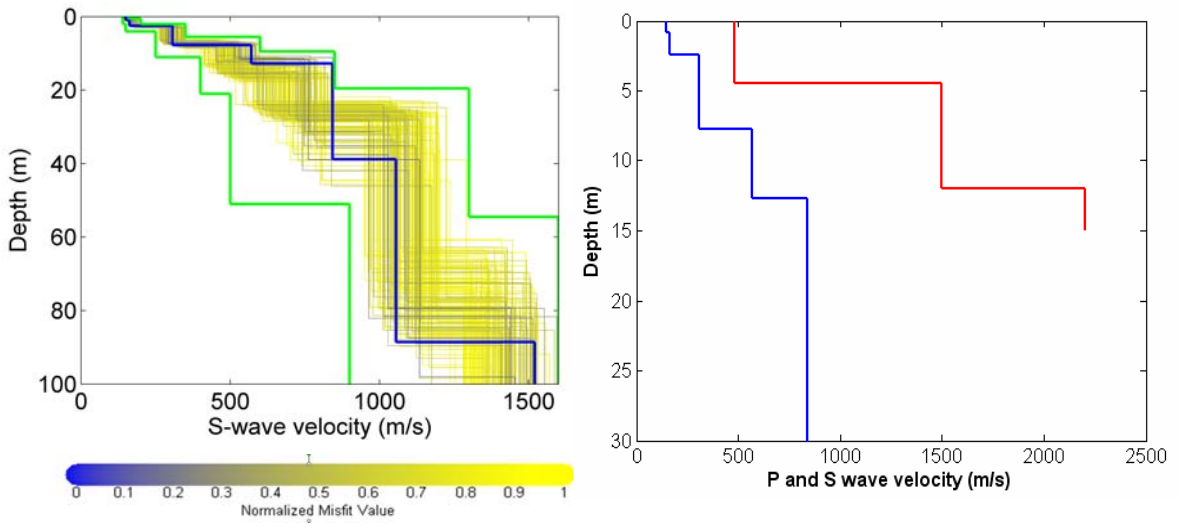

Figure 10 Tortona – left) Monte Carlo results (from yellow to blue) of the inversion with the boundaries (green). right) Tortona – Best fitting profile (blue) compared with the refraction tomography result (red).

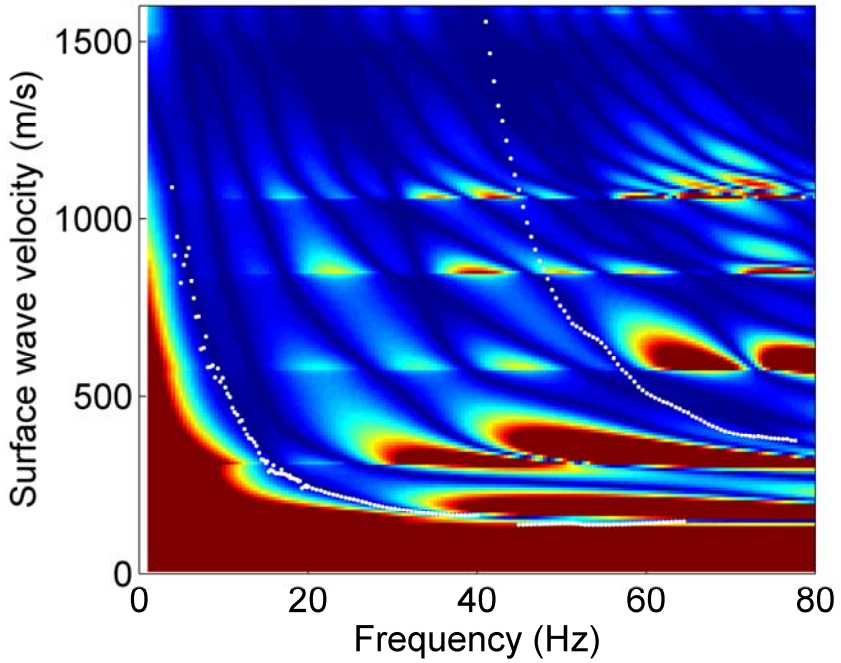

Figure 11 Tortona – Experimental dispersion curve compared with the misfit surface of the best fitting model

The parameters of the best fitting profile are summarized in Table 4.

Vs (m/s)	Thickness (m)	Poisson coefficient	Density (T/m^3)
150	0.9	0.3	1.8
160	1.6	0.3	1.8
305	5.3	0.3	1.8
570	4.9	0.3	1.8
840	26.1	0.3	1.8
1050	49.8	0.3	1.8
1520		0.3	1.8

Table 4 Tortona: subsoil parameters of the best fitting profile.

References

Project S4: ITALIAN STRONG MOTION DATA BASE, Deliverable # 6, Application of Surface wave methods for seismic site characterization, May 2009.

Foti S., Comina C., Boiero D., Socco L.V. (2009) "Non uniqueness in surface wave inversion and consequences on seismic site response analyses", Soil Dynamics and Earthquake Engineering, Vol. 29 (6), 982-993.

Haskell, N., 1964, Radiation pattern of surface waves from point sources in a multilayered medium: Bulletin of seismological society of America, 54, no. 1, 377-393.

Herrmann, R. B., and C. Y. Wang, 1980, A numerical study of p-, sv- and sh- wave generation in a plane layered medium: Bulletin of seismological society of America, 70, no. 4, 1015-1036.

Herrmann, R. B., 2002, SURF code, www.eas.slu.edu/People/RBHerrmann/.

Maraschini, M., F. Ernst, D. Boiero, S. Foti, and L.V. Socco, 2008, A new approach for multimodal inversion of Rayleigh and Scholte waves: Proceedings of EAGE Rome, expanded abstract.

Thomson, W. T, 1950., Transmission of elastic waves through a stratified solid medium: Journal of Applied Physics, 21, no. 89.

Dipartimento di Scienze della Terra
Università degli Studi di Siena
Via Laterina, 8 53100 Siena, Italy

APPLICATION OF SURFACE WAVES METHODS FOR SEISMIC SITE CHARACTERIZATION

L'Aquila – Colle dei Grilli RAN site (AQG)

Responsible
Prof.Dario Albarello

Co-Workers
Dott. Domenico Pileggi
Dott. David Rossi
Dott. Enrico Lunedei

FINAL REPORT

Siena 30 May 2010

The investigation protocol

It involves four major elements:

- *Detailed Geological survey of the study area resulting in a geo/lithologic map at the scale 1:5000 of the area surrounding the relevant RAN station. This also aimed at the evaluation of the degree of lateral heterogeneity present in the lithological structure paying major attention to faults and their relevant damage area (that can result in energy trapping phenomena)*
- *Extensive single station ambient vibration survey at the station and in the surrounding area to detect possible lateral variations potentially responsible for site effects*
- *Ambient vibration measurements carried on with a seismic array at the RAN site or at a site representative of the subsoil configuration at the RAN site. In this last case, suitable inversion procedures and test were carried on to warrant the representativeness of ambient vibration measurements*
- *Global interpretation of measurements to determine the V_S profile and of the resonance frequency at the RAN site by considering the whole set of collected data*

Details concerning experimental tools and processing techniques are given in the following sections.

Single station measurements

The goal of this kind of measurements is the retrieval of the HVSR curve that represents for each frequency, the average ratio between Horizontal (H) to vertical (V) ground motion components of ambient vibrations (SESAME, 2004). Each single-station measurement was executed with a three-directional digital tromograph Tromino Micromed (see www.tromino.it) with a sampling frequency of 128 Hz and an acquisition time length of 20 minutes. This value represents a good compromise between the celerity of the measurement execution (which is one of the main merits of this technique) and its accuracy, according to the SESAME guidelines and other studies (see, e.g., Picozzi et al., 2005). To provide HVSR curves, the time series relative to each ground motion component was subdivided in non-overlapping time windows of 30 s. For each of these, the signal was corrected for the base line, padded with zeros, and tapered with a Triangular window; the relevant spectrogram was smoothed through a triangular window with frequency dependent half-width (10% of central frequency) and the H/V ratio (HVSR) of the spectral components (the former being the geometric mean of North-South and East-West components) was computed for each frequency. Spectral ratios relative to all the time windows considered were then averaged, and a mean HVSR curve was computed along with the relevant 95% confidence interval.

Before interpreting HVSR curve in terms of subsoil dynamical properties, we checked the possible occurrence of spurious HVSR peaks (e.g., due to impulsive or strongly localized anthropic sources). To this purpose, we investigated both the time stability of spectral ratios over the recording length and their directionality. The latter was analyzed by estimating the HVSR curves derived by projecting the ground motion along different horizontal directions. If transient directional effects were identified in the directional HVSR curves, the relevant portions of the record were discarded.

Array Measurements

This technique consists in recording ambient vibration ground motion by means of an array of sensors (vertical geophones) distributed at the surface of the subsoil to be explored (see, e.g., Okada, 2003). Relevant information concerning phase velocities of waves propagating across the array are obtained from average cross-spectral matrixes relative to sensor pairs. In the present analysis, plane waves propagating across the array were considered only. Since vertical sensors were used only, these waves are interpreted as plane Rayleigh waves in their fundamental and higher propagation modes. Determination of Rayleigh wave phase velocities V_R as a function of frequency (dispersion curve) from cross-spectral matrixes can be carried on in several ways. In the present analysis, the Extended Spatial Auto Correlation (ESAC) technique (Ohori et al. , 2002; Okada, 2003)

was applied. The basic element of this analysis is the cross-correlation spectrum deduced by the analysis of ambient vibrations measured at a couple of sensors $\phi(f,r)$ where *f* is frequency and *r* is the distance between the relevant sensors .

To this purpose, registrations relative to each sensor are partitioned in a number of non overlapping time windows of fixed duration (20 sec). Time windows characterised by energy bursts were removed from the analysis. To this purpose, a time segment is considered in the analysis if standard deviation of all the traces of that time window do not exceed the threshold fixed in advance for each trace. In general, this threshold was fixed to be 2 times the standard deviation computed over the whole registration for the relevant trace. In each accepted time window, linear trend was removed and the resulting time series was padded and tapered (5% cosine windows). For each time window and couple of sensors, the cross spectrum was computed. The average cross spectrum was then computed for each couple of sensors by considering all the relevant time series. The resulting average cross-spectrum was thus smoothed in the frequency domain by a moving triangular window having an half-width proportional to the central value (usually 10%) and normalized to the relevant auto spectra.

In the assumption that ambient vibration wave field can be represented as a linear combination of statistically independent plane waves propagating with negligible attenuation in a horizontal plane in different directions with different powers, but with the same phase velocity for a given frequency, the normalized cross-spectrum $\phi_{ij}(f,r)$ relative to sensors located at a distance r, can be written in the form

$$\phi(f,r) = J_0\left(\frac{2\pi f r}{V_R(f)}\right)$$

where J_0 is the Bessel function of *0-th* order. In the ESAC approach, the value of V_R relative to each frequency *f* is retrieved by a grid search algorithm to optimized (in a RMS sense) the fit of the above function of r for the relevant frequency *f* (Ohori et al. , 2002; Okada, 2003). Robustness of this fitting procedure was enhanced by adopting the iterative procedure proposed by Parolai et al., 2006). By following these last Authors, uncertainty on "apparent" velocities was computed by means the second derivative of the misfit function relative to grid search procedure (see, Menke, 1989). However, since these estimate tend to be under-conservative in some cases, the lower bound of the confidence interval for experimental V_R values was fixed by using the relationship proposed by Zhang et al. (2004) as a function of the adopted sampling rate and array dimension.

The $V_R(f)$ value obtained in this way, is the "apparent" or "effective" Rayleigh waves phase velocity that coincides with the actual phase velocity only in the case that higher modes play a negligible role. In the other cases, a relationship can be established between actual phase velocities and the apparent one (Tokimatsu, 1997). The fact that the ESAC approach allows the determination of the apparent dispersion curve instead of the modal ones could represent an important limitation of this procedure with respect to other approaches (e.g., f-k techniques). On the other hand, this makes the approach here considered more robust with respect to the alternative procedures, since it does not require troublesome picking of existing propagation modes.

In the present study, ambient vibrations were recorded for 20 minutes at a 256 Hz sampling rate by using 16 vertical geophones (4.5 Hz) and a digital acquisition system produced by Micromed (http://micromed.com/brainspy1.htm). Geophones were placed along two crossing perpendicular branches (with maximum dimensions lower than 100 m) and irregularly spaced (in the range 0.5-30 m).

Inversion procedures

HVSR and apparent V_R curves have been jointly inverted to constrain to the local V_S profile. To this purpose, a genetic algorithm procedure was considered. This is an iterative procedure, consisting in sequence of steps miming the evolutionary selection of living being (see Picozzi and Albarello, 2007 and references therein). The formalization proposed by Lunedei and Albarello (2009) was used as the forward modelling modelling

implemented in the procedure. This procedure assumes the subsoil as a flat stratified viscoelastic medium where surface waves (Rayleigh and Love with relevant higher modes) propagate only. From this model, both theoretical HVSR and effective dispersion curves can be computed from a set of parameters representative of the hypothetical subsoil (V_S, V_P, density, Q_P and Q_S profiles). The discrepancy between theoretical and observed HVSR and dispersion curves were then evaluated in terms of a suitable misfit function, strictly linked to the well-known χ^2 function, that allowed different choices about the combination of the discrepancies of V_R and HVSR curves, with different weights as well. The confidence interval around preferred *Vs* values and layer thickness were evaluated by following Picozzi and Albarello (2007).

Geological Setting

A detailed geologic survey of the area surrounding the RAN site was carried on (Figure 1).

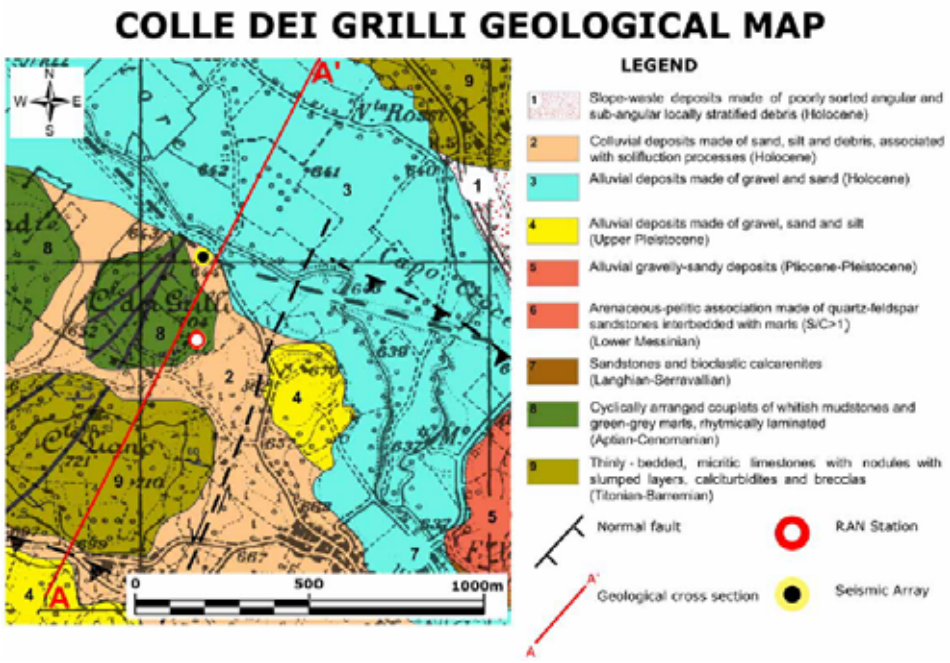

Figure 1*: Geologic map of the l'Aquila – Colle dei Grilli RAN site*

The Colle dei Grilli RAN site is located in the north-western portion of the l'Aquila plain to the hydrographical right of the Aterno river. The area is characterized by the outcropping of the Miocene and Upper Cretaceous successions. In particular the Miocene deposits over-thrust above the Cretaceous succession with an high angle SW-dipping thrust fault. The sedimentary successions recognized in the area were subdivided into nine different lithological formations as listed below: from the bottom 9) Thinly bedded micritic limestones with abundant nodules and slumped layers with dark-grey flint and biodetritic horizons. Several calciturbidites and breccias were recognized at different levels; 8) Cyclically arranged couplets of whitish mudstones and green-grey marls, rhythmically laminated with rare dark-grey flint, while to the top of the sequence planktonic biomicrite, limestones and yellowish and greenish marls. The upper side of the sequence is characterized by the thickness increasing of the strata; 7) Calcarenites with Briozoa has been distinguished. Whitish/gray calcarenites/calcirudites with Briozoa and fragments of Lithotamnium, interbedded with whitish saccaroid calcarenites laterally passing to gray-yellowish calcarenites with Briozoa and Pecten; 6) This arenaceous-pelitic association is constituted by the alternations of different facies association characterized by varying time/space relationships. In particular outcropping in the area quartz-feldspars sandstones, without sedimentary structures, intercalated with this politic levels. At different levels quartz-feldspar sandstones interbedded with marls (S/C>1); 5) Alluvial gravelly-sandy deposits terraces. This deposits is widespread in the area specially in the eastern sector with a variable thickness from few meters up to 20m; 4) Alluvial deposits made of gravel, sand and silt.

This deposits outcropping with little thickness; 3) Actual alluvial deposits mainly made of gravel and sand; 2) Colluvial deposits made of sand silt and debris associated with solifluction processes; 1) Slope-waste deposits made of poorly sorted angular and sub-angular locally stratified debris.

From a structural point of view the area is characterized by the presence of an important thrust fault NW-SE trending, and SW dipping, that favourite the over-thrusting of the cretaceous/Miocene succession above an upper cretaceous sequence. In particular inversion processes affect the whole area reactivating the thrust fault with an extensional movement, as demonstrated by the presence of Miocene deposits just above a cretaceous succession. This anomalous contact represent the effect of the inversion tectonic from positive (compression) to negative (extension) along the same fault plane. Furthermore the thrust plane is offset to the East by a N20° tear fault that favourite the complexity distribution of the thrust fault trace. Three normal fault were also recognized close to the RAN and ARRAY stations. These faults offset the compressional structures with a N30° strike direction with an high SE-dipping fault planes.

The Array station was realized above a thin colluvial deposits lie over the cretaceous marls (Figure 1), while the RAN station is located above the outcropping rocks. Despite the lithological differences the two sites are representative due to the very tin thickness of the cover deposits just below the ARRAY.

A representative geological section is reported in Figure2.

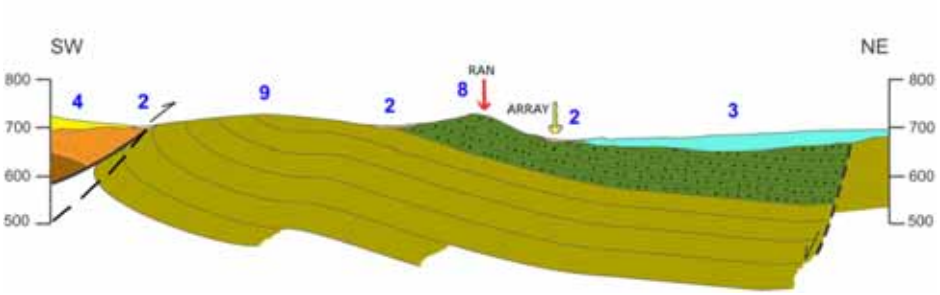

Figure 2 *Geological section across L'Aquila Colle dei Grilli area (see trace in Fig.1): RAN indicates location of the AQP accelerometric station. ARRAY indicates the position of the array*

Results of passive seismic survey

A single station measurement was carried nearby the RAN station (Figures 3 and 5) on 28th of July 2009. A significant resonance phenomenon was detected at the frequencies of about 6 Hz as a possible effect of a layer of rock alteration.

Figure3. *Location of the RAN station and of the corresponding single station ambient vibration measurement*

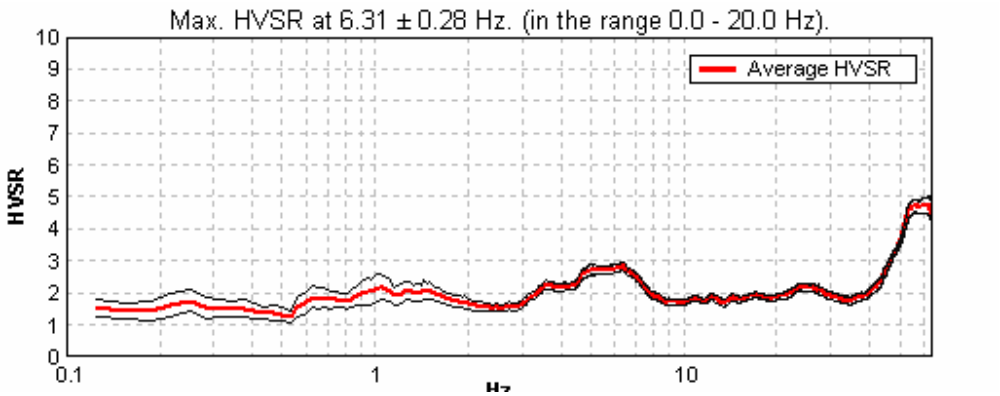

Figure 4. *HVSR curve obtained at the AQG RAN station. The red line indicates the average HVSR values, while the black thin lines indicate the relevant 95% confidence interval*

It was not possible to deploy the Array near the RAN station and thus it was located few hundreds meters apart in the flat area nearest to the station (Figure 1). HVSR measurements at the array sites revealed a sharp resonance that is absent at the RAN station. This implies that at the array, a layer of soft material overlies the rock formations present at the RAN station. Thus, HVSR at the Array site where jointly inverted to provide VS values at depth. Thus, this profile was varied (in its shallowest part) to best fit the HVSR curve at the RAN station. This analysis provided the VS profile in Figure 7 and Table 1. This indicate the presence of relatively low Vs values (altered rocks?) in the shallowest part of the profile, overlying more rigid formations.

Figure 5. *Location of the L'Aquila – Colle dei Grilli RAN station (in the background). On the bottom of the picture, the digital tromograph used for the single station ambient vibration measurements is shown*

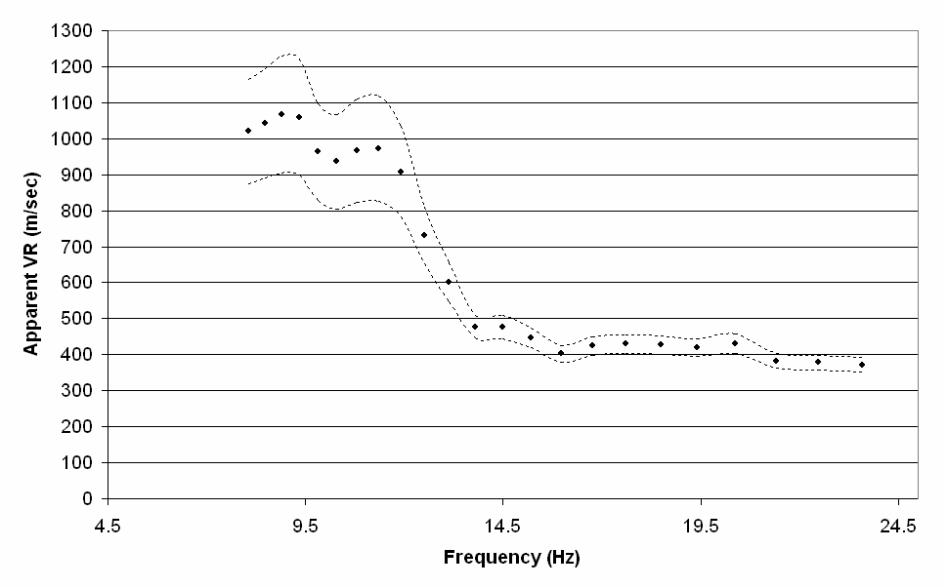

Figure 6. *Apparent VR curve deduced from array measurements. Dots indicate VR estimates while dashed lines bound the relevant 95% confidence interval*

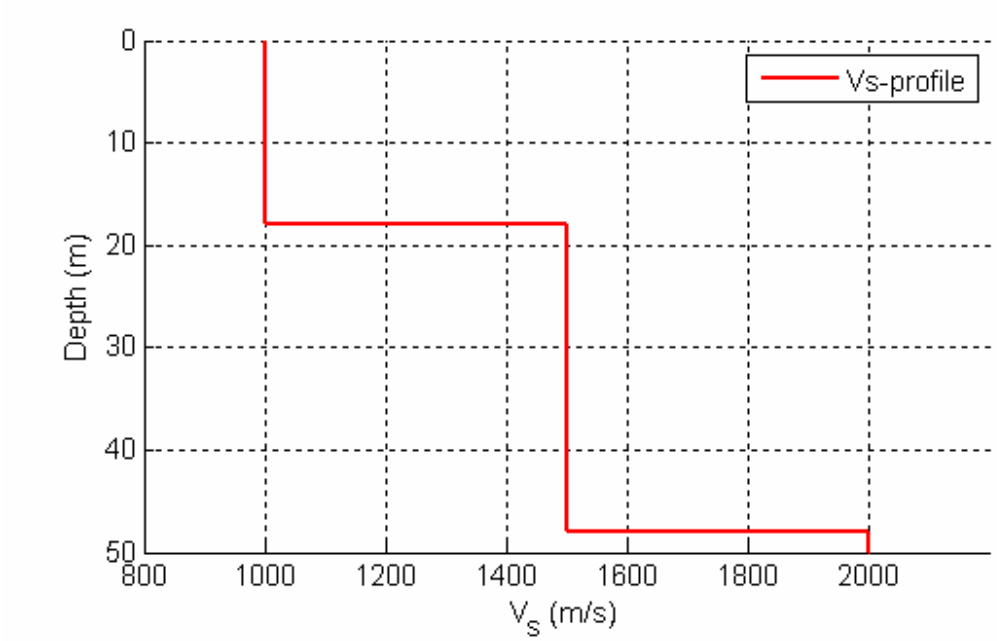

Figure 7. *Vs Velocity profile at the L'Aquila – Monte Colle dei Grilli RAN station*

***Table 1**: V_S profile at the AQG station*

Tickness (m)	S-Velocity (m/s)
18	**1000**
30	**1500**
7	**2000**
?	**2800**

Summary of subsoil basic features at the AQG RAN site

Vs30 = 1150 m/s
Soil Class = A
Topography classification = T2
Depth to bedrock = 0
Average Vs to bedrock = 0 m/s
f_0 from ambient vibrations = 6.3 Hz

References

Lunedei E., Albarello D. (2009). On the seismic noise wavefield in a weakly dissipative layered Earth. *Geophys. J. Int.* (2009) **177,** 1001–1014, doi: 10.1111/j.1365-246X.2008.04062.x

Menke,W., 1989. *Geophysical Data Analysis: Discrete Inverse Theory,* rev.ed. Academic, San Diego, CA.

Ohori M., Nobata A., Wakamatsu K. (2002). A comparison of ESAC and FK methods of estimating phasevelocity using arbitrarily shaped microtremor arrays. Bull.Seism.Soc.Am., 92, 6, 2323-2332

Okada, H. (2003). The microtremor survey method, *Geophys. Monograph Series,* Vol. 12, Society of Exploration Geohysicists, 129 pp.

Picozzi M., Parolai S., Albarello D.; 2005: Statistical analysis of noise Horizonatal-to-Vertical Specrtal Ratios (HVSR). Bull. Seism. Soc. Am., **95**, n. 5, 1779–1786, doi: 10.1785/0120040152

Picozzi M., Albarello D. (2007). Combining genetic and linearized algorithms for a two-step joint inversion of Rayleigh wave dispersion and *H/V* spectral ratio curves. *Geophys. J. Int.* (2007) **169,** 189–200, doi: 10.1111/j.1365-246X.2006.03282.x

SESAME; 2004: Guidelines for the implementation of the H/V spectral ratio technique on ambient vibrations. SESAME, European project, WP12, Deliverable D23.12, http://sesame-fp5.obs.ujfgrenoble.fr/SES TechnicalDoc.htm

Tokimatsu, K. (1997). “Geotechnical Site Characterization using Surface Waves.” *Proceedings, First International Conference on Earthquake Geotechnical Engineering, IS-Tokyo '95*, Tokyo, November 14-16, Balkema, Rotterdam, 1333-1368.

Zhang, S.H., Chan, L.S. and Xia, J. (2004). The selection of field acquisition parameters for dispersion images from multichannel surface wave data. *Pure and Applied Geophysics* 161, 185–201.

Dipartimento di Scienze della Terra
Università degli Studi di Siena
Via Laterina, 8 53100 Siena, Italy

APPLICATION OF SURFACE WAVES METHODS FOR SEISMIC SITE CHARACTERIZATION

L'Aquila - Pettino RAN site (AQP)

Responsible
Prof.Dario Albarello

Co-Workers
Dott. Domenico Pileggi
Dott. David Rossi
Dott. Enrico Lunedei

FINAL REPORT

Siena 30 May 2010

The investigation protocol

It involves four major elements:

- *Detailed Geological survey of the study area resulting in a geo/lithologic map at the scale 1:5000 of the area surrounding the relevant RAN station. This also aimed at the evaluation of the degree of lateral heterogeneity present in the lithological structure paying major attention to faults and their relevant damage area (that can result in energy trapping phenomena)*
- *Extensive single station ambient vibration survey at the station and in the surrounding area to detect possible lateral variations potentially responsible for site effects*
- *Ambient vibration measurements carried on with a seismic array at the RAN site or at a site representative of the subsoil configuration at the RAN site. In this last case, suitable inversion procedures and test were carried on to warrant the representativeness of ambient vibration measurements*
- *Global interpretation of measurements to determine the V_S profile and of the resonance frequency at the RAN site by considering the whole set of collected data*

Details concerning experimental tools and processing techniques are given in the following sections.

Single station measurements

The goal of this kind of measurements is the retrieval of the HVSR curve that represents for each frequency, the average ratio between Horizontal (H) to vertical (V) ground motion components of ambient vibrations (SESAME, 2004). Each single-station measurement was executed with a three-directional digital tromograph Tromino Micromed (see www.tromino.it) with a sampling frequency of 128 Hz and an acquisition time length of 20 minutes. This value represents a good compromise between the celerity of the measurement execution (which is one of the main merits of this technique) and its accuracy, according to the SESAME guidelines and other studies (see, e.g., Picozzi et al., 2005). To provide HVSR curves, the time series relative to each ground motion component was subdivided in non-overlapping time windows of 30 s. For each of these, the signal was corrected for the base line, padded with zeros, and tapered with a Triangular window; the relevant spectrogram was smoothed through a triangular window with frequency dependent half-width (10% of central frequency) and the H/V ratio (HVSR) of the spectral components (the former being the geometric mean of North-South and East-West components) was computed for each frequency. Spectral ratios relative to all the time windows considered were then averaged, and a mean HVSR curve was computed along with the relevant 95% confidence interval.

Before interpreting HVSR curve in terms of subsoil dynamical properties, we checked the possible occurrence of spurious HVSR peaks (e.g., due to impulsive or strongly localized anthropic sources). To this purpose, we investigated both the time stability of spectral ratios over the recording length and their directionality. The latter was analyzed by estimating the HVSR curves derived by projecting the ground motion along different horizontal directions. If transient directional effects were identified in the directional HVSR curves, the relevant portions of the record were discarded.

Array Measurements

This technique consists in recording ambient vibration ground motion by means of an array of sensors (vertical geophones) distributed at the surface of the subsoil to be explored (see, e.g., Okada, 2003). Relevant information concerning phase velocities of waves propagating across the array are obtained from average cross-spectral matrixes relative to sensor pairs. In the present analysis, plane waves propagating across the array were considered only. Since vertical sensors were used only, these waves are interpreted as plane Rayleigh waves in their fundamental and higher propagation modes. Determination of Rayleigh wave phase velocities V_R as a function of frequency (dispersion curve) from cross-spectral matrixes can be carried on in several ways. In the present analysis, the Extended Spatial Auto Correlation (ESAC) technique (Ohori et al. , 2002; Okada, 2003)

was applied. The basic element of this analysis is the cross-correlation spectrum deduced by the analysis of ambient vibrations measured at a couple of sensors $\phi(f,r)$ where *f* is frequency and *r* is the distance between the relevant sensors .

To this purpose, registrations relative to each sensor are partitioned in a number of non overlapping time windows of fixed duration (20 sec). Time windows characterised by energy bursts were removed from the analysis. To this purpose, a time segment is considered in the analysis if standard deviation of all the traces of that time window do not exceed the threshold fixed in advance for each trace. In general, this threshold was fixed to be 2 times the standard deviation computed over the whole registration for the relevant trace. In each accepted time window, linear trend was removed and the resulting time series was padded and tapered (5% cosine windows). For each time window and couple of sensors, the cross spectrum was computed. The average cross spectrum was then computed for each couple of sensors by considering all the relevant time series. The resulting average cross-spectrum was thus smoothed in the frequency domain by a moving triangular window having an half-width proportional to the central value (usually 10%) and normalized to the relevant auto spectra.

In the assumption that ambient vibration wave field can be represented as a linear combination of statistically independent plane waves propagating with negligible attenuation in a horizontal plane in different directions with different powers, but with the same phase velocity for a given frequency, the normalized cross-spectrum $\phi_{ij}(f,r)$ relative to sensors located at a distance r, can be written in the form

$$\phi(f,r) = J_0\left(\frac{2\pi f r}{V_R(f)}\right)$$

where J_0 is the Bessel function of *0-th* order. In the ESAC approach, the value of V_R relative to each frequency *f* is retrieved by a grid search algorithm to optimized (in a RMS sense) the fit of the above function of r for the relevant frequency *f* (Ohori et al. , 2002; Okada, 2003). Robustness of this fitting procedure was enhanced by adopting the iterative procedure proposed by Parolai et al., 2006). By following these last Authors, uncertainty on "apparent" velocities was computed by means the second derivative of the misfit function relative to grid search procedure (see, Menke, 1989). However, since these estimate tend to be under-conservative in some cases, the lower bound of the confidence interval for experimental V_R values was fixed by using the relationship proposed by Zhang et al. (2004) as a function of the adopted sampling rate and array dimension.

The $V_R(f)$ value obtained in this way, is the "apparent" or "effective" Rayleigh waves phase velocity that coincides with the actual phase velocity only in the case that higher modes play a negligible role. In the other cases, a relationship can be established between actual phase velocities and the apparent one (Tokimatsu, 1997). The fact that the ESAC approach allows the determination of the apparent dispersion curve instead of the modal ones could represent an important limitation of this procedure with respect to other approaches (e.g., f-k techniques). On the other hand, this makes the approach here considered more robust with respect to the alternative procedures, since it does not require troublesome picking of existing propagation modes.

In the present study, ambient vibrations were recorded for 20 minutes at a 256 Hz sampling rate by using 16 vertical geophones (4.5 Hz) and a digital acquisition system produced by Micromed (http://micromed.com/brainspy1.htm). Geophones were placed along two crossing perpendicular branches (with maximum dimensions lower than 100 m) and irregularly spaced (in the range 0.5-30 m).

Inversion procedures

HVSR and apparent V_R curves have been jointly inverted to constrain to the local V_S profile. To this purpose, a genetic algorithm procedure was considered. This is an iterative procedure, consisting in sequence of steps miming the evolutionary selection of living being (see Picozzi and Albarello, 2007 and references therein). The formalization proposed by Lunedei and Albarello (2009) was used as the forward modelling modelling

implemented in the procedure. This procedure assumes the subsoil as a flat stratified viscoelastic medium where surface waves (Rayleigh and Love with relevant higher modes) propagate only. From this model, both theoretical HVSR and effective dispersion curves can be computed from a set of parameters representative of the hypothetical subsoil (V_S, V_P, density, Q_P and Q_S profiles). The discrepancy between theoretical and observed HVSR and dispersion curves were then evaluated in terms of a suitable misfit function, strictly linked to the well-known χ^2 function, that allowed different choices about the combination of the discrepancies of V_R and HVSR curves, with different weights as well. The confidence interval around preferred *Vs* values and layer thickness were evaluated by following Picozzi and Albarello (2007).

Geological Setting

A detailed geologic survey of the area surrounding the RAN site was carried on (Figure 1).

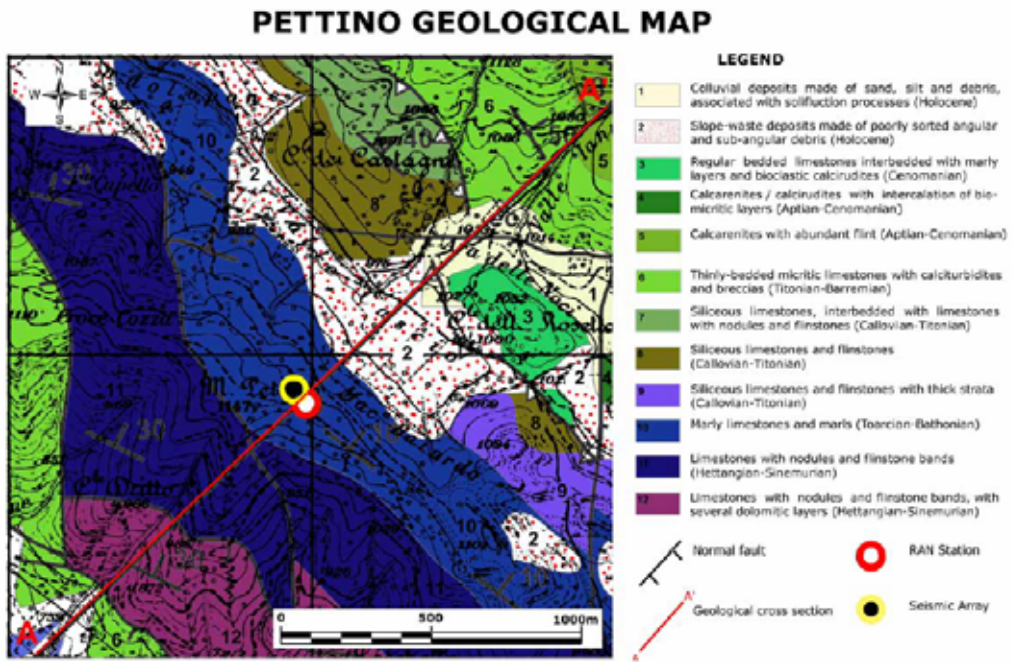

Figure 1*: Geologic map of the l'Aquila – Monte Pettino RAN site*

The Pettino RAN site is located in the northern sector of the l'Aquila plain at 1147m above the sea level at the top of an important apenninic carbonatic ridge. The whole area analyzed is characterized by the presence of a thrust fault in the NE and by an important interconnecting network of normal faults. These last shows a N130-140° direction with SW dipping. The main effect of the extensional tectonic is represented by the progressive SW-downwards of the whole sedimentary succession allowing the contact between middle Jurassic with the upper cretaceous. The sedimentary succession cropping out in the area is represented by a tick meso-cenozoic sedimentary succession mainly represented by limestones and calcarenites. The Jurassic succession is characterized by limestones with nodules and flinstone bands (12-11) while the upper part is represented by a tin thickness of marly limestones and marls (10). The whole Cretaceous sequence is mainly characterized by siliceous limestones interbedded with limestones and by thinly-bedded micritic limestones with calciturbidites and breccias (9-8-7-6-5-4-3). The main lithological difference within the Cretaceous succession is underlined by the upper portion, represented by a regularly bedded calcarenites and calcirudites with abundant flint.

The structural setting of the area is highlighted by the presence of a low angle thrust fault that favourite the overlapping of the upper Jurassic succession above the upper cretaceous sequence. The sedimentary succession in the hangingwall of the thrust fault is organized into an East verging anticline while the footwall is represented by an overturned recumbent syncline. These folds favorite the widespread development of an intense fracturation processes, both in the fault interface and along the hinge folds. An important interconnecting

network of normal faults were recognized. These last are kinematically characterized by dip-slip movements, N130° direction and 70-80° SW dipping. As result of the normal fault activity the whole sedimentary succession is progressively downwards offset to the SW.

Both the RAN and the ARRAY are located directly above the outcropping rocks with only few centimeter of quaternary deposits.

A representative geological section is reported in Figure2.

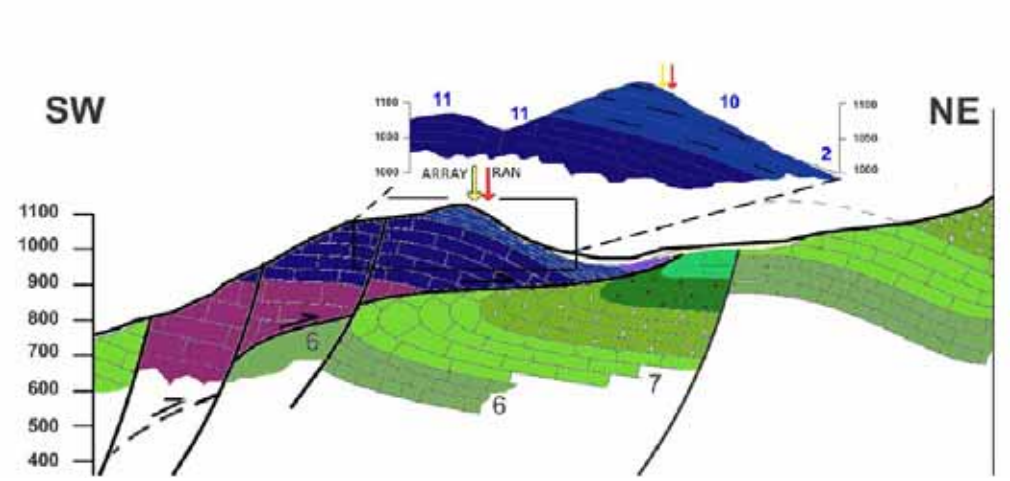

Figure 2 *Geological section across L'Aquila Monte Pettino area (see trace in Fig.1): RAN indicates location of the AQP accelerometric station. ARRAY indicates the position of the array*

Results of passive seismic survey

A single station measurement was carried nearby the RAN station (Figures 3 and 5) on 28th of July 2009. A significant resonance phenomenon was detected at the frequencies of about 2 Hz.

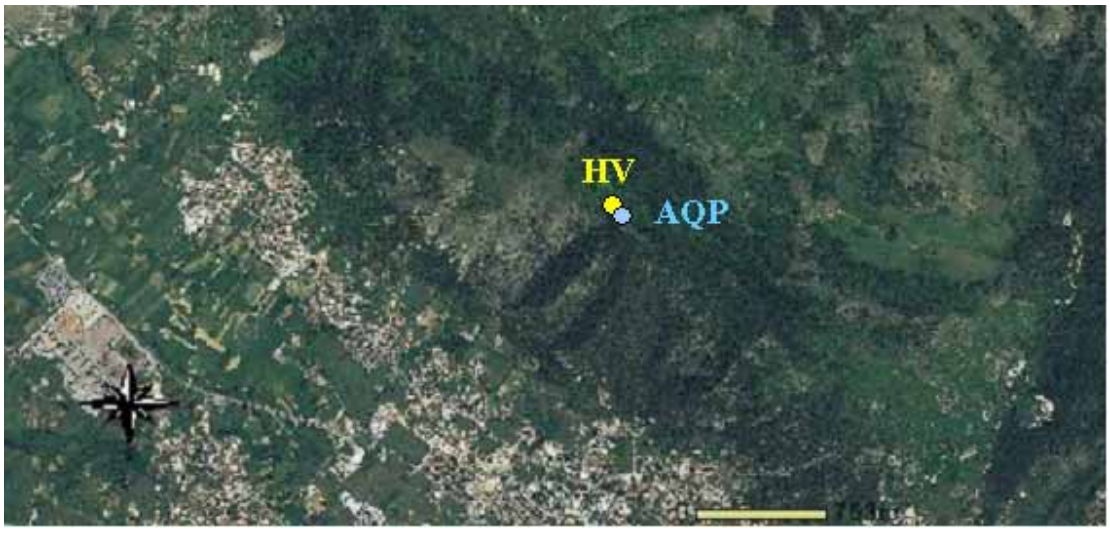

Figure3. *Location of the RAN station and of the corresponding single station ambient vibration measurement*

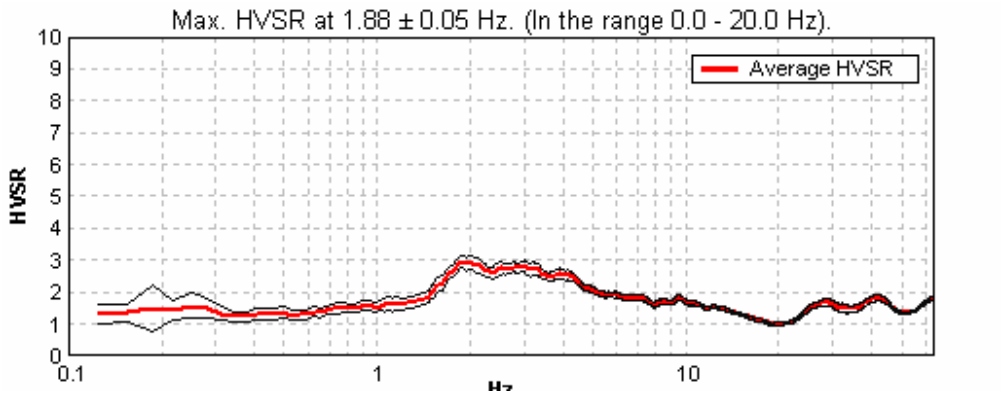

Figure 4. *HVSR curve obtained at the AQP RAN station. The red line indicates the average HVSR values, while the black thin lines indicate the relevant 95% confidence interval*

Array measurements were carried near RAN site (Figure 1). Results of these measurements (Fig. 6), however, resulted quite irregular and show a non monotonic trend and this prevents a simple interpretation. Several attempts were performed to jointly invert HVSR and Apparent dispersion curve. Neither of them resulted fully satisfactory. The one presented in Figure 7 and Table 1, represents the best compromise between inversion results and geological indications. The shallowest layer could correspond to altered materials that overly a rigid body. The possible further increase of VS values could be justified from the geological point of view (from Unit 10 to unit 11 in Figure 2).

Figure 5. *Location of the L'Aquila – Monte Pettino RAN station (on the right). On the left, the digital tromograph used for the single station ambient vibration measurements is shown*

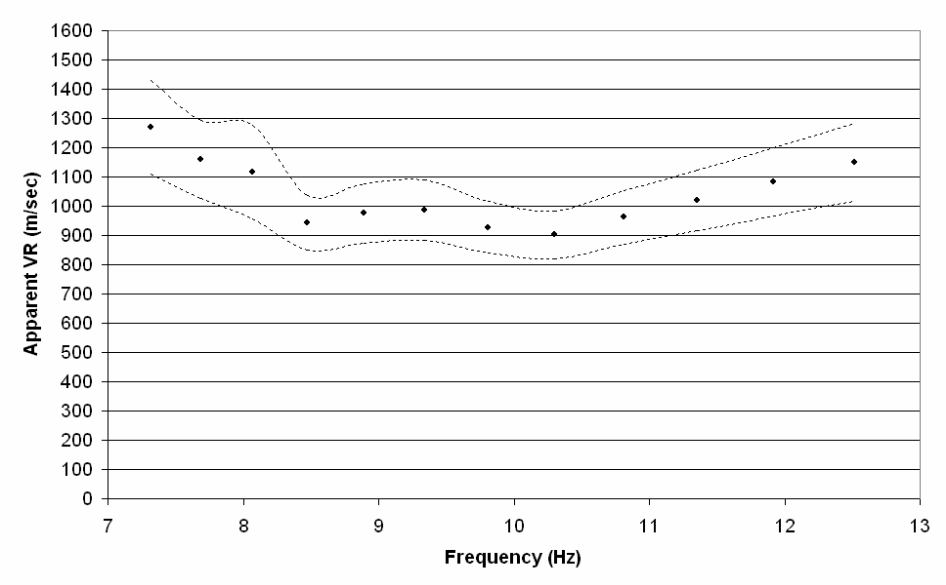

Figure 6. *Apparent VR curve deduced from array measurements. Dots indicate VR estimates while dashed lines bound the relevant 95% confidence interval*

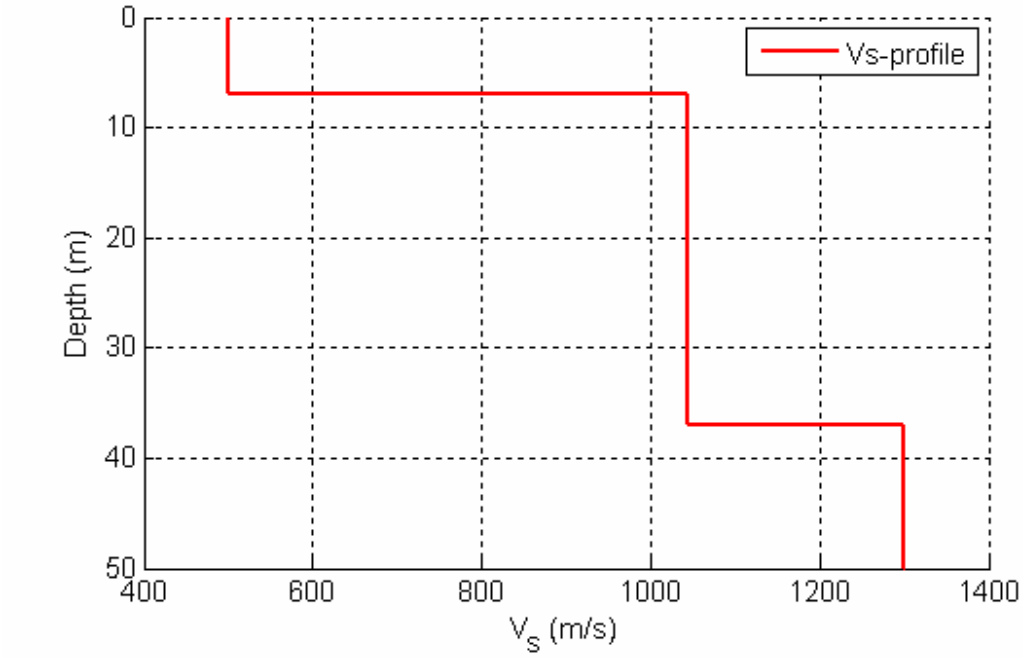

Figure 7. *Vs Velocity profile at the L'Aquila – Monte Pettino RAN station*

***Table 1**: V_S profile at the AQP station*

Tickness (m)	S-Velocity (m/s)
7	**500**
30	**1050**
?	**1300**

Summary of subsoil basic features at the AQP RAN site

Vs30 = 830 m/s
Soil Class = A
Topography classification = T3
Depth to bedrock = 7 m
Average Vs to bedrock = 500 m/s
f_0 from ambient vibrations = 1.9 Hz

References

Lunedei E., Albarello D. (2009). On the seismic noise wavefield in a weakly dissipative layered Earth. *Geophys. J. Int.* (2009) **177,** 1001–1014, doi: 10.1111/j.1365-246X.2008.04062.x

Menke,W., 1989. *Geophysical Data Analysis: Discrete Inverse Theory,* rev.ed. Academic, San Diego, CA.

Ohori M., Nobata A., Wakamatsu K. (2002). A comparison of ESAC and FK methods of estimating phasevelocity using arbitrarily shaped microtremor arrays. Bull.Seism.Soc.Am., 92, 6, 2323-2332

Okada, H. (2003). The microtremor survey method, *Geophys. Monograph Series,* Vol. 12, Society of Exploration Geohysicists, 129 pp.

Picozzi M., Parolai S., Albarello D.; 2005: Statistical analysis of noise Horizonatal-to-Vertical Specrtal Ratios (HVSR). Bull. Seism. Soc. Am., **95**, n. 5, 1779–1786, doi: 10.1785/0120040152

Picozzi M., Albarello D. (2007). Combining genetic and linearized algorithms for a two-step joint inversion of Rayleigh wave dispersion and *H/V* spectral ratio curves. *Geophys. J. Int.* (2007) **169,** 189–200, doi: 10.1111/j.1365-246X.2006.03282.x

SESAME; 2004: Guidelines for the implementation of the H/V spectral ratio technique on ambient vibrations. SESAME, European project, WP12, Deliverable D23.12, http://sesame-fp5.obs.ujfgrenoble.fr/SES TechnicalDoc.htm

Tokimatsu, K. (1997). “Geotechnical Site Characterization using Surface Waves.” *Proceedings, First International Conference on Earthquake Geotechnical Engineering, IS-Tokyo '95*, Tokyo, November 14-16, Balkema, Rotterdam, 1333-1368.

Zhang, S.H., Chan, L.S. and Xia, J. (2004). The selection of field acquisition parameters for dispersion images from multichannel surface wave data. *Pure and Applied Geophysics* 161, 185–201.

Dipartimento di Scienze della Terra
Università degli Studi di Siena
Via Laterina, 8 53100 Siena, Italy

APPLICATION OF SURFACE WAVES METHODS FOR SEISMIC SITE CHARACTERIZATION

CAPESTRANO RAN site (CPS)

Responsible
Prof.Dario Albarello

Co-Workers
Dott. Domenico Pileggi
Dott. David Rossi
Dott. Enrico Lunedei

FINAL REPORT

Siena 30 May 2010

The investigation protocol

It involves four major elements:

- *Detailed Geological survey of the study area resulting in a geo/lithologic map at the scale 1:5000 of the area surrounding the relevant RAN station. This also aimed at the evaluation of the degree of lateral heterogeneity present in the lithological structure paying major attention to faults and their relevant damage area (that can result in energy trapping phenomena)*
- *Extensive single station ambient vibration survey at the station and in the surrounding area to detect possible lateral variations potentially responsible for site effects*
- *Ambient vibration measurements carried on with a seismic array at the RAN site or at a site representative of the subsoil configuration at the RAN site. In this last case, suitable inversion procedures and test were carried on to warrant the representativeness of ambient vibration measurements*
- *Global interpretation of measurements to determine the V_S profile and of the resonance frequency at the RAN site by considering the whole set of collected data*

Details concerning experimental tools and processing techniques are given in the following sections.

Single station measurements

The goal of this kind of measurements is the retrieval of the HVSR curve that represents for each frequency, the average ratio between Horizontal (H) to vertical (V) ground motion components of ambient vibrations (SESAME, 2004). Each single-station measurement was executed with a three-directional digital tromograph Tromino Micromed (see www.tromino.it) with a sampling frequency of 128 Hz and an acquisition time length of 20 minutes. This value represents a good compromise between the celerity of the measurement execution (which is one of the main merits of this technique) and its accuracy, according to the SESAME guidelines and other studies (see, e.g., Picozzi et al., 2005). To provide HVSR curves, the time series relative to each ground motion component was subdivided in non-overlapping time windows of 30 s. For each of these, the signal was corrected for the base line, padded with zeros, and tapered with a Triangular window; the relevant spectrogram was smoothed through a triangular window with frequency dependent half-width (10% of central frequency) and the H/V ratio (HVSR) of the spectral components (the former being the geometric mean of North-South and East-West components) was computed for each frequency. Spectral ratios relative to all the time windows considered were then averaged, and a mean HVSR curve was computed along with the relevant 95% confidence interval.

Before interpreting HVSR curve in terms of subsoil dynamical properties, we checked the possible occurrence of spurious HVSR peaks (e.g., due to impulsive or strongly localized anthropic sources). To this purpose, we investigated both the time stability of spectral ratios over the recording length and their directionality. The latter was analyzed by estimating the HVSR curves derived by projecting the ground motion along different horizontal directions. If transient directional effects were identified in the directional HVSR curves, the relevant portions of the record were discarded.

Array Measurements

This technique consists in recording ambient vibration ground motion by means of an array of sensors (vertical geophones) distributed at the surface of the subsoil to be explored (see, e.g., Okada, 2003). Relevant information concerning phase velocities of waves propagating across the array are obtained from average cross-spectral matrixes relative to sensor pairs. In the present analysis, plane waves propagating across the array were considered only. Since vertical sensors were used only, these waves are interpreted as plane Rayleigh waves in their fundamental and higher propagation modes. Determination of Rayleigh wave phase velocities V_R as a function of frequency (dispersion curve) from cross-spectral matrixes can be carried on in several ways. In the present analysis, the Extended Spatial Auto Correlation (ESAC) technique (Ohori et al. , 2002; Okada, 2003)

was applied. The basic element of this analysis is the cross-correlation spectrum deduced by the analysis of ambient vibrations measured at a couple of sensors $\phi(f,r)$ where *f* is frequency and *r* is the distance between the relevant sensors .

To this purpose, registrations relative to each sensor are partitioned in a number of non overlapping time windows of fixed duration (20 sec). Time windows characterised by energy bursts were removed from the analysis. To this purpose, a time segment is considered in the analysis if standard deviation of all the traces of that time window do not exceed the threshold fixed in advance for each trace. In general, this threshold was fixed to be 2 times the standard deviation computed over the whole registration for the relevant trace. In each accepted time window, linear trend was removed and the resulting time series was padded and tapered (5% cosine windows). For each time window and couple of sensors, the cross spectrum was computed. The average cross spectrum was then computed for each couple of sensors by considering all the relevant time series. The resulting average cross-spectrum was thus smoothed in the frequency domain by a moving triangular window having an half-width proportional to the central value (usually 10%) and normalized to the relevant auto spectra.

In the assumption that ambient vibration wave field can be represented as a linear combination of statistically independent plane waves propagating with negligible attenuation in a horizontal plane in different directions with different powers, but with the same phase velocity for a given frequency, the normalized cross-spectrum $\phi_{ij}(f,r)$ relative to sensors located at a distance r, can be written in the form

$$\phi(f,r) = J_0\left(\frac{2\pi f r}{V_R(f)}\right)$$

where J_0 is the Bessel function of *0-th* order. In the ESAC approach, the value of V_R relative to each frequency *f* is retrieved by a grid search algorithm to optimized (in a RMS sense) the fit of the above function of r for the relevant frequency *f* (Ohori et al. , 2002; Okada, 2003). Robustness of this fitting procedure was enhanced by adopting the iterative procedure proposed by Parolai et al., 2006). By following these last Authors, uncertainty on "apparent" velocities was computed by means the second derivative of the misfit function relative to grid search procedure (see, Menke, 1989). However, since these estimate tend to be under-conservative in some cases, the lower bound of the confidence interval for experimental V_R values was fixed by using the relationship proposed by Zhang et al. (2004) as a function of the adopted sampling rate and array dimension.

The $V_R(f)$ value obtained in this way, is the "apparent" or "effective" Rayleigh waves phase velocity that coincides with the actual phase velocity only in the case that higher modes play a negligible role. In the other cases, a relationship can be established between actual phase velocities and the apparent one (Tokimatsu, 1997). The fact that the ESAC approach allows the determination of the apparent dispersion curve instead of the modal ones could represent an important limitation of this procedure with respect to other approaches (e.g., f-k techniques). On the other hand, this makes the approach here considered more robust with respect to the alternative procedures, since it does not require troublesome picking of existing propagation modes.

In the present study, ambient vibrations were recorded for 20 minutes at a 256 Hz sampling rate by using 16 vertical geophones (4.5 Hz) and a digital acquisition system produced by Micromed (http://micromed.com/brainspy1.htm). Geophones were placed along two crossing perpendicular branches (with maximum dimensions lower than 100 m) and irregularly spaced (in the range 0.5-30 m).

Inversion procedures

HVSR and apparent V_R curves have been jointly inverted to constrain to the local V_S profile. To this purpose, a genetic algorithm procedure was considered. This is an iterative procedure, consisting in sequence of steps miming the evolutionary selection of living being (see Picozzi and Albarello, 2007 and references therein). The formalization proposed by Lunedei and Albarello (2009) was used as the forward modelling modelling

implemented in the procedure. This procedure assumes the subsoil as a flat stratified viscoelastic medium where surface waves (Rayleigh and Love with relevant higher modes) propagate only. From this model, both theoretical HVSR and effective dispersion curves can be computed from a set of parameters representative of the hypothetical subsoil (V_S, V_P, density, Q_P and Q_S profiles). The discrepancy between theoretical and observed HVSR and dispersion curves were then evaluated in terms of a suitable misfit function, strictly linked to the well-known χ^2 function, that allowed different choices about the combination of the discrepancies of V_R and HVSR curves, with different weights as well. The confidence interval around preferred *Vs* values and layer thickness were evaluated by following Picozzi and Albarello (2007).

Geological Setting

The geologic setting around the CPS RAN site as deduced by a detailed geologic survey is reported in Figure 1.

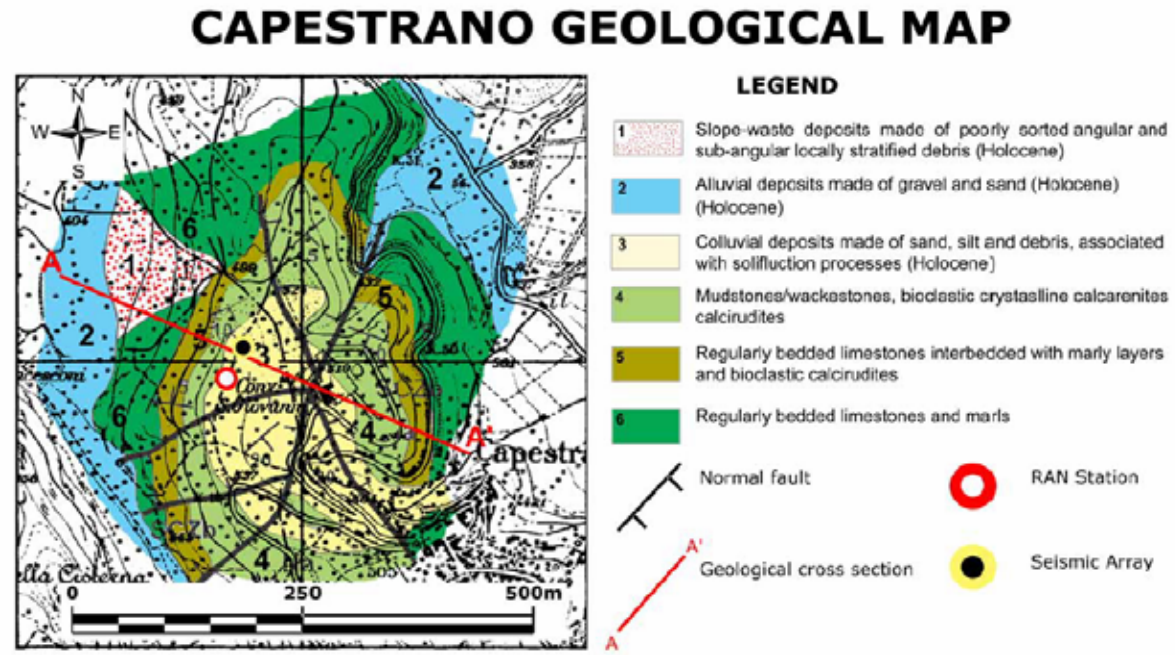

***Figure 1**: Geologic map of the Capestrano RAN site*

The Capestrano RAN station was realized on the top of a small hill at 537 m over the sea level. The station is located above a tin colluvial deposits just over the top of a cretaceous sedimentary succession belonging the laziale abruzzese domain. From a geometrically point of view the sedimentary succession is folded by a wide syncline with a sub-vertical fold plane. The average strata dip angle is always comprised between 5° to 10°. From the bottom of the cropping out formations it is possible to identify the following rocks: 6-5) regularly bedded limestones with nodules and flinstone bands, light brown micrite and bioclastic calcarenite, then wackestones with thin intercalations of clay and sporadic levels of flint. The base of the formation is characterized by a tick calcirudites horizon; 4) Mudstones and wackestones regularly bedded with intercalation of bioclastic crystalline calcarenites and calcirudites; 3) Colluvial deposits mainly composed of sand, silt and debris associated with solifluction processes; 2) Alluvial deposits made of gravel and sand with various thickness; 1) Slope-waste deposits made of poorly sorted angular and sub-angular. Locally the deposits present a well organized stratification.
The site is characterized by the presence of several normal faults offsetting the whole sedimentary succession. Despite the small offset (up to 40m) the fault planes recognized cross-cutting the whole zone with a main strike direction of N170°-20°. The main fault plane is characterized by a N20° trending, dip-slip W-dipping normal fault offsetting both the sedimentary succession and the other fault planes. Field analyses carried out allow us to identify and kinematically characterize up to 10 normal faults, but only 4 were mapped. Most of the un-mapped

faults planes was characterized by centimetric offset and very poor planimetric extension. Fracture sets were observed across the limbs and the hinge of the fold (limb dips range from 5° to 10°). The fracture sets recognized was identify as dissolution cleavage showing a sub-vertical planes sub-parallel to the fold hinge. A second sets of fracture were identified and linked to the faults mechanisms. Both the ARRAY and the RAN (very close each other) lie over the same tin cover deposits just above an intense fractured sedimentary succession. A representative geological section at the RAN station is reported in Figure 2.

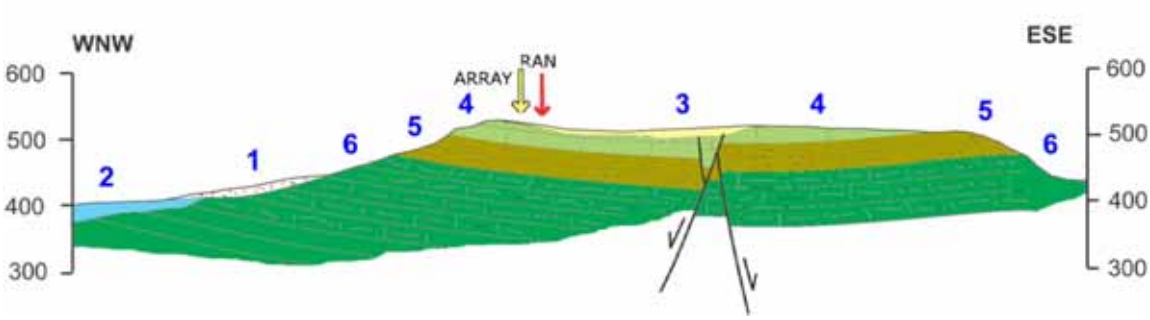

Figure 2 *Geological section across Capestrano area (see trace in Fig.9): RAN indicates location of the CPS accelerometric station. ARRAY indicates the position of the array*

In the case of the Capestrano site, both single station and array measurements were carried on nearby the RAN station (Figure 1). Resulting HVSR curve is reported in Figure 4 and, despite the presence of a marked directionality, reveals the presence of a broad resonance peak with a maximum at the frequency of about 2.7 Hz in the presence of electromagnetic disturbances around 5 Hz.

Figure 3. *HAVSR measurements at the CPS RAN station. The silver small object at the bottom of the picture in the tromograph Tromino used for single station ambient vibration measurements.*

Due to the relatively flat morphology around the RAN station, the deployment of the array did not present any particular problem. These measurements provided the dispersion curve in Figure 5, that seems compatible V_S velocities relatively high and increasing with depth.

The curve in figures 4 and 5 were jointly inverted by providing the V_S profile in Figure 6 and Table 1. This indicates the presence, below a very thin soft coverage (1 m) of two rigid layers. The shallower one (10 thick with a V_S of about 700 m/sec) nearly correspond to the unit 4 (see section in figure 2). This overlies a deeper more rigid layer (with V_S values of the order of 1000 m/sec) having a larger thickness (about 50 m that nearly corresponds to unit 5 in the section of Figure 2) overlaying a more rigid structure (unit 6 in figure 2).
In this case, an almost perfect convergence of outcomes provide by geophysical and geological was achieved.

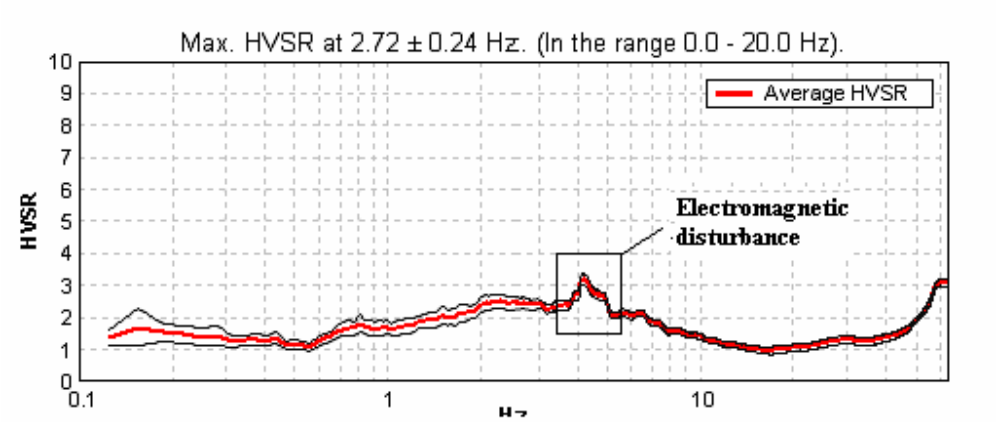

Figure 4. *HVSR curve obtained at the RAN station CPS. The red line indicates the average HVSR values, while the black thin lines indicate the relevant 95% confidence interval*

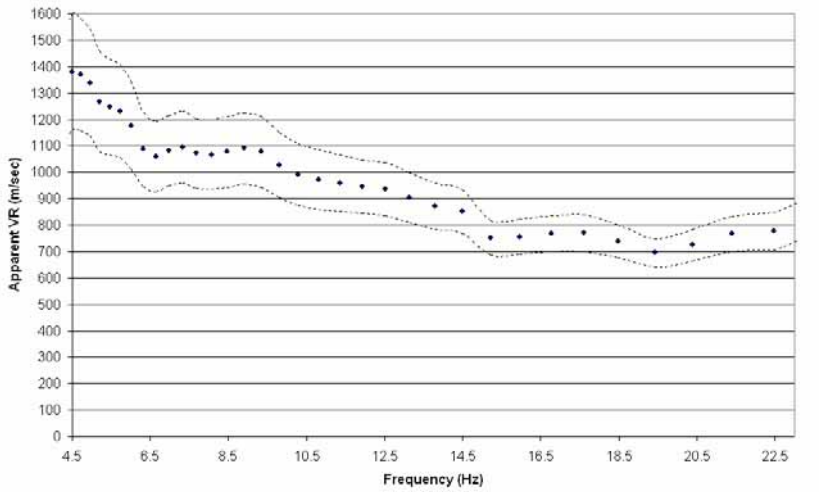

Figure 5. *Apparent VR curve deduced at the Cepestrano RAN site from array measurements. Dots indicate VR estimates while dashed lines bound the relevant 95% confidence interval*

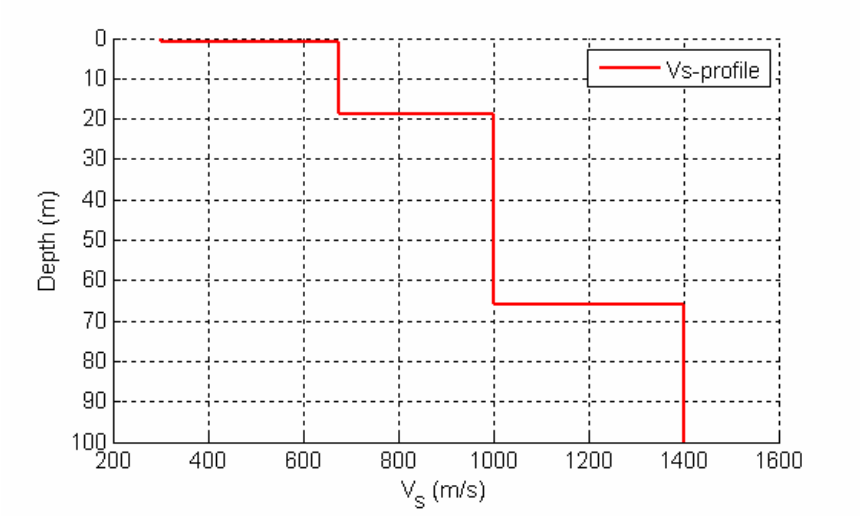

Figure 6. *Vs Velocity profile at the Capestrano RAN station*

Table 1*: V_S profile at the CPS RAN station*

Tickness (m)	S-Velocity (m/s)
1	**300**
18	**675**
47	**1000**
34	**1400**

Summary of subsoil basic features at the CPS RAN site

Vs30 = 730 m/s
Soil Class = B
Topography classification =T3
Depth to bedrock = 19 m
Average Vs to bedrock = 630 m/s
f_0 from ambient vibrations = 2.7 Hz

References

Lunedei E., Albarello D. (2009). On the seismic noise wavefield in a weakly dissipative layered Earth. *Geophys. J. Int.* (2009) **177,** 1001–1014, doi: 10.1111/j.1365-246X.2008.04062.x

Menke,W., 1989. *Geophysical Data Analysis: Discrete Inverse Theory,* rev.ed. Academic, San Diego, CA.

Ohori M., Nobata A., Wakamatsu K. (2002). A comparison of ESAC and FK methods of estimating phasevelocity using arbitrarily shaped microtremor arrays. Bull.Seism.Soc.Am., 92, 6, 2323-2332

Okada, H. (2003). The microtremor survey method, *Geophys. Monograph Series,* Vol. 12, Society of Exploration Geohysicists, 129 pp.

Picozzi M., Parolai S., Albarello D.; 2005: Statistical analysis of noise Horizonatal-to-Vertical Specrtal Ratios (HVSR). Bull. Seism. Soc. Am., **95**, n. 5, 1779–1786, doi: 10.1785/0120040152

Picozzi M., Albarello D. (2007). Combining genetic and linearized algorithms for a two-step joint inversion of Rayleigh wave dispersion and *H/V* spectral ratio curves. *Geophys. J. Int.* (2007) **169,** 189–200, doi: 10.1111/j.1365-246X.2006.03282.x

SESAME; 2004: Guidelines for the implementation of the H/V spectral ratio technique on ambient vibrations. SESAME, European project, WP12, Deliverable D23.12, http://sesame-fp5.obs.ujfgrenoble.fr/SES TechnicalDoc.htm

Tokimatsu, K. (1997). “Geotechnical Site Characterization using Surface Waves.” *Proceedings, First International Conference on Earthquake Geotechnical Engineering, IS-Tokyo '95*, Tokyo, November 14-16, Balkema, Rotterdam, 1333-1368.

Zhang, S.H., Chan, L.S. and Xia, J. (2004). The selection of field acquisition parameters for dispersion images from multichannel surface wave data. *Pure and Applied Geophysics* 161, 185–201.

Dipartimento di Scienze della Terra
Università degli Studi di Siena
Via Laterina, 8 53100 Siena, Italy

APPLICATION OF SURFACE WAVES METHODS FOR SEISMIC SITE CHARACTERIZATION

Montecassino RAN site (MTC)

Responsible
Prof.Dario Albarello

Co-Workers
Dott. Domenico Pileggi
Dott. David Rossi
Dott. Enrico Lunedei
Dott. Salomon Hailemikael

FINAL REPORT

Dipartimento di Scienze della Terra
Università degli Studi di Siena
Via Laterina, 8 53100 Siena, Italy

Siena 30 May 2010

The investigation protocol

It involves four major elements:

- *Detailed Geological survey of the study area resulting in a geo/lithologic map at the scale 1:5000 of the area surrounding the relevant RAN station. This also aimed at the evaluation of the degree of lateral heterogeneity present in the lithological structure paying major attention to faults and their relevant damage area (that can result in energy trapping phenomena)*
- *Extensive single station ambient vibration survey at the station and in the surrounding area to detect possible lateral variations potentially responsible for site effects*
- *Ambient vibration measurements carried on with a seismic array at the RAN site or at a site representative of the subsoil configuration at the RAN site. In this last case, suitable inversion procedures and test were carried on to warrant the representativeness of ambient vibration measurements*
- *Global interpretation of measurements to determine the V_S profile and of the resonance frequency at the RAN site by considering the whole set of collected data*

Details concerning experimental tools and processing techniques are given in the following sections.

Single station measurements

The goal of this kind of measurements is the retrieval of the HVSR curve that represents for each frequency, the average ratio between Horizontal (H) to vertical (V) ground motion components of ambient vibrations (SESAME, 2004). Each single-station measurement was executed with a three-directional digital tromograph Tromino Micromed (see www.tromino.it) with a sampling frequency of 128 Hz and an acquisition time length of 20 minutes. This value represents a good compromise between the celerity of the measurement execution (which is one of the main merits of this technique) and its accuracy, according to the SESAME guidelines and other studies (see, e.g., Picozzi et al., 2005). To provide HVSR curves, the time series relative to each ground motion component was subdivided in non-overlapping time windows of 30 s. For each of these, the signal was corrected for the base line, padded with zeros, and tapered with a Triangular window; the relevant spectrogram was smoothed through a triangular window with frequency dependent half-width (10% of central frequency) and the H/V ratio (HVSR) of the spectral components (the former being the geometric mean of North-South and East-West components) was computed for each frequency. Spectral ratios relative to all the time windows considered were then averaged, and a mean HVSR curve was computed along with the relevant 95% confidence interval.

Before interpreting HVSR curve in terms of subsoil dynamical properties, we checked the possible occurrence of spurious HVSR peaks (e.g., due to impulsive or strongly localized anthropic sources). To this purpose, we investigated both the time stability of spectral ratios over the recording length and their directionality. The latter was analyzed by estimating the HVSR curves derived by projecting the ground motion along different horizontal directions. If transient directional effects were identified in the directional HVSR curves, the relevant portions of the record were discarded.

Array Measurements

This technique consists in recording ambient vibration ground motion by means of an array of sensors (vertical geophones) distributed at the surface of the subsoil to be explored (see, e.g., Okada, 2003). Relevant information concerning phase velocities of waves propagating across the array are obtained from average cross-spectral matrixes relative to sensor pairs. In the present analysis, plane waves propagating across the array were considered only. Since vertical sensors were used only, these waves are interpreted as plane Rayleigh waves in their fundamental and higher propagation modes. Determination of Rayleigh wave phase velocities V_R

as a function of frequency (dispersion curve) from cross-spectral matrixes can be carried on in several ways. In the present analysis, the Extended Spatial Auto Correlation (ESAC) technique (Ohori et al. , 2002; Okada, 2003) was applied. The basic element of this analysis is the cross-correlation spectrum deduced by the analysis of ambient vibrations measured at a couple of sensors $\phi(f,r)$ where *f* is frequency and *r* is the distance between the relevant sensors .

To this purpose, registrations relative to each sensor are partitioned in a number of non overlapping time windows of fixed duration (20 sec). Time windows characterised by energy bursts were removed from the analysis. To this purpose, a time segment is considered in the analysis if standard deviation of all the traces of that time window do not exceed the threshold fixed in advance for each trace. In general, this threshold was fixed to be 2 times the standard deviation computed over the whole registration for the relevant trace. In each accepted time window, linear trend was removed and the resulting time series was padded and tapered (5% cosine windows). For each time window and couple of sensors, the cross spectrum was computed. The average cross spectrum was then computed for each couple of sensors by considering all the relevant time series. The resulting average cross-spectrum was thus smoothed in the frequency domain by a moving triangular window having an half-width proportional to the central value (usually 10%) and normalized to the relevant auto spectra.

In the assumption that ambient vibration wave field can be represented as a linear combination of statistically independent plane waves propagating with negligible attenuation in a horizontal plane in different directions with different powers, but with the same phase velocity for a given frequency, the normalized cross-spectrum $\phi_{ij}(f,r)$ relative to sensors located at a distance r, can be written in the form

$$\phi(f,r) = J_0\left(\frac{2\pi f r}{V_R(f)}\right)$$

where J_0 is the Bessel function of *0-th* order. In the ESAC approach, the value of V_R relative to each frequency *f* is retrieved by a grid search algorithm to optimized (in a RMS sense) the fit of the above function of r for the relevant frequency *f* (Ohori et al. , 2002; Okada, 2003). Robustness of this fitting procedure was enhanced by adopting the iterative procedure proposed by Parolai et al., 2006). By following these last Authors, uncertainty on "apparent" velocities was computed by means the second derivative of the misfit function relative to grid search procedure (see, Menke, 1989). However, since these estimate tend to be under-conservative in some cases, the lower bound of the confidence interval for experimental V_R values was fixed by using the relationship proposed by Zhang et al. (2004) as a function of the adopted sampling rate and array dimension.

The $V_R(f)$ value obtained in this way, is the "apparent" or "effective" Rayleigh waves phase velocity that coincides with the actual phase velocity only in the case that higher modes play a negligible role. In the other cases, a relationship can be established between actual phase velocities and the apparent one (Tokimatsu, 1997). The fact that the ESAC approach allows the determination of the apparent dispersion curve instead of the modal ones could represent an important limitation of this procedure with respect to other approaches (e.g., f-k techniques). On the other hand, this makes the approach here considered more robust with respect to the alternative procedures, since it does not require troublesome picking of existing propagation modes.

In the present study, ambient vibrations were recorded for 20 minutes at a 256 Hz sampling rate by using 16 vertical geophones (4.5 Hz) and a digital acquisition system produced by Micromed (http://micromed.com/brainspy1.htm). Geophones were placed along two crossing perpendicular branches (with maximum dimensions lower than 100 m) and irregularly spaced (in the range 0.5-30 m).

Inversion procedures

HVSR and apparent V_R curves have been jointly inverted to constrain to the local V_S profile. To this purpose, a genetic algorithm procedure was considered. This is an iterative procedure, consisting in sequence of steps

miming the evolutionary selection of living being (see Picozzi and Albarello, 2007 and references therein). The formalization proposed by Lunedei and Albarello (2009) was used as the forward modelling modelling implemented in the procedure. This procedure assumes the subsoil as a flat stratified viscoelastic medium where surface waves (Rayleigh and Love with relevant higher modes) propagate only. From this model, both theoretical HVSR and effective dispersion curves can be computed from a set of parameters representative of the hypothetical subsoil (V_S, V_P, density, Q_P and Q_S profiles). The discrepancy between theoretical and observed HVSR and dispersion curves were then evaluated in terms of a suitable misfit function, strictly linked to the well-known χ^2 function, that allowed different choices about the combination of the discrepancies of V_R and HVSR curves, with different weights as well. The confidence interval around preferred *Vs* values and layer thickness were evaluated by following Picozzi and Albarello (2007).

Geological Setting

A detailed geologic survey of the area surrounding the RAN site was carried on (Figure 1).

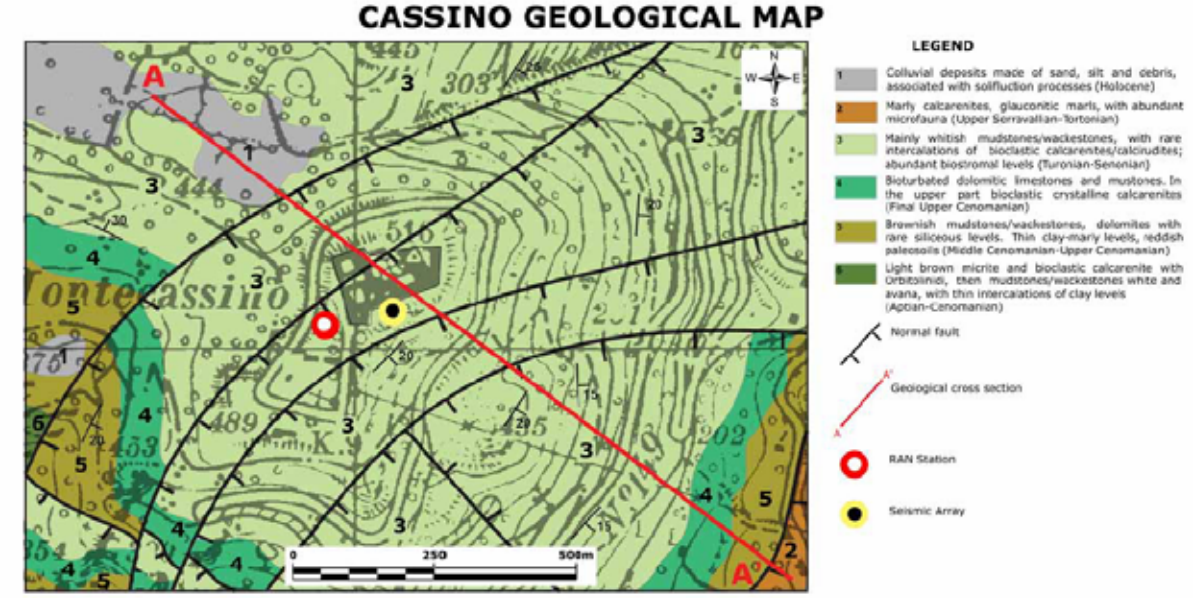

***Figure 1**: Geologic map of the Montecassino RAN site*

The Montecassino RAN station is located in the South-Eastern sector of Monte Cairo (Southern Latium). The site is characterized by the cropping out of a thick Cretaceous inner platform succession belonging to the Laziale-abruzzse domain. The sedimentary succession is characterized by bioclastic limestones, brownish limestones, marls, bio-clastic calcarenites dolomitic limestones and dolomites. Field analyses carried out in the site allow us to identify up to 6 different formations as listed below: 6) Downward light brown micrite and bioclastic calcarenite with Orbitoidi, then mudstones/wackestones white and avana, with thin intercalations of clay and sporadic levels of flint. Middle portion is characterized by laminated dolomicrite and light brown mudstones/wackestones and marly-conglomeratic levels with large quantity of quartz. Upward dolomite with laminations and saccaroid dolomites. 5) Brownish mudstones/wackestones, dolomitic limestones, dolomites with rare siliceous levels. Thin clay-marly levels, reddish paleosoils. Conglomerates, reddish calcareous hard-ground and dark dolomites. 4)Bioturbated dolomitic limestones and mudstones/wackestones. In the upper part bioclastic crystalline calcarenites/calcurydites. 3) Mainly whitish mudstones/wackestones, with rare intercalations of bioclastic calcarenites/calcirudites; abundant bioclastic calcarenites/calcirudites; abundant biostromal levels and dissolution processes. 2) Calcareniti a Briozoa member has been distinguished. Whitish/gray calcarenites/calcirudites with Briozoa and fragments of Lithotamnium, interbedded with whitish saccaroids calcarenites laterally passing to gray-yellowish calcarenites with Briozoa and Pecten. 1) Continental deposits mainly characterized by alluvial/colluvial deposits.

The site is characterized by the presence of several faults. These last has been kinematically caracterized as normal faults, mainly dip-slip, with an anti-Apenninic SW-NE trend. The average deep angle is 70-80° SE that gradually offset toward the South-Eastern sector the whole sedimentary succession. An important normal fault N-S trending offset to the E the upper portion of the succession as demonstrated by the cropping out of the Miocene formation at the base of the M. Cassino hill.

A representative geological section is reported in Figure2.

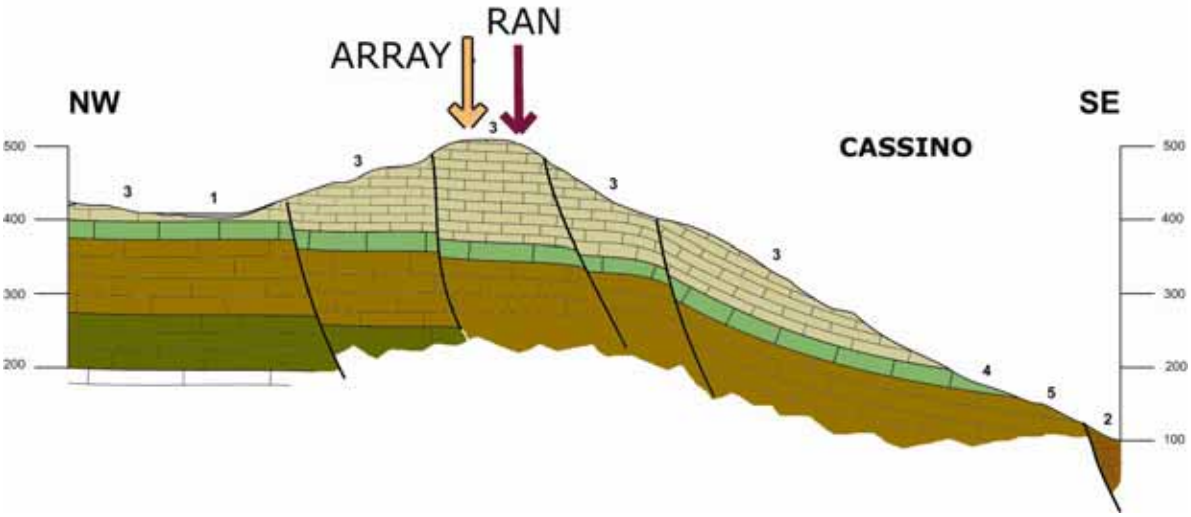

Figure 2 *Geological section across Montecassino area (see trace in Fig.2): RAN indicates location of the MTC accelerometric station. ARRAY indicates the position of the array*

Results of passive seismic survey

A single station measurement was carried nearby the RAN station (Figure 3) on 15th of May 2009. The analysis of this measurement revealed the presence of strong electromagnetic noise affecting a significant range of frequencies.

Figure3. *Location of the RAN station and of the corresponding single station ambient vibration measurement*

The resulting HVSR curve is reported in Figure 4. One can see that, if one discards the apparent peak around 1-2 Hz induced by electromagnetic noise, a sharp peak only emerges in the high frequency range (just above 18 Hz) that can be attributed to a very thin soft coverage of the rock that constitutes the bulk of the hill.

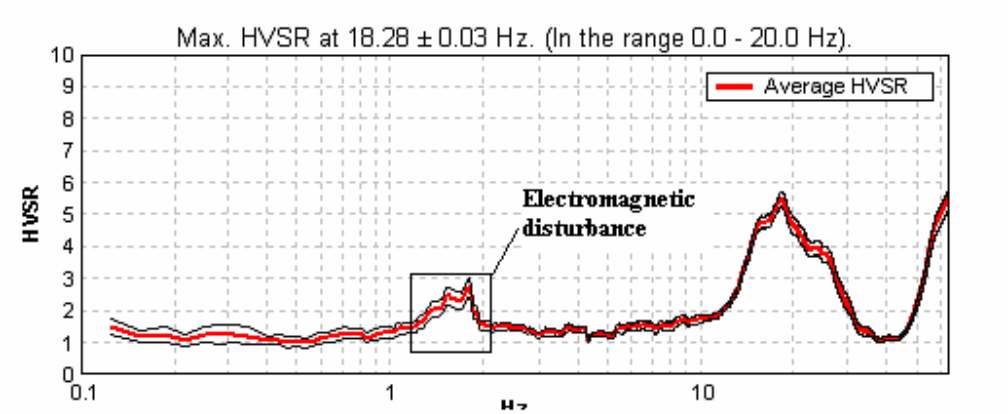

Figure 4. *HVSR curve obtained at the RAN station. The red line indicates the average HVSR values, while the black thin lines indicate the relevant 95% confidence interval*

Due to the very difficult topographic situation (the RAN station is located at the edge of the terrace where the Montecassino Abbey is located , Fig 5), array measurements were carried on at the foothill, few hundreds meters apart (Fig. 1).

The apparent V_R pattern is shown in Figure 6. Geological analyses indicate that at the array, bedrock is nearly outcropping. In fact, the shape of apparent V_R values is compatible with a uniform rock formation characterised by a *Vs* value of the order of 1400 m/sec. At the site were array was located, a number of HVSR measurements were carried on to reveal possible lateral variations in the subsoil around the array. These allowed to exclude such variations: all the relevant HVSR curves resulted flat, confirming geological indications and suggesting that a uniform rock body constitutes the local subsoil.

Figure 5. *Location of the MTC RAN station, at the edge of the terrace where the Montecassino Abbey is located*

However, a uniform subsoil is incompatible with the HVSR curve at the RAN station, where a resonance frequency was detected by HVSR measurements, that is compatible with the presence of a sharp shallow transition between a soft coverage (possibly landfill of anthropic origin) and the underlying bedrock.

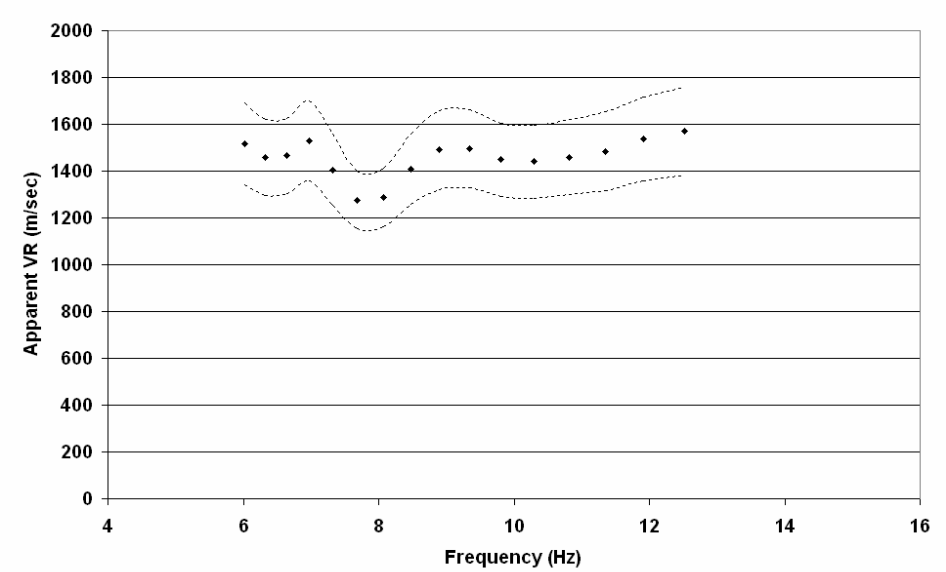

Figure 6. *Apparent VR curve deduced from array measurements. Dots indicate VR estimates while dashed lines bound the relevant 95% confidence interval*

In order to make these results compatible, an inversion of HVSR curve in Figure 4 (after that electromagnetic noise was discarded) was attempted by using Genetic Algorithms technique. In this inversion, V_S values of the bedrock was kept fixed to the value deduced from array measurements and a soft coverage configuration was searched for, that is compatible with HVSR measurements at the RAN station.

Outcomes of this inversion are reported in Figure 7 and Table 1. The presence of thin soft layer (about 5 m thick possibly representative of onthropic landfill) is revealed above the seismic bedrock

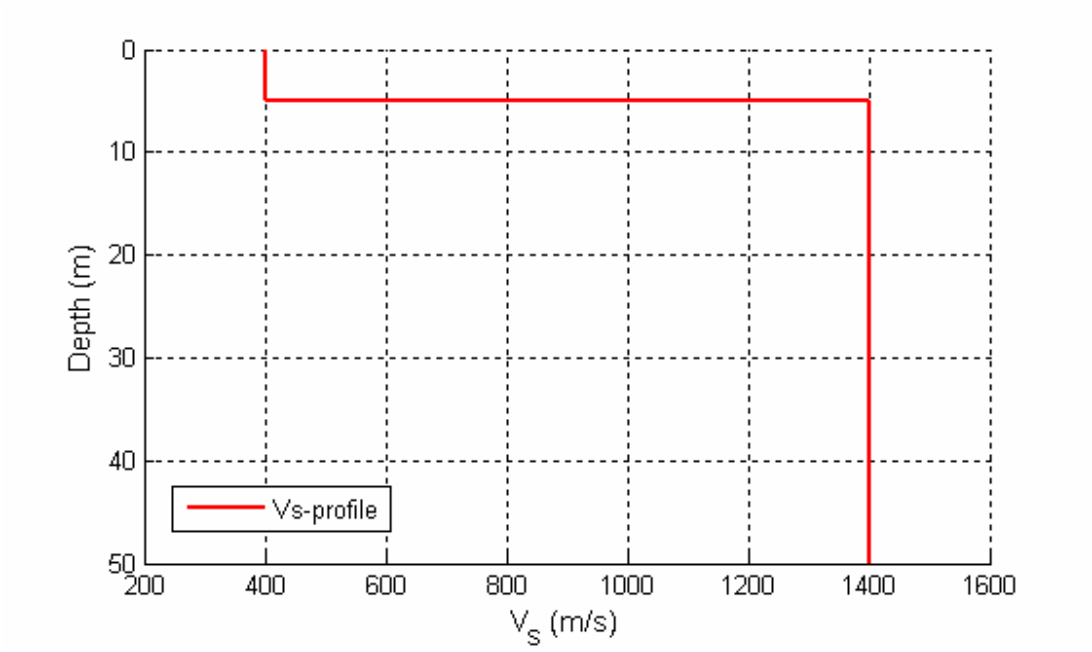

Figure 7. *Vs Velocity profile at the Montecassino RAN station*

***Table 1**: V_S profile at the MTC RAN station*

Tickness (m)	S-Velocity (m/s)
5	**400**
?	**1400**

Summary of subsoil basic features at the MTC RAN site

Vs30 = 1000 m/s
Soil Class = A
Topography classification = T4
Depth to bedrock = 2.5 m
Average Vs to bedrock = 400 m/s
f_0 from ambient vibrations = 18.3 Hz

References

Lunedei E., Albarello D. (2009). On the seismic noise wavefield in a weakly dissipative layered Earth. *Geophys. J. Int.* (2009) **177,** 1001–1014, doi: 10.1111/j.1365-246X.2008.04062.x

Menke,W., 1989. *Geophysical Data Analysis: Discrete Inverse Theory,* rev.ed. Academic, San Diego, CA.

Ohori M., Nobata A., Wakamatsu K. (2002). A comparison of ESAC and FK methods of estimating phasevelocity using arbitrarily shaped microtremor arrays. Bull.Seism.Soc.Am., 92, 6, 2323-2332

Okada, H. (2003). The microtremor survey method, *Geophys. Monograph Series,* Vol. 12, Society of Exploration Geohysicists, 129 pp.

Picozzi M., Parolai S., Albarello D.; 2005: Statistical analysis of noise Horizonatal-to-Vertical Specrtal Ratios (HVSR). Bull. Seism. Soc. Am., **95**, n. 5, 1779–1786, doi: 10.1785/0120040152

Picozzi M., Albarello D. (2007). Combining genetic and linearized algorithms for a two-step joint inversion of Rayleigh wave dispersion and *H/V* spectral ratio curves. *Geophys. J. Int.* (2007) **169,** 189–200, doi: 10.1111/j.1365-246X.2006.03282.x

SESAME; 2004: Guidelines for the implementation of the H/V spectral ratio technique on ambient vibrations. SESAME, European project, WP12, Deliverable D23.12, http://sesame-fp5.obs.ujfgrenoble.fr/SES TechnicalDoc.htm

Tokimatsu, K. (1997). “Geotechnical Site Characterization using Surface Waves.” *Proceedings, First International Conference on Earthquake Geotechnical Engineering, IS-Tokyo '95*, Tokyo, November 14-16, Balkema, Rotterdam, 1333-1368.

Zhang, S.H., Chan, L.S. and Xia, J. (2004). The selection of field acquisition parameters for dispersion images from multichannel surface wave data. *Pure and Applied Geophysics* 161, 185–201.

Dipartimento di Scienze della Terra
Università degli Studi di Siena
Via Laterina, 8 53100 Siena, Italy

APPLICATION OF SURFACE WAVES METHODS FOR SEISMIC SITE CHARACTERIZATION

Mormanno RAN site (MRM)

Responsible
Prof.Dario Albarello

Co-Workers
Dott. Domenico Pileggi
Dott. David Rossi
Dott. Enrico Lunedei

FINAL REPORT

Siena 30 May 2010

The investigation protocol

It involves four major elements:

- *Detailed Geological survey of the study area resulting in a geo/lithologic map at the scale 1:5000 of the area surrounding the relevant RAN station. This also aimed at the evaluation of the degree of lateral heterogeneity present in the lithological structure paying major attention to faults and their relevant damage area (that can result in energy trapping phenomena)*
- *Extensive single station ambient vibration survey at the station and in the surrounding area to detect possible lateral variations potentially responsible for site effects*
- *Ambient vibration measurements carried on with a seismic array at the RAN site or at a site representative of the subsoil configuration at the RAN site. In this last case, suitable inversion procedures and test were carried on to warrant the representativeness of ambient vibration measurements*
- *Global interpretation of measurements to determine the V_S profile and of the resonance frequency at the RAN site by considering the whole set of collected data*

Details concerning experimental tools and processing techniques are given in the following sections.

Single station measurements

The goal of this kind of measurements is the retrieval of the HVSR curve that represents for each frequency, the average ratio between Horizontal (H) to vertical (V) ground motion components of ambient vibrations (SESAME, 2004). Each single-station measurement was executed with a three-directional digital tromograph Tromino Micromed (see www.tromino.it) with a sampling frequency of 128 Hz and an acquisition time length of 20 minutes. This value represents a good compromise between the celerity of the measurement execution (which is one of the main merits of this technique) and its accuracy, according to the SESAME guidelines and other studies (see, e.g., Picozzi et al., 2005). To provide HVSR curves, the time series relative to each ground motion component was subdivided in non-overlapping time windows of 30 s. For each of these, the signal was corrected for the base line, padded with zeros, and tapered with a Triangular window; the relevant spectrogram was smoothed through a triangular window with frequency dependent half-width (10% of central frequency) and the H/V ratio (HVSR) of the spectral components (the former being the geometric mean of North-South and East-West components) was computed for each frequency. Spectral ratios relative to all the time windows considered were then averaged, and a mean HVSR curve was computed along with the relevant 95% confidence interval.

Before interpreting HVSR curve in terms of subsoil dynamical properties, we checked the possible occurrence of spurious HVSR peaks (e.g., due to impulsive or strongly localized anthropic sources). To this purpose, we investigated both the time stability of spectral ratios over the recording length and their directionality. The latter was analyzed by estimating the HVSR curves derived by projecting the ground motion along different horizontal directions. If transient directional effects were identified in the directional HVSR curves, the relevant portions of the record were discarded.

Array Measurements

This technique consists in recording ambient vibration ground motion by means of an array of sensors (vertical geophones) distributed at the surface of the subsoil to be explored (see, e.g., Okada, 2003). Relevant information concerning phase velocities of waves propagating across the array are obtained from average cross-spectral matrixes relative to sensor pairs. In the present analysis, plane waves propagating across the array were considered only. Since vertical sensors were used only, these waves are interpreted as plane Rayleigh waves in their fundamental and higher propagation modes. Determination of Rayleigh wave phase velocities V_R as a function of frequency (dispersion curve) from cross-spectral matrixes can be carried on in several ways. In the present analysis, the Extended Spatial Auto Correlation (ESAC) technique (Ohori et al. , 2002; Okada, 2003)

was applied. The basic element of this analysis is the cross-correlation spectrum deduced by the analysis of ambient vibrations measured at a couple of sensors $\phi(f,r)$ where *f* is frequency and *r* is the distance between the relevant sensors .

To this purpose, registrations relative to each sensor are partitioned in a number of non overlapping time windows of fixed duration (20 sec). Time windows characterised by energy bursts were removed from the analysis. To this purpose, a time segment is considered in the analysis if standard deviation of all the traces of that time window do not exceed the threshold fixed in advance for each trace. In general, this threshold was fixed to be 2 times the standard deviation computed over the whole registration for the relevant trace. In each accepted time window, linear trend was removed and the resulting time series was padded and tapered (5% cosine windows). For each time window and couple of sensors, the cross spectrum was computed. The average cross spectrum was then computed for each couple of sensors by considering all the relevant time series. The resulting average cross-spectrum was thus smoothed in the frequency domain by a moving triangular window having an half-width proportional to the central value (usually 10%) and normalized to the relevant auto spectra.

In the assumption that ambient vibration wave field can be represented as a linear combination of statistically independent plane waves propagating with negligible attenuation in a horizontal plane in different directions with different powers, but with the same phase velocity for a given frequency, the normalized cross-spectrum $\phi_{ij}(f,r)$ relative to sensors located at a distance r, can be written in the form

$$\phi(f,r) = J_0\left(\frac{2\pi f r}{V_R(f)}\right)$$

where J_0 is the Bessel function of *0-th* order. In the ESAC approach, the value of V_R relative to each frequency *f* is retrieved by a grid search algorithm to optimized (in a RMS sense) the fit of the above function of r for the relevant frequency *f* (Ohori et al. , 2002; Okada, 2003). Robustness of this fitting procedure was enhanced by adopting the iterative procedure proposed by Parolai et al., 2006). By following these last Authors, uncertainty on "apparent" velocities was computed by means the second derivative of the misfit function relative to grid search procedure (see, Menke, 1989). However, since these estimate tend to be under-conservative in some cases, the lower bound of the confidence interval for experimental V_R values was fixed by using the relationship proposed by Zhang et al. (2004) as a function of the adopted sampling rate and array dimension.

The $V_R(f)$ value obtained in this way, is the "apparent" or "effective" Rayleigh waves phase velocity that coincides with the actual phase velocity only in the case that higher modes play a negligible role. In the other cases, a relationship can be established between actual phase velocities and the apparent one (Tokimatsu, 1997). The fact that the ESAC approach allows the determination of the apparent dispersion curve instead of the modal ones could represent an important limitation of this procedure with respect to other approaches (e.g., f-k techniques). On the other hand, this makes the approach here considered more robust with respect to the alternative procedures, since it does not require troublesome picking of existing propagation modes.

In the present study, ambient vibrations were recorded for 20 minutes at a 256 Hz sampling rate by using 16 vertical geophones (4.5 Hz) and a digital acquisition system produced by Micromed (http://micromed.com/brainspy1.htm). Geophones were placed along two crossing perpendicular branches (with maximum dimensions lower than 100 m) and irregularly spaced (in the range 0.5-30 m).

Inversion procedures

HVSR and apparent V_R curves have been jointly inverted to constrain to the local V_S profile. To this purpose, a genetic algorithm procedure was considered. This is an iterative procedure, consisting in sequence of steps miming the evolutionary selection of living being (see Picozzi and Albarello, 2007 and references therein). The formalization proposed by Lunedei and Albarello (2009) was used as the forward modelling modelling

implemented in the procedure. This procedure assumes the subsoil as a flat stratified viscoelastic medium where surface waves (Rayleigh and Love with relevant higher modes) propagate only. From this model, both theoretical HVSR and effective dispersion curves can be computed from a set of parameters representative of the hypothetical subsoil (V_S, V_P, density, Q_P and Q_S profiles). The discrepancy between theoretical and observed HVSR and dispersion curves were then evaluated in terms of a suitable misfit function, strictly linked to the well-known χ^2 function, that allowed different choices about the combination of the discrepancies of V_R and HVSR curves, with different weights as well. The confidence interval around preferred *Vs* values and layer thickness were evaluated by following Picozzi and Albarello (2007).

Geological Setting

A detailed geologic survey of the area surrounding the RAN site was carried on (Figure 1).

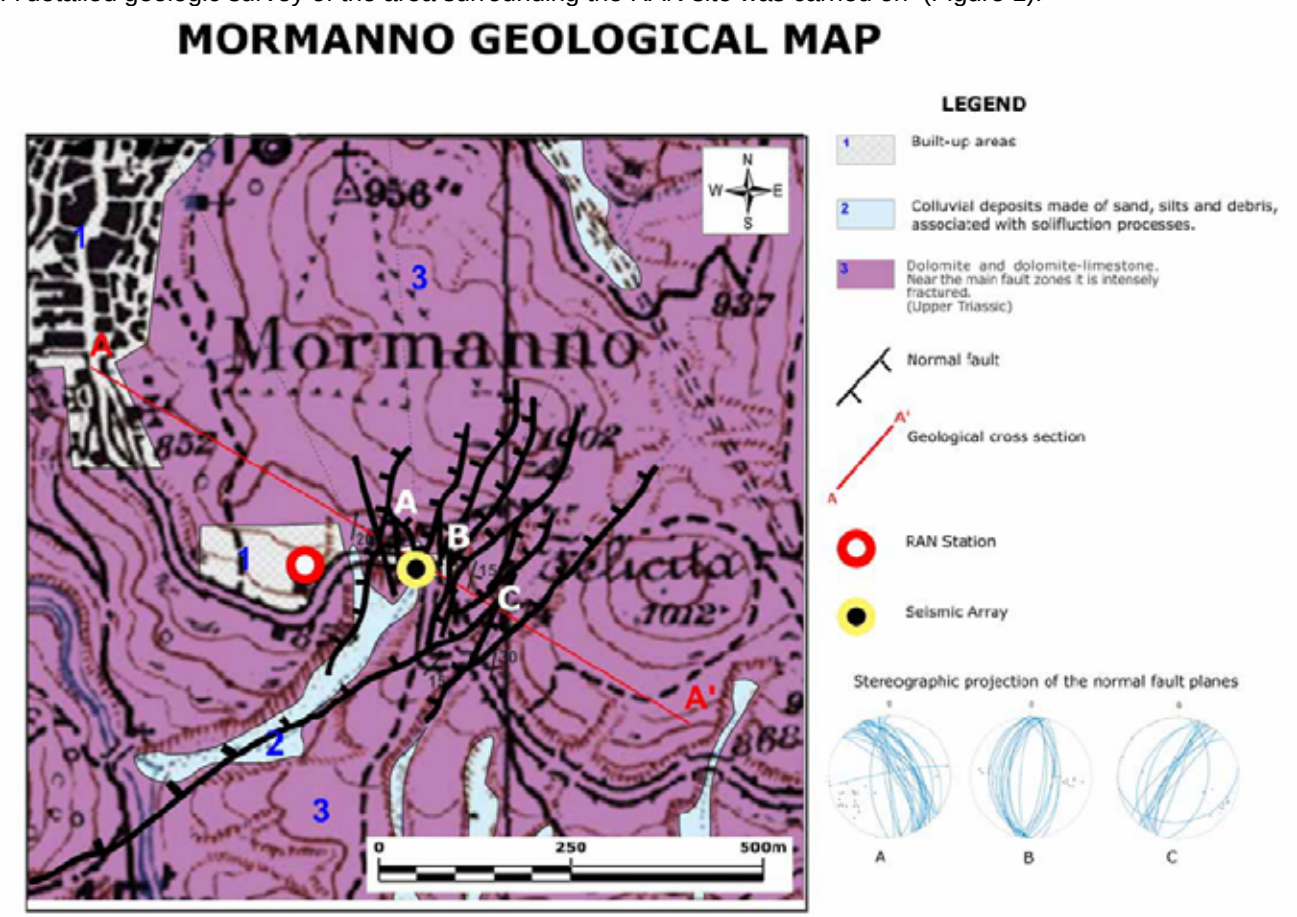

***Figure 1**: Geologic map of the Mormanno RAN site*

The Mormanno RAN station is located in the northern sector of the Calabria region (southern Italy). Lithostratigraphic units and structures in the area were mapped at a 1:5,000 scale to determine the relationship between tectonic structures, fracturing processes and stratigraphy. Majority of the mapping was conducted along a NE-SW trending fault system, exceptionally well exposed along the Eastern sector of the Mormanno town. The site is characterized by the outcropping of a thick sedimentary succession, mainly composed by dolomitic limestones, yellowish dolomites and dark grey dolomites layers. Both the Ran and the seismic array are close to an important normal fault system characterized by an average direction of N20°. The analyses carried out in field allow us to identify 3 main fault sub-zones characterized by different dip and direction as show in the stereographic projections of the fault planes. From East to West were identified a C zone characterized by a set of NW dipping fault planes (80°-90°) showing a main direction of N30°; a B zone characterized by N-S fault

planes dipping East and West with an average dip angle of 60-70°, and an A zone showing NNW-SSE trending faults with an ENE dipping. The whole fault area shows up to 400m wide fractured zone mainly composed by tension gashes filled by calcite cements. Two fracture network type was distinguished using the spatial distribution and the aperture width: a very strongly fractured zone showing subvertical, irregularly spaced and connected tension gashes (East sector of the study area) and a strongly fractured zone with subvertical and irregularly spaced tension gashes (West sector).

Despite the distance both the RAN and the ARRAY are located above the same rocks type with same bedding geometry and fracturing processes (both lie in the strongly fractured zone).

A representative geological section is reported in Figure2.

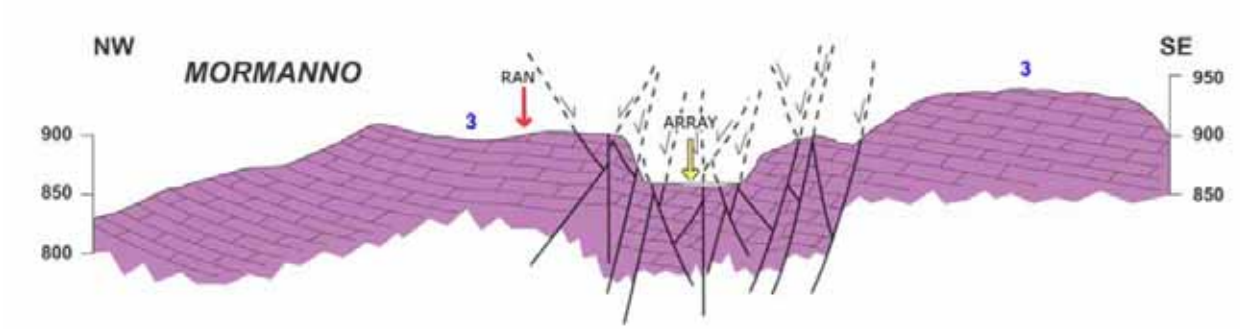

Figure 2 *Geological section across Mormanno area (see trace in Fig.2): RAN indicates location of the MRM accelerometric station. ARRAY indicates the position of the array*

Results of passive seismic survey

A single station measurement was carried nearby the RAN station (Figure 3) on 15th of April 2009. No resonance was detected at his site in the frequency range of interest (Figure 4), in line with the rock character of the subsoil deduced from the geologic survey.

Figure3. *Location of the RAN station and of the corresponding single station ambient vibration measurement*

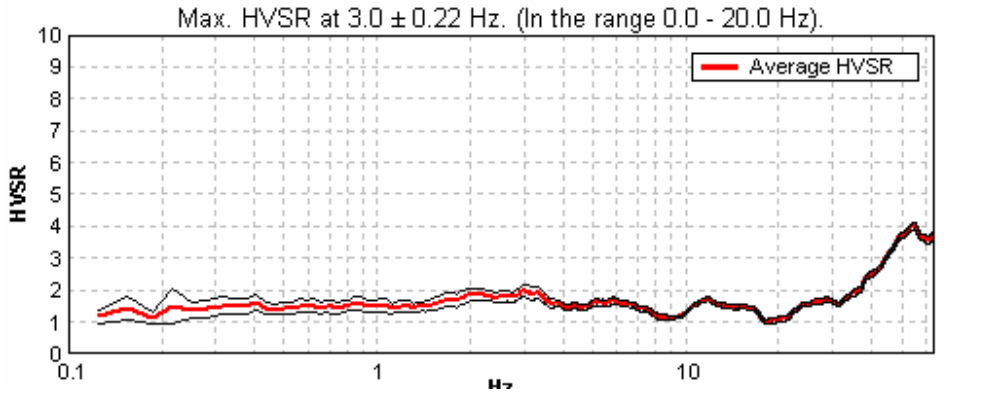

Figure 4. *HVSR curve obtained at the MRM RAN station. The red line indicates the average HVSR values, while the black thin lines indicate the relevant 95% confidence interval*

Due to logistic problems, array measurements were carried on about 100m away from the RAN site (Figure 1). Geological setting and HVSR measurements carried on all around the area did not reveal any significant difference with respect to the situation at the RAN site. Thus, array measurements were considered fully representative of the situation at the RAN site. Results of these measurements are reported in Figure 6 and are compatible with a uniform subsoil characterized by V_S values of the order of 1400 m/sec (see Figure 7 and Table 1).

Figure 5. *Location of the Mormanno RAN station*

It is worth noting that, despite of the ubiquitous presence of faults and fracture nearly uniformly oriented NNE ward, no indication of azimuthal differences was revealed by ambient vibration measurements. Thus, the MRM site can be safely used as a reference site for seismological and seismic engineering studies.

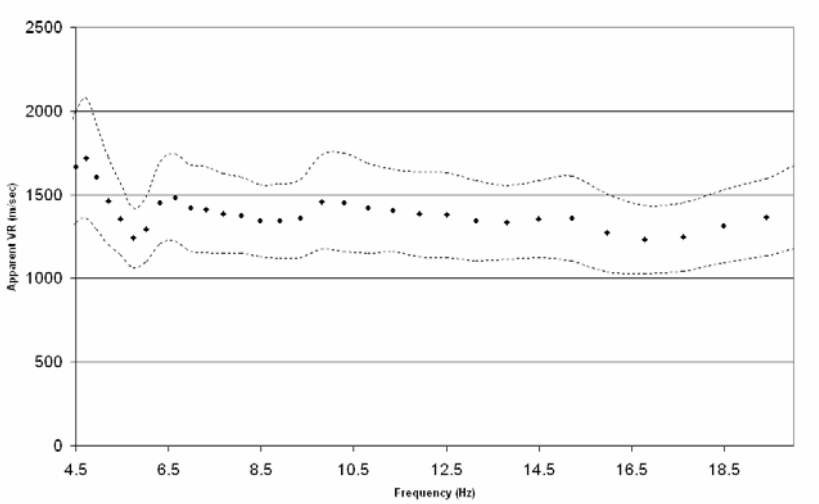

Figure 6. *Apparent VR curve deduced from array measurements. Dots indicate VR estimates while dashed lines bound the relevant 95% confidence interval*

Table 1*: V_S profile at the MRM RAN station*

Tickness (m)	S-Velocity (m/s)
?	**1400**

Summary of subsoil basic features at the MRM RAN site

Vs30 = 1400 m/s
Soil Class = A
Topography classification = T3
Depth to bedrock = 0 m
Average Vs to bedrock = 0 m/s
f_0 from ambient vibrations = flat measurement

References

Lunedei E., Albarello D. (2009). On the seismic noise wavefield in a weakly dissipative layered Earth. *Geophys. J. Int.* (2009) **177,** 1001–1014, doi: 10.1111/j.1365-246X.2008.04062.x

Menke,W., 1989. *Geophysical Data Analysis: Discrete Inverse Theory,* rev.ed. Academic, San Diego, CA.

Ohori M., Nobata A., Wakamatsu K. (2002). A comparison of ESAC and FK methods of estimating phasevelocity using arbitrarily shaped microtremor arrays. Bull.Seism.Soc.Am., 92, 6, 2323-2332

Okada, H. (2003). The microtremor survey method, *Geophys. Monograph Series,* Vol. 12, Society of Exploration Geohysicists, 129 pp.

Picozzi M., Parolai S., Albarello D.; 2005: Statistical analysis of noise Horizonatal-to-Vertical Specrtal Ratios (HVSR). Bull. Seism. Soc. Am., **95**, n. 5, 1779–1786, doi: 10.1785/0120040152

Picozzi M., Albarello D. (2007). Combining genetic and linearized algorithms for a two-step joint inversion of Rayleigh wave dispersion and *H/V* spectral ratio curves. *Geophys. J. Int.* (2007) **169,** 189–200, doi: 10.1111/j.1365-246X.2006.03282.x

SESAME; 2004: Guidelines for the implementation of the H/V spectral ratio technique on ambient vibrations. SESAME, European project, WP12, Deliverable D23.12, http://sesame-fp5.obs.ujfgrenoble.fr/SES TechnicalDoc.htm

Tokimatsu, K. (1997). “Geotechnical Site Characterization using Surface Waves.” *Proceedings, First International Conference on Earthquake Geotechnical Engineering, IS-Tokyo '95*, Tokyo, November 14-16, Balkema, Rotterdam, 1333-1368.

Zhang, S.H., Chan, L.S. and Xia, J. (2004). The selection of field acquisition parameters for dispersion images from multichannel surface wave data. *Pure and Applied Geophysics* 161, 185–201.

Dipartimento di Scienze della Terra
Università degli Studi di Siena
Via Laterina, 8 53100 Siena, Italy

APPLICATION OF SURFACE WAVES METHODS FOR SEISMIC SITE CHARACTERIZATION

Scanno RAN site (SCN)

Responsible
Prof.Dario Albarello

Co-Workers
Dott. Domenico Pileggi
Dott. David Rossi
Dott. Enrico Lunedei

FINAL REPORT

Siena 30 May 2010

The investigation protocol

It involves four major elements:

- *Detailed Geological survey of the study area resulting in a geo/lithologic map at the scale 1:5000 of the area surrounding the relevant RAN station. This also aimed at the evaluation of the degree of lateral heterogeneity present in the lithological structure paying major attention to faults and their relevant damage area (that can result in energy trapping phenomena)*
- *Extensive single station ambient vibration survey at the station and in the surrounding area to detect possible lateral variations potentially responsible for site effects*
- *Ambient vibration measurements carried on with a seismic array at the RAN site or at a site representative of the subsoil configuration at the RAN site. In this last case, suitable inversion procedures and test were carried on to warrant the representativeness of ambient vibration measurements*
- *Global interpretation of measurements to determine the V_S profile and of the resonance frequency at the RAN site by considering the whole set of collected data*

Details concerning experimental tools and processing techniques are given in the following sections.

Single station measurements

The goal of this kind of measurements is the retrieval of the HVSR curve that represents for each frequency, the average ratio between Horizontal (H) to vertical (V) ground motion components of ambient vibrations (SESAME, 2004). Each single-station measurement was executed with a three-directional digital tromograph Tromino Micromed (see www.tromino.it) with a sampling frequency of 128 Hz and an acquisition time length of 20 minutes. This value represents a good compromise between the celerity of the measurement execution (which is one of the main merits of this technique) and its accuracy, according to the SESAME guidelines and other studies (see, e.g., Picozzi et al., 2005). To provide HVSR curves, the time series relative to each ground motion component was subdivided in non-overlapping time windows of 30 s. For each of these, the signal was corrected for the base line, padded with zeros, and tapered with a Triangular window; the relevant spectrogram was smoothed through a triangular window with frequency dependent half-width (10% of central frequency) and the H/V ratio (HVSR) of the spectral components (the former being the geometric mean of North-South and East-West components) was computed for each frequency. Spectral ratios relative to all the time windows considered were then averaged, and a mean HVSR curve was computed along with the relevant 95% confidence interval.

Before interpreting HVSR curve in terms of subsoil dynamical properties, we checked the possible occurrence of spurious HVSR peaks (e.g., due to impulsive or strongly localized anthropic sources). To this purpose, we investigated both the time stability of spectral ratios over the recording length and their directionality. The latter was analyzed by estimating the HVSR curves derived by projecting the ground motion along different horizontal directions. If transient directional effects were identified in the directional HVSR curves, the relevant portions of the record were discarded.

Array Measurements

This technique consists in recording ambient vibration ground motion by means of an array of sensors (vertical geophones) distributed at the surface of the subsoil to be explored (see, e.g., Okada, 2003). Relevant information concerning phase velocities of waves propagating across the array are obtained from average cross-spectral matrixes relative to sensor pairs. In the present analysis, plane waves propagating across the array were considered only. Since vertical sensors were used only, these waves are interpreted as plane Rayleigh waves in their fundamental and higher propagation modes. Determination of Rayleigh wave phase velocities V_R as a function of frequency (dispersion curve) from cross-spectral matrixes can be carried on in several ways. In the present analysis, the Extended Spatial Auto Correlation (ESAC) technique (Ohori et al. , 2002; Okada, 2003)

was applied. The basic element of this analysis is the cross-correlation spectrum deduced by the analysis of ambient vibrations measured at a couple of sensors $\phi(f,r)$ where *f* is frequency and *r* is the distance between the relevant sensors .

To this purpose, registrations relative to each sensor are partitioned in a number of non overlapping time windows of fixed duration (20 sec). Time windows characterised by energy bursts were removed from the analysis. To this purpose, a time segment is considered in the analysis if standard deviation of all the traces of that time window do not exceed the threshold fixed in advance for each trace. In general, this threshold was fixed to be 2 times the standard deviation computed over the whole registration for the relevant trace. In each accepted time window, linear trend was removed and the resulting time series was padded and tapered (5% cosine windows). For each time window and couple of sensors, the cross spectrum was computed. The average cross spectrum was then computed for each couple of sensors by considering all the relevant time series. The resulting average cross-spectrum was thus smoothed in the frequency domain by a moving triangular window having an half-width proportional to the central value (usually 10%) and normalized to the relevant auto spectra.

In the assumption that ambient vibration wave field can be represented as a linear combination of statistically independent plane waves propagating with negligible attenuation in a horizontal plane in different directions with different powers, but with the same phase velocity for a given frequency, the normalized cross-spectrum $\phi_{ij}(f,r)$ relative to sensors located at a distance r, can be written in the form

$$\phi(f,r) = J_0\left(\frac{2\pi f r}{V_R(f)}\right)$$

where J_0 is the Bessel function of *0-th* order. In the ESAC approach, the value of V_R relative to each frequency *f* is retrieved by a grid search algorithm to optimized (in a RMS sense) the fit of the above function of r for the relevant frequency *f* (Ohori et al. , 2002; Okada, 2003). Robustness of this fitting procedure was enhanced by adopting the iterative procedure proposed by Parolai et al., 2006). By following these last Authors, uncertainty on "apparent" velocities was computed by means the second derivative of the misfit function relative to grid search procedure (see, Menke, 1989). However, since these estimate tend to be under-conservative in some cases, the lower bound of the confidence interval for experimental V_R values was fixed by using the relationship proposed by Zhang et al. (2004) as a function of the adopted sampling rate and array dimension.

The $V_R(f)$ value obtained in this way, is the "apparent" or "effective" Rayleigh waves phase velocity that coincides with the actual phase velocity only in the case that higher modes play a negligible role. In the other cases, a relationship can be established between actual phase velocities and the apparent one (Tokimatsu, 1997). The fact that the ESAC approach allows the determination of the apparent dispersion curve instead of the modal ones could represent an important limitation of this procedure with respect to other approaches (e.g., f-k techniques). On the other hand, this makes the approach here considered more robust with respect to the alternative procedures, since it does not require troublesome picking of existing propagation modes.

In the present study, ambient vibrations were recorded for 20 minutes at a 256 Hz sampling rate by using 16 vertical geophones (4.5 Hz) and a digital acquisition system produced by Micromed (http://micromed.com/brainspy1.htm). Geophones were placed along two crossing perpendicular branches (with maximum dimensions lower than 100 m) and irregularly spaced (in the range 0.5-30 m).

Inversion procedures

HVSR and apparent V_R curves have been jointly inverted to constrain to the local V_S profile. To this purpose, a genetic algorithm procedure was considered. This is an iterative procedure, consisting in sequence of steps miming the evolutionary selection of living being (see Picozzi and Albarello, 2007 and references therein). The formalization proposed by Lunedei and Albarello (2009) was used as the forward modelling modelling

implemented in the procedure. This procedure assumes the subsoil as a flat stratified viscoelastic medium where surface waves (Rayleigh and Love with relevant higher modes) propagate only. From this model, both theoretical HVSR and effective dispersion curves can be computed from a set of parameters representative of the hypothetical subsoil (V_S, V_P, density, Q_P and Q_S profiles). The discrepancy between theoretical and observed HVSR and dispersion curves were then evaluated in terms of a suitable misfit function, strictly linked to the well-known χ^2 function, that allowed different choices about the combination of the discrepancies of V_R and HVSR curves, with different weights as well. The confidence interval around preferred *Vs* values and layer thickness were evaluated by following Picozzi and Albarello (2007).

Geological Setting

A detailed geologic survey of the area surrounding the RAN site was carried on (Figure 1).

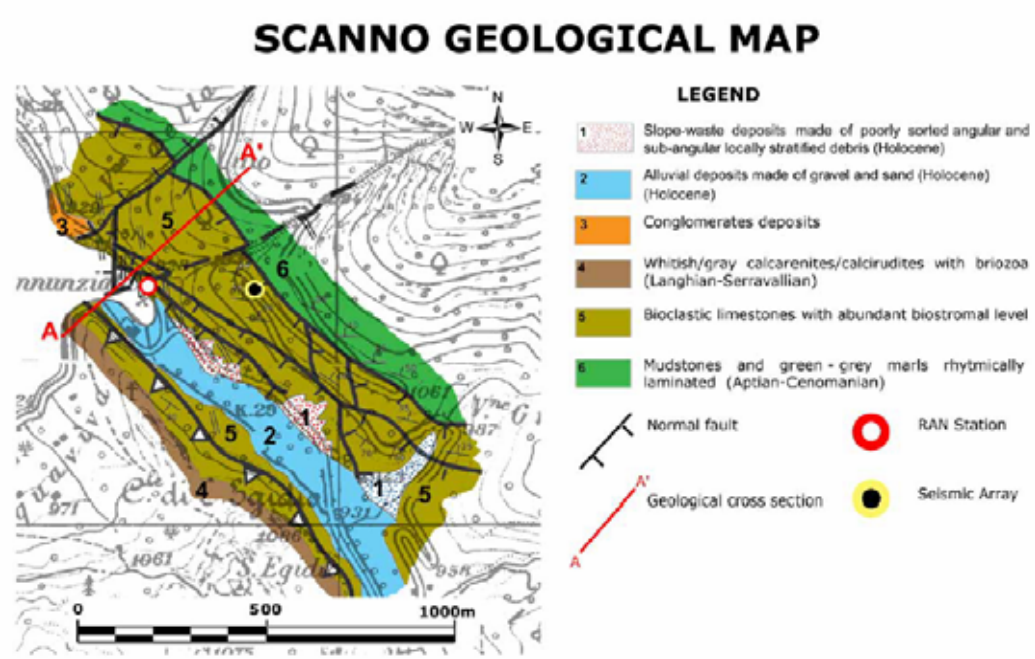

***Figure 1**: Geologic map of the Scanno RAN site*

The Scanno RAN site is located into the South Eastern edge of the Scanno lake. The whole site is affected by an intense and widespread tectonic processes. The site is characterized by the outcropping of a Cretaceous and Miocene sedimentary succession. In details the Cretaceous succession is characterized by mudstones, green-grey marls rhythmically laminated and by bioclastic limestones with abundant biostromal levels (6-5). The Miocene deposits is constituted by whitish/gray clacarenites and calcirudites with abundant briozoa. This deposits present also at different levels whitish saccaroid calcarenites laterally passing to gray-yellowish calcarenites. The main tectonical feature is represented by the presence of an important thrust fault, SW dipping that favorite the over-thrusting of the upper cretaceous-lower Miocene succession above the upper Cretaceous sequence. The hanging-wall of the thrust fault is characterized by the presence of an asymmetric overturned syncline with the southern limb completely verticalized locally overturned. The RAN station is located exactly above the vertical strata. The NE sector of the area is represented by the northern syncline limb NE gently dipping with average dip angle of 25-30°. The ARRAY station was realized in this last sector. Despite the distance between the RAN and the ARRAY, both are located above the same sedimentary succession with the only difference represented by the dip angle of the strata (sub-vertical in the RAN and gently dipping toward NE in the ARRAY). The whole area is also characterized by the presence of several normal faults, most of them SW dipping and with a N130° main strike direction. These last are offset by two set of N40° normal faults that cross cutting the whole area. The presence of the fault network within the cretaceous succession favorite the

development of a widespread intense fracturation processes. Field data acquired allow us to identify up to 4 different generation fracture systems sub-parallel to the main faults. The fracturation density progressively increase toward the fault plane with a maximum concentration in the linking fault sectors.

A representative geological section is reported in Figure2.

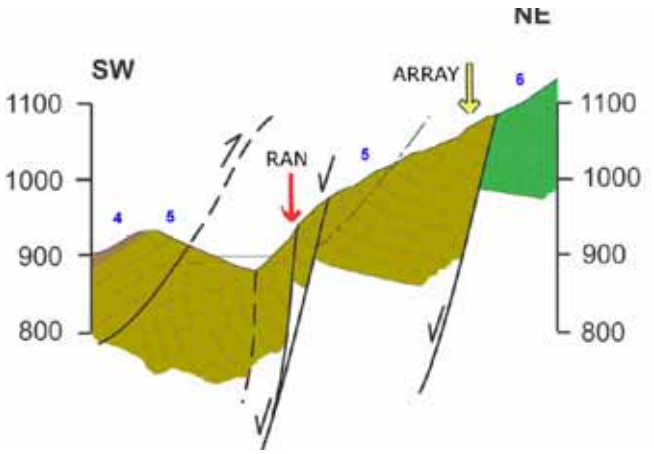

Figure 2 *Geological section across Scanno area (see trace in Fig.1): RAN indicates location of the SCN accelerometric station. ARRAY indicates the position of the array*

Results of passive seismic survey

A single station measurement was carried nearby the RAN station (Figures 3 and 5) on 3rd of July 2009. A strong resonance phenomenon was detected at the frequencies of about 4 Hz. HVSR measurements carried on the the RAN site and all around results affected by strong directionality, that is the possible effect of fault structures located immediately nearby the RAN station (Figure 2).

Figure3. *Location of the RAN station and of the corresponding single station ambient vibration measurement*

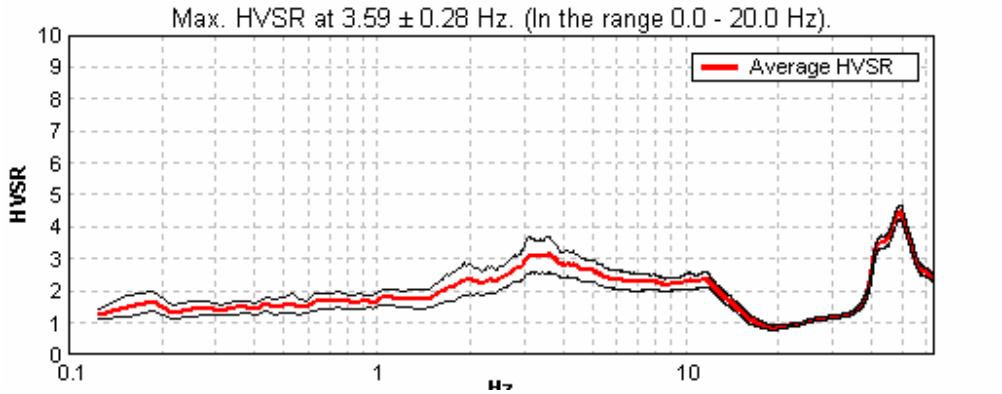

Figure 4. *HVSR curve obtained at the SCN RAN station. The red line indicates the average HVSR values, while the black thin lines indicate the relevant 95% confidence interval*

Due to the complex topography, array measurements were carried several hundreds of meters apart from the RAN site (Figure 1). Results of these measurements (Fig. 6) suggest that at the array, a V_S increase with depth is expected. Since geological survey suggests that both array and RAN site share the same subsoil configuration, HVSR and array results (Figure 4 and 6 respectively) were jointly inverted to deduce the local V_S profile (Figure 7 and Table 1). Results of the joint inversion of the HVSR and Rayleigh waves dispersion curve are reported in figure 6 and table 1. These results suggest that a relatively thick alteration layer overlies the bedrock and is responsible for possible resonance phenomena. This interpretation, however, does not account for possible resonance phenomena induced by energy trapping in the damaged areas surrounding the faults present in the area. However, such an hypothesis would require more complex modelling that is beyond the scope of the present survey.

Figure 5. *Location of the Scanno RAN station (in the background). On the bottom, the digital tromograph used for the single station ambient vibration measurements is shown*

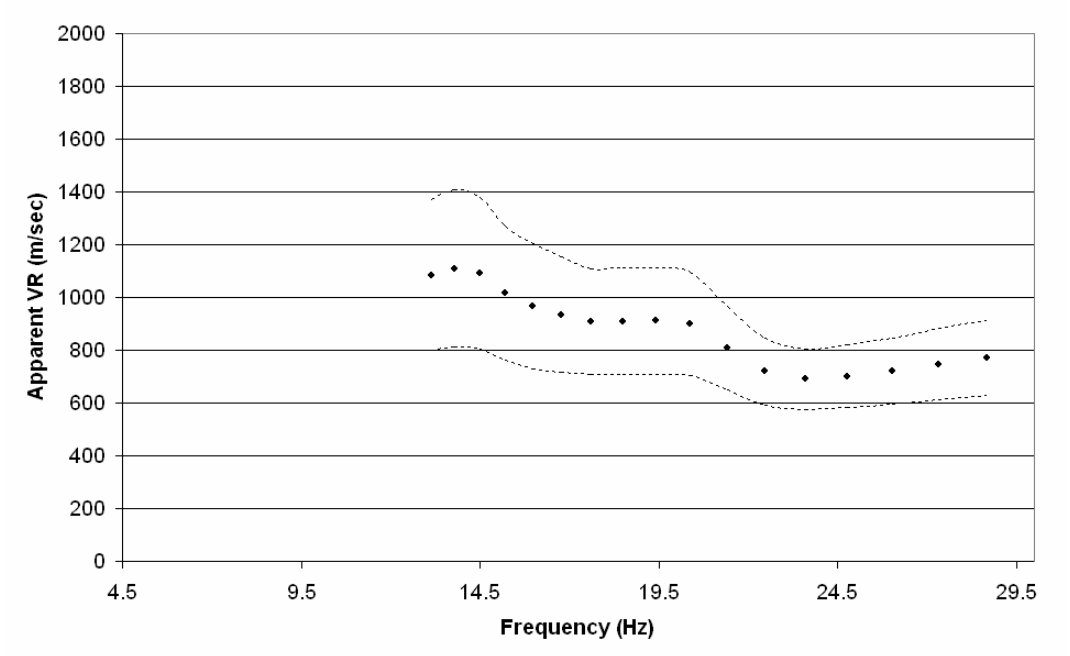

Figure 6. *Apparent VR curve deduced from array measurements. Dots indicate VR estimates while dashed lines bound the relevant 95% confidence interval*

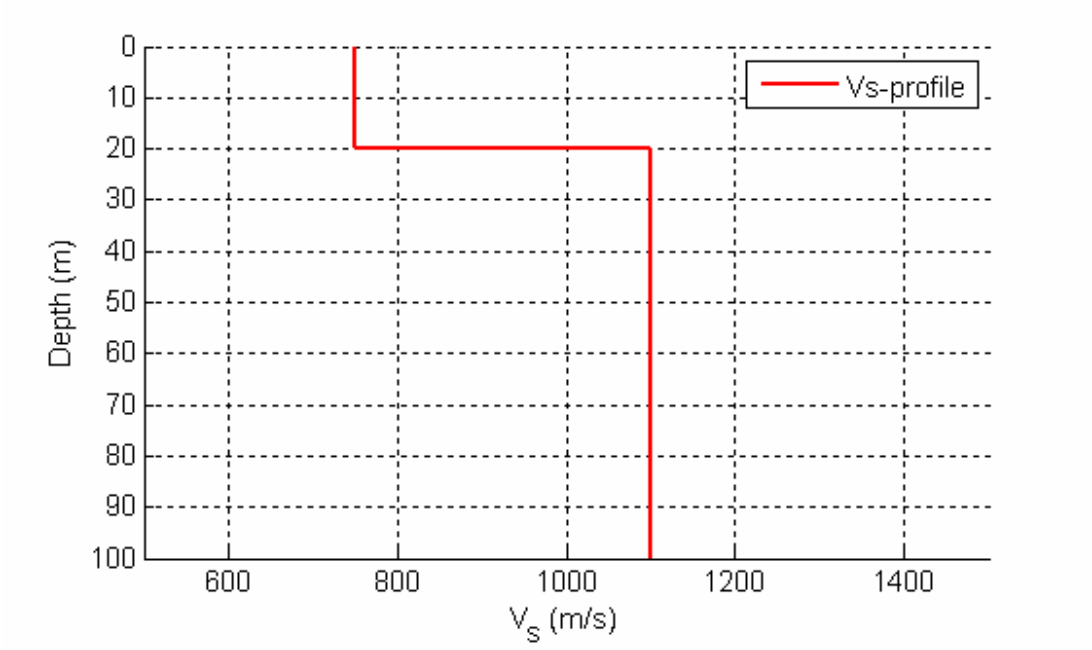

Figure 7. *Vs Velocity profile at the Scanno RAN station*

***Table 1**: V_S profile at the SCN station*

Tickness (m)	S-Velocity (m/s)
20	**750**
?	**1100**

Summary of subsoil basic features at the SCN RAN site

Vs30 = 840 m/s
Soil Class = A
Topography classification = T4
Depth to bedrock = 20 m
Average Vs to bedrock = 750 m/s
f_0 from ambient vibrations = 3.6 Hz

References

Lunedei E., Albarello D. (2009). On the seismic noise wavefield in a weakly dissipative layered Earth. *Geophys. J. Int.* (2009) **177,** 1001–1014, doi: 10.1111/j.1365-246X.2008.04062.x

Menke,W., 1989. *Geophysical Data Analysis: Discrete Inverse Theory,* rev.ed. Academic, San Diego, CA.

Ohori M., Nobata A., Wakamatsu K. (2002). A comparison of ESAC and FK methods of estimating phasevelocity using arbitrarily shaped microtremor arrays. Bull.Seism.Soc.Am., 92, 6, 2323-2332

Okada, H. (2003). The microtremor survey method, *Geophys. Monograph Series,* Vol. 12, Society of Exploration Geohysicists, 129 pp.

Picozzi M., Parolai S., Albarello D.; 2005: Statistical analysis of noise Horizonatal-to-Vertical Specrtal Ratios (HVSR). Bull. Seism. Soc. Am., **95**, n. 5, 1779–1786, doi: 10.1785/0120040152

Picozzi M., Albarello D. (2007). Combining genetic and linearized algorithms for a two-step joint inversion of Rayleigh wave dispersion and *H/V* spectral ratio curves. *Geophys. J. Int.* (2007) **169,** 189–200, doi: 10.1111/j.1365-246X.2006.03282.x

SESAME; 2004: Guidelines for the implementation of the H/V spectral ratio technique on ambient vibrations. SESAME, European project, WP12, Deliverable D23.12, http://sesame-fp5.obs.ujfgrenoble.fr/SES TechnicalDoc.htm

Tokimatsu, K. (1997). “Geotechnical Site Characterization using Surface Waves.” *Proceedings, First International Conference on Earthquake Geotechnical Engineering, IS-Tokyo '95*, Tokyo, November 14-16, Balkema, Rotterdam, 1333-1368.

Zhang, S.H., Chan, L.S. and Xia, J. (2004). The selection of field acquisition parameters for dispersion images from multichannel surface wave data. *Pure and Applied Geophysics* 161, 185–201.

Dipartimento di Scienze della Terra
Università degli Studi di Siena
Via Laterina, 8 53100 Siena, Italy

APPLICATION OF SURFACE WAVES METHODS FOR SEISMIC SITE CHARACTERIZATION

Spezzano Sila RAN site (SPS)

Responsible
Prof.Dario Albarello

Co-Workers
Dott. Domenico Pileggi
Dott. David Rossi
Dott. Enrico Lunedei

FINAL REPORT

Siena 30 May 2010

The investigation protocol

It involves four major elements:

- *Detailed Geological survey of the study area resulting in a geo/lithologic map at the scale 1:5000 of the area surrounding the relevant RAN station. This also aimed at the evaluation of the degree of lateral heterogeneity present in the lithological structure paying major attention to faults and their relevant damage area (that can result in energy trapping phenomena)*
- *Extensive single station ambient vibration survey at the station and in the surrounding area to detect possible lateral variations potentially responsible for site effects*
- *Ambient vibration measurements carried on with a seismic array at the RAN site or at a site representative of the subsoil configuration at the RAN site. In this last case, suitable inversion procedures and test were carried on to warrant the representativeness of ambient vibration measurements*
- *Global interpretation of measurements to determine the V_S profile and of the resonance frequency at the RAN site by considering the whole set of collected data*

Details concerning experimental tools and processing techniques are given in the following sections.

Single station measurements

The goal of this kind of measurements is the retrieval of the HVSR curve that represents for each frequency, the average ratio between Horizontal (H) to vertical (V) ground motion components of ambient vibrations (SESAME, 2004). Each single-station measurement was executed with a three-directional digital tromograph Tromino Micromed (see www.tromino.it) with a sampling frequency of 128 Hz and an acquisition time length of 20 minutes. This value represents a good compromise between the celerity of the measurement execution (which is one of the main merits of this technique) and its accuracy, according to the SESAME guidelines and other studies (see, e.g., Picozzi et al., 2005). To provide HVSR curves, the time series relative to each ground motion component was subdivided in non-overlapping time windows of 30 s. For each of these, the signal was corrected for the base line, padded with zeros, and tapered with a Triangular window; the relevant spectrogram was smoothed through a triangular window with frequency dependent half-width (10% of central frequency) and the H/V ratio (HVSR) of the spectral components (the former being the geometric mean of North-South and East-West components) was computed for each frequency. Spectral ratios relative to all the time windows considered were then averaged, and a mean HVSR curve was computed along with the relevant 95% confidence interval.

Before interpreting HVSR curve in terms of subsoil dynamical properties, we checked the possible occurrence of spurious HVSR peaks (e.g., due to impulsive or strongly localized anthropic sources). To this purpose, we investigated both the time stability of spectral ratios over the recording length and their directionality. The latter was analyzed by estimating the HVSR curves derived by projecting the ground motion along different horizontal directions. If transient directional effects were identified in the directional HVSR curves, the relevant portions of the record were discarded.

Array Measurements

This technique consists in recording ambient vibration ground motion by means of an array of sensors (vertical geophones) distributed at the surface of the subsoil to be explored (see, e.g., Okada, 2003). Relevant information concerning phase velocities of waves propagating across the array are obtained from average cross-spectral matrixes relative to sensor pairs. In the present analysis, plane waves propagating across the array were considered only. Since vertical sensors were used only, these waves are interpreted as plane Rayleigh waves in their fundamental and higher propagation modes. Determination of Rayleigh wave phase velocities V_R as a function of frequency (dispersion curve) from cross-spectral matrixes can be carried on in several ways. In the present analysis, the Extended Spatial Auto Correlation (ESAC) technique (Ohori et al. , 2002; Okada, 2003)

was applied. The basic element of this analysis is the cross-correlation spectrum deduced by the analysis of ambient vibrations measured at a couple of sensors $\phi(f,r)$ where *f* is frequency and *r* is the distance between the relevant sensors .

To this purpose, registrations relative to each sensor are partitioned in a number of non overlapping time windows of fixed duration (20 sec). Time windows characterised by energy bursts were removed from the analysis. To this purpose, a time segment is considered in the analysis if standard deviation of all the traces of that time window do not exceed the threshold fixed in advance for each trace. In general, this threshold was fixed to be 2 times the standard deviation computed over the whole registration for the relevant trace. In each accepted time window, linear trend was removed and the resulting time series was padded and tapered (5% cosine windows). For each time window and couple of sensors, the cross spectrum was computed. The average cross spectrum was then computed for each couple of sensors by considering all the relevant time series. The resulting average cross-spectrum was thus smoothed in the frequency domain by a moving triangular window having an half-width proportional to the central value (usually 10%) and normalized to the relevant auto spectra.

In the assumption that ambient vibration wave field can be represented as a linear combination of statistically independent plane waves propagating with negligible attenuation in a horizontal plane in different directions with different powers, but with the same phase velocity for a given frequency, the normalized cross-spectrum $\phi_{ij}(f,r)$ relative to sensors located at a distance r, can be written in the form

$$\phi(f,r) = J_0\left(\frac{2\pi f r}{V_R(f)}\right)$$

where J_0 is the Bessel function of *0-th* order. In the ESAC approach, the value of V_R relative to each frequency *f* is retrieved by a grid search algorithm to optimized (in a RMS sense) the fit of the above function of r for the relevant frequency *f* (Ohori et al. , 2002; Okada, 2003). Robustness of this fitting procedure was enhanced by adopting the iterative procedure proposed by Parolai et al., 2006). By following these last Authors, uncertainty on "apparent" velocities was computed by means the second derivative of the misfit function relative to grid search procedure (see, Menke, 1989). However, since these estimate tend to be under-conservative in some cases, the lower bound of the confidence interval for experimental V_R values was fixed by using the relationship proposed by Zhang et al. (2004) as a function of the adopted sampling rate and array dimension.

The $V_R(f)$ value obtained in this way, is the "apparent" or "effective" Rayleigh waves phase velocity that coincides with the actual phase velocity only in the case that higher modes play a negligible role. In the other cases, a relationship can be established between actual phase velocities and the apparent one (Tokimatsu, 1997). The fact that the ESAC approach allows the determination of the apparent dispersion curve instead of the modal ones could represent an important limitation of this procedure with respect to other approaches (e.g., f-k techniques). On the other hand, this makes the approach here considered more robust with respect to the alternative procedures, since it does not require troublesome picking of existing propagation modes.

In the present study, ambient vibrations were recorded for 20 minutes at a 256 Hz sampling rate by using 16 vertical geophones (4.5 Hz) and a digital acquisition system produced by Micromed (http://micromed.com/brainspy1.htm). Geophones were placed along two crossing perpendicular branches (with maximum dimensions lower than 100 m) and irregularly spaced (in the range 0.5-30 m).

Inversion procedures

HVSR and apparent V_R curves have been jointly inverted to constrain to the local V_S profile. To this purpose, a genetic algorithm procedure was considered. This is an iterative procedure, consisting in sequence of steps miming the evolutionary selection of living being (see Picozzi and Albarello, 2007 and references therein). The formalization proposed by Lunedei and Albarello (2009) was used as the forward modelling modelling

implemented in the procedure. This procedure assumes the subsoil as a flat stratified viscoelastic medium where surface waves (Rayleigh and Love with relevant higher modes) propagate only. From this model, both theoretical HVSR and effective dispersion curves can be computed from a set of parameters representative of the hypothetical subsoil (V_S, V_P, density, Q_P and Q_S profiles). The discrepancy between theoretical and observed HVSR and dispersion curves were then evaluated in terms of a suitable misfit function, strictly linked to the well-known χ^2 function, that allowed different choices about the combination of the discrepancies of V_R and HVSR curves, with different weights as well. The confidence interval around preferred *Vs* values and layer thickness were evaluated by following Picozzi and Albarello (2007).

Geological Setting

A detailed geologic survey of the area surrounding the RAN site was carried on (Figure 1).

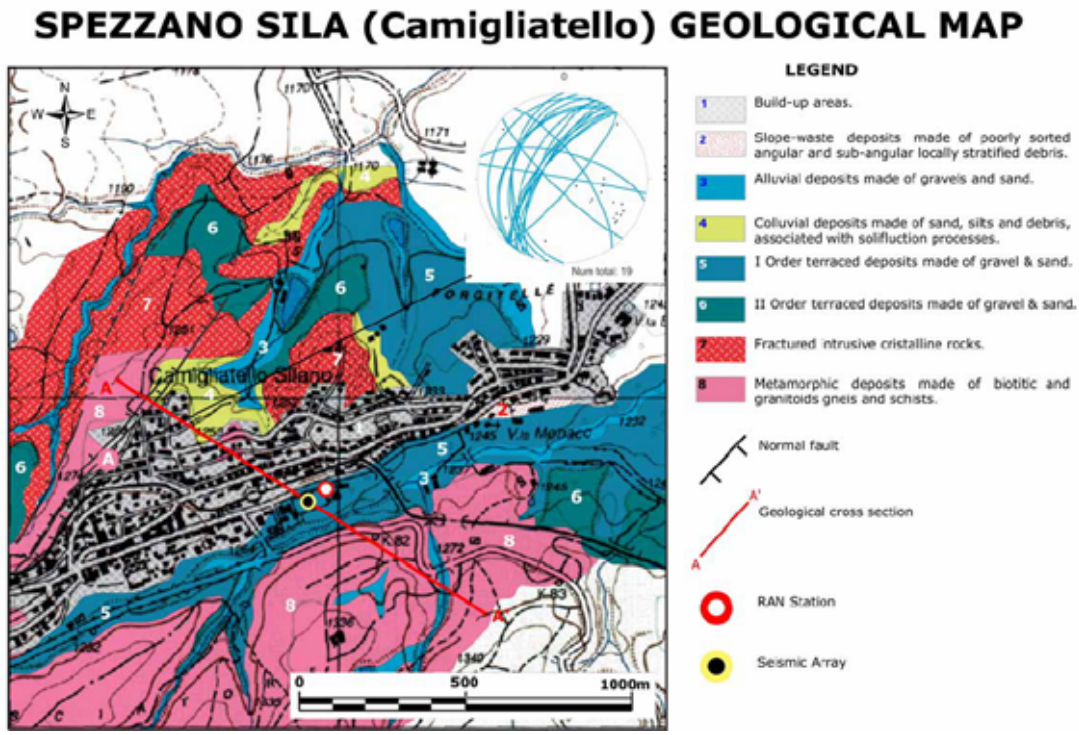

***Figure 1**: Geologic map of the Spezzano Sila RAN site*

The Spezzano Sila RAN (Camigliatello) site is located at the top of the Sila ridge (central Calabria). Both the RAN and the ARRAY (very close each other) are located above a tick alluvial deposits mainly composed by gravel and sand. The analyses carried out in field allow us to identify up to two different terraced orders at different topographic levels. The two station are localized over the I Order terraced at an altitude of 1245m. The two terraced order lie directly over the metamorphic succession, outcropping both in the southern and northern sector of the studied area. The metamorphic complex is made of biotitic gneiss and granodioritic schists extremely fractured. The fracturation process in several cases it is so widespread and pervasive that in most of the outcrops it is very difficult to identify a main scistosity planes, in other sites the metamorphic complex it is associable to a sandy deposit. Tectonic processes are pervasive in the whole area but due to the intense build-up areas affecting the whole Camigliatello Silano town district only in the northern sector were recognized several faults. The fault system is represented by a set of normal faults NW dipping and with N20° average strike direction as shown in the geological map stereograms. These last mesoscale fault system is linked to a main fault recognized in the NW sector of the studied site where it is possible to identify the tectonical contact

between the metamorphic complex and the intrusive crystalline rocks. The crystalline instrusive complex it is also extremely fractured and altered with a main set of fracture family sub-parallel to the main fault lineament.

The area it is also characterized by the presence of recent deposits as colluvial deposits, alluvial deposits and slope-waste deposits made of poorly sorted angular and sub-angular clasts. In the geological cross section it is possible to observe also in detail both the thickness of the order terraced and the relationships with the metamorphic complex.

A representative geological section is reported in Figure2.

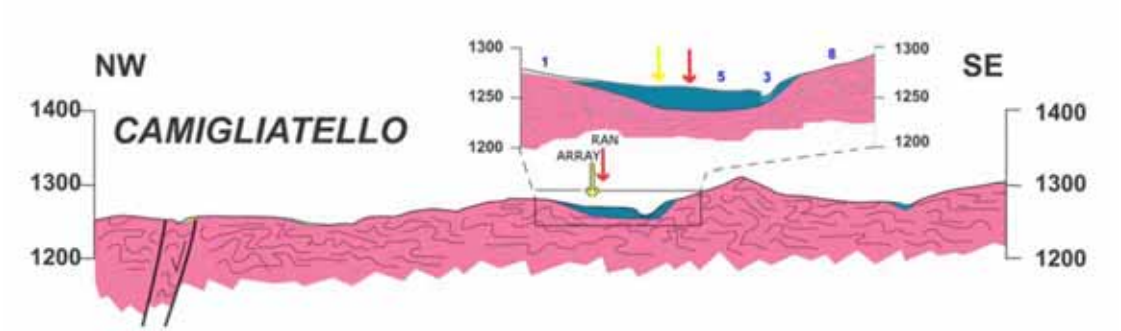

Figure 2 *Geological section across Spezzano Sila area (see trace in Fig.2): RAN indicates location of the SPS accelerometric station. ARRAY indicates the position of the array*

Results of passive seismic survey

A single station measurement was carried nearby the RAN station (Figure 3 and 5) on 10th of April 2009. A strong significant resonance was detected at his site (Figure 4), in line with the what expected from the geological survey.

Figure3. *Location of the RAN station and of the corresponding single station ambient vibration measurement*

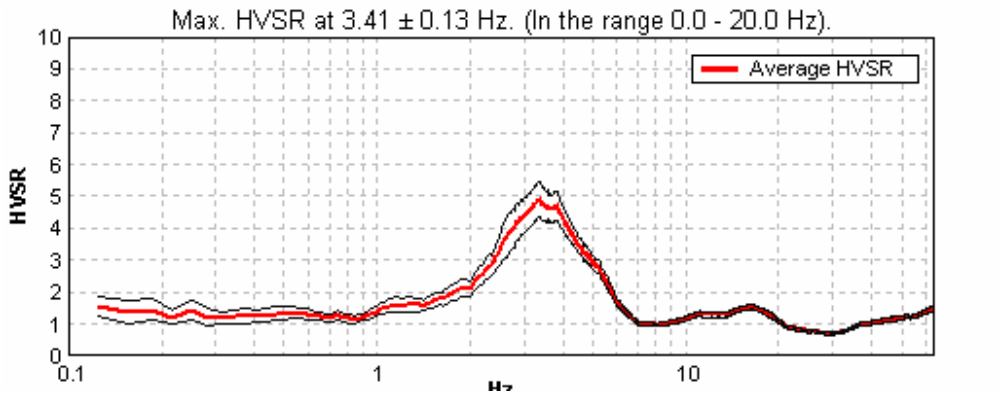

Figure 4. *HVSR curve obtained at the SPS RAN station. The red line indicates the average HVSR values, while the black thin lines indicate the relevant 95% confidence interval*

Due to the nearly flat morphology, array measurements were carried on nearby the RAN site (Figure 1). Results of these measurements are reported in Figure 6 and are compatible with a subsoil characterized by V_S values increasing with depth. Results obtained from the joint inversion of the HVSR and Apparent Rayleigh waves dispersion curves are reported in Figure 7 and Table 1. These are in line with results provided by the geologic survey that indicate the presence of a relatively thick sedimentary cover overlying a rigid bedrock.

Figure 5. *Location of the Spezzano Sila RAN station*

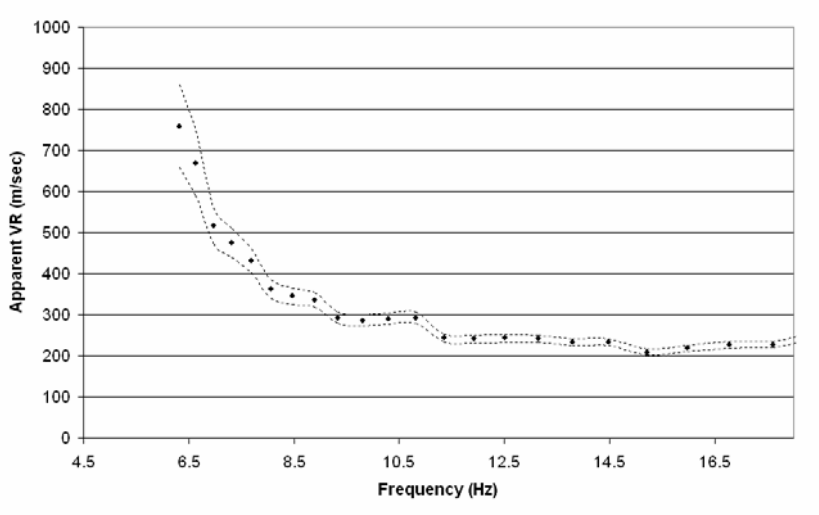

Figure 6. *Apparent VR curve deduced from array measurements. Dots indicate VR estimates while dashed lines bound the relevant 95% confidence interval*

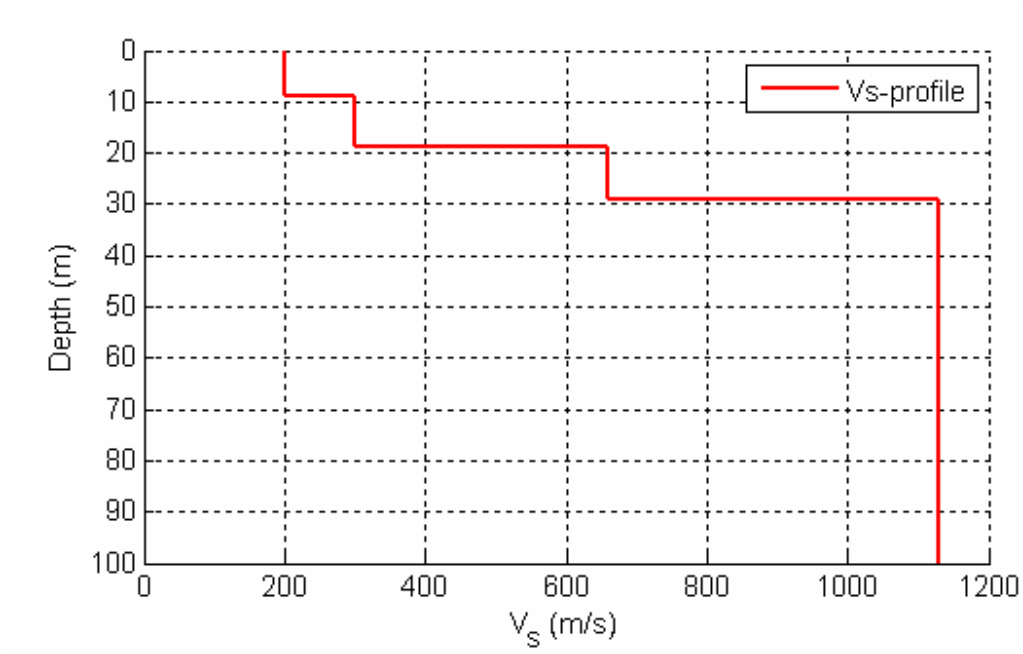

Figure 7. *Vs Velocity profile at the Spezzano Sila RAN station*

Table 1*: V_S profile at the SPS station (confidence intervals are reported in parenthesis)*

Tickness (m)	S-Velocity (m/s)
9	**200**
10	**300**
10	**660 (600-660)**
?	**1130 (1130-1160)**

Summary of subsoil basic features at the SPS RAN site

Vs30 = 320 m/s
Soil Class = C
Topography classification = T1
Depth to bedrock = 29 m
Average Vs to bedrock = 310 m/s
f_0 from ambient vibrations = 3.4 Hz

References

Lunedei E., Albarello D. (2009). On the seismic noise wavefield in a weakly dissipative layered Earth. *Geophys. J. Int.* (2009) **177,** 1001–1014, doi: 10.1111/j.1365-246X.2008.04062.x

Menke,W., 1989. *Geophysical Data Analysis: Discrete Inverse Theory,* rev.ed. Academic, San Diego, CA.

Ohori M., Nobata A., Wakamatsu K. (2002). A comparison of ESAC and FK methods of estimating phasevelocity using arbitrarily shaped microtremor arrays. Bull.Seism.Soc.Am., 92, 6, 2323-2332

Okada, H. (2003). The microtremor survey method, *Geophys. Monograph Series,* Vol. 12, Society of Exploration Geohysicists, 129 pp.

Picozzi M., Parolai S., Albarello D.; 2005: Statistical analysis of noise Horizonatal-to-Vertical Specrtal Ratios (HVSR). Bull. Seism. Soc. Am., **95**, n. 5, 1779–1786, doi: 10.1785/0120040152

Picozzi M., Albarello D. (2007). Combining genetic and linearized algorithms for a two-step joint inversion of Rayleigh wave dispersion and *H/V* spectral ratio curves. *Geophys. J. Int.* (2007) **169,** 189–200, doi: 10.1111/j.1365-246X.2006.03282.x

SESAME; 2004: Guidelines for the implementation of the H/V spectral ratio technique on ambient vibrations. SESAME, European project, WP12, Deliverable D23.12, http://sesame-fp5.obs.ujfgrenoble.fr/SES TechnicalDoc.htm

Tokimatsu, K. (1997). “Geotechnical Site Characterization using Surface Waves.” *Proceedings, First International Conference on Earthquake Geotechnical Engineering, IS-Tokyo '95*, Tokyo, November 14-16, Balkema, Rotterdam, 1333-1368.

Zhang, S.H., Chan, L.S. and Xia, J. (2004). The selection of field acquisition parameters for dispersion images from multichannel surface wave data. *Pure and Applied Geophysics* 161, 185–201.

Dipartimento di Scienze della Terra
Università degli Studi di Siena
Via Laterina, 8 53100 Siena, Italy

APPLICATION OF SURFACE WAVES METHODS FOR SEISMIC SITE CHARACTERIZATION

Vibo Marina RAN site (VBM)

Responsible
Prof.Dario Albarello

Co-Workers
Dott. Domenico Pileggi
Dott. David Rossi
Dott. Enrico Lunedei

FINAL REPORT

Siena 30 May 2010

The investigation protocol

It involves four major elements:

- *Detailed Geological survey of the study area resulting in a geo/lithologic map at the scale 1:5000 of the area surrounding the relevant RAN station. This also aimed at the evaluation of the degree of lateral heterogeneity present in the lithological structure paying major attention to faults and their relevant damage area (that can result in energy trapping phenomena)*
- *Extensive single station ambient vibration survey at the station and in the surrounding area to detect possible lateral variations potentially responsible for site effects*
- *Ambient vibration measurements carried on with a seismic array at the RAN site or at a site representative of the subsoil configuration at the RAN site. In this last case, suitable inversion procedures and test were carried on to warrant the representativeness of ambient vibration measurements*
- *Global interpretation of measurements to determine the V_S profile and of the resonance frequency at the RAN site by considering the whole set of collected data*

Details concerning experimental tools and processing techniques are given in the following sections.

Single station measurements

The goal of this kind of measurements is the retrieval of the HVSR curve that represents for each frequency, the average ratio between Horizontal (H) to vertical (V) ground motion components of ambient vibrations (SESAME, 2004). Each single-station measurement was executed with a three-directional digital tromograph Tromino Micromed (see www.tromino.it) with a sampling frequency of 128 Hz and an acquisition time length of 20 minutes. This value represents a good compromise between the celerity of the measurement execution (which is one of the main merits of this technique) and its accuracy, according to the SESAME guidelines and other studies (see, e.g., Picozzi et al., 2005). To provide HVSR curves, the time series relative to each ground motion component was subdivided in non-overlapping time windows of 30 s. For each of these, the signal was corrected for the base line, padded with zeros, and tapered with a Triangular window; the relevant spectrogram was smoothed through a triangular window with frequency dependent half-width (10% of central frequency) and the H/V ratio (HVSR) of the spectral components (the former being the geometric mean of North-South and East-West components) was computed for each frequency. Spectral ratios relative to all the time windows considered were then averaged, and a mean HVSR curve was computed along with the relevant 95% confidence interval.

Before interpreting HVSR curve in terms of subsoil dynamical properties, we checked the possible occurrence of spurious HVSR peaks (e.g., due to impulsive or strongly localized anthropic sources). To this purpose, we investigated both the time stability of spectral ratios over the recording length and their directionality. The latter was analyzed by estimating the HVSR curves derived by projecting the ground motion along different horizontal directions. If transient directional effects were identified in the directional HVSR curves, the relevant portions of the record were discarded.

Array Measurements

This technique consists in recording ambient vibration ground motion by means of an array of sensors (vertical geophones) distributed at the surface of the subsoil to be explored (see, e.g., Okada, 2003). Relevant information concerning phase velocities of waves propagating across the array are obtained from average cross-spectral matrixes relative to sensor pairs. In the present analysis, plane waves propagating across the array were considered only. Since vertical sensors were used only, these waves are interpreted as plane Rayleigh waves in their fundamental and higher propagation modes. Determination of Rayleigh wave phase velocities V_R as a function of frequency (dispersion curve) from cross-spectral matrixes can be carried on in several ways. In the present analysis, the Extended Spatial Auto Correlation (ESAC) technique (Ohori et al. , 2002; Okada, 2003)

was applied. The basic element of this analysis is the cross-correlation spectrum deduced by the analysis of ambient vibrations measured at a couple of sensors $\phi(f,r)$ where *f* is frequency and *r* is the distance between the relevant sensors .

To this purpose, registrations relative to each sensor are partitioned in a number of non overlapping time windows of fixed duration (20 sec). Time windows characterised by energy bursts were removed from the analysis. To this purpose, a time segment is considered in the analysis if standard deviation of all the traces of that time window do not exceed the threshold fixed in advance for each trace. In general, this threshold was fixed to be 2 times the standard deviation computed over the whole registration for the relevant trace. In each accepted time window, linear trend was removed and the resulting time series was padded and tapered (5% cosine windows). For each time window and couple of sensors, the cross spectrum was computed. The average cross spectrum was then computed for each couple of sensors by considering all the relevant time series. The resulting average cross-spectrum was thus smoothed in the frequency domain by a moving triangular window having an half-width proportional to the central value (usually 10%) and normalized to the relevant auto spectra.

In the assumption that ambient vibration wave field can be represented as a linear combination of statistically independent plane waves propagating with negligible attenuation in a horizontal plane in different directions with different powers, but with the same phase velocity for a given frequency, the normalized cross-spectrum $\phi_{ij}(f,r)$ relative to sensors located at a distance r, can be written in the form

$$\phi(f,r) = J_0\left(\frac{2\pi f r}{V_R(f)}\right)$$

where J_0 is the Bessel function of *0-th* order. In the ESAC approach, the value of V_R relative to each frequency *f* is retrieved by a grid search algorithm to optimized (in a RMS sense) the fit of the above function of r for the relevant frequency *f* (Ohori et al. , 2002; Okada, 2003). Robustness of this fitting procedure was enhanced by adopting the iterative procedure proposed by Parolai et al., 2006). By following these last Authors, uncertainty on "apparent" velocities was computed by means the second derivative of the misfit function relative to grid search procedure (see, Menke, 1989). However, since these estimate tend to be under-conservative in some cases, the lower bound of the confidence interval for experimental V_R values was fixed by using the relationship proposed by Zhang et al. (2004) as a function of the adopted sampling rate and array dimension.

The $V_R(f)$ value obtained in this way, is the "apparent" or "effective" Rayleigh waves phase velocity that coincides with the actual phase velocity only in the case that higher modes play a negligible role. In the other cases, a relationship can be established between actual phase velocities and the apparent one (Tokimatsu, 1997). The fact that the ESAC approach allows the determination of the apparent dispersion curve instead of the modal ones could represent an important limitation of this procedure with respect to other approaches (e.g., f-k techniques). On the other hand, this makes the approach here considered more robust with respect to the alternative procedures, since it does not require troublesome picking of existing propagation modes.

In the present study, ambient vibrations were recorded for 20 minutes at a 256 Hz sampling rate by using 16 vertical geophones (4.5 Hz) and a digital acquisition system produced by Micromed (http://micromed.com/brainspy1.htm). Geophones were placed along two crossing perpendicular branches (with maximum dimensions lower than 100 m) and irregularly spaced (in the range 0.5-30 m).

Inversion procedures

HVSR and apparent V_R curves have been jointly inverted to constrain to the local V_S profile. To this purpose, a genetic algorithm procedure was considered. This is an iterative procedure, consisting in sequence of steps miming the evolutionary selection of living being (see Picozzi and Albarello, 2007 and references therein). The formalization proposed by Lunedei and Albarello (2009) was used as the forward modelling modelling

implemented in the procedure. This procedure assumes the subsoil as a flat stratified viscoelastic medium where surface waves (Rayleigh and Love with relevant higher modes) propagate only. From this model, both theoretical HVSR and effective dispersion curves can be computed from a set of parameters representative of the hypothetical subsoil (V_S, V_P, density, Q_P and Q_S profiles). The discrepancy between theoretical and observed HVSR and dispersion curves were then evaluated in terms of a suitable misfit function, strictly linked to the well-known χ^2 function, that allowed different choices about the combination of the discrepancies of V_R and HVSR curves, with different weights as well. The confidence interval around preferred *Vs* values and layer thickness were evaluated by following Picozzi and Albarello (2007).

Geological Setting

A detailed geologic survey of the area surrounding the RAN site was carried on (Figure 1).

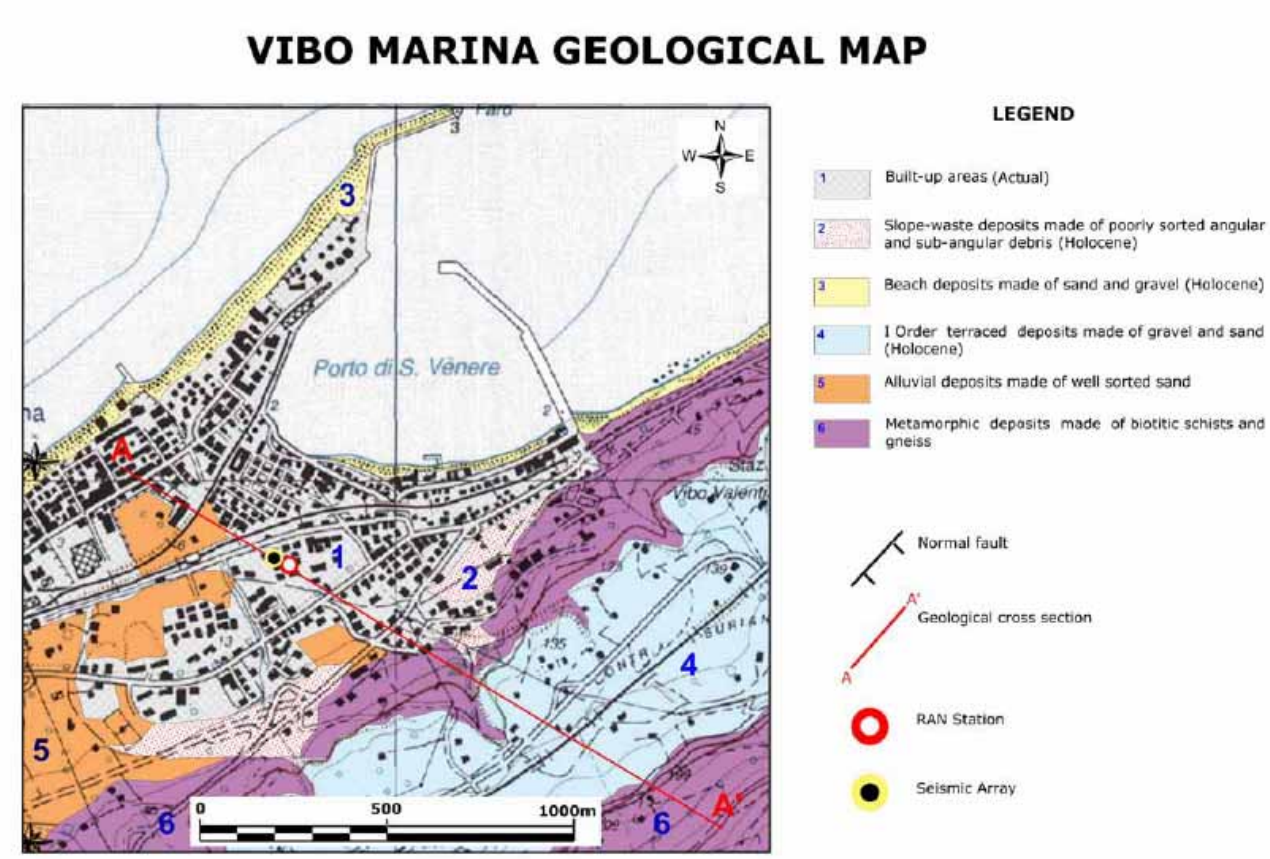

***Figure 1**: Geologic map of the Vibo Marina RAN site*

The Vibo Marina RAN site represent the coastal line area of the Vibo Valentia district. As for the other site in the area (Vibo Valentia – VBV RAN site), especially in the SE sector a metamorphic substrata complex were recognized. The metamorphic deposits is mainly composed by biotitic schists and gneiss with an high alteration grade. Despite this both the RAN and the ARRAY (close each other) lie over a tick alluvial deposits mainly made of well sorted sand and silt. Due to the complete absence of outcropping sediments all around the station it is not possible to better define both the sediment internal organization and thickness. No well were identified and no log stratigaphy available. Simply on the base of the morphological overview and by the analyses of the hills shape and ridge slope it is possible to hypothesize an average thickness up to 50 meters. No faults were recognized directly in field, but two main normal fault, north-west dipping were supposed, that progressively NW-downwards the whole substrata.

A representative geological section is reported in Figure2.

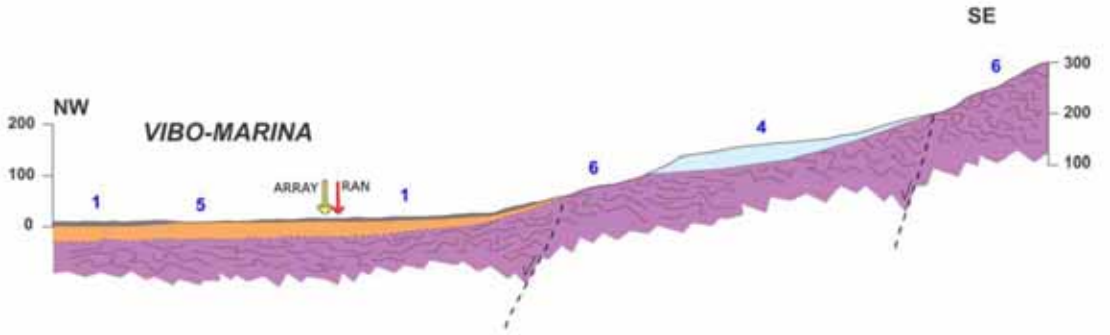

Figure 2 *Geological section across Vibo Marina area (see trace in Fig.1): RAN indicates location of the VBM accelerometric station. ARRAY indicates the position of the array*

Results of passive seismic survey

A single station measurement was carried nearby the RAN station (Figures 3 and 5) on 3rd of March 2009. A strong resonance phenomenon was detected at the frequencies of 5 Hz. These could be the effect of the sedimentary cover detected by the geological analysis (Figure 2).

Figure3. *Location of the RAN station and of the corresponding single station ambient vibration measurement*

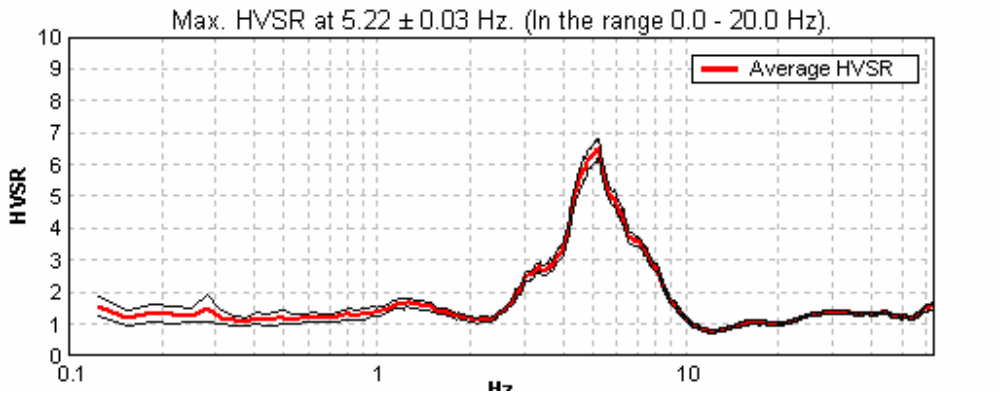

Figure 4. *HVSR curve obtained at the VBM RAN station. The red line indicates the average HVSR values, while the black thin lines indicate the relevant 95% confidence interval*

Due to the nearly flat morphology, array measurements were carried nearby the RAN site (Figure 1). Results of these measurements are reported in Figure 6 and are compatible with a subsoil characterized by V_S values increasing with depth (see Figure 7 and Table 1). Results of the joint inversion of the HVSR and Rayleigh waves dispersion curve are reported in figure 6 and table 1. These result compatible with results of the geological survey that indicates the presence of a relatively thick sedimentary cover overlying a rigid bedrock.

Figure 5. *Location of the Vibo Marina RAN station. On the bottom, the digital tromograph used for the single station ambient vibration measurements is shown*

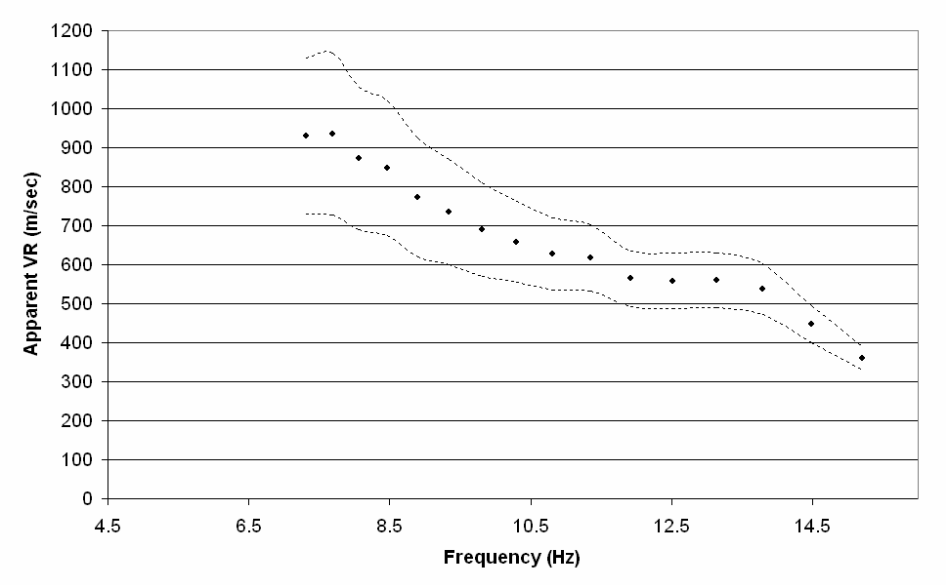

Figure 6. *Apparent VR curve deduced from array measurements. Dots indicate VR estimates while dashed lines bound the relevant 95% confidence interval*

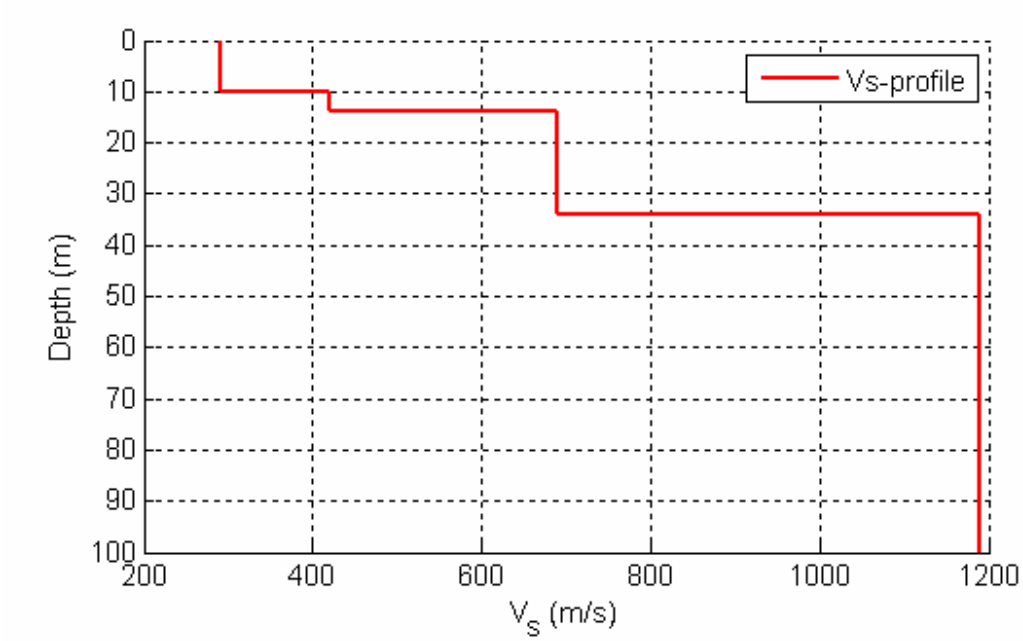

Figure 7. *Vs Velocity profile at the Vibo Marina RAN station*

Table 1*: V_S profile at the VBM station*

Tickness (m)	S-Velocity (m/s)
10	**290**
4	**420**
20	**690**
?	**1180**

Summary of subsoil basic features at the VBM RAN site

Vs30 = 450 m/s
Soil Class = B
Topography category = T1
Depth to bedrock = 34 m
Average Vs to bedrock = 460 m/s
f_0 from ambient vibrations = 5.2 Hz

References

Lunedei E., Albarello D. (2009). On the seismic noise wavefield in a weakly dissipative layered Earth. *Geophys. J. Int.* (2009) **177,** 1001–1014, doi: 10.1111/j.1365-246X.2008.04062.x

Menke,W., 1989. *Geophysical Data Analysis: Discrete Inverse Theory,* rev.ed. Academic, San Diego, CA.

Ohori M., Nobata A., Wakamatsu K. (2002). A comparison of ESAC and FK methods of estimating phasevelocity using arbitrarily shaped microtremor arrays. Bull.Seism.Soc.Am., 92, 6, 2323-2332

Okada, H. (2003). The microtremor survey method, *Geophys. Monograph Series,* Vol. 12, Society of Exploration Geohysicists, 129 pp.

Picozzi M., Parolai S., Albarello D.; 2005: Statistical analysis of noise Horizonatal-to-Vertical Specrtal Ratios (HVSR). Bull. Seism. Soc. Am., **95**, n. 5, 1779–1786, doi: 10.1785/0120040152

Picozzi M., Albarello D. (2007). Combining genetic and linearized algorithms for a two-step joint inversion of Rayleigh wave dispersion and *H/V* spectral ratio curves. *Geophys. J. Int.* (2007) **169,** 189–200, doi: 10.1111/j.1365-246X.2006.03282.x

SESAME; 2004: Guidelines for the implementation of the H/V spectral ratio technique on ambient vibrations. SESAME, European project, WP12, Deliverable D23.12, http://sesame-fp5.obs.ujfgrenoble.fr/SES TechnicalDoc.htm

Tokimatsu, K. (1997). “Geotechnical Site Characterization using Surface Waves.” *Proceedings, First International Conference on Earthquake Geotechnical Engineering, IS-Tokyo '95*, Tokyo, November 14-16, Balkema, Rotterdam, 1333-1368.

Zhang, S.H., Chan, L.S. and Xia, J. (2004). The selection of field acquisition parameters for dispersion images from multichannel surface wave data. *Pure and Applied Geophysics* 161, 185–201.

Dipartimento di Scienze della Terra
Università degli Studi di Siena
Via Laterina, 8 53100 Siena, Italy

APPLICATION OF SURFACE WAVES METHODS FOR SEISMIC SITE CHARACTERIZATION

Vibo Valentia RAN site (VBV)

Responsible
Prof.Dario Albarello

Co-Workers
Dott. Domenico Pileggi
Dott. David Rossi
Dott. Enrico Lunedei

FINAL REPORT

Siena 30 May 2010

The investigation protocol

It involves four major elements:

- *Detailed Geological survey of the study area resulting in a geo/lithologic map at the scale 1:5000 of the area surrounding the relevant RAN station. This also aimed at the evaluation of the degree of lateral heterogeneity present in the lithological structure paying major attention to faults and their relevant damage area (that can result in energy trapping phenomena)*
- *Extensive single station ambient vibration survey at the station and in the surrounding area to detect possible lateral variations potentially responsible for site effects*
- *Ambient vibration measurements carried on with a seismic array at the RAN site or at a site representative of the subsoil configuration at the RAN site. In this last case, suitable inversion procedures and test were carried on to warrant the representativeness of ambient vibration measurements*
- *Global interpretation of measurements to determine the V_S profile and of the resonance frequency at the RAN site by considering the whole set of collected data*

Details concerning experimental tools and processing techniques are given in the following sections.

Single station measurements

The goal of this kind of measurements is the retrieval of the HVSR curve that represents for each frequency, the average ratio between Horizontal (H) to vertical (V) ground motion components of ambient vibrations (SESAME, 2004). Each single-station measurement was executed with a three-directional digital tromograph Tromino Micromed (see www.tromino.it) with a sampling frequency of 128 Hz and an acquisition time length of 20 minutes. This value represents a good compromise between the celerity of the measurement execution (which is one of the main merits of this technique) and its accuracy, according to the SESAME guidelines and other studies (see, e.g., Picozzi et al., 2005). To provide HVSR curves, the time series relative to each ground motion component was subdivided in non-overlapping time windows of 30 s. For each of these, the signal was corrected for the base line, padded with zeros, and tapered with a Triangular window; the relevant spectrogram was smoothed through a triangular window with frequency dependent half-width (10% of central frequency) and the H/V ratio (HVSR) of the spectral components (the former being the geometric mean of North-South and East-West components) was computed for each frequency. Spectral ratios relative to all the time windows considered were then averaged, and a mean HVSR curve was computed along with the relevant 95% confidence interval.

Before interpreting HVSR curve in terms of subsoil dynamical properties, we checked the possible occurrence of spurious HVSR peaks (e.g., due to impulsive or strongly localized anthropic sources). To this purpose, we investigated both the time stability of spectral ratios over the recording length and their directionality. The latter was analyzed by estimating the HVSR curves derived by projecting the ground motion along different horizontal directions. If transient directional effects were identified in the directional HVSR curves, the relevant portions of the record were discarded.

Array Measurements

This technique consists in recording ambient vibration ground motion by means of an array of sensors (vertical geophones) distributed at the surface of the subsoil to be explored (see, e.g., Okada, 2003). Relevant information concerning phase velocities of waves propagating across the array are obtained from average cross-spectral matrixes relative to sensor pairs. In the present analysis, plane waves propagating across the array were considered only. Since vertical sensors were used only, these waves are interpreted as plane Rayleigh waves in their fundamental and higher propagation modes. Determination of Rayleigh wave phase velocities V_R as a function of frequency (dispersion curve) from cross-spectral matrixes can be carried on in several ways. In the present analysis, the Extended Spatial Auto Correlation (ESAC) technique (Ohori et al. , 2002; Okada, 2003)

was applied. The basic element of this analysis is the cross-correlation spectrum deduced by the analysis of ambient vibrations measured at a couple of sensors $\phi(f,r)$ where *f* is frequency and *r* is the distance between the relevant sensors .

To this purpose, registrations relative to each sensor are partitioned in a number of non overlapping time windows of fixed duration (20 sec). Time windows characterised by energy bursts were removed from the analysis. To this purpose, a time segment is considered in the analysis if standard deviation of all the traces of that time window do not exceed the threshold fixed in advance for each trace. In general, this threshold was fixed to be 2 times the standard deviation computed over the whole registration for the relevant trace. In each accepted time window, linear trend was removed and the resulting time series was padded and tapered (5% cosine windows). For each time window and couple of sensors, the cross spectrum was computed. The average cross spectrum was then computed for each couple of sensors by considering all the relevant time series. The resulting average cross-spectrum was thus smoothed in the frequency domain by a moving triangular window having an half-width proportional to the central value (usually 10%) and normalized to the relevant auto spectra.

In the assumption that ambient vibration wave field can be represented as a linear combination of statistically independent plane waves propagating with negligible attenuation in a horizontal plane in different directions with different powers, but with the same phase velocity for a given frequency, the normalized cross-spectrum $\phi_{ij}(f,r)$ relative to sensors located at a distance r, can be written in the form

$$\phi(f,r) = J_0\left(\frac{2\pi f r}{V_R(f)}\right)$$

where J_0 is the Bessel function of *0-th* order. In the ESAC approach, the value of V_R relative to each frequency *f* is retrieved by a grid search algorithm to optimized (in a RMS sense) the fit of the above function of r for the relevant frequency *f* (Ohori et al. , 2002; Okada, 2003). Robustness of this fitting procedure was enhanced by adopting the iterative procedure proposed by Parolai et al., 2006). By following these last Authors, uncertainty on "apparent" velocities was computed by means the second derivative of the misfit function relative to grid search procedure (see, Menke, 1989). However, since these estimate tend to be under-conservative in some cases, the lower bound of the confidence interval for experimental V_R values was fixed by using the relationship proposed by Zhang et al. (2004) as a function of the adopted sampling rate and array dimension.

The $V_R(f)$ value obtained in this way, is the "apparent" or "effective" Rayleigh waves phase velocity that coincides with the actual phase velocity only in the case that higher modes play a negligible role. In the other cases, a relationship can be established between actual phase velocities and the apparent one (Tokimatsu, 1997). The fact that the ESAC approach allows the determination of the apparent dispersion curve instead of the modal ones could represent an important limitation of this procedure with respect to other approaches (e.g., f-k techniques). On the other hand, this makes the approach here considered more robust with respect to the alternative procedures, since it does not require troublesome picking of existing propagation modes.

In the present study, ambient vibrations were recorded for 20 minutes at a 256 Hz sampling rate by using 16 vertical geophones (4.5 Hz) and a digital acquisition system produced by Micromed (http://micromed.com/brainspy1.htm). Geophones were placed along two crossing perpendicular branches (with maximum dimensions lower than 100 m) and irregularly spaced (in the range 0.5-30 m).

Inversion procedures

HVSR and apparent V_R curves have been jointly inverted to constrain to the local V_S profile. To this purpose, a genetic algorithm procedure was considered. This is an iterative procedure, consisting in sequence of steps miming the evolutionary selection of living being (see Picozzi and Albarello, 2007 and references therein). The formalization proposed by Lunedei and Albarello (2009) was used as the forward modelling modelling

implemented in the procedure. This procedure assumes the subsoil as a flat stratified viscoelastic medium where surface waves (Rayleigh and Love with relevant higher modes) propagate only. From this model, both theoretical HVSR and effective dispersion curves can be computed from a set of parameters representative of the hypothetical subsoil (V_S, V_P, density, Q_P and Q_S profiles). The discrepancy between theoretical and observed HVSR and dispersion curves were then evaluated in terms of a suitable misfit function, strictly linked to the well-known χ^2 function, that allowed different choices about the combination of the discrepancies of V_R and HVSR curves, with different weights as well. The confidence interval around preferred *Vs* values and layer thickness were evaluated by following Picozzi and Albarello (2007).

Geological Setting

A detailed geologic survey of the area surrounding the RAN site was carried on (Figure 1).

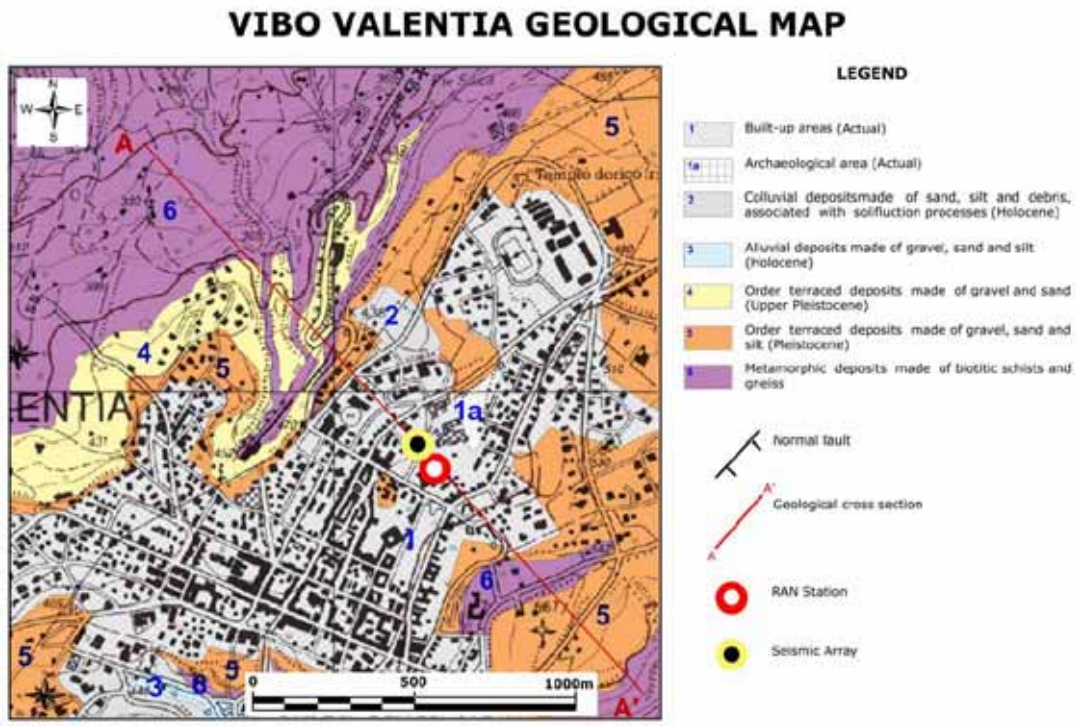

Figure 1*: Geologic map of the Vibo Valentia RAN site*

The Vibo valentia RAN site is located in the South-western sector of the Calabria region close to the Mar Tirreno coastal line. Both the RAN and the ARRAY (very close each other) lie over an important order terraced deposit widespread in the whole western side of the southern Calabria. With a thickness of 50-60m this deposit represent an important stage during the quaternary evolution of the whole region. In this site were recognized two main order terraced identified at different topographic levels at 430m and 530 m above the sea level. Both terraced deposits are mainly made of gravel and sand with several levels of silt. The RAN site it is located above the topographically highest order terraced. The substrata outcropping in the area is mainly composed by a metamorphic complex deposits composed by biotitic schists and gneiss. The contact between the terraced deposits with the metamorphic substrata is well defined by an unconformities erosional surfaces cropping out in the NW sector of the studied area. Both the contact surfaces and the terraced bedding allow us to identify and better understanding the relationships between the cover sediments and the substrata as shown in the geological cross sections. In regard to the Holocene and recent deposits in the area were recognized also alluvial deposits made of gravel and sand, colluvial deposits and an Archaeological area very close to the ran station. Despite the intense built-up areas, due to several building excavation (still in progress) it was possible to

better understanding the thickness of the terraced and the internal configuration mainly composed by crossing strata and by an alternation at different levels of gravels.
In the area no fault system were recognized but we do not exclude the presence of buried lineaments cross cutting the metamorphic substrata.

A representative geological section is reported in Figure2.

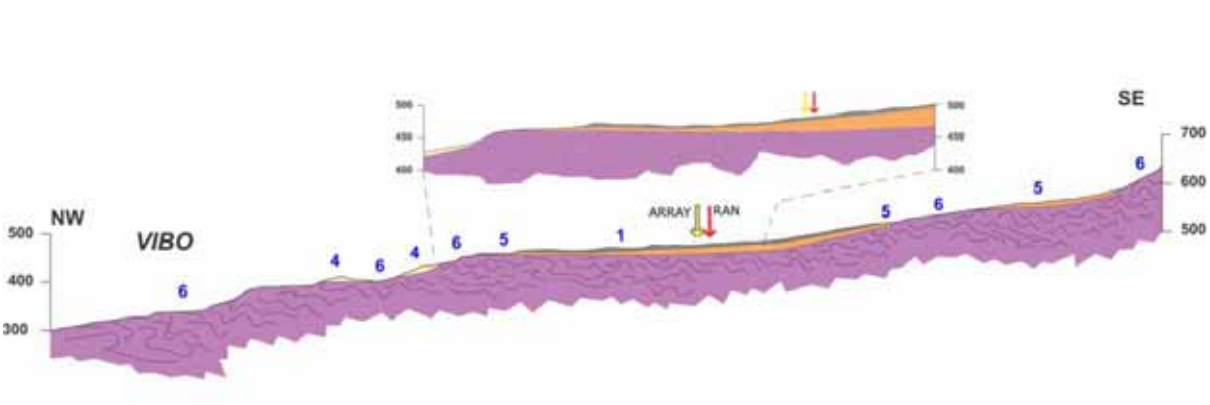

Figure 2 *Geological section across Vibo Valentia area (see trace in Fig.1): RAN indicates location of the VBV accelerometric station. ARRAY indicates the position of the array*

Results of passive seismic survey

A single station measurement was carried nearby the RAN station (Figure 3 and 5) on 3rd of March 2009. Light resonance phenomena were detected at the frequencies of 5 and 13 Hz. These could be the effect of the sedimentary cover detected by the geological analysis.

Figure3. *Location of the RAN station and of the corresponding single station ambient vibration measurement*

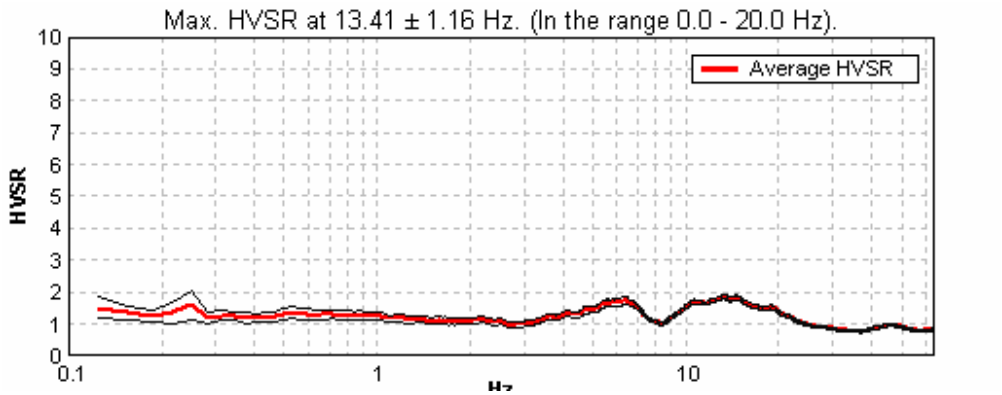

Figure 4. *HVSR curve obtained at the VBV RAN station. The red line indicates the average HVSR values, while the black thin lines indicate the relevant 95% confidence interval*

Due to the nearly flat morphology, array measurements were carried nearby the RAN site (Figure 1). Results of these measurements are reported in Figure 6 and are compatible with a subsoil characterized by V_S values increasing with depth (see Figure 7 and Table 1). Results of the joint inversion of the HVSR and Rayleigh waves dispersion curve are reported in figure 6 and table 1. These result compatible with results of the geological survey that indicates the presence of a relatively thick sedimentary cover overlying a rigid bedrock.

Figure 5. *Location of the Vibo Valentia RAN station. On the bottom, the digital tromograph used for the single station ambient vibration measurements is shown*

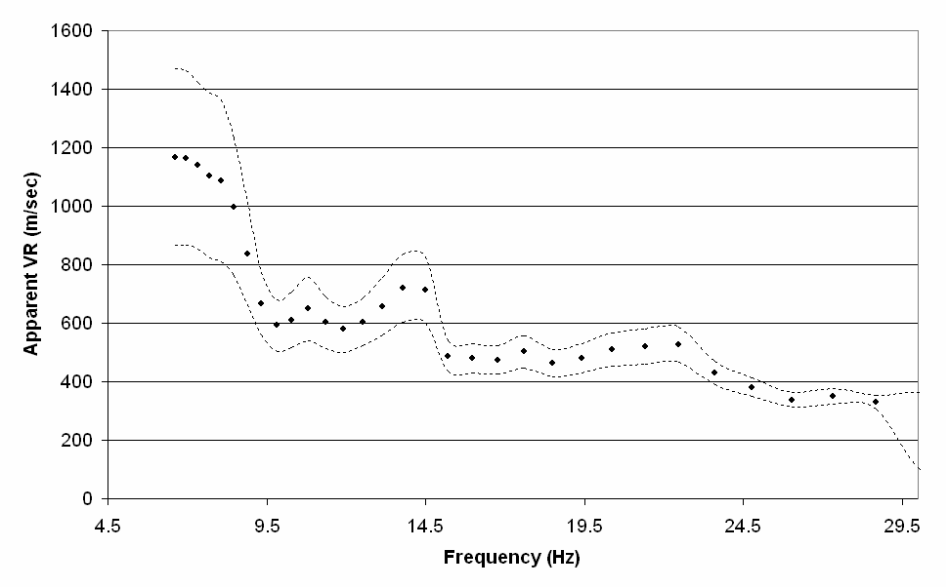

Figure 6. *Apparent VR curve deduced from array measurements. Dots indicate VR estimates while dashed lines bound the relevant 95% confidence interval*

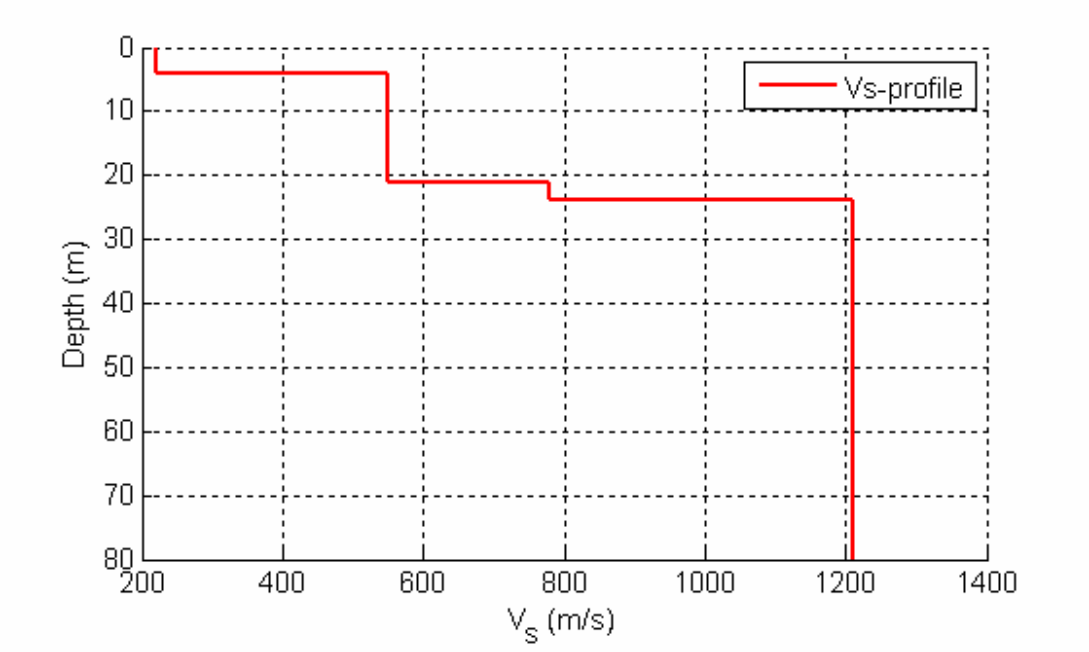

Figure 7. *Vs Velocity profile at the Vibo Valentia RAN station*

***Table 1**: V_S profile at the VBV station (confidence intervals are reported in parenthesis)*

Tickness (m)	S-Velocity (m/s)
4	**220**
17	**550**
3 (2-5)	**780 (700-750)**
?	**1210 (1260-1360)**

Summary of subsoil basic features at the VBV RAN site

Vs30 = 510 m/s
Soil Class = B
Topography classification = T1
Depth to bedrock = 24 m
Average Vs to bedrock = 450 m/s
f_0 from ambient vibrations = 13.5 Hz

References

Lunedei E., Albarello D. (2009). On the seismic noise wavefield in a weakly dissipative layered Earth. *Geophys. J. Int.* (2009) **177,** 1001–1014, doi: 10.1111/j.1365-246X.2008.04062.x

Menke,W., 1989. *Geophysical Data Analysis: Discrete Inverse Theory,* rev.ed. Academic, San Diego, CA.

Ohori M., Nobata A., Wakamatsu K. (2002). A comparison of ESAC and FK methods of estimating phasevelocity using arbitrarily shaped microtremor arrays. Bull.Seism.Soc.Am., 92, 6, 2323-2332

Okada, H. (2003). The microtremor survey method, *Geophys. Monograph Series,* Vol. 12, Society of Exploration Geohysicists, 129 pp.

Picozzi M., Parolai S., Albarello D.; 2005: Statistical analysis of noise Horizonatal-to-Vertical Specrtal Ratios (HVSR). Bull. Seism. Soc. Am., **95**, n. 5, 1779–1786, doi: 10.1785/0120040152

Picozzi M., Albarello D. (2007). Combining genetic and linearized algorithms for a two-step joint inversion of Rayleigh wave dispersion and *H/V* spectral ratio curves. *Geophys. J. Int.* (2007) **169,** 189–200, doi: 10.1111/j.1365-246X.2006.03282.x

SESAME; 2004: Guidelines for the implementation of the H/V spectral ratio technique on ambient vibrations. SESAME, European project, WP12, Deliverable D23.12, http://sesame-fp5.obs.ujfgrenoble.fr/SES TechnicalDoc.htm

Tokimatsu, K. (1997). “Geotechnical Site Characterization using Surface Waves.” *Proceedings, First International Conference on Earthquake Geotechnical Engineering, IS-Tokyo '95*, Tokyo, November 14-16, Balkema, Rotterdam, 1333-1368.

Zhang, S.H., Chan, L.S. and Xia, J. (2004). The selection of field acquisition parameters for dispersion images from multichannel surface wave data. *Pure and Applied Geophysics* 161, 185–201.

APPLICATION OF SURFACE WAVE METHODS

FOR SEISMIC SITE CHARACTERIZATION

STATION CODE:

ARG

Responsible: Stefano Parolai[1]

Co-workers: Rodolfo Puglia[2], Matteo Picozzi[1]

1) Helmholtz Centre Potsdam - German Research Centre For Geosciences (GFZ), Helmholtzstraße 7, 14467 Potsdam, Germany
2) Istituto Nazionale di Geofisica e Vulcanologia (INGV), Sezione di Milano-Pavia, via Bassini 15, 20133 Milano, Italy

Introduction note

Details and references about *in-situ* measurement, Rayleigh wave dispersion and H/V curves estimate and inversion procedure here reported, can be found in the research reports of DPC-INGV S4 Project 2007-2009: Deliverables 6 and 7 at http://esse4.mi.ingv.it .

Testing equipment

The array measurements were performed using 17 EDL 24bit acquisition systems equipped with short-period Mark-L4-C-3D 1Hz sensors and GPS timing (**Figure 1**). However, due to malfunctioning, only the data of 16 stations (depicted as blue squares) could be used for the processing. The inter-station distances in the array ranged between 7.8 m to 151 meters. The stations worked contemporary for about 2 hours, recording noise at 200 s.p.s., which is adequate for the short inter-station distances considered.

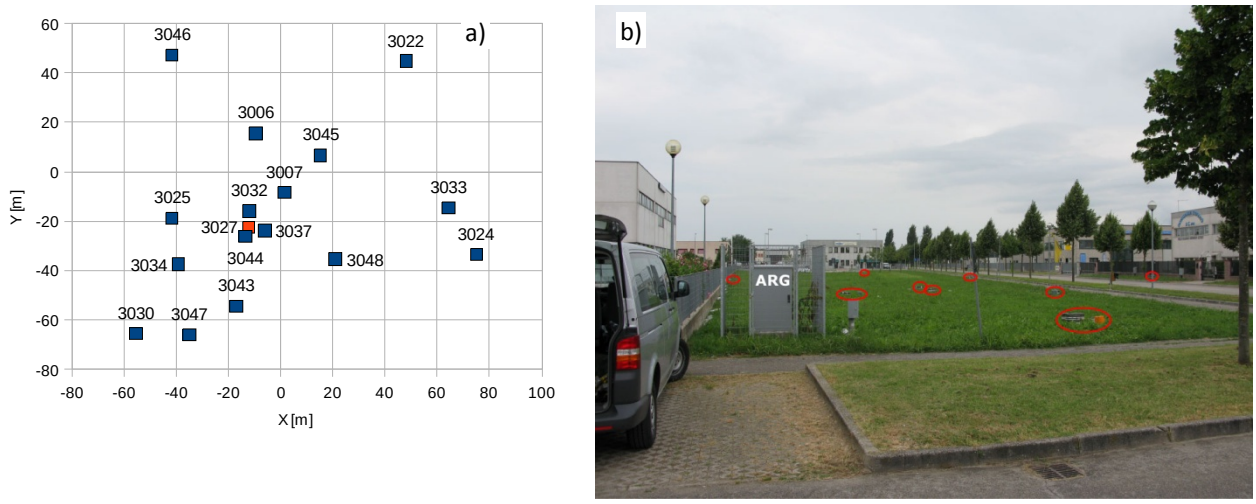

Figure 1: a) Geometry of the array. Stations which had problems are evidenced with the red color: in particular, GPS of 3027 did not work properly. b) The field measurements.

Processing overview

The Rayleigh wave dispersion curve was estimated by analysing the vertical component of the recorded microtremors. In particular, the Extended Spatial Auto Correlation (ESAC) and the Frequency-Wavenumber (f-k) methods were adopted.

Rayleigh wave dispersion and *H/V* ratio curves were both used to estimate the local S-wave velocity profile, using a joint inversion scheme. The non-linear inversions were performed using a genetic algorithm which does not rely upon an explicit starting model and allows the identification of a solution close to the global minimum. The forward modeling of Rayleigh wave phase velocities and *H/V* curves was performed using the modified Thomson-Haskell method, under the assumption of vertically heterogeneous 1D earth models. The validity of this assumption was investigated by computing the *H/V* curve for each station of the array using the recorded data. The modeling of both the dispersion and *H/V* ratio curves during the inversions was not restricted to the fundamental mode only, but the possibility that higher modes can participate to define the observed dispersion and *H/V* curves is allowed.

Data analysis

The first step of the analysis consists in a visual inspection of the recordings at all stations. In particular, in order to identify malfunctioning of one station or channel and to select signal windows suitable for the H/V analysis, the quality of the recording was evaluated analysing (1) the signal stationarity in the time domain (**Figure 2a**), (2) the relevant unfiltered Fourier spectra (**Figure 2b**), and (3) the *H/V* variation over time (**Figure 2a**).

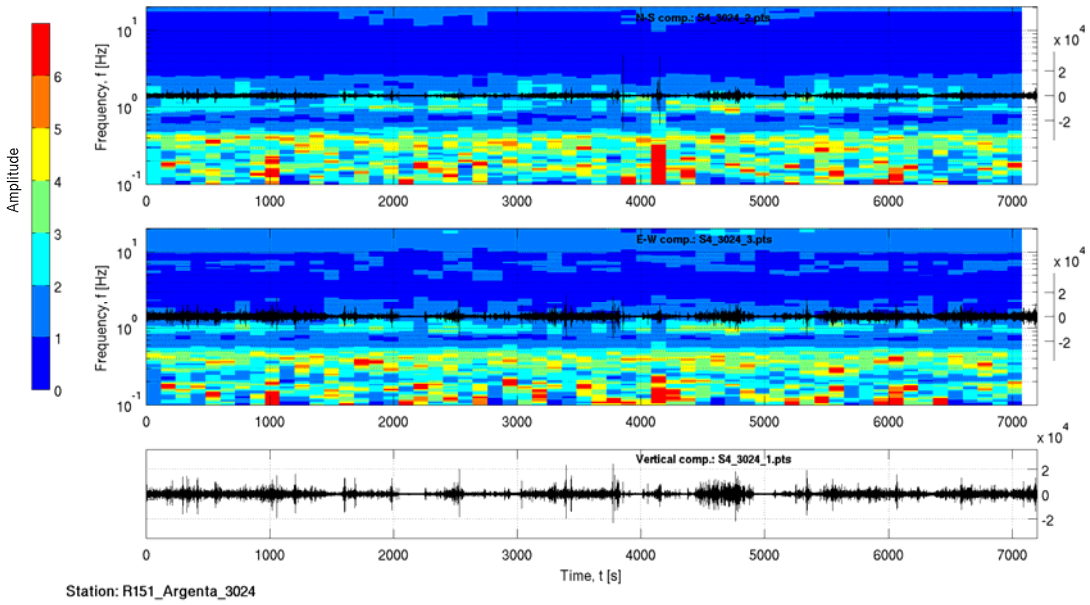

Figure 2a: *H/V* spectral ratios versus time (top and central panel for the NS and EW component, respectively) and corresponding time histories for station 3024.

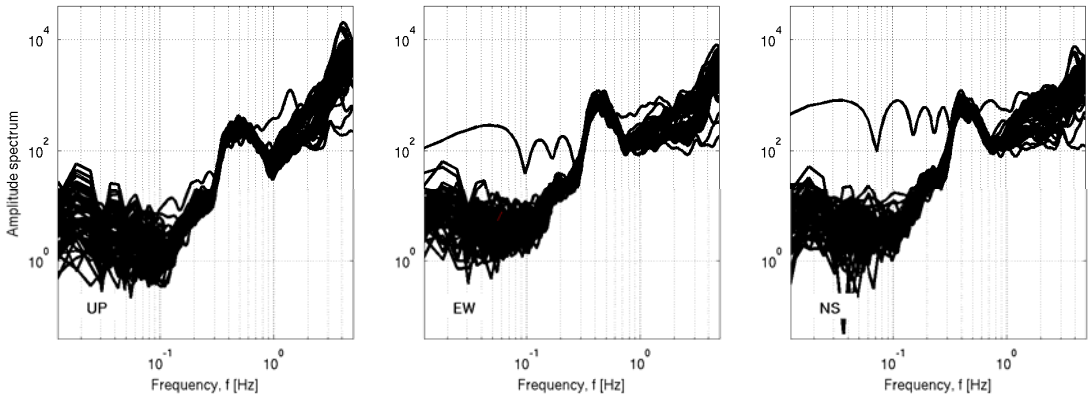

Figure 2b: Fourier spectra for each noise window at station 3024. Left) Vertical component spectra, center) E-W component spectra, right) N-S component spectra.

For each of the 16 used stations, 68 synchronized signal windows of 60 seconds were selected avoiding windows affected by local disturbance. These windows were in turn used to estimate the experimental Rayleigh-wave dispersion curves (using the vertical component only) both by f-k and ESAC analysis.

The ESAC Rayleigh-wave dispersion curve was obtained minimizing the root mean square (RMS) of the differences between experimental and theoretical Bessel function values (**Figure 3**). Values that differ more than two standard deviations from those estimated by the best fitting functions (red circles in **Figure 3**) are automatically discarded and the procedure iteratively repeated. Furthermore, data are discarded also when their inter-station distance is longer than 1.8 times the relevant wavelength.

In the ESAC analysis, only the couples of stations characterized by paths with azimuth between 30° and 120° Nord were used. These paths are strongly contaminated by the industrial noise generated by a waste compactor. On the other hand, the couple of stations characterized by paths within the 120°-210° azimuthal range were discarded in order to avoid data for which a low energy content could furnish a wrong phase velocity estimate. The source of the strong directional noise, coming from about 75° N, is identified in the plot of **Figure 4** (frequency-wavenumber analysis by Maximum Likelihood Method) and **Figure 5** (frequency-wavenumber analysis by Beam Forming) and its location is depicted in **Figure 6**. The industrial noise affected in particular the frequency band between 2 and 5 Hz.

Figure 7 shows the good agreement between the Rayleigh wave dispersion curves estimated both with ESAC and f-k approaches. Only below 2 Hz the f-k analysis provides larger phase velocities.

An average *H/V* for the selected stations was computed by averaging the *H/V* calculated for each signal window (**Figure 8a**). The average *H/V* curves for the selected stations were in turn averaged to obtain a single *H/V* spectral ratio representative for the array, which was then used as input in the joint inversion procedure for the estimation of the S-wave velocity profile (**Figure 8b**).

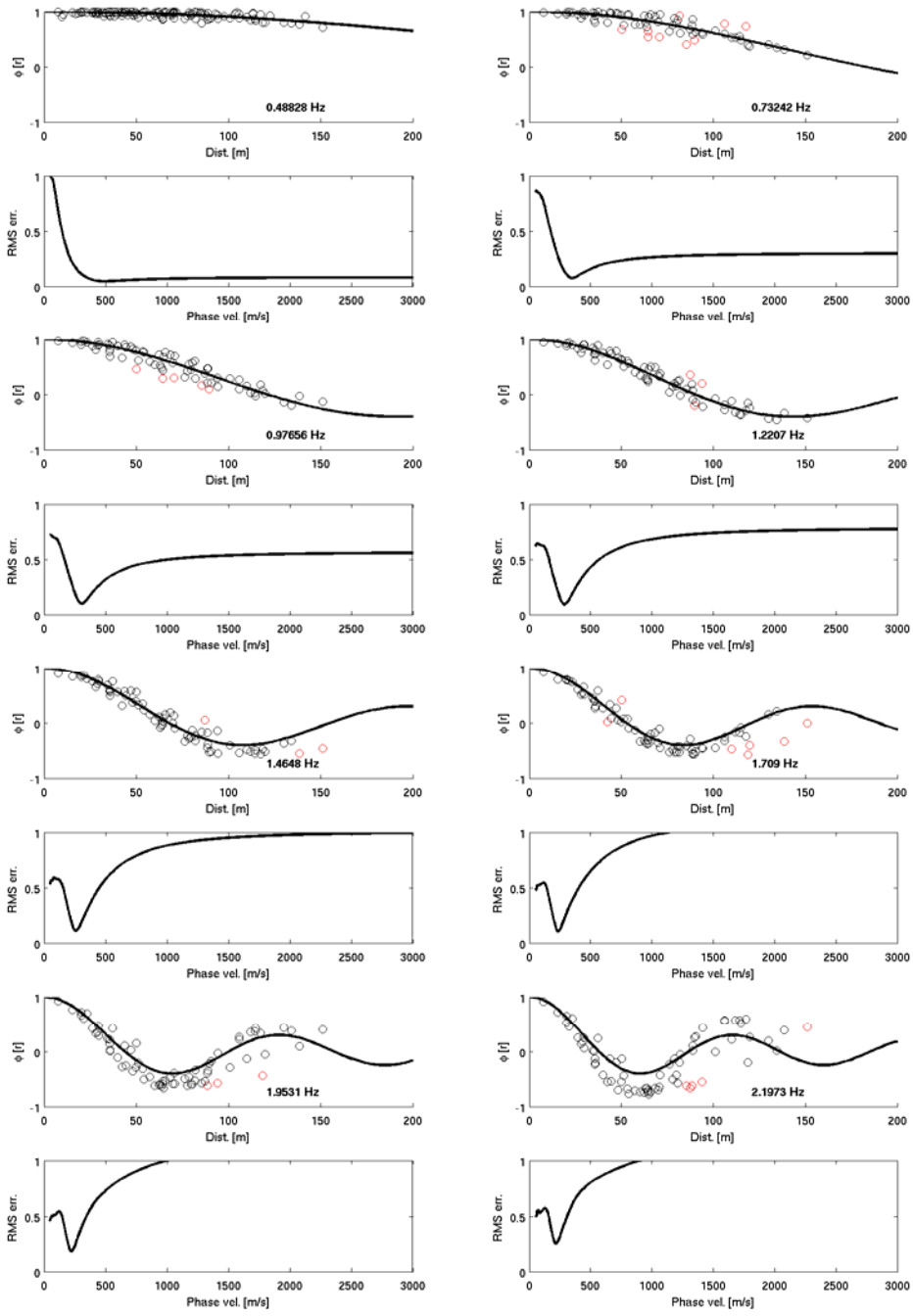

Figure 3: Experimental space-correlation function values versus distance (circles) for different frequencies. The red circles indicate values discarded. The black lines depict the estimated space-correlation function values for the phase velocity showing the best fit to the data. The bottom panels show the relevant root-mean square errors (RMS) versus phase velocity tested.

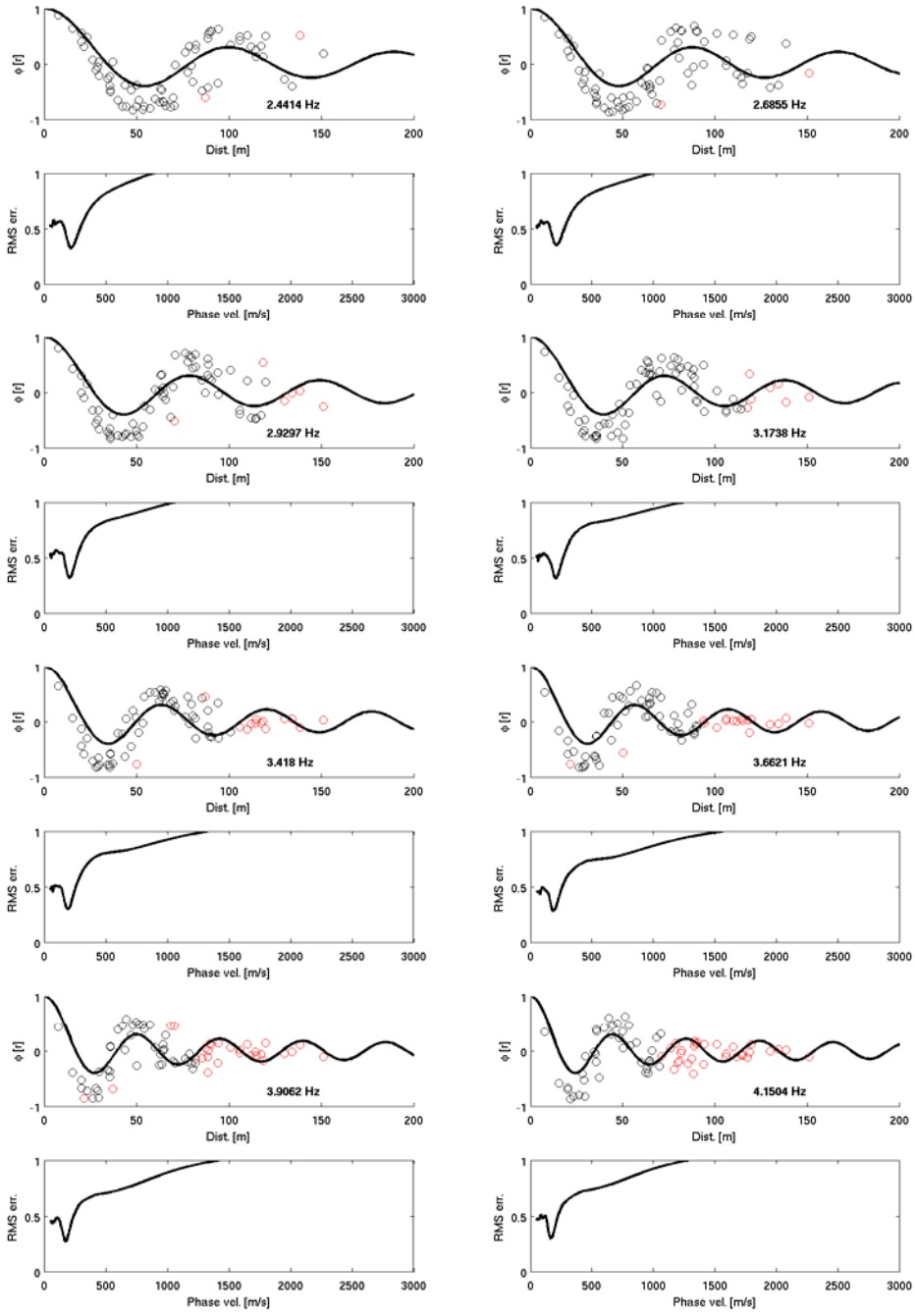

Figure 3: See previous caption.

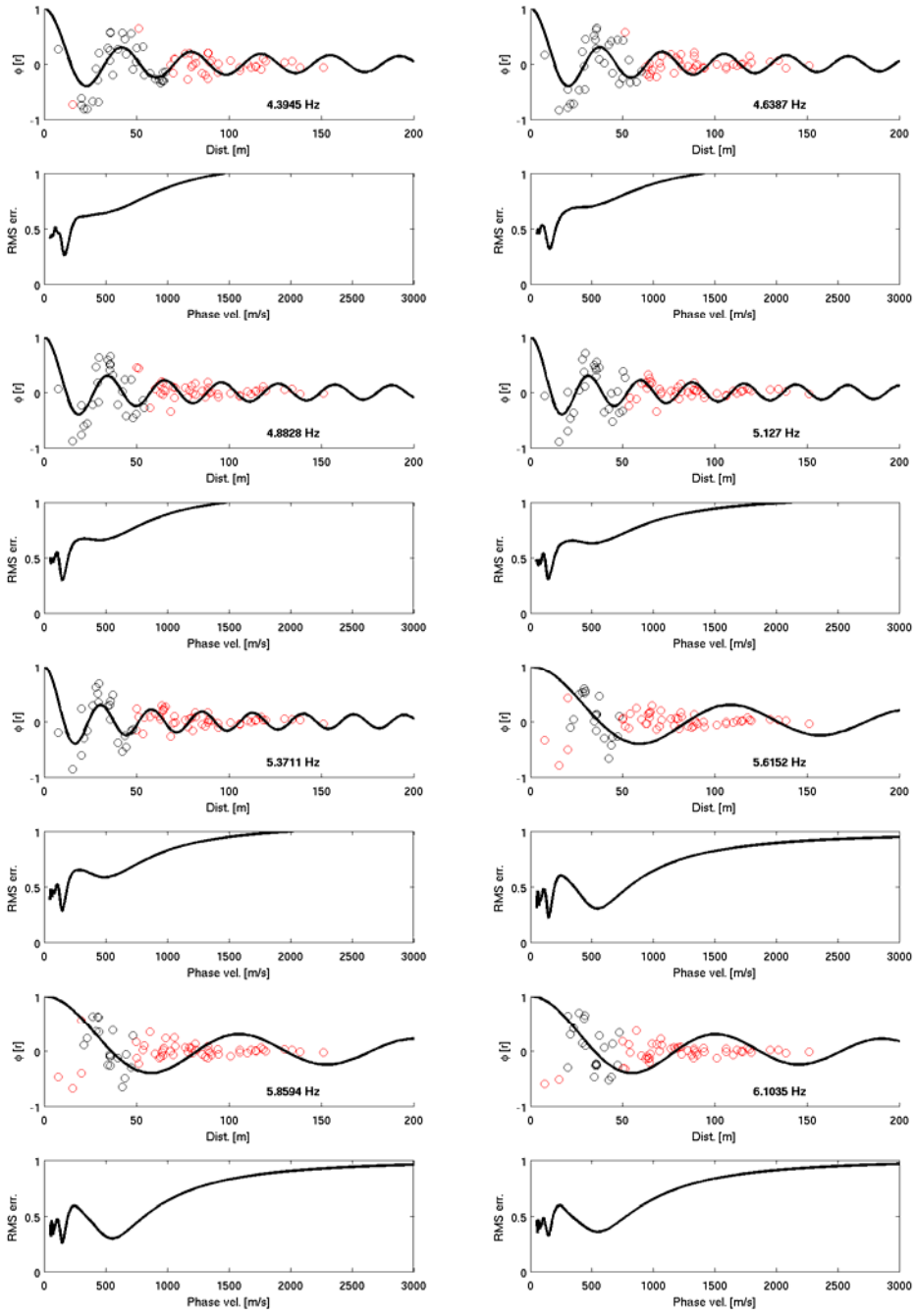

Figure 3: See previous caption.

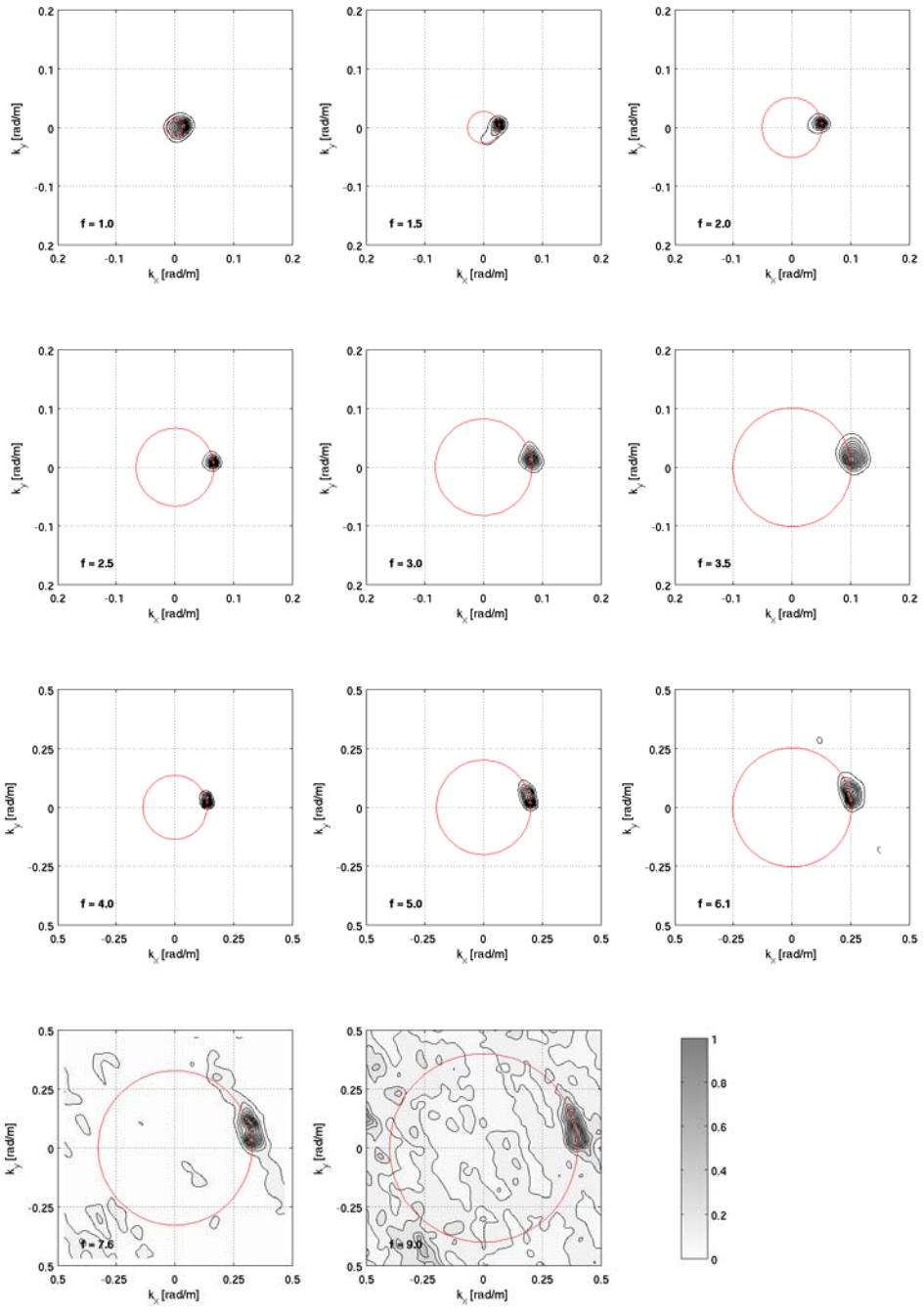

Figure 4: f-k power density function (MLM) at different frequencies (f, expressed in Hz). The red circles joints points with the same *k* value, corresponding to the maximum used to estimate the phase velocity.

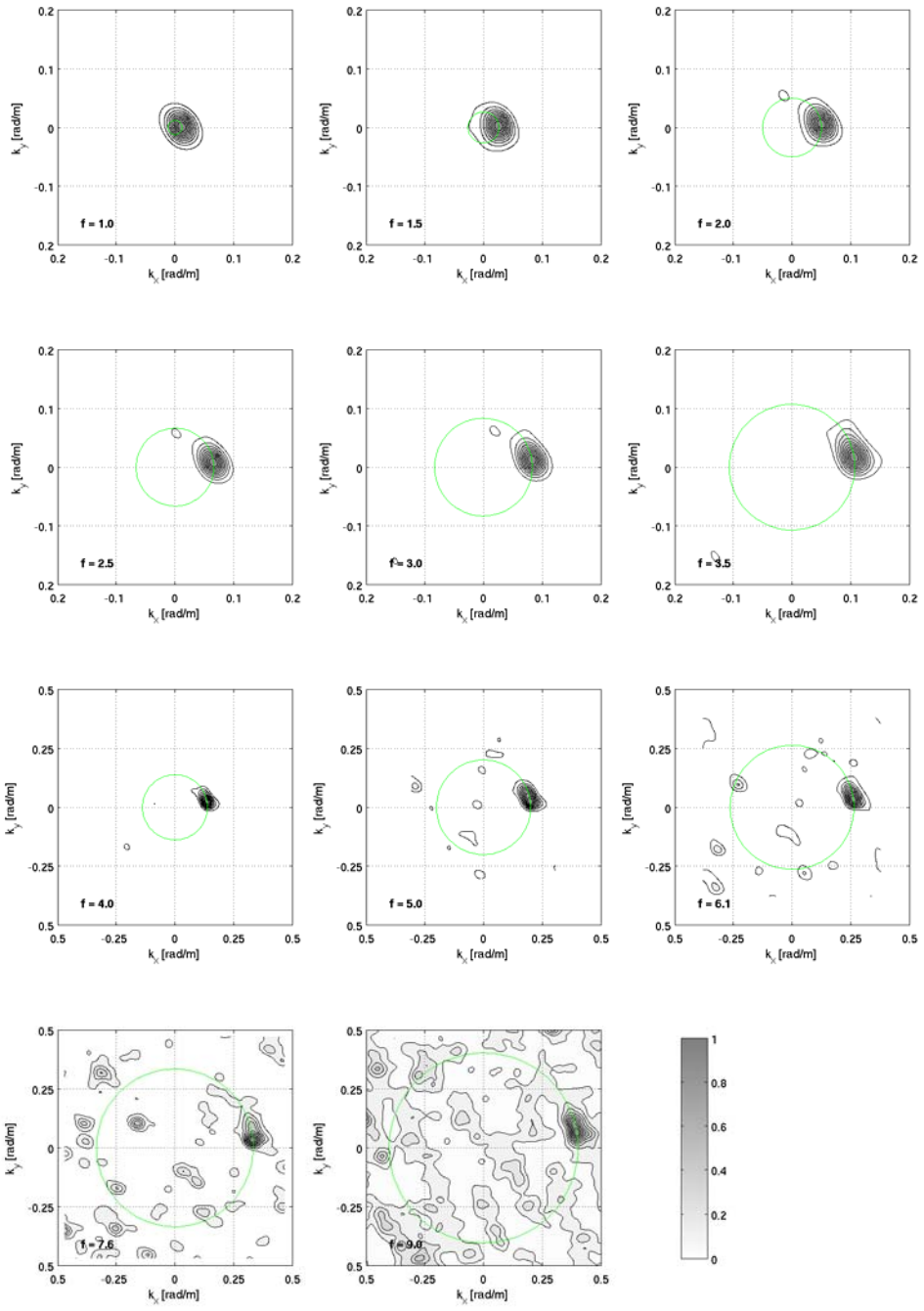

Figure 5: f-k power density function (BF) at different frequencies (f, expressed in Hz). The green circles joints points with the same *k* value, corresponding to the maximum used to estimate the phase velocity.

Figure 6: The industry identified as the source of the persistent noise in the frequency range 2-5 Hz is highlighted by the yellow circle.

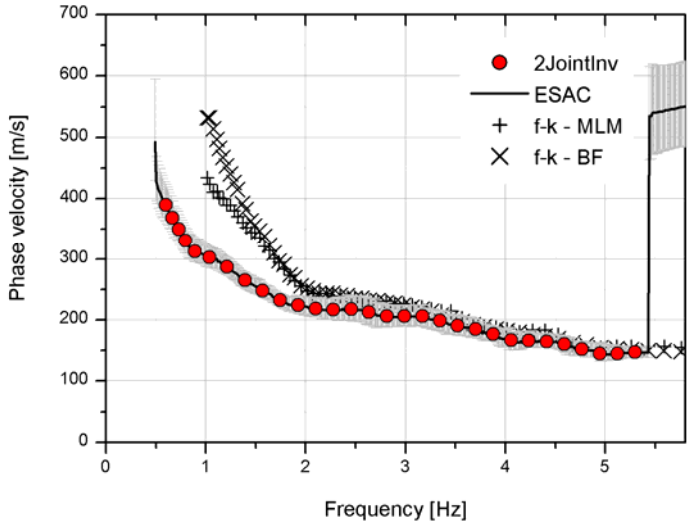

Figure 7: Comparison of experimental phase velocity estimated by the ESAC and the f-k (both for Beam Forming and Maximum Likelihood Method) methods. The red circles represent the values used for the joint inversion. The intervals (grey lines) around the observed ESAC phase velocities representing estimated uncertainties are obtained by calculating the square root of the covariance of the error function.

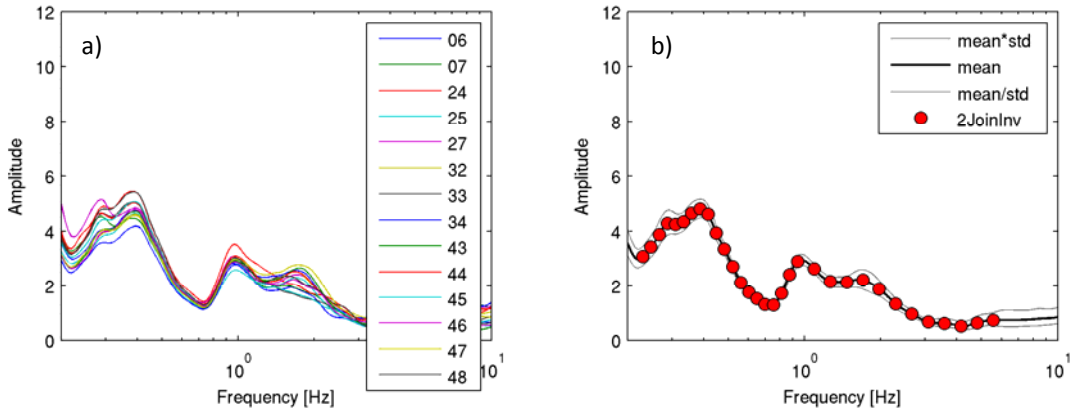

Figure 8: a) average *H/V* for the selected stations of the array (e.g. 06 stands for station 3006, etc.) and b) the average H/V of the array. The red circles represent the values used for the joint inversion.

The inversion of dispersion and *H/V* curves to estimate the S-wave velocity profile was carried out fixing to 8 the number of layers overlying the half-space in the model (**Table 1**). Through a genetic algorithm a search over 80000 models was carried out. The inversion was repeated several times starting from different seed numbers, that is to say from a different population of initial models. In this way it was possible to better explore the space of the solution.

Table 1: Ranges of values defined for the parameters used in the joint inversion.

	Shear wave velocity, V_S [m/s]		Thickness, h [m]		Density, ρ [ton/m^3]
Layer	MIN	MAX	MIN	MAX	
#1	75	300	10	30	1.9
#2	100	400	20	80	1.9
#3	150	450	30	120	2.1
#4	200	500	30	120	2.1
#5	250	550	40	160	2.2
#6	300	750	80	300	2.2
#7	400	850	300	900	2.2
#8	600	1200	100	400	2.2
Half-space	1000	2000	Infinite		2.3

During the inversion procedure the thickness and the shear wave velocity for each layer could be varied within the pre-defined ranges. On the contrary, for each layer, density was assigned *a priori*, while P-wave velocity (V_P) was calculated through the values of the S-wave velocity Vs via the equation: $V_P\,[\mathrm{m/s}] = 1.1 \cdot V_S + 1290$.

The models are selected by means of a cost function which take in account the agreement between the theoretical *H/V* and Rayleigh-wave dispersion curves with the observed ones. In this application, after trial and error test, the weight of 0.05, that allowed the best balanced fit of dispersion and H/V curves, was adopted.

Discussion of the results

In **Figure 9a** all the models tested during the inversion are depicted (gray lines). The best fit model (white line) and the models lying inside the 10% range of the minimum cost (black lines) function are highlighted. The agreement between experimental and theoretical Rayleigh wave dispersion curves (**Figure 9c**) is good and, considering the wavelengths related to the dispersion curve frequency range, the V_S profile between 15 to about 300 metres is likely to be well constrained. Therefore, since below this depth the profile is constrained by the H/V curve alone, we prefer to show, in **Figure 9a** and **Table 2**, the V_S profile only within the depth range were both curves contribute to the inversion.

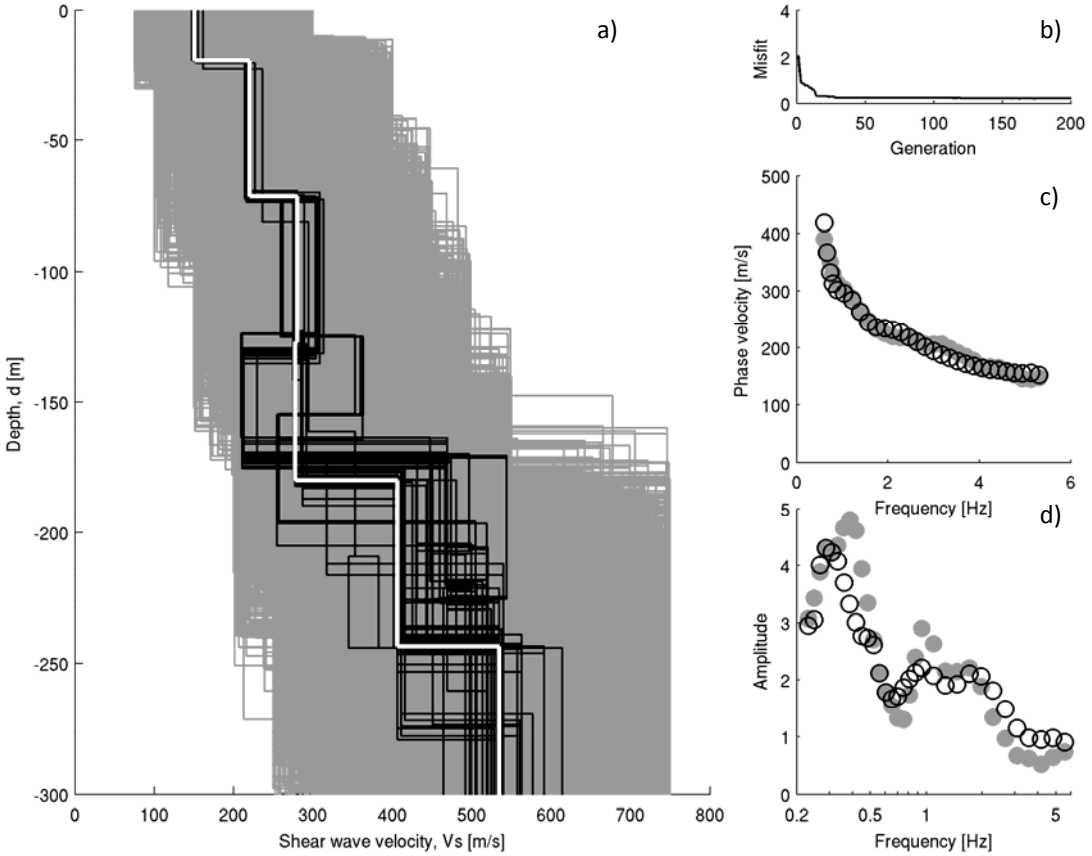

Figure 9: a) Tested models (grey lines), the minimum cost model (white line) and models lying inside the minimum cost + 10% range (black lines) for the ARG station; b) the misfit versus generation values; c) experimental (grey circles) and estimated (white circles – relevant to the minimum cost model) phase velocities; d) experimental (grey circles) and estimated (white circles – relevant to the minimum cost model) *H/V* ratio curves.

Table 2: Shear wave velocity model at the ARG station.

Shear wave velocity, V_S [m/s]	Thickness, h [m]
150.9	19.2
220.0	52.2
280.6	55.5
277.6	52.8
406.5	63.8
534.7	

APPLICATION OF SURFACE WAVE METHODS

FOR SEISMIC SITE CHARACTERIZATION

STATION CODE:

BVG

Responsible: Stefano Parolai[1]

Co-workers: Rodolfo Puglia[2], Matteo Picozzi[1]

1) Helmholtz Centre Potsdam - German Research Centre For Geosciences (GFZ), Helmholtzstraße 7, 14467 Potsdam, Germany
2) Istituto Nazionale di Geofisica e Vulcanologia (INGV), Sezione di Milano-Pavia, via Bassini 15, 20133 Milano, Italy

Introduction note

Details and references about *in-situ* measurement, Rayleigh wave dispersion and H/V curves estimate and inversion procedure here reported, can be found in the research reports of DPC-INGV S4 Project 2007-2009: Deliverables 6 and 7 at http://esse4.mi.ingv.it .

Testing equipment

The array measurements were performed using 15 Reftek 130 acquisition systems equipped with short-period Lennartz LE-3D/5s sensors and GPS timing. The BVG station (**Figure 1a**) was installed on a clayey formation (fluvial sediments in **Figure 1b-c**). The inter-station distances in the array ranged between 9.2 m to 170 meters. The stations worked contemporary for more than 3 hours, recording noise at 500 s.p.s., which is adequate for the short inter-station distances considered.

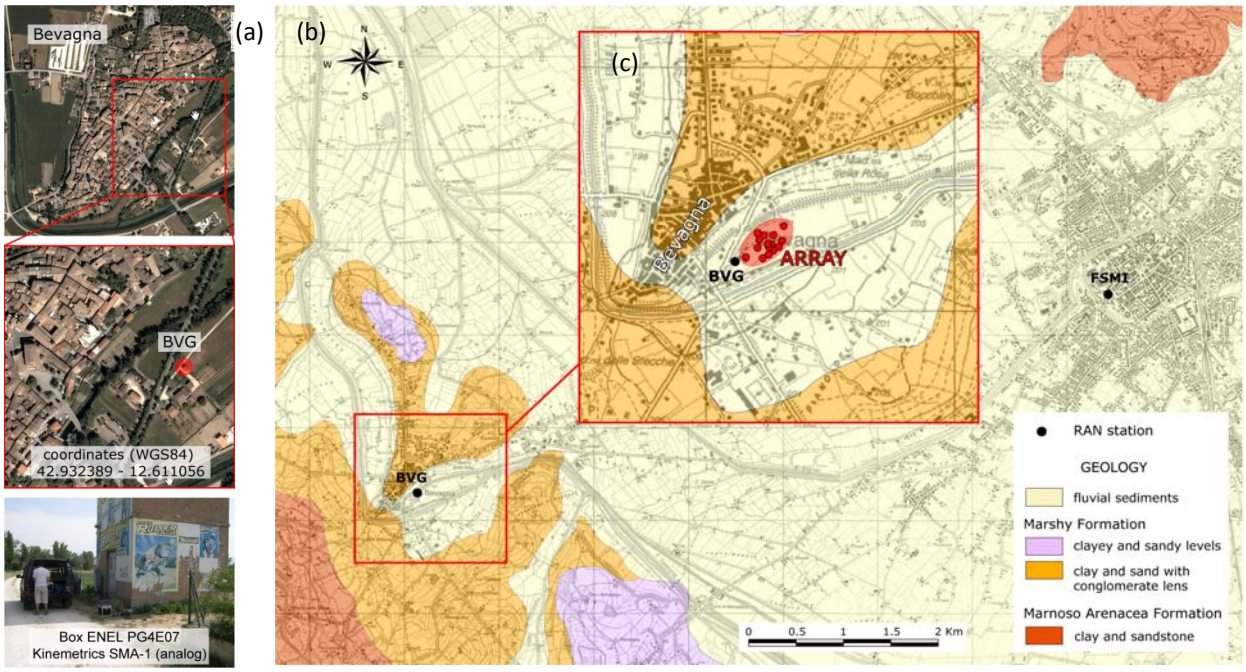

Figure 1: a) Location of the BVG station. b) Geological settings of the study area. c) Relative position between BVG and the array measurements.

Processing overview

The Rayleigh wave dispersion curve was estimated by analysing the vertical component of the recorded microtremors. In particular, the Extended Spatial Auto Correlation (ESAC) and the Frequency-Wavenumber (f-k) methods were adopted.

Rayleigh wave dispersion and *H/V* ratio curves were both used to estimate the local S-wave velocity profile, using a joint inversion scheme. The non-linear inversions were performed using a genetic algorithm which does not rely upon an explicit starting model and allows the identification of a solution close to the global minimum. The forward modeling of Rayleigh wave phase velocities and *H/V* curves was performed using the modified Thomson-Haskell method, under the assumption of vertically heterogeneous 1D earth models. The validity of this assumption was investigated by computing the *H/V* curve for each station of the array using the recorded data. The modeling of both the dispersion and *H/V* ratio curves during the inversions was not restricted to the fundamental mode only, but the possibility that higher modes can participate to define the observed dispersion and *H/V* curves is allowed.

Data analysis

The first step of the analysis consists in a visual inspection of the recordings at all stations. In particular, in order to identify malfunctioning of one station or channel and to select signal windows suitable for the H/V analysis, the quality of the recording was evaluated analysing (1) the signal stationarity in the time domain, (2) the relevant unfiltered Fourier spectra, and (3) the *H/V* variation over time.

For each of the 15 used stations, 46 synchronized signal windows of 60 seconds were selected avoiding windows affected by local disturbance. These windows were in turn used to estimate the experimental Rayleigh-wave dispersion curves (using the vertical component of ground motion only) both by f-k and ESAC analysis.

The ESAC Rayleigh-wave dispersion curve was obtained minimizing the root mean square (RMS) of the differences between experimental and theoretical Bessel function values (**Figure 2**). Values that differ more than two standard deviations from those estimated by the best fitting functions (red circles in **Figure 2**) are automatically discarded and the procedure iteratively repeated. Furthermore, data are discarded also when their inter-station distance is longer than 1.5 times the relevant wavelength.

The f-k analysis offers the opportunity to verify if the requirements on the noise source distribution, necessary for the application of the ESAC method, were fulfilled. **Figure 3a** shows examples of the results for several frequencies of the frequency-wavenumber analysis using the Maximum Likelihood Method (MLM).

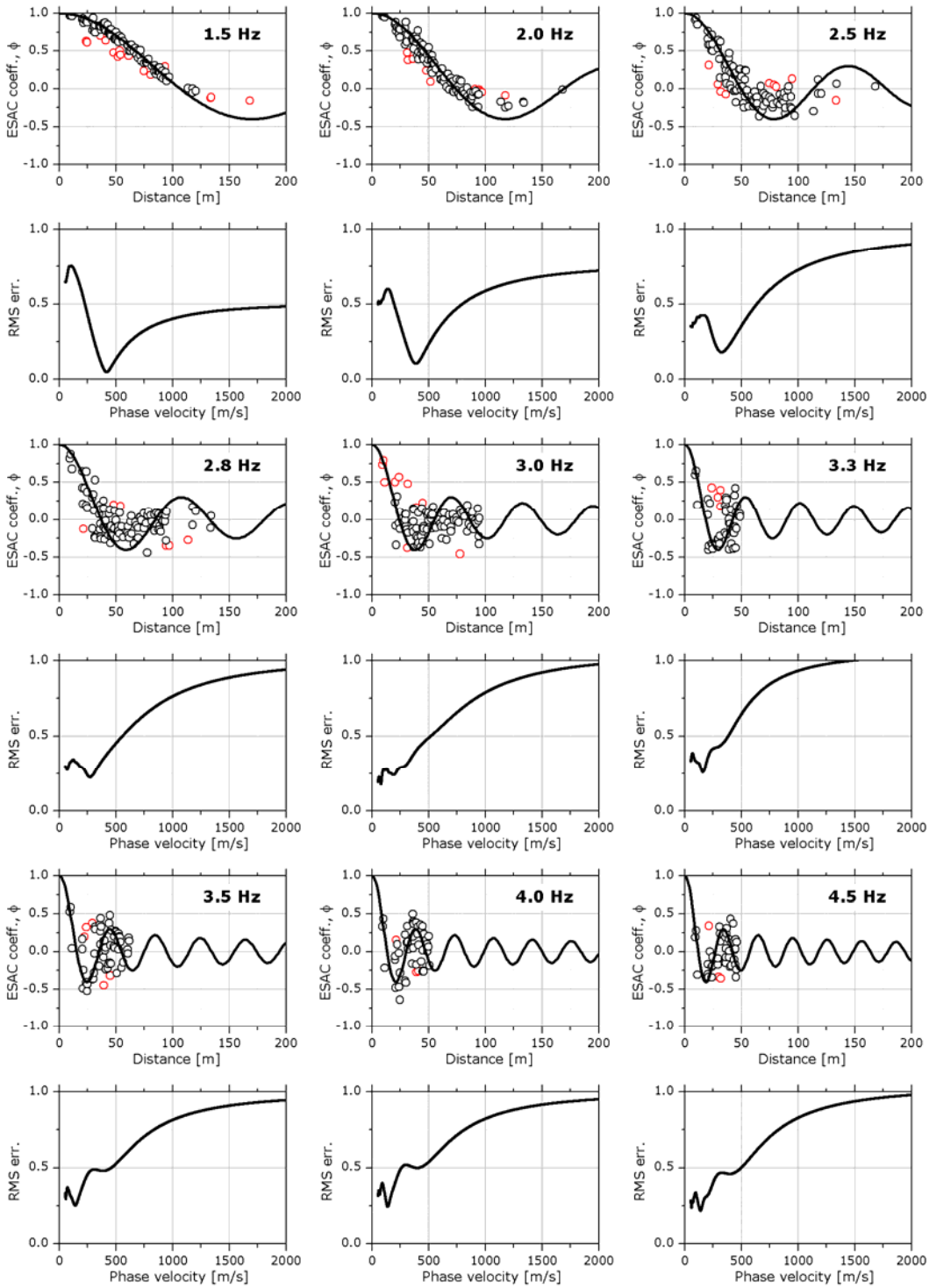

Figure 2: Experimental space-correlation function values versus distance (circles) for different frequencies. The red circles indicate values discarded. The black lines depict the estimated space-correlation function values for the phase velocity showing the best fit to the data. The bottom panels show the relevant root-mean square errors (RMS) versus phase velocity tested.

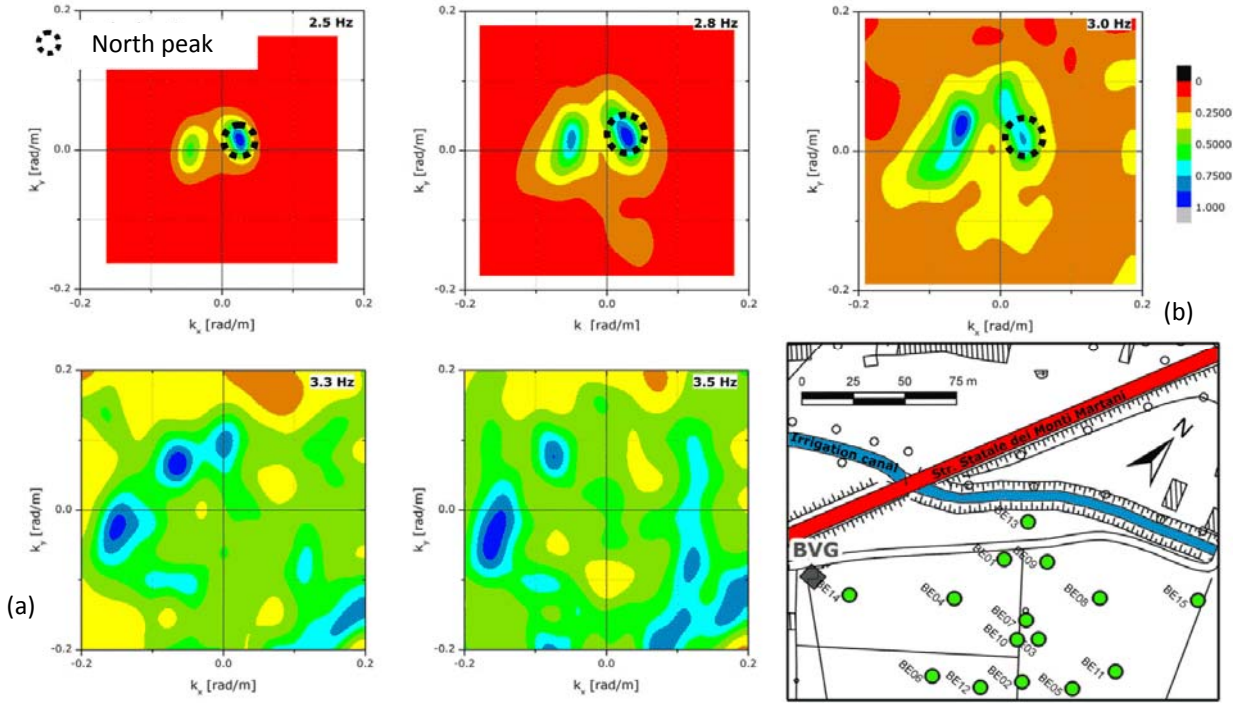

Figure 3: a) f-k power density function (MLM) at different frequencies. b) map showing the geometry of the array measurement. The respective positions of the "Statale dei Monti Martani" street and of an irrigation channel is highlighted.

Figure 4 shows the good agreement between the Rayleigh wave dispersion curves estimated both with ESAC and f-k MLM approaches. Only below 2.5 Hz the f-k analysis provides larger phase velocities.

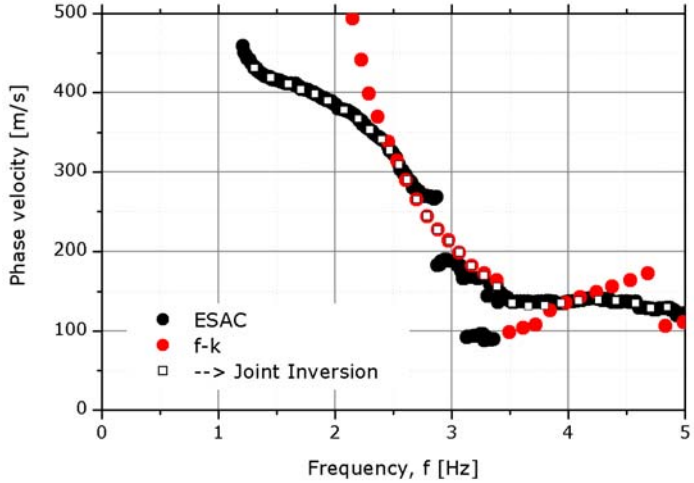

Figure 4: Comparison of experimental phase velocity estimated by the ESAC and the f-k (MLM) approaches. The white squares represent the values used for the joint inversion.

An average *H/V* for the selected stations was computed by averaging the *H/V* calculated for each signal window (**Figure 5**). The average *H/V* curves for the selected stations were in turn averaged to obtain a single *H/V* spectral ratio representative for the array, which was then used as input in the joint inversion procedure for the estimation of the S-wave velocity profile (**Figure 6d**).

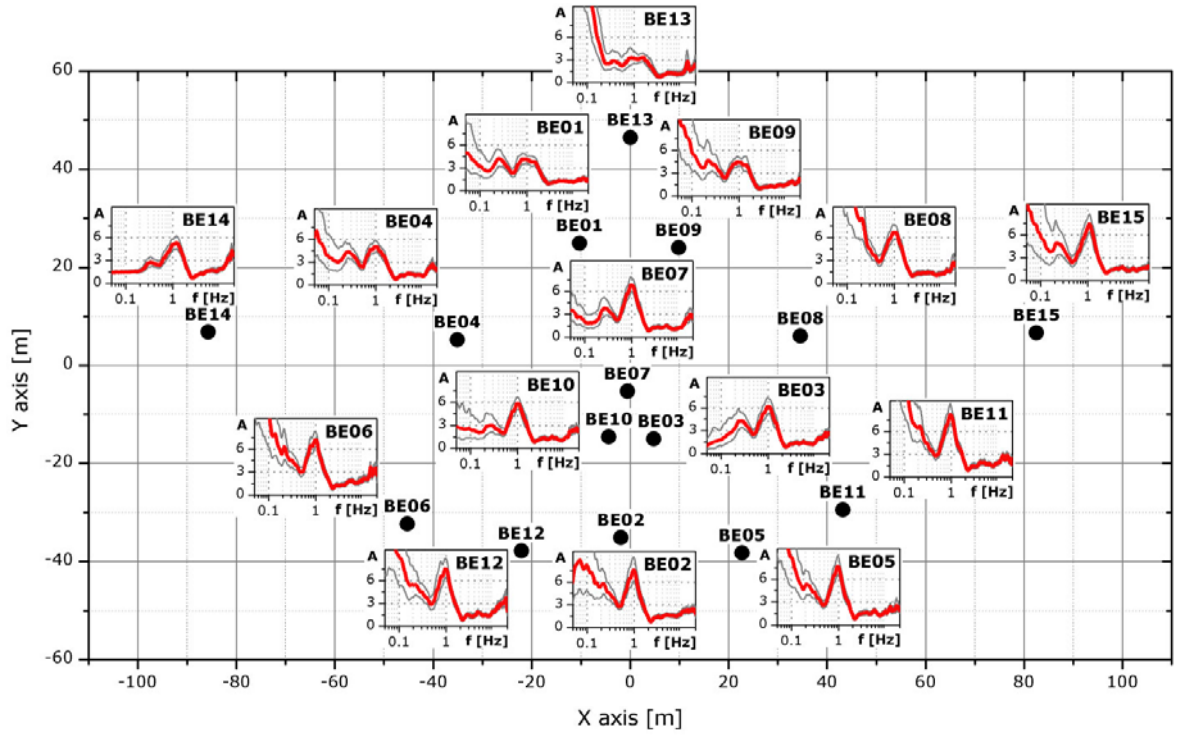

Figure 5: Average *H/V* for each station of the array.

The inversion of dispersion and *H/V* curves to estimate the S-wave velocity profile was carried out fixing to 5 the number of layers overlying the half-space in the model (**Table 1**). Through a genetic algorithm a search over 80000 models was carried out. The inversion was repeated several times starting from different seed numbers, that is to say from a different population of initial models. In this way it was possible to better explore the space of the solution.

Table 1: Ranges of values defined for the parameters used in the joint inversion.

	Shear wave velocity, V_S [m/s]		Thickness, h [m]		Density, ρ [ton/m^3]
Layer	MIN	MAX	MIN	MAX	
#1	100	300	10	30	1.9
#2	200	600	20	80	1.9
#3	300	800	30	120	2.1
#4	400	900	30	120	2.2
#5	500	1200	50	400	2.2
Half-space	600	2500	Infinite		2.3

During the inversion procedure the thickness and the shear wave velocity for each layer could be varied within the pre-defined ranges. On the contrary, for each layer, density was assigned *a priori*, while P-wave velocity (V_P) was calculated through the values of the S-wave velocity Vs via the equation: $V_P\,[\mathrm{m/s}] = 1.1 \cdot V_S + 1290$.

The models are selected by means of a cost function which take in account the agreement between the theoretical *H/V* and Rayleigh-wave dispersion curves with the observed ones. In this application, after trial and error test, the weight of 0.05, that allowed the best balanced fit of dispersion and H/V curves, was adopted.

Discussion of the results

In **Figure 6a** all the models tested during the inversion are depicted (gray lines). The best fit model (white line) and the models lying inside the 10% range of the minimum cost (black lines) function are highlighted. The agreement between experimental and theoretical Rayleigh wave dispersion curves (**Figure 6c**) is good and, considering the wavelengths related to the dispersion curve frequency range, the V_S profile between 10 to about 120 metres is likely to be well constrained. Therefore, since below this depth the profile is constrained by the H/V curve alone, we prefer to show, in **Figure 6a** and **Table 2**, the V_S profile only within the depth range were both curves contribute to the inversion.

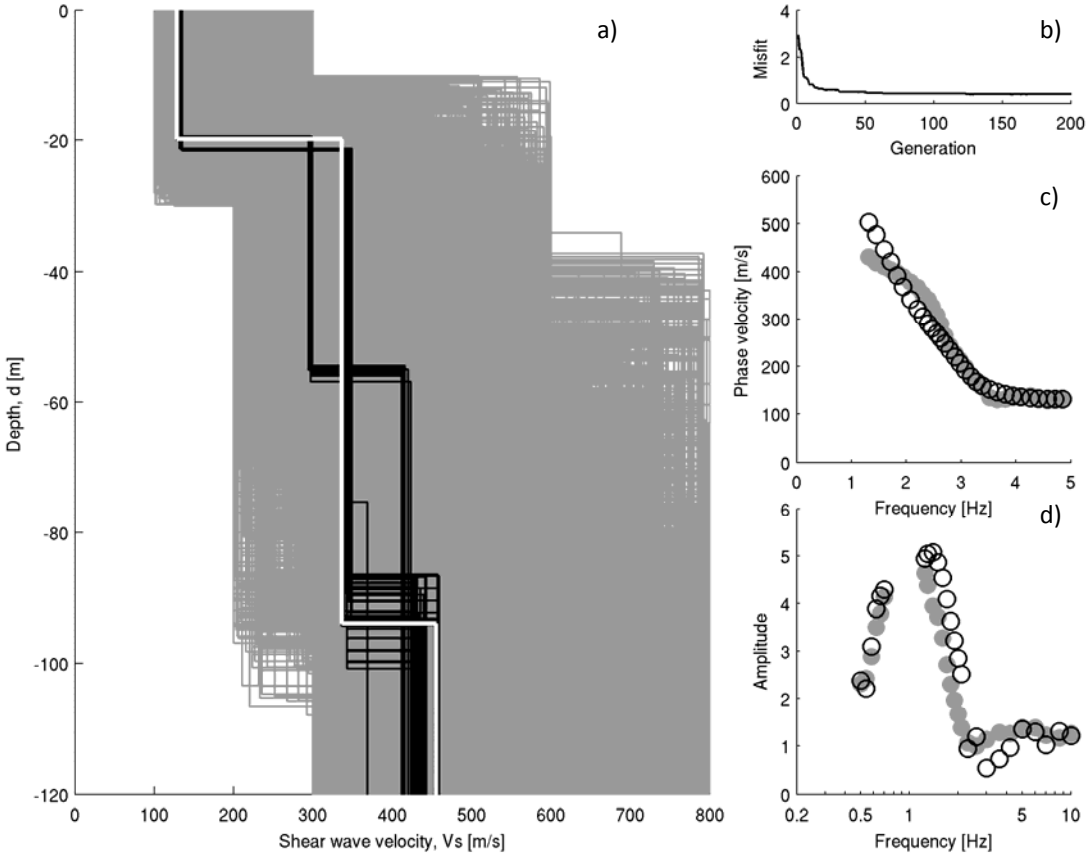

Figure 6: a) Tested models (grey lines), the minimum cost model (white line) and models lying inside the minimum cost + 10% range (black lines) for the BVG station; b) the misfit versus generation values; c) experimental (grey circles) and estimated (white circles – relevant to the minimum cost model) phase velocities; d) experimental (grey circles) and estimated (white circles – relevant to the minimum cost model) *H/V* ratio curves.

Table 2: Shear wave velocity model at the BVG station.

Shear wave velocity, V_S [m/s]	Thickness, h [m]
128	19.8
336	74.1
455	

APPLICATION OF SURFACE WAVE METHODS

FOR SEISMIC SITE CHARACTERIZATION

STATION CODE:

BZZ

Responsible: Stefano Parolai[1]

Co-workers: Rodolfo Puglia[2], Matteo Picozzi[1]

1) Helmholtz Centre Potsdam - German Research Centre For Geosciences (GFZ), Helmholtzstraße 7, 14467 Potsdam, Germany
2) Istituto Nazionale di Geofisica e Vulcanologia (INGV), Sezione di Milano-Pavia, via Bassini 15, 20133 Milano, Italy

Introduction note

Details and references about *in-situ* measurement, Rayleigh wave dispersion and H/V curves estimate and inversion procedure here reported, can be found in the research reports of DPC-INGV S4 Project 2007-2009: Deliverables 6 and 7 at http://esse4.mi.ingv.it .

Testing equipment

The array measurements were performed using 17 EDL 24bit acquisition systems equipped with short-period Mark-L4-C-3D 1Hz sensors and GPS timing. The stations worked contemporary for about 2 hour, recording noise at 200 s.p.s., which is adequate for the short inter-station distances considered.

Processing overview

The Rayleigh wave dispersion curve was estimated by analysing the vertical component of the recorded microtremors. In particular, the Extended Spatial Auto Correlation (ESAC) and the Frequency-Wavenumber (f-k) methods were adopted.

Only Rayleigh wave dispersion curve were used to estimate the local S-wave velocity profile. The non-linear inversions were performed using a genetic algorithm which does not rely upon an explicit starting model and allows the identification of a solution close to the global minimum. The forward modeling of Rayleigh wave phase velocities curve was performed using the modified Thomson-Haskell method, under the assumption of vertically heterogeneous 1D earth models. The validity of this assumption was investigated by computing the *H/V* curve for each station of the array using the recorded data. The *H/V* curves were not used in the inversion analysis due to their flat appearance. The modeling of the dispersion curve during the inversions was not restricted to the fundamental mode only, but the possibility that higher modes can participate to define the observed dispersion curve is allowed.

Data analysis

For each of the 17 used stations, more than 60 synchronized signal windows of 60 seconds were selected avoiding windows affected by local disturbance. These windows were used to estimate the experimental Rayleigh-wave dispersion curves by the ESAC analysis using the vertical component of ground motion only.

The ESAC Rayleigh-wave dispersion curve was obtained minimizing the root mean square (RMS) of the differences between experimental and theoretical Bessel function values (**Figure 1b**). Values that differ

more than two standard deviations from those estimated by the best fitting functions were discarded and the procedure iteratively repeated.

The inversion of dispersion curve to estimate the S-wave velocity profile was carried out through a genetic algorithm. The inversion was repeated several times starting from different seed numbers, that is to say from a different population of initial models. In this way it was possible to better explore the space of the solution.

During the inversion procedure the thickness and the shear wave velocity for each layer could be varied within pre-defined ranges. On the contrary, for each layer, density was assigned *a priori*, while P-wave velocity (V_P) was calculated through the values of the S-wave velocity Vs via the equation: $V_P\,[\mathrm{m/s}] = 1.1 \cdot V_S + 1290$.

Discussion of the results

In **Figure 1a** all the models tested during the inversion are depicted (grey lines). The best fit model (black line) and the models lying inside the 10% range of the minimum cost (dark-grey lines) function are highlighted. The agreement between experimental and theoretical Rayleigh wave dispersion curves (**Figure 1b**) is good and, considering the wavelengths related to the dispersion curve frequency range, the V_S profile between 20 to about 150 metres is likely to be well constrained. Therefore, we prefer to show, in **Figure 1a** and **Table 1**, the V_S profile only within this depth range.

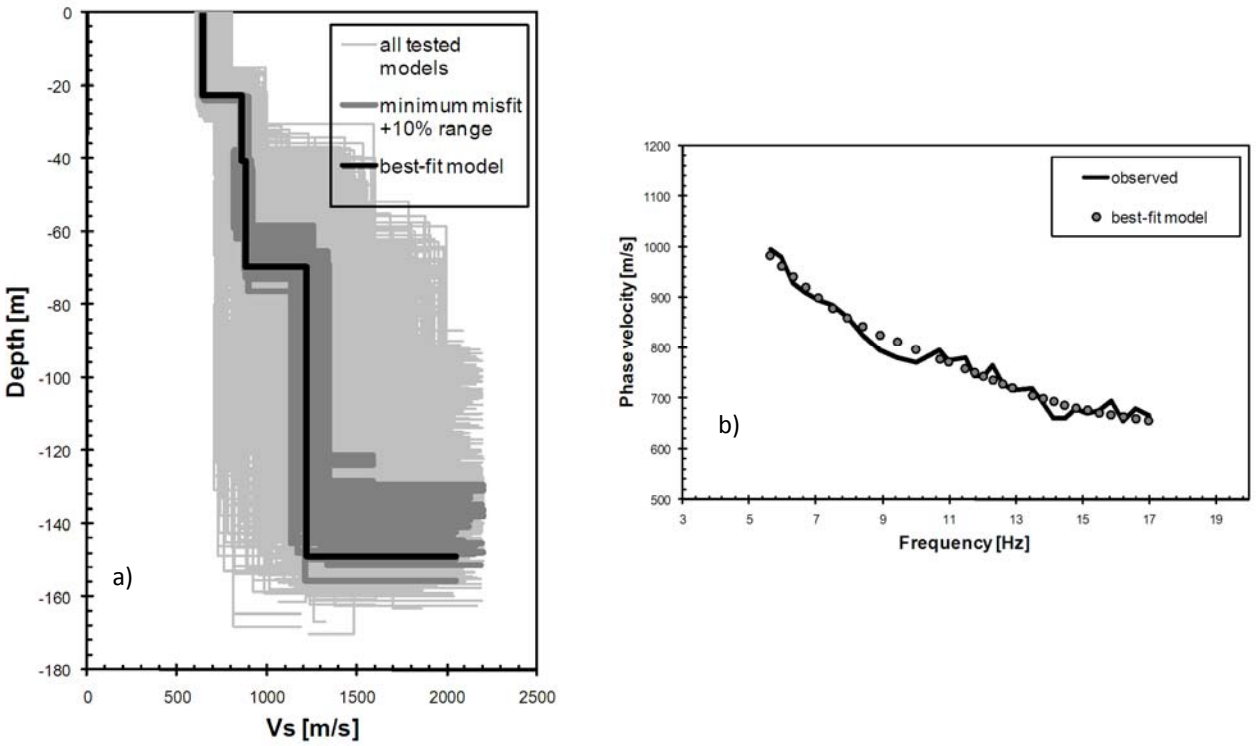

Figure 1: a) Tested models (grey lines), the minimum cost model (black line) and models lying inside the minimum cost + 10% range (dark grey lines) for the BZZ station; b) experimental (black line) and estimated (grey circles – relevant to the minimum cost model) phase velocities.

Table 1: Shear wave velocity model at the BZZ station.

Shear wave velocity, V_S [m/s]	Thickness, h [m]
640	23
850	18
880	29
1210	79
2050	

APPLICATION OF SURFACE WAVE METHODS

FOR SEISMIC SITE CHARACTERIZATION

STATION CODE:

CTL

Responsible: Stefano Parolai[1]

Co-workers: Rodolfo Puglia[2], Matteo Picozzi[1]

1) Helmholtz Centre Potsdam - German Research Centre For Geosciences (GFZ), Helmholtzstraße 7, 14467 Potsdam, Germany
2) Istituto Nazionale di Geofisica e Vulcanologia (INGV), Sezione di Milano-Pavia, via Bassini 15, 20133 Milano, Italy

Introduction note

Details and references about *in-situ* measurement, Rayleigh wave dispersion and H/V curves estimate and inversion procedure here reported, can be found in the research reports of DPC-INGV S4 Project 2007-2009: Deliverables 6 and 7 at http://esse4.mi.ingv.it .

Testing equipment

The array measurements were performed using 17 EDL 24bit acquisition systems equipped with short-period Mark-L4-C-3D 1Hz sensors and GPS timing (**Figure 1**). However, due to malfunctioning, only the data of 14 stations (depicted as blue squares) could be used for the processing. The inter-station distances in the array ranged between 5.4 m to 115 meters. The stations worked contemporary for about 2 hours, recording noise at 200 s.p.s., which is adequate for the short inter-station distances considered.

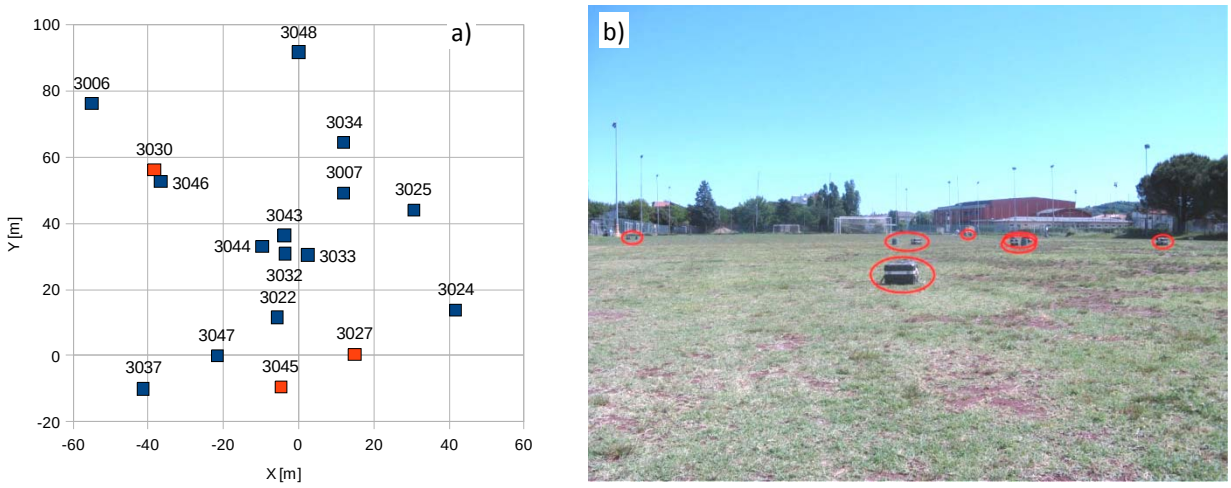

Figure 1: a) Geometry of the array. Stations that did not work properly are evidenced with the red color. b) Stations in the field.

Processing overview

The Rayleigh wave dispersion curve was estimated by analysing the vertical component of the recorded microtremors. In particular, the Extended Spatial Auto Correlation (ESAC) and the Frequency-Wavenumber (f-k) methods were adopted.

Rayleigh wave dispersion and *H/V* ratio curves were both used to estimate the local S-wave velocity profile, using a joint inversion scheme. The non-linear inversions were performed using a genetic algorithm which does not rely upon an explicit starting model and allows the identification of a solution close to the global minimum. The forward modeling of Rayleigh wave phase velocities and *H/V* curves was performed using the modified Thomson-Haskell method, under the assumption of vertically heterogeneous 1D earth models. The validity of this assumption was investigated by computing the *H/V* curve for each station of the array using the recorded data. The modeling of both the dispersion and *H/V* ratio curves during the inversions was not restricted to the fundamental mode only, but the possibility that higher modes can participate to define the observed dispersion and *H/V* curves is allowed.

Data analysis

The first step of the analysis consists in a visual inspection of the recordings at all stations. In particular, in order to identify malfunctioning of one station or channel and to select signal windows suitable for the H/V analysis, the quality of the recording was evaluated analysing (1) the signal stationarity in the time domain (**Figure 2a**), (2) the relevant unfiltered Fourier spectra (**Figure 2b**), and (3) the *H/V* variation over time (**Figure 2a**).

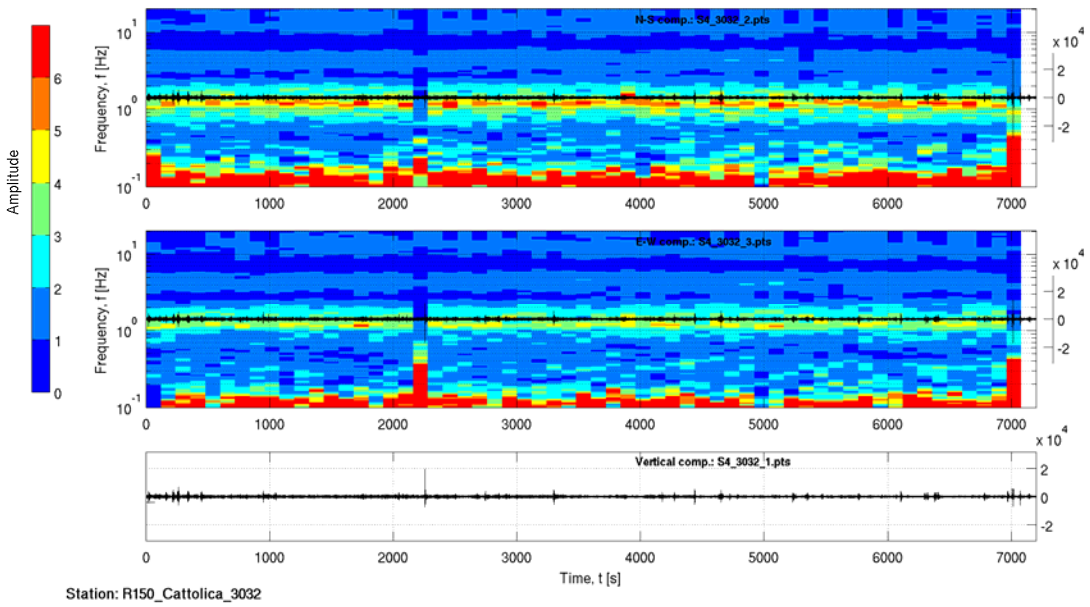

Figure 2a: *H/V* spectral ratios versus time (top and central panel for the NS and EW component, respectively) and corresponding time histories for station 3032.

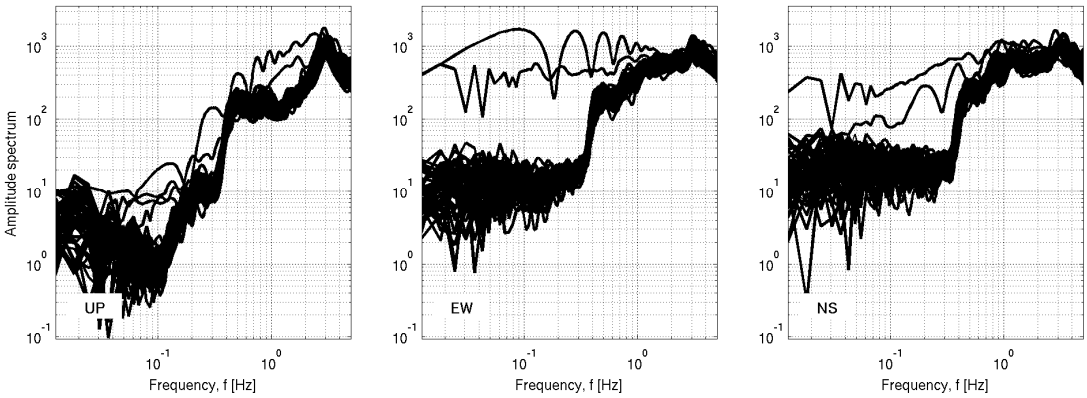

Figure 2b: Fourier spectra for each noise window at station 3032. Left) Vertical component spectra, center) E-W component spectra, right) N-S component spectra.

For each of the 14 used stations, 44 synchronized signal windows of 60 seconds were selected avoiding windows affected by local disturbance. These windows were in turn used to estimate the experimental Rayleigh-wave dispersion curves (using the vertical component of ground motion only) both by f-k and ESAC analysis.

The ESAC Rayleigh-wave dispersion curve was obtained minimizing the root mean square (RMS) of the differences between experimental and theoretical Bessel function values (**Figure 3**). Values that differ more than two standard deviations from those estimated by the best fitting functions (red circles in **Figure 3**) are automatically discarded and the procedure iteratively repeated. Furthermore, data are discarded also when their inter-station distance is longer than the relevant wavelength.

The f-k analysis offers the opportunity to verify if the requirements on the noise source distribution, necessary for the application of the ESAC method, were fulfilled. **Figure 4** and **Figure 5** show examples of the results for several frequencies of the frequency-wavenumber analysis using the Maximum Likelihood Method (MLM) and the Beam Forming (BF) respectively.

Figure 6 shows the good agreement between the Rayleigh wave dispersion curves estimated both with ESAC and f-k approaches. Only below 3 Hz the f-k analysis provides larger phase velocities.

An average *H/V* for the selected stations was computed by averaging the *H/V* calculated for each signal window (**Figure 7a**). The average *H/V* curves for the selected stations were in turn averaged to obtain a single *H/V* spectral ratio representative for the array, which was then used as input in the joint inversion procedure for the estimation of the S-wave velocity profile (**Figure 7b**).

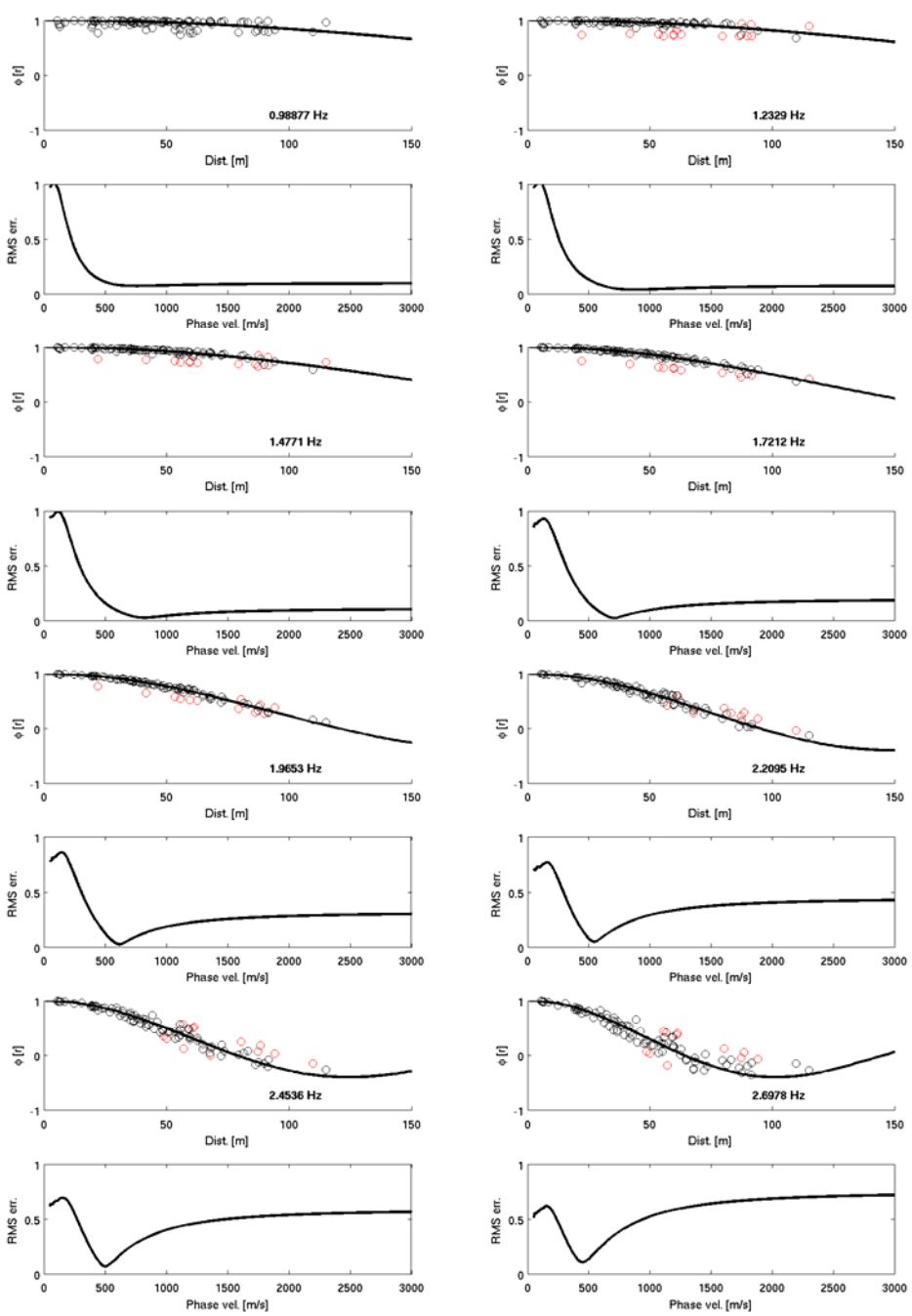

Figure 3: Experimental space-correlation function values versus distance (circles) for different frequencies. The red circles indicate values discarded. The black lines depict the estimated space-correlation function values for the phase velocity showing the best fit to the data. The bottom panels show the relevant root-mean square errors (RMS) versus phase velocity tested.

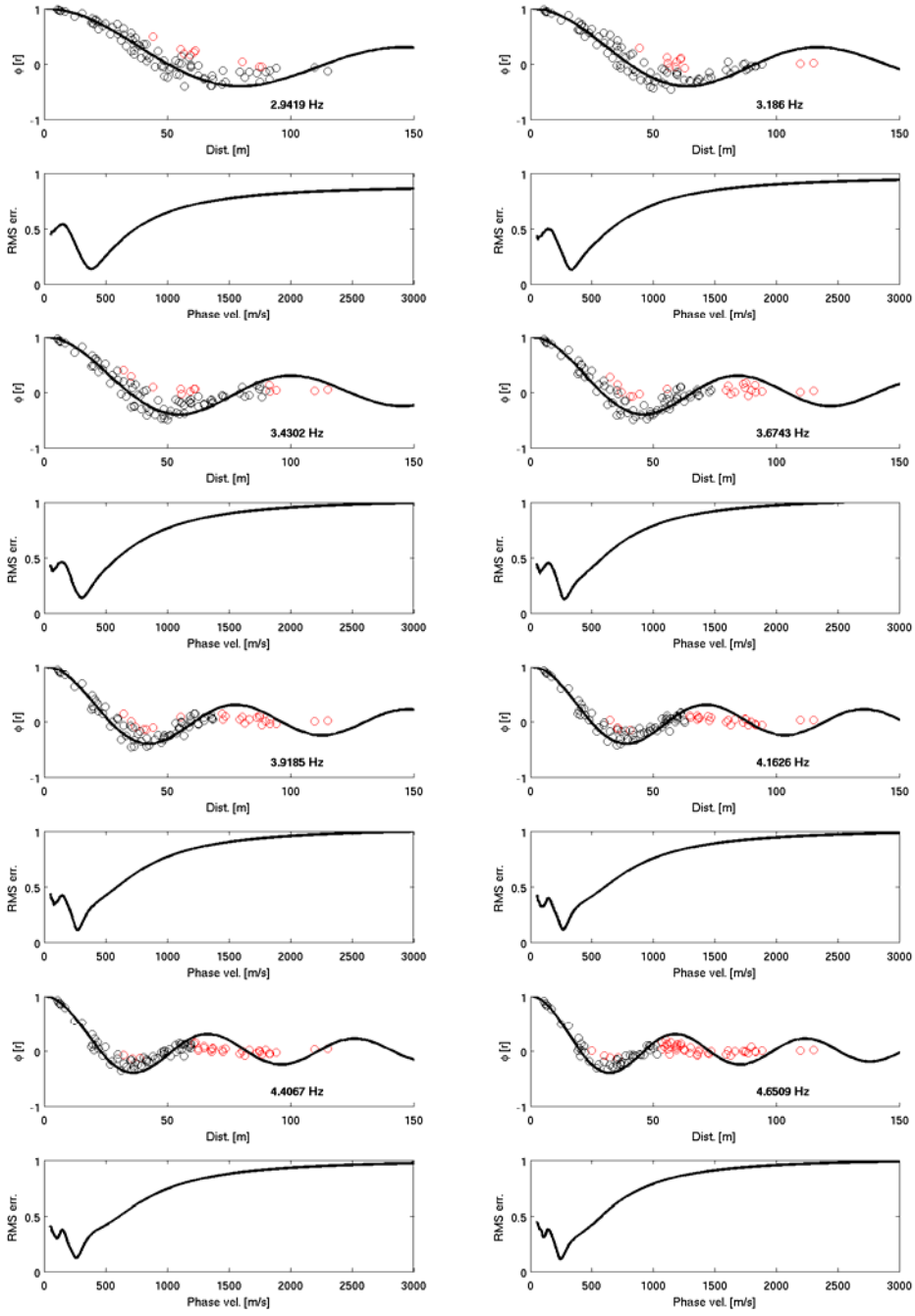

Figure 3: See previous caption.

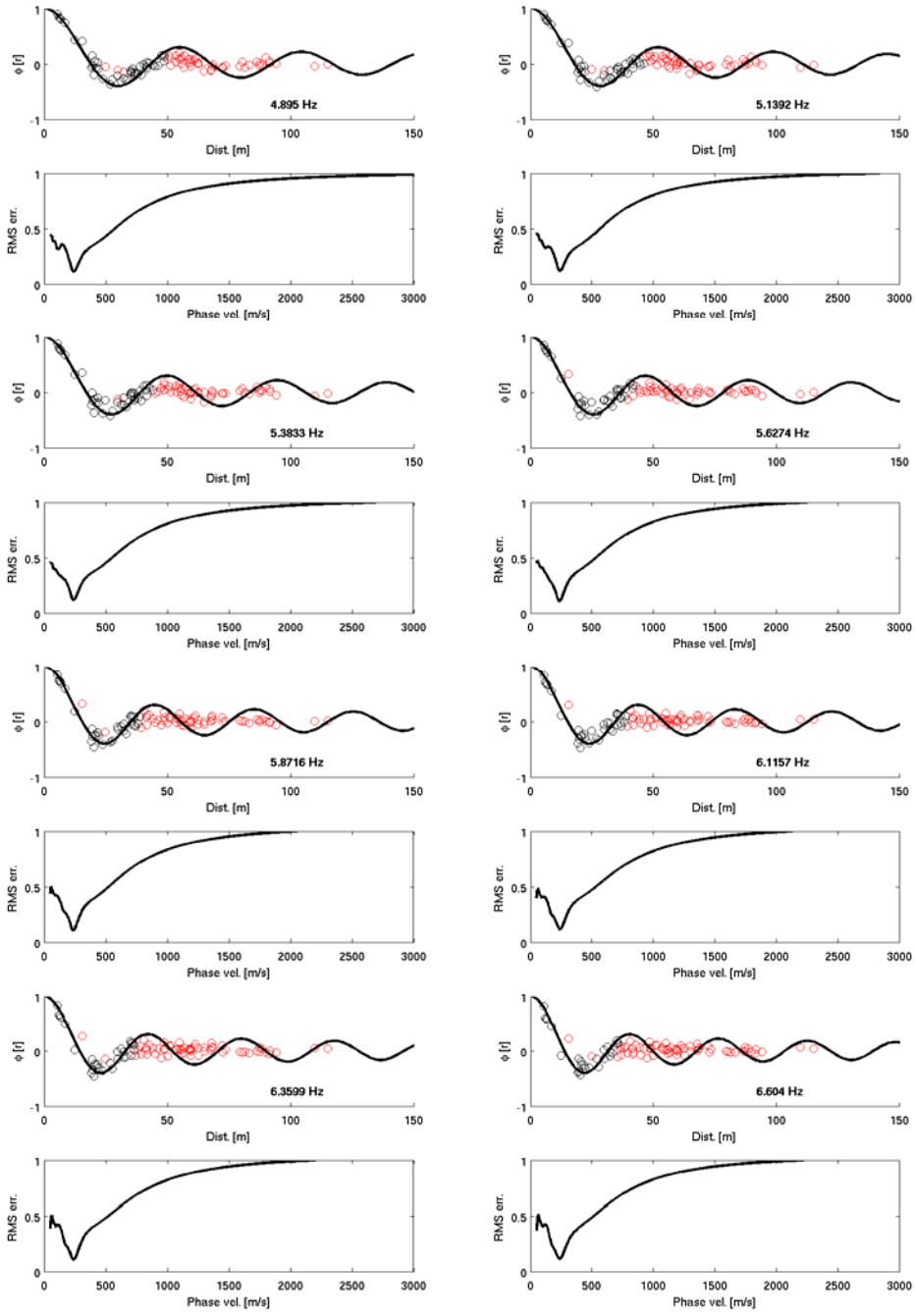

Figure 3: See previous caption.

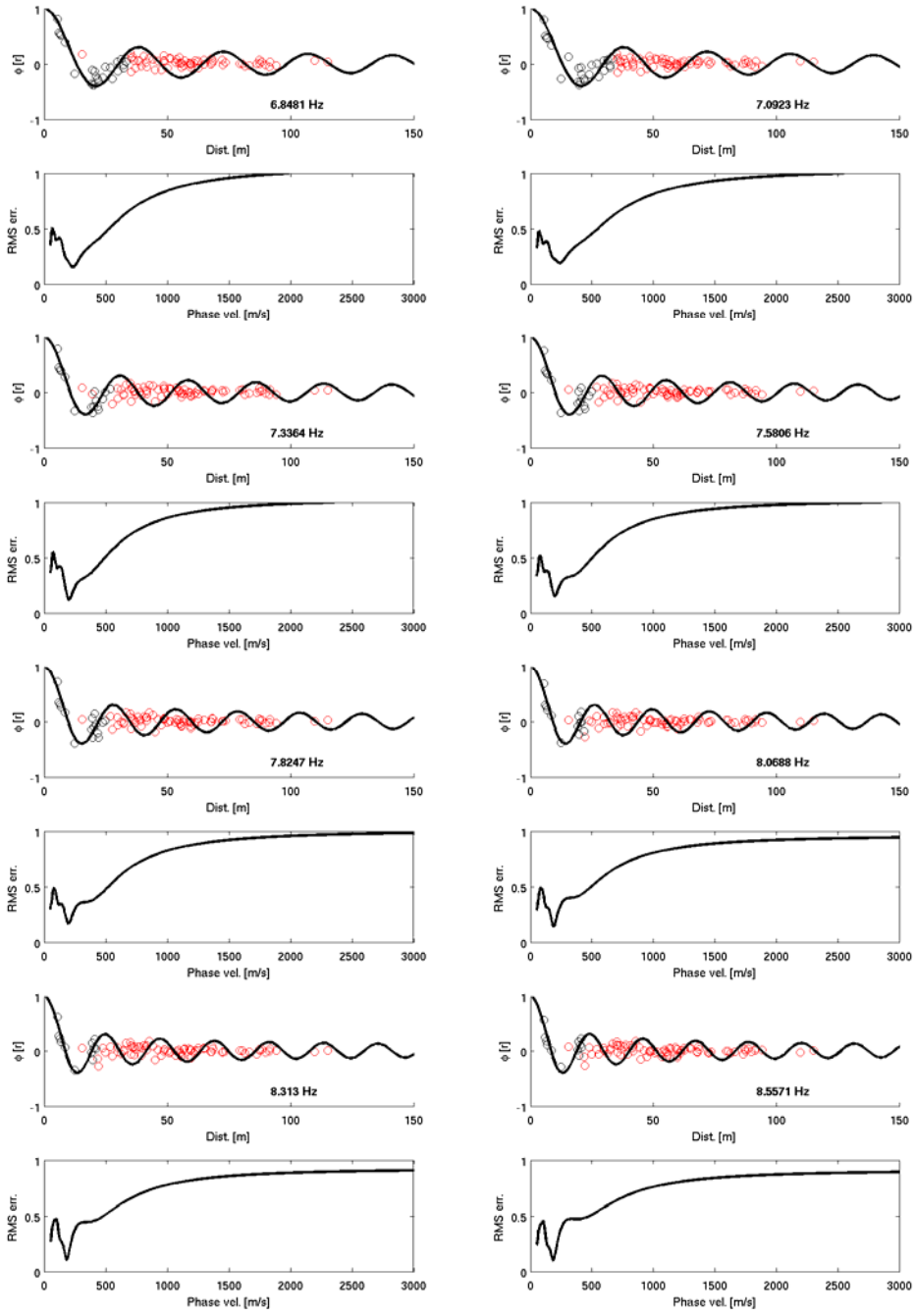

Figure 3: See previous caption.

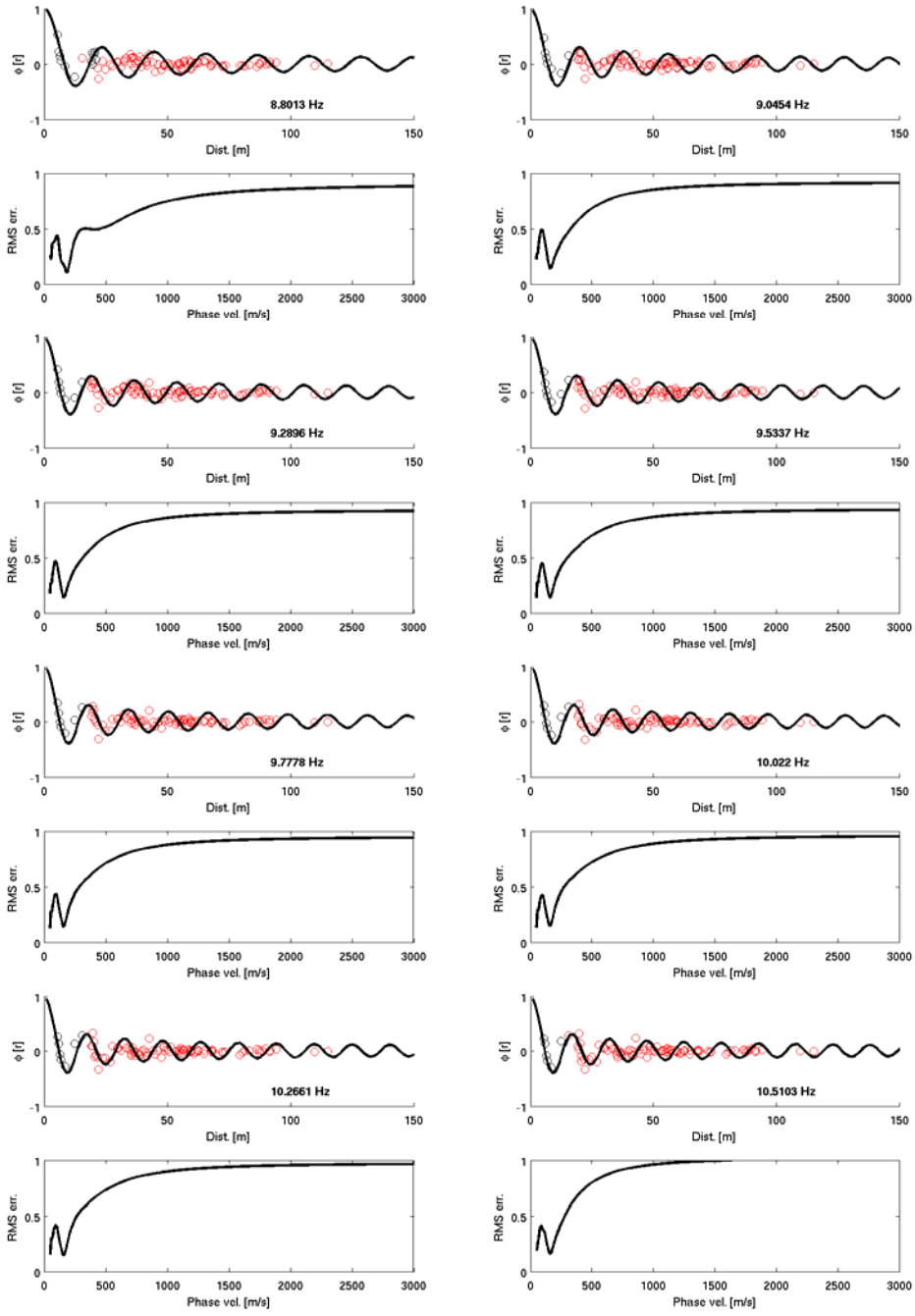

Figure 3: See previous caption.

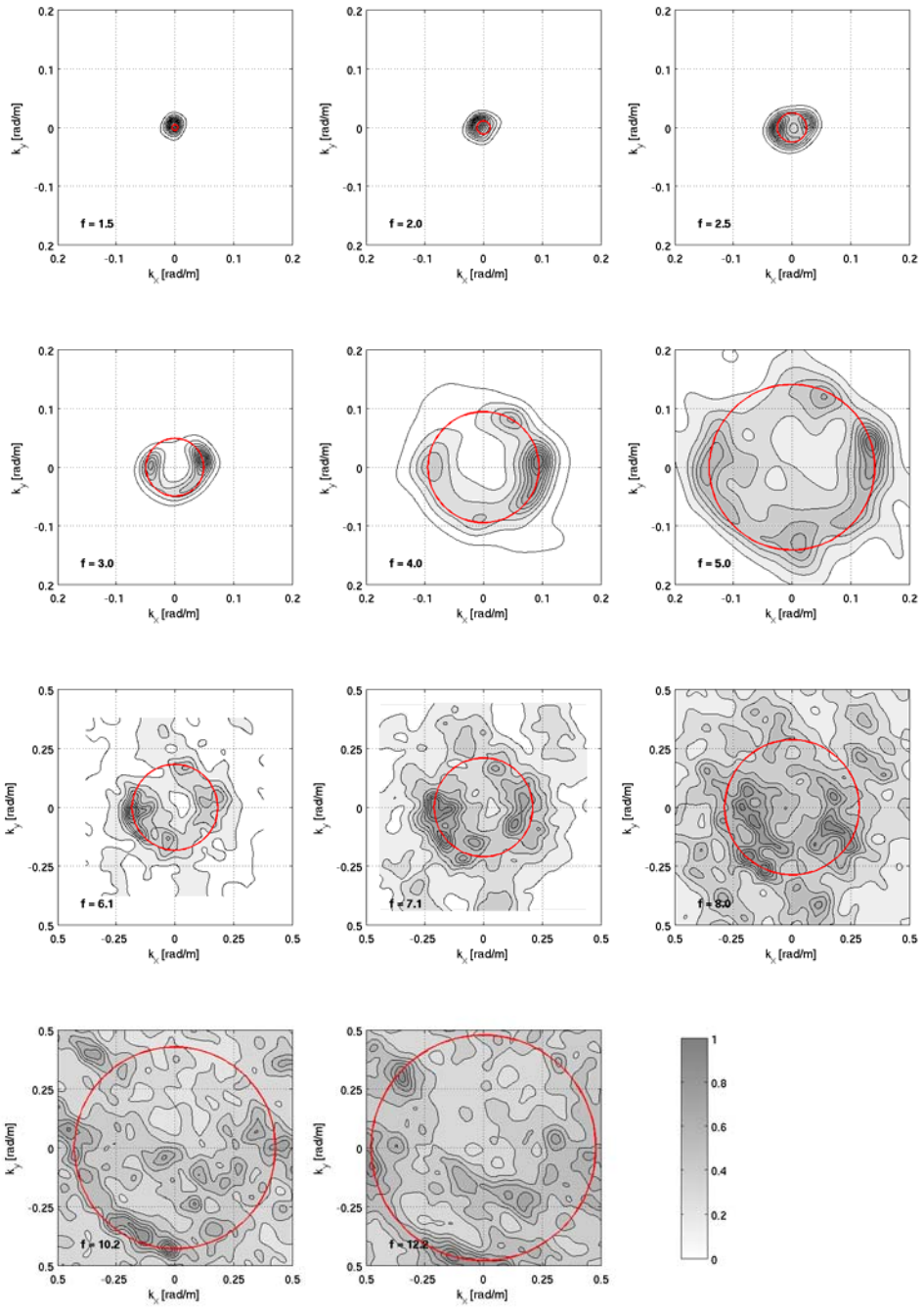

Figure 4: f-k power density function (MLM) at different frequencies (f, expressed in Hz). The red circles joints points with the same *k* value, corresponding to the maximum used to estimate the phase velocity.

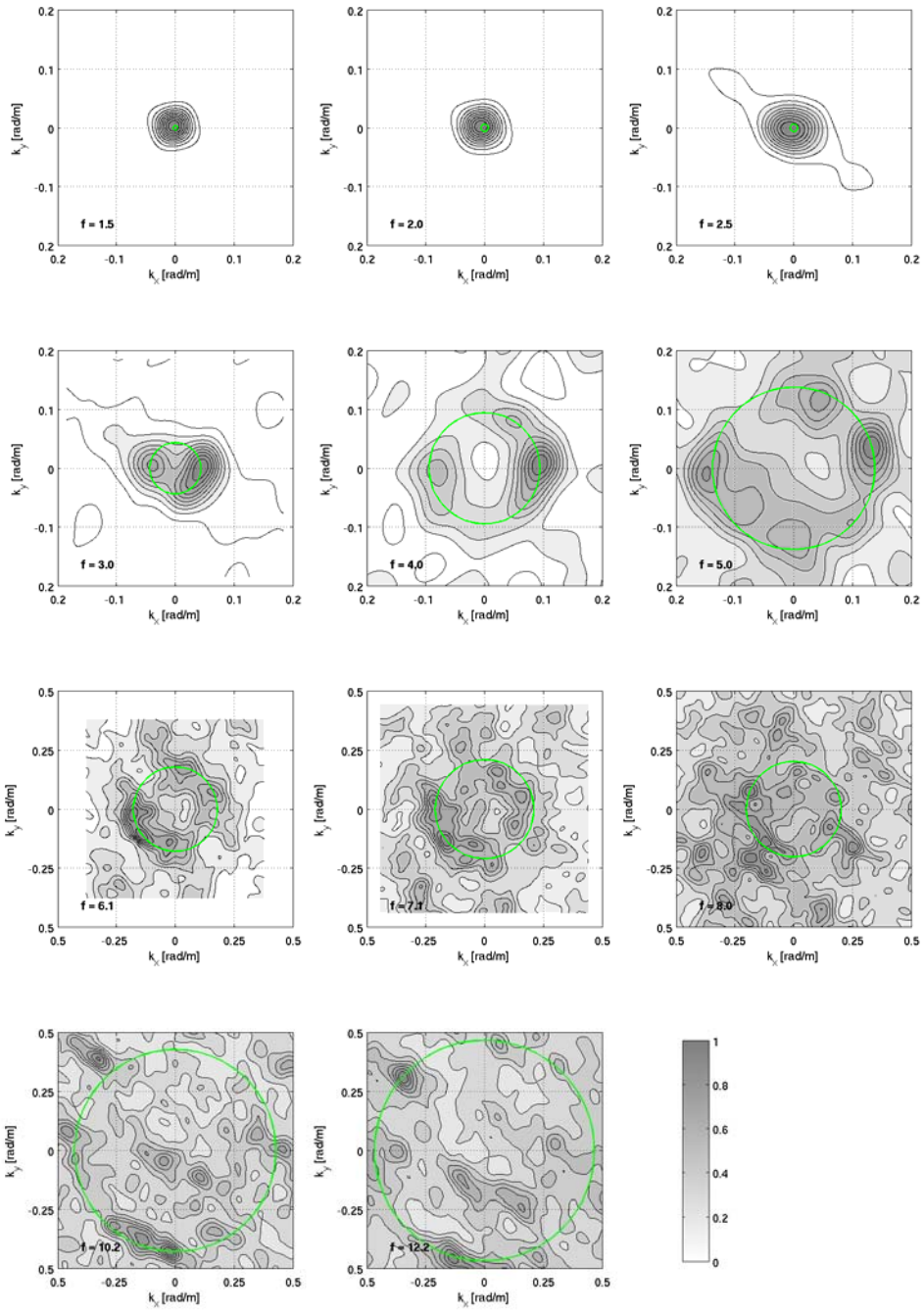

Figure 5: f-k power density function (BF) at different frequencies (f, expressed in Hz). The green circles joints points with the same *k* value, corresponding to the maximum used to estimate the phase velocity.

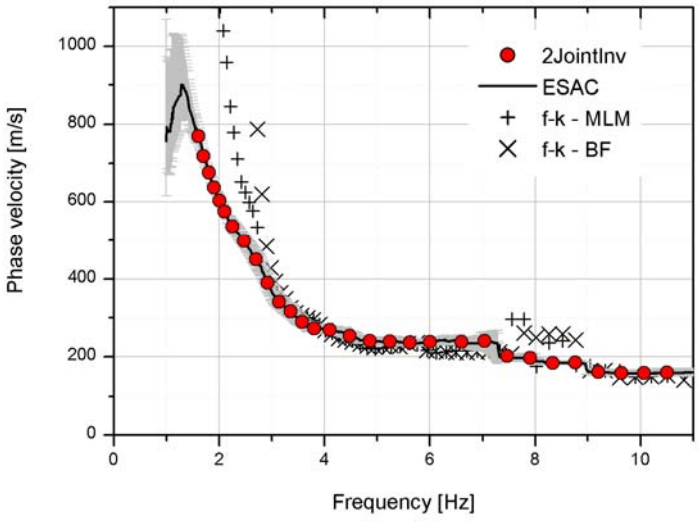

Figure 6: Comparison of experimental phase velocity estimated by the ESAC and the f-k (both for Beam Forming and Maximum Likelihood Method) methods. The red circles represent the values used for the joint inversion. The intervals (grey lines) around the observed ESAC phase velocities representing estimated uncertainties are obtained by calculating the square root of the covariance of the error function.

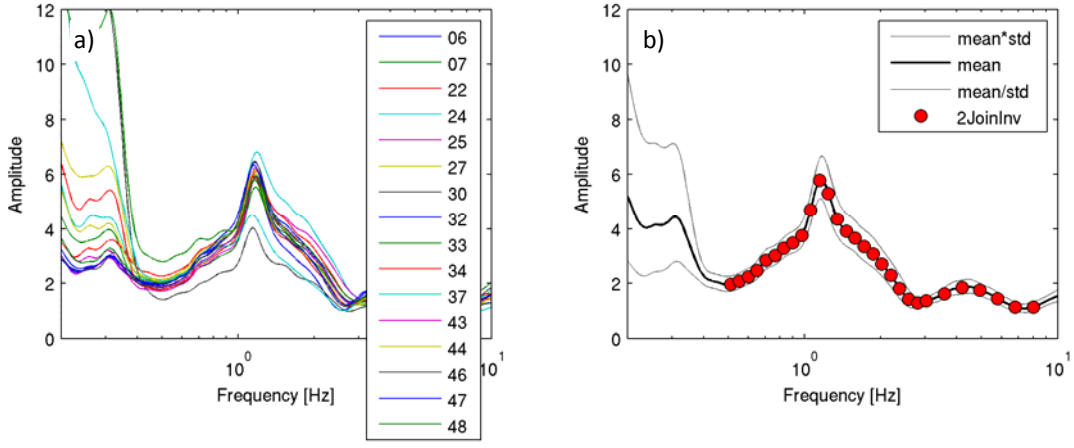

Figure 7: a) average *H/V* for the selected stations of the array (e.g. 06 stands for station 3006, 32 stands for station 3032, etc.) and b) the average H/V of the array. The red circles represent the values used for the joint inversion.

The inversion of dispersion and *H/V* curves to estimate the S-wave velocity profile was carried out fixing to 7 the number of layers overlying the half-space in the model (**Table 1**). Through a genetic algorithm a search over 80000 models was carried out. The inversion was repeated several times starting from different

seed numbers, that is to say from a different population of initial models. In this way it was possible to better explore the space of the solution.

Table 1: Ranges of values defined for the parameters used in the joint inversion.

	Shear wave velocity, V_S [m/s]		Thickness, h [m]		Density, ρ [ton/m^3]
Layer	MIN	MAX	MIN	MAX	
#1	100	250	5	20	1.9
#2	150	400	10	40	2.0
#3	250	650	20	80	2.1
#4	300	800	30	120	2.1
#5	400	900	50	200	2.2
#6	400	900	50	200	2.2
#7	500	1200	250	1000	2.2
Half-space	1000	2500	Infinite		2.3

During the inversion procedure the thickness and the shear wave velocity for each layer could be varied within the pre-defined ranges. On the contrary, for each layer, density was assigned *a priori*, while P-wave velocity (V_P) was calculated through the values of the S-wave velocity Vs via the equation: $V_P\,[\mathrm{m/s}] = 1.1 \cdot V_S + 1290$.

The models are selected by means of a cost function which take in account the agreement between the theoretical *H/V* and Rayleigh-wave dispersion curves with the observed ones. In this application, after trial and error test, the weight of 0.05, that allowed the best balanced fit of dispersion and H/V curves, was adopted.

Discussion of the results

In **Figure 8a** all the models tested during the inversion are depicted (gray lines). The best fit model (white line) and the models lying inside the 10% range of the minimum cost (black lines) function are highlighted. The agreement between experimental and theoretical Rayleigh wave dispersion curves (**Figure 8c**) is good and, considering the wavelengths related to the dispersion curve frequency range, the V_S profile between 5 to about 100 metres is likely to be well constrained. Therefore, since below this depth the profile is constrained by the H/V curve alone, we prefer to show, in **Figure 8a** and **Table 2**, the V_S profile only within the depth range were both curves contribute to the inversion.

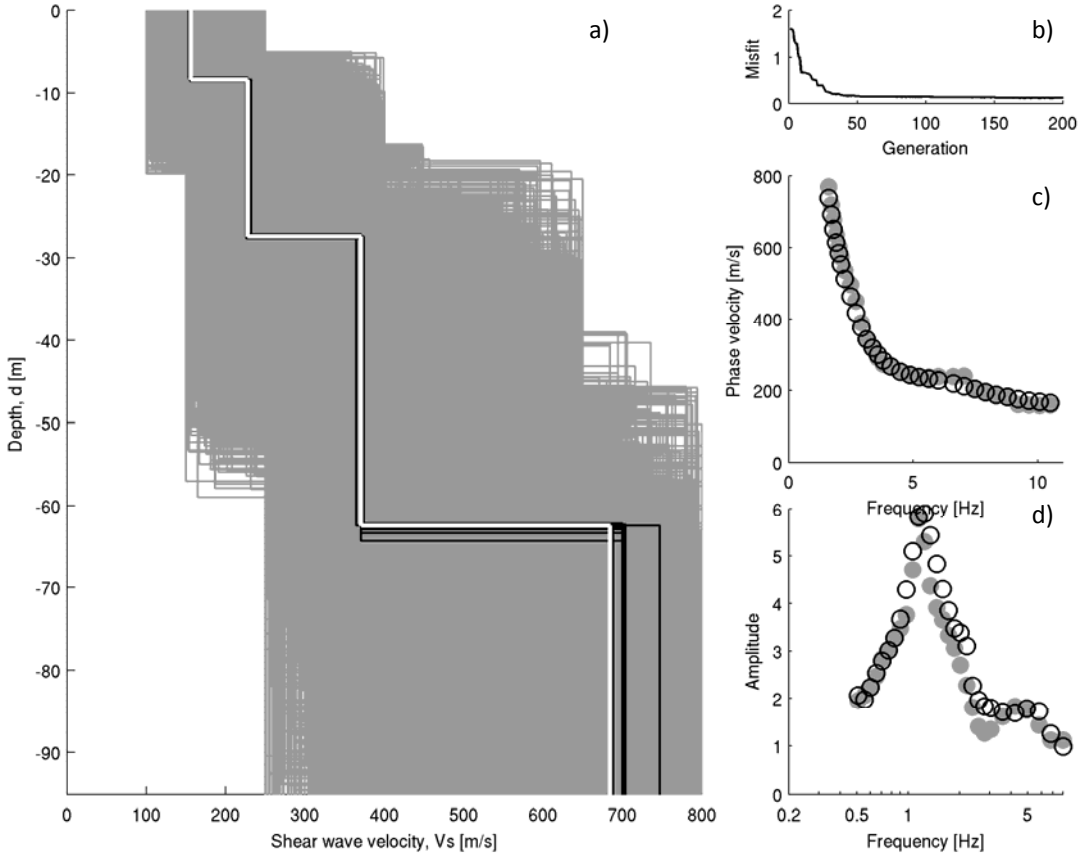

Figure 8: a) Tested models (grey lines), the minimum cost model (white line) and models lying inside the minimum cost + 10% range (black lines) for the CTL station; b) the misfit versus generation values; c) experimental (grey circles) and estimated (white circles – relevant to the minimum cost model) phase velocities; d) experimental (grey circles) and estimated (white circles – relevant to the minimum cost model) *H/V* ratio curves.

Table 2: Shear wave velocity model at the CTL station.

Shear wave velocity, V_S [m/s]	Thickness, h [m]
156	8.4
227	19.1
371	35.1
684	

APPLICATION OF SURFACE WAVE METHODS

FOR SEISMIC SITE CHARACTERIZATION

STATION CODE:

FAZ

Responsible: Stefano Parolai[1]

Co-workers: Rodolfo Puglia[2], Matteo Picozzi[1]

1) Helmholtz Centre Potsdam - German Research Centre For Geosciences (GFZ), Helmholtzstraße 7, 14467 Potsdam, Germany
2) Istituto Nazionale di Geofisica e Vulcanologia (INGV), Sezione di Milano-Pavia, via Bassini 15, 20133 Milano, Italy

Introduction note

Details and references about *in-situ* measurement, Rayleigh wave dispersion and H/V curves estimate and inversion procedure here reported, can be found in the research reports of DPC-INGV S4 Project 2007-2009: Deliverables 6 and 7 at http://esse4.mi.ingv.it .

Testing equipment

The array measurements were performed using 17 EDL 24bit acquisition systems equipped with short-period Mark-L4-C-3D 1Hz sensors and GPS timing (**Figure 1**). However, due to malfunctioning, only the data of 16 stations (depicted as blue squares) could be used for the processing. The inter-station distances in the array ranged between 5.0 m to 201 meters. The stations worked contemporary for about 4 hours, recording noise at 200 s.p.s., which is adequate for the short inter-station distances considered.

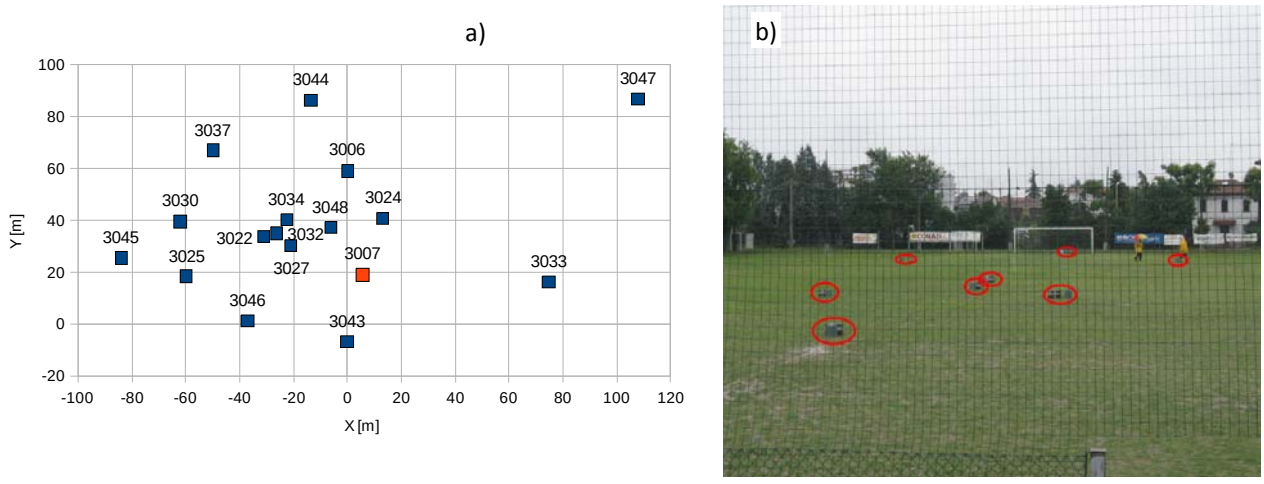

Figure 1: a) Geometry of the array. Stations which had problems are evidenced with the red color: in particular, 3007 did not work properly. b) The field measurements.

Processing overview

The Rayleigh wave dispersion curve was estimated by analysing the vertical component of the recorded microtremors. In particular, the Extended Spatial Auto Correlation (ESAC) and the Frequency-Wavenumber (f-k) methods were adopted.

Rayleigh wave dispersion and *H/V* ratio curves were both used to estimate the local S-wave velocity profile, using a joint inversion scheme. The non-linear inversions were performed using a genetic algorithm which does not rely upon an explicit starting model and allows the identification of a solution close to the global minimum. The forward modeling of Rayleigh wave phase velocities and *H/V* curves was performed using the modified Thomson-Haskell method, under the assumption of vertically heterogeneous 1D earth models. The validity of this assumption was investigated by computing the *H/V* curve for each station of the array using the recorded data. The modeling of both the dispersion and *H/V* ratio curves during the inversions was not restricted to the fundamental mode only, but the possibility that higher modes can participate to define the observed dispersion and *H/V* curves is allowed.

Data analysis

The first step of the analysis consists in a visual inspection of the recordings at all stations. In particular, in order to identify malfunctioning of one station or channel and to select signal windows suitable for the H/V analysis, the quality of the recording was evaluated analysing (1) the signal stationarity in the time domain (**Figure 2a**), (2) the relevant unfiltered Fourier spectra (**Figure 2b**), and (3) the *H/V* variation over time (**Figure 2a**).

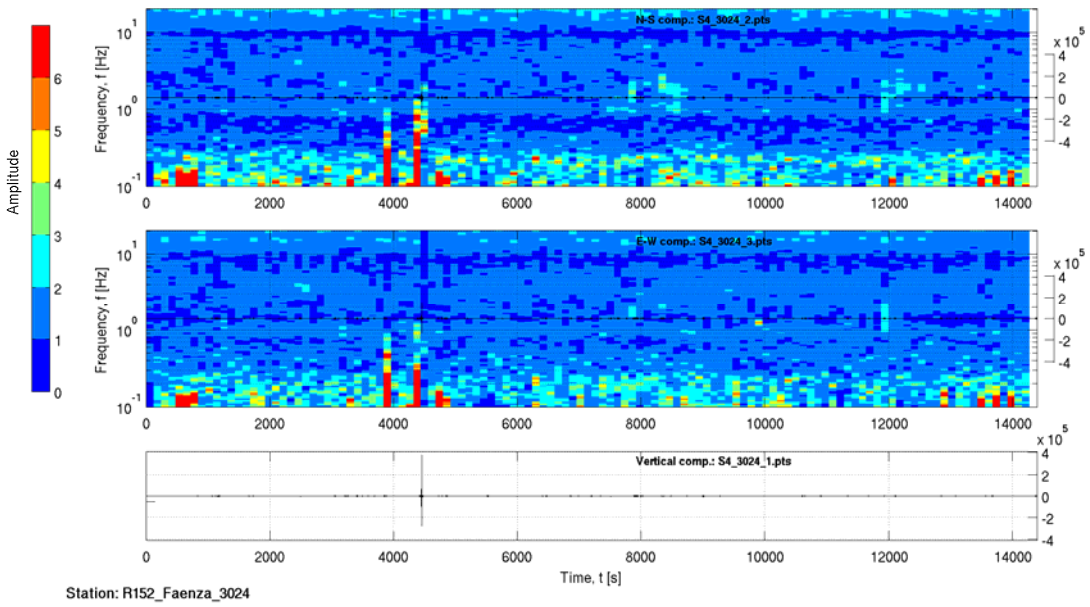

Figure 2a: *H/V* spectral ratios versus time (top and central panel for the NS and EW component, respectively) and corresponding time histories for station 3024.

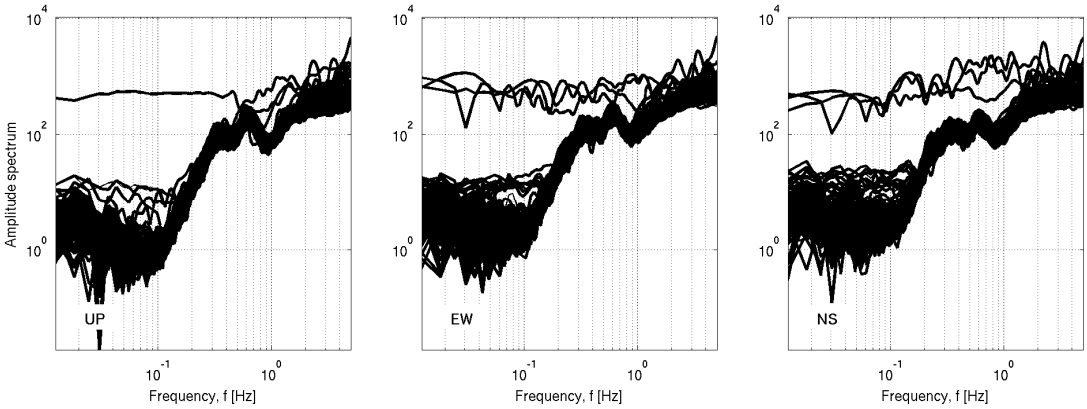

Figure 2b: Fourier spectra for each noise window at station 3024. Left) Vertical component spectra, center) E-W component spectra, right) N-S component spectra.

For each of the 16 used stations, 62 synchronized signal windows of 60 seconds were selected, avoiding windows affected by local disturbance. These windows were in turn used to estimate the experimental Rayleigh-wave dispersion curves (using the vertical component of ground motion only) both by f-k and ESAC analysis.

The ESAC Rayleigh-wave dispersion curve was obtained minimizing the root mean square (RMS) of the differences between experimental and theoretical Bessel function values (**Figure 3**). Values that differ more than two standard deviations from those estimated by the best fitting functions (red circles in **Figure 3**) are automatically discarded and the procedure iteratively repeated. Furthermore, data are discarded also when their inter-station distance is longer than the relevant wavelength.

The f-k analysis offers the opportunity to verify if the requirements on the noise source distribution, necessary for the application of the ESAC method, were fulfilled. **Figure 4** and **Figure 5** show examples of the results for several frequencies of the frequency-wavenumber analysis using the Maximum Likelihood Method (MLM) and the Beam Forming (BF) respectively.

Figure 6 shows the good agreement between the Rayleigh wave dispersion curves estimated both with ESAC and f-k approaches. Only below 3 Hz the f-k analysis provides larger phase velocities.

An average *H/V* for the selected stations was computed by averaging the *H/V* calculated for each signal window (**Figure 7a**). The average *H/V* curves for the selected stations were in turn averaged to obtain a single *H/V* spectral ratio representative for the array, which was then used as input in the joint inversion procedure for the estimation of the S-wave velocity profile (**Figure 7b**).

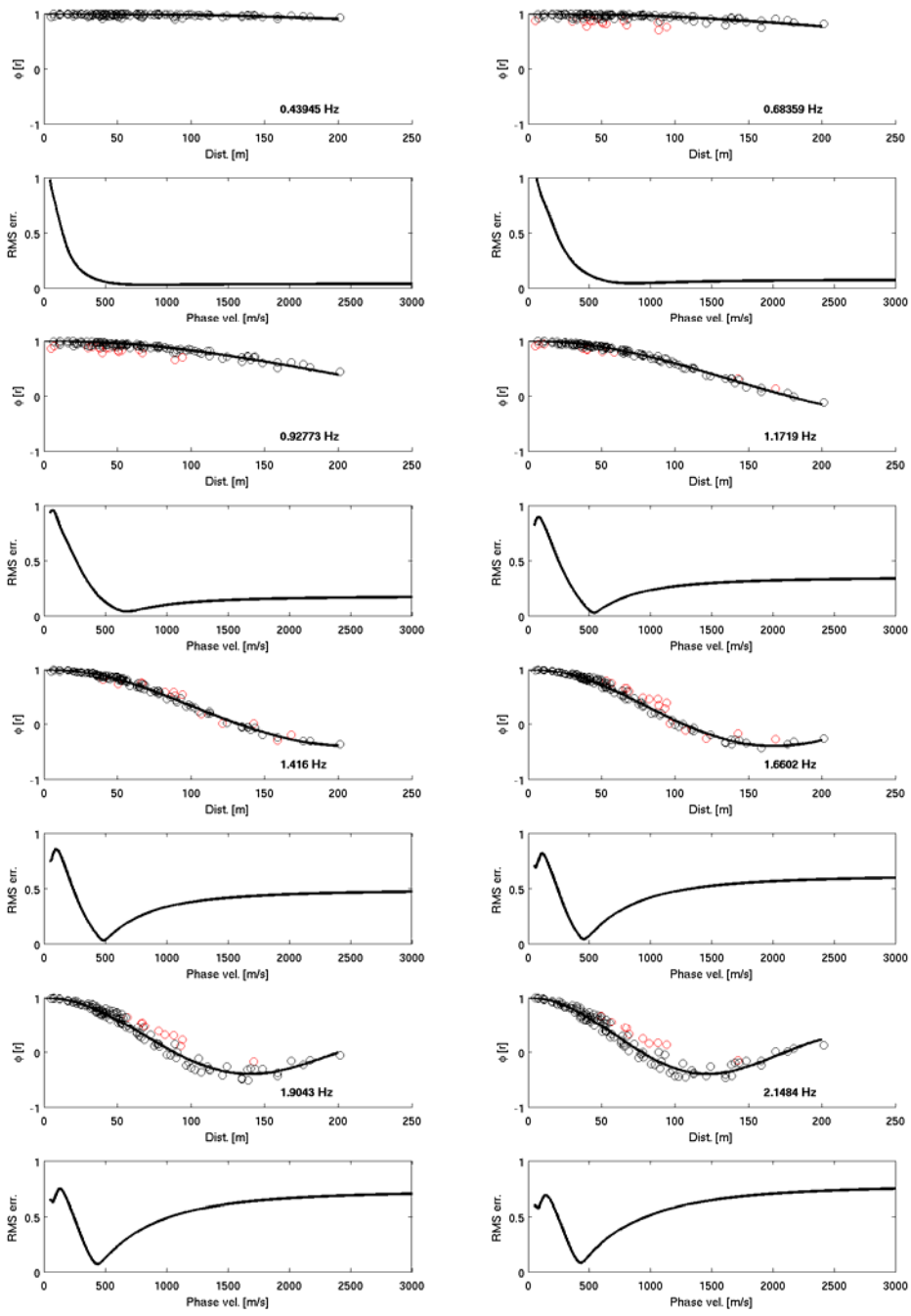

Figure 3: Experimental space-correlation function values versus distance (circles) for different frequencies. The red circles indicate values discarded. The black lines depict the estimated space-correlation function values for the phase velocity showing the best fit to the data. The bottom panels show the relevant root-mean square errors (RMS) versus phase velocity tested.

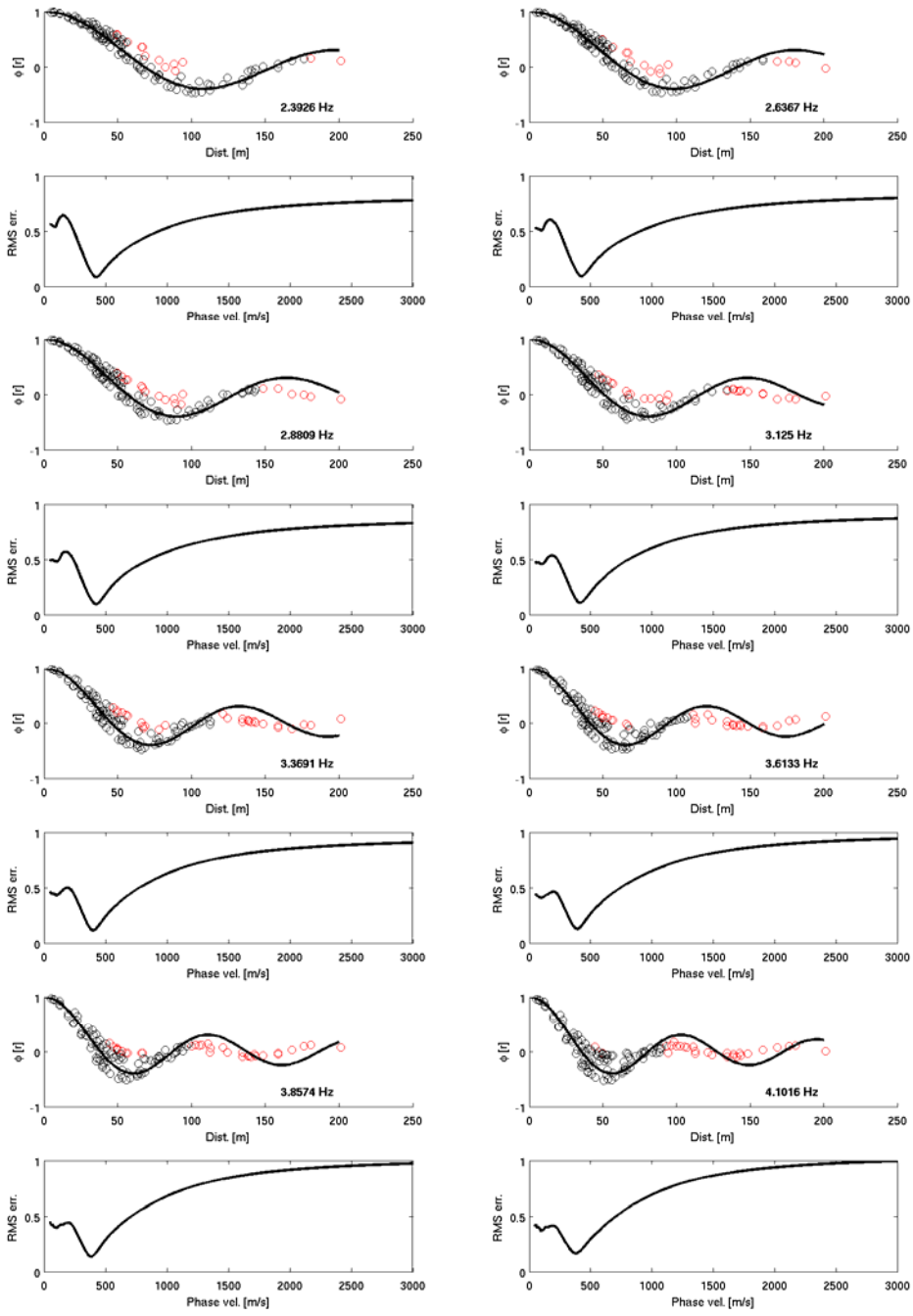

Figure 3: See previous caption.

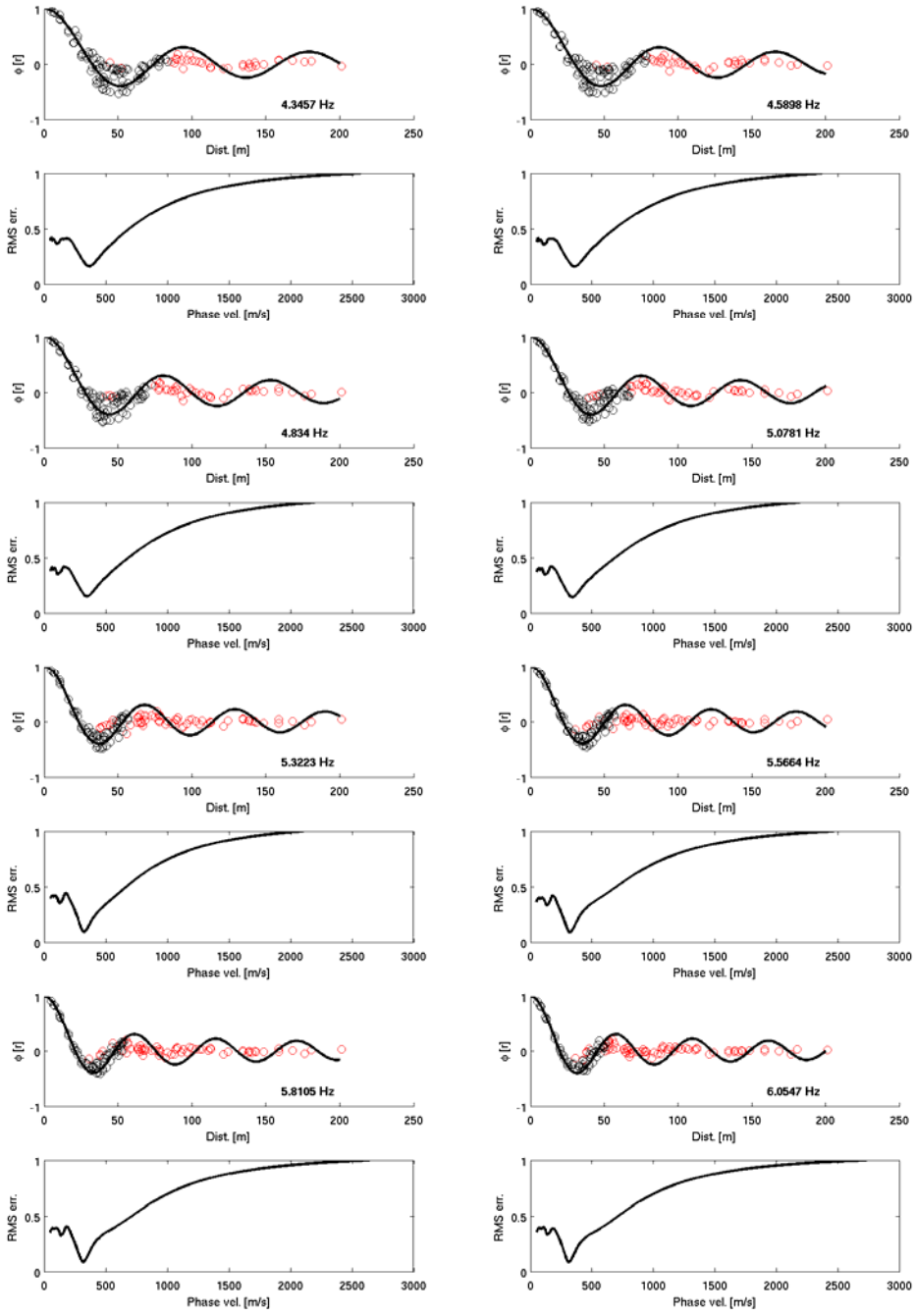

Figure 3: See previous caption.

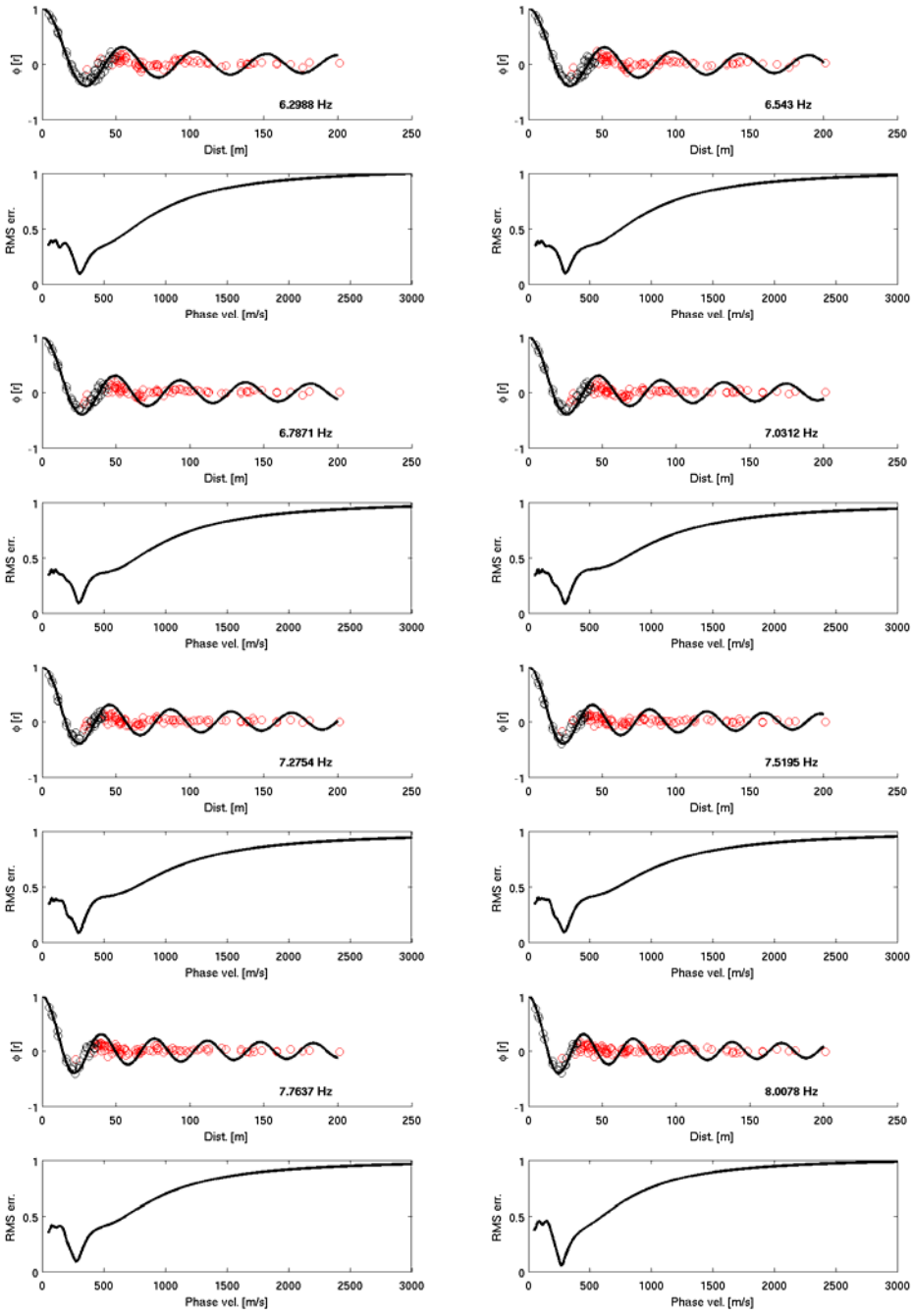

Figure 3: See previous caption.

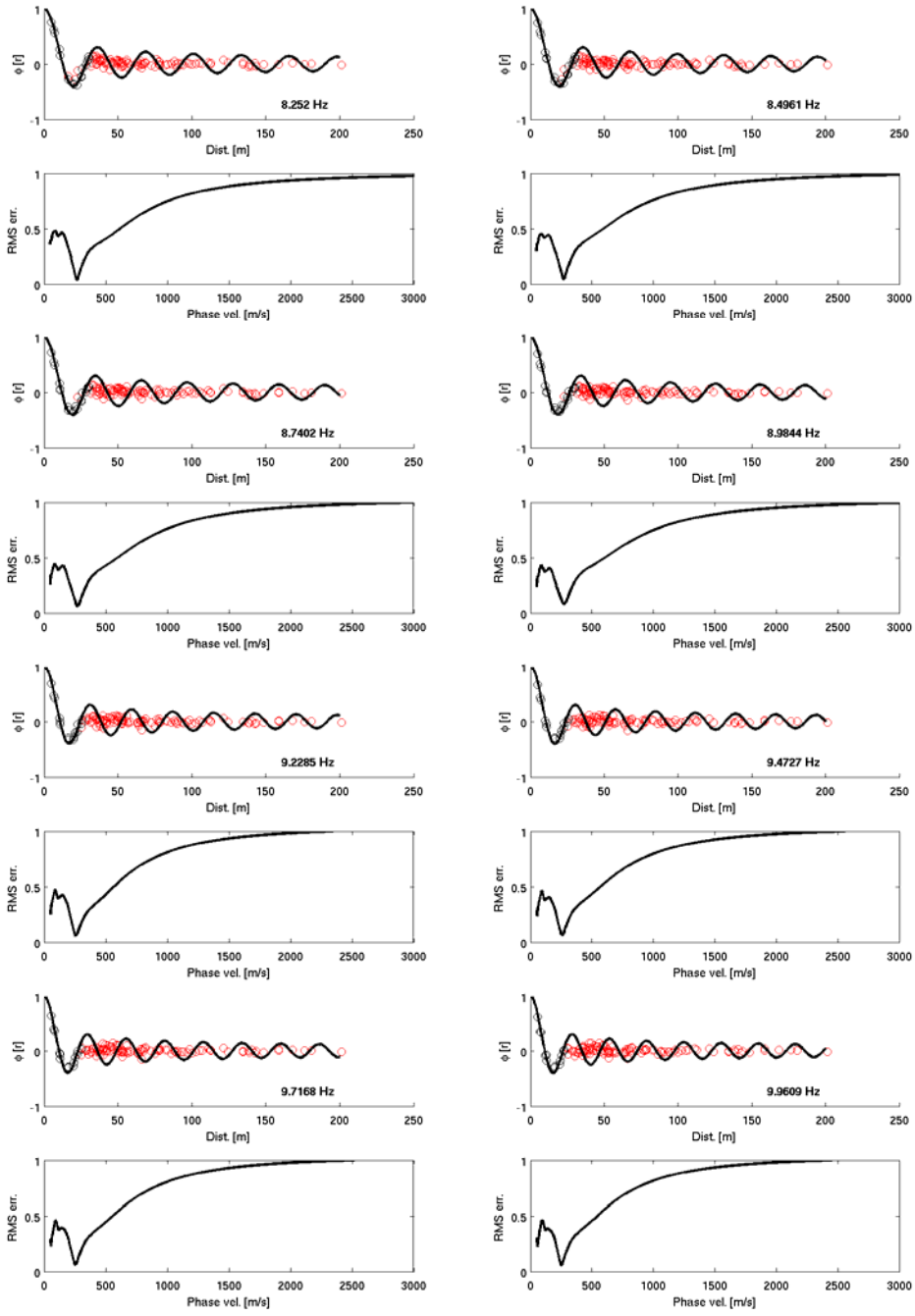

Figure 3: See previous caption.

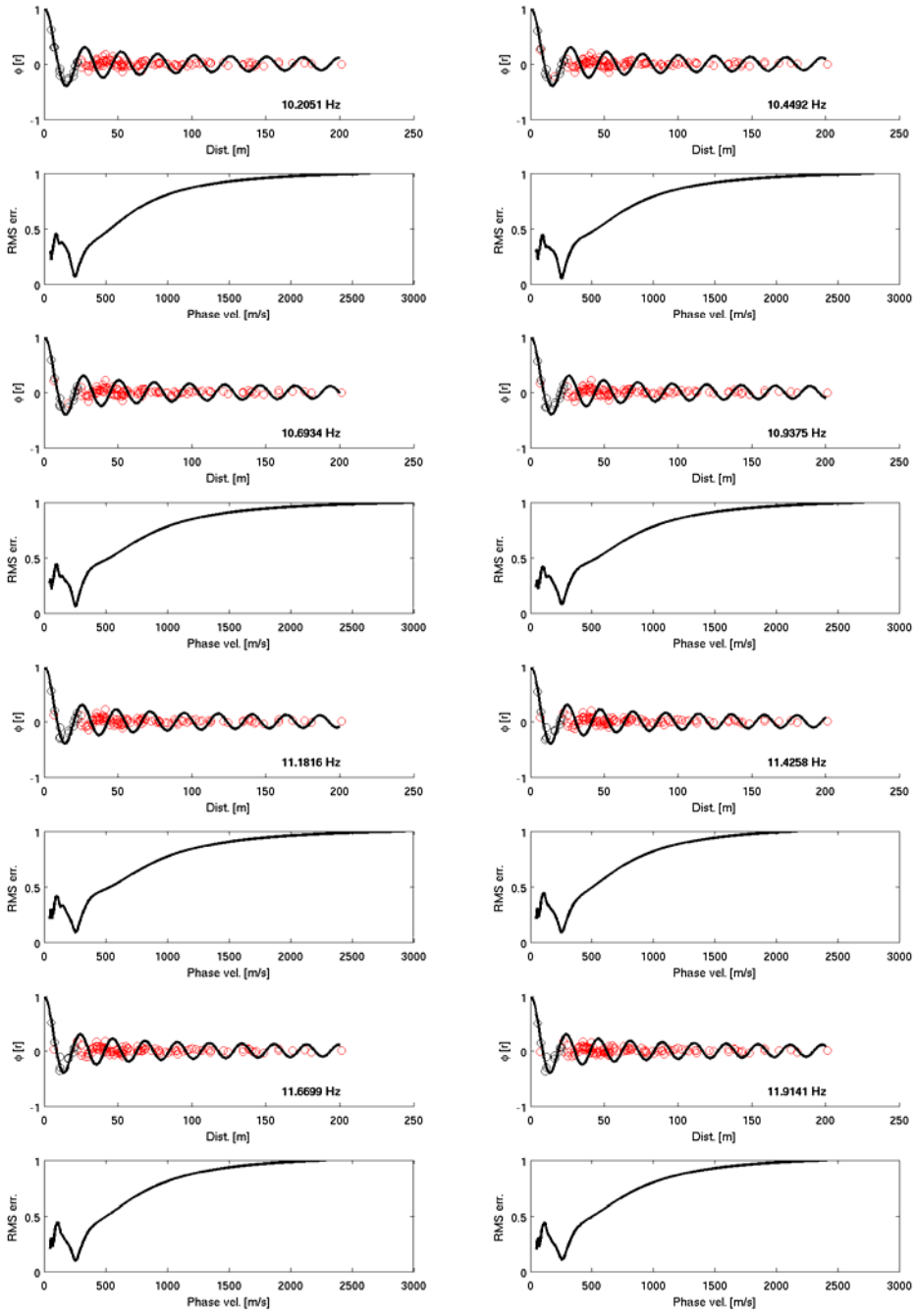

Figure 3: See previous caption.

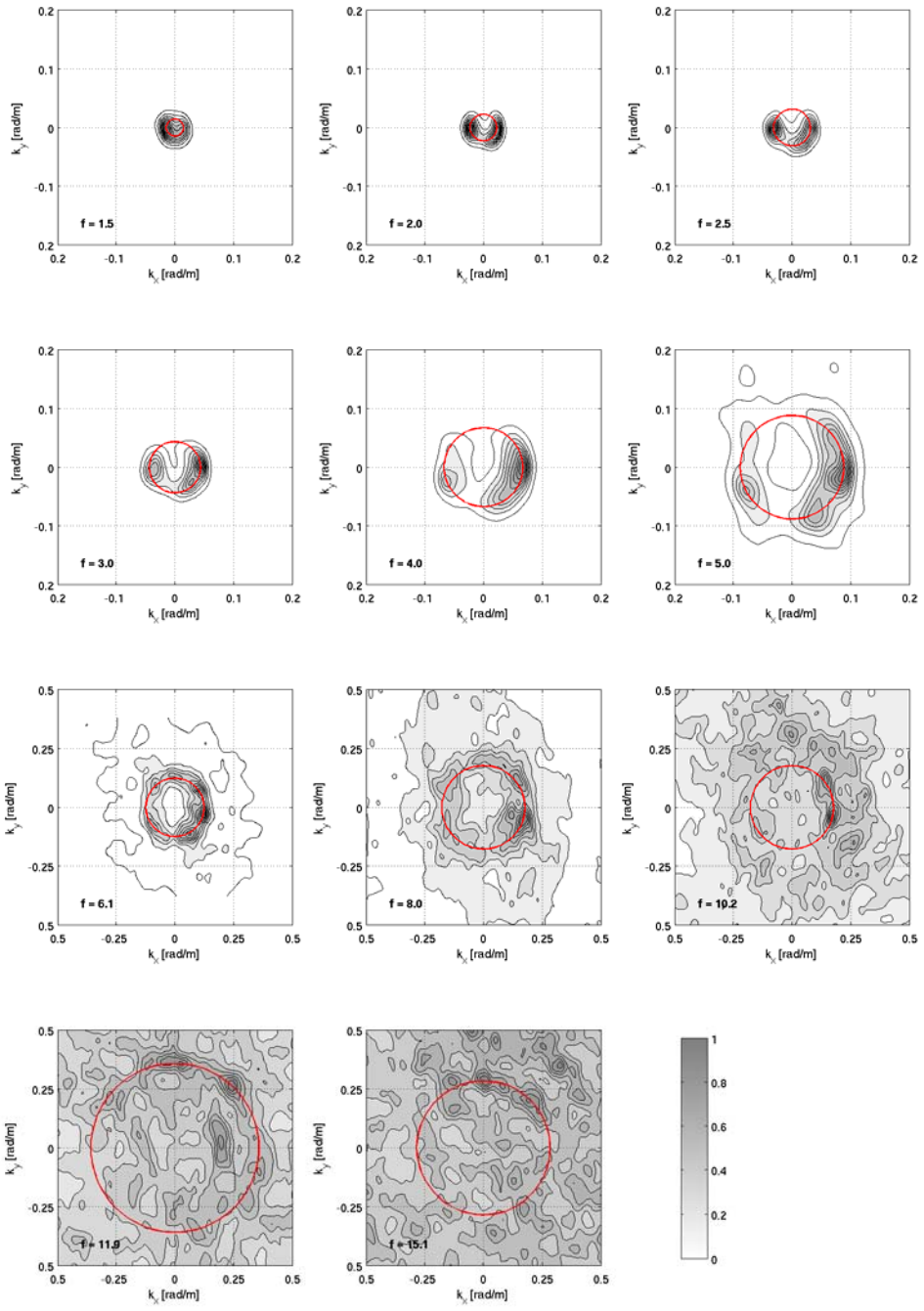

Figure 4: f-k power density function (MLM) at different frequencies (f, expressed in Hz). The red circles joints points with the same *k* value, corresponding to the maximum used to estimate the phase velocity.

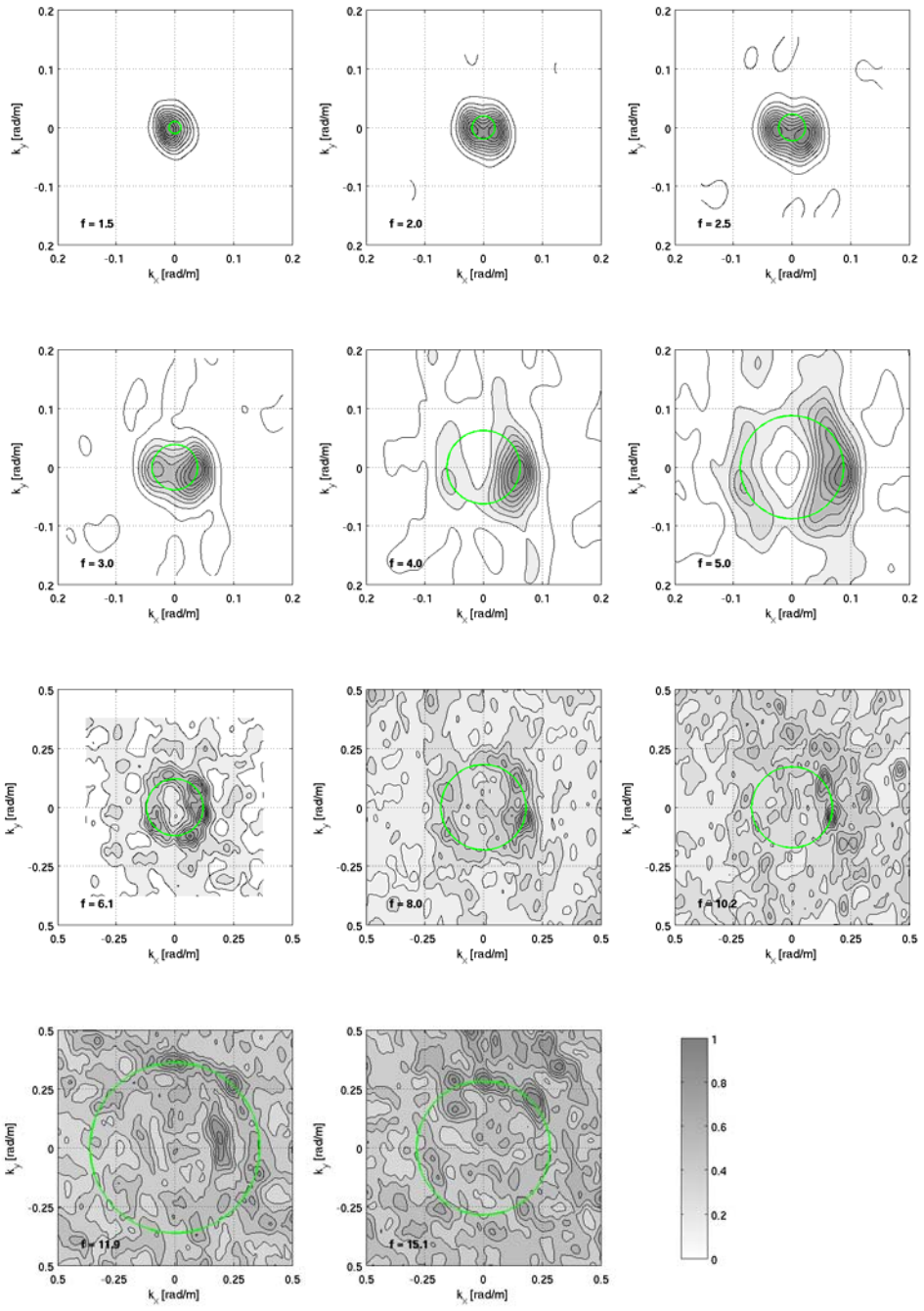

Figure 5: f-k power density function (BF) at different frequencies (f, expressed in Hz). The green circles joints points with the same *k* value, corresponding to the maximum used to estimate the phase velocity.

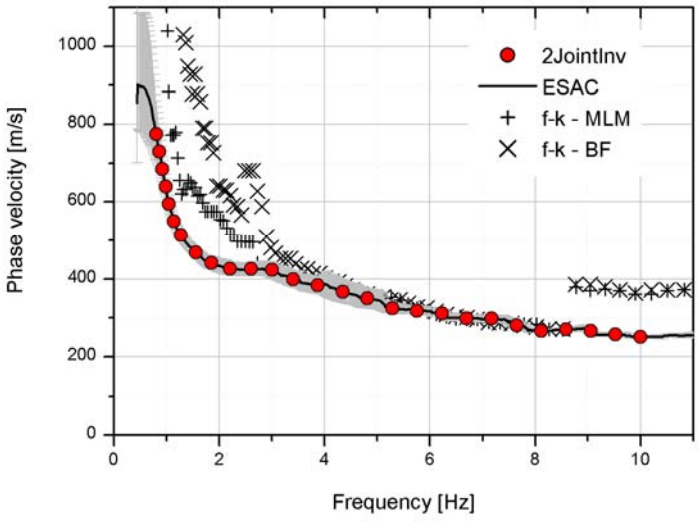

Figure 6: Comparison of experimental phase velocity estimated by the ESAC and the f-k (both for Beam Forming and Maximum Likelihood Method) methods. The red circles represent the values used for the joint inversion. The intervals (grey lines) around the observed ESAC phase velocities representing estimated uncertainties are obtained by calculating the square root of the covariance of the error function.

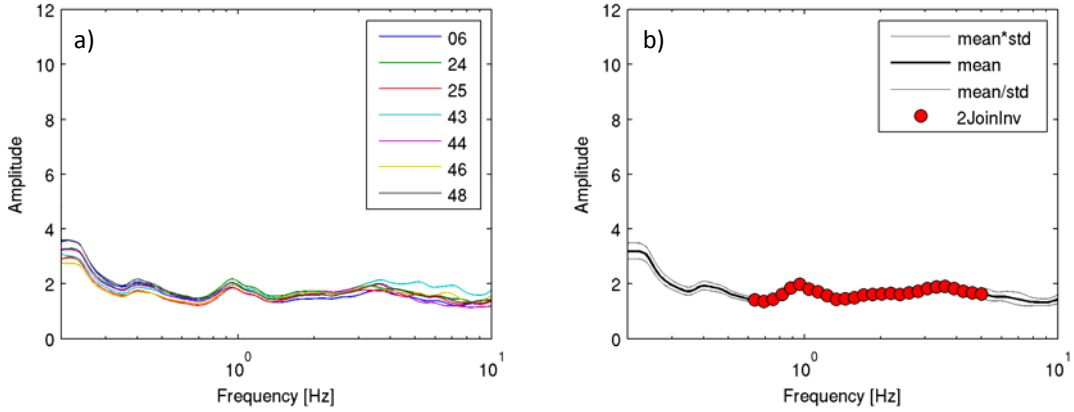

Figure 7: a) average *H/V* for some selected stations of the array (e.g. 06 stands for station 3006, etc.) and b) the average H/V of the array. The red circles represent the values used for the joint inversion.

The inversion of dispersion and *H/V* curves to estimate the S-wave velocity profile was carried out fixing to 7 the number of layers overlying the half-space in the model (**Table 1**). Through a genetic algorithm a search over 80000 models was carried out. The inversion was repeated several times starting from different

seed numbers, that is to say from a different population of initial models. In this way it was possible to better explore the space of the solution.

Table 1: Ranges of values defined for the parameters used in the joint inversion.

	Shear wave velocity, V_S [m/s]		Thickness, h [m]		Density, ρ [ton/m^3]
Layer	MIN	MAX	MIN	MAX	
#1	150	450	5	30	1.9
#2	200	500	5	40	2.0
#3	250	600	20	80	2.1
#4	300	700	20	80	2.1
#5	350	750	30	120	2.2
#6	400	900	50	350	2.2
#7	450	1000	50	350	2.2
Half-space	1000	2200	Infinite		2.3

During the inversion procedure the thickness and the shear wave velocity for each layer could be varied within the pre-defined ranges. On the contrary, for each layer, density was assigned *a priori*, while P-wave velocity (V_P) was calculated through the values of the S-wave velocity Vs via the equation: $V_P\,[\mathrm{m/s}] = 1.1 \cdot V_S + 1290$.

The models are selected by means of a cost function which take in account the agreement between the theoretical *H/V* and Rayleigh-wave dispersion curves with the observed ones. In this application, after trial and error test, the weight of 0.05, that allowed the best balanced fit of dispersion and H/V curves, was adopted.

Discussion of the results

In **Figure 8a** all the models tested during the inversion are depicted (gray lines). The best fit model (white line) and the models lying inside the 10% range of the minimum cost (black lines) function are highlighted. The agreement between experimental and theoretical Rayleigh wave dispersion curves (**Figure 8c**) is good and, considering the wavelengths related to the dispersion curve frequency range, the V_S profile between 10 to about 300 metres is likely to be fairly well constrained. Therefore, since below this depth the profile is constrained by the H/V curve alone, we prefer to show, in **Figure 8a** and **Table 2**, the V_S profile only within the depth range were both curves contribute to the inversion.

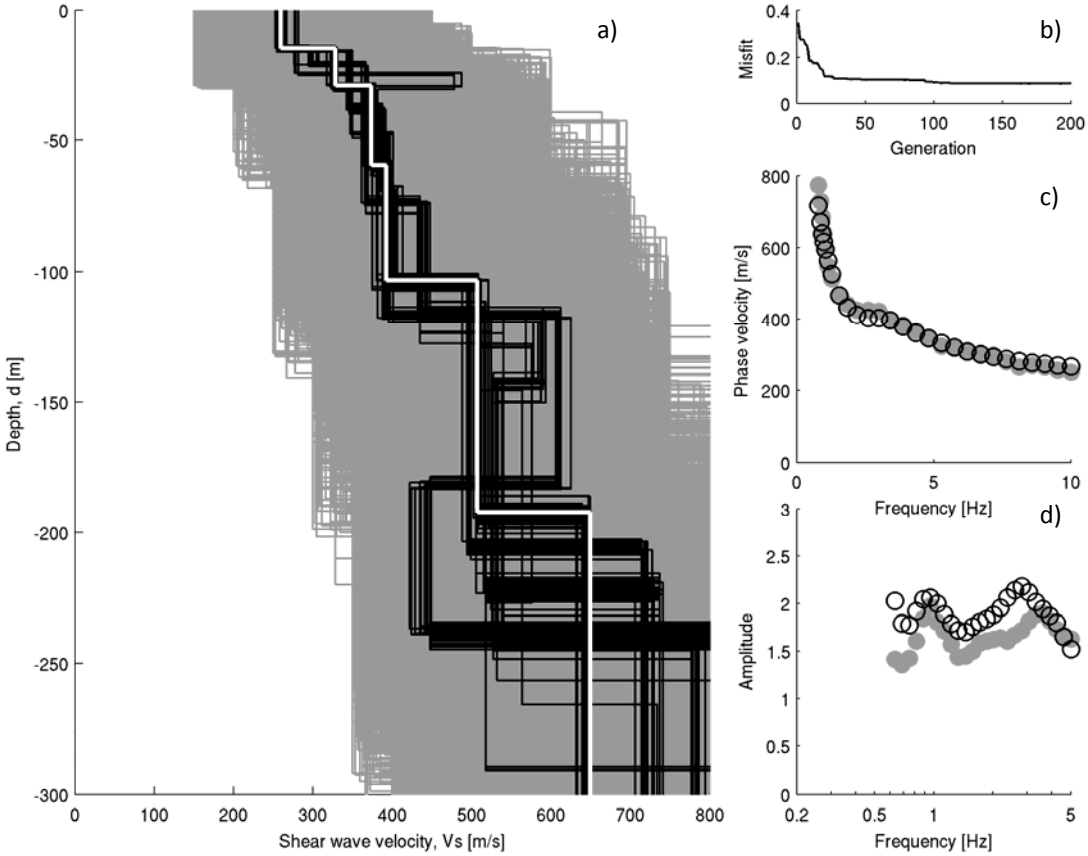

Figure 8: a) Tested models (grey lines), the minimum cost model (white line) and models lying inside the minimum cost + 10% range (black lines) for the FAZ station; b) the misfit versus generation values; c) experimental (grey circles) and estimated (white circles – relevant to the minimum cost model) phase velocities; d) experimental (grey circles) and estimated (white circles – relevant to the minimum cost model) *H/V* ratio curves.

Table 2: Shear wave velocity model at the FAZ station.

Shear wave velocity, V_S [m/s]	Thickness, h [m]
259.4	14.3
328.2	14.5
373.5	30.8
392.5	43.8
506.9	88.6
649.0	

APPLICATION OF SURFACE WAVE METHODS

FOR SEISMIC SITE CHARACTERIZATION

STATION CODE:

GRM

Responsible: Stefano Parolai[1]

Co-workers: Rodolfo Puglia[2], Matteo Picozzi[1]

1) Helmholtz Centre Potsdam - German Research Centre For Geosciences (GFZ), Helmholtzstraße 7, 14467 Potsdam, Germany
2) Istituto Nazionale di Geofisica e Vulcanologia (INGV), Sezione di Milano-Pavia, via Bassini 15, 20133 Milano, Italy

Introduction note

Details and references about *in-situ* measurement, Rayleigh wave dispersion and H/V curves estimate and inversion procedure here reported, can be found in the research reports of DPC-INGV S4 Project 2007-2009: Deliverables 6 and 7 at http://esse4.mi.ingv.it .

Testing equipment

The array measurements were performed using 15 EDL 24bit acquisition systems equipped with short-period Mark-L4-C-3D 1Hz sensors and GPS timing (**Figure 1**). The inter-station distances in the array ranged between 5.0 m to 127 meters. The stations worked contemporary for about 3 hours, recording noise at 200 s.p.s., which is adequate for the short inter-station distances considered.

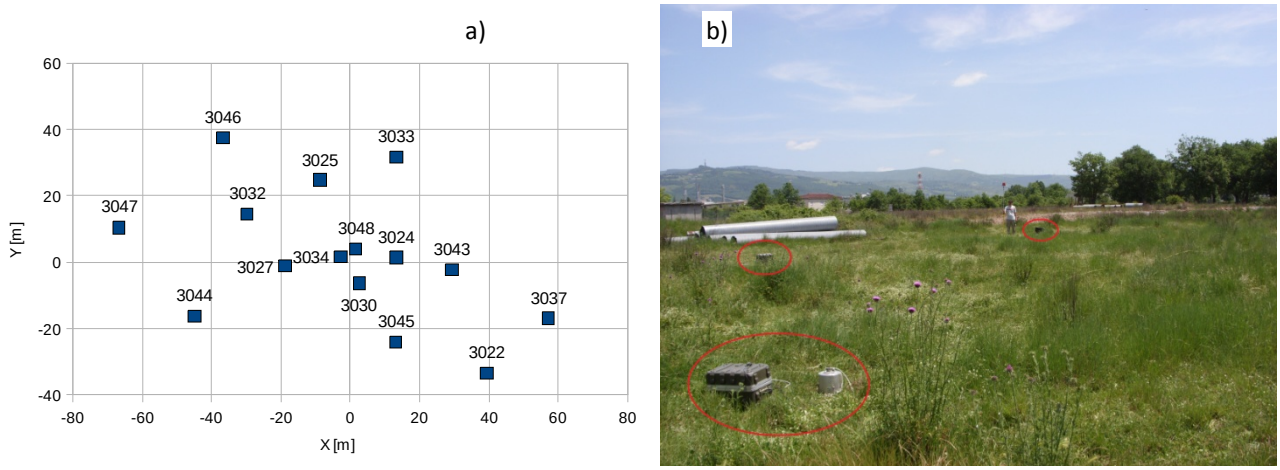

Figure 1: a) Geometry of the array. b) The field measurements.

Processing overview

The Rayleigh wave dispersion curve was estimated by analysing the vertical component of the recorded microtremors. In particular, the Extended Spatial Auto Correlation (ESAC) and the Frequency-Wavenumber (f-k) methods were adopted.

Rayleigh wave dispersion and *H/V* ratio curves were both used to estimate the local S-wave velocity profile, using a joint inversion scheme. The non-linear inversions were performed using a genetic algorithm which does not rely upon an explicit starting model and allows the identification of a solution close to the global minimum. The forward modeling of Rayleigh wave phase velocities and *H/V* curves was performed using the modified Thomson-Haskell method, under the assumption of vertically heterogeneous 1D earth models. The validity of this assumption was investigated by computing the *H/V* curve for each station of the array using the recorded data. The modeling of both the dispersion and *H/V* ratio curves during the inversions was not restricted to the fundamental mode only, but the possibility that higher modes can participate to define the observed dispersion and *H/V* curves is allowed.

Data analysis

The first step of the analysis consists in a visual inspection of the recordings at all stations. In particular, in order to identify malfunctioning of one station or channel and to select signal windows suitable for the H/V analysis, the quality of the recording was evaluated analysing (1) the signal stationarity in the time domain (**Figure 2a**), (2) the relevant unfiltered Fourier spectra (**Figure 2b**), and (3) the *H/V* variation over time (**Figure 2a**).

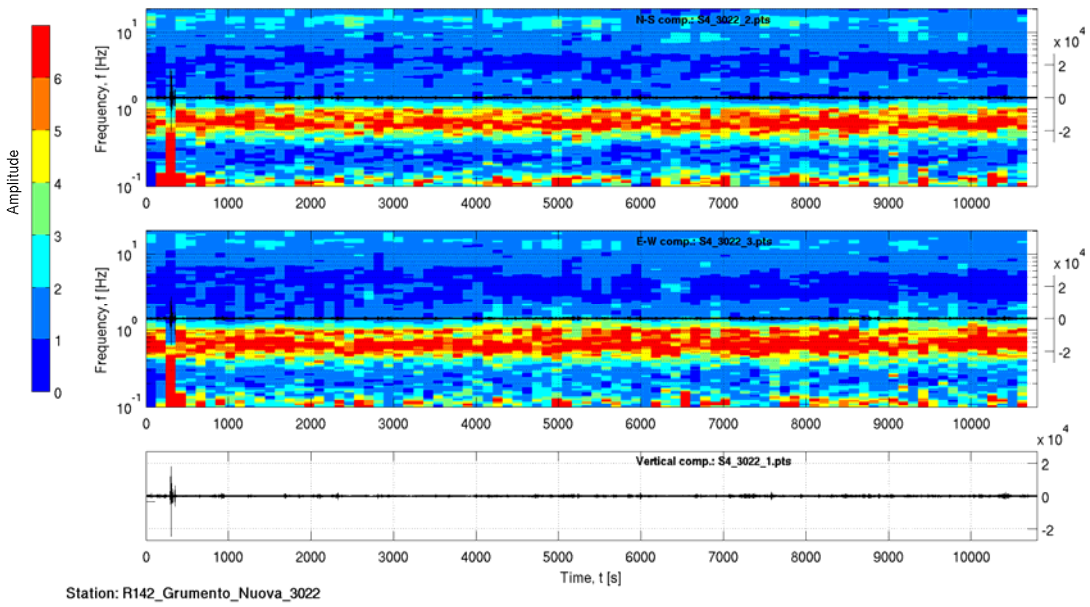

Figure 2a: *H/V* spectral ratios versus time (top and central panel for the NS and EW component, respectively) and corresponding time histories for station 3022.

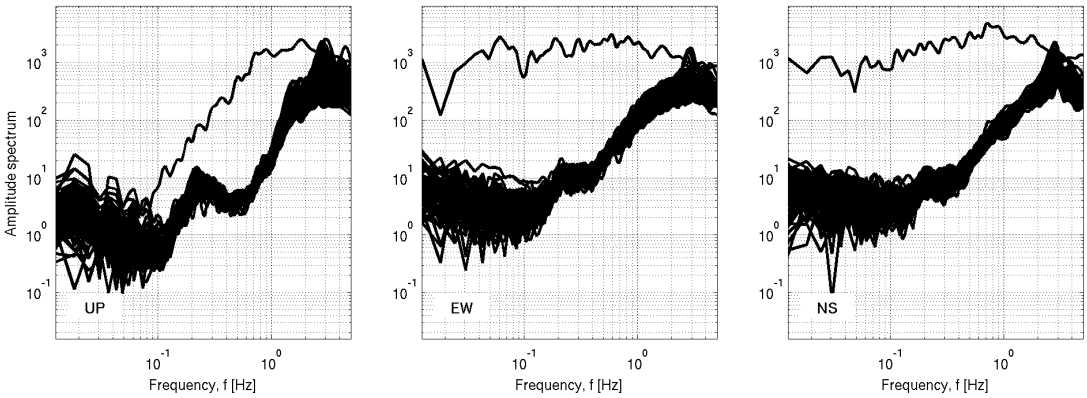

Figure 2b: Fourier spectra for each noise window at station 3022. Left) Vertical component spectra, center) E-W component spectra, right) N-S component spectra.

For each of the 15 used stations, 48 synchronized signal windows of 60 seconds were selected avoiding windows affected by local disturbance. These windows were in turn used to estimate the experimental Rayleigh-wave dispersion curves (using the vertical component of ground motion only) both by f-k and ESAC analysis.

The ESAC Rayleigh-wave dispersion curve was obtained minimizing the root mean square (RMS) of the differences between experimental and theoretical Bessel function values (**Figure 3**). Values that differ more than two standard deviations from those estimated by the best fitting functions (red circles in **Figure 3**) are automatically discarded and the procedure iteratively repeated. Furthermore, data are discarded also when their inter-station distance is longer than 1.5 times the relevant wavelength.

The f-k analysis offers the opportunity to verify if the requirements on the noise source distribution, necessary for the application of the ESAC method, were fulfilled. **Figure 4** and **Figure 5** show examples of the results for several frequencies of the frequency-wavenumber analysis using the Maximum Likelihood Method (MLM) and the Beam Forming (BF) respectively.

Figure 6 shows the good agreement between the Rayleigh wave dispersion curves estimated both with ESAC and f-k approaches. Only below 2.5 Hz the f-k analysis provides larger phase velocities.

An average *H/V* for the selected stations was computed by averaging the *H/V* calculated for each signal window (**Figure 7a**). The average *H/V* curves for the selected stations were in turn averaged to obtain a single *H/V* spectral ratio representative for the array, which was then used as input in the joint inversion procedure for the estimation of the S-wave velocity profile (**Figure 7b**).

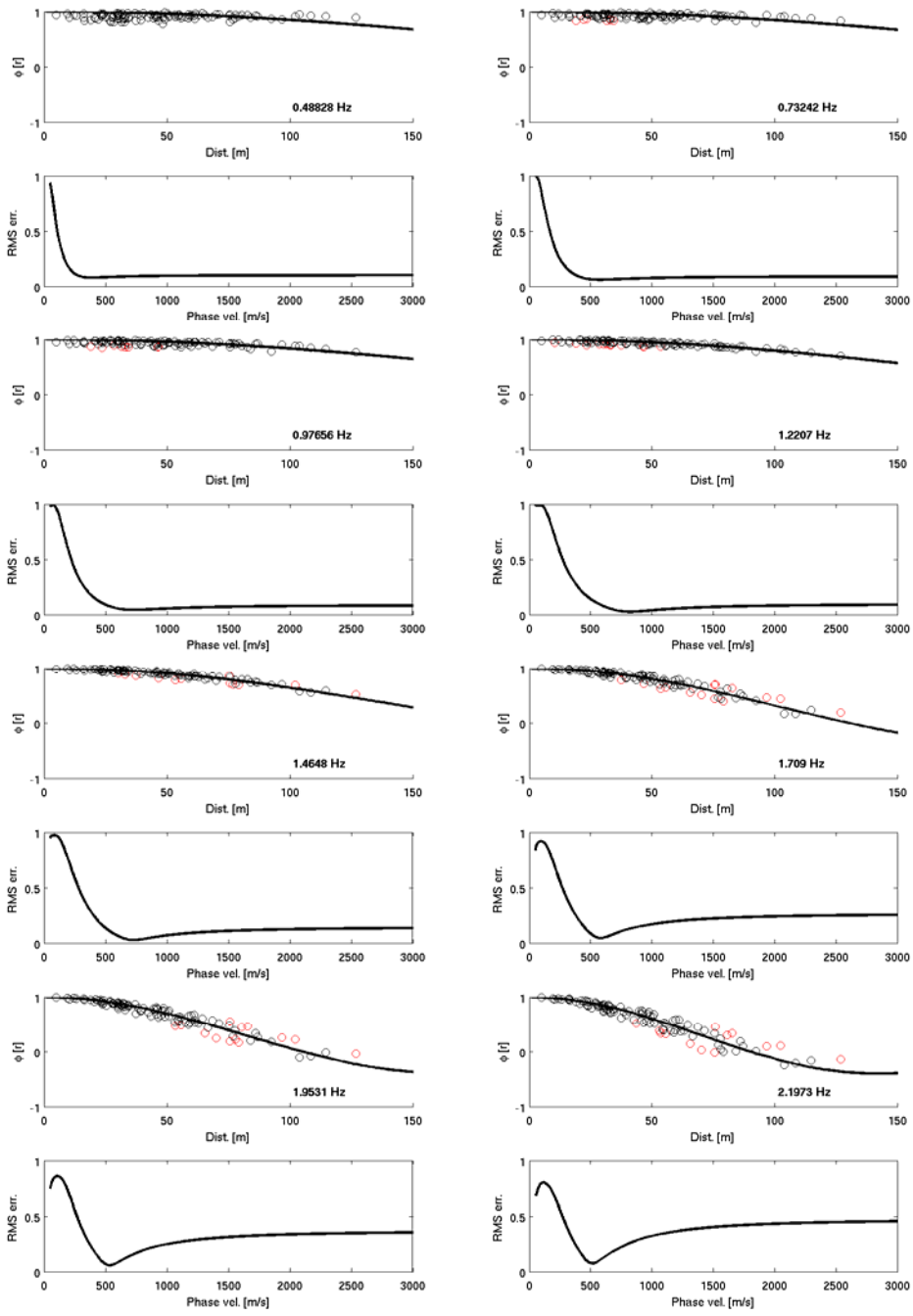

Figure 3: Experimental space-correlation function values versus distance (circles) for different frequencies. The red circles indicate values discarded. The black lines depict the estimated space-correlation function values for the phase velocity showing the best fit to the data. The bottom panels show the relevant root-mean square errors (RMS) versus phase velocity tested.

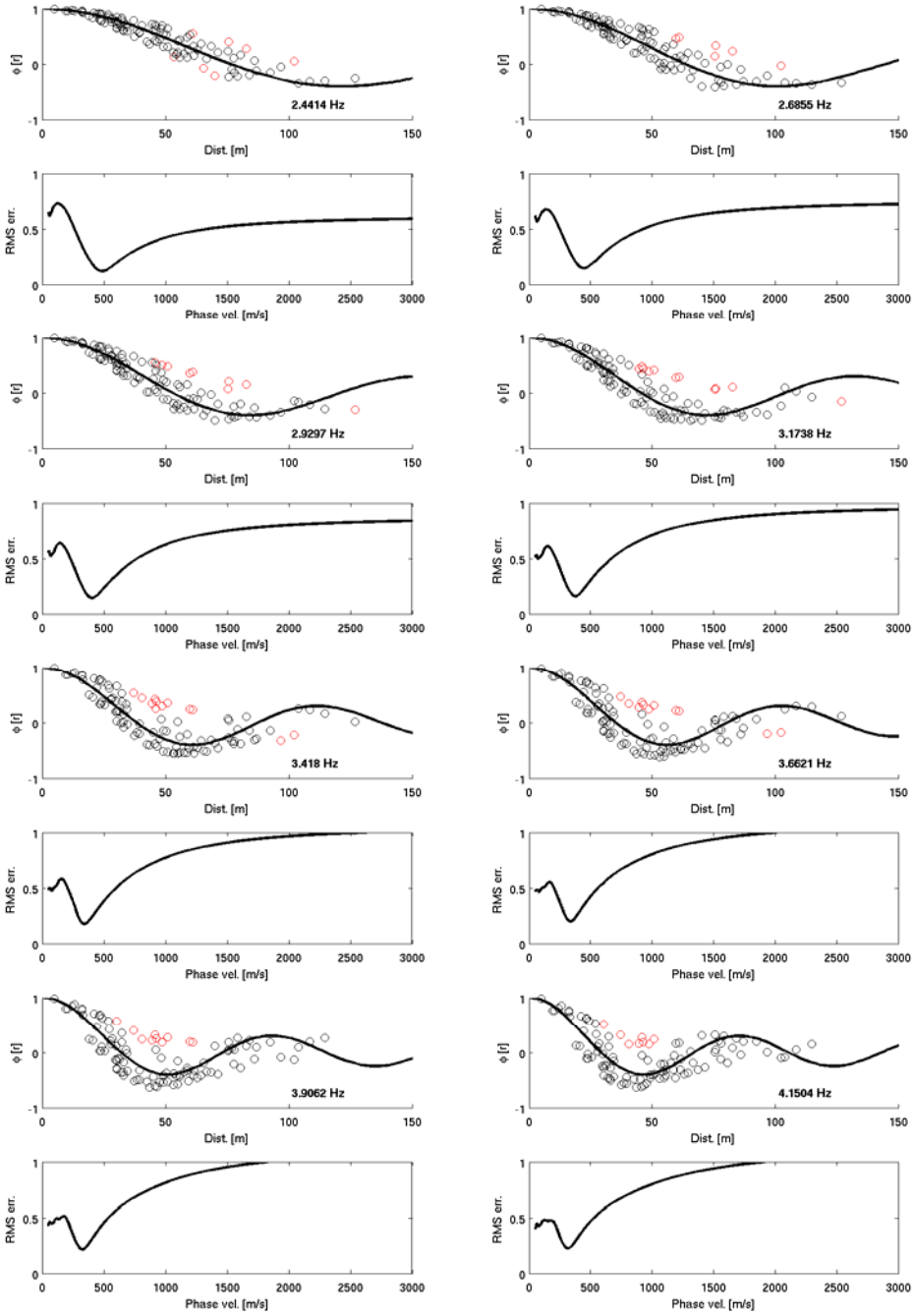

Figure 3: See previous caption.

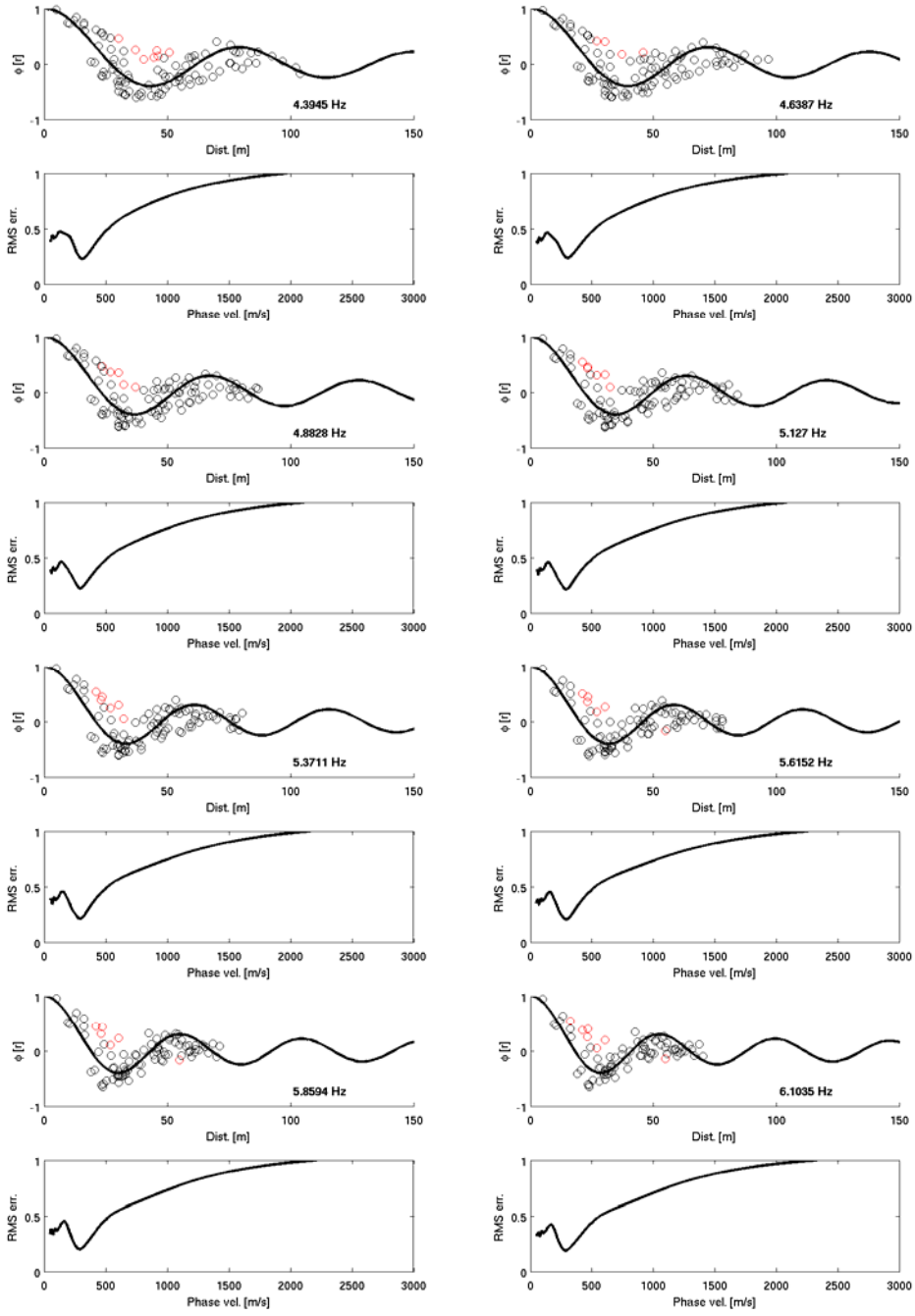

Figure 3: See previous caption.

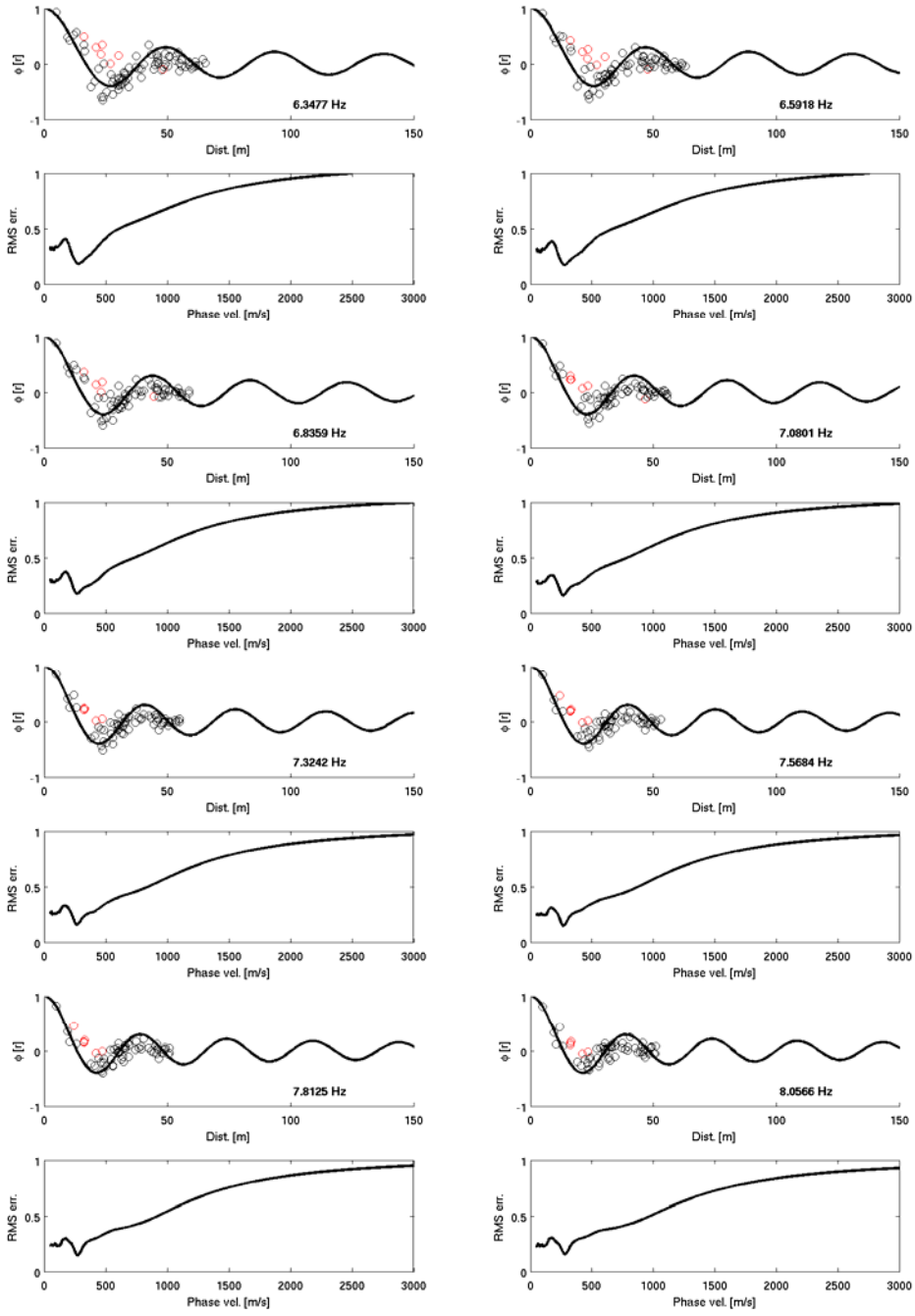

Figure 3: See previous caption.

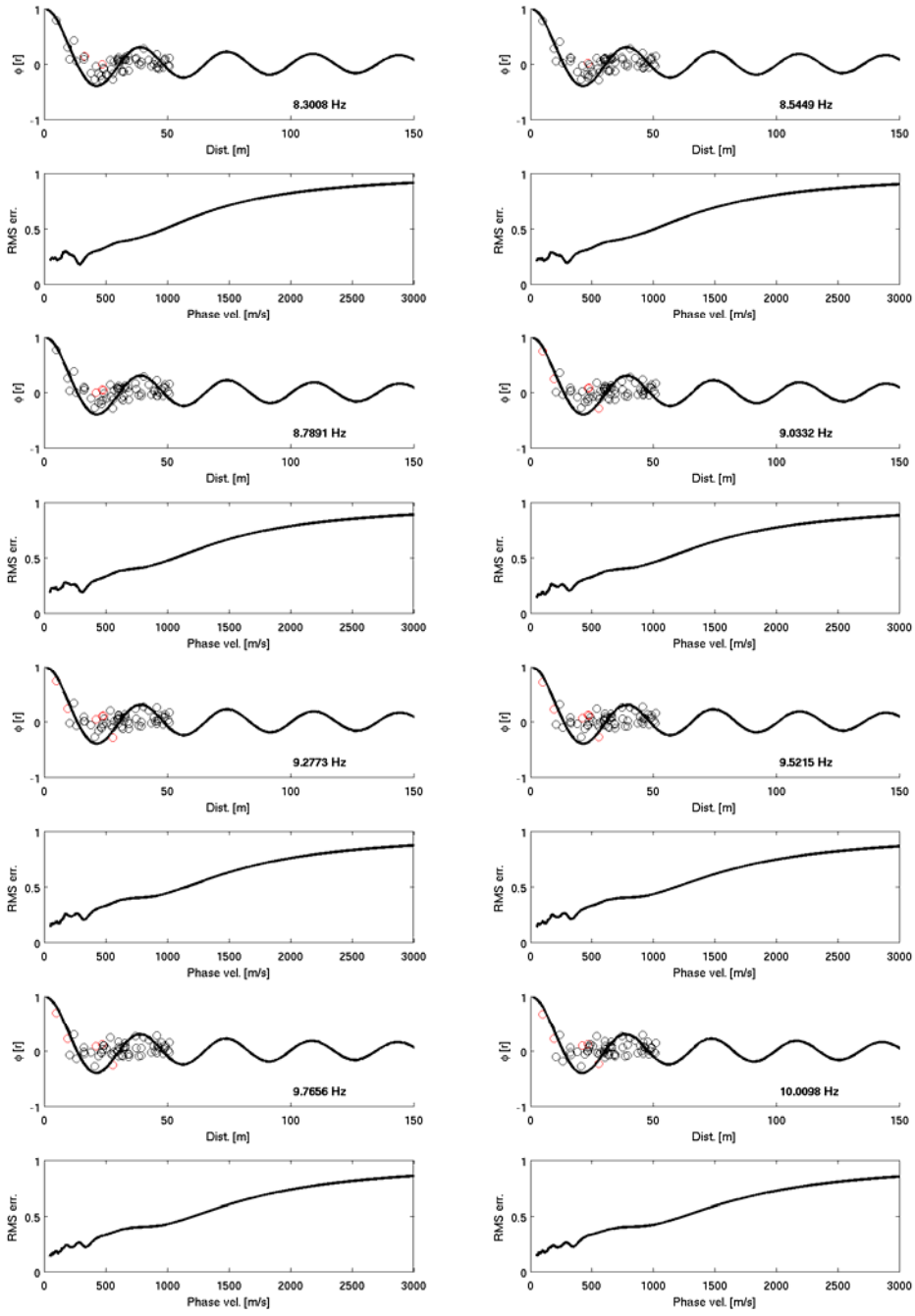

Figure 3: See previous caption.

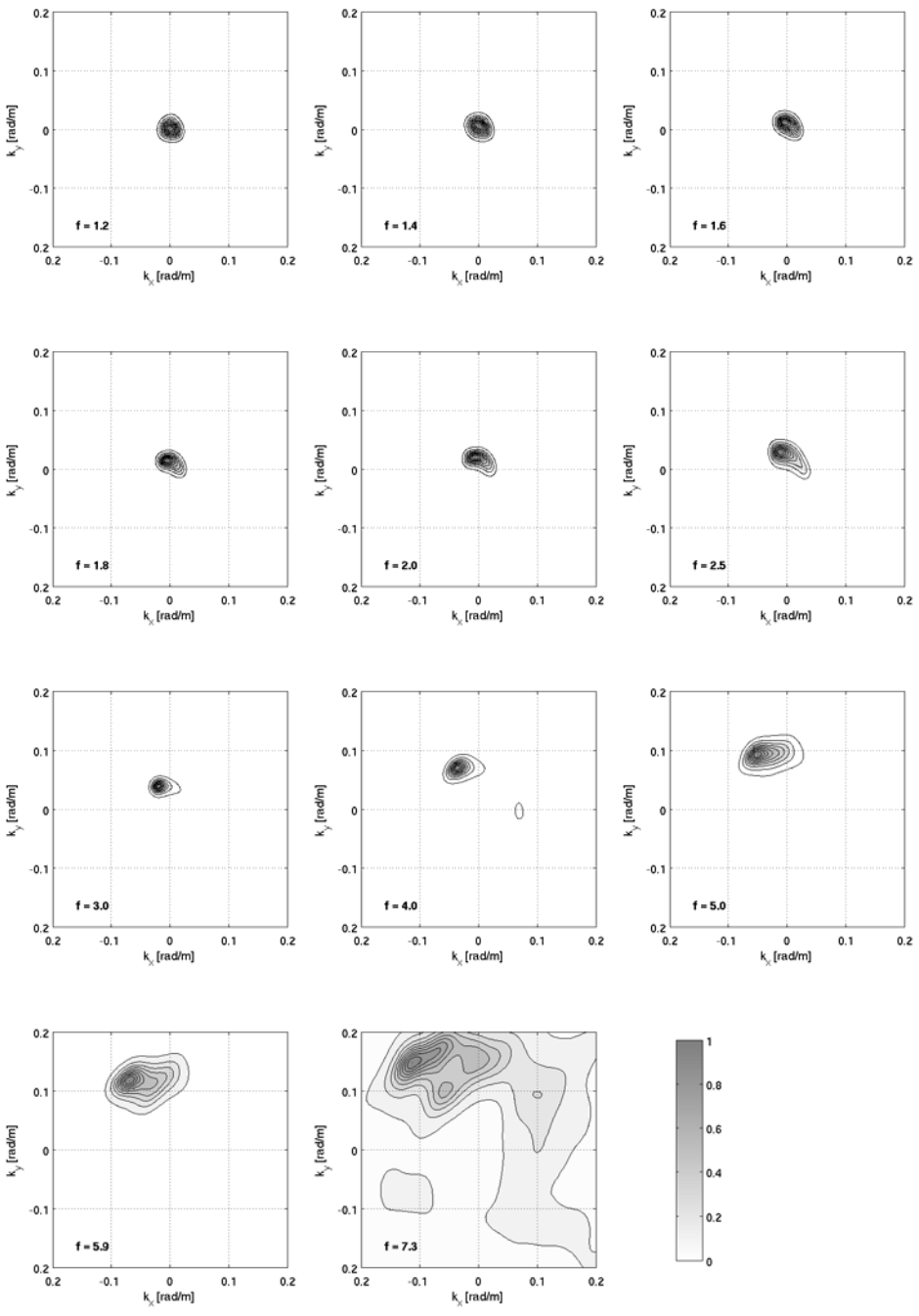

Figure 4: f-k power density function (MLM) at different frequencies (f, expressed in Hz).

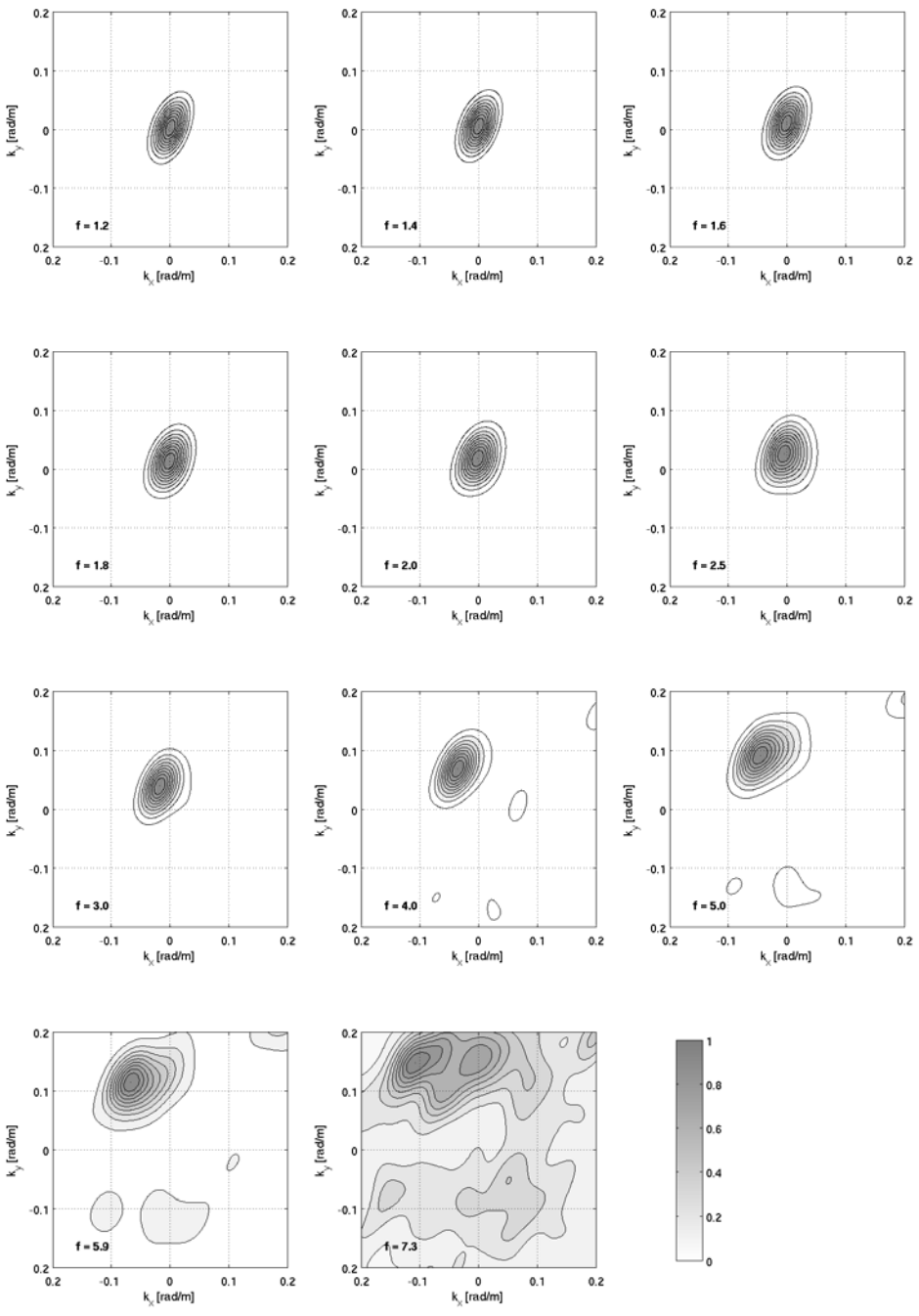

Figure 5: f-k power density function (BF) at different frequencies (f, expressed in Hz).

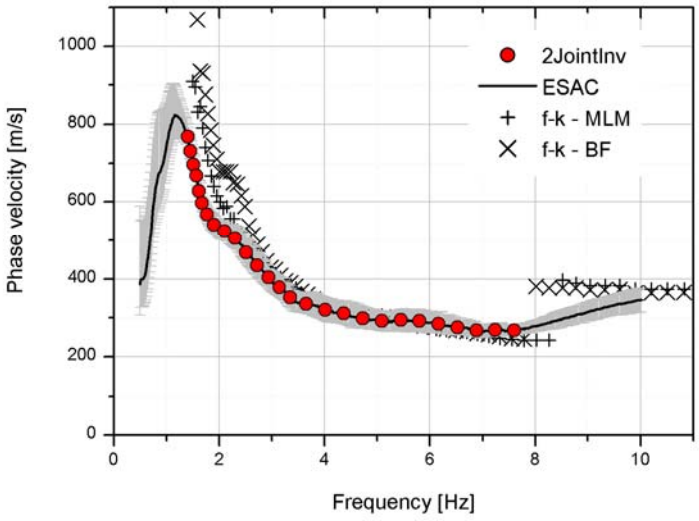

Figure 6: Comparison of experimental phase velocity estimated by the ESAC and the f-k (both for Beam Forming and Maximum Likelihood Method) methods. The red circles represent the values used for the joint inversion. The intervals (grey lines) around the observed ESAC phase velocities representing estimated uncertainties are obtained by calculating the square root of the covariance of the error function.

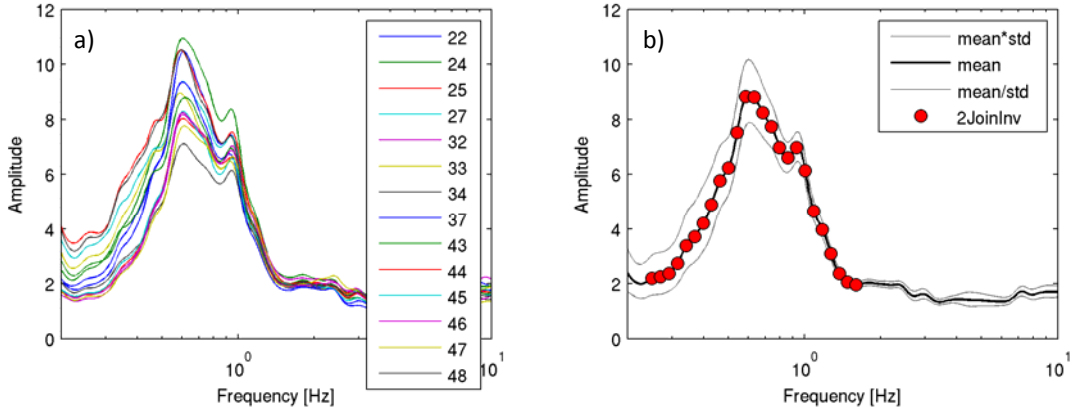

Figure 7: a) average *H/V* for the selected stations of the array (e.g. 06 stands for station 3006, 32 stands for station 3032, etc.) and b) the average H/V of the array. The red circles represent the values used for the joint inversion.

The inversion of dispersion and *H/V* curves to estimate the S-wave velocity profile was carried out fixing to 6 the number of layers overlying the half-space in the model (**Table 1**). Through a genetic algorithm a search over 80000 models was carried out. The inversion was repeated several times starting from different

seed numbers, that is to say from a different population of initial models. In this way it was possible to better explore the space of the solution.

Table 1: Ranges of values defined for the parameters used in the joint inversion.

	Shear wave velocity, V_S [m/s]		Thickness, h [m]		Density, ρ [ton/m^3]
Layer	MIN	MAX	MIN	MAX	
#1	150	400	10	40	1.9
#2	200	500	10	50	1.9
#3	250	600	10	60	2.0
#4	300	700	20	100	2.1
#5	400	800	20	100	2.2
#6	500	900	50	350	2.2
Half-space	600	1800	Infinite		2.3

During the inversion procedure the thickness and the shear wave velocity for each layer could be varied within the pre-defined ranges. On the contrary, for each layer, density was assigned *a priori*, while P-wave velocity (V_P) was calculated through the values of the S-wave velocity Vs via the equation: $V_P\,[\mathrm{m/s}] = 1.1 \cdot V_S + 1290$.

The models are selected by means of a cost function which take in account the agreement between the theoretical *H/V* and Rayleigh-wave dispersion curves with the observed ones. In this application, after trial and error test, the weight of 0.05, that allowed the best balanced fit of dispersion and H/V curves, was adopted.

Discussion of the results

In **Figure 8a** all the models tested during the inversion are depicted (gray lines). The best fit model (white line) and the models lying inside the 10% range of the minimum cost (black lines) function are highlighted. The agreement between experimental and theoretical Rayleigh wave dispersion curves (**Figure 8c**) is very good and, considering the wavelengths related to the dispersion curve frequency range, the V_S profile between 15 to about 180 metres is likely to be well constrained. Therefore, since below this depth the profile is constrained by the H/V curve alone, we prefer to show, in **Figure 8a** and **Table 2**, the V_S profile only within the depth range were both curves contribute to the inversion.

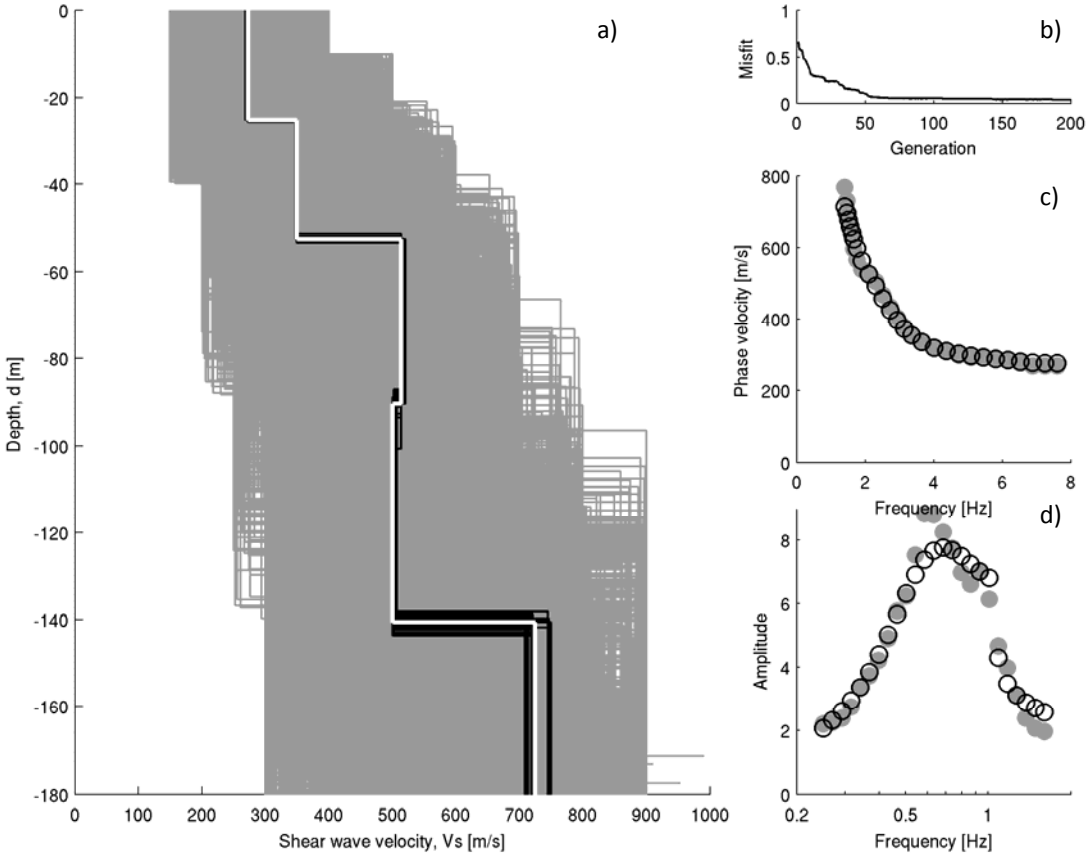

Figure 8: a) Tested models (grey lines), the minimum cost model (white line) and models lying inside the minimum cost + 10% range (black lines) for the GRM station; b) the misfit versus generation values; c) experimental (grey circles) and estimated (white circles – relevant to the minimum cost model) phase velocities; d) experimental (grey circles) and estimated (white circles – relevant to the minimum cost model) *H/V* ratio curves.

Table 2: Shear wave velocity model at the GRM station.

Shear wave velocity, V_S [m/s]	Thickness, h [m]
272.5	25.2
349.4	27.4
513.5	37.8
500.8	50.1
724.7	

APPLICATION OF SURFACE WAVE METHODS

FOR SEISMIC SITE CHARACTERIZATION

STATION CODE:

LGN

Responsible: Stefano Parolai[1]

Co-workers: Rodolfo Puglia[2], Matteo Picozzi[1]

1) Helmholtz Centre Potsdam - German Research Centre For Geosciences (GFZ), Helmholtzstraße 7, 14467 Potsdam, Germany
2) Istituto Nazionale di Geofisica e Vulcanologia (INGV), Sezione di Milano-Pavia, via Bassini 15, 20133 Milano, Italy

Introduction note

Details and references about *in-situ* measurement, Rayleigh wave dispersion and H/V curves estimate and inversion procedure here reported, can be found in the research reports of DPC-INGV S4 Project 2007-2009: Deliverables 6 and 7 at http://esse4.mi.ingv.it .

Testing equipment

The array measurements were performed using 15 EDL 24bit acquisition systems equipped with short-period Mark-L4-C-3D 1Hz sensors and GPS timing (**Figure 1**). The inter-station distances in the array ranged between 3.5 m to 102 meters. The stations worked contemporary for about 1 hour, recording noise at 200 s.p.s., which is adequate for the short inter-station distances considered.

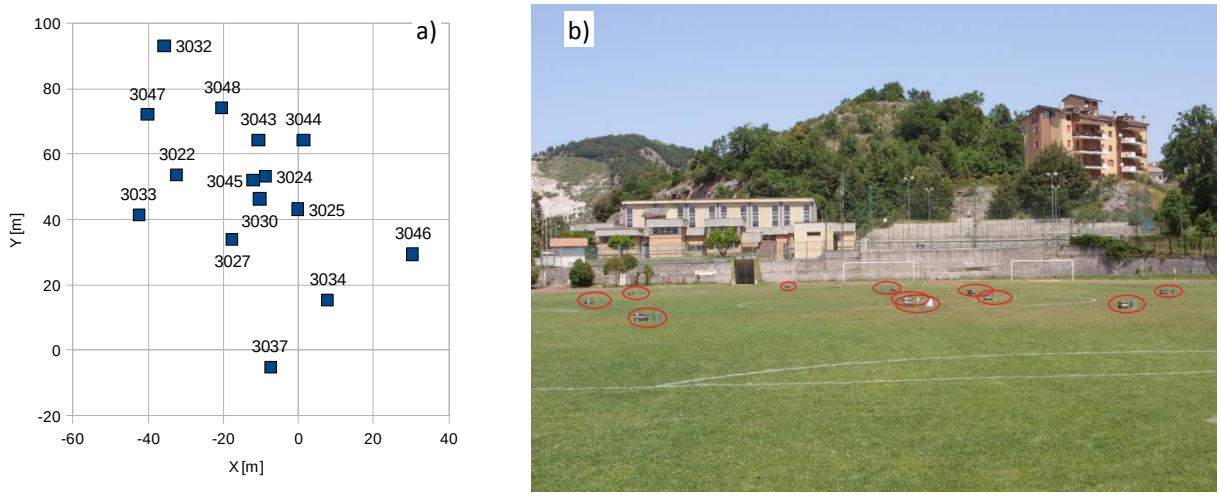

Figure 1: a) Geometry of the array. b) The field measurements.

Processing overview

The Rayleigh wave dispersion curve was estimated by analysing the vertical component of the recorded microtremors. In particular, the Extended Spatial Auto Correlation (ESAC) and the Frequency-Wavenumber (f-k) methods were adopted.

Only Rayleigh wave dispersion curve were used to estimate the local S-wave velocity profile. The non-linear inversions were performed using a genetic algorithm which does not rely upon an explicit starting model

and allows the identification of a solution close to the global minimum. The forward modeling of Rayleigh wave phase velocities curve was performed using the modified Thomson-Haskell method, under the assumption of vertically heterogeneous 1D earth models. The validity of this assumption was investigated by computing the *H/V* curve for each station of the array using the recorded data. The modeling of the dispersion curve during the inversions was not restricted to the fundamental mode only, but the possibility that higher modes can participate to define the observed dispersion curve is allowed.

Data analysis

The first step of the analysis consists in a visual inspection of the recordings at all stations. In particular, in order to identify malfunctioning of one station or channel and to select signal windows suitable for the H/V analysis, the quality of the recording was evaluated analysing (1) the signal stationarity in the time domain (**Figure 2a**), (2) the relevant unfiltered Fourier spectra (**Figure 2b**), and (3) the *H/V* variation over time (**Figure 2a**).

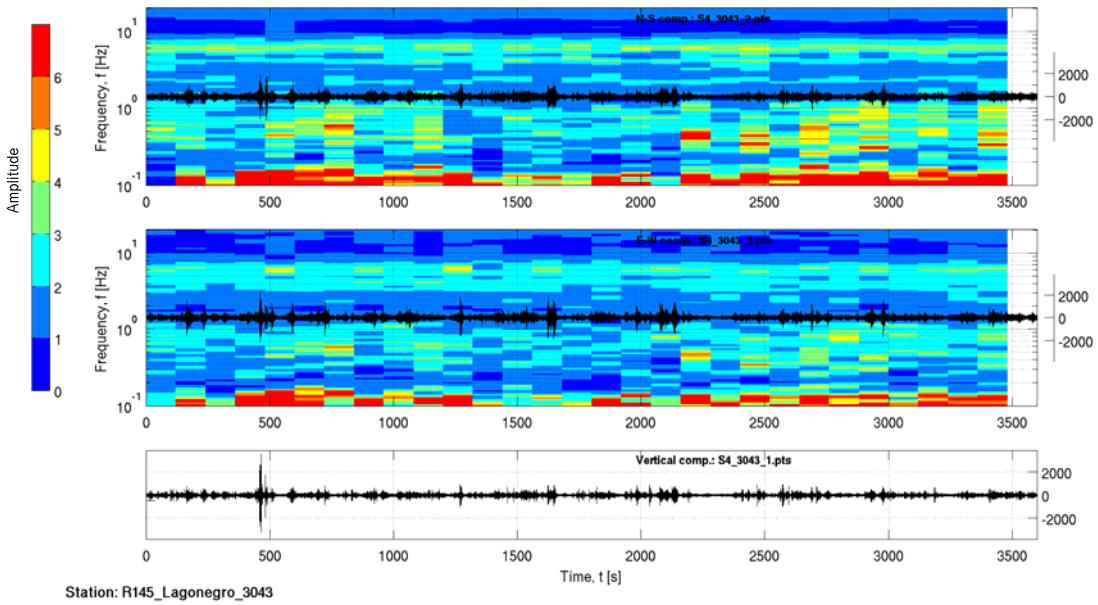

Figure 2a: *H/V* spectral ratios versus time (top and central panel for the NS and EW component, respectively) and corresponding time histories for station 3043.

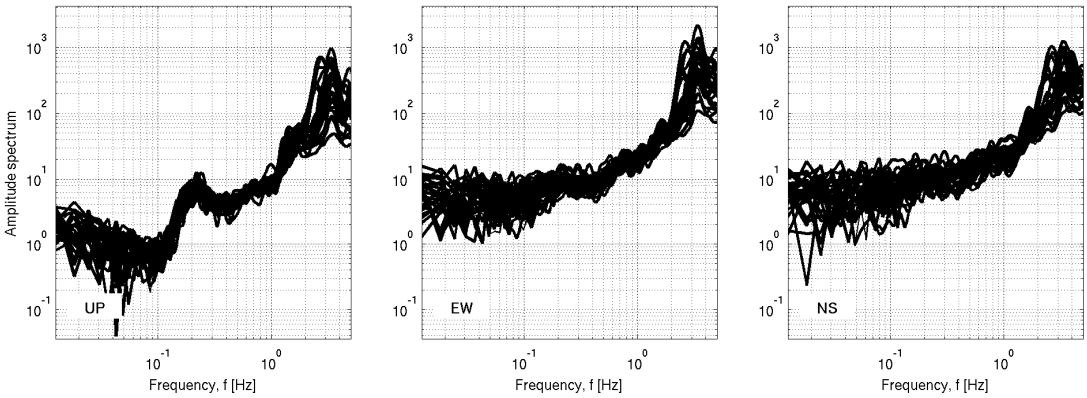

Figure 2b: Fourier spectra for each noise window at station 3043. Left) Vertical component spectra, center) E-W component spectra, right) N-S component spectra.

For each of the 15 used stations, 30 synchronized signal windows of 60 seconds were selected avoiding windows affected by local disturbance. These windows were in turn used to estimate the experimental Rayleigh-wave dispersion curves (using the vertical component of ground motion only) both by f-k and ESAC analysis.

The ESAC Rayleigh-wave dispersion curve was obtained minimizing the root mean square (RMS) of the differences between experimental and theoretical Bessel function values (**Figure 3**). Values that differ more than two standard deviations from those estimated by the best fitting functions (red circles in **Figure 3**) are automatically discarded and the procedure iteratively repeated. Furthermore, data are discarded also when their inter-station distance is longer than the relevant wavelength.

The f-k analysis offers the opportunity to verify if the requirements on the noise source distribution, necessary for the application of the ESAC method, were fulfilled. **Figure 4** and **Figure 5** show examples of the results for several frequencies of the frequency-wavenumber analysis using the Maximum Likelihood Method (MLM) and the Beam Forming (BF) respectively.

Figure 6 shows the roughly good agreement between the Rayleigh wave dispersion curves estimated both with ESAC and f-k MLM approaches. Already below 5 Hz the f-k MLM analysis provides larger phase velocities.

An average *H/V* for the selected stations was computed by averaging the *H/V* calculated for each signal window (**Figure 7**). Due to the significant differences between the *H/V* curves under 1Hz, a single *H/V* spectral ratio representative for the array could not be estimated, then the estimation of the S-wave velocity profile was based only on the Rayleigh wave dispersion curve. Anyway, observing the *H/V* curves above 1 Hz, the vertically heterogeneous 1D earth model assumption seems to be satisfied at least in the investigated soil volume.

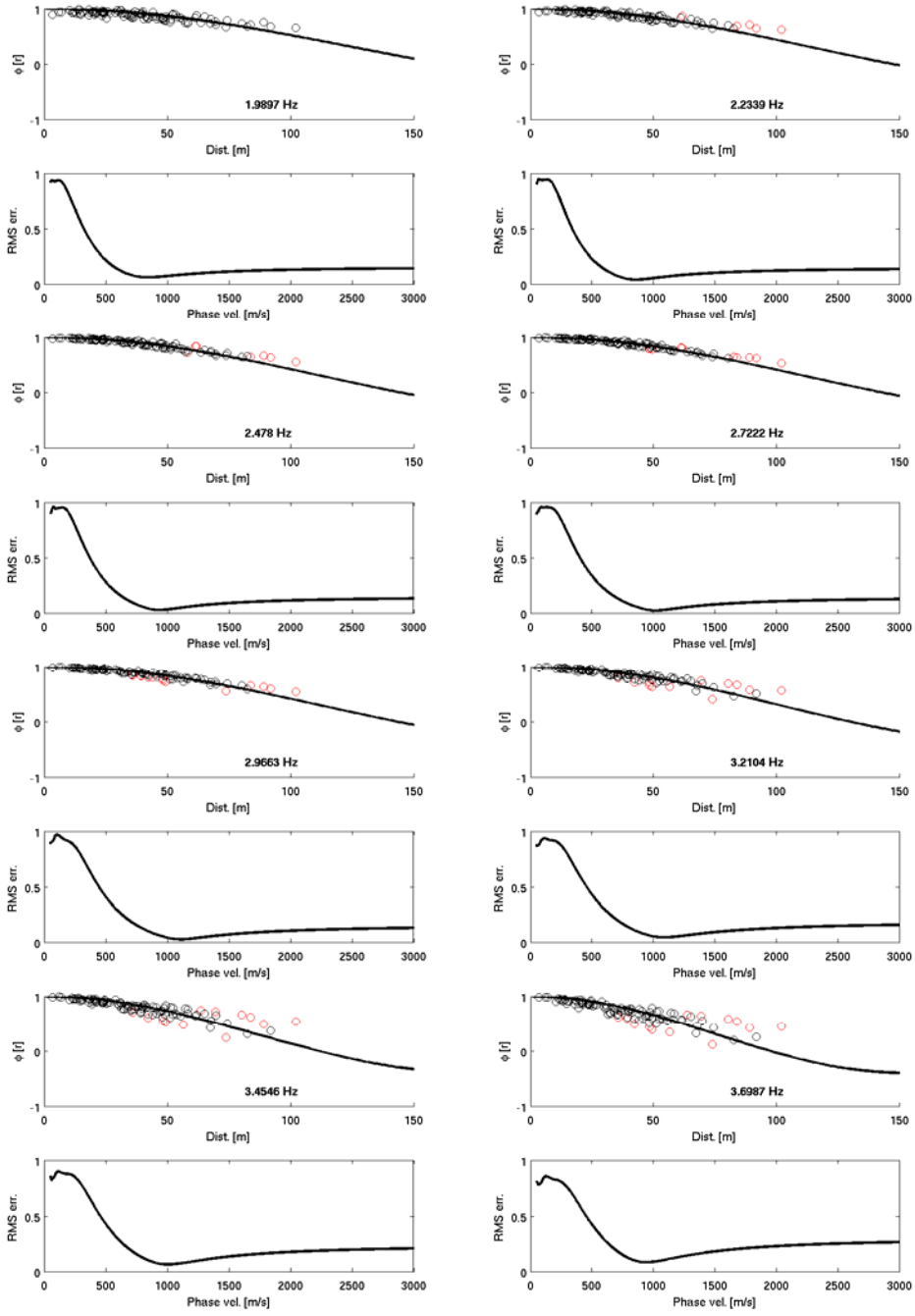

Figure 3: Experimental space-correlation function values versus distance (circles) for different frequencies. The red circles indicate values discarded. The black lines depict the estimated space-correlation function values for the phase velocity showing the best fit to the data. The bottom panels show the relevant root-mean square errors (RMS) versus phase velocity tested.

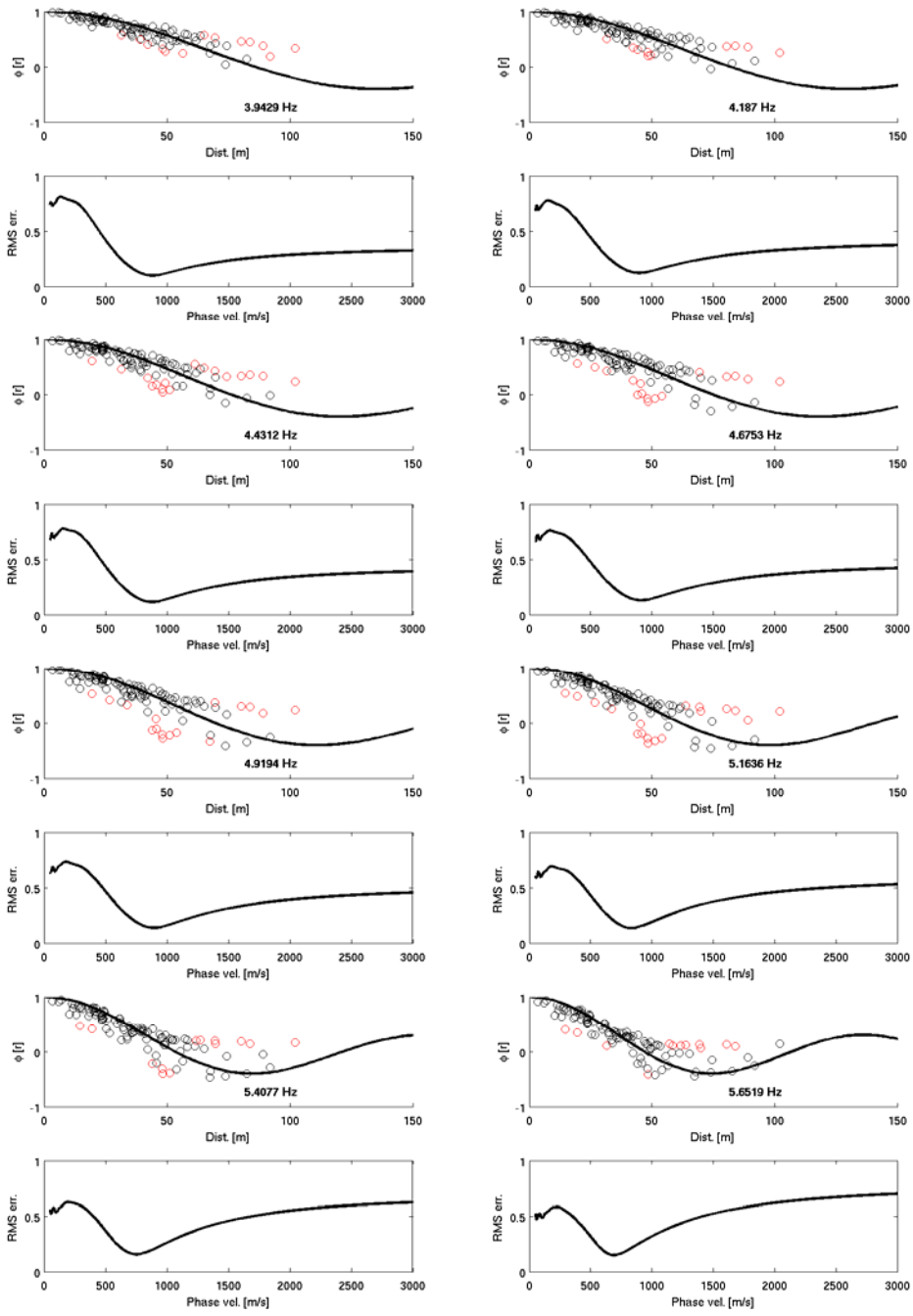

Figure 3: See previous caption.

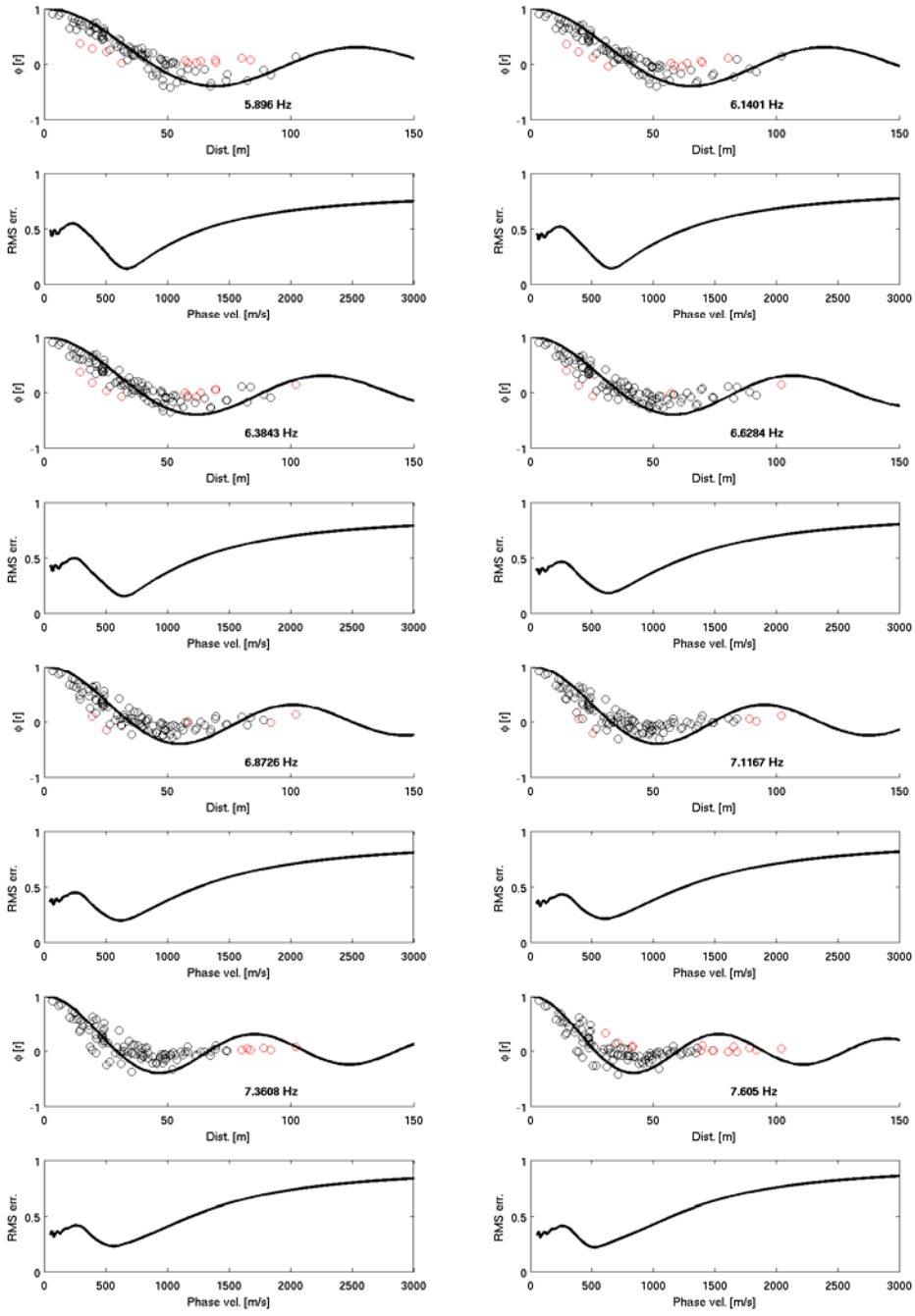

Figure 3: See previous caption.

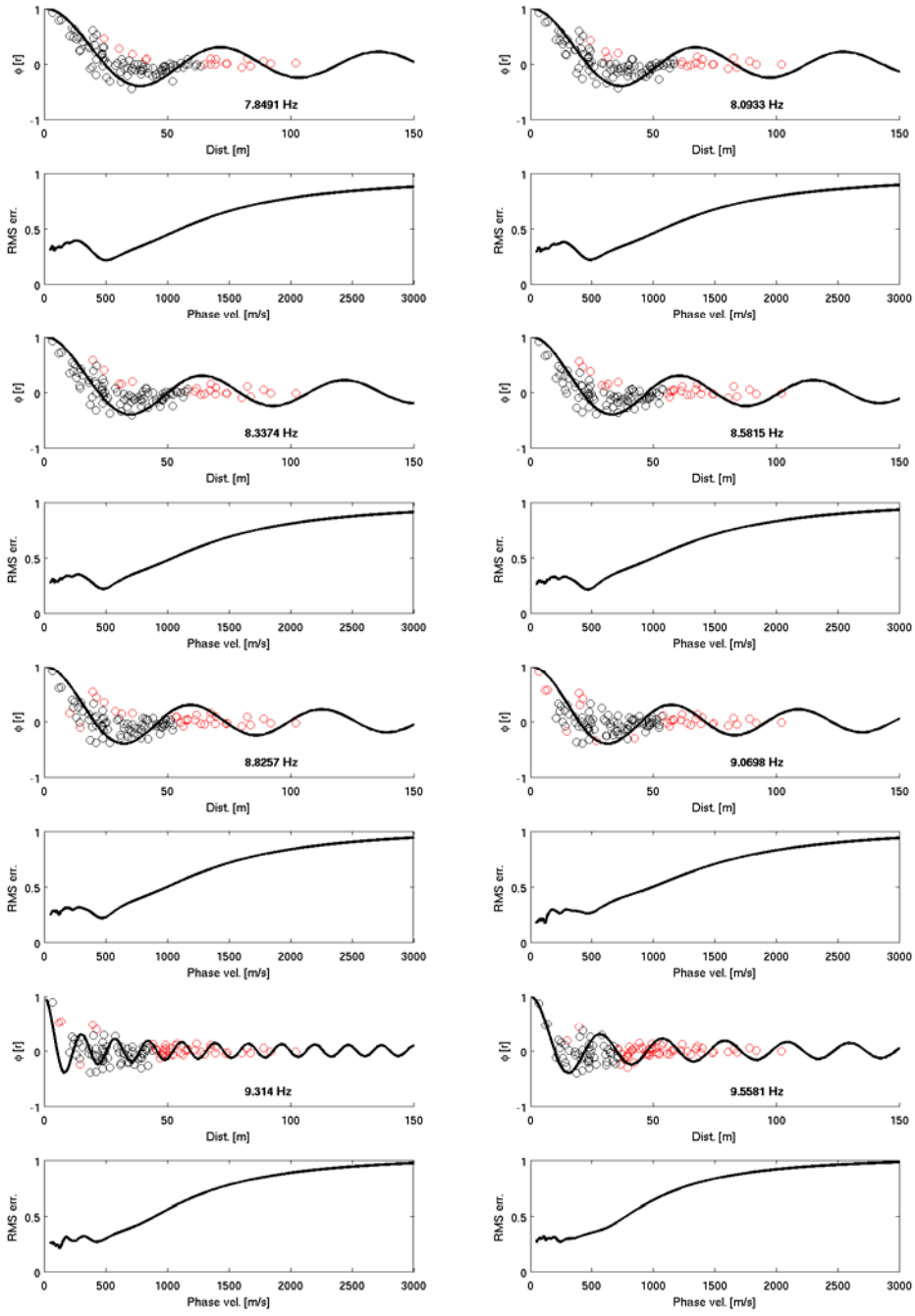

Figure 3: See previous caption.

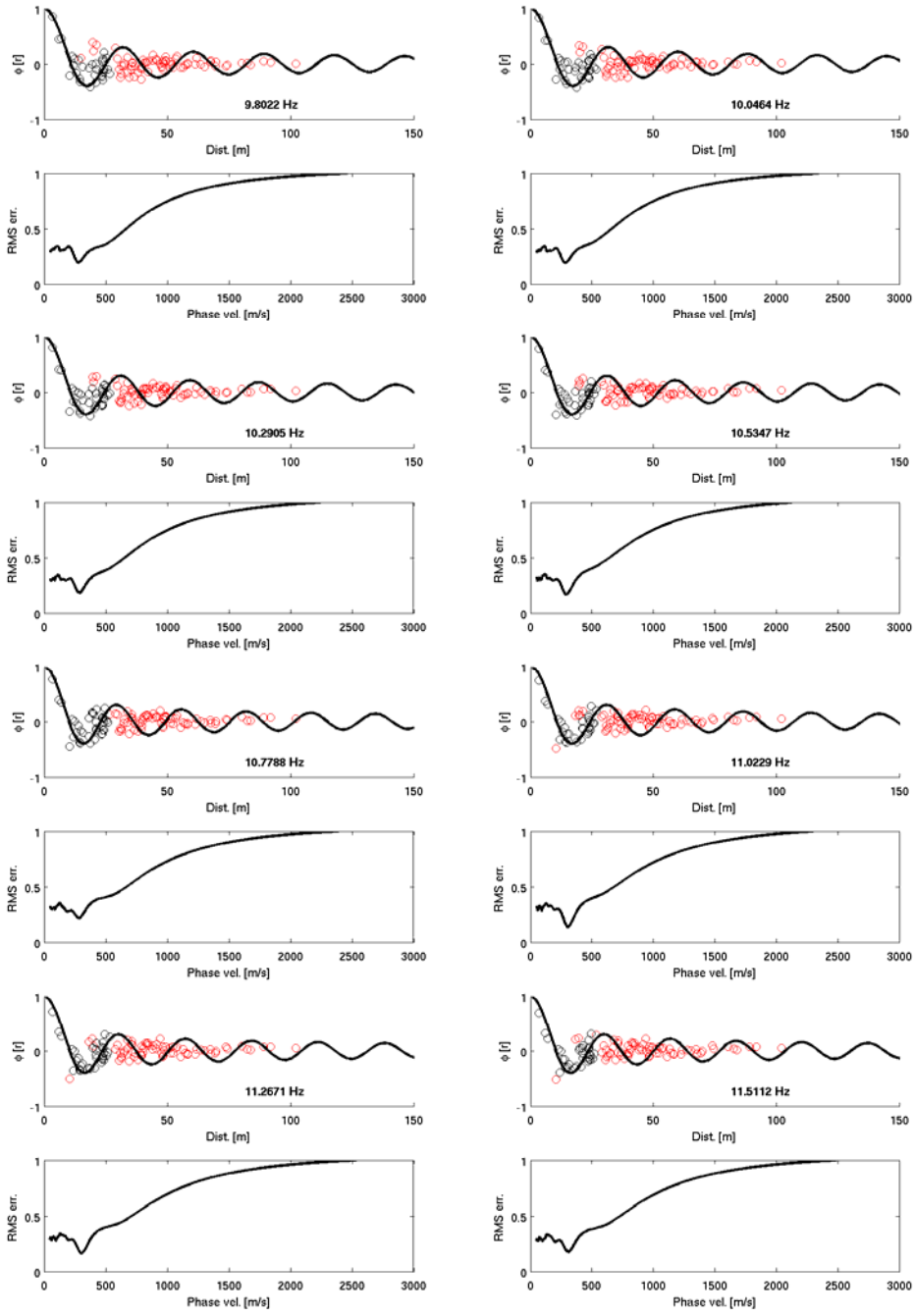

Figure 3: See previous caption.

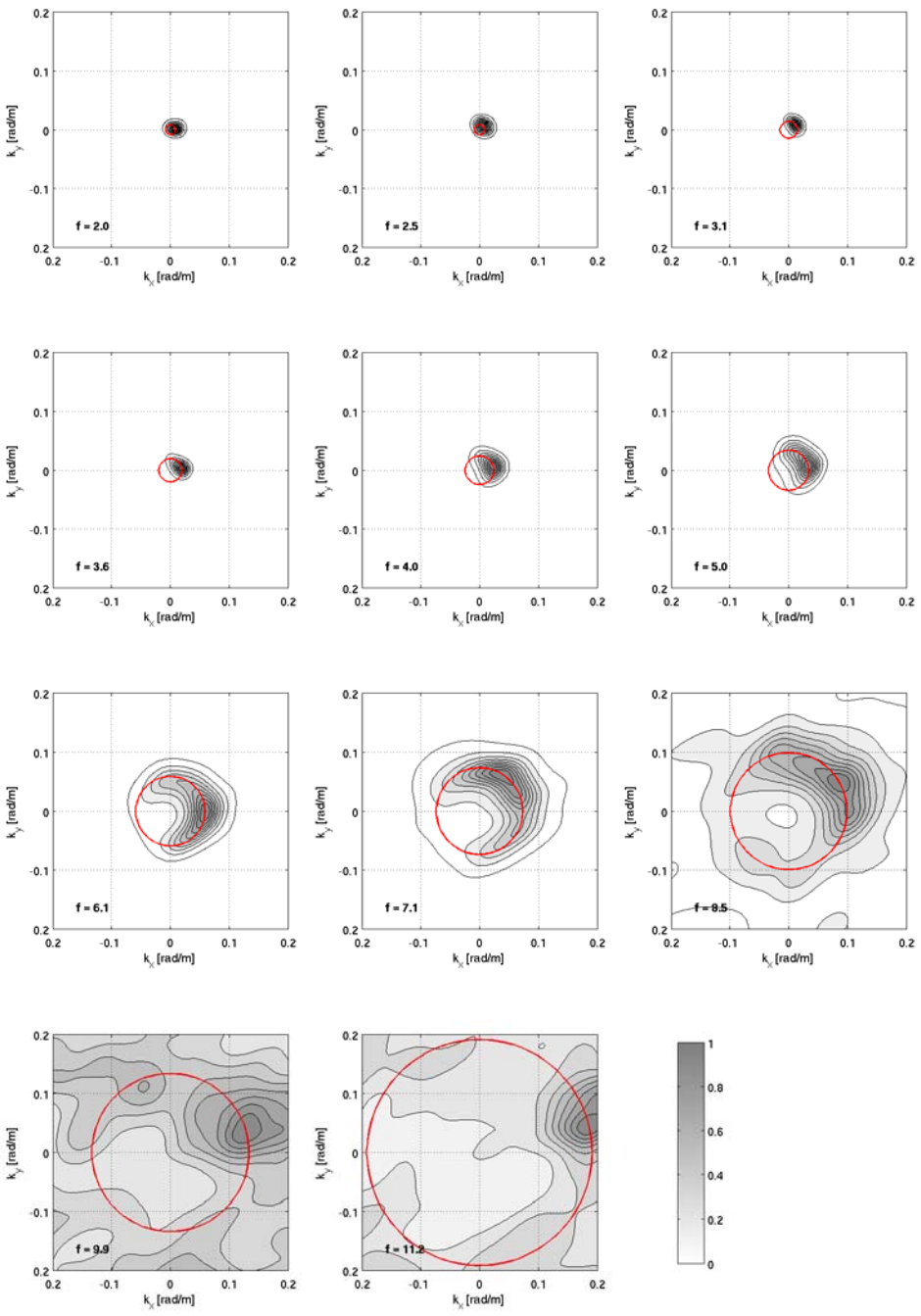

Figure 4: f-k power density function (MLM) at different frequencies (f, expressed in Hz). The red circles joints points with the same *k* value, corresponding to the maximum used to estimate the phase velocity.

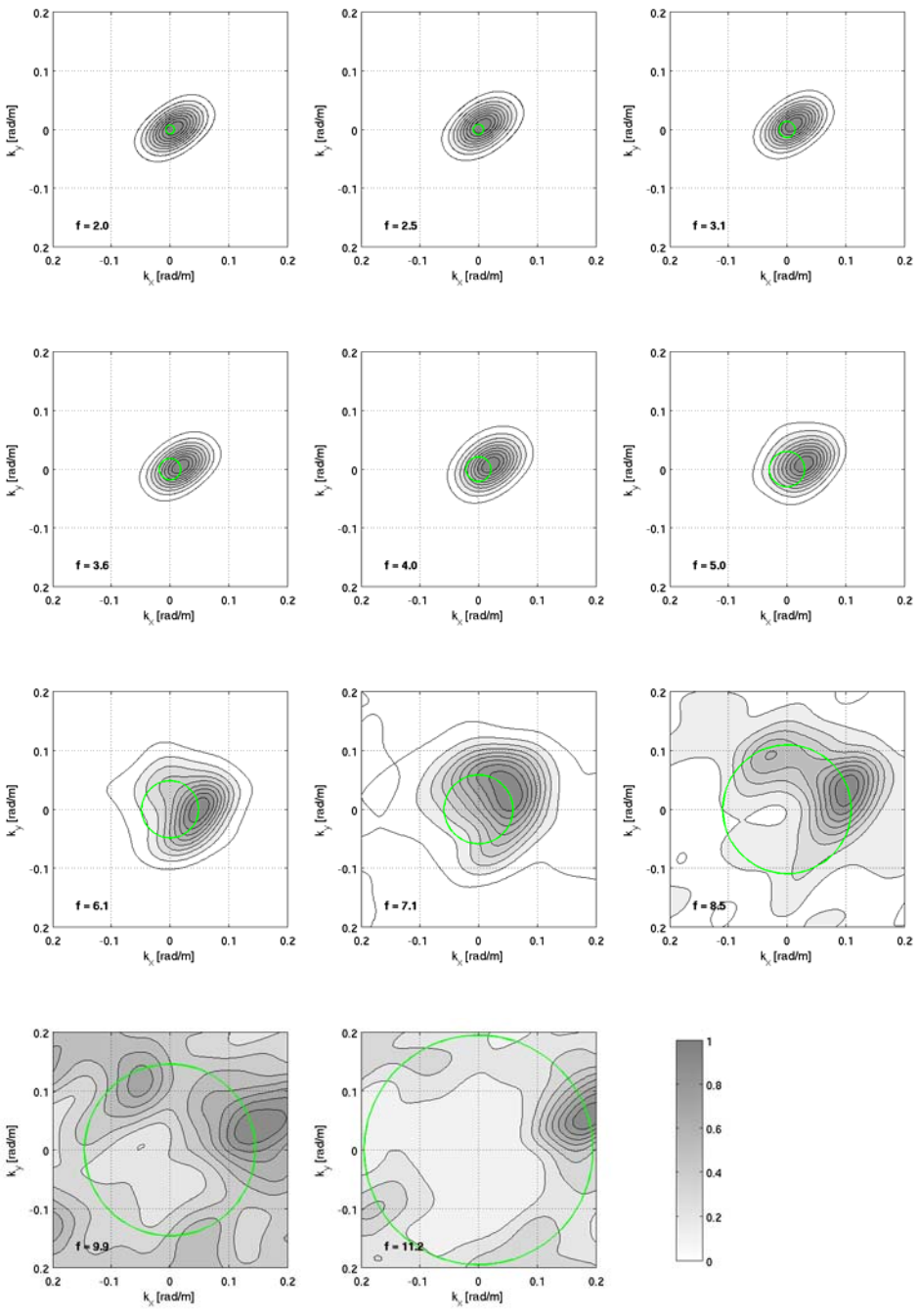

Figure 5: f-k power density function (BF) at different frequencies (f, expressed in Hz). The green circles joints points with the same *k* value, corresponding to the maximum used to estimate the phase velocity.

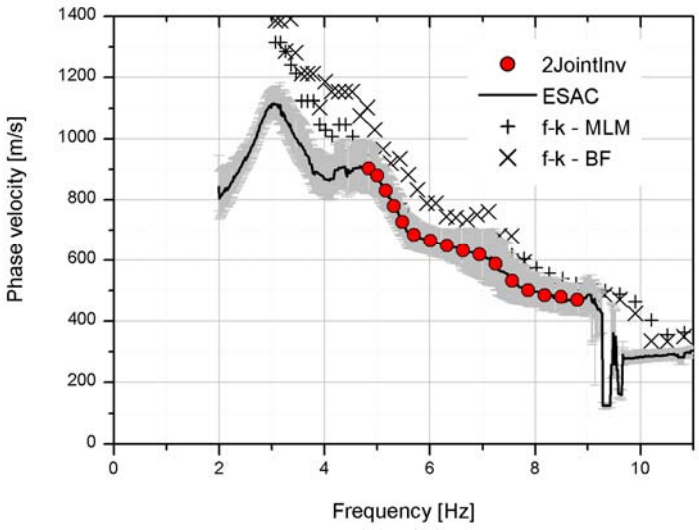

Figure 6: Comparison of experimental phase velocity estimated by the ESAC and the f-k (both for Beam Forming and Maximum Likelihood Method) methods. The red circles represent the values used for the joint inversion. The intervals (grey lines) around the observed ESAC phase velocities representing estimated uncertainties are obtained by calculating the square root of the covariance of the error function.

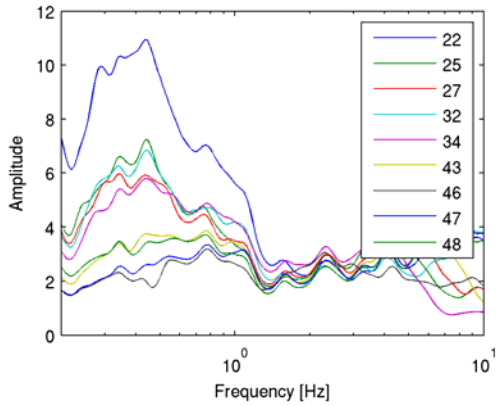

Figure 7: average *H/V* for the selected stations of the array (e.g. 22 stands for station 3022, etc.).

The inversion of dispersion curve to estimate the S-wave velocity profile was carried out fixing to 4 the number of layers overlying the half-space in the model (**Table 1**). Through a genetic algorithm a search over 40000 models was carried out. The inversion was repeated several times starting from different seed

numbers, that is to say from a different population of initial models. In this way it was possible to better explore the space of the solution.

Table 1: Ranges of values defined for the parameters used in the joint inversion.

	Shear wave velocity, V_S [m/s]		Thickness, h [m]		Density, ρ [ton/m^3]
Layer	MIN	MAX	MIN	MAX	
#1	200	500	10	40	1.9
#2	400	800	10	50	1.9
#3	500	950	10	50	2.0
#4	600	1150	20	80	2.1
Half-space	1000	2500	Infinite		2.3

During the inversion procedure the thickness and the shear wave velocity for each layer could be varied within the pre-defined ranges. On the contrary, for each layer, density was assigned *a priori*, while P-wave velocity (V_P) was calculated through the values of the S-wave velocity Vs via the equation: $V_P\,[\mathrm{m/s}] = 1.1 \cdot V_S + 1290$.

Discussion of the results

In **Figure 8a** all the models tested during the inversion are depicted (gray lines). The best fit model (white line) and the models lying inside the 10% range of the minimum cost (black lines) function are highlighted. The agreement between experimental and theoretical Rayleigh wave dispersion curves (**Figure 8c**) is good and, considering the wavelengths related to the dispersion curve frequency range, the V_S profile between 15 to about 55 metres is likely to be well constrained. Therefore, we prefer to show, in **Figure 8a** and **Table 2**, the V_S profile only within this depth range.

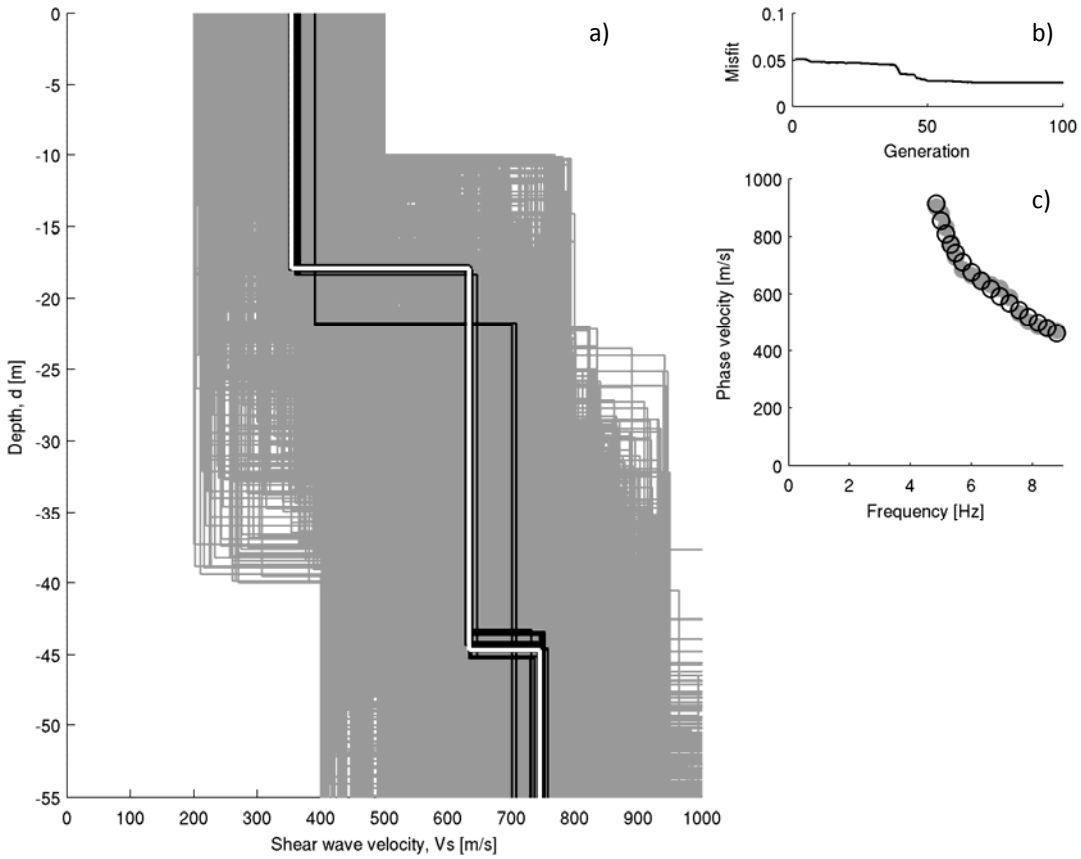

Figure 8: a) Tested models (grey lines), the minimum cost model (white line) and models lying inside the minimum cost + 10% range (black lines) for the LGN station; b) the misfit versus generation values; c) experimental (grey circles) and estimated (white circles – relevant to the minimum cost model) phase velocities.

Table 2: Shear wave velocity model at the LGN station.

Shear wave velocity, V_S [m/s]	Thickness, h [m]
354.1	17.9
633.7	26.8
745.3	

APPLICATION OF SURFACE WAVE METHODS

FOR SEISMIC SITE CHARACTERIZATION

STATION CODE:

MDN

Responsible: Stefano Parolai[1]

Co-workers: Rodolfo Puglia[2], Matteo Picozzi[1]

1) Helmholtz Centre Potsdam - German Research Centre For Geosciences (GFZ), Helmholtzstraße 7, 14467 Potsdam, Germany
2) Istituto Nazionale di Geofisica e Vulcanologia (INGV), Sezione di Milano-Pavia, via Bassini 15, 20133 Milano, Italy

Introduction note

Details and references about *in-situ* measurement, Rayleigh wave dispersion and H/V curves estimate and inversion procedure here reported, can be found in the research reports of DPC-INGV S4 Project 2007-2009: Deliverables 6 and 7 at http://esse4.mi.ingv.it .

Testing equipment

The array measurements were performed using 17 EDL 24bit acquisition systems equipped with short-period Mark-L4-C-3D 1Hz sensors and GPS timing (**Figure 1**). The inter-station distances in the array ranged between 5.0 m to 218 meters. The stations worked contemporary for about 1 hour and 30 minutes, recording noise at 200 s.p.s., which is adequate for the short inter-station distances considered.

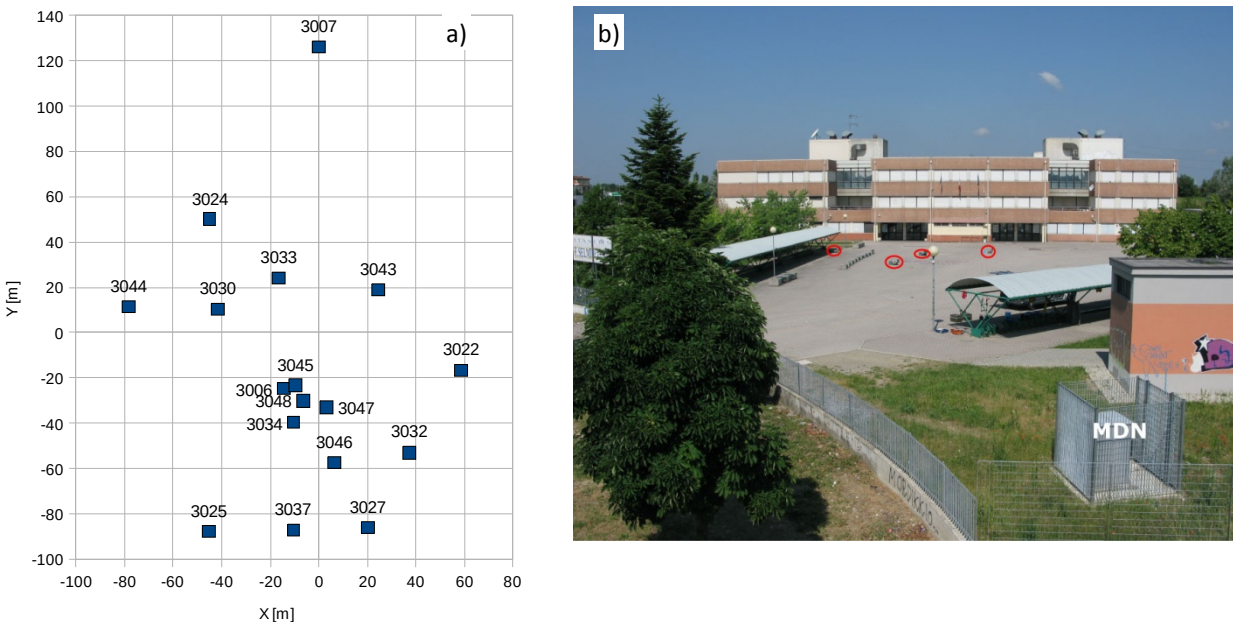

Figure 1: a) Geometry of the array. b) The field measurements.

Processing overview

The Rayleigh wave dispersion curve was estimated by analysing the vertical component of the recorded microtremors. In particular, the Extended Spatial Auto Correlation (ESAC) and the Frequency-Wavenumber (f-k) methods were adopted.

Rayleigh wave dispersion and *H/V* ratio curves were both used to estimate the local S-wave velocity profile, using a joint inversion scheme. The non-linear inversions were performed using a genetic algorithm which does not rely upon an explicit starting model and allows the identification of a solution close to the global minimum. The forward modeling of Rayleigh wave phase velocities and *H/V* curves was performed using the modified Thomson-Haskell method, under the assumption of vertically heterogeneous 1D earth models. The validity of this assumption was investigated by computing the *H/V* curve for each station of the array using the recorded data. The modeling of both the dispersion and *H/V* ratio curves during the inversions was not restricted to the fundamental mode only, but the possibility that higher modes can participate to define the observed dispersion and *H/V* curves is allowed.

Data analysis

The first step of the analysis consists in a visual inspection of the recordings at all stations. In particular, in order to identify malfunctioning of one station or channel and to select signal windows suitable for the H/V analysis, the quality of the recording was evaluated analysing (1) the signal stationarity in the time domain (**Figure 2a**), (2) the relevant unfiltered Fourier spectra (**Figure 2b**), and (3) the *H/V* variation over time (**Figure 2a**).

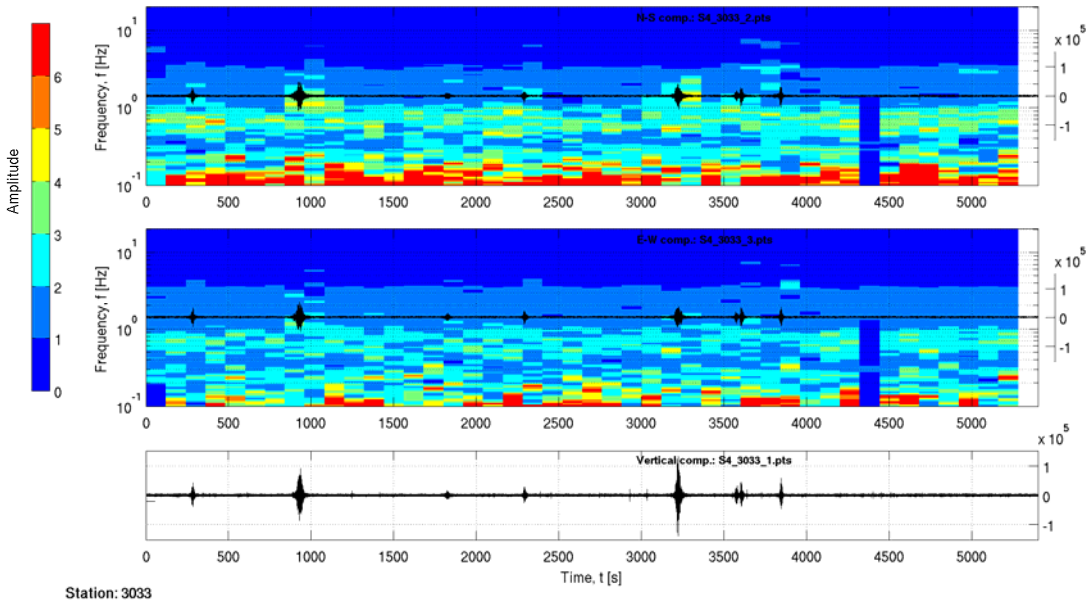

Figure 2a: *H/V* spectral ratios versus time (top and central panel for the NS and EW component, respectively) and corresponding time histories for station 3033.

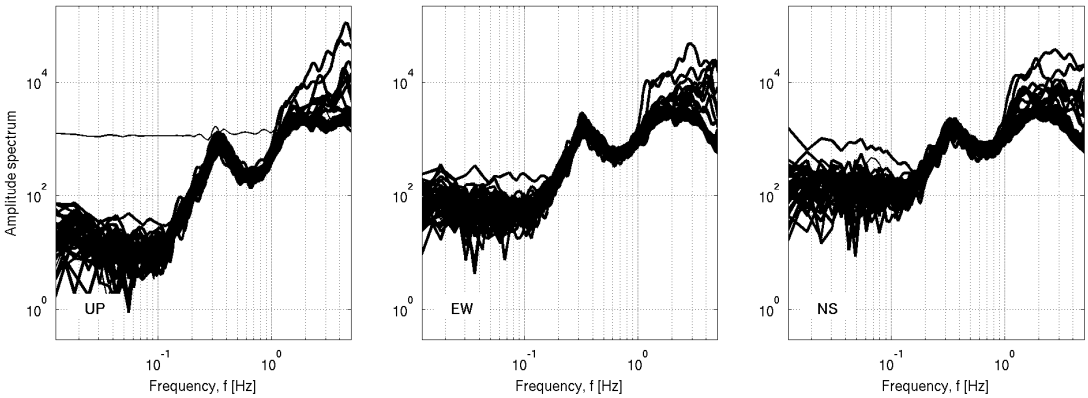

Figure 2b: Fourier spectra for each noise window at station 3033. Left) Vertical component spectra, center) E-W component spectra, right) N-S component spectra.

For each of the 17 used stations, 60 synchronized signal windows of 60 seconds were selected avoiding windows affected by local disturbance. These windows were in turn used to estimate the experimental Rayleigh-wave dispersion curves (using the vertical component of ground motion only) both by f-k and ESAC analysis.

The ESAC Rayleigh-wave dispersion curve was obtained minimizing the root mean square (RMS) of the differences between experimental and theoretical Bessel function values (**Figure 3**). Values that differ more than two standard deviations from those estimated by the best fitting functions (red circles in **Figure 3**) are automatically discarded and the procedure iteratively repeated. Furthermore, data are discarded also when their inter-station distance is longer than 1.5 times the relevant wavelength.

The f-k analysis offers the opportunity to verify if the requirements on the noise source distribution, necessary for the application of the ESAC method, were fulfilled. **Figure 4** and **Figure 5** show examples of the results for several frequencies of the frequency-wavenumber analysis using the Maximum Likelihood Method (MLM) and the Beam Forming (BF) respectively.

Figure 6 shows the good agreement between the Rayleigh wave dispersion curves estimated both with ESAC and f-k approaches. Only below 2.5 Hz the f-k analysis provides larger phase velocities.

An average *H/V* for the selected stations was computed by averaging the *H/V* calculated for each signal window (**Figure 7a**). The average *H/V* curves for the selected stations were in turn averaged to obtain a single *H/V* spectral ratio representative for the array, which was then used as input in the joint inversion procedure for the estimation of the S-wave velocity profile (**Figure 7b**).

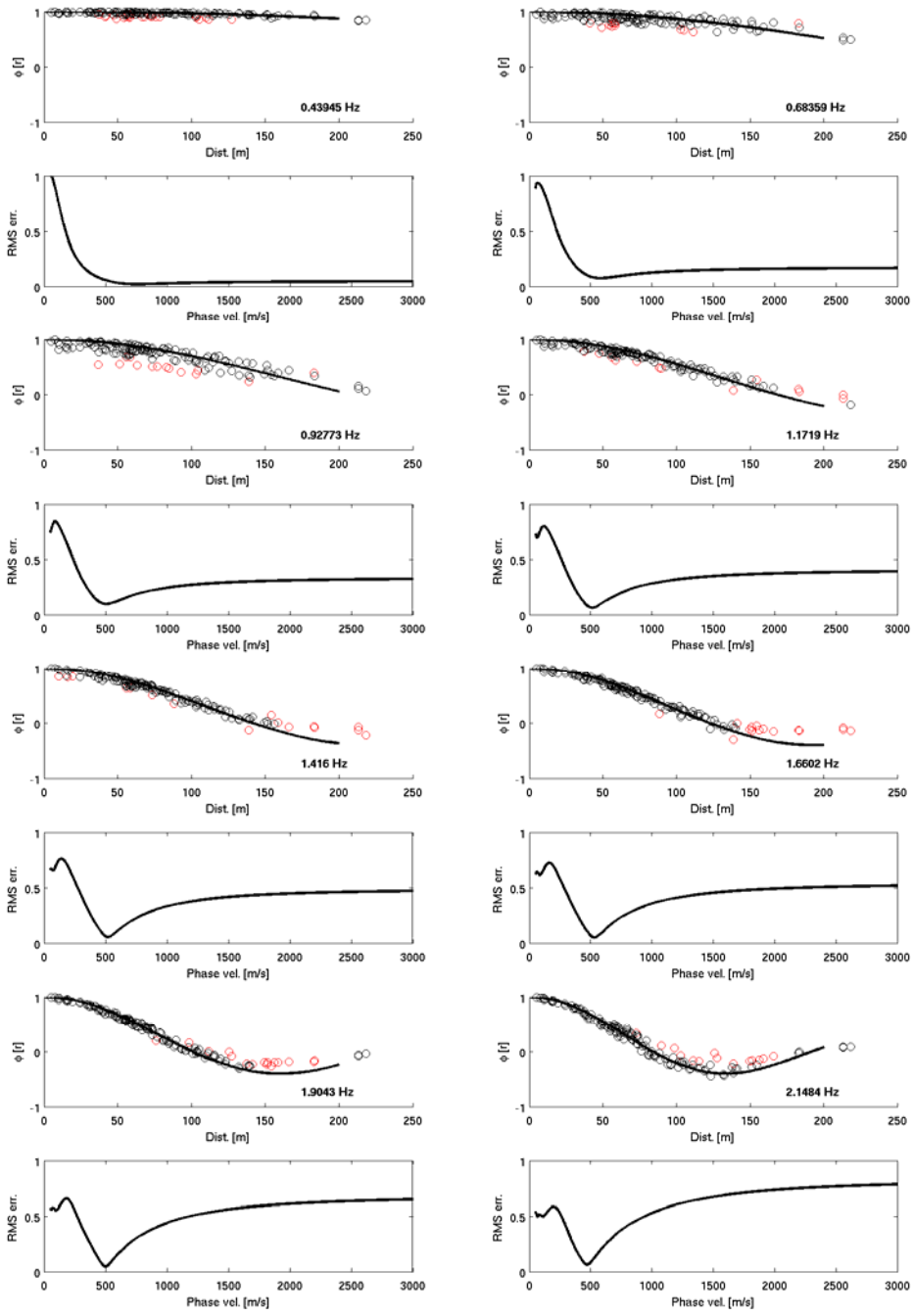

Figure 3: Experimental space-correlation function values versus distance (circles) for different frequencies. The red circles indicate values discarded. The black lines depict the estimated space-correlation function values for the phase velocity showing the best fit to the data. The bottom panels show the relevant root-mean square errors (RMS) versus phase velocity tested.

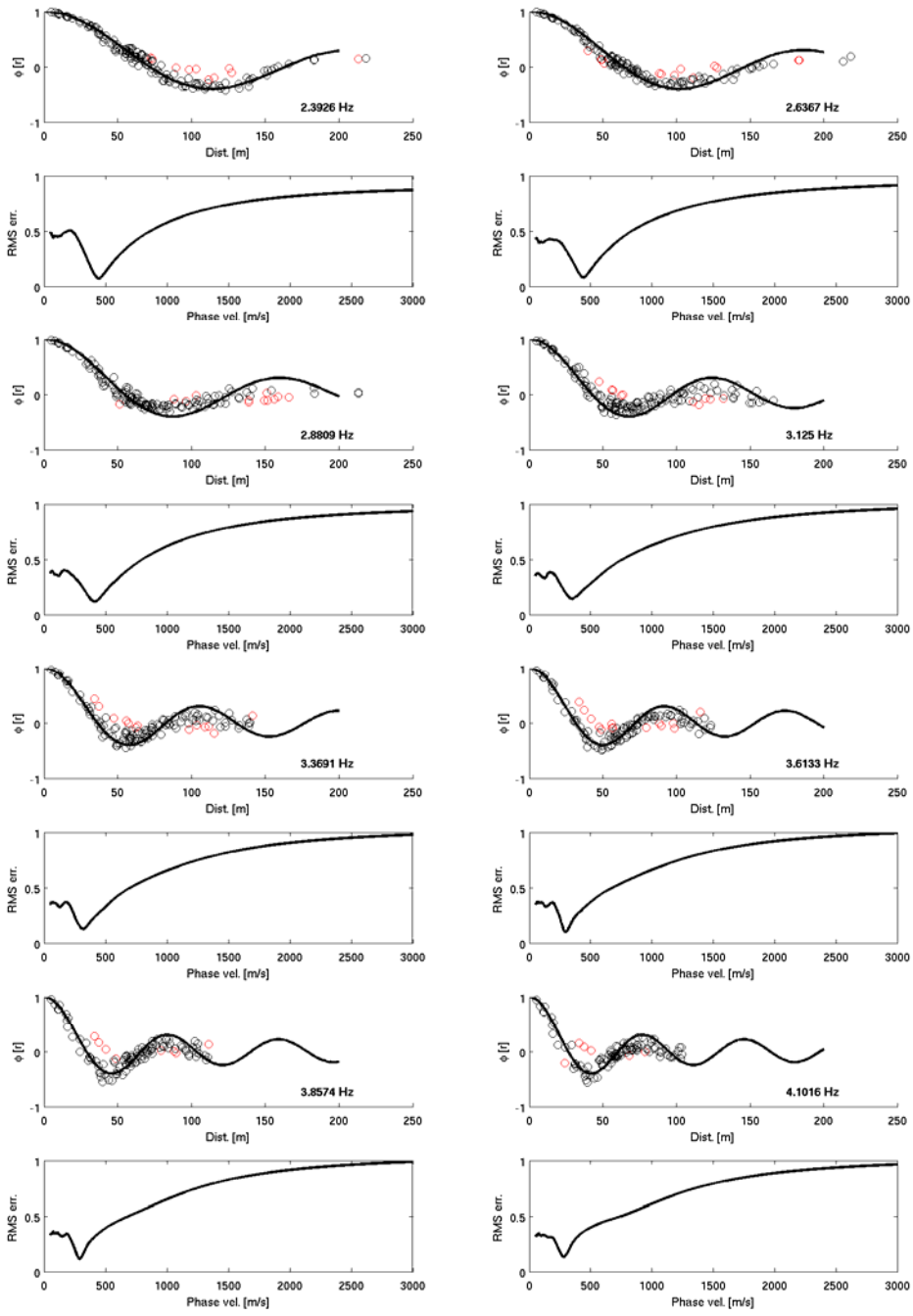

Figure 3: See previous caption.

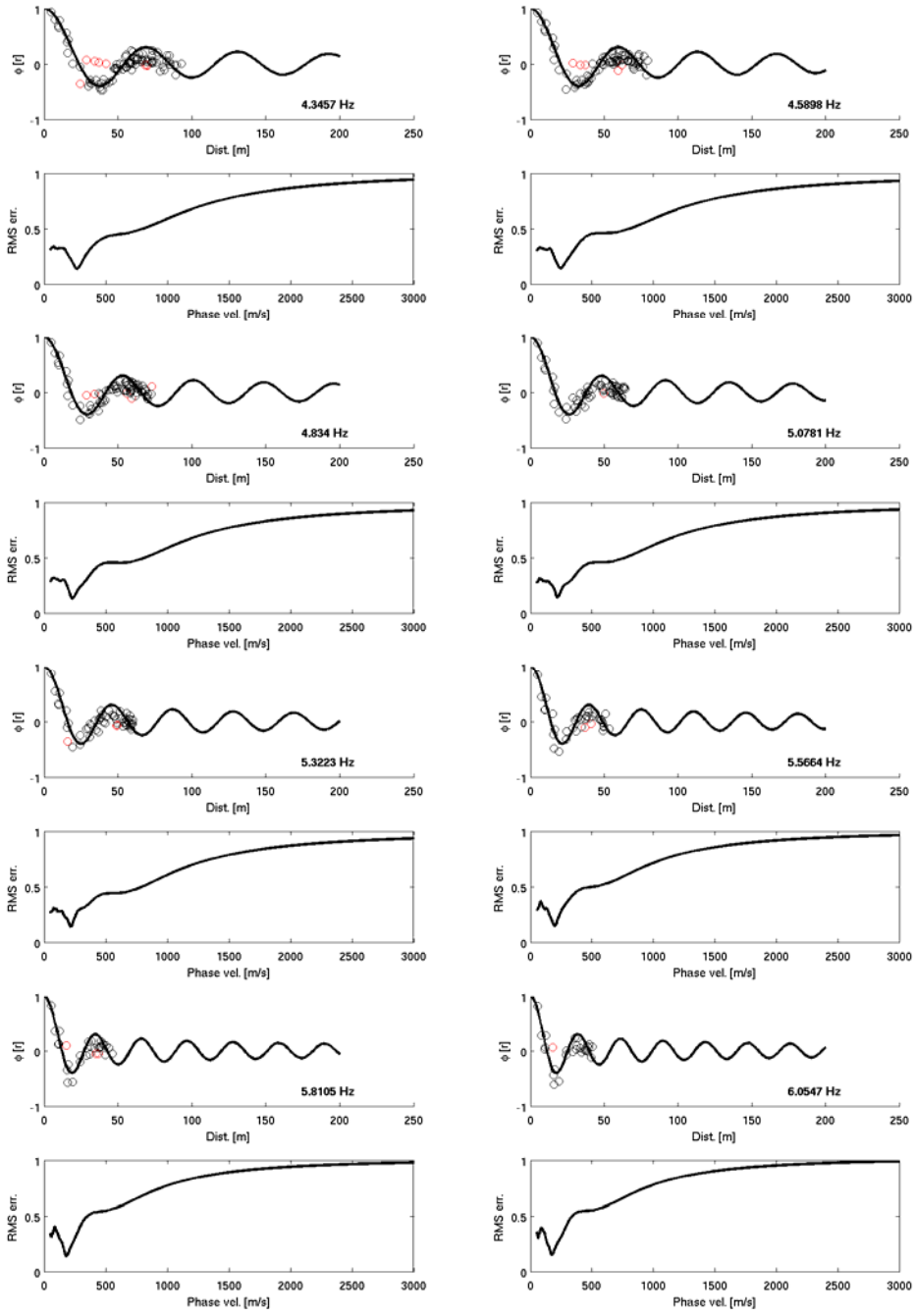

Figure 3: See previous caption.

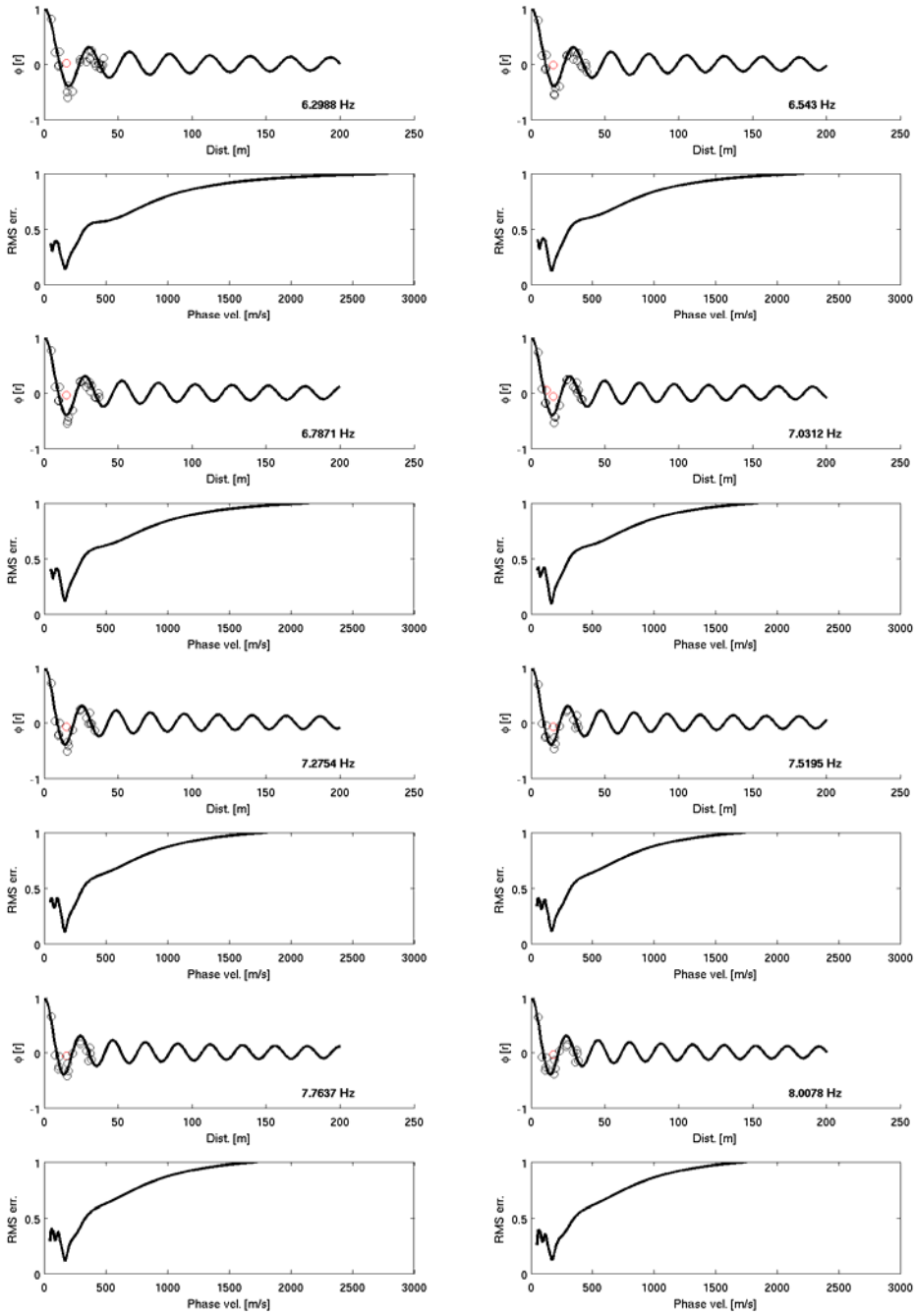

Figure 3: See previous caption.

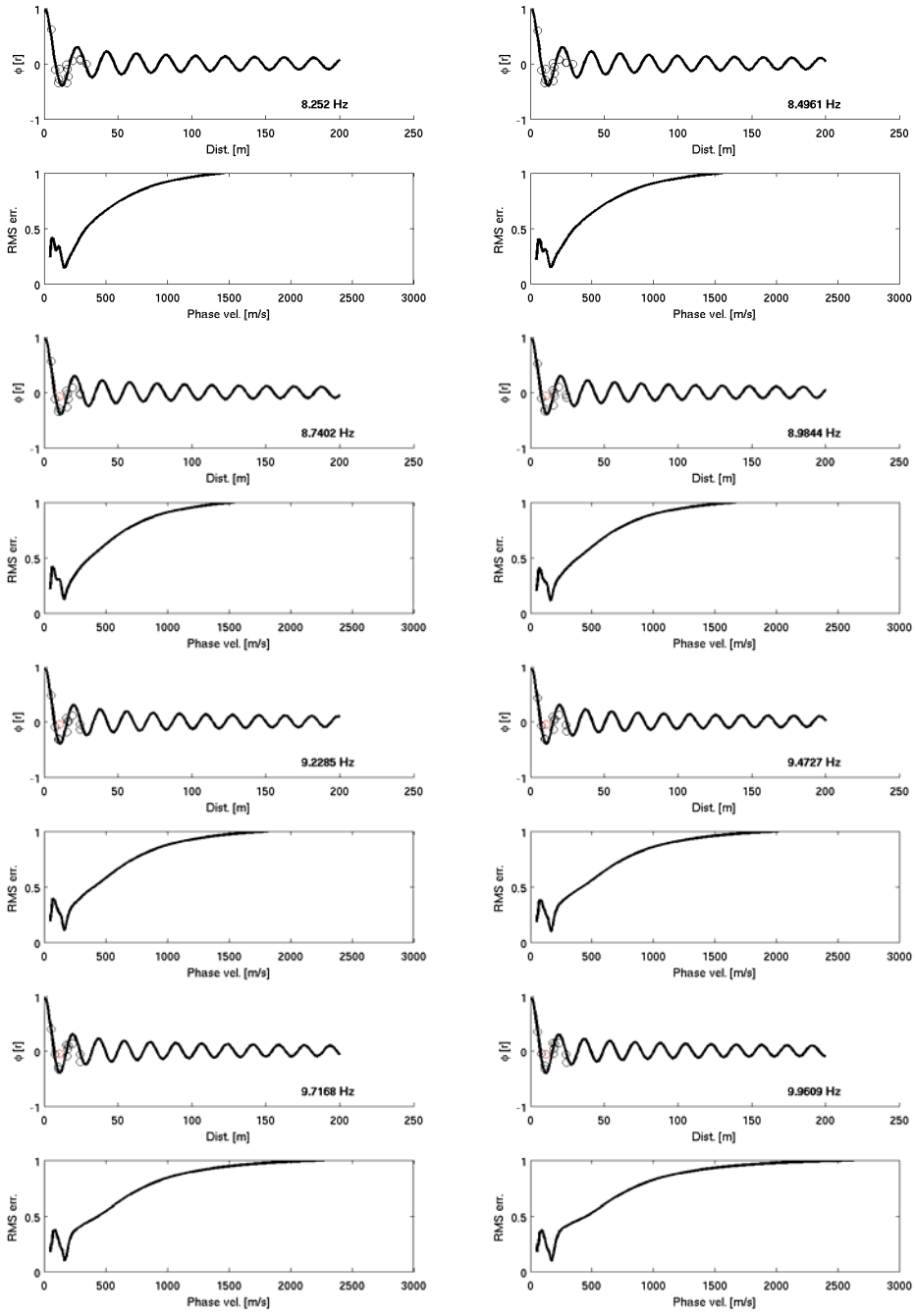

Figure 3: See previous caption.

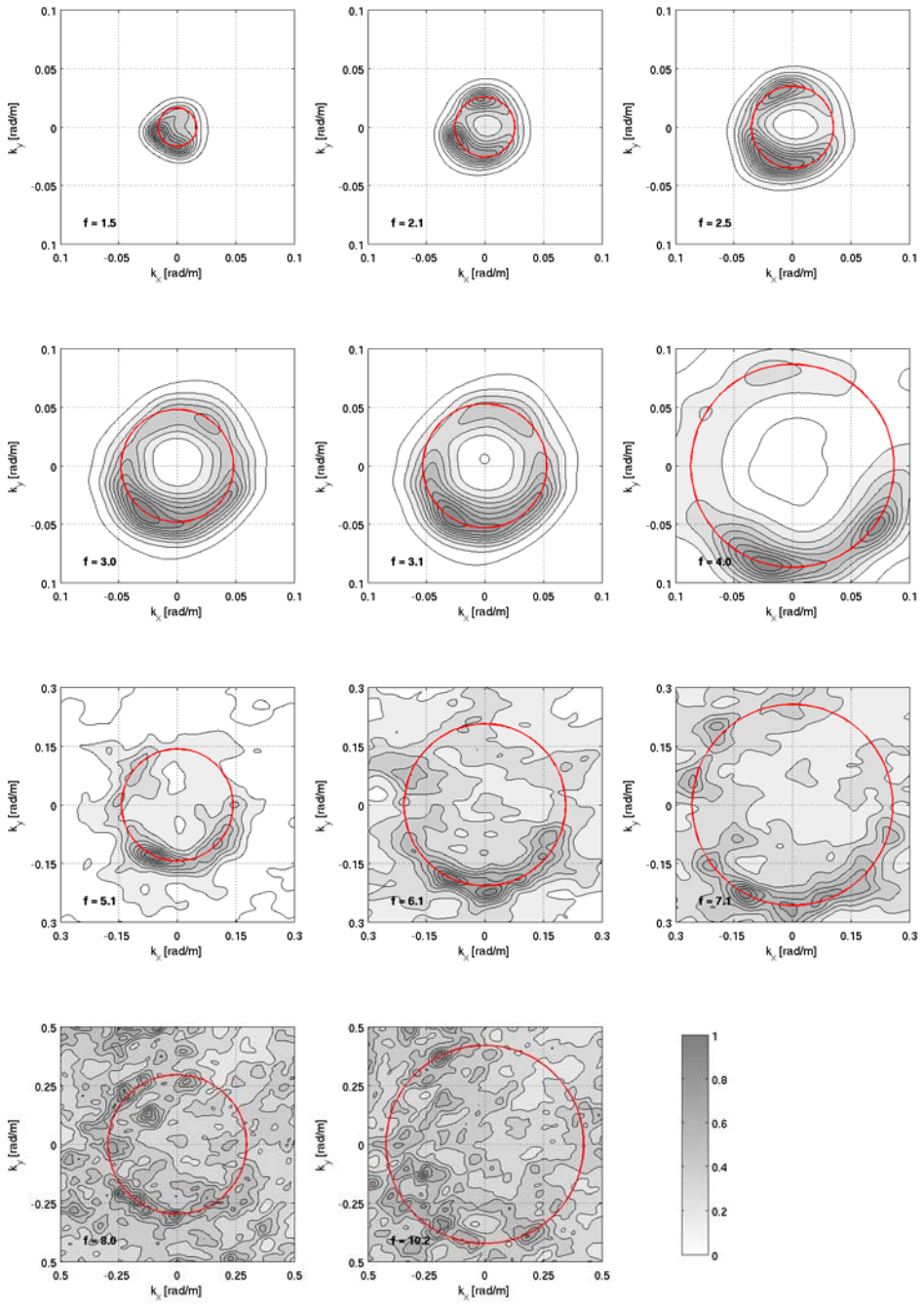

Figure 4: f-k power density function (MLM) at different frequencies (f, expressed in Hz). The red circles joints points with the same *k* value, corresponding to the maximum used to estimate the phase velocity.

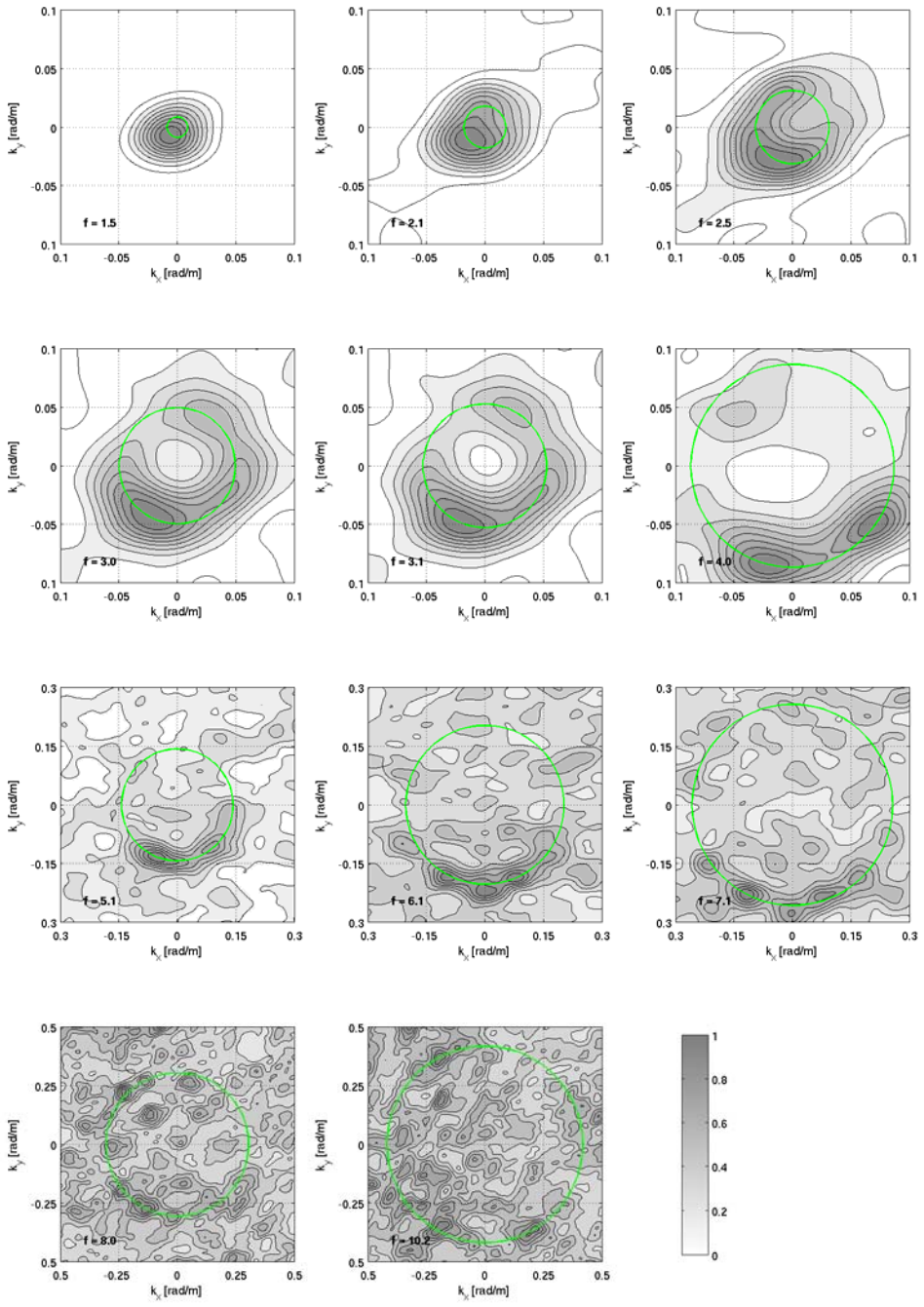

Figure 5: f-k power density function (BF) at different frequencies (f, expressed in Hz). The green circles joints points with the same *k* value, corresponding to the maximum used to estimate the phase velocity.

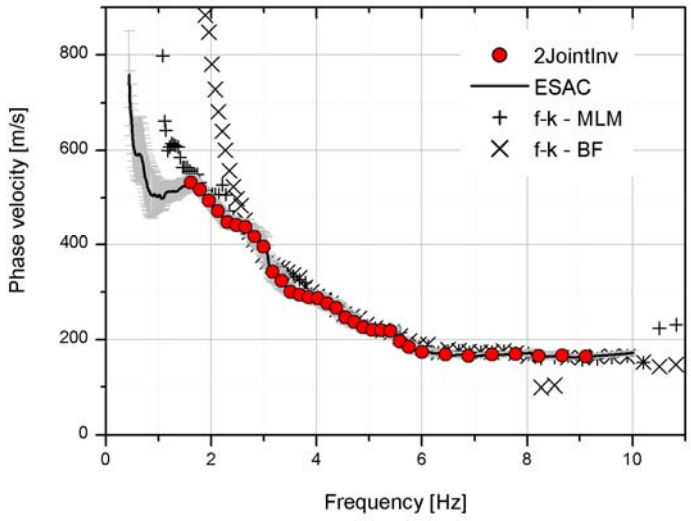

Figure 6: Comparison of experimental phase velocity estimated by the ESAC and the f-k (both for Beam Forming and Maximum Likelihood Method) methods. The red circles represent the values used for the joint inversion. The intervals (grey lines) around the observed ESAC phase velocities representing estimated uncertainties are obtained by calculating the square root of the covariance of the error function.

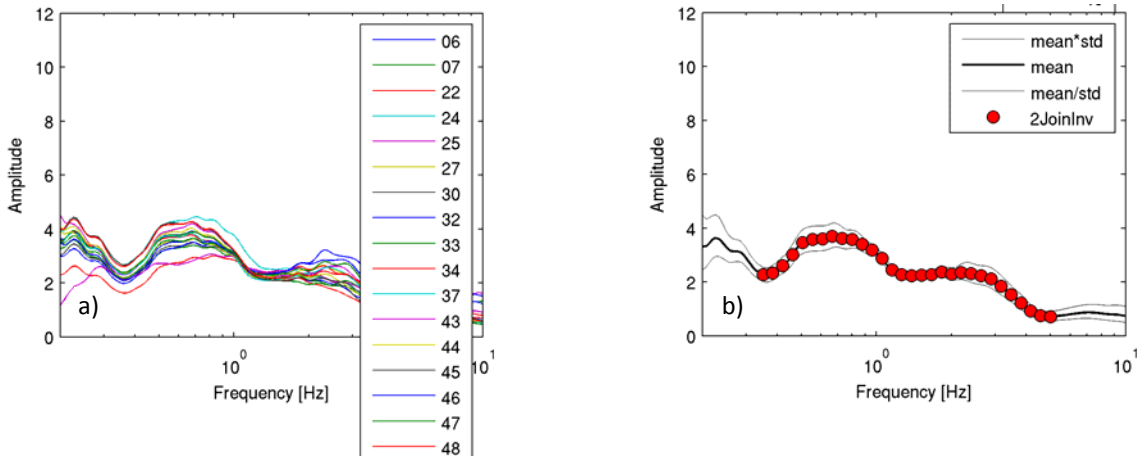

Figure 7: a) average *H/V* for the selected stations of the array (e.g. 06 stands for station 3006, 32 stands for station 3032, etc.) and b) the average H/V of the array. The red circles represent the values used for the joint inversion.

The inversion of dispersion and *H/V* curves to estimate the S-wave velocity profile was carried out fixing to 7 the number of layers overlying the half-space in the model (**Table 1**). Through a genetic algorithm a search over 80000 models was carried out. The inversion was repeated several times starting from different

seed numbers, that is to say from a different population of initial models. In this way it was possible to better explore the space of the solution.

Table 1: Ranges of values defined for the parameters used in the joint inversion.

	Shear wave velocity, V_S [m/s]		Thickness, h [m]		Density, ρ [ton/m^3]
Layer	MIN	MAX	MIN	MAX	
#1	100	300	10	30	1.9
#2	200	400	10	50	1.9
#3	250	500	20	80	2.0
#4	300	600	40	160	2.1
#5	450	900	60	240	2.2
#6	500	1000	100	400	2.2
#7	600	1200	300	800	2.2
Half-space	1000	2500	Infinite		2.3

During the inversion procedure the thickness and the shear wave velocity for each layer could be varied within the pre-defined ranges. On the contrary, for each layer, density was assigned *a priori*, while P-wave velocity (V_P) was calculated through the values of the S-wave velocity Vs via the equation: $V_P\,[\mathrm{m/s}] = 1.1 \cdot V_S + 1290$.

The models are selected by means of a cost function which take in account the agreement between the theoretical *H/V* and Rayleigh-wave dispersion curves with the observed ones. In this application, after trial and error test, the weight of 0.01, that allowed the best balanced fit of dispersion and H/V curves, was adopted.

Discussion of the results

In **Figure 8a** all the models tested during the inversion are depicted (gray lines). The best fit model (white line) and the models lying inside the 10% range of the minimum cost (black lines) function are highlighted. The agreement between experimental and theoretical Rayleigh wave dispersion curves (**Figure 8c**) is good and, considering the wavelengths related to the dispersion curve frequency range, the V_S profile between 10 to about 200 metres is likely to be well constrained. Therefore, since below this depth the profile is constrained by the H/V curve alone, we prefer to show, in **Figure 8a** and **Table 2**, the V_S profile only within the depth range were both curves contribute to the inversion.

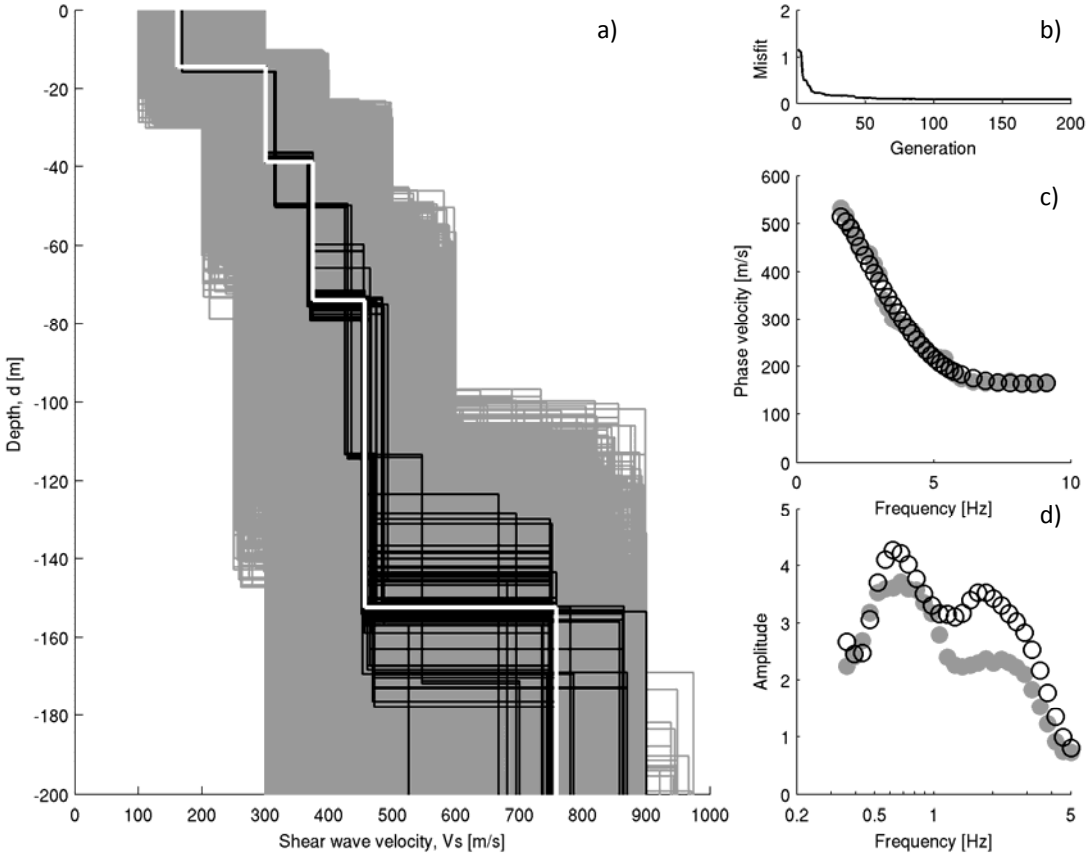

Figure 8: a) Tested models (grey lines), the minimum cost model (white line) and models lying inside the minimum cost + 10% range (black lines) for the MDN station; b) the misfit versus generation values; c) experimental (grey circles) and estimated (white circles – relevant to the minimum cost model) phase velocities; d) experimental (grey circles) and estimated (white circles – relevant to the minimum cost model) *H/V* ratio curves.

Table 2: Shear wave velocity model at the MDN station.

Shear wave velocity, V_S [m/s]	Thickness, h [m]
161.2	14.3
300.4	24.6
374.5	35.1
456.5	78.6
758.8	

APPLICATION OF SURFACE WAVE METHODS

FOR SEISMIC SITE CHARACTERIZATION

STATION CODE:

MI03

Responsible: Stefano Parolai[1]

Co-workers: Rodolfo Puglia[2], Matteo Picozzi[1]

1) Helmholtz Centre Potsdam - German Research Centre For Geosciences (GFZ), Helmholtzstraße 7, 14467 Potsdam, Germany
2) Istituto Nazionale di Geofisica e Vulcanologia (INGV), Sezione di Milano-Pavia, via Bassini 15, 20133 Milano, Italy

Introduction note

Details and references about *in-situ* measurement, Rayleigh wave dispersion and H/V curves estimate and inversion procedure here reported, can be found in the research reports of DPC-INGV S4 Project 2007-2009: Deliverables 6 and 7 at http://esse4.mi.ingv.it .

Testing equipment

The array measurements were performed using 17 EDL 24bit acquisition systems equipped with short-period Mark-L4-C-3D 1Hz sensors and GPS timing. The stations worked contemporary for more than 2 hours, recording noise at 200 s.p.s., which is adequate for the short inter-station distances considered.

Processing overview

The Rayleigh wave dispersion curve was estimated by analysing the vertical component of the recorded microtremors. In particular, the Extended Spatial Auto Correlation (ESAC) and the Frequency-Wavenumber (f-k) methods were adopted.

Rayleigh wave dispersion and *H/V* ratio curves were both used to estimate the local S-wave velocity profile, using a joint inversion scheme. The non-linear inversions were performed using a genetic algorithm which does not rely upon an explicit starting model and allows the identification of a solution close to the global minimum. The forward modeling of Rayleigh wave phase velocities and *H/V* curves was performed using the modified Thomson-Haskell method, under the assumption of vertically heterogeneous 1D earth models. The validity of this assumption was investigated by computing the *H/V* curve for each station of the array using the recorded data. The modeling of both the dispersion and *H/V* ratio curves during the inversions was not restricted to the fundamental mode only, but the possibility that higher modes can participate to define the observed dispersion and *H/V* curves is allowed.

Data analysis

For each of the 17 used stations, more than 60 synchronized signal windows of 60 seconds were selected avoiding windows affected by local disturbance. These windows were used to estimate the experimental Rayleigh-wave dispersion curves by the ESAC analysis, using the vertical component of ground motion only.

The ESAC Rayleigh-wave dispersion curve was obtained minimizing the root mean square (RMS) of the differences between experimental and theoretical Bessel function values (**Figure 1b**). Values that differ

more than two standard deviations from those estimated by the best fitting functions were discarded and the procedure iteratively repeated.

To obtain a single *H/V* spectral ratio representative for the array an average *H/V* for each window of each station was computed (**Figure 1c**). This curve was then used as input in the joint inversion procedure for the estimation of the S-wave velocity profile.

The inversion of dispersion and *H/V* curves to estimate the S-wave velocity profile was carried out through a genetic algorithm. The inversion was repeated several times starting from different seed numbers, that is to say from a different population of initial models. In this way it was possible to better explore the space of the solution.

During the inversion procedure the thickness and the shear wave velocity for each layer could be varied within pre-defined ranges. On the contrary, for each layer, density was assigned *a priori*, while P-wave velocity (V_P) was calculated through the values of the S-wave velocity Vs via the equation: $V_P\,[\mathrm{m/s}] = 1.1 \cdot V_S + 1290$.

The models are selected by means of a cost function which take in account the agreement between the theoretical *H/V* and Rayleigh-wave dispersion curves with the observed ones.

Discussion of the results

In **Figure 1a** all the models tested during the inversion are depicted (grey lines). The best fit model (black line) and the models lying inside the 10% range of the minimum cost (dark-grey lines) function are highlighted. The agreement between experimental and theoretical Rayleigh wave dispersion curves (**Figure 1b**) is good and, considering the wavelengths related to the dispersion curve frequency range, the V_S profile between 10 to about 80 metres is likely to be well constrained. Therefore, we prefer to show, in **Figure 1a** and **Table 1**, the V_S profile only within this depth range.

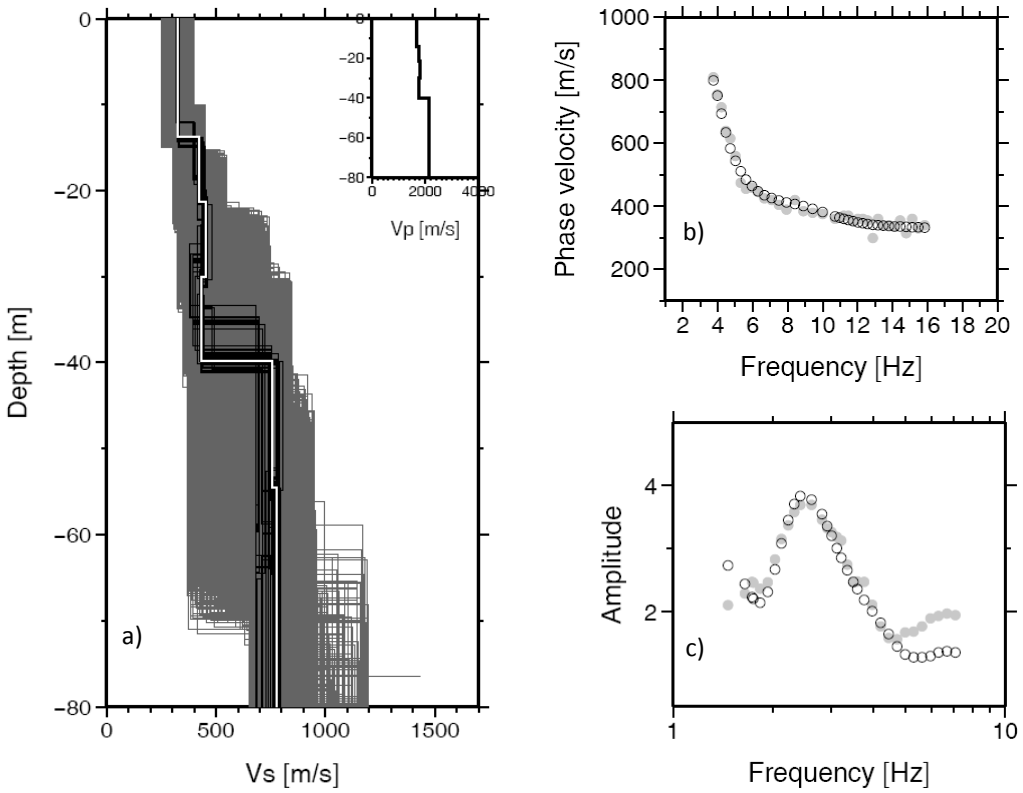

Figure 1: a) Tested models (grey lines), the minimum cost model (white line) and models lying inside the minimum cost + 10% range (black lines) for the MI03 station; b) experimental (grey circles) and estimated (white circles – relevant to the minimum cost model) phase velocities; c) experimental (grey circles) and estimated (white circles – relevant to the minimum cost model) *H/V* ratio curves.

Table 1: Shear wave velocity model at the MI03 station.

Shear wave velocity, V_S [m/s]	Thickness, h [m]
325	13.8
422	7.5
453	8.7
432	9.8
756	14.8
778	

APPLICATION OF SURFACE WAVE METHODS

FOR SEISMIC SITE CHARACTERIZATION

STATION CODE:

NRZI

Responsible: Stefano Parolai[1]

Co-workers: Rodolfo Puglia[2], Matteo Picozzi[1]

1) Helmholtz Centre Potsdam - German Research Centre For Geosciences (GFZ), Helmholtzstraße 7, 14467 Potsdam, Germany
2) Istituto Nazionale di Geofisica e Vulcanologia (INGV), Sezione di Milano-Pavia, via Bassini 15, 20133 Milano, Italy

Introduction note

Details and references about *in-situ* measurement, Rayleigh wave dispersion and H/V curves estimate and inversion procedure here reported, can be found in the research reports of DPC-INGV S4 Project 2007-2009: Deliverables 6 and 7 at http://esse4.mi.ingv.it .

Testing equipment

The array measurements were performed using 15 EDL 24bit acquisition systems equipped with short-period Mark-L4-C-3D 1Hz sensors and GPS timing (**Figure 1**). However, due to malfunctioning, only the data of 14 stations (depicted as blue squares) could be used for the processing. The inter-station distances in the array ranged between 4.6 m to 83 meters. The stations worked contemporary for about 2 hours, recording noise at 200 s.p.s., which is adequate for the short inter-station distances considered.

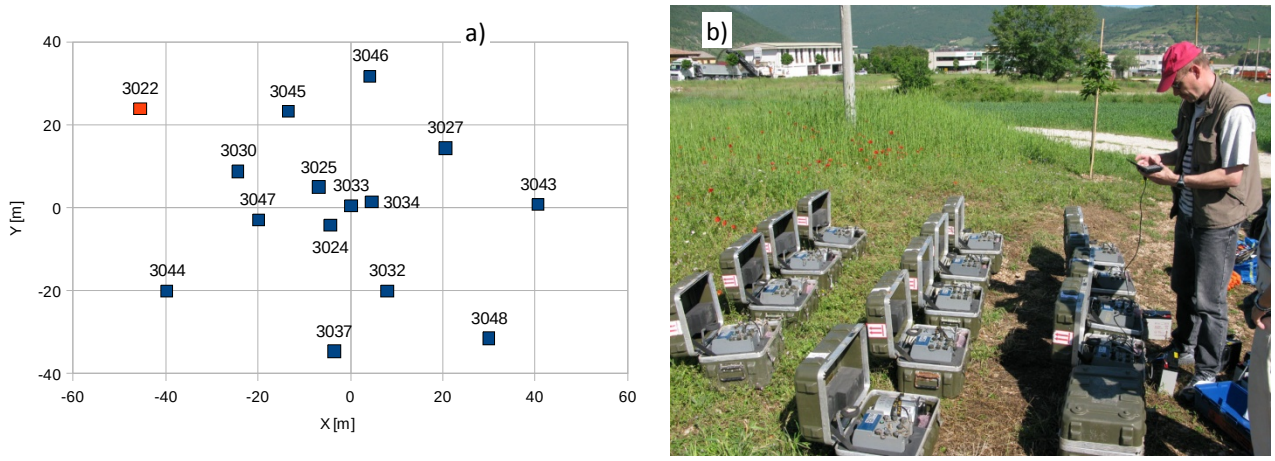

Figure 1: a) Geometry of the array. Stations which had problems are evidenced with the red color, in particular: 3022 did not work. b) The field measurements.

Processing overview

The Rayleigh wave dispersion curve was estimated by analysing the vertical component of the recorded microtremors. In particular, the Extended Spatial Auto Correlation (ESAC) and the Frequency-Wavenumber (f-k) methods were adopted.

Rayleigh wave dispersion and *H/V* ratio curves were both used to estimate the local S-wave velocity profile, using a joint inversion scheme. The non-linear inversions were performed using a genetic algorithm which does not rely upon an explicit starting model and allows the identification of a solution close to the global minimum. The forward modeling of Rayleigh wave phase velocities and *H/V* curves was performed using the modified Thomson-Haskell method, under the assumption of vertically heterogeneous 1D earth models. The validity of this assumption was investigated by computing the *H/V* curve for each station of the array using the recorded data. The modeling of both the dispersion and *H/V* ratio curves during the inversions was not restricted to the fundamental mode only, but the possibility that higher modes can participate to define the observed dispersion and *H/V* curves is allowed.

Data analysis

The first step of the analysis consists in a visual inspection of the recordings at all stations. In particular, in order to identify malfunctioning of one station or channel and to select signal windows suitable for the H/V analysis, the quality of the recording was evaluated analysing (1) the signal stationarity in the time domain (**Figure 2a**), (2) the relevant unfiltered Fourier spectra (**Figure 2b**), and (3) the *H/V* variation over time (**Figure 2a**).

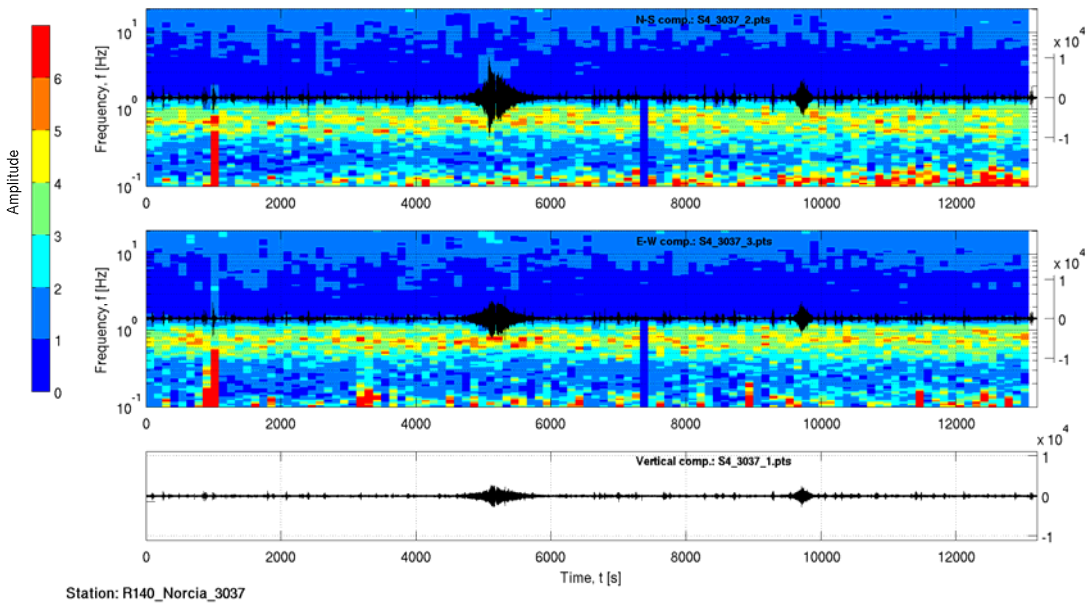

Figure 2a: *H/V* spectral ratios versus time (top and central panel for the NS and EW component, respectively) and corresponding time histories for station 3037.

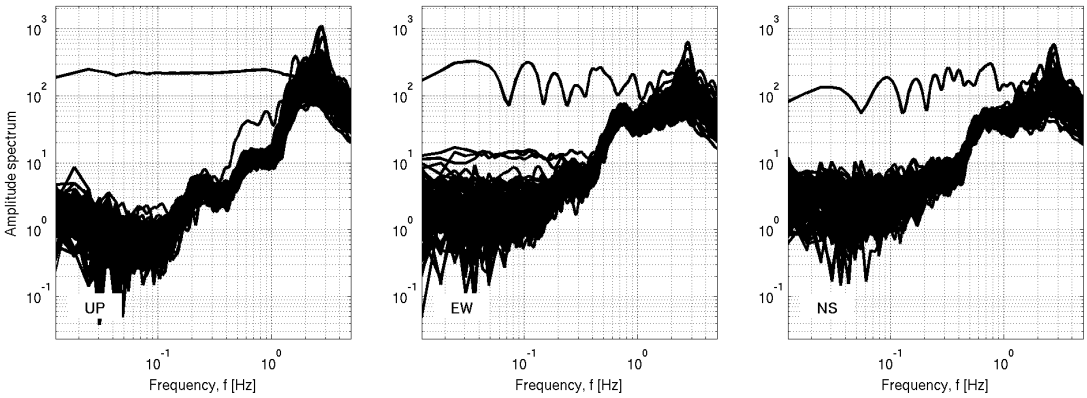

Figure 2b: Fourier spectra for each noise window at station 3037. Left) Vertical component spectra, center) E-W component spectra, right) N-S component spectra.

For each of the 14 used stations, 60 synchronized signal windows of 60 seconds were selected avoiding windows affected by local disturbance. These windows were in turn used to estimate the experimental Rayleigh-wave dispersion curves (using the vertical component of ground motion only) both by f-k and ESAC analysis.

The ESAC Rayleigh-wave dispersion curve was obtained minimizing the root mean square (RMS) of the differences between experimental and theoretical Bessel function values (**Figure 3**). Values that differ more than two standard deviations from those estimated by the best fitting functions (red circles in **Figure 3**) are automatically discarded and the procedure iteratively repeated. Furthermore, data are discarded also when their inter-station distance is longer than 1.5 times the relevant wavelength.

The f-k analysis offers the opportunity to verify if the requirements on the noise source distribution, necessary for the application of the ESAC method, were fulfilled. **Figure 4** and **Figure 5** show examples of the results for several frequencies of the frequency-wavenumber analysis using the Maximum Likelihood Method (MLM) and the Beam Forming (BF) respectively.

Figure 6 shows the good agreement between the Rayleigh wave dispersion curves estimated both with ESAC and f-k MLM approaches. Only below 4 Hz the f-k analysis provides larger phase velocities.

An average *H/V* for the selected stations was computed by averaging the *H/V* calculated for each signal window (**Figure 7a**). The average *H/V* curves for the selected stations were in turn averaged to obtain a single *H/V* spectral ratio representative for the array, which was then used as input in the joint inversion procedure for the estimation of the S-wave velocity profile (**Figure 7b**).

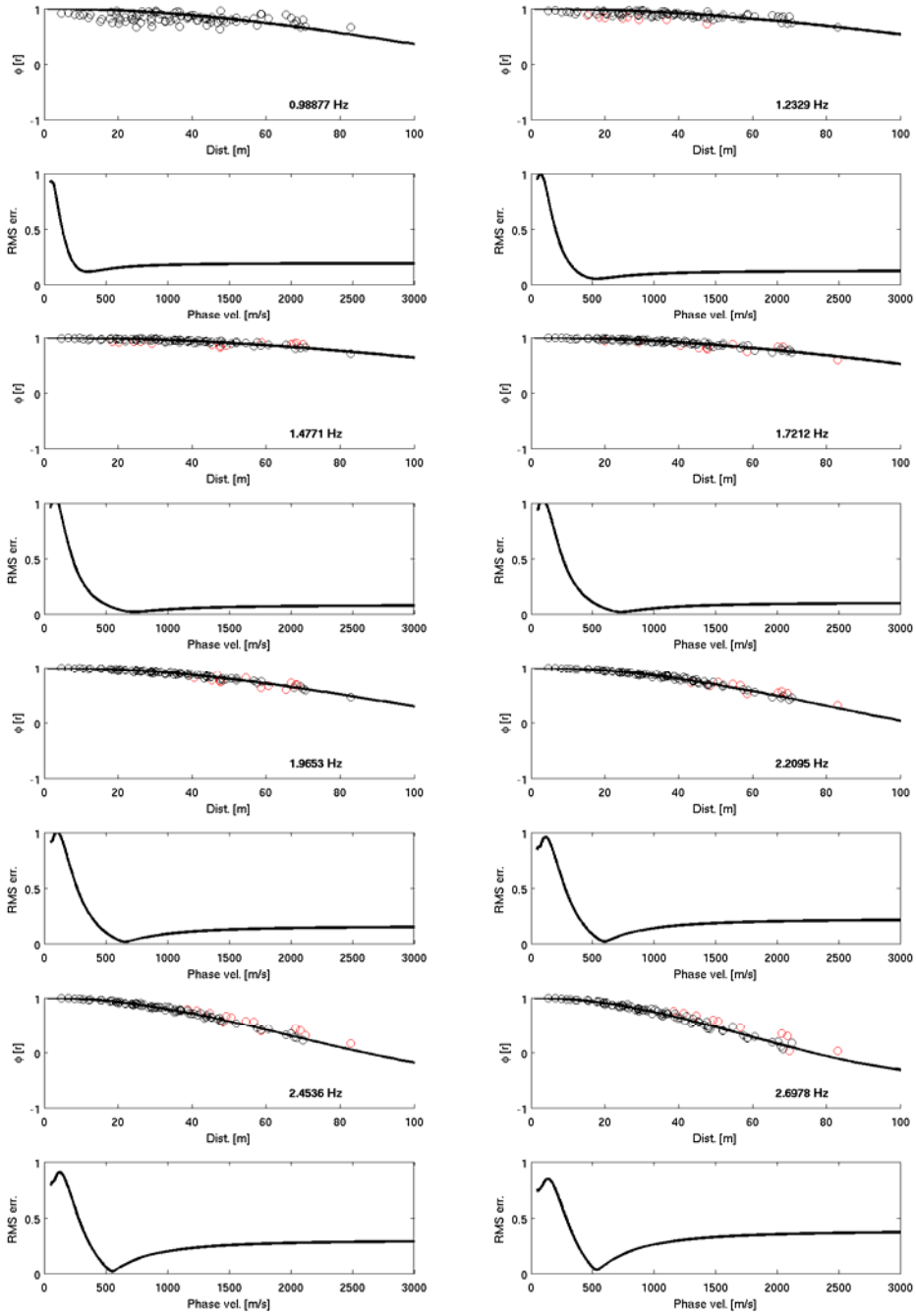

Figure 3: Experimental space-correlation function values versus distance (circles) for different frequencies. The red circles indicate values discarded. The black lines depict the estimated space-correlation function values for the phase velocity showing the best fit to the data. The bottom panels show the relevant root-mean square errors (RMS) versus phase velocity tested.

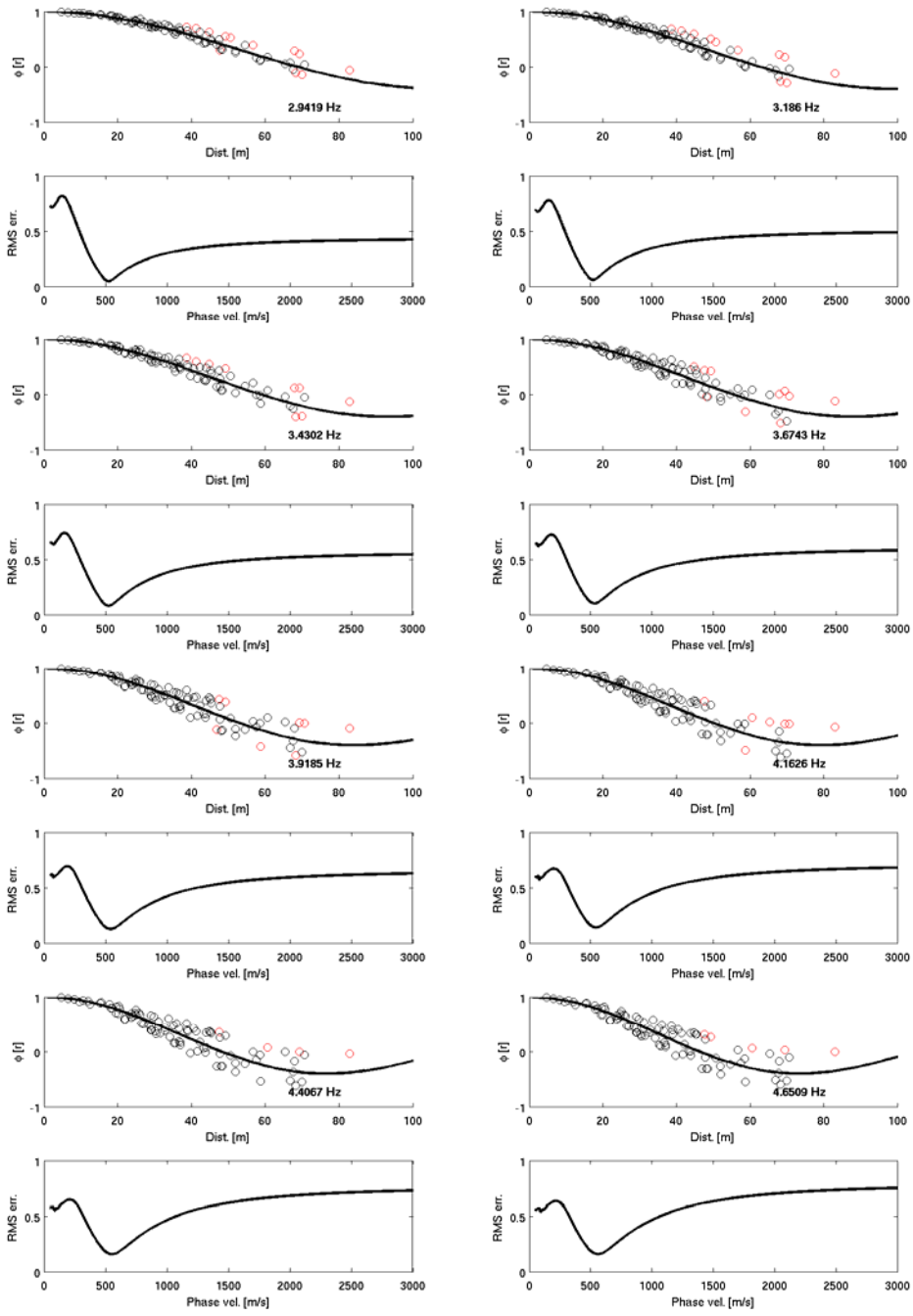

Figure 3: See previous caption.

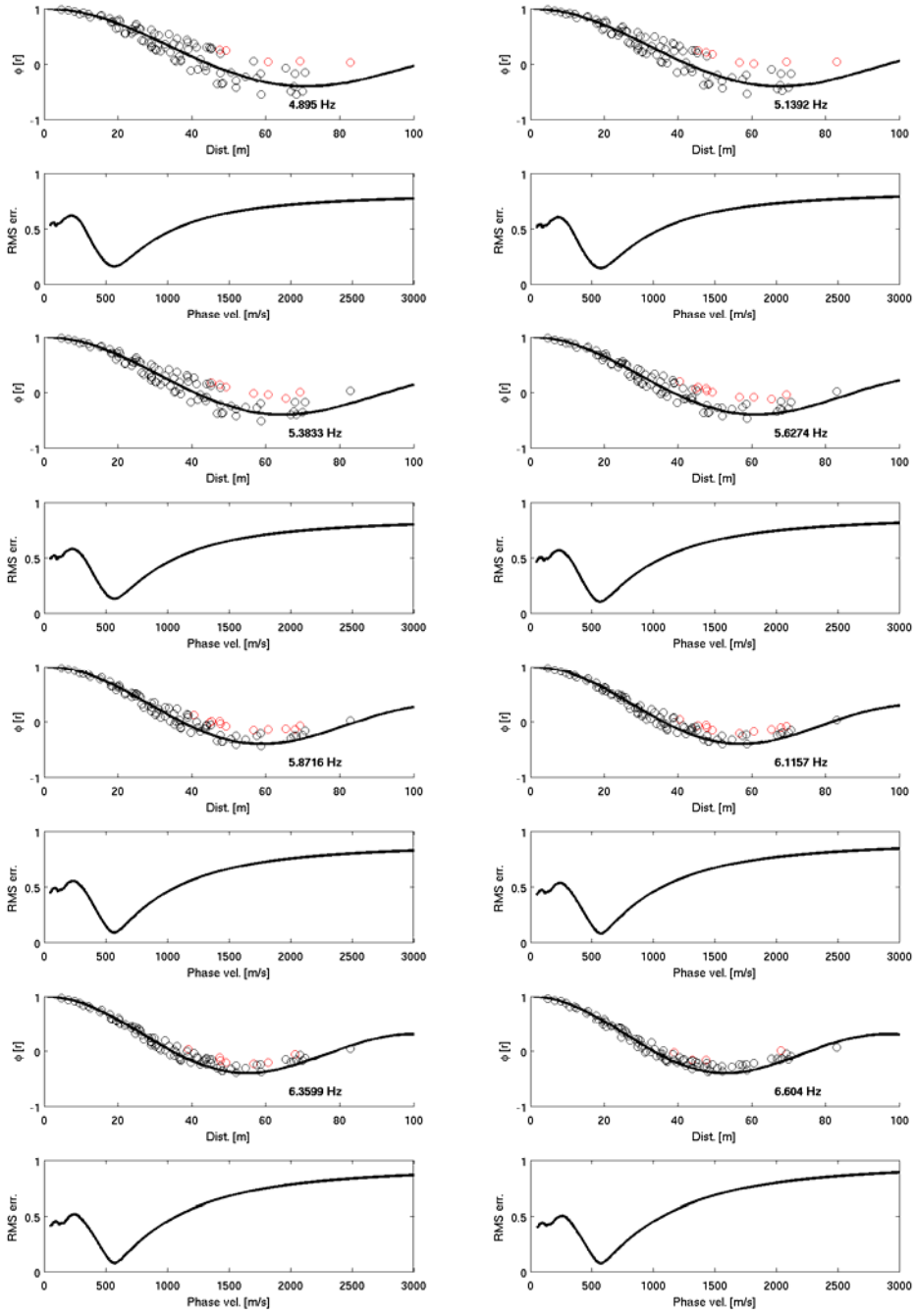

Figure 3: See previous caption.

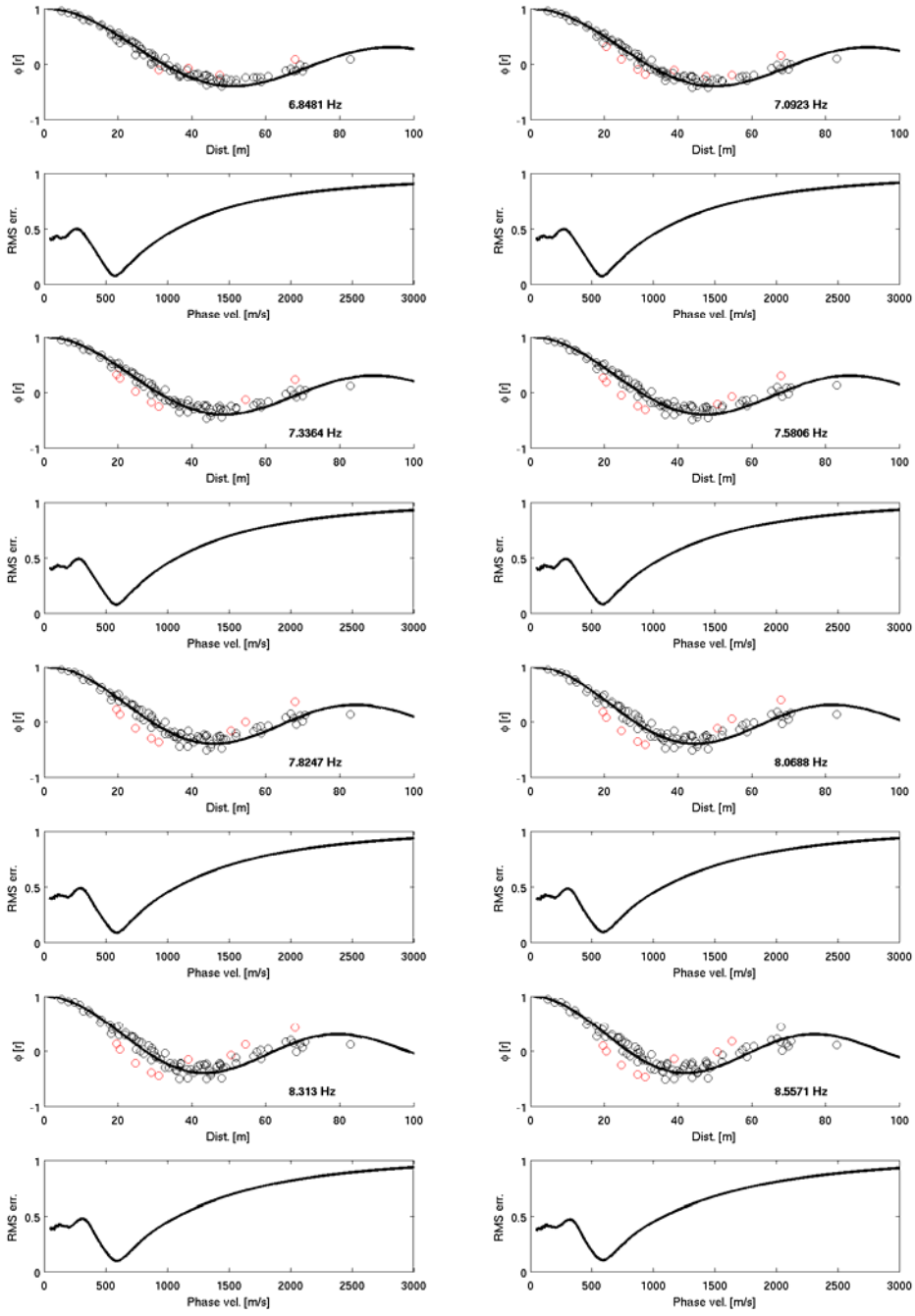

Figure 3: See previous caption.

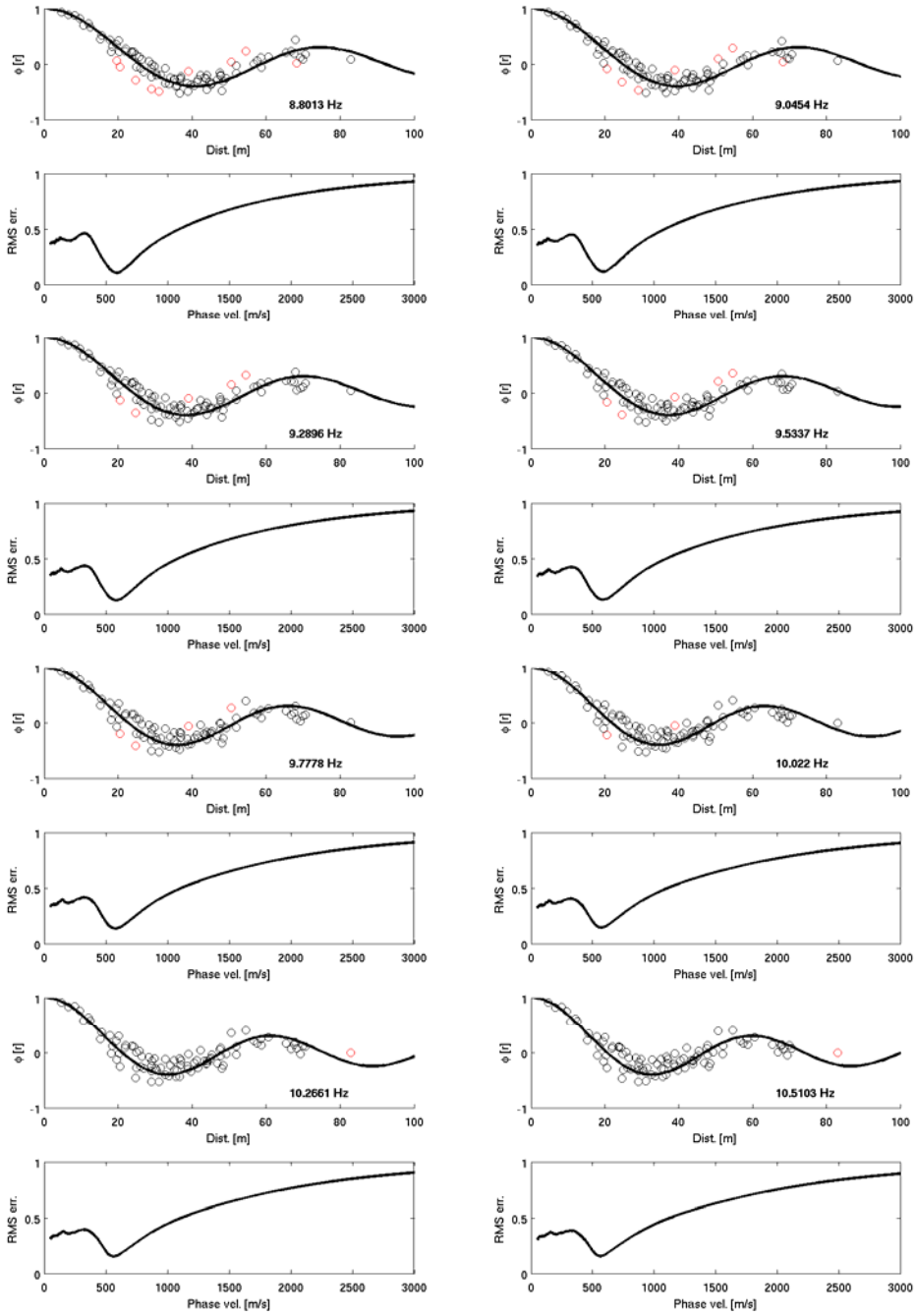

Figure 3: See previous caption.

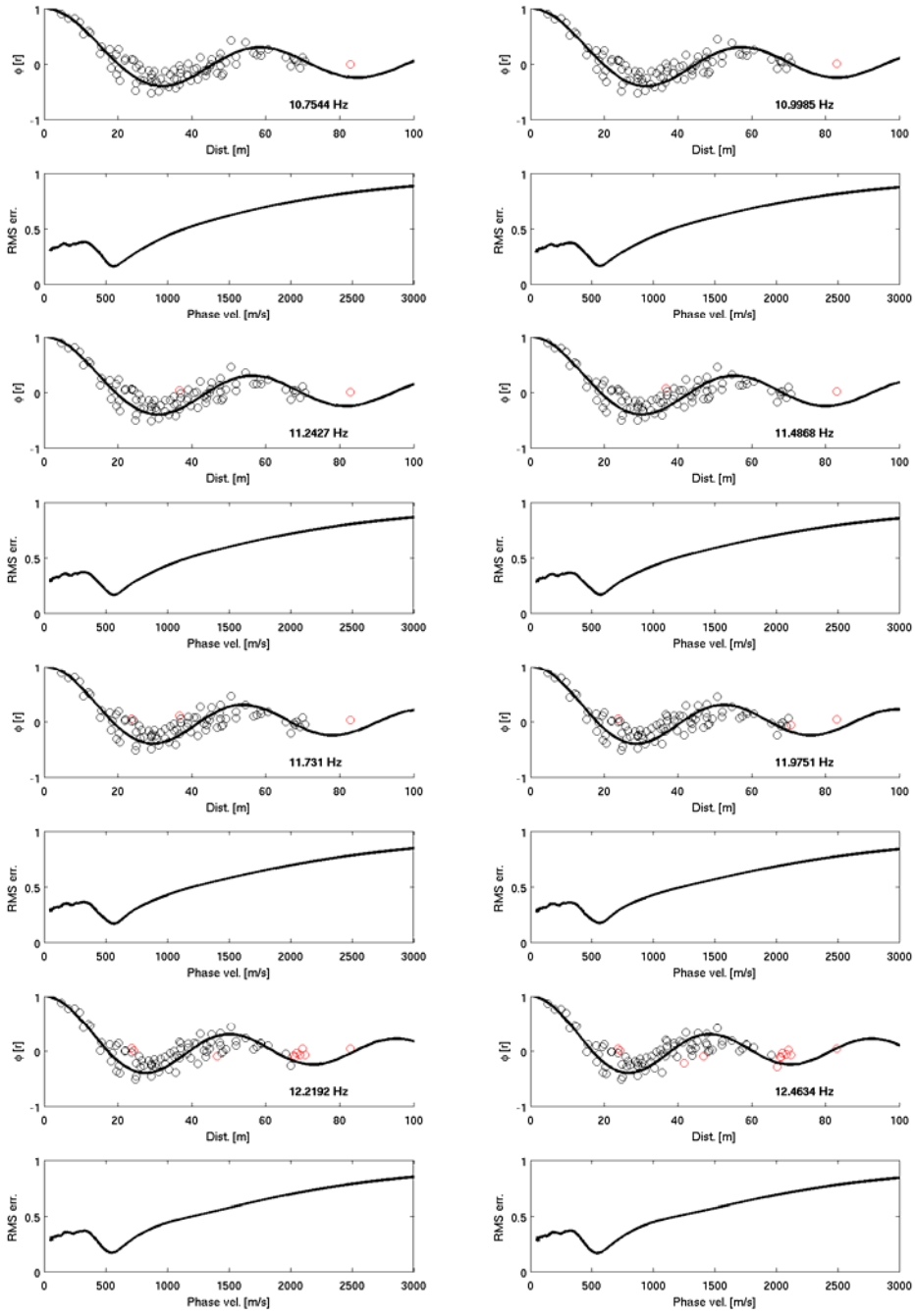

Figure 3: See previous caption.

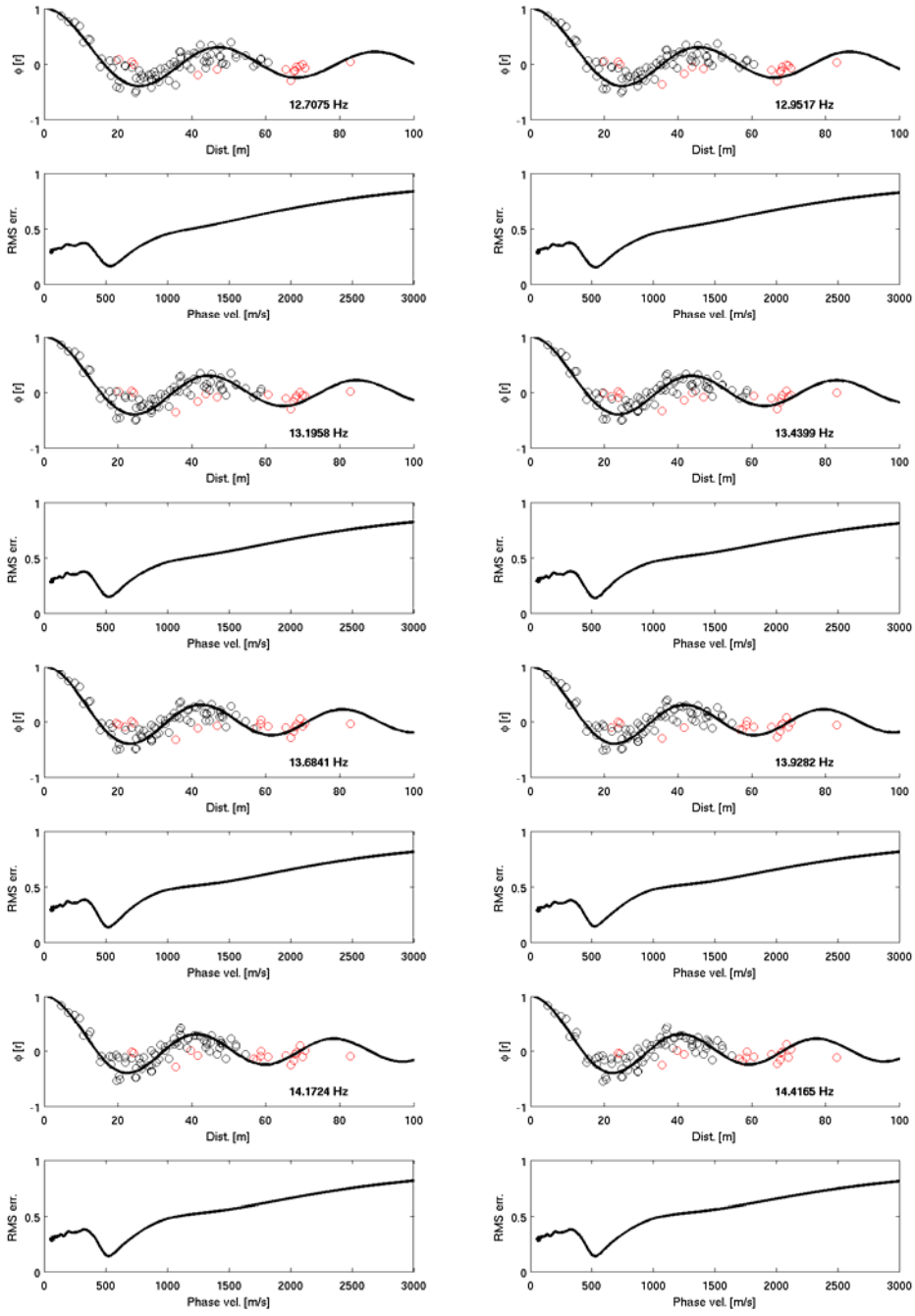

Figure 3: See previous caption.

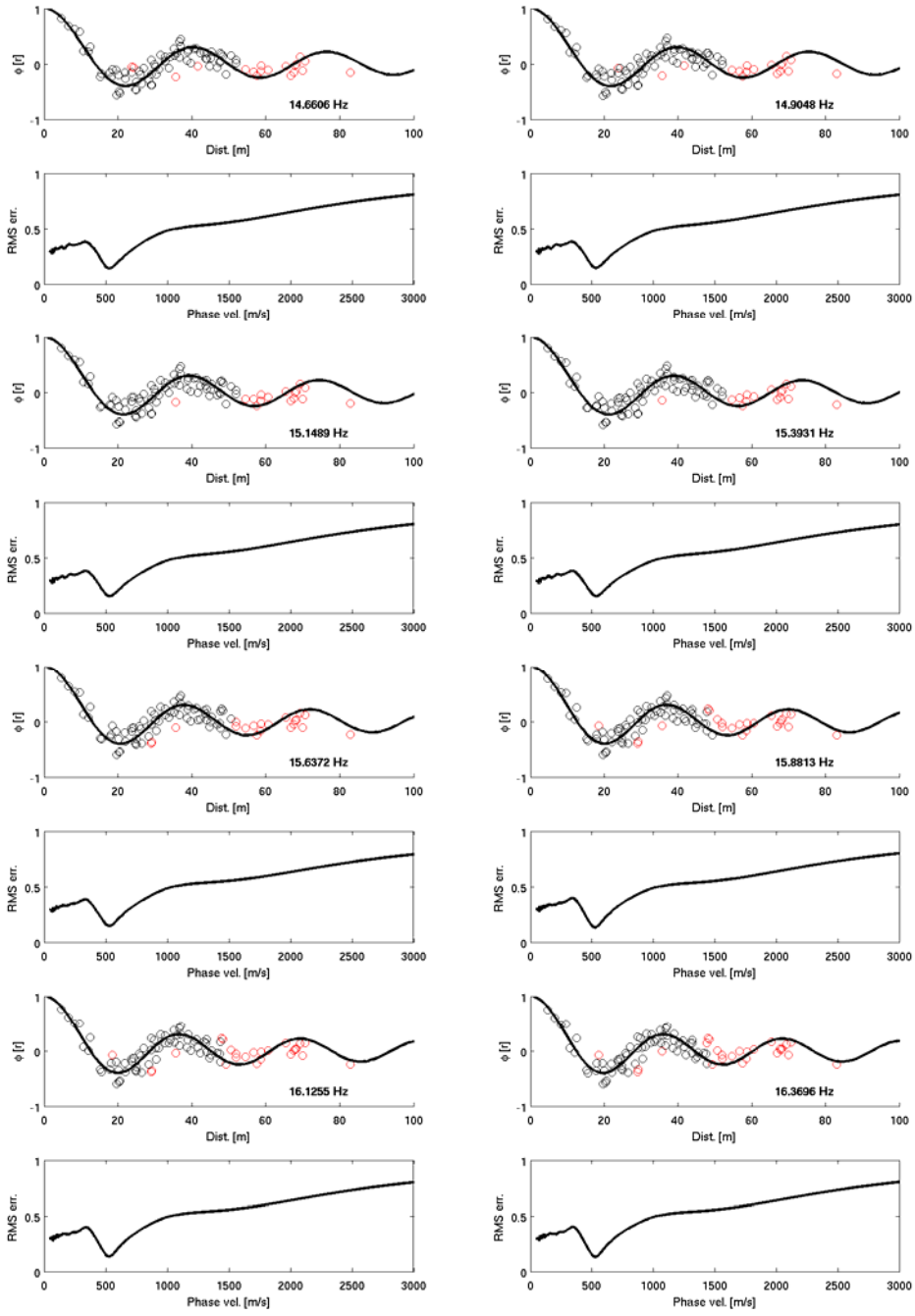

Figure 3: See previous caption.

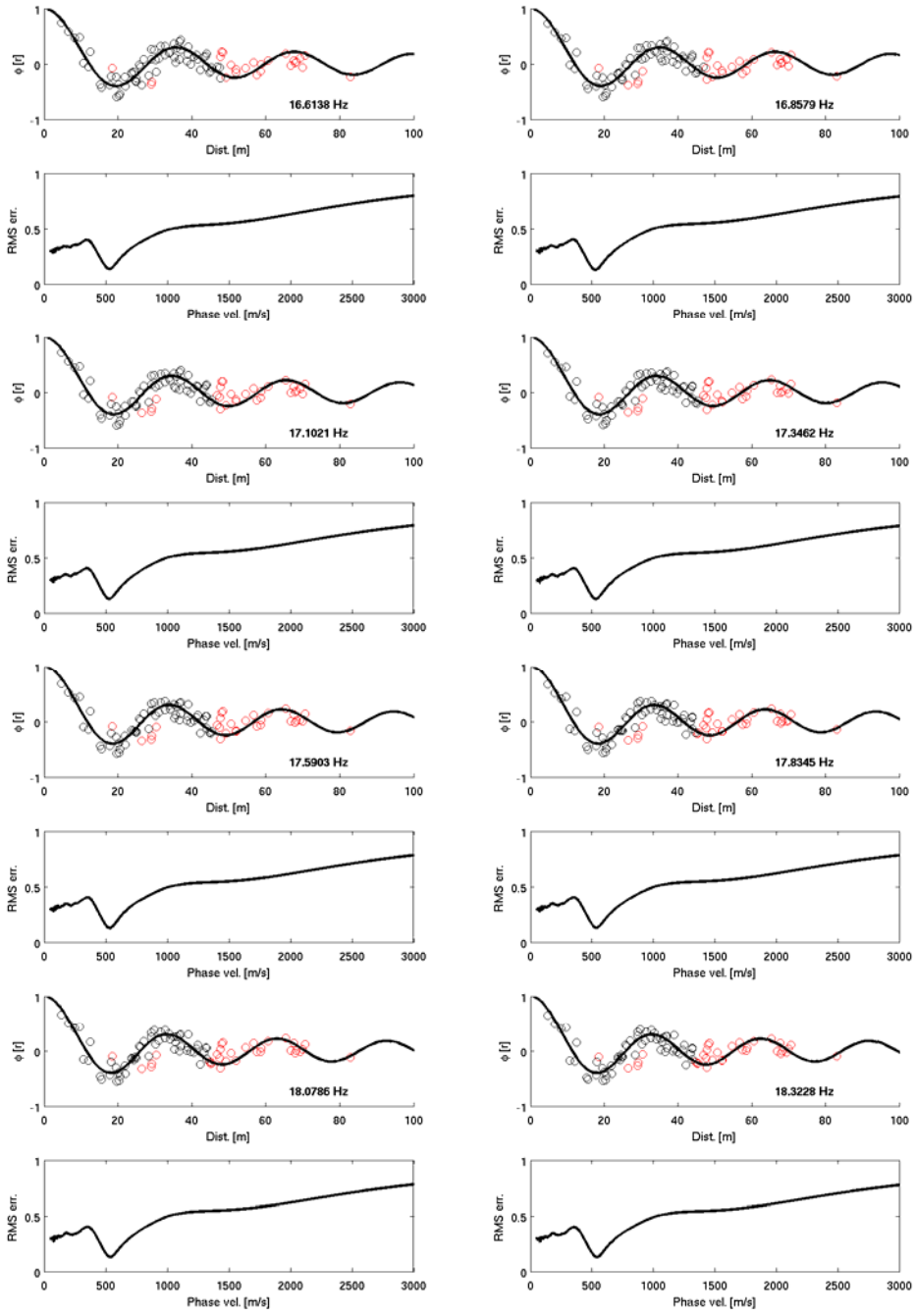

Figure 3: See previous caption.

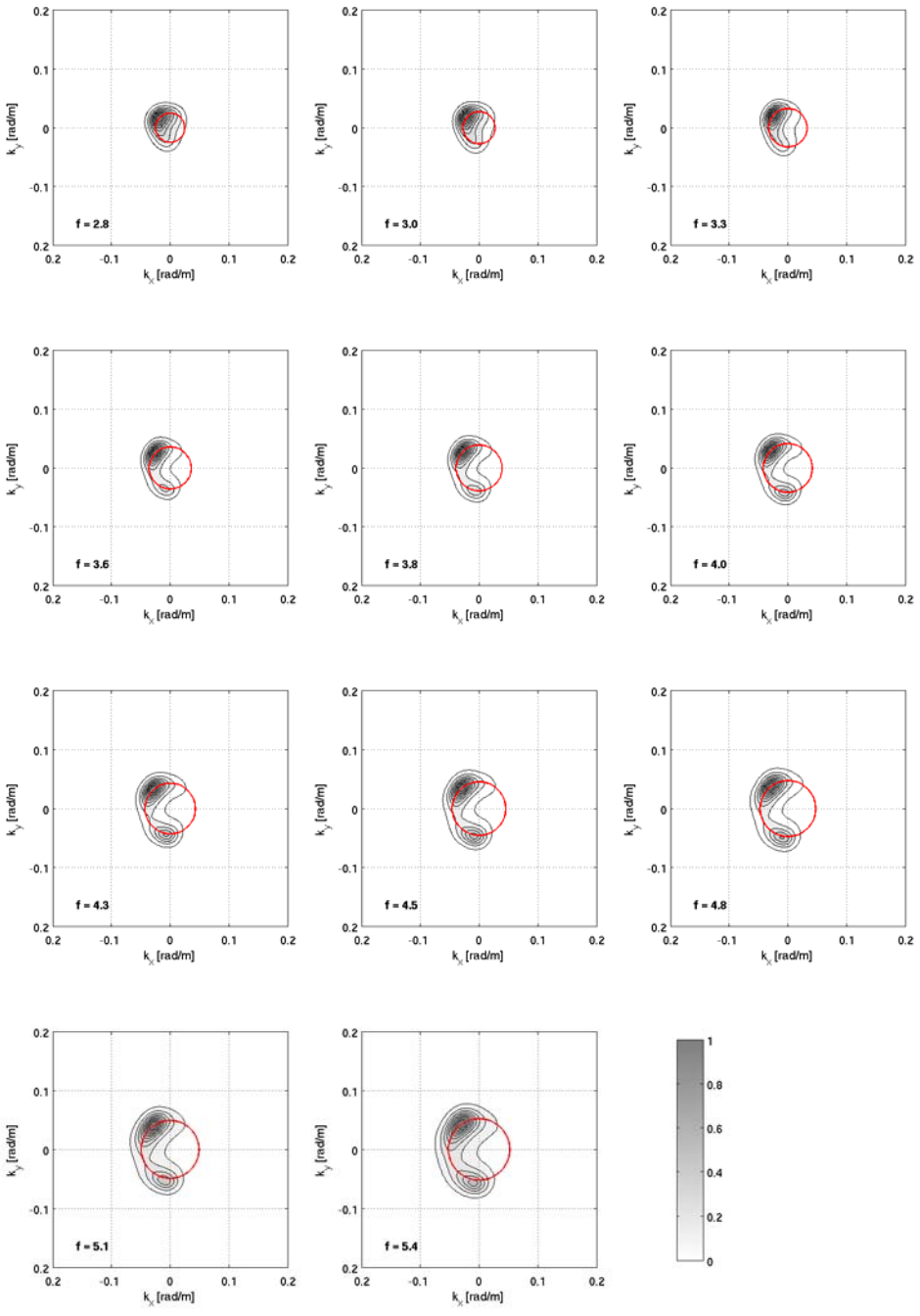

Figure 4: f-k power density function (MLM) at different frequencies (f, expressed in Hz). The red circles joints points with the same *k* value, corresponding to the maximum used to estimate the phase velocity.

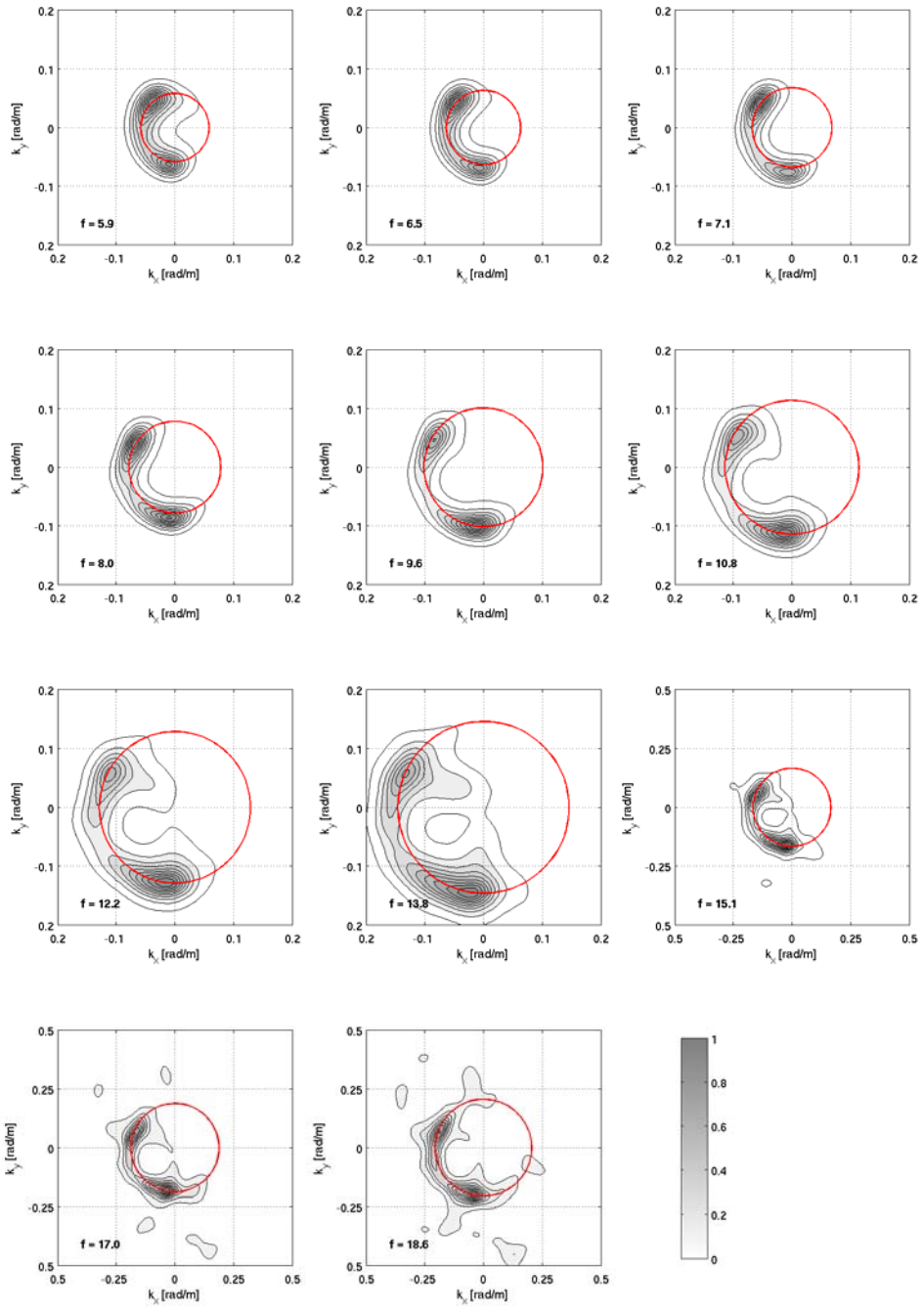

Figure 4: See previous caption.

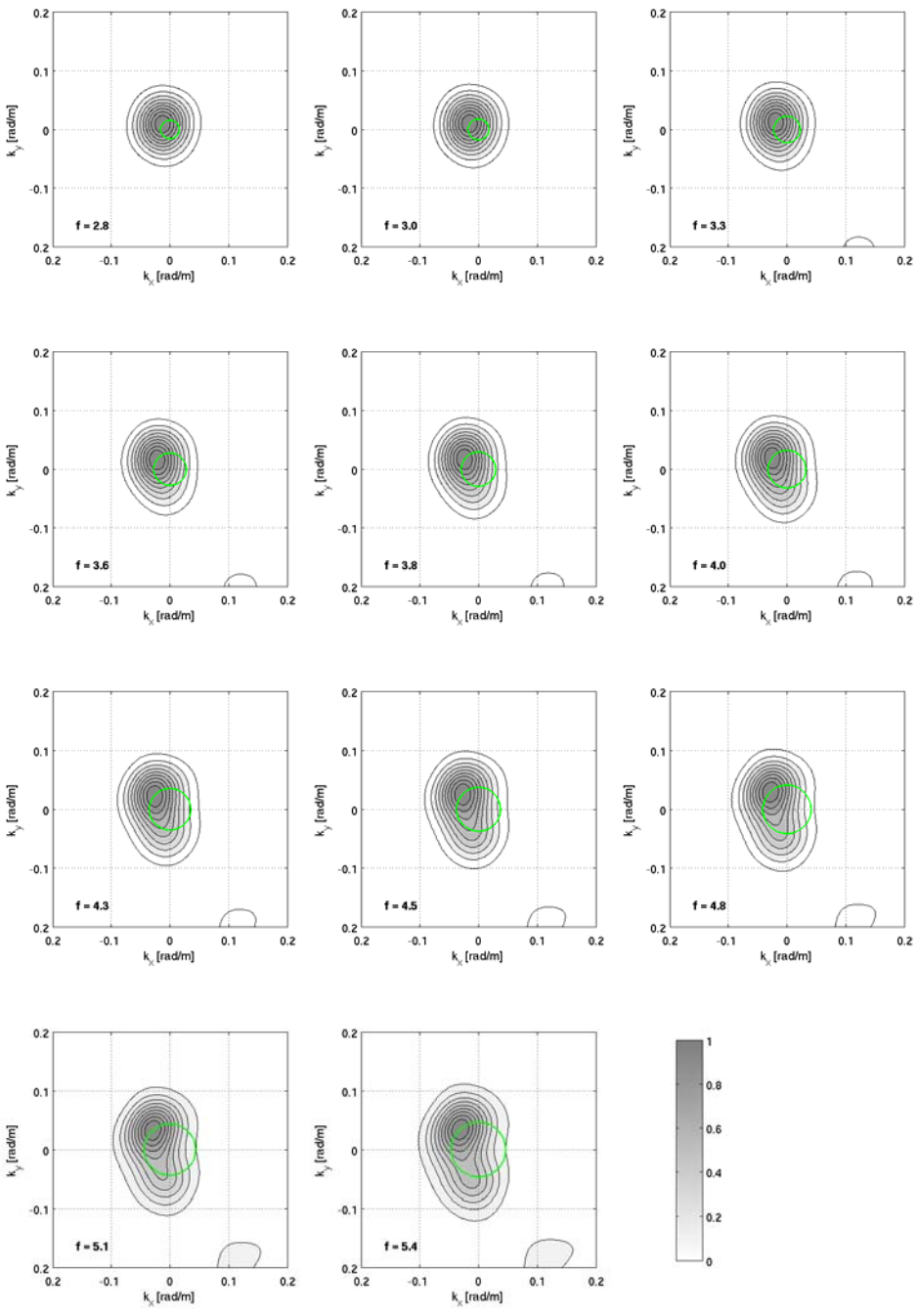

Figure 5: f-k power density function (BF) at different frequencies (f, expressed in Hz). The green circles joints points with the same *k* value, corresponding to the maximum used to estimate the phase velocity.

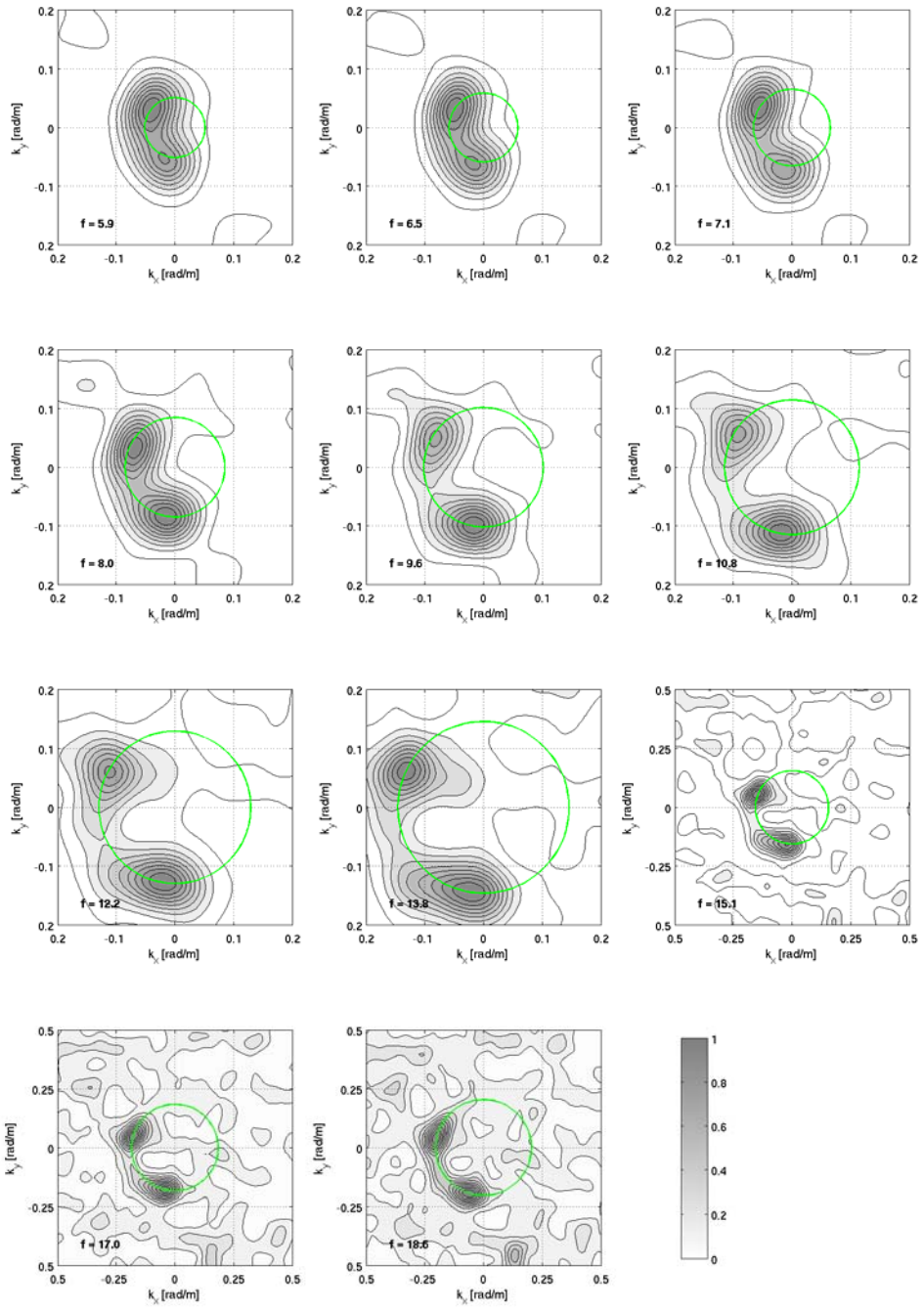

Figure 5: See previous caption.

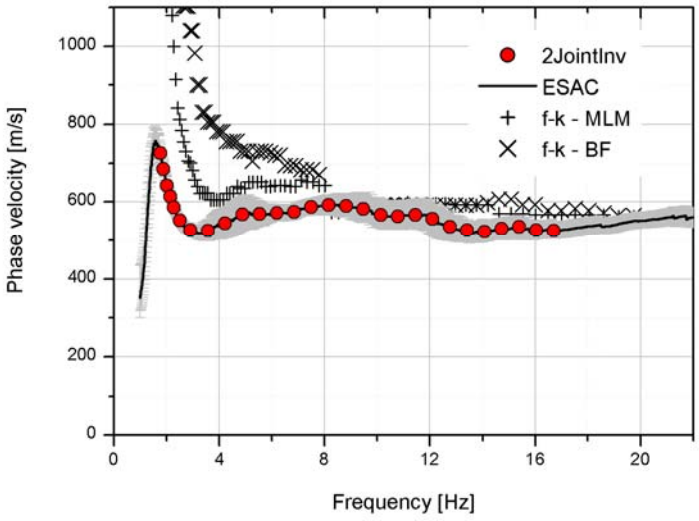

Figure 6: Comparison of experimental phase velocity estimated by the ESAC and the f-k (both for Beam Forming and Maximum Likelihood Method) methods. The red circles represent the values used for the joint inversion. The intervals (grey lines) around the observed ESAC phase velocities representing estimated uncertainties are obtained by calculating the square root of the covariance of the error function.

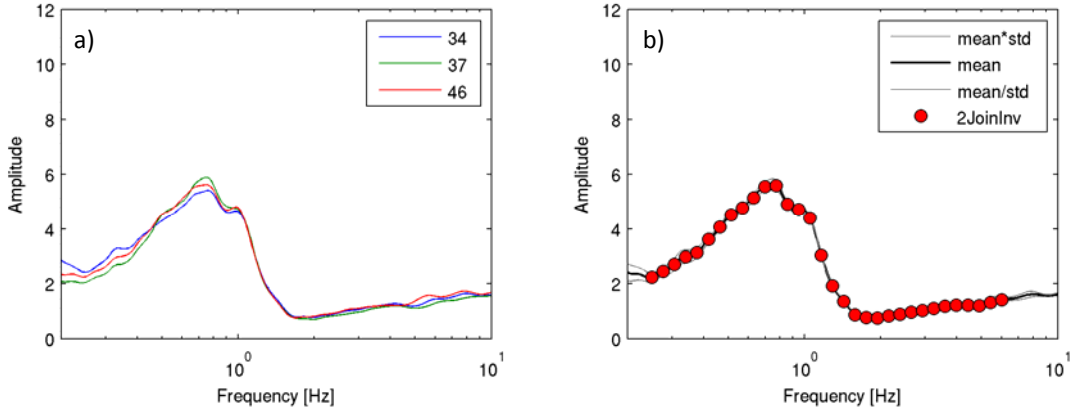

Figure 7: a) average *H/V* for some selected stations of the array (e.g. 34 stands for station 3034, etc.) and b) the average H/V of the array. The red circles represent the values used for the joint inversion.

The inversion of dispersion and *H/V* curves to estimate the S-wave velocity profile was carried out fixing to 7 the number of layers overlying the half-space in the model (**Table 1**). Through a genetic algorithm a search over 80000 models was carried out. The inversion was repeated several times starting from different

seed numbers, that is to say from a different population of initial models. In this way it was possible to better explore the space of the solution.

Table 1: Ranges of values defined for the parameters used in the joint inversion.

	Shear wave velocity, V_S [m/s]		Thickness, h [m]		Density, ρ [ton/m^3]	P wave velocity, V_P [m/s]
Layer	MIN	MAX	MIN	MAX		
#1	400	650	10	30	1.9	1400
#2	400	700	10	50	1.9	2050
#3	400	700	10	50	1.9	2200
#4	450	800	10	50	2.0	1800
#5	500	1000	30	100	2.1	1900
#6	600	1200	40	160	2.2	2400
#7	700	1300	50	400	2.2	2400
Half-space	1000	2000	Infinite		2.3	2600

During the inversion procedure the thickness and the shear wave velocity for each layer could be varied within the pre-defined ranges. On the contrary, for each layer, density was assigned *a priori*, while and P-wave velocity (V_P) was fixed considering the results of a seismic reflection tomography made nearby the NRZI station by Böhm (2009).

The models are selected by means of a cost function which take in account the agreement between the theoretical *H/V* and Rayleigh-wave dispersion curves with the observed ones. In this application, after trial and error test, the weight of 0.03, that allowed the best balanced fit of dispersion and H/V curves, was adopted.

Discussion of the results

In **Figure 8a** all the models tested during the inversion are depicted (gray lines). The best fit model (white line) and the models lying inside the 10% range of the minimum cost (black lines) function are highlighted. The agreement between experimental and theoretical Rayleigh wave dispersion curves (**Figure 8c**) is very good and, considering the wavelengths related to the dispersion curve frequency range, the V_S profile between 15 to about 180 metres is likely to be well constrained. Therefore, since below this depth the profile is constrained by the H/V curve alone, we prefer to show, in **Figure 8a** and **Table 2**, the V_S profile only within the depth range were both curves contribute to the inversion.

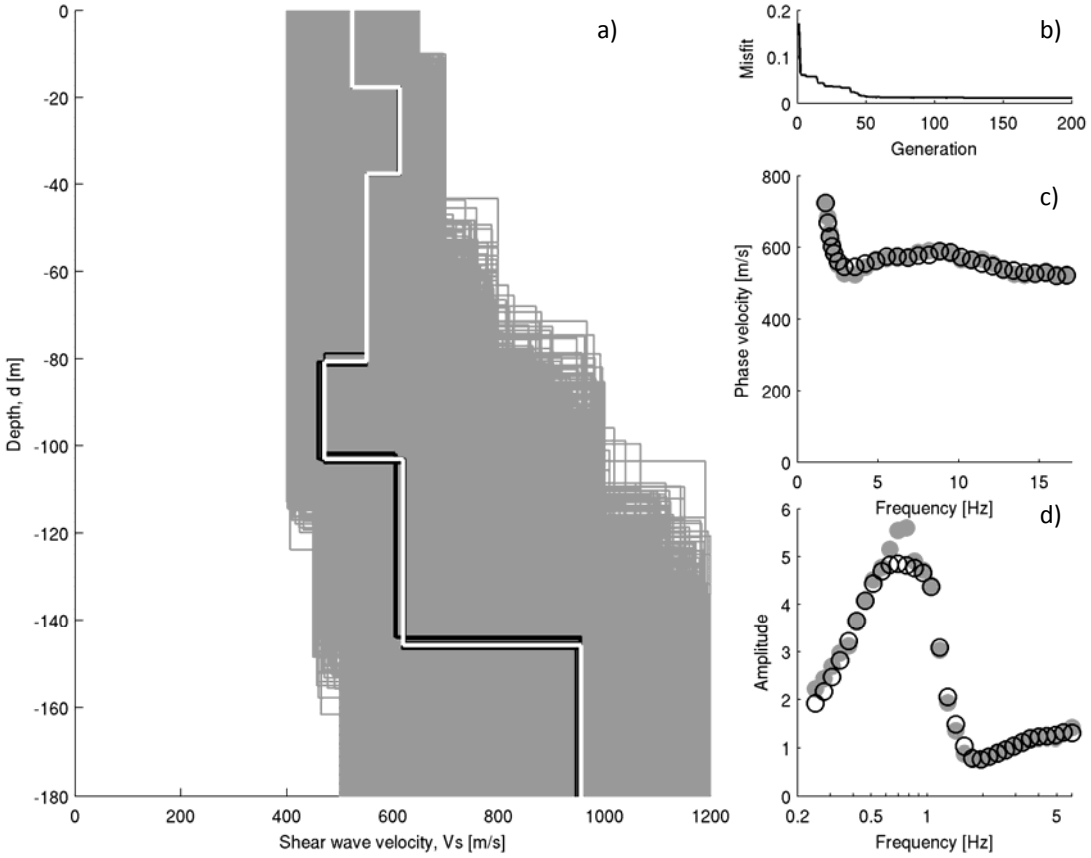

Figure 8: a) Tested models (grey lines), the minimum cost model (white line) and models lying inside the minimum cost + 10% range (black lines) for the NRZI station; b) the misfit versus generation values; c) experimental (grey circles) and estimated (white circles – relevant to the minimum cost model) phase velocities; d) experimental (grey circles) and estimated (white circles – relevant to the minimum cost model) *H/V* ratio curves.

Table 2: Shear wave velocity model at the NRZI station.

Shear wave velocity, V_S [m/s]	Thickness, h [m]
523.5	17.7
614.1	20.0
550.6	42.9
470.6	22.4
619.6	42.6
955.3	

APPLICATION OF SURFACE WAVE METHODS

FOR SEISMIC SITE CHARACTERIZATION

STATION CODE:

NVL

Responsible: Stefano Parolai[1]

Co-workers: Rodolfo Puglia[2], Matteo Picozzi[1]

1) Helmholtz Centre Potsdam - German Research Centre For Geosciences (GFZ), Helmholtzstraße 7, 14467 Potsdam, Germany
2) Istituto Nazionale di Geofisica e Vulcanologia (INGV), Sezione di Milano-Pavia, via Bassini 15, 20133 Milano, Italy

Introduction note

Details and references about *in-situ* measurement, Rayleigh wave dispersion and H/V curves estimate and inversion procedure here reported, can be found in the research reports of DPC-INGV S4 Project 2007-2009: Deliverables 6 and 7 at http://esse4.mi.ingv.it .

Testing equipment

The array measurements were performed using 17 EDL 24bit acquisition systems equipped with short-period Mark-L4-C-3D 1Hz sensors and GPS timing (**Figure 1**). The inter-station distances in the array ranged between 6.0 m to 182 meters. The stations worked contemporary for about 2 hours and 30 minutes, recording noise at 200 s.p.s., which is adequate for the short inter-station distances considered.

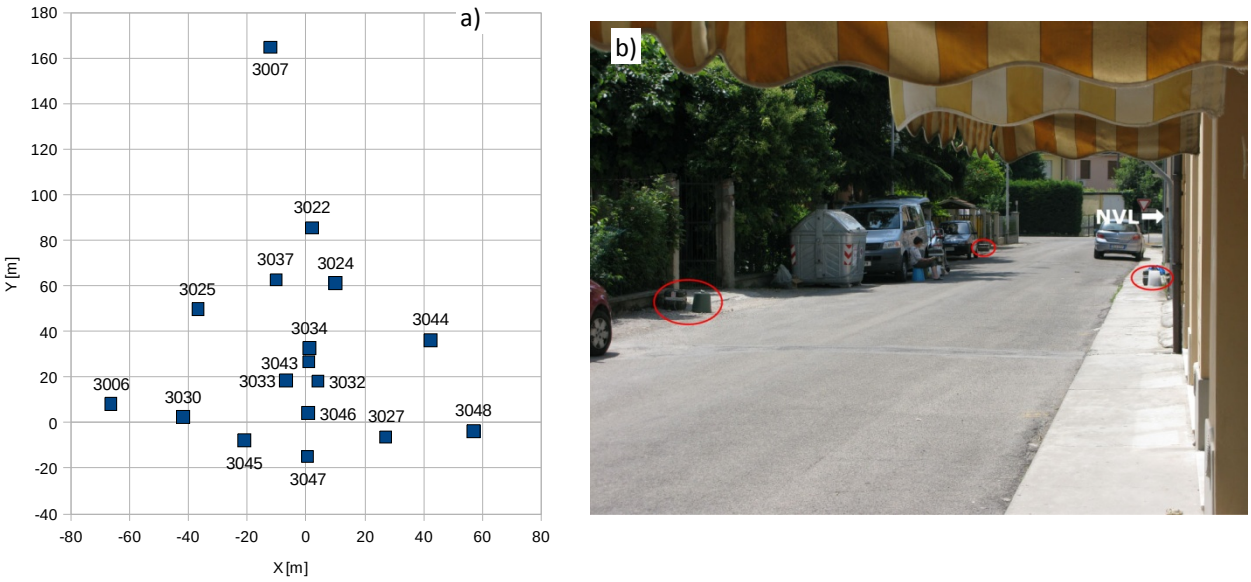

Figure 1: a) Geometry of the array. b) The field measurements.

Processing overview

The Rayleigh wave dispersion curve was estimated by analysing the vertical component of the recorded microtremors. In particular, the Extended Spatial Auto Correlation (ESAC) and the Frequency-Wavenumber (f-k) methods were adopted.

Rayleigh wave dispersion and *H/V* ratio curves were both used to estimate the local S-wave velocity profile, using a joint inversion scheme. The non-linear inversions were performed using a genetic algorithm which does not rely upon an explicit starting model and allows the identification of a solution close to the global minimum. The forward modeling of Rayleigh wave phase velocities and *H/V* curves was performed using the modified Thomson-Haskell method, under the assumption of vertically heterogeneous 1D earth models. The validity of this assumption was investigated by computing the *H/V* curve for each station of the array using the recorded data. The modeling of both the dispersion and *H/V* ratio curves during the inversions was not restricted to the fundamental mode only, but the possibility that higher modes can participate to define the observed dispersion and *H/V* curves is allowed.

Data analysis

The first step of the analysis consists in a visual inspection of the recordings at all stations. In particular, in order to identify malfunctioning of one station or channel and to select signal windows suitable for the H/V analysis, the quality of the recording was evaluated analysing (1) the signal stationarity in the time domain (**Figure 2a**), (2) the relevant unfiltered Fourier spectra (**Figure 2b**), and (3) the *H/V* variation over time (**Figure 2a**).

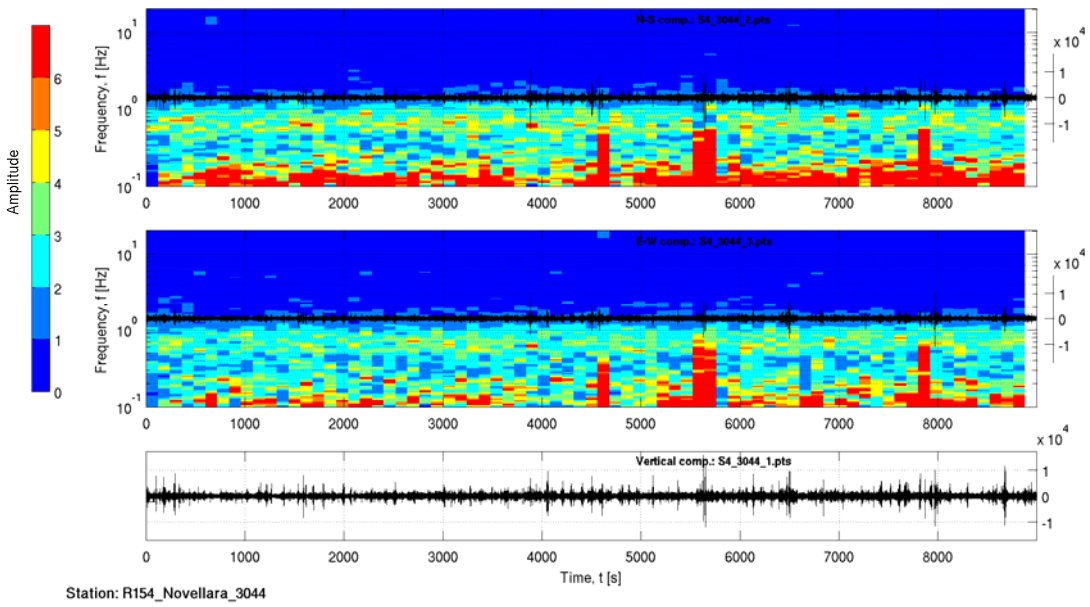

Figure 2a: *H/V* spectral ratios versus time (top and central panel for the NS and EW component, respectively) and corresponding time histories for station 3044.

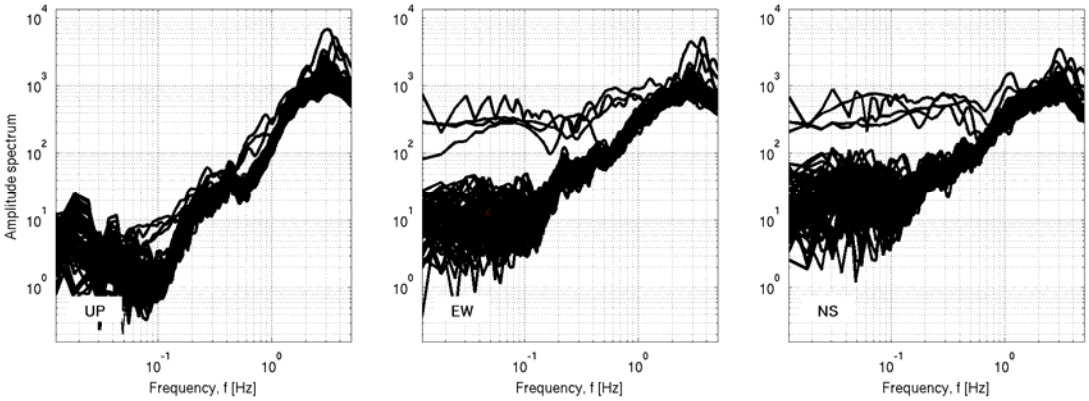

Figure 2b: Fourier spectra for each noise window at station 3044. Left) Vertical component spectra, center) E-W component spectra, right) N-S component spectra.

For each of the 17 used stations, 44 synchronized signal windows of 60 seconds were selected avoiding windows affected by local disturbance. These windows were in turn used to estimate the experimental Rayleigh-wave dispersion curves (using the vertical component of ground motion only) both by f-k and ESAC analysis.

The ESAC Rayleigh-wave dispersion curve was obtained minimizing the root mean square (RMS) of the differences between experimental and theoretical Bessel function values (**Figure 3**). Values that differ more than two standard deviations from those estimated by the best fitting functions (red circles in **Figure 3**) are automatically discarded and the procedure iteratively repeated. Furthermore, data are discarded also when their inter-station distance is longer than 1.5 times the relevant wavelength.

The f-k analysis offers the opportunity to verify if the requirements on the noise source distribution, necessary for the application of the ESAC method, were fulfilled. **Figure 4** and **Figure 5** show examples of the results for several frequencies of the frequency-wavenumber analysis using the Maximum Likelihood Method (MLM) and the Beam Forming (BF) respectively.

Figure 6 shows the very good agreement between the Rayleigh wave dispersion curves estimated both with ESAC and f-k approaches. Only below 2 Hz the f-k analysis provides larger phase velocities.

An average *H/V* for the selected stations was computed by averaging the *H/V* calculated for each signal window (**Figure 7a**). The average *H/V* curves for the selected stations were in turn averaged to obtain a single *H/V* spectral ratio representative for the array, which was then used as input in the joint inversion procedure for the estimation of the S-wave velocity profile (**Figure 7b**).

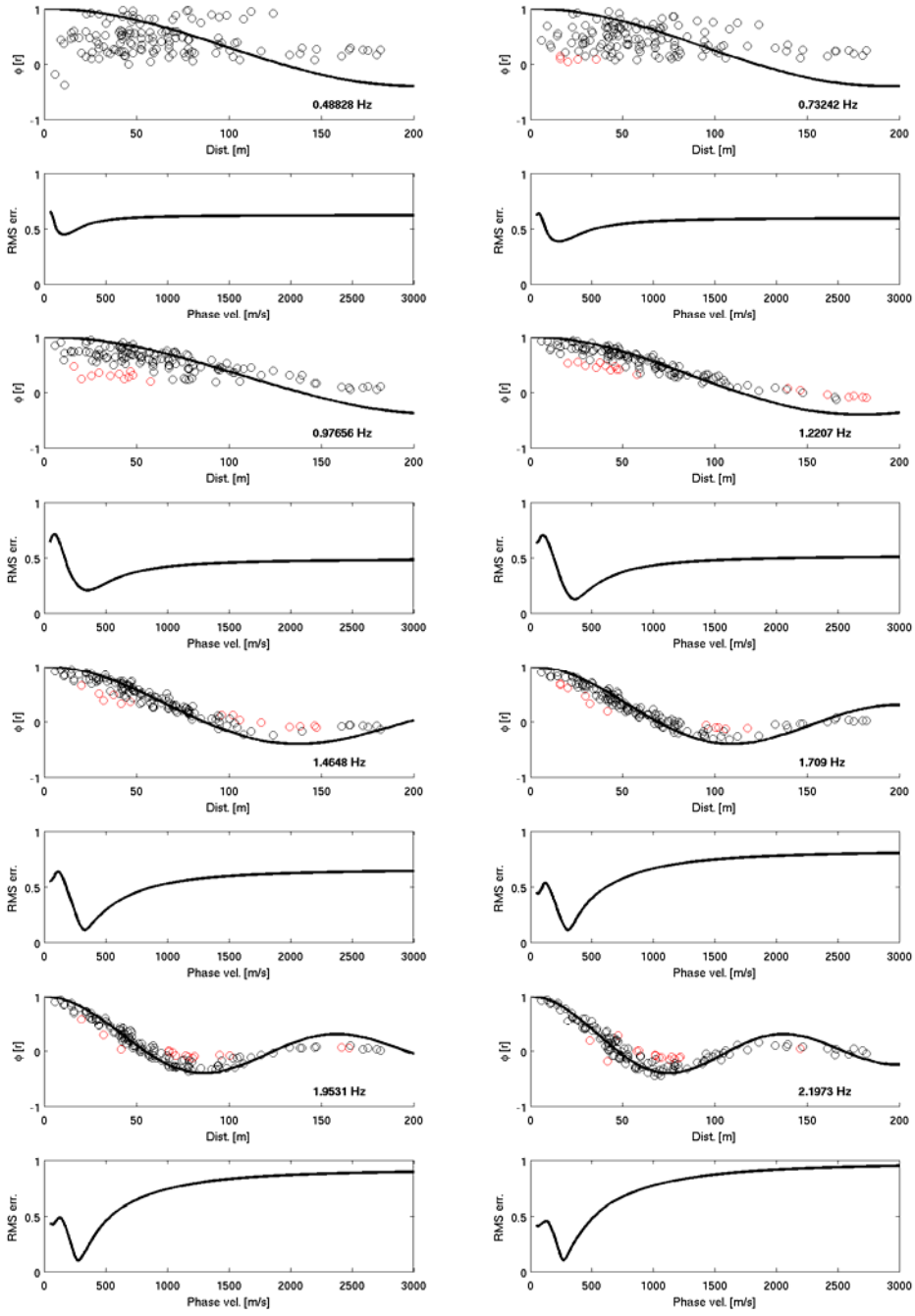

Figure 3: Experimental space-correlation function values versus distance (circles) for different frequencies. The red circles indicate values discarded. The black lines depict the estimated space-correlation function values for the phase velocity showing the best fit to the data. The bottom panels show the relevant root-mean square errors (RMS) versus phase velocity tested.

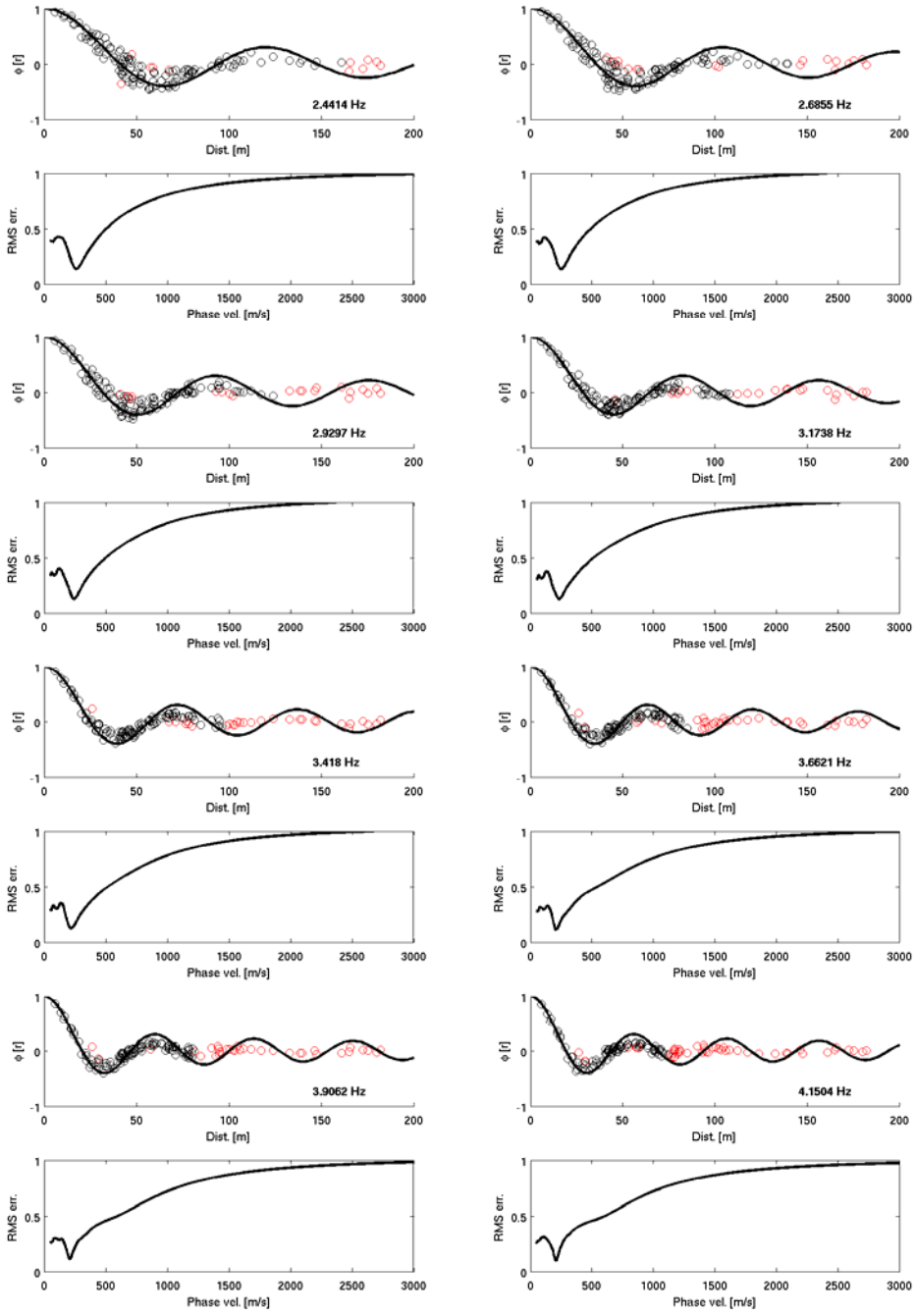

Figure 3: See previous caption.

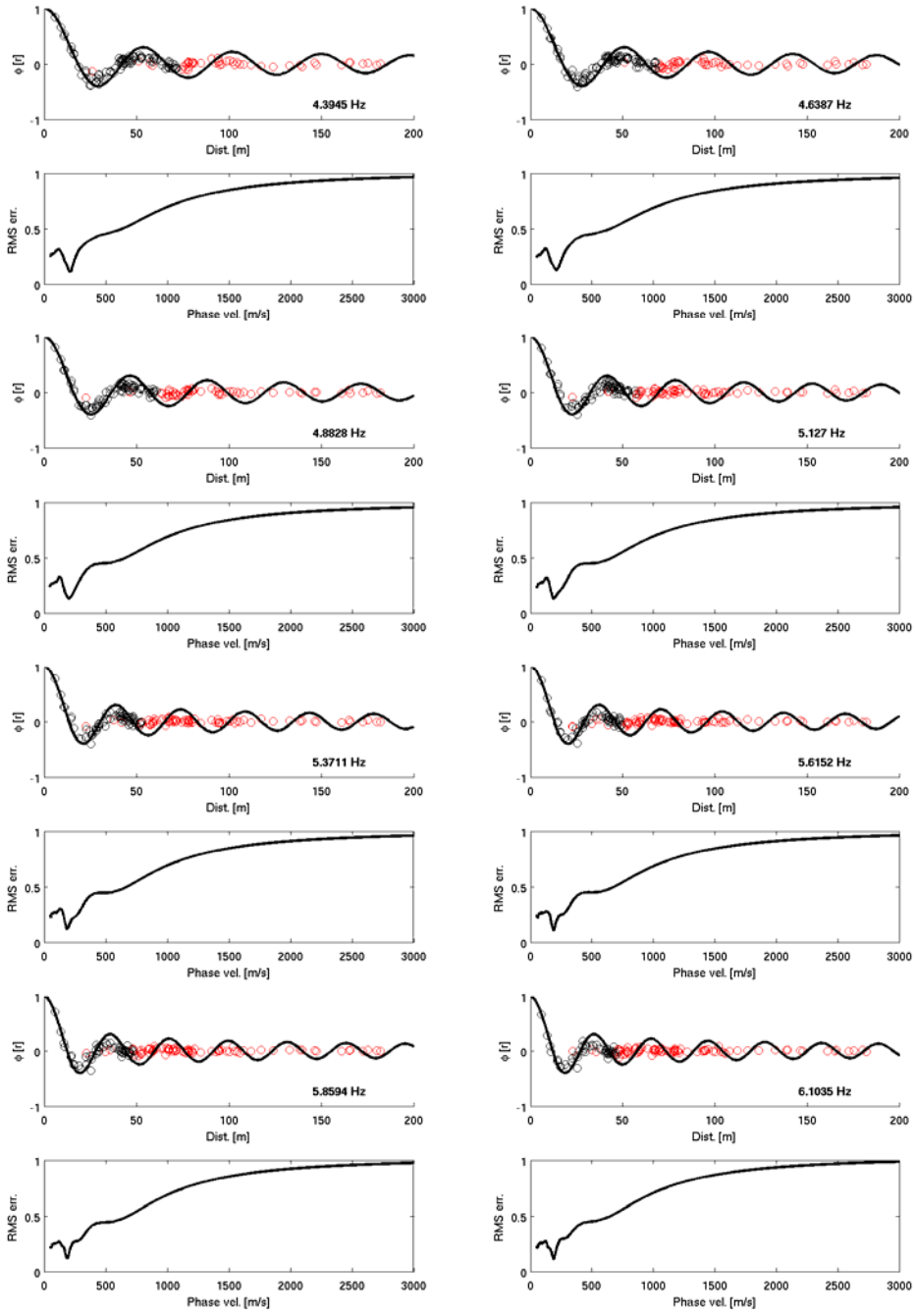

Figure 3: See previous caption.

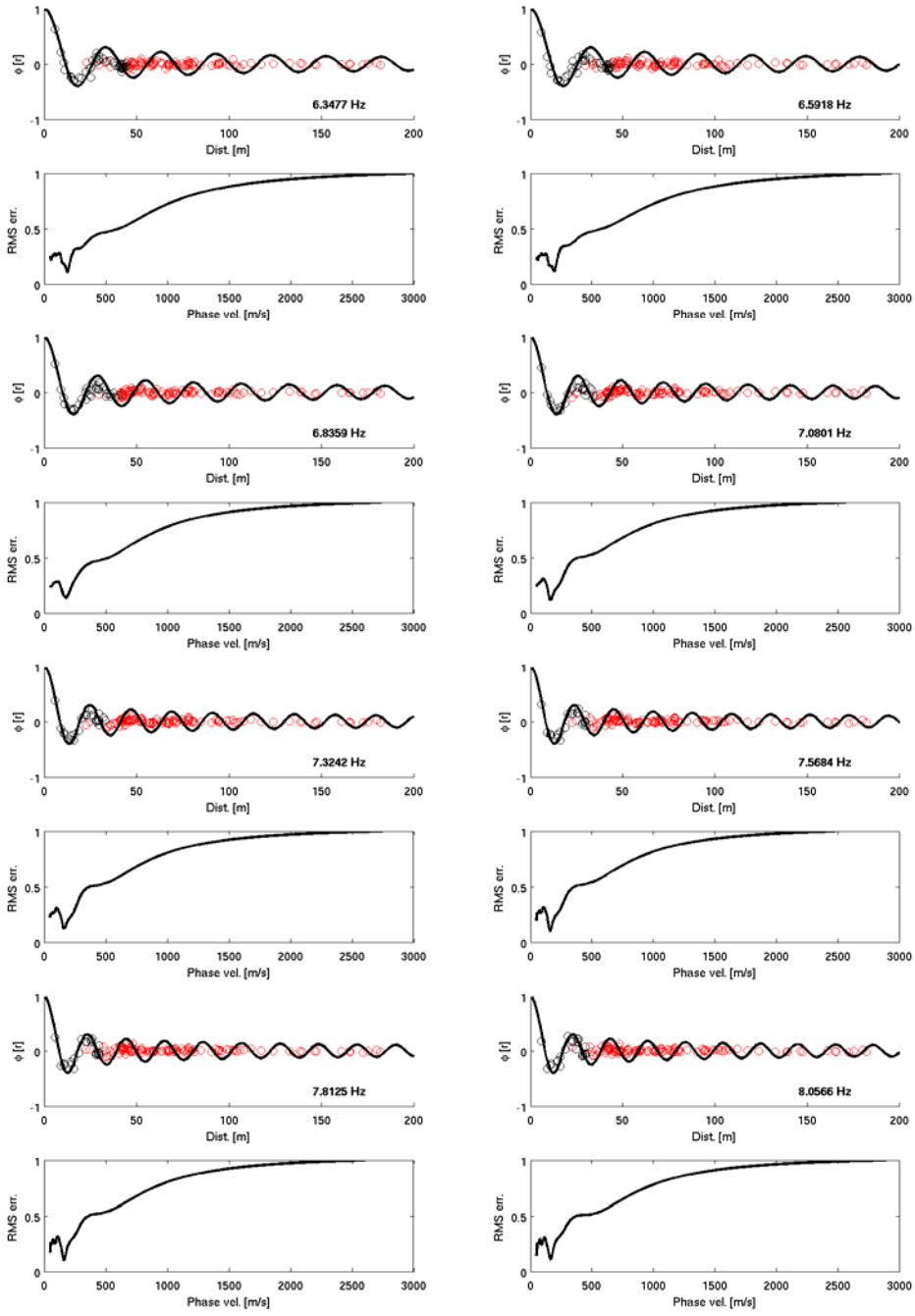

Figure 3: See previous caption.

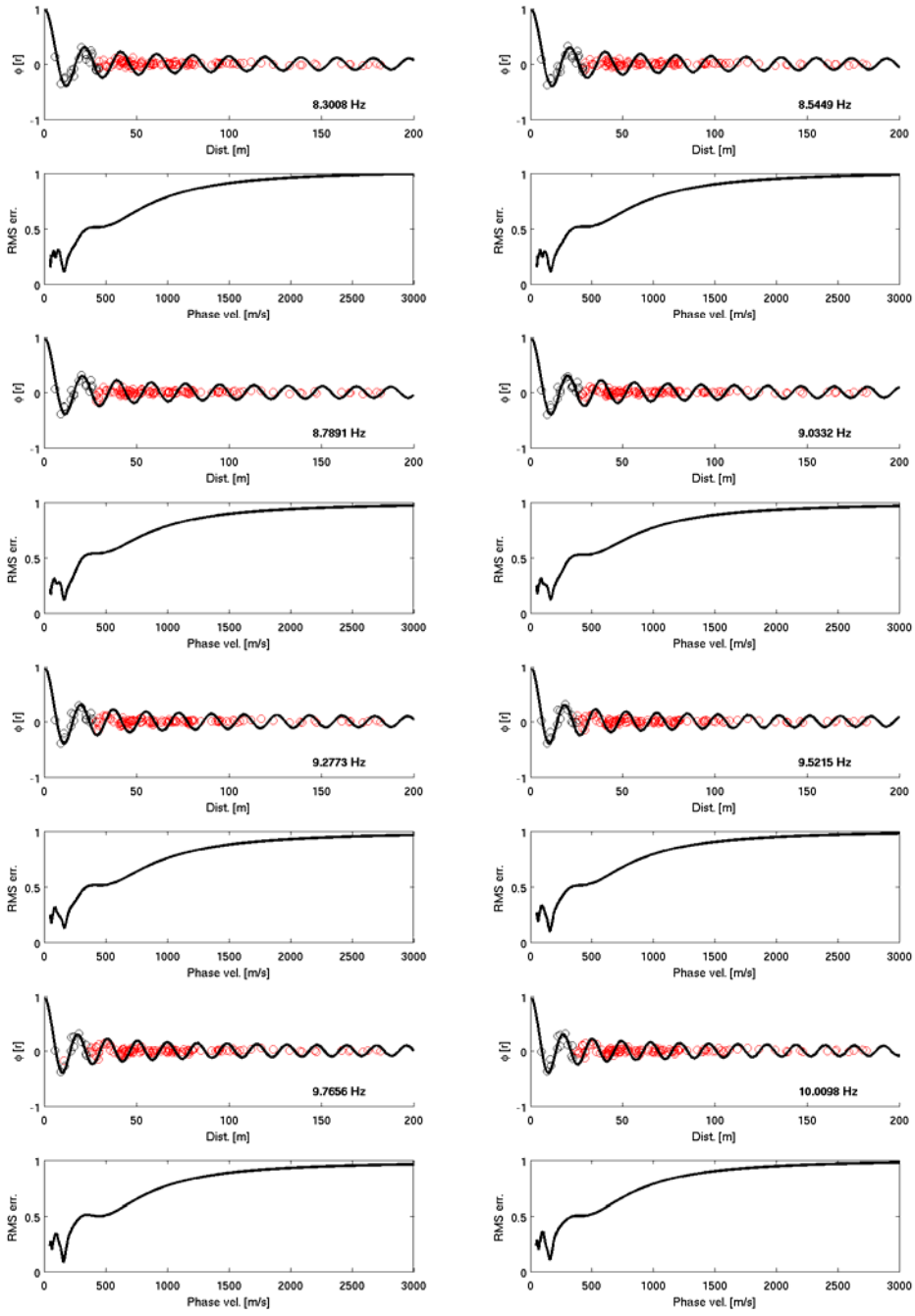

Figure 3: See previous caption.

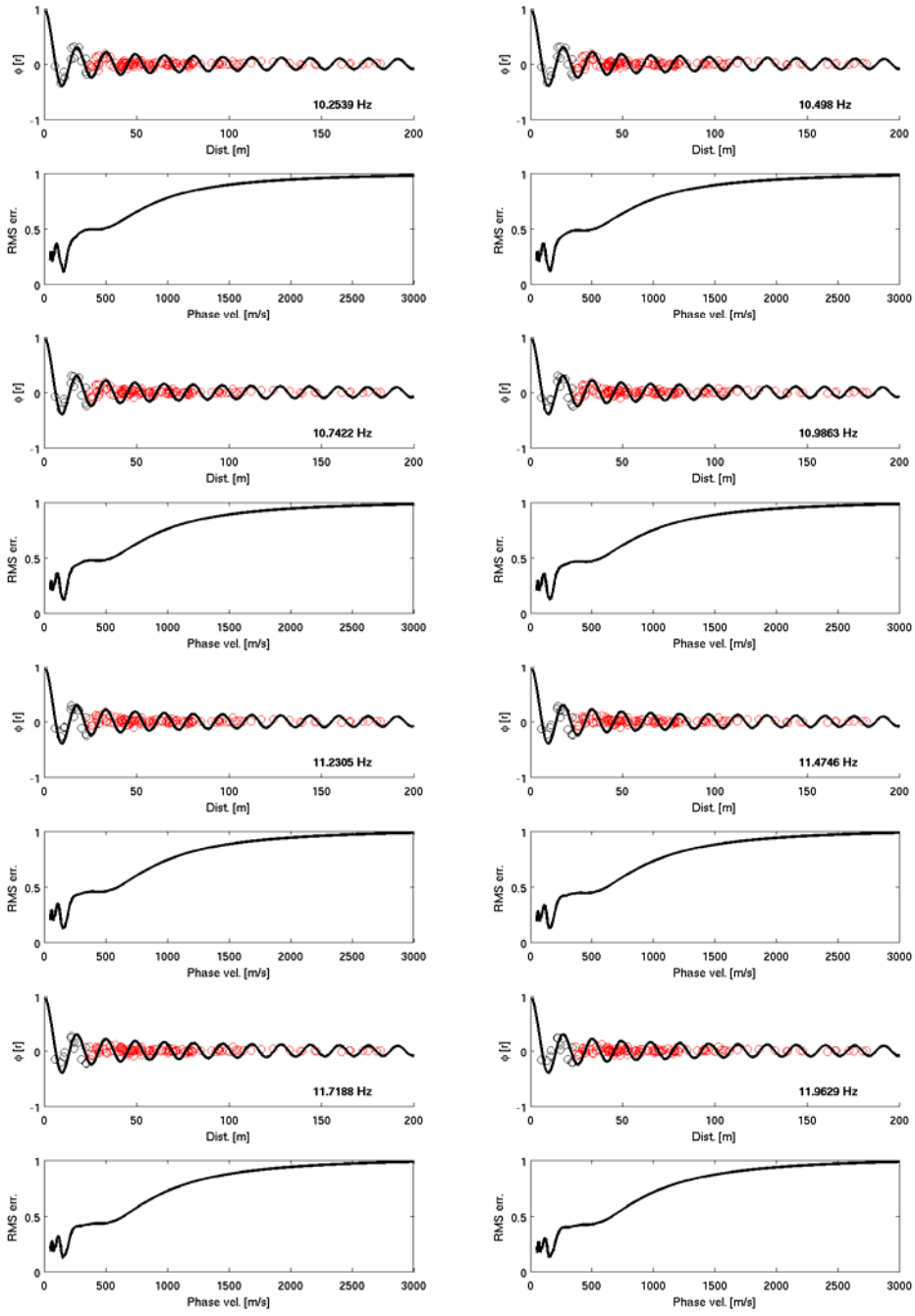

Figure 3: See previous caption.

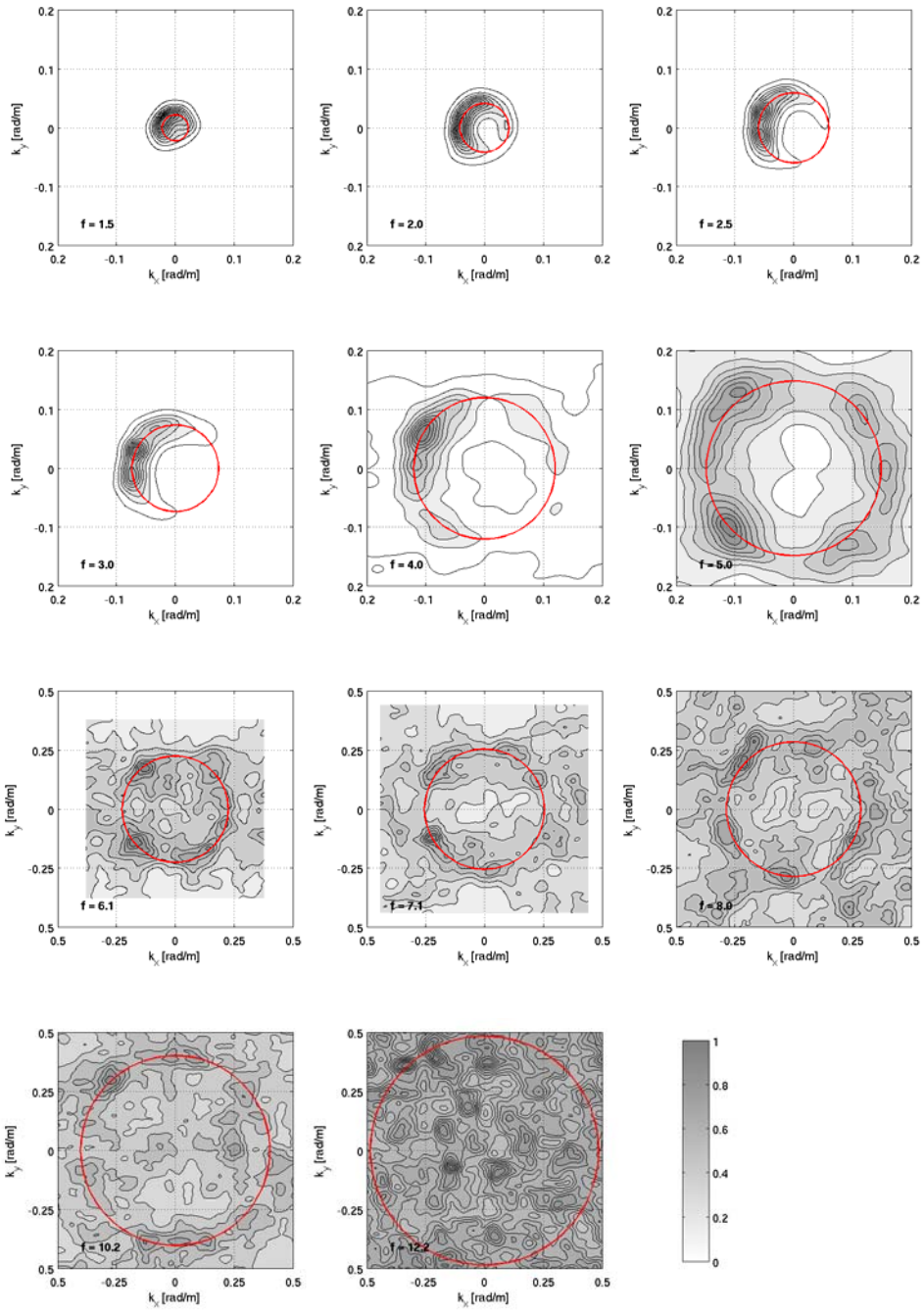

Figure 4: f-k power density function (MLM) at different frequencies (f, expressed in Hz). The red circles joints points with the same *k* value, corresponding to the maximum used to estimate the phase velocity.

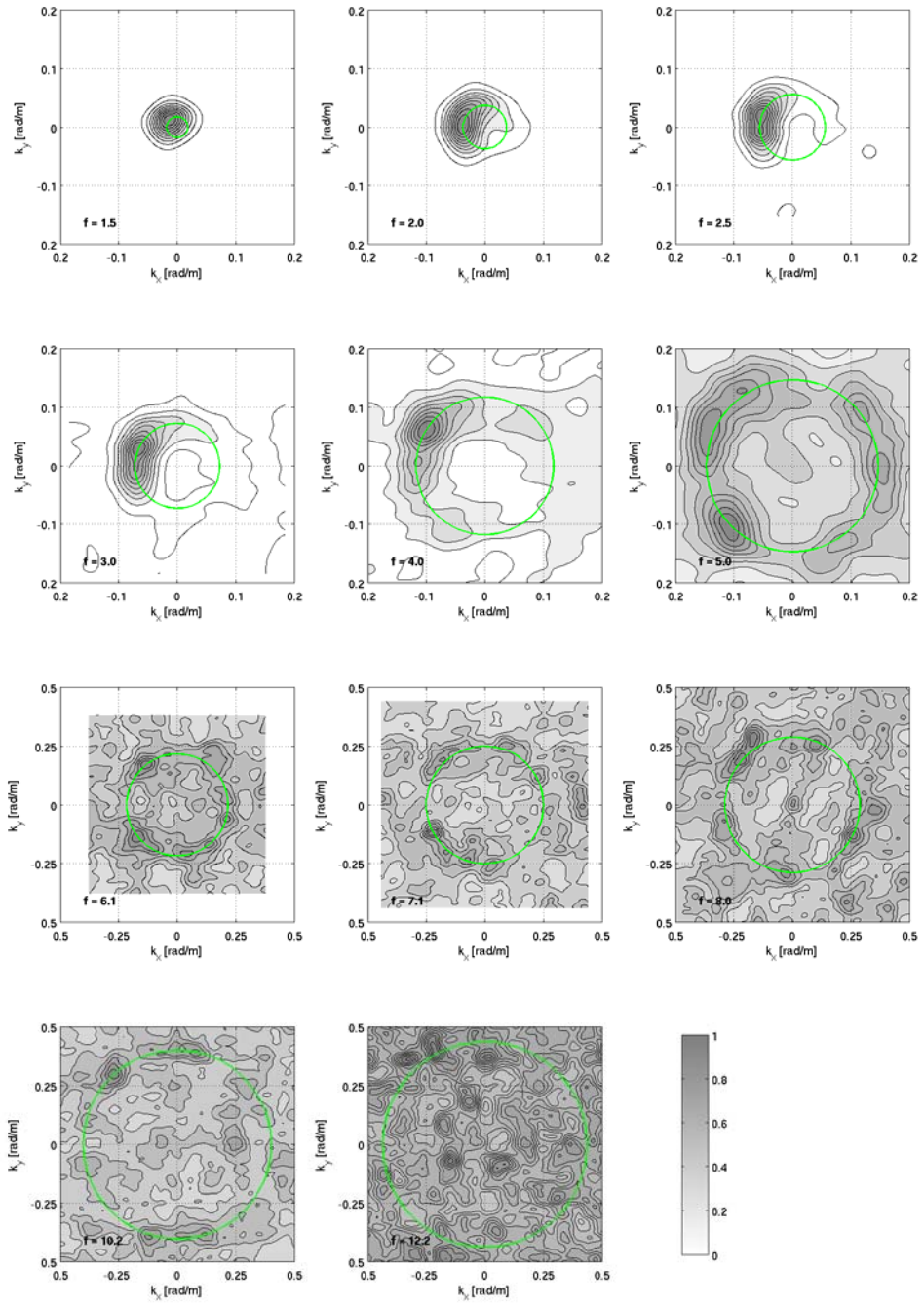

Figure 5: f-k power density function (BF) at different frequencies (f, expressed in Hz). The green circles joints points with the same *k* value, corresponding to the maximum used to estimate the phase velocity.

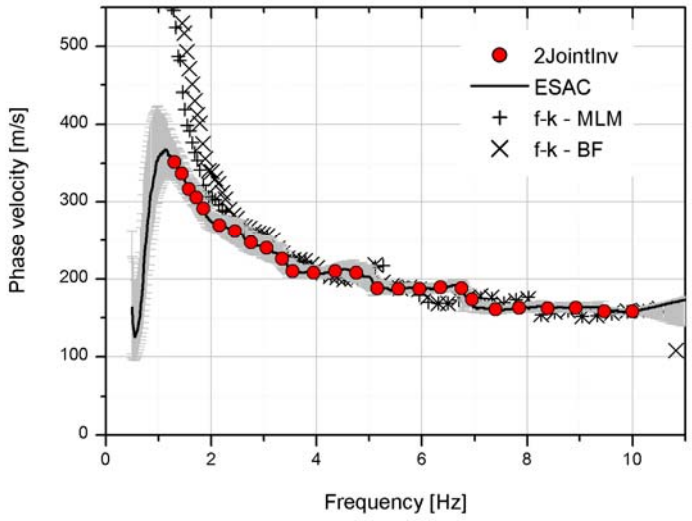

Figure 6: Comparison of experimental phase velocity estimated by the ESAC and the f-k (both for Beam Forming and Maximum Likelihood Method) methods. The red circles represent the values used for the joint inversion. The intervals (grey lines) around the observed ESAC phase velocities representing estimated uncertainties are obtained by calculating the square root of the covariance of the error function.

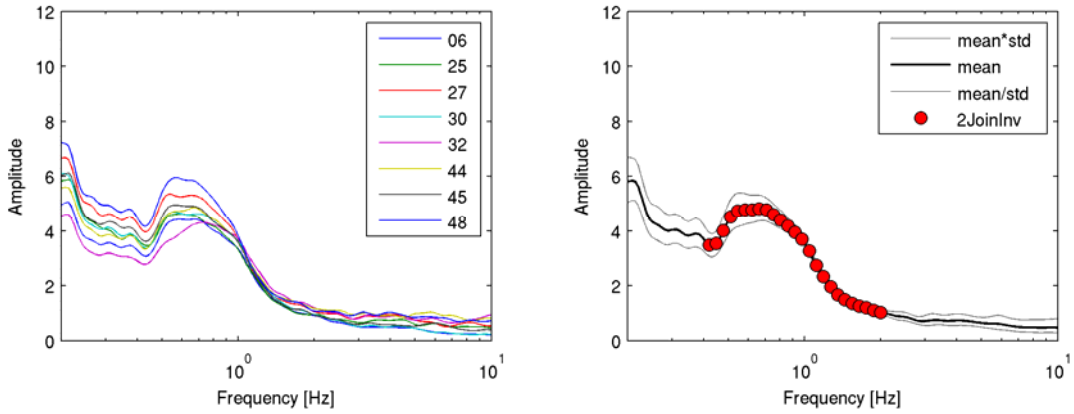

Figure 7: a) average *H/V* for the selected stations of the array (e.g. 06 stands for station 3006, etc.) and b) the average H/V of the array. The red circles represent the values used for the joint inversion.

The inversion of dispersion and *H/V* curves to estimate the S-wave velocity profile was carried out fixing to 6 the number of layers overlying the half-space in the model (**Table 1**). Through a genetic algorithm a search over 80000 models was carried out. The inversion was repeated several times starting from different

seed numbers, that is to say from a different population of initial models. In this way it was possible to better explore the space of the solution.

Table 1: Ranges of values defined for the parameters used in the joint inversion.

	Shear wave velocity, V_S [m/s]		Thickness, h [m]		Density, ρ [ton/m^3]
Layer	MIN	MAX	MIN	MAX	
#1	100	250	5	30	1.9
#2	100	300	10	50	2.0
#3	150	400	10	50	2.1
#4	250	500	30	100	2.2
#5	350	800	50	300	2.2
#6	350	800	200	700	2.2
Half-space	800	1800	Infinite		2.3

During the inversion procedure the thickness and the shear wave velocity for each layer could be varied within the pre-defined ranges. On the contrary, for each layer, density was assigned *a priori*, while P-wave velocity (V_P) was calculated through the values of the S-wave velocity Vs via the equation: $V_P\,[\mathrm{m/s}] = 1.1 \cdot V_S + 1290$.

The models are selected by means of a cost function which take in account the agreement between the theoretical *H/V* and Rayleigh-wave dispersion curves with the observed ones. In this application, after trial and error test, the weight of 0.05, that allowed the best balanced fit of dispersion and H/V curves, was adopted.

Discussion of the results

In **Figure 8a** all the models tested during the inversion are depicted (gray lines). The best fit model (white line) and the models lying inside the 10% range of the minimum cost (black lines) function are highlighted. The agreement between experimental and theoretical Rayleigh wave dispersion curves (**Figure 8c**) is good and, considering the wavelengths related to the dispersion curve frequency range, the V_S profile between 5 to about 200 metres is likely to be well constrained. Therefore, since below this depth the profile is constrained by the H/V curve alone, we prefer to show, in **Figure 8a** and **Table 2**, the V_S profile only within the depth range were both curves contribute to the inversion.

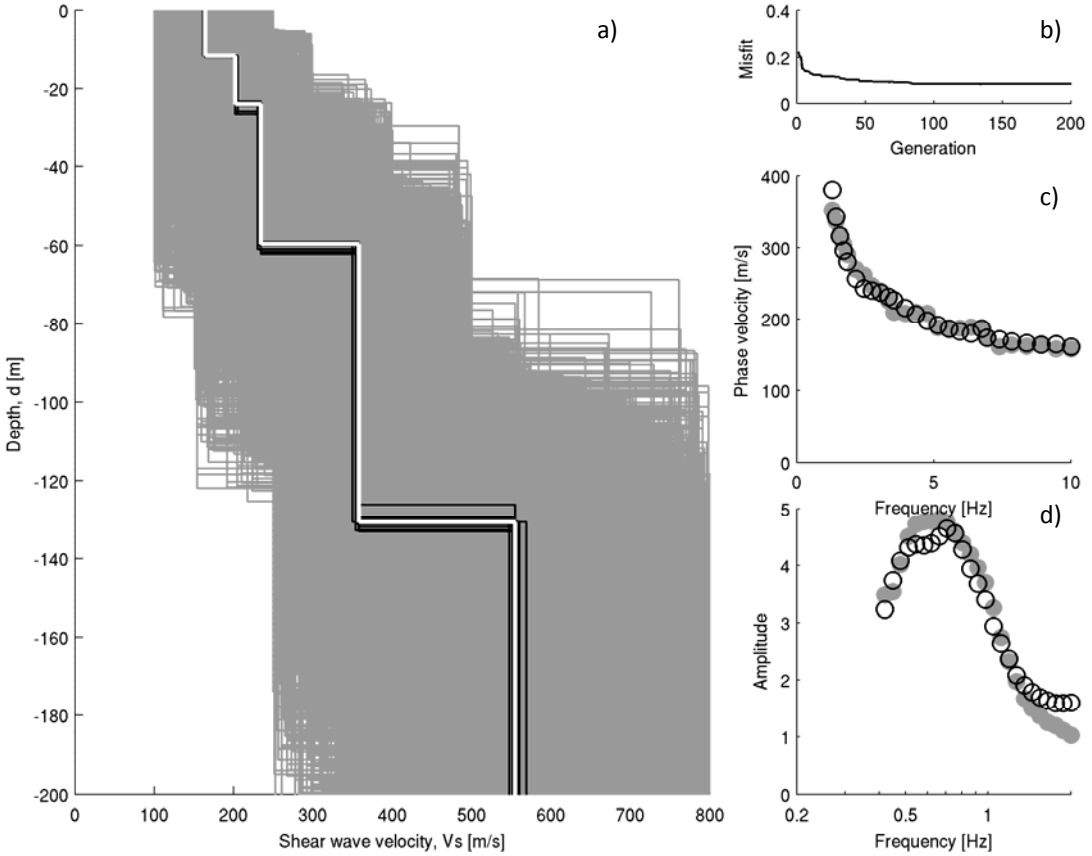

Figure 8: a) Tested models (grey lines), the minimum cost model (white line) and models lying inside the minimum cost + 10% range (black lines) for the NVL station; b) the misfit versus generation values; c) experimental (grey circles) and estimated (white circles – relevant to the minimum cost model) phase velocities; d) experimental (grey circles) and estimated (white circles – relevant to the minimum cost model) *H/V* ratio curves.

Table 2: Shear wave velocity model at the NVL station.

Shear wave velocity, V_S [m/s]	Thickness, h [m]
164.1	11.6
202.0	12.4
234.3	35.7
357.8	70.9
554.7	

APPLICATION OF SURFACE WAVE METHODS

FOR SEISMIC SITE CHARACTERIZATION

STATION CODE:

SNA

Responsible: Stefano Parolai[1]

Co-workers: Rodolfo Puglia[2], Matteo Picozzi[1]

1) Helmholtz Centre Potsdam - German Research Centre For Geosciences (GFZ), Helmholtzstraße 7, 14467 Potsdam, Germany
2) Istituto Nazionale di Geofisica e Vulcanologia (INGV), Sezione di Milano-Pavia, via Bassini 15, 20133 Milano, Italy

Introduction note

Details and references about *in-situ* measurement, Rayleigh wave dispersion and H/V curves estimate and inversion procedure here reported, can be found in the research reports of DPC-INGV S4 Project 2007-2009: Deliverables 6 and 7 at http://esse4.mi.ingv.it .

Testing equipment

The array measurements were performed using 15 EDL 24bit acquisition systems equipped with short-period Mark-L4-C-3D 1Hz sensors and GPS timing (**Figure 1**). However, due to malfunctioning, only the data of 13 stations (depicted as blue squares) could be used for the processing. The inter-station distances in the array ranged between 6.0 m to 61 meters. The stations worked contemporary for about 1 hour and 40 minutes, recording noise at 200 s.p.s., which is adequate for the short inter-station distances considered.

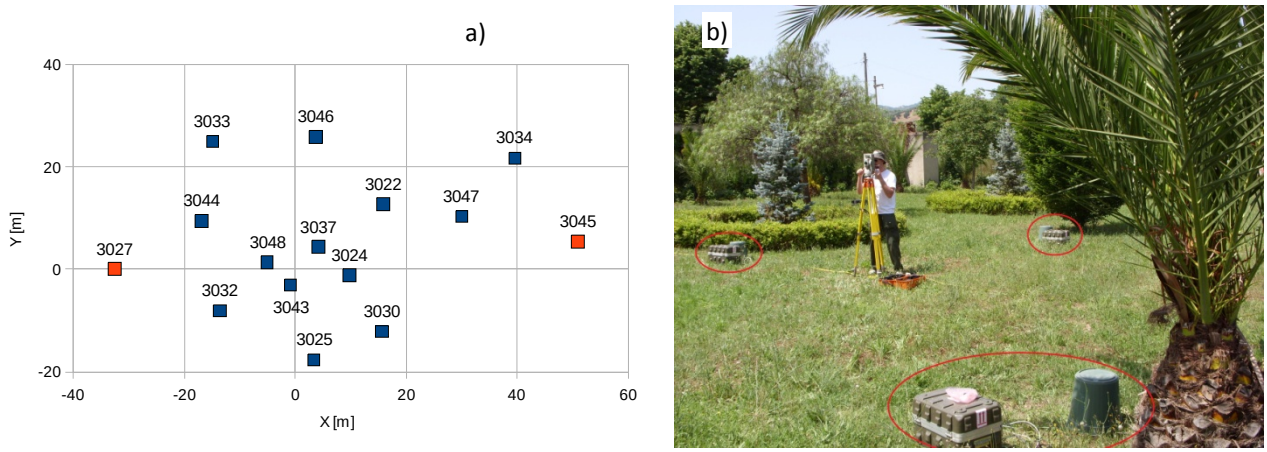

Figure 1: a) Geometry of the array. Stations that did not work properly are evidenced with the red color. b) The field measurements.

Processing overview

The Rayleigh wave dispersion curve was estimated by analysing the vertical component of the recorded microtremors. In particular, the Extended Spatial Auto Correlation (ESAC) and the Frequency-Wavenumber (f-k) methods were adopted.

Rayleigh wave dispersion and *H/V* ratio curves were both used to estimate the local S-wave velocity profile, using a joint inversion scheme. The non-linear inversions were performed using a genetic algorithm which does not rely upon an explicit starting model and allows the identification of a solution close to the global minimum. The forward modeling of Rayleigh wave phase velocities and *H/V* curves was performed using the modified Thomson-Haskell method, under the assumption of vertically heterogeneous 1D earth models. The validity of this assumption was investigated by computing the *H/V* curve for each station of the array using the recorded data. The modeling of both the dispersion and *H/V* ratio curves during the inversions was not restricted to the fundamental mode only, but the possibility that higher modes can participate to define the observed dispersion and *H/V* curves is allowed.

Data analysis

The first step of the analysis consists in a visual inspection of the recordings at all stations. In particular, in order to identify malfunctioning of one station or channel and to select signal windows suitable for the H/V analysis, the quality of the recording was evaluated analysing (1) the signal stationarity in the time domain (**Figure 2a**), (2) the relevant unfiltered Fourier spectra (**Figure 2b**), and (3) the *H/V* variation over time (**Figure 2a**).

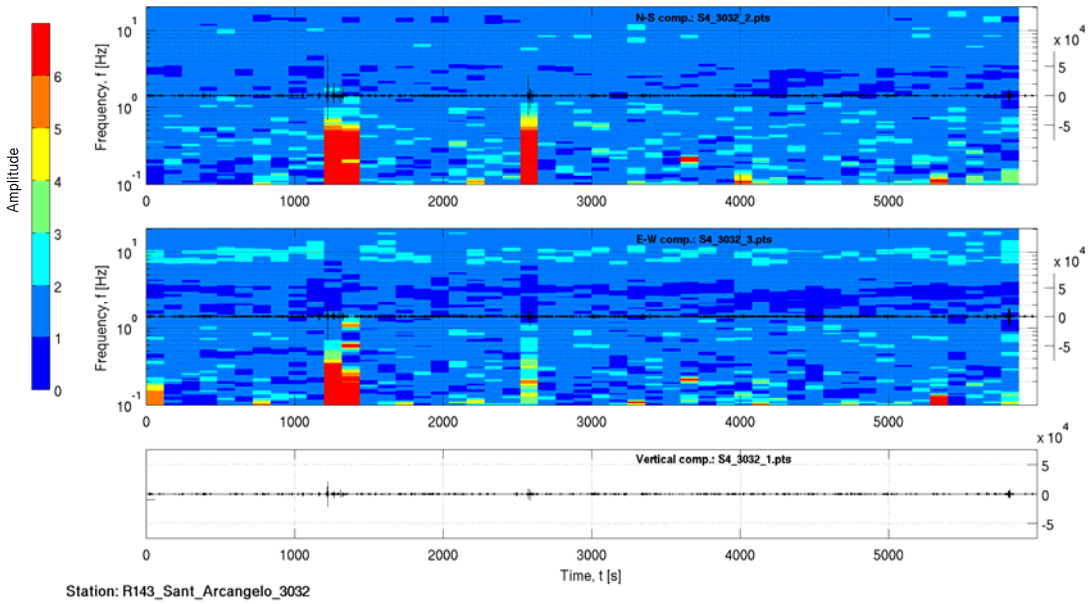

Figure 2a: *H/V* spectral ratios versus time (top and central panel for the NS and EW component, respectively) and corresponding time histories for station 3032.

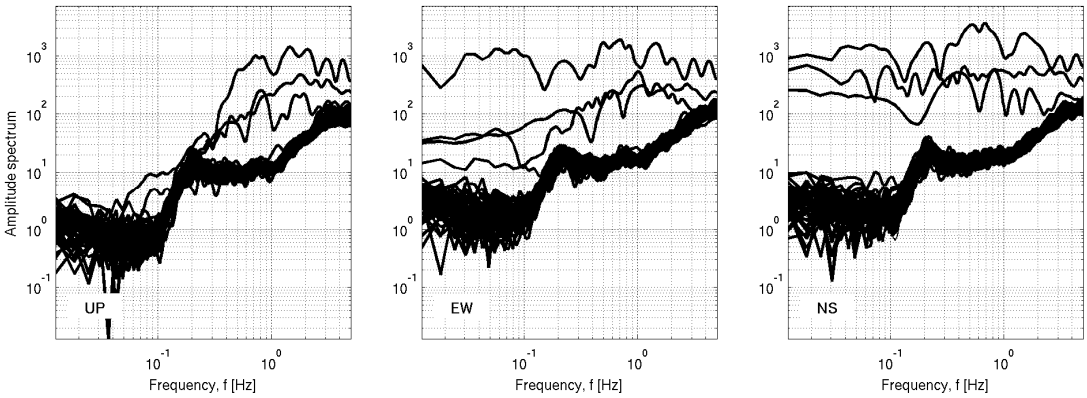

Figure 2b: Fourier spectra for each noise window at station 3032. Left) Vertical component spectra, center) E-W component spectra, right) N-S component spectra.

For each of the 13 used stations, 44 synchronized signal windows of 60 seconds were selected avoiding windows affected by local disturbance. These windows were in turn used to estimate the experimental Rayleigh-wave dispersion curves (using the vertical component of ground motion only) both by f-k and ESAC analysis.

The ESAC Rayleigh-wave dispersion curve was obtained minimizing the root mean square (RMS) of the differences between experimental and theoretical Bessel function values (**Figure 3**). Values that differ more than two standard deviations from those estimated by the best fitting functions (red circles in **Figure 3**) are automatically discarded and the procedure iteratively repeated. Furthermore, data are discarded also when their inter-station distance is longer than 1.5 times the relevant wavelength.

The f-k analysis offers the opportunity to verify if the requirements on the noise source distribution, necessary for the application of the ESAC method, were fulfilled. **Figure 4** and **Figure 5** show examples of the results for several frequencies of the frequency-wavenumber analysis using the Maximum Likelihood Method (MLM) and the Beam Forming (BF) respectively.

Figure 6 shows a not very good agreement between the Rayleigh wave dispersion curves estimated both with ESAC and f-k approaches. Already below 6 Hz the f-k -MLM analysis provides larger phase velocities.

An average *H/V* for the selected stations was computed by averaging the *H/V* calculated for each signal window (**Figure 7a**). The average *H/V* curves for the selected stations were in turn averaged to obtain a single *H/V* spectral ratio representative for the array, which was then used as input in the joint inversion procedure for the estimation of the S-wave velocity profile (**Figure 7b**).

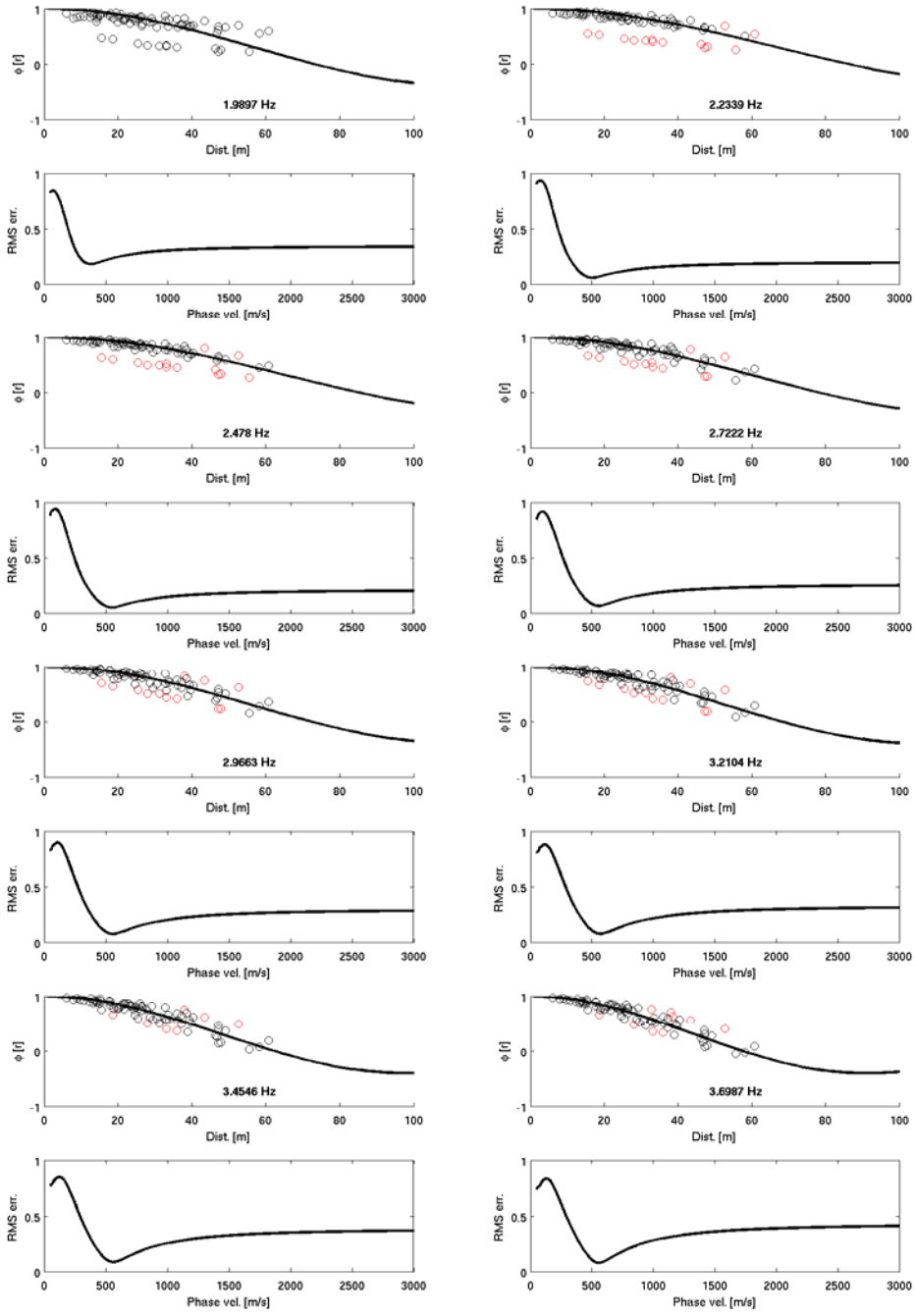

Figure 3: Experimental space-correlation function values versus distance (circles) for different frequencies. The red circles indicate values discarded. The black lines depict the estimated space-correlation function values for the phase velocity showing the best fit to the data. The bottom panels show the relevant root-mean square errors (RMS) versus phase velocity tested.

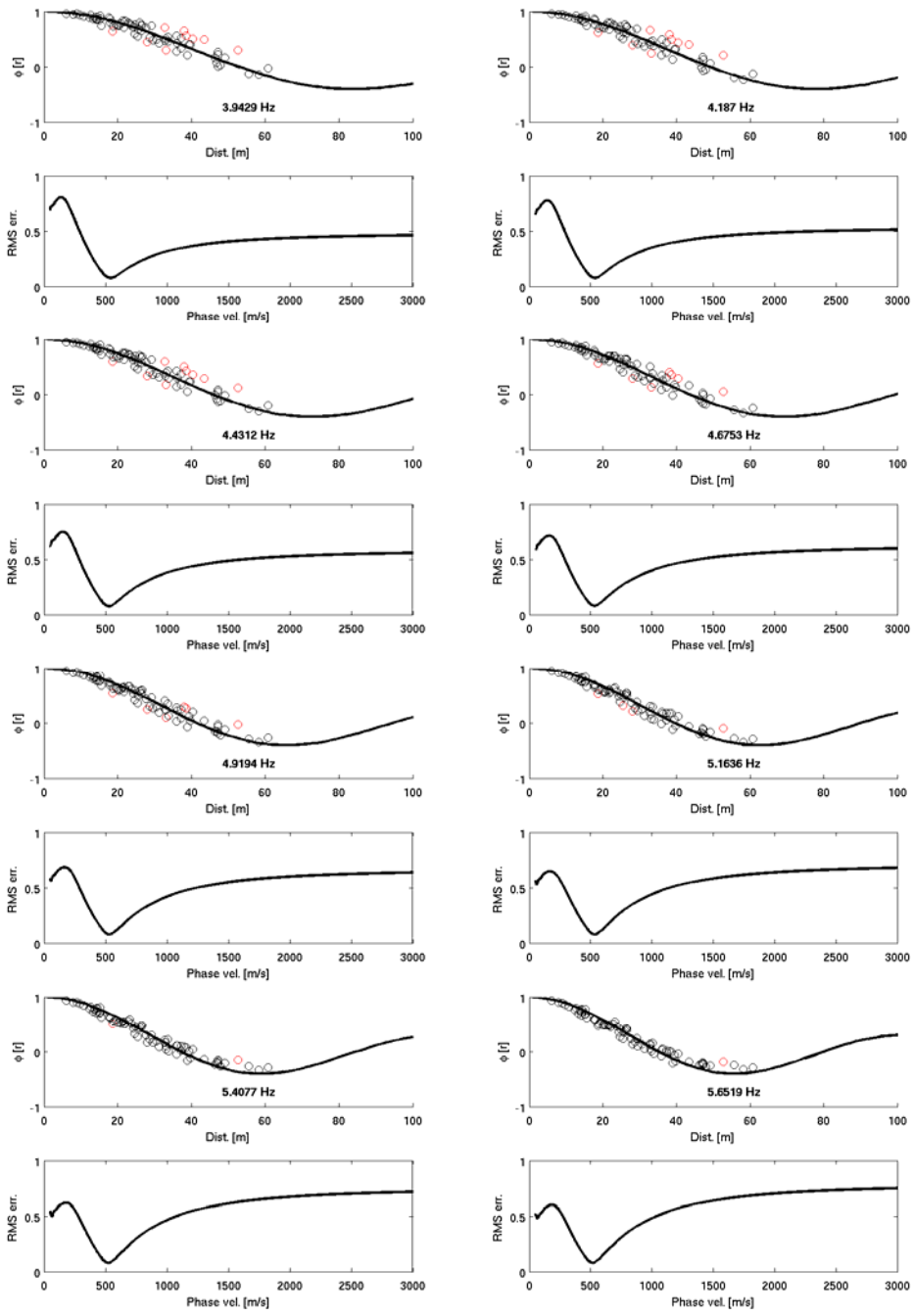

Figure 3: See previous caption.

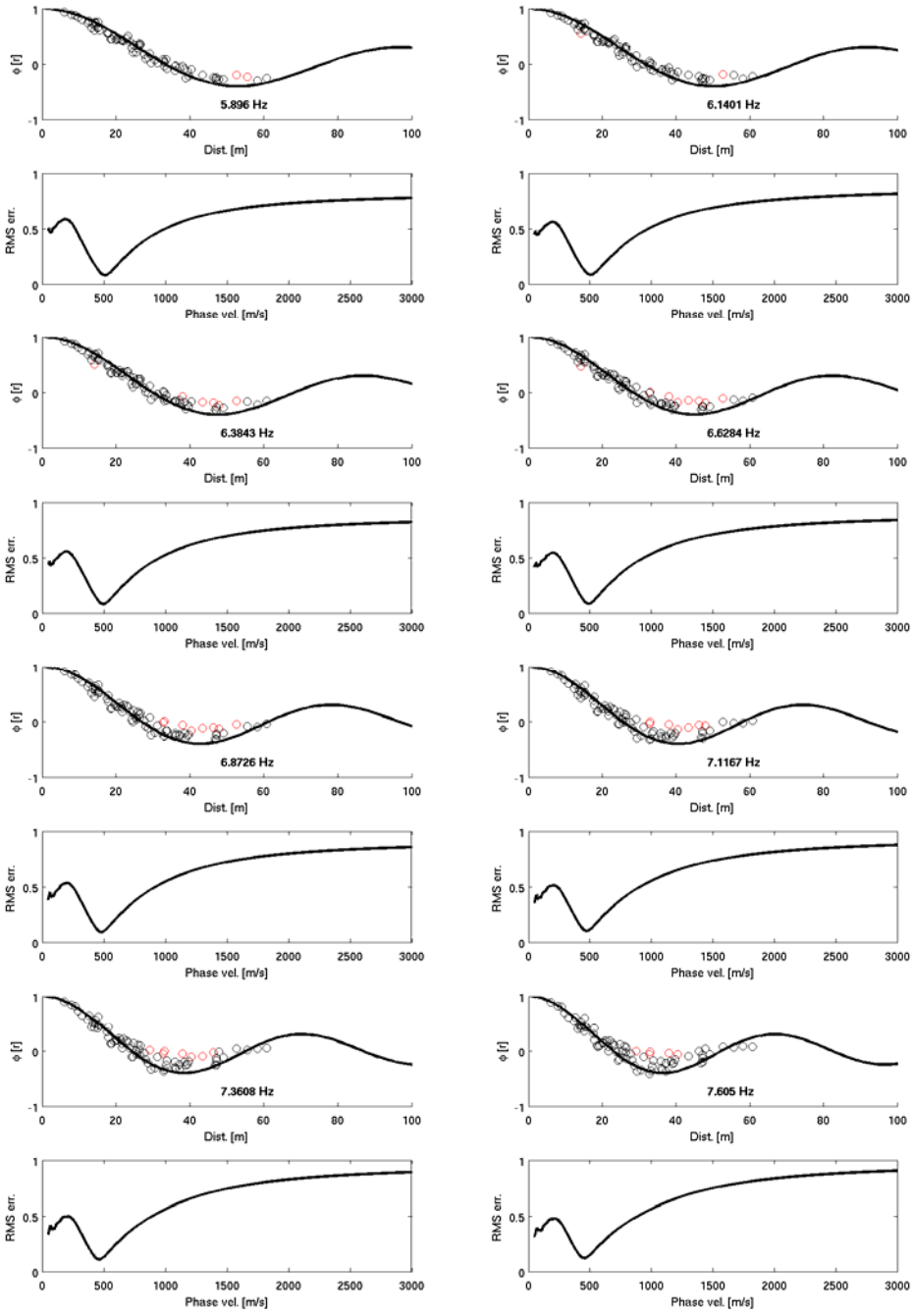

Figure 3: See previous caption.

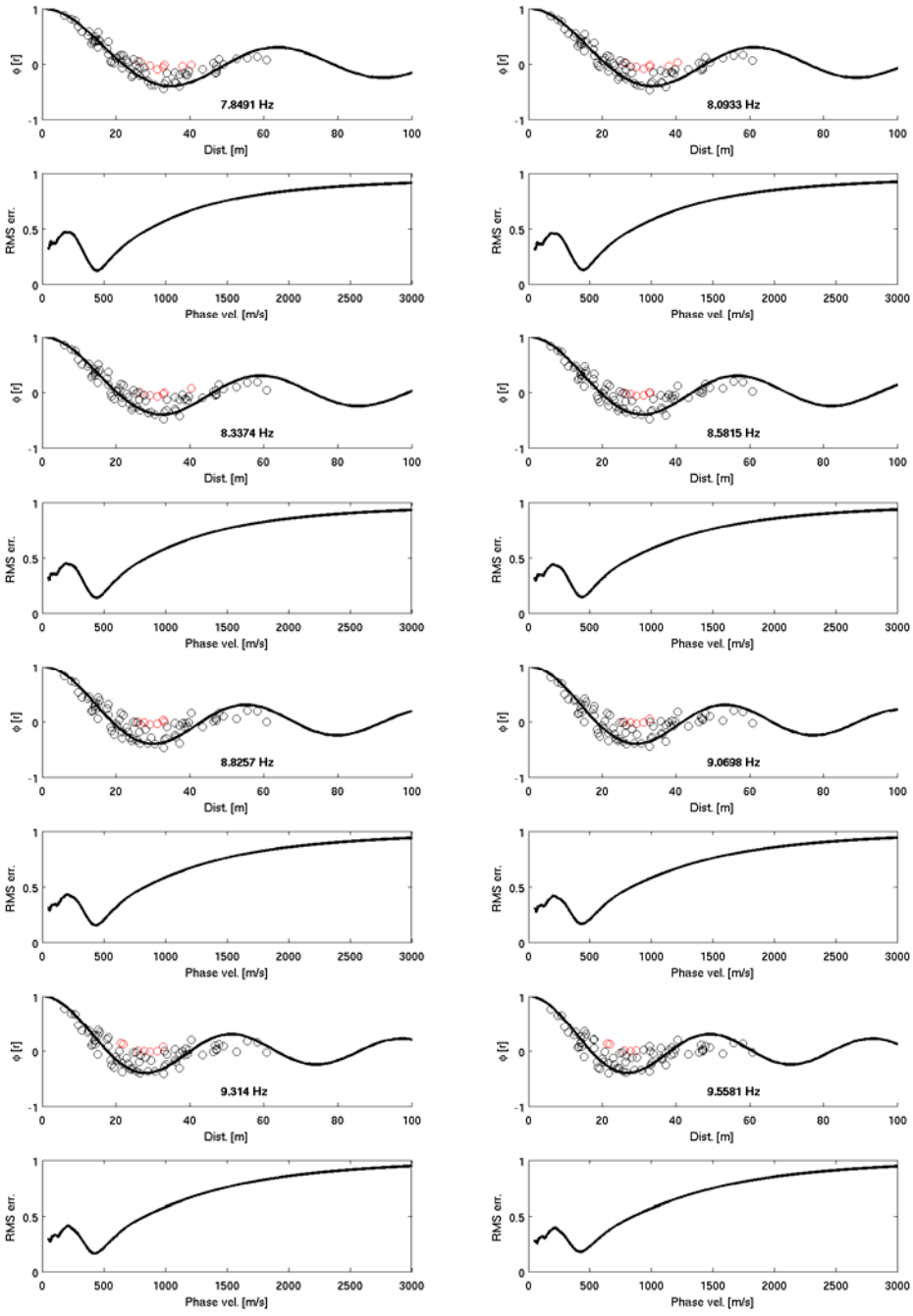

Figure 3: See previous caption.

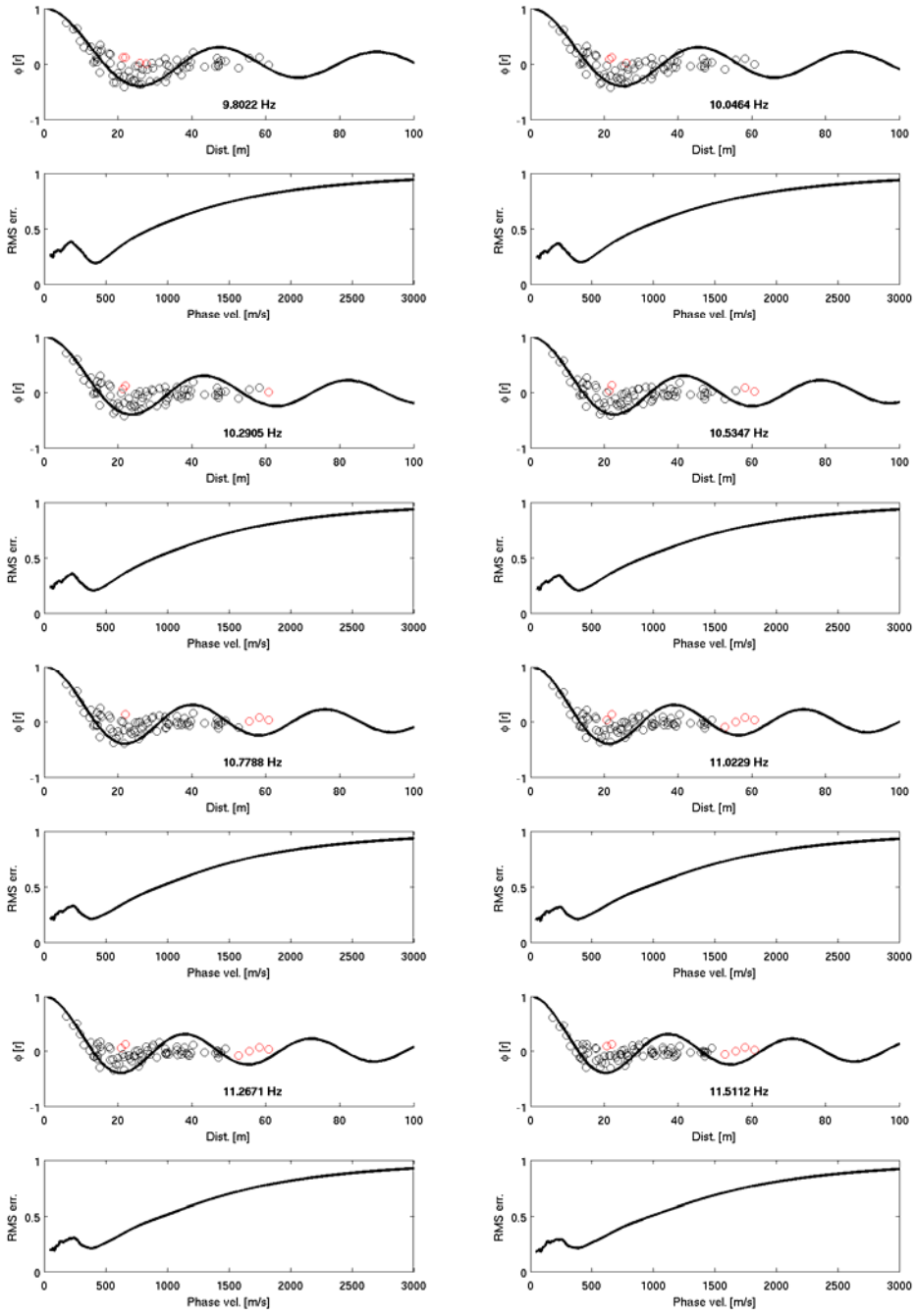

Figure 3: See previous caption.

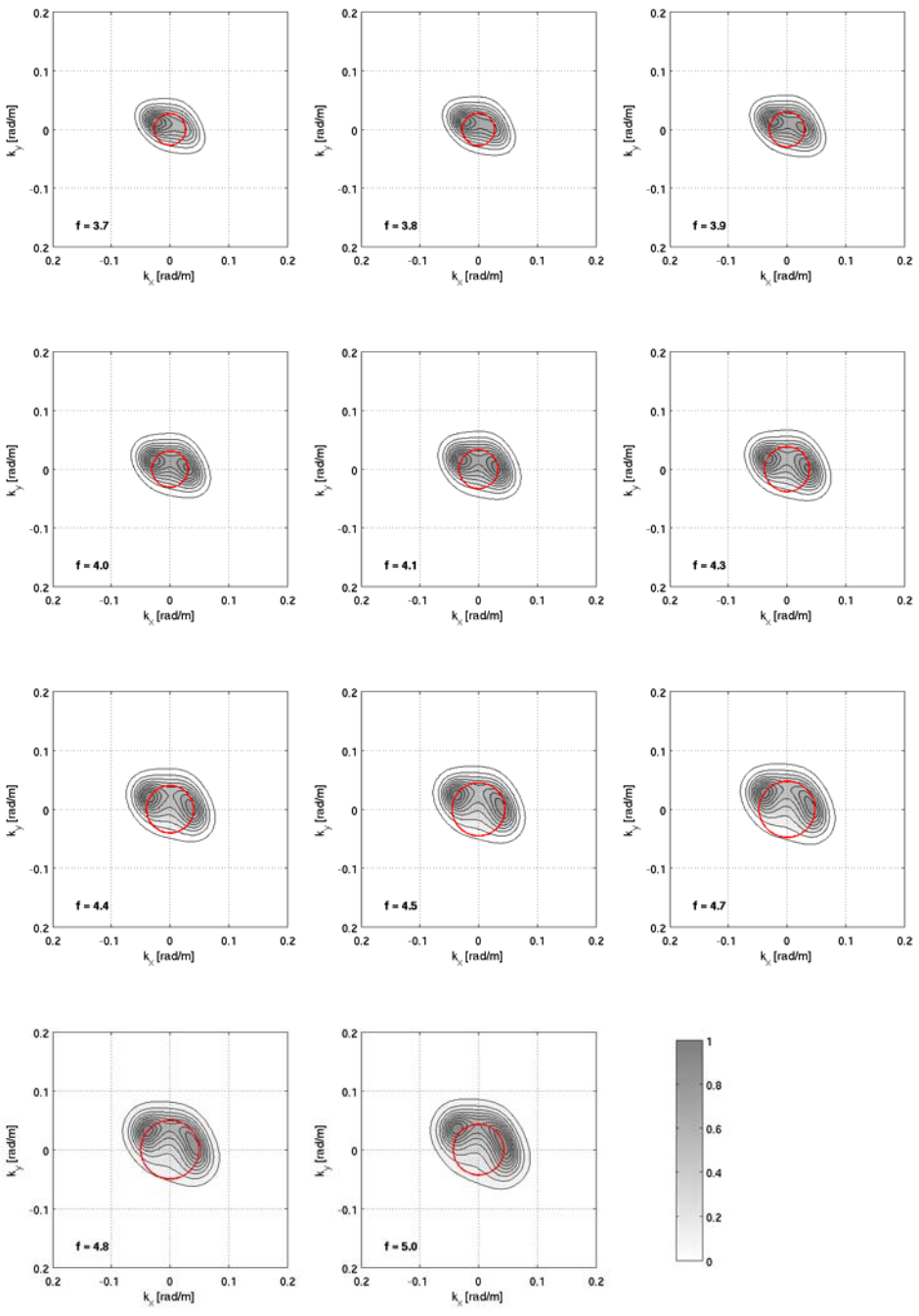

Figure 4: f-k power density function (MLM) at different frequencies (f, expressed in Hz). The red circles joints points with the same *k* value, corresponding to the maximum used to estimate the phase velocity.

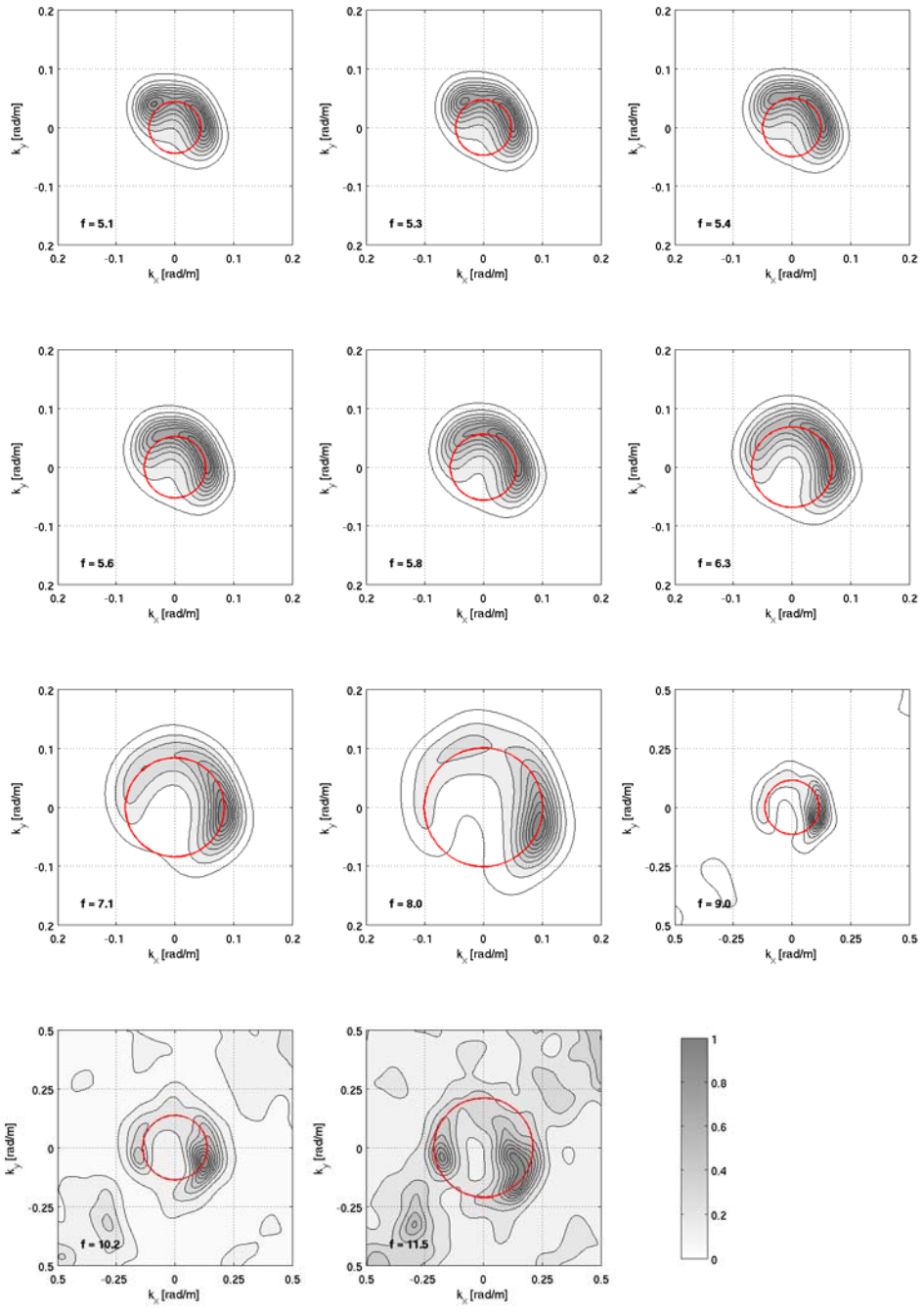

Figure 4: See previous caption.

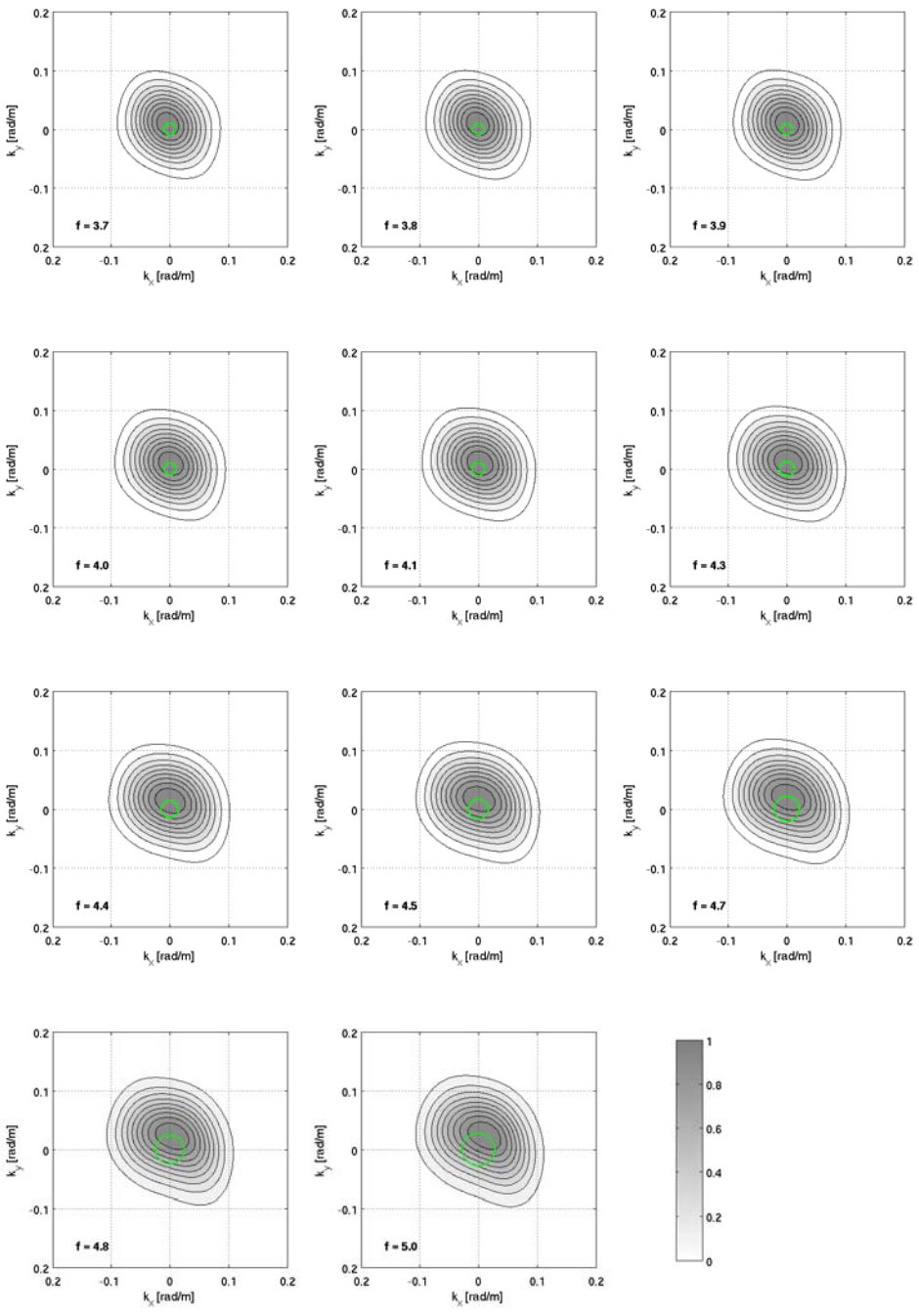

Figure 5: f-k power density function (BF) at different frequencies (f, expressed in Hz). The green circles joints points with the same *k* value, corresponding to the maximum used to estimate the phase velocity.

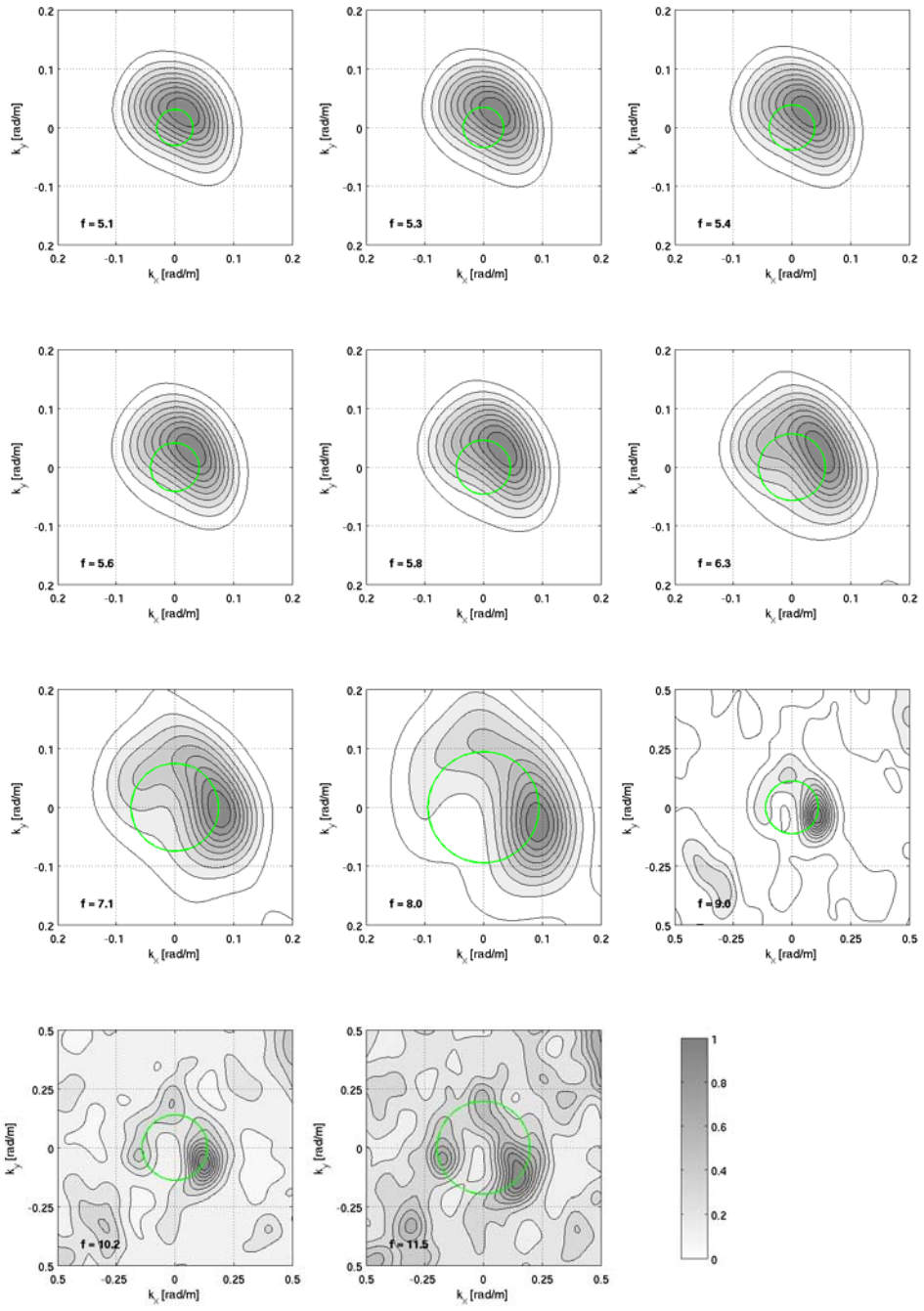

Figure 5: See previous caption.

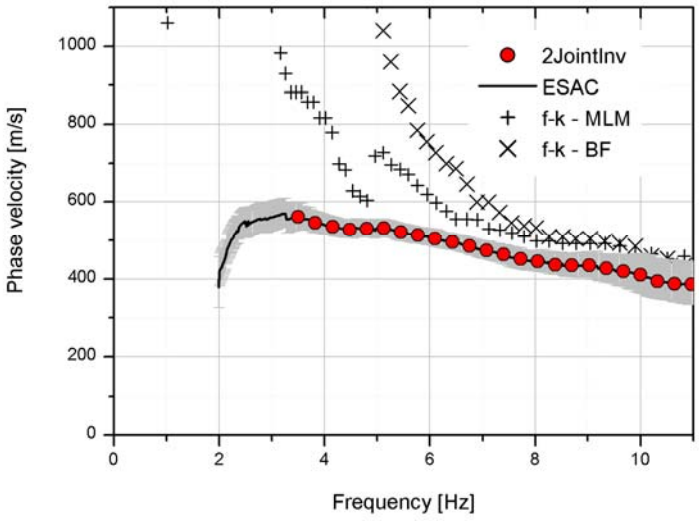

Figure 6: Comparison of experimental phase velocity estimated by the ESAC and the f-k (both for Beam Forming and Maximum Likelihood Method) methods. The red circles represent the values used for the joint inversion. The intervals (grey lines) around the observed ESAC phase velocities representing estimated uncertainties are obtained by calculating the square root of the covariance of the error function.

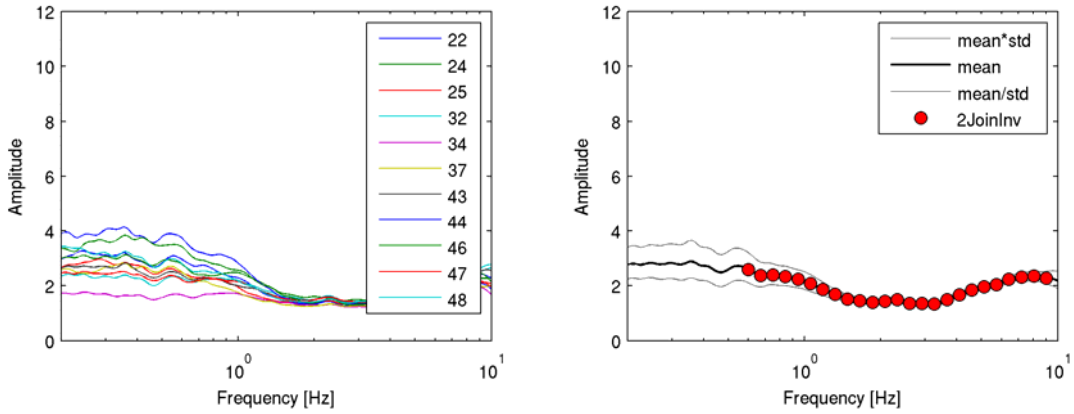

Figure 7: a) average *H/V* for the selected stations of the array (e.g. 22 stands for station 3022, etc.) and b) the average H/V of the array. The red circles represent the values used for the joint inversion.

The inversion of dispersion and *H/V* curves to estimate the S-wave velocity profile was carried out fixing to 5 the number of layers overlying the half-space in the model (**Table 1**). Through a genetic algorithm a search over 80000 models was carried out. The inversion was repeated several times starting from different

seed numbers, that is to say from a different population of initial models. In this way it was possible to better explore the space of the solution.

Table 1: Ranges of values defined for the parameters used in the joint inversion.

	Shear wave velocity, V_S [m/s]		Thickness, h [m]		Density, ρ [ton/m^3]
Layer	MIN	MAX	MIN	MAX	
#1	250	450	10	40	1.9
#2	300	700	30	100	1.9
#3	350	800	40	150	1.9
#4	400	900	50	200	2
#5	500	1500	80	700	2.2
Half-space	800	3500	Infinite		2.3

During the inversion procedure the thickness and the shear wave velocity for each layer could be varied within the pre-defined ranges. On the contrary, for each layer, density was assigned *a priori*, while P-wave velocity (V_P) was calculated through the values of the S-wave velocity Vs via the equation: $V_P\,[\mathrm{m/s}] = 1.1 \cdot V_S + 1290$.

The models are selected by means of a cost function which take in account the agreement between the theoretical *H/V* and Rayleigh-wave dispersion curves with the observed ones. In this application, after trial and error test, the weight of 0.01, that allowed the best balanced fit of dispersion and H/V curves, was adopted.

Discussion of the results

In **Figure 8a** all the models tested during the inversion are depicted (gray lines). The best fit model (white line) and the models lying inside the 10% range of the minimum cost (black lines) function are highlighted. The agreement between experimental and theoretical Rayleigh wave dispersion curves (**Figure 8c**) is good and, considering the wavelengths related to the dispersion curve frequency range, the V_S profile between 15 to about 60 metres is likely to be well constrained. Therefore, since below this depth the profile is constrained by the H/V curve alone, we prefer to show, in **Figure 8a** and **Table 2**, the V_S profile only within the depth range were both curves contribute to the inversion.

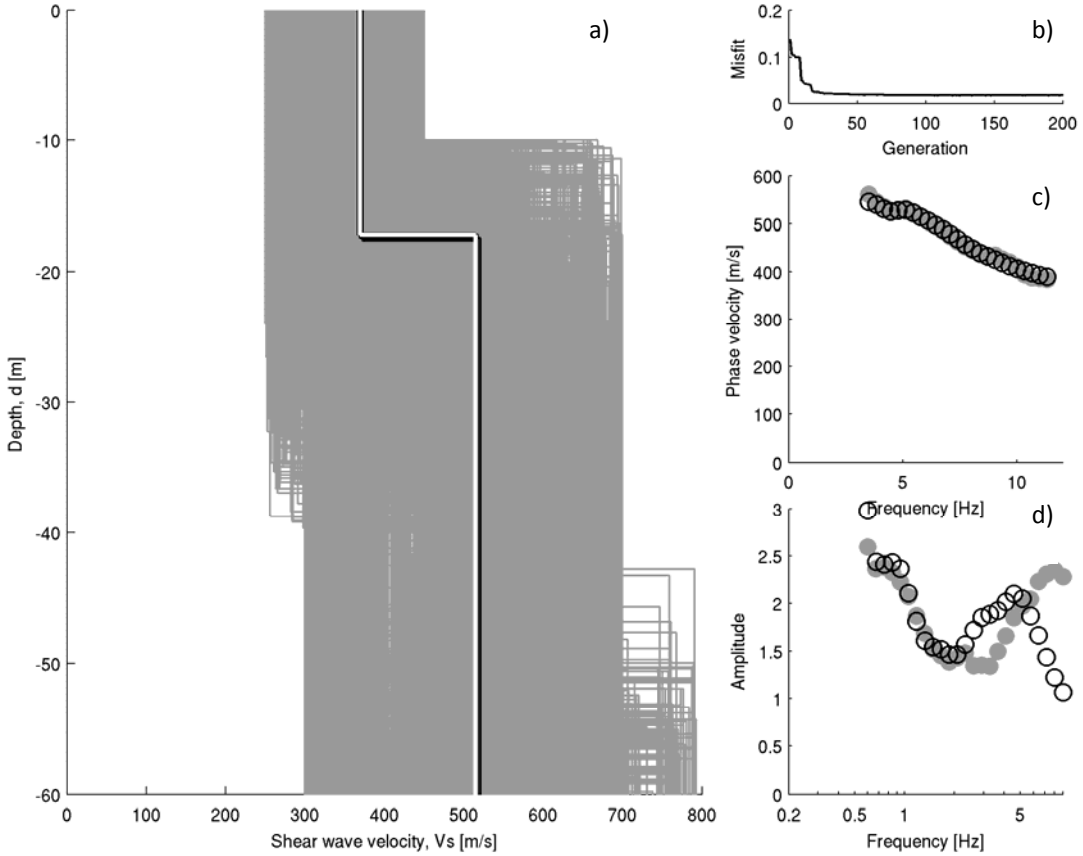

Figure 8: a) Tested models (grey lines), the minimum cost model (white line) and models lying inside the minimum cost + 10% range (black lines) for the SNA station; b) the misfit versus generation values; c) experimental (grey circles) and estimated (white circles – relevant to the minimum cost model) phase velocities; d) experimental (grey circles) and estimated (white circles – relevant to the minimum cost model) *H/V* ratio curves.

Table 2: Shear wave velocity model at the SNA station.

Shear wave velocity, V_S [m/s]	Thickness, h [m]
369.2	17.2
514.9	